[redacted]

Z65·11248

SINGLE COPY ONLY

(NASA-CR-82899) APOLLO REQUIREMENTS MANUAL. ENVIRONMENTAL AND THERMAL CONTROL AND THERMAL ANALYSIS (North American Aviation, Inc.) 314 p

N75-76076

Unclas

00/98 29778

Copy No.

ARM 2-5

APOLLO REQUIREMENTS MANUAL
Environmental and Thermal Control
and Thermal Analysis [U]

15 January 1964

NAS-9-150

Apollo

X67·82103

(ACCESSION NUMBER) (THRU)

314 (PAGES) 58 (CODE)

CR-82899 (NASA CR OR TMX OR AD NUMBER) (CATEGORY)

FACILITY FORM 602

CLASSIFICATION CHANGE

To UNCLASSIFIED
By authority of GDS-GP-4 Date 7-75
Changed by L. Shirley
Classified Document Master Control Station, NASA
Scientific and Technical Information Facility

RECEIVED
NASA STI FACILITY
INPUT BRANCH

[redacted]

[redacted]

Accession No. _____

Copy No.

ARM 2-5

APOLLO REQUIREMENTS MANUAL
Environmental and Thermal Control and Thermal Analysis [U]

15 January 1964

NAS-9-150

AVAILABLE TO NASA HEADQUARTERS ONLY

This document contains information affecting the national defense of the United States within the meaning of the Espionage Laws. Title 18 U.S.C. Section 793 and 794. Its transmission or revelation of its contents in any manner to an unauthorized person is prohibited by law.

NORTH AMERICAN AVIATION, INC.
SPACE and INFORMATION SYSTEMS DIVISION

Downgraded at 3-year intervals: declassified after 12 years; DOD DIR 5200.10.

[redacted]

[redacted]

FOREWORD

Apollo Requirements Manual (ARM 2) is an official source of reference data and material related to the tasks of the Thermo. and Fluid Dynamics section. The contents of this manual supersedes all previous criteria and transmittals, with the exception of those specifically mentioned in the text.

Apollo Requirements Manual 2 consists of five volumes:

ARM 2-1	Aerodynamics
ARM 2-2	Aerodynamic Loads Data
ARM 2-3	Environmental and Power Analysis
ARM 2-4	Propulsion Analysis
ARM 2-5	Thermal Analysis

The method of operation for making revisions to the manual is as follows:

Preliminary copies of additions or revisions are forwarded as enclosures to an IOL to all manual holders and other interested parties. The Manual Review Board reviews the preliminary data and with suitable revisions, if any, returns the data for inclusion in the manual. Comments on the preliminary data from other interested parties are welcome. Comments should be directed to the undersigned, or E.J. Alexander, 041-695-220.

M. R. Kinsler
Manager
Thermo. and Fluid Dynamics

[redacted]

~~CONFIDENTIAL~~

CONTENTS

Section		Page
1.0	LAUNCH ESCAPE SYSTEM	1-1
1.1	Preliminary Estimate of Escape Tower Truss Member Temperature as a Function of Ablative Thickness	1-1
1.2	Maximum Temperature of Nose Cone Ballast	1-1
1.3	Launch Escape System Skirt	1-1
1.4	LES Skirt-to-Rocket Interface Bolt Temperature	1-2
1.5	Expected LES Temperature for Wire Selection Purposes	1-2
1.6	Temperature of the Lockhead LES Casing Ring During Boost-Abort	1-3
1.7	Maximum Surface Temperature of the LES Skirt-to-Motor Attaching Bolts	1-3
1.8	Launch Escape Tower Maximum Temperature as a Function of Insulation Thickness	1-4
2.0	COMMAND MODULE	2-1
2.1	Heat Protection System Preliminary Ablation Shield Design	2-1
2.2	Heat Protection System Preliminary Ablation Shield Design	2-1
2.3	Preliminary Thermal Study of the C/M Fiberglass Stringers (Crew Compartment Heat Shield) During Reentry	2-1
2.4	Command Module Minimum Temperature Predictions	2-1
2.5	Expected Environment Temperatures in the Food and Fecal Storage Compartment	2-3
2.6	Attitude Control Rockets on C/M - Temperature During Reentry	2-3
2.7	Expected C/M Parachute Compartment Temperature During Flight	2-3
2.8	Temperature of Observation Windows, Uncovered During Reentry	2-3
2.9	Maximum Bondline Temperatures for HSE-3A and Depth of Char for a C-5 Direct Lunar Boost	2-3
2.10	Substructure Temperature History for Trajectory HSE-3A and HSE-6	2-4
2.11	Expected Maximum Bondline Temperature During Entry From HSA-3, HSE-1, HSE-2, and Nominal Suborbital Trajectory	2-4
2.12	Temperature Predictions of Repaired Honeycomb Panels	2-7
2.13	Temperatures of the Stainless Steel and Aluminum Honeycombs of Airframe 011 for Reentry Trajectory HSE-1	2-8
2.14	Thermal Analysis of Forward Heat Shield Skin Panels at Station X_c = 112.25 and X_c = 81.0	2-9

[redacted]

~~CONFIDENTIAL~~

Section | Page

2.15 Ablator-Bondline Temperatures at Body Points 8, 17, 24, and 32 2-9
2.16 Dead-Ended Holes for Heat Shield Penetrations . . 2-9
2.17 Preliminary Thermal Analysis of Aft Heat Shield Tie-Down Bolt 2-9
2.18 Thermal Analysis of C/M to S/M Umbilical During Boost and Reentry 2-10
2.19 Thermal Analysis of Scimitar Antenna Housings on Spacecraft for Boost and Atmospheric Reentry . . 2-10
2.20 Thermal Analysis of the Elastomer Seals Located on Various Equipment Penetrations in the C/M Inner Structure 2-11
2.21 Thermal Analysis of the Forward Heat Shield Thruster . 2-11
2.22 Preliminary Thermal Study of the Forward Compartment Heat Shield Separation System Components During Reentry 2-14
2.23 Preliminary Thermal Analysis of the Main Parachute Fittings and Steel Cable Risers 2-15
2.24 Typical Temperature Histories for the Command Module Air Vent Components 2-15
2.25 Thermal Analysis of the Teflon Covering of the Command Module Vent 2-16
2.26 Thermal Analysis of the C/M RCS Yaw, Roll, and Aft Pitch Engine Mounting Structures 2-16
2.27 Temperature Histories of the C/M RCS Tanks and Lines for Space Flight, Reentry, and Post-Landing Phases . 2-16
2.28 Minimum C/M Outer Structure Temperatures in Earth Orbit 2-18
2.29 Command Module Surface Temperature Extremes During Lunar Orbit 2-19
2.30 Oxygen Temperatures at C/M Pressure Bulkhead . . 2-19
2.31 Temperature Histories of the C/M RCS Propellant Tanks 2-19
2.32 Temperature Extremes of C/M Antennas in Spaceflight . 2-19
2.33 Command Module Environmental Heat Exchanger (Various Mission Phases) 2-19
2.34 Command Module LEM Docking Study, Space Heat Transfer Analysis 2-22
2.35 Polaroid Filter Proposed for C/M Windows . . . 2-23
2.36 Heat Loads Through C/M C-Band Antennas . . . 2-23
2.37 Heat Loads to C/M 2-24
2.38 Temperature Extremes of C/M RCS Rocket Engines . . 2-24
2.39 Command Module Heat Shield Steady-State Circumferential Temperature Distributions in Space 2-25

[redacted]

Section | Page

2.40 Total Heat Loads to C/M 2-25
2.41 Heat Transfer Coefficient Through C/M Walls . . . 2-25
2.42 Command Module Space Flight Transient Circumferential Temperature Distribution 2-25
2.43 Minimum Temperature of Harmonic Drive Mechanism of Astro-Sextant Door 2-27
2.44 Space Flight Temperature Extremes of Scimitar Antenna 2-28
2.45 Temperature Distributions Through the Heat Shield, About C-Band Antenna Window 2-28
2.46 Steady-State Temperature Distribution for ECS Water Dump Line 2-28
2.47 Temperature Extremes of Airlock Seals for Space Flight Conditions 2-29
2.48 C-Band Antenna Window Temperatures in Space Flight . . 2-30
2.49 Command Module Space Flight Transient Circumference Temperature Distribution 2-30
2.50 Temperature Extremes of Parachutes During Space Flight Conditions 2-31
2.51 Insulation Requirements for the LES Tower-to-C/M Forward Heat Shield Pull-Off Tubes 2-31
2.52 Temperature Distribution of the C/M Structural I-Beam Spacer and Outer Structure for Space Operation . . . 2-32
2.53 Thermal Data for Heat Shield Substructure and Attachments 2-33

3.0 SERVICE MODULE 3-1
3.1 Expected Temperatures During Space Operations for the S/M Shell Structure and for Some Components 3-1
3.2 Service Module Honeycomb Shell Structure (Boost) . . 3-1
3.3 Thermal Requirements of Storable Propellants During Prelaunch Phase 3-1
3.4 Heating Requirement for S/M Main Engine Injector Plate 3-1
3.5 Maximum and Minimum Expected Surface Temperatures of the S/M Cryogenic Tanks During the Lunar Mission . . 3-7
3.6 Heat Transfer Analysis of Solenoid Valve 3-7
3.7 Expected Environmental Temperature Extremes for Electrical Cables 3-8
3.8 Thermal Data for Mechanical Docking Arms 3-8
3.9 Service Module Outer Shell Temperatures During Translunar Flight 3-8

[redacted]

Section | Page

3.10 Summary of S/M SPS Propellant Thermal Protection Requirements 3-11
3.11 Service Module Surface Insulation Requirements Due to Plume Impingement From the S/M RCS Engines . . . 3-11
3.12 Oxygen and Hydrogen Cryogenic Storage Tank Temperatures 3-12
3.13 Thermal Evaluation of 2 KMC Scimitar Antennas Located on the S/M Firing 3-12
3.14 Temperature Response of S/M RCS Composite Thermal Protection for Variable RCS Firings 3-15
3.15 Sensor Locations for AFRM 011 S/M 3-15
3.16 Thermal Analysis of Flexible Boot and Aft Heat Shield Attachment Techniques 3-16
3.17 Thermal Design Requirements of the LEM Tracking Antenna 3-17
3.18 Temperature Histories of the Service Module High-Gain Antenna and Boom During 60-Second Firing of RCS Rocket Engine 3-17
3.19 Service Module RCS Nozzle Radiation Reflector on the S/M Surface 3-18
3.20 Service Module Interior Coating and Finish Requirements 3-19
3.21 Service Module SPS Nozzle Extension Temperatures During Abort Firing With S-IVB Adapter Attached 3-19
3.22 Temperature Time History of RCS Tanks During S/M Atmosphere Reentry 3-19
3.23 Cooling Requirements for S/M RCS Inboard Configuration . 3-19

4.0 INTERFACE 4-1
4.1 Maximum Surface Temperatures of the Honeycomb Adapter During Boost Heating 4-1

5.0 BOILERPLATES
5.1 Thermal Requirements During C-1 Boost (Boilerplates 9, 13, 15, 16, and 18) 5-1
5.2 Temperature Histories of the C-Band Antenna Windows (at X_c = 77) During Maximum-Q and High-Altitude Abort Missions 5-2
5.3 Boilerplate Shell Structure Temperatures During C-1 Boost 5-2
5.4 Shell Structure Temperatures During the Little Joe II Boost (Boilerplates 12, 22, and 23) 5-2
5.5 Command Module Forward Heat Shield Separation Bolt Temperature Histories (Boilerplates 6 and 12) . . . 5-2
5.6 Maximum Temperatures of the LES, Nose Cone, Motor Casing and Structural Skirt Skin (Boilerplate 22) . . 5-3

Section | Page

5.7 Thermal Analysis of the C/M R&D Radome (Boilerplates 13, 15, and 18) 5-3
5.8 Thermal Protection for Boilerplates 12 and 23 . . . 5-4
5.9 Thermal Protection for C/M to S/M Umbilical Cover on Boilerplate 13 5-4
5.10 Thermal Analysis of Selected Points on the C/M of Boilerplate 15 (During Boost) 5-4
5.11 Minimum Insulation Requirements of the LES Tower-to-C/M Umbilical Conduit Shroud 5-5
5.12 Thermal Analysis of the C/M Tower Leg Wells for Boilerplates 13, 15, 16, 18, and 26 5-6
5.13 Thermal Protection (for Boilerplate 22) 5-7
5.14 Insulation Requirements for the LES Tower-to-C/M Forward Heat Shield Pull-Off Tubes 5-8
5.15 Temperature Histories of Telemetry Antenna Cover on Boilerplate 22 5-8
5.16 Maximum Temperatures of S/M RCS Fiberglass Nozzles for a Saturn-I Boost Trajectory of Boilerplates 13 and 15 . 5-8
5.17 Shaped Charges for C-1 Adapter 5-8
5.18 Environmental Temperature Extremes for the LEM Adapter . 5-9
5.19 Thermal Environment of Radiation Sensor During Lunar Mission 5-9
5.20 Thermal Characteristics of the Forward Heat Shield/LET Ejection System. 5-9
5.21 Parametric Thermal Analysis of the LEM Adapter During Boost 5-10
5.22 Heating Rates for C/M During a 100-Nautical-Mile Tumbling Earth Orbit 5-11
5.23 Expected Inside Wall Temperatures of Boilerplate 13 for a Tumbling-Earth Orbit 5-12

6.0 GROUND SUPPORT EQUIPMENT 6-1

[redacted]

ILLUSTRATIONS

Figure		Page
1-1	Preliminary Estimate of Escape Tower Truss Member Temperature as a Function of Ablative Thickness	1-5
1-2	LES Skirt-to-Motor Interface, Showing Bolt and Nut Locations	1-6
1-3	Temperature History of the LES Skirt-to-Motor Interface Bolt-Head Surface During a Saturn-V Boost/High-Altitude Abort	1-7
1-4	Temperature History of the LES Skirt-to-Motor Interface Nut Surface During a Saturn-V Boost/High-Altitude Abort	1-8
1-5	LES Tower, Showing Data Tube Locations and Cross Sections	1-9
1-6	LES Tower Buna-N Ablative Insulation Versus Maximum Tube Temperature for a Typical 2.5-Inch Horizontal Tube (During a Saturn-V Boost/High-Altitude Abort)	1-10
1-7	LES Tower Buna-N Ablative Insulation Versus Maximum Tube Temperature for a Typical 3.5-Inch Horizontal Tube (During a Saturn-V Boost/High-Altitude Abort)	1-11
2-1	Typical Structure for Ablation and Transient Heat Transfer Analysis	2-34
2-2	Schematic Diagram of the Command Module	2-35
2-3	Command Module Ablator Stainless Steel Interface Temperature Histories for Reentry Trajectories (Indicated at Body Location 8)	2-36
2-4	Command Module Ablator Stainless Steel Interface Temperature Histories for Reentry Trajectories (Indicated at Body Location 13)	2-37
2-5	Command Module Ablator Stainless Steel Interface Temperature Histories for Reentry Trajectories (Indicated at Body Location 24)	2-38
2-6	Temperature History at Inner Structure	2-39
2-7	Temperature Histories of Front Facesheet S/S Honeycomb as a Function of Distance From the Pin	2-40
2-8	Temperature Versus Time	2-41
2-9	Forward Heat Shield Skin Panel	2-68
2-10	Bondline Temperature History HSE-3A Body Point 17 Initial Temperature 250°F	2-71
2-11	Bondline Temperature History HSE-3A Body Point 31 Initial Temperature 250°F	2-72
2-12	Bondline Temperature History HSE-3A Body Point 24 Initial Temperature -260°F	2-73
2-13	Bondline Temperature History HSE-3A Body Point 8 Initial Temperature -260°F	2-74
2-14	Sketch of Aft Heat Shield Tie-Down Bolt	2-75
2-15	Temperature Histories of Aft Heat Shield Tie-Down Bolt and Supporting Substructure	2-76

[redacted]

[redacted]

Figure		Page
2-16	Sketch of C/M - S/M Umbilical Wire Package	2-77
2-17	Temperature Histories of Referenced C/M to S/M Umbilical Locations	2-78
2-18	Schematic Diagram of Scimitar Antenna Housings	2-79
2-19	Sections Through Windward Antenna Housing	2-80
2-20	Sections Through Leeward Antenna Housing	2-81
2-21	Temperature Histories for Windward Antenna Housing During S-V Boost	2-83
2-22	Temperature Histories for Leeward Antenna Housing During S-V Boost	2-87
2-23	Temperature Histories With Severe Initial Gradients During Reentry Trajectory HSE-3A	2-89
2-24	Temperature Histories With Severe Initial Gradients During Reentry Trajectory HSE-6	2-93
2-25	Diagram of Elastomer Seal Locations on the Command Module Inner Structure	2-95
2-26	Forward Heat Shield Thruster	2-96
2-27	Schematic of the Command Module Air Vent Components	2-97
2-28	Typical Reentry Temperature-Histories for the C/M Air Vent Copper Heat Exchanger - Trajectory HSE-6	2-98
2-29	Typical Temperature Histories for the Tapered Ablation Outer Structure of the Air Vent Copper Grid Trajectory HSE-6	2-99
2-30	Vent Tube Bondline Temperature History of Point 1 for a Saturn V Boost	2-100
2-31	Vent Tube Bondline Temperature History of Point 2 for a Saturn V Boost	2-101
2-32	Vent Tube Bondline Temperature History of Point 3 for a Saturn V Boost	2-102
2-33	Vent Tube Bondline Temperature History of Point 4 for a Saturn V Boost	2-103
2-34	Command Module Air Vent System Sketch	2-104
2-35	Typical Yaw Engine Mounting Can Configuration	2-105
2-36	Typical Roll Engine Cast Mount Configuration	2-106
2-37	Typical Aft Pitch Engine Mounting Can Configuration	2-107
2-38	Temperature Histories of the RCS Yaw Engine Mounting Structure Reentry Trajectory HSE-3A	2-108
2-39	Temperature Histories of the RCS Engine Mounting Structure Reentry Trajectory, HSE-3A	2-109
2-40	Command Module/RCS Temperatures	2-111
2-41	Command Module/RCS Propellant Tanks Temperature History	2-116
2-42	Command Module Environmental Heat Exchange, Earth Orbit (Launch Time: June 21, 7 AM)	2-117
2-43	Command Module Environmental Heat Exchange, Earth Orbit (Launch Time: June 21, 12 AM)	2-118
2-44	Command Module Environmental Heat Exchange, Translunar Mission	2-119
2-45	Command Module Environmental Heat Exchange, Transit - Cold Case	2-120

[redacted]

Figure		Page
2-46	Command Module Environmental Heat Exchange, Lunar Orbit	2-121
2-47	Command Module Environmental Heat Exchange, Transearth Mission	2-122
2-48	Command Module Steady-State Circumferential Temperature Distributions (at X_c = 23)	2-123
2-49	Command Module Steady-State Circumferential Temperature Distributions (at X_c = 112)	2-124
2-50	Forward Heat Shield Space Flight Transient Circumferential Temperature Distributions	2-125
2-51	Forward Heat Shield Temperature Distribution After Start of Heating	2-126
2-52	Distribution at 0 Hours: Heating From Steady-State Cold	2-138
2-53	Forward Hatch Assembly Showing Location of Seals	2-155
2-54	Hot-Soak Space Flight Conditions	2-156
2-55	Cold-Soak Space Flight Conditions	2-157
2-56	Airlock Seal Extreme Temperature History	2-158
2-57	Forward Heat Shield Space Flight Transient Circumferential Temperature Distributions	2-159
2-58	Forward Heat Shield Temperature Distribution After Start Cooling Period	2-160
2-59	Schematic of the LES Tower, Showing the Location of the Forward Heat Shield Pull-off Tubes; and a Tube Cross-Section, Showing the Insulation Requirements for These Tubes	2-174
2-60	Command Module Steady-State Temperature Distribution of I-Beam Spacer for Space Flight	2-175
2-61	Command Module Steady-State Temperature Distribution of I-Beam Spacer for Space Flight	2-176
3-1	Heating Requirement for S/M Main Engine Injector Plate (Part 1)	3-20
3-2	Heating Requirement for S/M Main Engine Injector Plate (Part 2)	3-21
3-3	Time-Temperature History of Solenoid Valve	3-22
3-4	Configurations Analyzed During Thermal Analysis	3-23
3-5	Isothermal Profile Map Caused by RCS Plume Impingement on S/M Surface	3-24
3-6	Area on S/M Covered by Q-Felt Plus Cover Sheet to Prevent the Surface Temperature of the Aluminum Honeycomb From Exceeding 400 F	3-25
3-7	Temperature History for the Outer Surface of the Oxygen and Hydrogen Cryogenic Storage Tanks	3-26
3-8	Temperature at End of Firing Cycle and Maximum Temperature of Interface Between Service Module and RCS Composite Thermal Protection as a Function of RCS Firing Time	3-27
3-9	Time Required for the Temperature of Interface Between Service Module and RCS Composite Thermal Protection to Reach a Maximum as a Function of RCS Firing Time	3-28
3-10	Placement of Insulation at Section E-E and All Similar Sections Shown in Drawing V17-931118	3-29

Figure		Page
3-11	Placement of Thermal Protection for Section A-A and All Similar Sections Shown in Drawing V17-331739	3-29
3-12	Placement of Thermal Protection for Section D-D and All Similar Sections Shown in Drawing V17-331739	3-30
3-13	Thermal Design Criterion for the X-Band Radar Antenna Dish	3-31
3-14	Thermal Design Criterion for the VHF Radar Antenna	3-32
3-15	Temperature History of End Fire Element - René 41	3-33
3-16	Temperature History of End Fire Element - Columbium	3-34
3-17	Temperature History of Gimbal Housing and Shield	3-35
3-18	Temperature History of Earth Sensor With Stainless Steel Shield	3-36
3-19	Temperature History of Earth Sensor With Columbium Shield	3-37
3-20	Temperature History of Antenna Boom, Stainless Steel	3-38
3-21	Temperature History of Antenna Boom, Inconel	3-39
3-22	Temperature History of Antenna Boom at Deployment Point - No Shield	3-40
3-23	S/M RCS Nozzle Temperatures From Marquardt Test	3-41
3-24	S/M Radiation Shield Configuration	3-42
3-25	Summary of RCS and S/M Temperatures for a 60-Second RCS Engine Fire Cycle, With an RCS Mount Wall ϵ of 0.05	3-43
3-26	Summary of RCS and S/M Temperatures for a 60-Second RCS Engine Fire Cycle, With an RCS Mount Wall ϵ of 0.20	3-44
3-27	Summary of RCS and S/M Temperatures for a 300-Second RCS Engine Fire Cycle, With an RCS Mount Wall ϵ of 0.05	3-45
3-28	Summary of RCS and S/M Temperatures for a 300-Second RCS Engine Fire Cycle, With an RCS Mount Wall ϵ of 0.20	3-46
3-29	Summary of RCS and S/M Temperatures for a 500-Second RCS Engine Fire Cycle, With an RCS Mount Wall ϵ of 0.05	3-47
3-30	Summary of RCS and S/M Temperatures for a 500-Second RCS Engine Fire Cycle, With an RCS Mount Wall ϵ of 0.20	3-48
3-31	Temperature-Time History of RCS Tanks for S/M Reentry Temperature	3-49
5-1	Typical Boilerplate (With X_c Locations Shown)	5-13
5-2	Temperature History of Aluminum Skin During a C-1 Boost (X_c = 23.87)	5-14
5-3	Temperature History of Aluminum Skin During a C-1 Boost (X_c = 115.938)	5-15
5-4	C-Band Antenna Schematic	5-16
5-5	Maximum-Q Abort Temperature Histories of Front and Back Faces of C-Band Antenna Windows (X_c = 77)	5-16
5-6	High-Altitude Abort Temperature Histories of Front and Back Faces of C-Band Antenna Windows (X_c = 77)	5-17
5-7	Temperature Profile of Boilerplate Shell Structure During C-1 Boost	5-18
5-8	Temperature Profile of Boilerplate 22 During Little Joe II Boost	5-19
5-9	Command Module Forward Heat Shield Separation Bolt	5-19

[redacted]

Figure		Page
5-10	Temperature History at Point A of C/M Forward Heat Shield Separation Bolt During a Pad Abort	5-20
5-11	Temperature History at Point B of C/M Forward Heat Shield Separation Bolt During a Pad Abort	5-21
5-12	Temperature History at Point C of C/M Forward Heat Shield Separation Bolt During a Pad Abort	5-22
5-13	Maximum Expected Temperatures of the LES Nose Cone, Motor Casing, and Skirt Skin	5-23
5-14	Schematic of the C/M Radome for Boilerplates 13, 15, and 18 Showing Locations of Four Data Points	5-24
5-15	Temperature History at Point A of Figure 5-14	5-25
5-16	Temperature History at Point B of Figure 5-14	5-26
5-17	Temperature History at Point C of Figure 5-14	5-27
5-18	Temperature History at Point D of Figure 5-14	5-28
5-19	Diagram of the C/M Boilerplate, Showing X_c Locations	5-29
5-20	Temperature History of Aluminum, 0.08-Inch Skin (With and Without Thermal Protection), During Little Joe II Boost/ Maximum-Q Abort	5-30
5-21	Temperature History of Aluminum, 0.19-Inch Skin (With and Without Thermal Protection), During Little Joe II Boost/ Maximum-Q Abort	5-31
5-22	Schematic Diagram of C/M-to-S/M Umbilical Cover on Boilerplate 13	5-32
5-23	Temperature History of the Umbilical Cover, From $X_c = 43.9$ to $X_c = 40.2$	5-33
5-24	Temperature History of the Umbilical Cover, From $X_c = 40.2$ to $X_c = 356.5$	5-34
5-25	Locations for Thermal Analysis on Boilerplate 15	5-35
5-26	Temperature Histories of Bondlines at $X_c = 88.00$	5-36
5-27	Schematic of the LES Tower-to-C/M Umbilical Electrical Installation, Showing the Locations of the Wire Conduit and Connector Shroud	5-37
5-28	Locations of Data Points on the C/M Tower Leg Well	5-38
5-29	Temperature History of the C/M Tower Leg Well for Boilerplates 13, 16, and 26 (No Insulation)	5-39
5-30	Temperature History of the C/M Tower Leg Well for Boilerplates 13, 16, and 26 (Minimum Insulation)	5-40
5-31	Temperature History of the C/M Tower Leg Well for Boilerplate 15 (No Insulation)	5-41
5-32	Temperature History of the C/M Tower Leg Well for Boilerplate 15 (Minimum Insulation)	5-42
5-33	Temperature History of the C/M Tower Leg Well for Boilerplate 18 (No Insulation)	5-43
5-34	Temperature History of the C/M Tower Leg Well for Boilerplate 18 (Minimum Insulation)	5-44
5-35	Diagram of the C/M Boilerplate	5-45

[redacted]

Figure		Page
5-36	Temperature History of Aluminum Skin—With and Without Thermal Protection—(X_c= 115.938) During Little Joe II Boost/60,000-ft Abort	5-46
5-37	Temperature History of Tower Leg Well—With and Without Insulation—During Little Joe II Boost/60,000-ft Abort	5-47
5-38	Temperature History of the Telemetry Antenna Window Surfaces—With and Without Insulation—During Little Joe II Boost/60,000-ft Abort	5-48
5-39	Schematic of the LES Tower (Showing the Location of the Forward Heat Shield Pull-Off Tubes) and a Tubular Cross-Section (Showing the Insulation Requirement for these Tubes)	5-49
5-40	Approximate Location of Telemetry Antennas for Boilerplate 22	5-50
5-41	Temperature Histories of Teflon Cover of Telemetry Antenna for Boilerplate 22 (Little Joe II Boost/60,000-ft Abort)	5-51
5-42	Maximum Temperature of Fiberglass S/M RCS Nozzles (During Saturn-I Boost Trajectory	5-52
5-43	Radiation Sensor Temperature History, Lunar Mission	5-53
5-44	Forward Heat Shield/LET Ejection System	5-54
5-45	Schematic Diagram of the LEM Adapter	5-55
5-46	Maximum Temperature of LEM Adapter: Honeycomb Surface Facesheet Versus Insulation (Cork) Thickness and Facesheet Thickness (X_a = 838)	5-56
5-47	Maximum Temperature of LEM Adapter: Honeycomb Surface Facesheet Versus Insulation (Cork) Thickness and Facesheet Thickness (X_a = 510)	5-57
5-48	Temperature History of LEM Adapter Aluminum Honeycomb Facesheet During Saturn-V Boost Heating	5-58

[redacted]

TABLES

Table		Page
1-1	Expected LES Temperatures	1-2
1-2	Maximum Expected Temperatures of the LES Skirt-to-Motor Interface: Bolt-Head and Nut Surfaces	1-3
2-1	Heat Protection System, Ablation Shield Design	2-2
2-2	Insulation Material Layer, Ablation Shield Design	2-2
2-3	Maximum Expected Temperatures of the Nozzles on Command Module Attitude Control Engines	2-4
2-4	Average Inner Wall Temperatures of the C/M Parachute Compartment	2-5
2-5	Bondline Temperatures at Time of Earth Impact for HSE-3A (Ablator Avcoat 5026-39) Subliming Ablator Program	2-6
2-6	Ablation Material Char Depth for A C-5 Direct Lunar Boost	2-7
2-7	Maximum Bondline Temperatures	2-8
2-8	Maximum Temperatures During S-V Boost, Additional Data Points	2-12
2-9	Maximum Temperatures for Leeward Scimitar Antenna Housing During Atmospheric Reentry	2-13
2-10	Additional Temperature Gradients Possible in Leeward Scimitar Antenna Housing Prior to Reentry	2-14
2-11	Thicknesses of Teflon-Like Ablator Remaining on Scimitar Antenna Housings Following S-V Boost	2-15
2-12	Command Module RCS Tanks and Lines Temperature Extremes	2-17
2-13	Apex Lunar-Oriented (Positive X-Axis Pointed Toward Lunar Center at All Times)	2-20
2-14	Apex Orbit-Oriented (Positive X-Axis Pointed Along Orbit Path at All Times)	2-21
2-15	Base Sun-Oriented (Negative X-Axis Pointed Toward Sun at All Times)	2-21
2-16	Oxygen Temperature at C/M Pressure Bulkhead	2-22
2-17	Antenna Temperature Extremes	2-22
2-18	Heat Gains and Losses Through C/M Antenna Cables	2-23
2-19	Heat Loads to C/M	2-24
2-20	C/M-RCS Rocket Engine Temperature Distribution During Space Flight	2-26
2-21	Total Heat Loads to C/M	2-27
2-22	Steady-State Temperature Distribution for ECS Water Dump Line	2-29
2-23	Temperature Distribution of the C/M I-Beam	2-32
3-1	Expected Component Temperatures During Translunar Phase, S/M Surface (Part 1)	3-2
3-2	Expected Component Temperatures During Translunar Phase, S/M Surface (Part 2)	3-3
3-3	Expected Component Temperatures During Translunar Phase, S/M Surface (Part 3)	3-4

[redacted]

[redacted]

Table		Page
3-4	Maximum and Minimum Surface Temperatures of S/M Cryogenic Tanks During Lunar Mission (Part 1)	3-5
3-5	Maximum Surface Temperatures of Honeycomb Adapter During Boost Heating	3-6
3-6	Maximum and Minimum Surface Temperatures of S/M Cryogenic Tanks During Lunar Mission (Part 2)	3-7
3-7	Summary of Expected Environmental Temperature Extremes for Electrical Cables in the C/M and S/M (Preliminary)	3-9
3-8	Results of Thermal Analysis of Mechanical Docking Arms	3-10
3-9	Summary of Insulation Requirements for S/M SPS Propellant Thermal Protection	3-11
3-10	Summary of Maximum Temperature and Insulation Requirements for S/M Surface After 60 Seconds of RCS Plume Impingement	3-13
3-11	Comparison of Composite Insulation Weights of Min-K and Q-Felt	3-14
3-12	Thermal Evaluation Results	3-15
4-1	Maximum Surface Temperatures of the Honeycomb Adapter During Boost Heating	4-1
5-1	Minimum Thermal Requirements (Various Boilerplates)	5-1
5-2	Maximum Expected Temperatures for Four Data Points	5-3
5-3	Minimum Buna-N Ablative Insulation Requirements of the LES Tower-to-C/M Umbilical Conduit and Shroud	5-5
5-4	Maximum Temperatures to Minimum Insulation Requirements for the C/M Tower Leg Well	5-6
5-5	Thermal Protection Requirements for Boilerplate 22	5-7
5-6	Temperature Extremes for Shaped Charges of C-1 Adapter	5-9
5-7	Temperature History of Tension Tie Rod	5-10
5-8	Command Module Average Heating Rates During a 100-Nautical-Mile Tumbling Earth Orbit	5-11

[redacted]

1.0 LAUNCH ESCAPE SYSTEM

1.1 Preliminary Estimate of Escape Tower Truss Member Temperature as a Function of Ablative Thickness

1.1.1 The LES truss will be subjected to aerodynamic heating during launch and in an abort, to escape rocket plume heating. The required thickness of two ablative materials, Teflon and Thermolag T-500, as a function of temperature, has been estimated for these conditions. These values are shown in Figure 1-1. The method of analysis involved the use of a finite difference ablative program, 9K-118, in an idealization which considered the flow normal to the surface of a tube. This resulted in an unrealistic uniform heating rate for the entire structure.

1.1.2 These thicknesses must be revised upon development of:

a. Realistic aerodynamic heating rates

b. The extent and nature of the damage as a result of rocket-exhaust, hot-particle impingement upon the truss

c. Refined physical property values of the ablative material

1.2 Maximum Temperature of Nose Cone Ballast

1.2.1 The maximum temperature that the lead ballast will reach during the LES trajectory is 160 F. If a copper ballast is used, the maximum temperature will be 110 F. These temperature predictions are preliminary and should be used accordingly.

1.3 Launch Escape System Skirt (Boost and Abort)

1.3.1 To maintain LES skirt temperature below 600 F during boost and abort conditions, the skirt thickness must either be increased from 0.140 inches to 0.282 inches or be thermally protected (e.g., 0.05 inches of Thermolag T-500) on all surfaces.

1.3.2 The maximum expected (unprotected) skirt temperatures during boost-abort conditions are 1070 F and 815 F for skirt thicknesses of 0.140 inches and 0.188 inches, respectively. These values are preliminary in nature and should be used accordingly.

[redacted]

1.4 LES Skirt-to-Rocket Interface Bolt Temperature

1.4.1 The maximum expected LES skirt-to-rocket interface bolt temperatures during boost-abort for various designs are as follows:

Design	Bolt Temperature
0.14 in. (unprotected skirt)	680 F
0.188 in. (unprotected skirt)	620 F
0.14 in. (protected skirt)	470 F

The above values are preliminary in nature and should be used accordingly.

1.5 Expected LES Temperature for Wire Selection Purposes

1.5.1 Based on information received from Lockheed Aircraft Corporation and previous thermal studies, the expected LES temperatures, for use in the selection of electrical wiring and connectors, are listed in Table 1-1.

Table 1-1. Expected LES Temperatures

Location	Temperature (°F)	Time (sec)	Phase
LES Rocket Base (Skirt Area)	80	0	pre-launch
	130	80	boost
	175	84	LES rocket firing
	450	354	coast
LES Rocket Casing	80	0	pre-launch
	140	80	boost
	200	84	LES rocket firing
	400	354	coast
Tower Jettison Motor Casing	80	0	pre-launch
	260	80	boost
	300	354	coast

1.5.2 The firing of the tower jettison motor is taken to occur after the coast phase. It is understood that no impingement heating occurs in the vicinity of the electrical equipment. The above values are preliminary in nature and should be used accordingly. Base heating rates, rocket exhaust information and detailed design of the LES are required before a more thorough study can be made. This information is currently unavailable.

1.6 Temperature of the Lockheed LES Casing Ring During Boost-Abort

1.6.1 During boost-abort, the expected temperature at the Lockheed LES casing ring (point A) is about 175 F. This information is preliminary in nature and should be used accordingly.

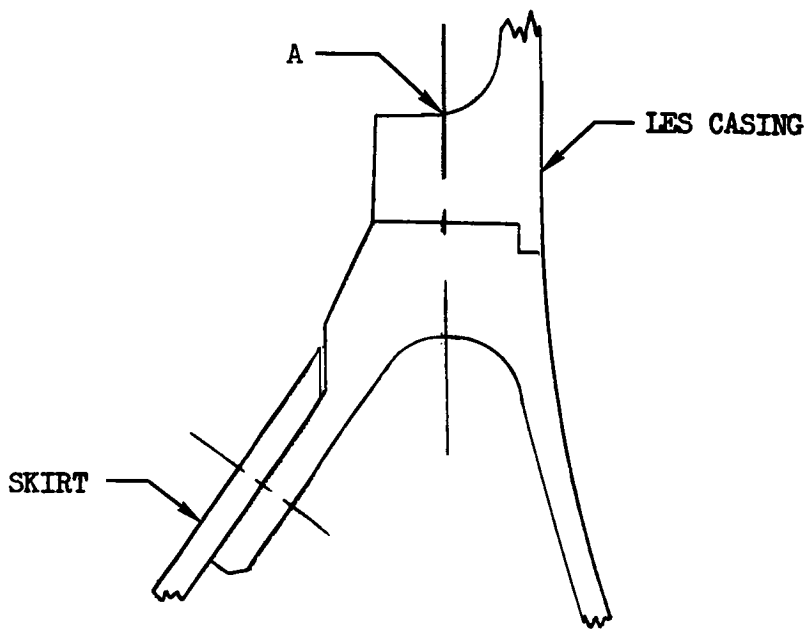

1.7 Maximum Surface Temperature of the LES Skirt-to-Motor Attaching Bolts

1.7.1 A thermal analysis of the LES skirt-to-motor attaching bolts (Figure 1-2) resulted in establishing maximum expected surface temperatures at 375 F for the bolt leads and 380 F for the nuts. These valves are for a Saturn-V boost/high-altitude abort mission. Table 1-2 lists temperatures for both the S-V boost and S-V boost/high-altitude abort missions. Temperature histories of the bolt-head and nut surfaces for S-V boost/abort heating are included in Figures 1-3 and 1-4.

Table 1-2. Maximum Expected Temperatures of the LES Skirt-to-Motor Interface: Bolt-head and Nut Surfaces (See Figure 1-2)

Data Point or Location -	Maximum Temperature (°F)	
	S-V Boost	S-V Boost/Hi-Altitude Abort
Bolt-head surface	375	375
Nut surface	295	380

1.8 Launch Escape Tower Maximum Temperature as a Function of Insulation Thickness (for Boost-Abort Only)

1.8.1 A thermal analysis was performed for horizontal tubes having diameters of 2.5 and 3.5 inches (Figure 1-5). Figures 1-6 and 1-7 reveal that the insulation weight, due to raising the maximum tower design temperature from its present 550 F, may not be significant.

[redacted]

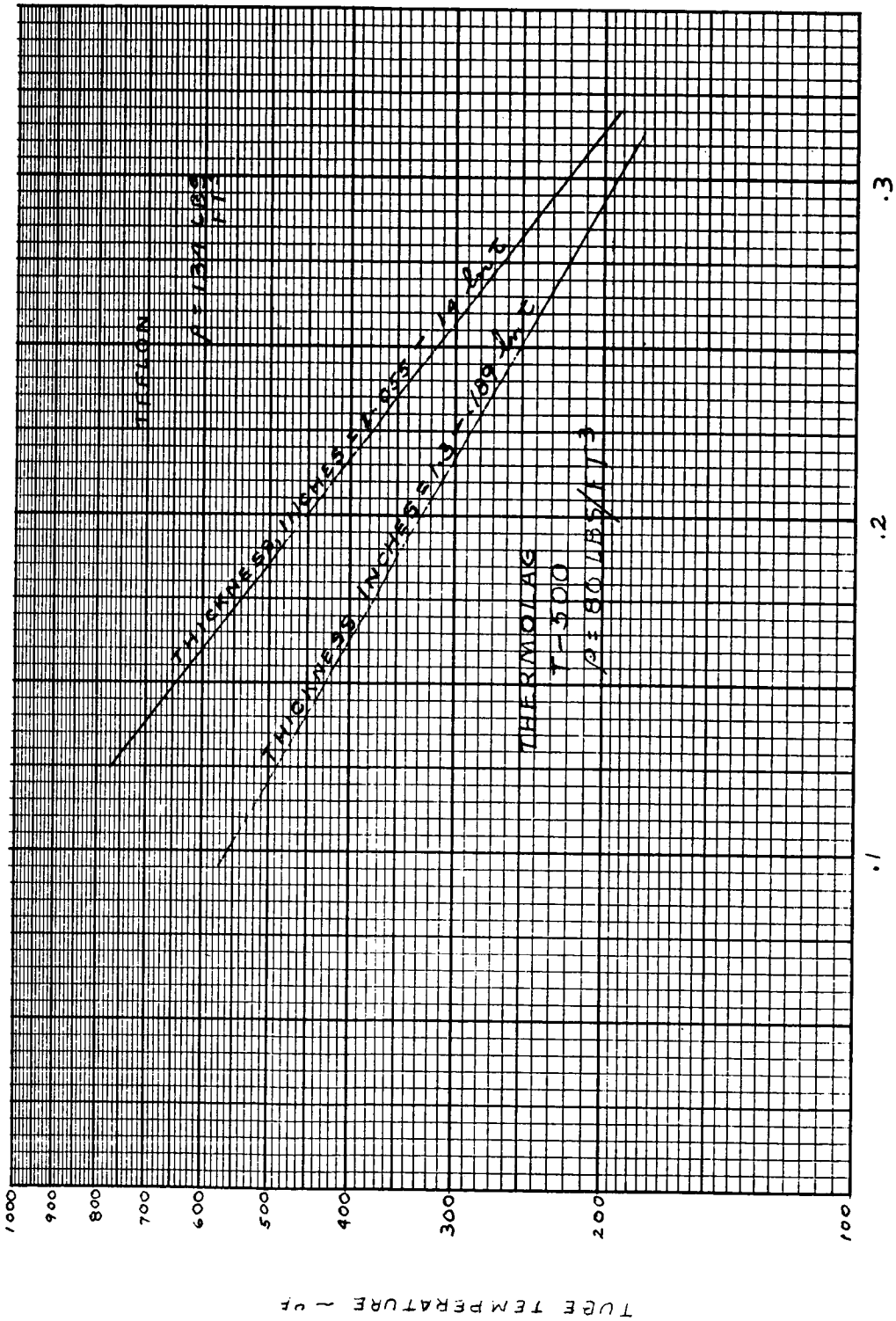

Figure 1-1. Preliminary Estimate of Escape Tower Truss Member Temperature as a Function of Ablative Thickness

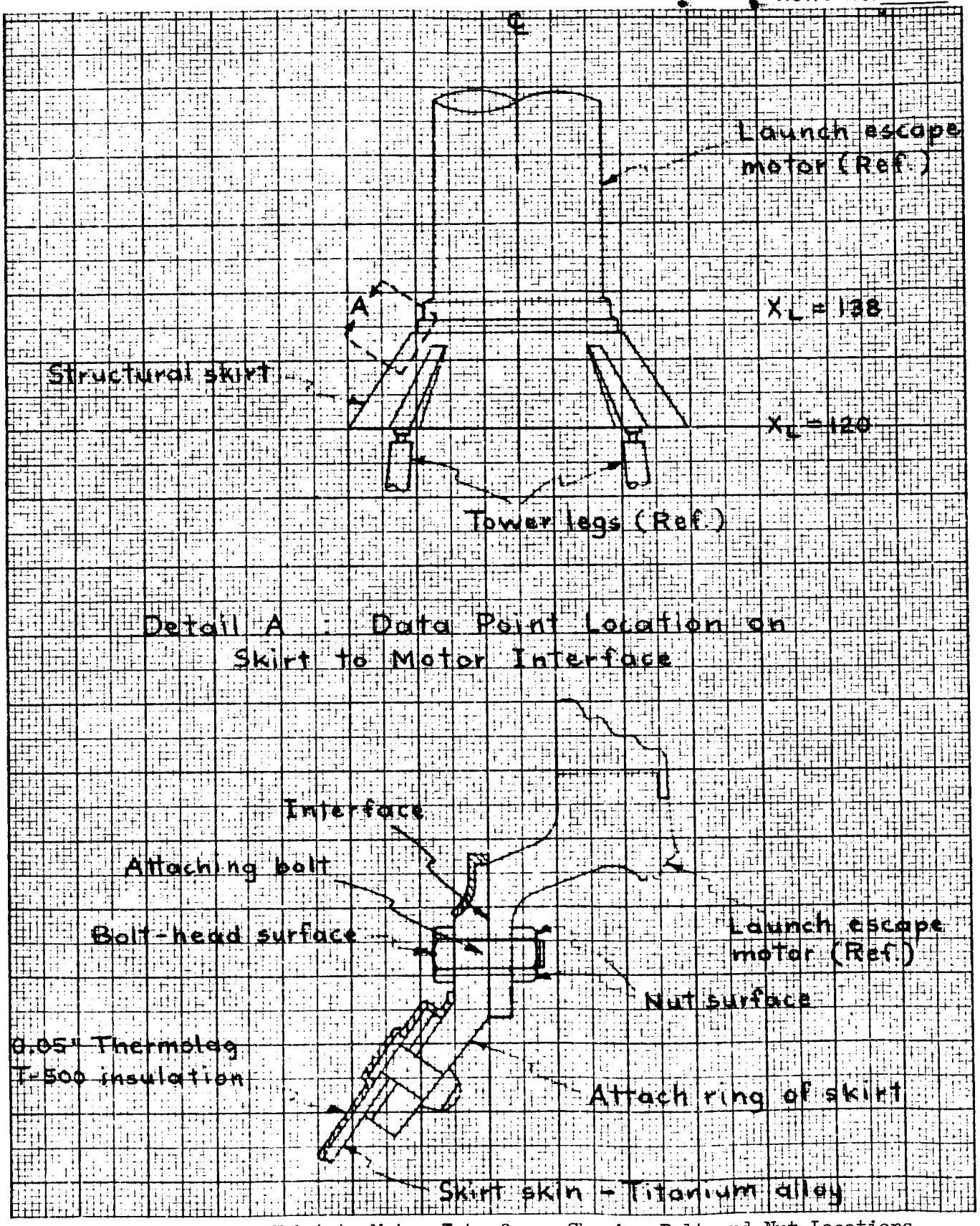

Figure 1-2. LES Skirt-to-Motor Interface, Showing Bolt and Nut Locations

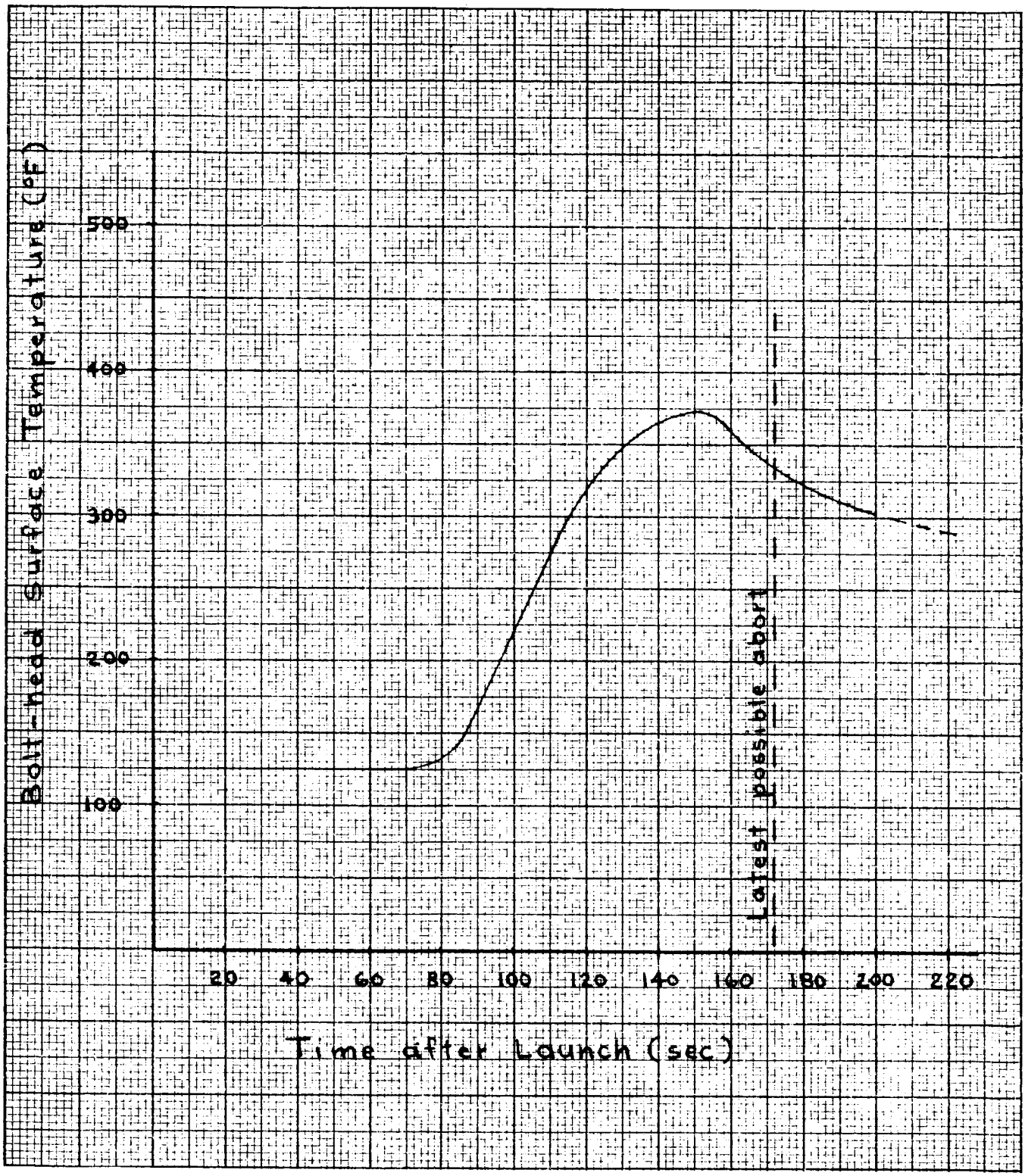

Figure 1-3. Temperature History of the LES Skirt-to-Motor Interface Bolt-Head Surface During a Saturn-V Boost/High-Altitude Abort

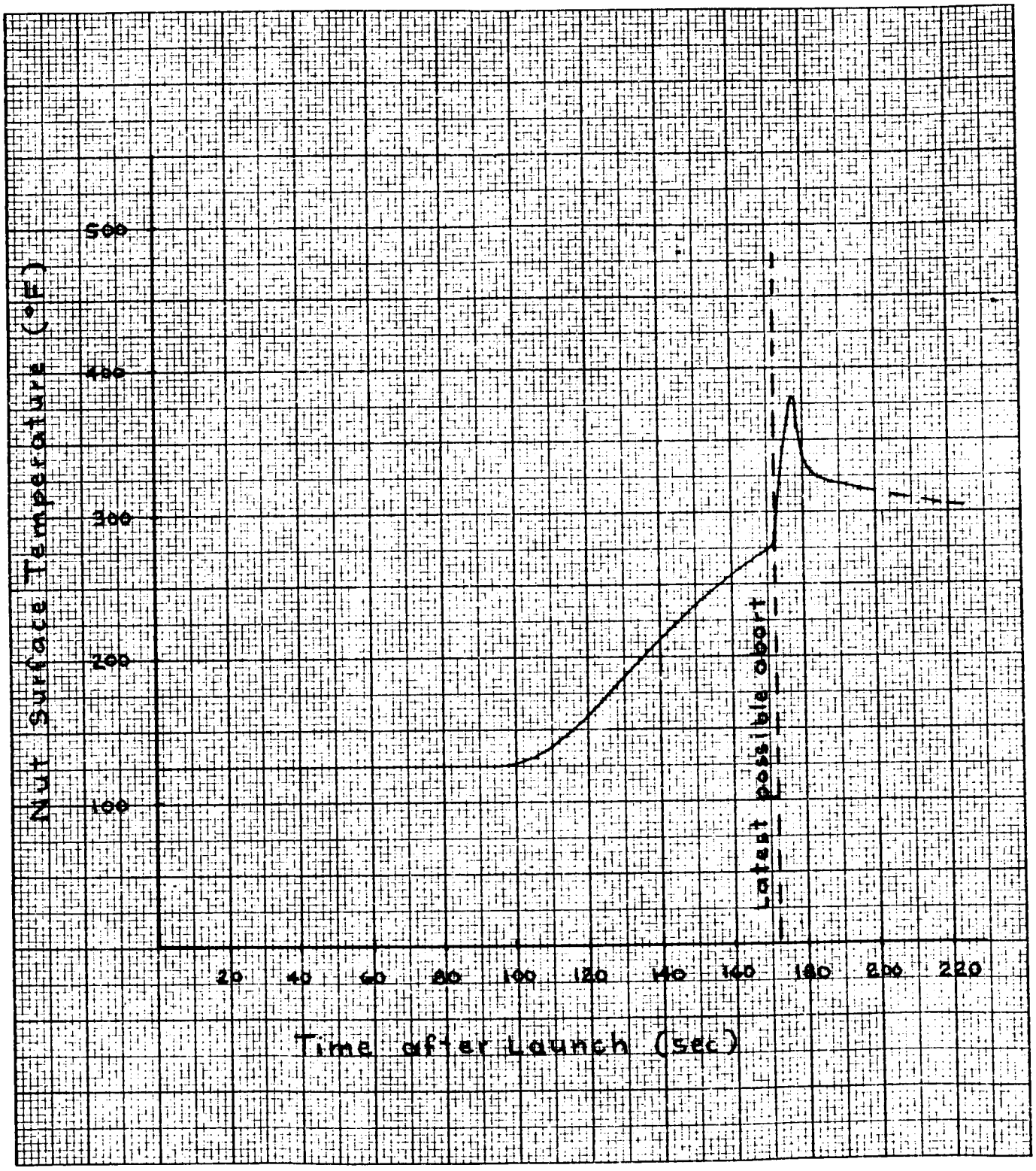

Figure 1-4. Temperature History of the LES Skirt-to-Motor Interface Nut Surface During a Saturn-V Boost/High-Altitude Abort

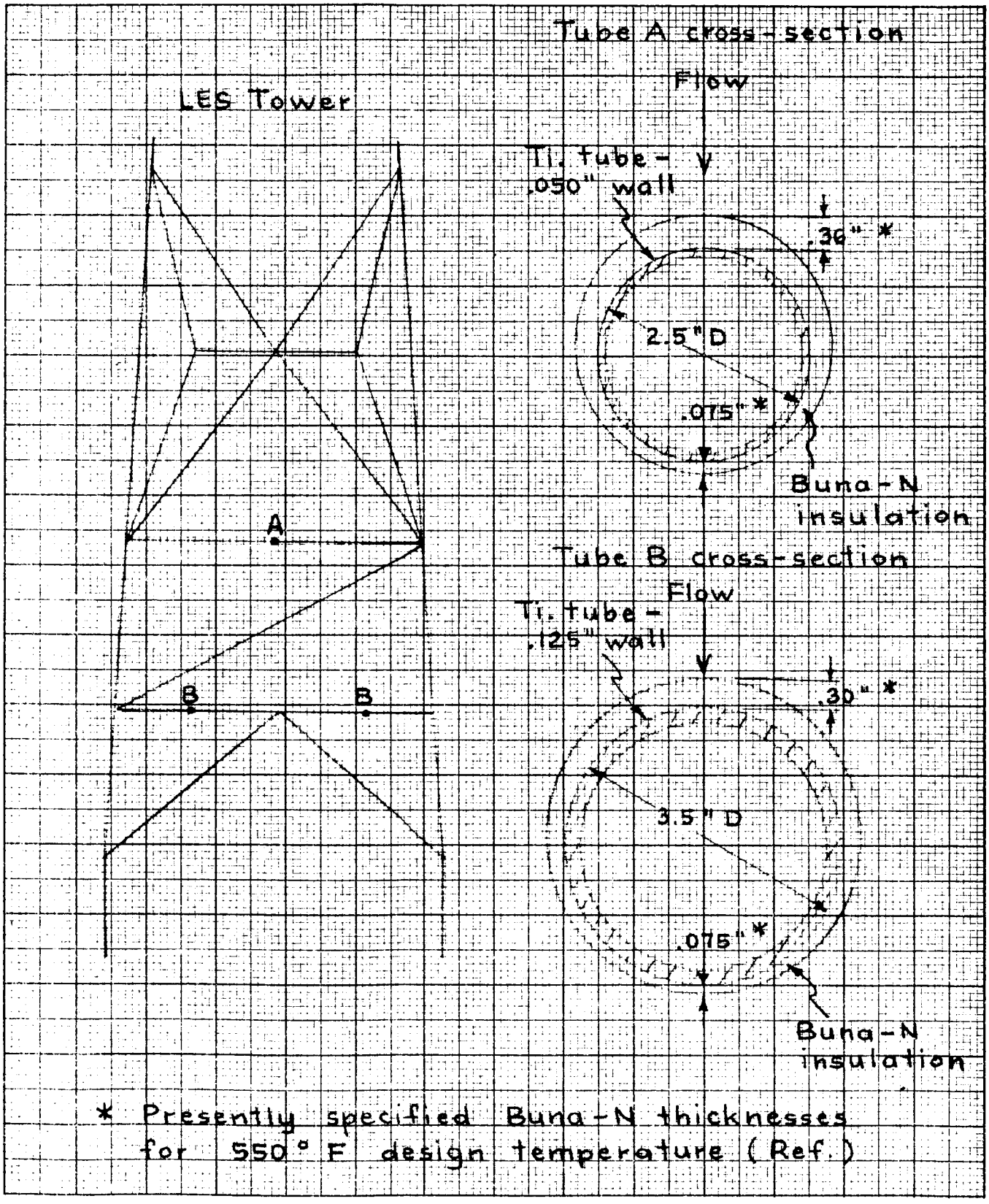

Figure 1-5. LES Tower, Showing Data Tube Locations and Cross Sections

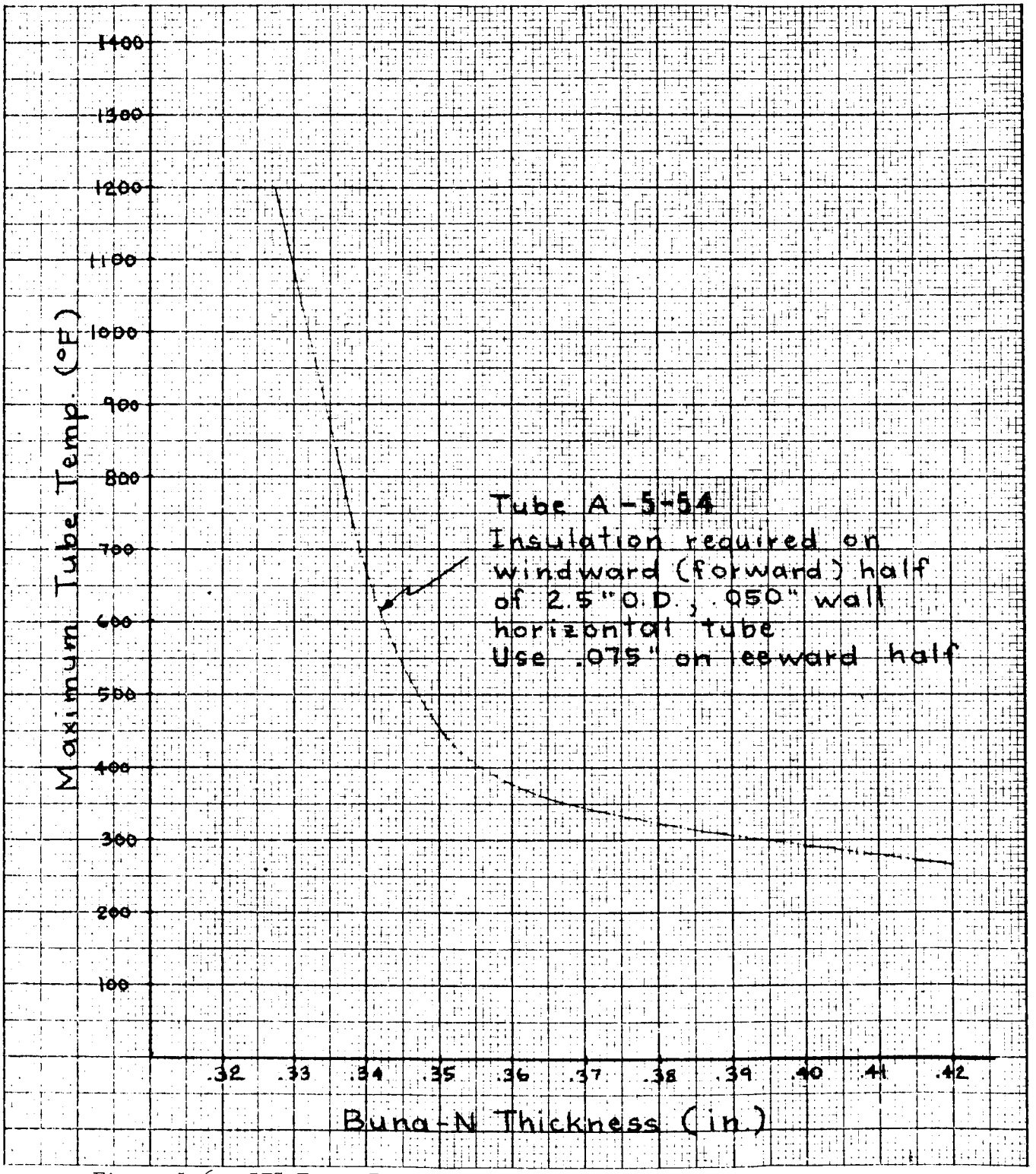

Figure 1-6. LES Tower Buna-N Ablative Insulation Versus Maximum Tube Temperature for a Typical 2.5-Inch Horizontal Tube (During a Saturn-V Boost/High-Altitude Abort)

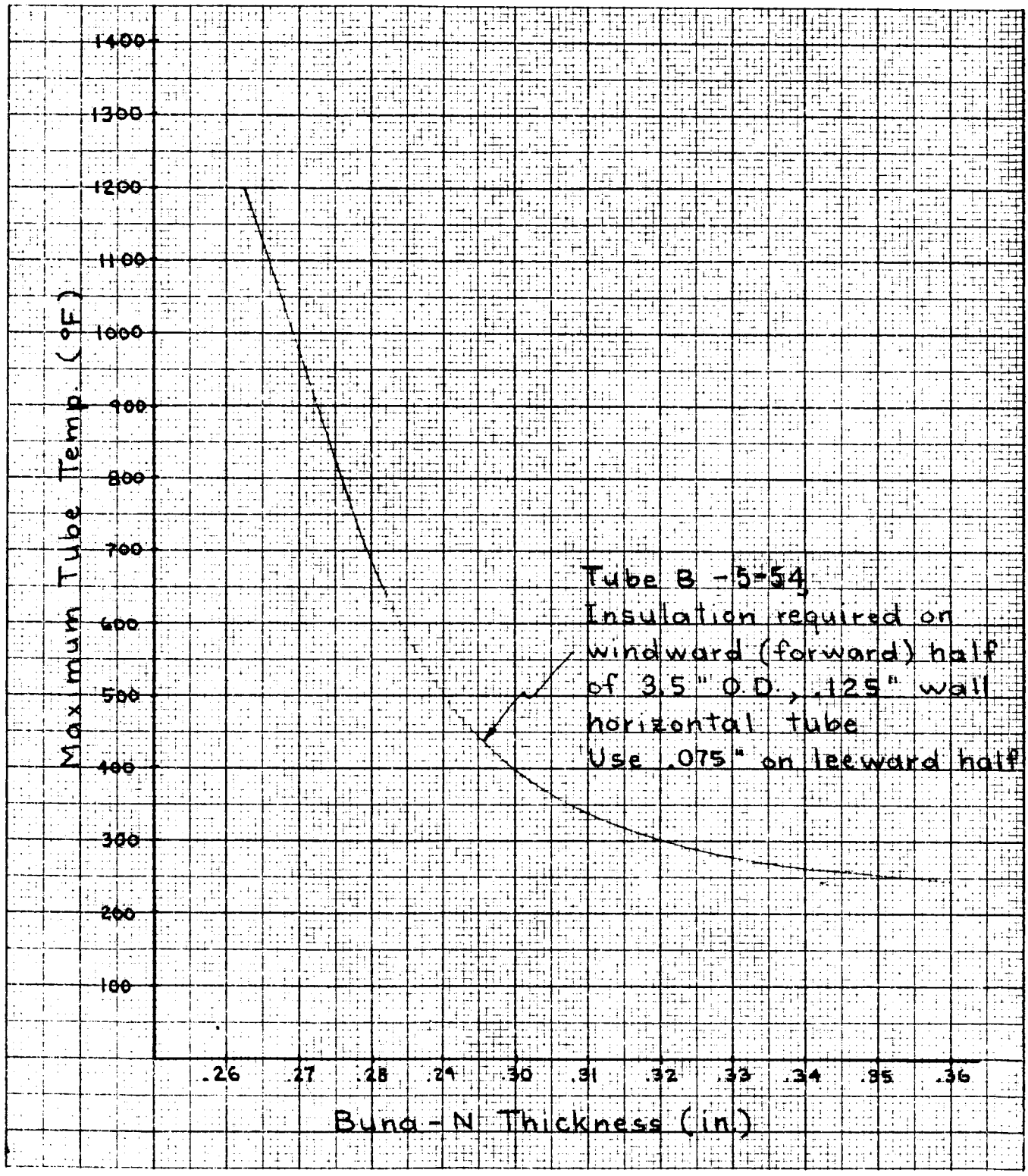

Figure 1-7. LES Tower Buna-N Ablative Insulation Versus Maximum Tube Temperature for a Typical 3.5-Inch Horizontal Tube (During a Saturn-V Boost/High-Altitude Abort)

[redacted]

2.0 COMMAND MODULE

2.1 Heat Protection System Preliminary Ablation Shield Design

2.1.1 The information presented here summarizes a preliminary thermal design of the ablation shield for the command module. This analysis was performed only to establish the approximate insulation layer requirements and should be considered as such. The materials that were considered will not be considered further for use on Apollo. Their ablation characteristics and thermal properties were available and this permitted the analysis. More efficient, but proprietary materials will be utilized by AVCO Corporation, the shield subcontractor, per Apollo design.

The sketch presented in Figure 2-1 shows the typical structure for which the ablation and transient heat transfer analysis was performed.

2.2 Heat Protection System Preliminary Ablation Shield Design

2.2.1 Table 2-1 lists the ablation shield dimensions which, on the basis of this preliminary analysis, should prevent the temperature of the back face of the ablative panels from exceeding 600 F. The insulation material given in Table 2-2 was designed to maintain the inner honeycomb inner face sheet surface from exceeding 250 F.

2.3 Preliminary Thermal Study of the Command Module Fiberglass Stringers (Crew Compartment Heat Shield) During Reentry

2.3.1 The maximum expected temperature at the outer surface of the stringers, during reentry, is 520 F. The inner surface of the stringers is expected to reach a maximum temperature of 140 F. The temperature drop across the stringers (outer surface to inner surface) during reentry is expected to reach a maximum of 430 F. A schematic diagram of the command module is shown in Figure 2-2.

2.4 Command Module Minimum Temperature Predictions

2.4.1 Preliminary predictions for the steady-state relationship between the thermal conductivity of the insulation and the temperature of the stainless steel honeycomb sandwich are tabulated below for no external heat source. An expected value for the thermal conductivity is about 10^{-7} Btu/ft/sec/°F.

No External Heat Source

$\epsilon = 1$, cabin temperature = 75° F Insulation Thickness = 0.111 feet

Thermal conductivity (Btu/ft/sec/°F)	10^{-5}	10^{-6}	10^{-7}	10^{-8}	10^{-9}
Minimum surface temperature, °F	-62	-194	-297	-365	-405

[redacted]

Table 2-1. Heat Protection System, Ablation Shield Design

Ablation Shield		
Location	Thickness (inches)	Material
1	3.00	Phenolic - Material
2	1.10	Phenolic - Nylon Microballoons, 38 lbs/ft^3
4	0.60	Phenolic - Nylon Microballoons, 38 lbs/ft^3
6	0.75	Phenolic - Nylon Microballoons, 38 lbs/ft^3
10	0.35	Phenolic - Nylon Microballoons, 38 lbs/ft^3
12, 16, 19	0.125	Phenolic - Nylon Microballoons, 38 lbs/ft^3

Table 2-2. Insulation Material Layer, Ablation Shield Design

Insulation Material Layer		
Location	Thickness (inches)	Material
Spherical face	0.80	Q - Felt, 6 lbs/ft^3
Conical surface	1.50	Q - Felt, 6 lbs/ft^3

2.5 Expected Environmental Temperatures in the Food and Fecal Storage Compartment

2.5.1 The environmental temperature in the food and fecal storage compartment is expected to be 69 F at steady-state conditions during lunar transit with normal pressurization. This result is based on an air flow of 50 feet per minute at the compartment wall. Under the conditions of emergency depressurization, a minimum steady-state temperature of 45 F can be expected on the upper outer wall of the compartment after a 24-hour period. This latter result is based on an orientation where the apex of the command module is solar oriented, with no consideration given to the presence of the LEM. The above minimum temperature of 45 F can be expected to be lower when the LEM is considered, since the command module would be shielded from solar radiation by the LEM. The maximum expected temperature for the compartment wall for the reentry portion of the flight is 132 F.

2.6 Attitude Control Rockets on Command Module - Temperature During Reentry

2.6.1 The maximum expected temperatures of the nozzles on the command module attitude control engines due to re-entry heating alone are given in Table 2-3.

2.7 Expected Command Module Parachute Compartment Temperature During Flight

2.7.1 The average inner wall temperatures of the command module parachute compartment during the various mission phases are shown in Table 2-4.

2.8 Temperature of Observation Windows, Uncovered During Reentry

2.8.1 Using undershoot trajectory HSE-2, for the analysis, the estimated surface temperature for an exposed observation window for the command module will exceed the maximum allowable temperature of 1500 F for Corning 7940 fuzed quartz. Interior convective cooling does not seem feasible to reduce the surface temperature because this method of cooling will further increase the severe thermal strain. It is doubtful that such a design can be adequately qualified to insure the integrity necessary to survive reentry heating.

2.9 Maximum Bondline Temperatures for HSE-3A and Depth of Char for a C-5 Direct Lunar Boost

2.9.1 Maximum bondline temperatures at time of earth impact were determined at body locations 1, 4, 8, 13, and 17 for emissivities of 0.75 and 0.9, using the subliming ablator program. An initial temperature of 100 F was assumed on the dished portion of the vehicle and 250 F in other areas. For purposes of this analysis, the temperature of sublimation was set at 4840 F. For body points located on the conic section, 0.2 inches was subtracted from the thickness requiremements stated by AVCO to account for mass loss during the missions boost phase. The results are tabulated in Tables 2-5 and 2-6.

Table 2-3. Maximum Expected Temperatures of the Nozzles on the Command Module Attitude Control Engines

Nozzle Temperature (degrees F)*	Engine
2710	Yaw rocket 92 degrees from stagnation point
2620	Yaw rocket 100 degrees from stagnation point
2160	Roll rocket facing the stagnation point
1630	Roll rocket facing away from stagnation point
1150	Pitch rocket 176 degrees from stagnation point
1060	Pitch rocket in parachute compartment

*These values are based on preliminary aerodynamic heating rates and are subject to change pending experimentation.

2.10 Substructure Temperature History for Trajectory HSE-3A and HSE-6

2.10.1 For purposes of the investigation, structural temperature response was determined for overshoot and undershoot trajectories HSE-3A and HSE-6 at command module body locations 8, 13, and 24. The ablator-stainless steel interface (bondline) temperature histories are presented in Figures 2-3 through 2-5.

2.11 Expected Maximum Bondline Temperature During Entry from HSA-3, HSE-1, HSE-2, and Nominal Suborbital Trajectory

2.11.1 A study was conducted to determine the maximum bondline temperature that could be expected at or before time of earth impact for entry trajectories HSA-3, HSE-1, HSE-2, and a nominal suborbital reentry. Temperatures were determined at body locations 1, 5, 6, 10, 12, 15, 17, and 19. A thickness

Table 2-4. Average Inner Wall Temperatures of the C/M Parachute Compartment

Sequence of Events	Length of Time (hours)	Bound	Temperature of Wall A (degrees F)	Temperature of Wall B (degrees F)	Temperature of Wall C (degrees F)
Prelaunch	10.0	Maximum	120	95	80
		Minimum	30	40	65
Boost	0.05	Maximum	175	145	80
		Minimum	60	40	65
Coast (to moon)	84.0	Maximum	120	65	80
		Minimum	-65	20	40
Lunar orbit	168.0	Maximum	120	80	80
		Minimum	-65	-20	40
Coast (return to earth)	84.0	Maximum	120	65	80
		Minimum	-65	20	40
Reentry	0.4	Maximum	250	65	80
		Minimum	0	20	40

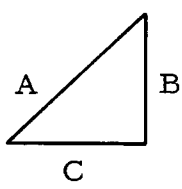

Parachute Compartment

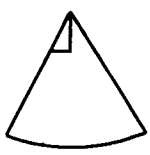

Command Module

of 0.2 inch was subtracted from the ablator thicknesses stated by AVCO at body points 6 through 19 to account for material loss during boost. The results of this analysis are presented in Table 2-7.

Table 2-5. Bondline Temperatures at Time of Earth Impact for HSE-3A (Ablator Avcoat 5026-39) Subliming Ablator Program

Command Module Body Location	Emissivity	Ablator Thickness (inches)	Bondline Temperature (F)	Initial Temperature (F)	Mass Lose from Subliming Program (pounds per square foot)	Mass Lose Predicted (pounds per square foot)
1	0.9	1.54	586	100	0.232	3.93
1	0.75	1.54	695	100	0.570	3.93
4	0.9	1.24	633	100	0	3.16
4	0.75	1.24	663	100	0	3.16
8	0.9	1.21	581	250	0	3.09
8	0.75	1.21	599	250	0	3.09
13	0.9	0.7	544	250	0	1.49
13	0.75	0.7	573	250	0	1.49
17	0.9	0.29	576	250	0	0.74

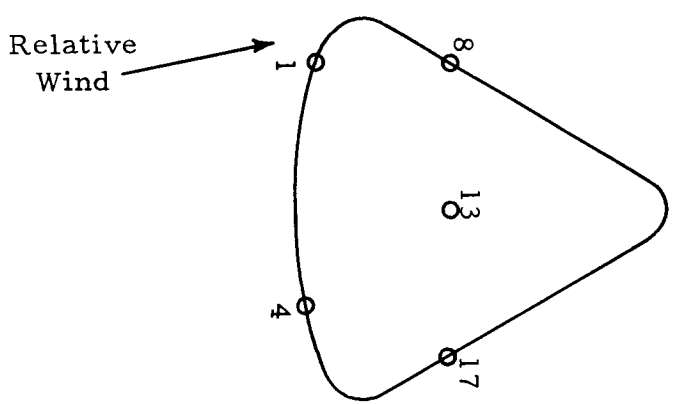

Input Data to Program	
Conductivity	0.07 Btu/ft hr °F
Density	36 lb/ft^3
Specific Heat	0.36 Btu/lb
Ablation Temperature	4840 F

~~CONFIDENTIAL~~

~~CONFIDENTIAL~~

Table 2-6. Ablation Material Char Depth for a C-5 Direct Lunar Boost

Command Module χ Location	Emissivity	Char Depth (Inches)
10.32	0.9	0.208
10.32	0.75	0.231
6.70	0.9	0.210
6.70	0.75	0.232
4.58	0.9	0.128
4.58	0.75	0.171

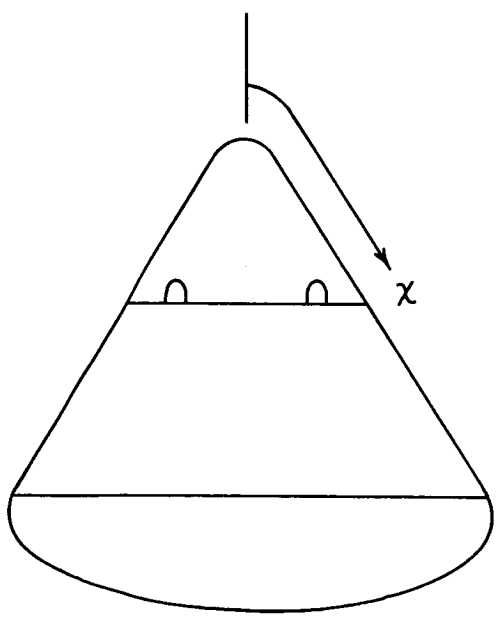

2.12 Temperature Predictions of Repaired Honeycomb Panels

2.12.1 A study was performed to determine the thermal effects of repairing stainless steel honeycomb sandwich panels when the condition known as "core-to-face-sheet void" develops. It was found that as more pins and doublers were added to repair a section of honeycomb, the

Table 2-7. Maximum Bondline Temperatures

Body Location	HSE-1	HSE-2	HSA-3	Suborbital
1	600	116	134	156
5	600	148	151	201
6	562	252	139	200
10	540	283	201	205
12	511	286	171	147
15	474		323	278
17	265		314	329
19	487		587	388

temperatures of the honeycomb and the inner cabin structure decreased. However, the introduction of pins and doublers to the honeycomb structure resulted in localized cold spots. The problems analyzed were:

1. The maximum amount of pins and doublers that could be added and still keep the temperatures of the steel honeycomb (heat shield bondline) and the inner cabin structure below their thermal design limits.

2. The maximum thermal gradients that a repair causes at the face sheets.

2.12.2 It was found that as the density of pins and doublers were increased to repair the structure, the temperatures of the steel honeycomb (heat shield bondline) and the inner cabin structure decreased. Figure 2-6 shows that if the honeycomb structure were replaced by a solid piece of steel, the temperatures decrease throughout the inner structure. This result is due to the ability of the steel pins and doublers to absorb the heat and act as heat sinks. The thermal gradients caused by repairing the steel honeycomb will vary as a function of the quantity of pins and doublers added to repair an area. Figure 2-7 shows temperature histories at various locations in the vicinity of a typical repair.

2.13 Temperatures of the Stainless Steel and Aluminum Honeycombs of Airframe 011 for Reentry Trajectory HSE-1

2.13.1 Figure 2-8 presents bondline temperature, stainless steel honeycomb interior face sheet temperature and insulation backface temperature versus time for 27 body points. The command module body points

forward of X_c = 16.5 are assumed to have an initial temperature of 250 F. The body points which are aft of X_c = 16.5 are assumed to be at 100 F. The time from 400,000 feet to earth impact for HSE-1 is 2950 seconds with drogue deployment at approximately 2400 seconds.

2.14 Thermal Analysis of Forward Heat Shield Skin Panels at Station X_c = 112.25 and X_c = 81.0

2.14.1 The skin panels and their locations on the C/M are shown in Figure 2-9. Tables showing maximum expected temperatures during reentry at the points shown in the diagrams are also presented. It is recommended that maximum temperatures be used as design criteria.

2.15 Ablator-Bondline Temperatures at Body Points 8, 17, 24, and 31

2.15.1 The ablator-stainless steel honeycomb bondline temperature histories for body points 8, 17, 24, and 31 have been calculated for trajectory HSE-3A and are presented in Figures 2-10 through 2-13. The initial temperature of body points 8 and 24 was assumed to be -260 F and +250 F for body points 17 and 31.

2.16 Dead-Ended Holes for Heat Shield Penetrations

2.16.1 It is feasible to permit holes to penetrate the ablative heat shield on the command module if certain design limitations are observed. One of the more critical limitations is that all holes be dead-ended (to prevent passage of plasma during reentry). This requirement is based on the necessity of maintaining a stagnant air column in the hole in order to maintain as low a heat transfer coefficient as possible. If the air column is not stagnant, i.e., a velocity gradient exists, then the heat transfer coefficient becomes increasingly large. In the extreme case where hot plasma actually flows in the hole, the heat transfer coefficient and temperature gradient would increase sufficiently that failure of the ablator and substructure in the vicinity of the plasma flow should be anticipated.

2.16.2 Temperature predictions for heat shield penetrations are, therefore, based on a stagnant air column with no plasma flow. In general, these thermal analysis considerations have limited the design of heat shield penetrations to holes dead-ended at or near the substructure-ablator bondline.

2.17 Preliminary Thermal Analysis of Aft Heat Shield Tie-Down Bolt

2.17.1 The maximum expected temperature of the aft heat shield tie down bolt (Figure 2-14) located near command module coordinates X_c 11.8, Z_c 72.3 is 200 F. Temperature time histories for various other points on the supporting substructure are shown in Figure 2-15. The structure shown in Figure 2-14 with exception of the ablative material thickness of 1.54 inches was obtained from Layout Drawing V16-932704H.

2.18 Thermal Analysis of C/M to S/M Umbilical During Boost and Reentry

2.18.1 During reentry (trajectory HSE-3A) the maximum expected temperature of three referenced locations (Figure 2-16) along the C/M-S/M umbilical wire bundle are given below.

Severed End of Bundle (Point 1)	Mid Point of Bundle (Point 2)	Point of Entrance into Command Module (Point 3)
740 F	370 F	230 F

2.18.2 Assuming an initial temperature of 150 F, and no plasma leakage through the braided wires, temperature histories (Figure 2-17) have been calculated at three points along the wire bundle for a reentry from a lunar mission on trajectory HSE-3A.

2.18.3 There is no appreciable temperature rise during a normal Saturn-V boost. The initial temperature prior to boost is 125 F.

2.19 Thermal Analysis of Scimitar Antenna Housings on Spacecraft for Boost and Atmospheric Reentry

2.19.1 The required thickness of this boost coat varies from 0.11 inch to 0.30 inch on the most windward housing and ranges from 0.08 inch to 0.22 inch on the leeward antenna housing. For protection against the heating of atmospheric reentry, charring ablator protection consisting of 0.65 inch of Avcoat 5026-39 on the faces and 0.85 inch of the same ablator on the outer edge of the leeward housing has been recommended in addition to the aforementioned boost coat.

2.19.2 A charred surface surrounding the scimitar antennas cannot be tolerated because of its interference with radio transmissions from deep space. The recommended thicknesses are 0.21 inch on the faces and tapering from 0.11 inch to 0.30 inch on the outer edges of the windward housing and 0.15 inch on the faces and from 0.08 inch to 0.22 inch on the external edges of the leeward antenna housing (see Figures 2-18 and 2-19). With these thicknesses of ablator the fiber-glass structure of the windward antenna housing is not expected to exceed 450 F during S-V boost. It was assumed that fiber-glass would begin to char above this temperature. The Avcoat 5026-39 recommended to protect the leeward housing during reentry is not expected to exceed 500 F and char during S-V boost. Temperature histories at a number of locations in

both scimitar antenna housings during S-V boost are shown in Figures 2-21 and 2-22. Temperatures at significant times during boost for some additional data points which were not plotted are listed in Table 2-8. The assumed initial temperature for the boost analysis was 125 F.

2.19.3 For reentry survival the leeward scimitar antenna housing should be protected with Avcoat 5026-39: 0.65 inch on the faces and 0.85 inch on the external edge. With these thicknesses of ablator, the maximum temperature attained by any section of the fiber-glass housing structure is expected to be 570 F during reentry trajectory HSE-3A. Since teflon-like materials may be subject to radiation damage and since immunity to high vacuum and cold soak is not certain, it was assumed that the boost coat was lost during space flight. The design thicknesses of Avcoat 5026-39 were obtained using an overall initial temperature of 250 F. Maximum temperatures during reentry are shown in Table 2-9. Table 2-9 also contains temperatures at other significant times during trajectories HSE-3A and HSE-6.

2.19.4 Specific information was requested on the maximum temperature gradients which could be expected in the leeward antenna housing during atmospheric reentry. There is a multitude of initial gradients which are possible depending upon the orientation with respect to the sun of the C/M during the hours just prior to reentry. Many of these initial gradients could be considered to be severe since they span a major portion of the temperature range from approximately -300 F to +250 F. Temperature histories using the chosen initial gradient are plotted in Figure 2-23 for trajectory HSE-3A and in Figure 2-24 for trajectory HSE-6. Other possible initial temperature gradients are outlined in Table 2-10.

2.19.5 As shown in Table 2-11, the approximate thickness of the teflon-like ablator remaining on the housings following S-V boost ranges from 0.08 inch to 0.20 inch.

2.20 Thermal Analysis of the Elastomer Seals Located on Various Equipment Penetrations in the Command Module Inner Structure

2.20.1 A thermal analysis was made on the elastomer seals located on the various equipment penetrations in the command module inner structure. It is estimated that a temperature of 190 F will be reached at an elevation of 15,000 feet during an HSE-3A reentry trajectory. These various equipment penetrations are shown in Figure 2-25 and are as follows: (1) electrical insulator feed-through (side wall), (2) main crew hatch, (3) hatch actuating mechanisms, (4) coax insulator feed-through (side wall), (5) electrical insulator to structure (forward bulkhead), and (6) coax insulator feed-through (forward bulkhead). The numbers in parenthesis correspond to the numbers in Figure 2-25.

2.21 Thermal Analysis of the Forward Heat Shield Thruster

[redacted]

Table 2-8. Maximum Temperatures During S-V Boost, Additional Data Points

Windward Scimitar Antenna Housing at Section B-B (See Figure 2-19)*					Leeward Scimitar Antenna Housing at Section H-H (See Figure 2-20)*				
Data Point	Maximum Temperature (F)	Time of Maximum Temperature (Seconds)	Temperature at Time = 77 Seconds (F)	Temperature at Time = 173 Seconds (F)	Data Point	Maximum Temperature (F)	Time of Maximum Temperature (Seconds)	Temperature at Time = 77 Seconds (F)	Temperature at Time = 173 Seconds (F)
Q7	800	119-173	119	800	A7	530	164	120	519
R7	416	269	125	282	B4	388	212	124	341
S6	365	**	124	259	B10	388	212	124	341
S8	365	**	124	259	C7	145	**	125	126
T2	800	128-158	123	726	D2	800	128-158	126	744
T6	419	251	124	325	D3	435	233	123	371
T7	267	**	125	149	D6	158	**	125	129
T8	419	251	124	325	D7	130	**	125	125
T12	800	128-158	123	726	D8	158	**	125	129
					D11	435	233	123	371
					D12	800	128-158	126	744

(*) Initial temperature for all data points = 125 F.

(**) Temperature rising slightly at elapsed time of 305 seconds.

[redacted]

[redacted]

Table 2-9. Maximum Temperatures for Leeward Scimitar Antenna Housing During Atmospheric Reentry

Data Point[2]	Trajectory HSE-3A[1]						Trajectory HSE-6[1]			
	Maximum Temperature (F)	Time of Maximum Temperature (Seconds)	Temperature at Time = 84 Seconds (F)	Temperature at Time = 1380 Seconds (F)	Temperature at Time = 1640 Seconds (F)	Temperature at Time = 2100 Seconds (F)	Maximum Temperature (F)	Time of Maximum Temperature (Seconds)	Temperature at Time = 50 Seconds (F)	Temperature at Time = 240 Seconds (F)
C4	613	1240	284	603	525	444	508	180	278	484
C7	570	1680	250	544	570	540	355	**	250	283
C10	613	1240	284	603	525	444	508	180	278	484
D3	1150	108	1036	566	378	321	2114	51	2114	446
D4	591	1220	281	581	506	426	505	180	276	484
D6	552	1500	251	547	545	485	381	460	250	340
D7	544	1640	250	526	544	506	375	**	250	281
D8	552	1500	251	547	545	485	381	460	250	340
D10	591	1220	281	581	506	426	505	180	276	484
D11	1150	108	1036	566	378	321	2114	51	2114	446
E3	1268	114	1101	619	403	353	2348	51	2348	516
E5	493	1560	251	485	492	473	350	400	251	332
E9	493	1560	251	485	492	473	350	400	251	332
E11	1268	114	1101	619	403	353	2348	51	2348	516
F1	566	1460	251	563	553	494	390	440	250	353
F7	492	1960	250	446	479	490	335	**	250	258
F13	566	1460	251	563	553	494	390	440	250	353
C7*	549	1620	250	534	549	513	---	---	---	---
D7*	486	1660	250	472	486	470	---	---	---	---

1 Initial temperature for all data points = 250 F.
2 Unless noted otherwise, see Figure 2-20, Section G-G for data point locations.
(*) See Figure 2-20, Section I-I for data point locations.
(**) Estimated at touchdown.

[redacted]

Table 2-10. Additional Temperature Gradients Possible in Leeward Scimitar Antenna Housing Prior to Reentry

Gradient	Data Point*								
	B3	B7	B11	D3	D7	D11	F3	F7	F11
	Initial Temperature (F)								
I	200	250	200	0	-50	0	150	0	150
II	0	100	200	-200	0	200	-290	-100	200
III	50	100	150	-150	-100	-50	-290	-260	-220

*See Figure 2-20

2.21.1 Results of a thermal analysis made on the forward heat shield ejector system indicate that the maximum temperature reached at the bondline between the steel honeycomb and the heat shield is expected to be 425 F (point 1, Figure 2-26). Results also indicate that the maximum temperature reached by point 2 (Figure 2-26) is 265 F. These temperatures are reached at times of 1450 and 1650 seconds, respectively, during reentry trajectory HSE-3A.

2.22 Preliminary Thermal Study of the Forward Compartment Heat Shield Separation System Components During Reentry

2.22.1 A thermal analysis was conducted to determine the maximum predicted temperatures of the thrusters, breech, and the cartridges at forward compartment separation altitude (25,000 feet). The determined values for reentry trajectory HSE-3A are as follows:

Part	Maximum Temperature
Thrusters	250 F
Cartridges	200 F
Breeches	200 F

Table 2-11. Thickness of Teflon-Like Ablator Remaining on Scimitar Antenna Housings Following S-V Boost

Surface Covered with Teflon-Like Ablator	Thickness Remaining (Inches)
Windward Antenna Housing	
On faces (grid lines 6 and 8) at Sections A-A, B-B, C-C, and D-D*	0.20
On outer edge (grid line R)	
At Section A-A*	0.18
At Section B-B*	0.16
At Section C-C*	0.11
Leeward Antenna Housing	
On faces (grid lines 3 and 11) at Sections E-E, F-F, and H-H**	0.14
On outer edge (grid line B)	
At Section E-E**	0.15
At Section F-F**	0.12
At Section H-H**	0.08

*See Figure 2-19
**See Figure 2-20

2.23 Preliminary Thermal Analysis of the Main Parachute Fittings and Steel Cable Risers

2.23.1 The maximum expected temperatures reached during normal reentry will be 110 F initially, and 250 F at time of touchdown. During a pad abort the maximum expected temperature is 150 F, and during a low altitude abort the maximum expected temperature is also 150 F.

2.24 Typical Temperature Histories for the Command Module Air Vent Components

2.24.1 Typical temperature histories for the command module air vent heat exchange (Figure 2-27) were determined and transmitted for preliminary design considerations. Figure 2-28 presents the best available design temperature limits.

2.24.2 On the basis of the heating rates to the entrance region of the heat exchanger copper grid, the temperature histories of the tapered ablative outer structure have been determined and are shown in Figure 2-29. Figure 2-29 also indicates that the outer surface of laminate structure may reach 310 F at touchdown for reentry trajectory HSE-6, with no appreciable charring on the inside.

2.25 Thermal Analysis of the Teflon Covering of the Command Module Vent

2.25.1 The bondline between the teflon and fiber-glass air vent tube is expected to reach a maximum temperature of 598 F during a Saturn-V boost.

2.25.2 Time-temperature histories of four referenced locations are shown in Figures 2-30 through 2-33. The thickness of the teflon was assumed to be 0.05 inch thick and the initial temperature was assumed to be 125 F. Figure 2-34 shows the command module air vent systems.

2.26 Thermal Analysis of the Command Module RCS Yaw, Roll, and Aft Pitch Engine Mounting Structures

2.26.1 A thermal analysis was conducted to determine the maximum temperatures experienced by the command module RCS yaw, roll, and aft pitch engine mounting structures during an HSE-3A reentry trajectory. These temperatures were obtained by considering heating due to engine operation along with aerodynamic heating.

Results indicate that the maximum expected temperatures reached by these mounting structures are 840 F, 830 F, and 820 F for the yaw, roll, and aft pitch engines respectively (point 3, Figures 2-34 through 2-36). These temperatures occur at touchdown which is at a time of approximately 2150 seconds. For the analysis, a representative RCS engine duty cycle, and reentry heating rates for trajectory HSE-3A were obtained. Also, an initial reentry temperature of 250 F was obtained. Figures 2-37 through 2-39 show temperature histories of selected points on the mounting structures of the yaw, roll, and aft pitch engines respectively. These selected points are shown on Figures 2-34 through 2-36.

2.27 Temperature Histories of the C/M RCS Tanks and Lines for Space Flight, Reentry, and Post-Landing Phases

2.27.1 A thermal analysis was performed to determine temperature extremes of the C/M RCS fuel, oxidizer and helium tanks (and related lines) during space flight, reentry and post-landing mission phases. The results (Table 2-12) show the minimum (no solar input) and maximum (full solar input) temperatures of the subject tanks and lines for the space portion of the LOR mission. Also shown are the maximum tank (full and empty) and line temperatures which occur during the reentry and post-landing phases (Figure 2-40).

Table 2-12. C/M RCS Tanks and Lines Temperature Extremes

		Minimum Temperature - °F (No Solar Input)		Maximum Temperature - °F (Full Solar Input)	
Space Portion of LOR Mission:	Helium Tanks	47		67	
	Fuel Tanks	60		75	
	Oxidizer Tanks	57		77	
		Full Tanks		Empty Tanks	
		Maximum Temperature - °F	Time After Start of Reentry (sec)	Maximum Temperature - °F	Time After Start of Reentry (sec)
Reentry and Post Landing Portion of LOR Mission:	Propellant Tanks	84	6000	141	6500
	Propellant Lines	149	5500	149	5500

2.27.2 The analysis was conducted assuming no insulation on the tanks, lines and S/M fairing. The effect of firing the RCS rockets was not considered. The crew compartment was assumed to be pressurized at all times.

2.27.3 Minimum temperatures for space flight occur at the end of the translunar or transearth coast, with no solar energy incident on the surface of the C/M. The temperatures can become as cold as 47 F, 57 F, and 60 F for the helium, oxidizer, and fuel tanks, respectively.

2.27.4 Maximum temperatures of 75 F and 77 F for the fuel and oxidizer tanks, respectively, occur at the end of translunar coast, for the condition of maximum solar heating of the outer surface surrounding these tanks and lines. However, the maximum temperature of 67 F for the helium tanks is reached at the end of the lunar orbit phase.

2.27.5 Maximum temperatures of the tanks and lines after space flight are reached during the post-landing phase due to heat soakback. For reentry trajectory HSE-3A, the maximum expected temperature of the full propellant tanks is 84 F, which is reached 6000 seconds after the beginning of reentry (3915 seconds after landing). For the same reentry trajectory, the maximum temperature of the empty propellant tanks can be as high as 141 F at 6500 seconds following the initiation of reentry (4415 seconds after landing). The peak line temperature during the post-landing phase is 149 F.

2.28 Minimum C/M Outer Structure Temperatures in Earth Orbit

2.28.1 The following are minimum C/M outer structure temperatures in an earth orbit:

The lowest cyclic steady-state temperature experienced by a portion of the C/M outer structure in the earth orbit studies conducted to the present is -121 F. For this earth orbit mission, the X-axis was maintained tangent to the orbit path.

The minimum temperature at the end of three orbits for the same orbit orientation is expected to be -103 F.

After five orbits the temperature is expected to be -114 F.

2.28.2 The following data and assumptions were applied to the calculations in order to obtain the temperatures:

No roll about the X-axis
Orbit inclination angle of 33° with the equator
100-nautical-mile circular orbit
Crew compartment temperature held constant at 75 F
Initial earth orbit temperature 270 F
Solar absorptivity and emissivity of surface is 0.9

2.29 Command Module Surface Temperature Extremes During Lunar Orbit

2.29.1 The results of a thermal analysis on the C/M crew compartment section are presented in Tables 2-13 through 2-15, and are based on a 1.33-inch thickness of Q-felt insulation (thermal conductivity of 6.0×10^{-3} Btu/in./Hr-F-ft^2). Thermal effects of the windows were not considered.

2.29.2 This analysis was performed for three sets of surface characteristics, three orbit inclinations and three different orientations. The most probable value of solar absorptivity and emissivity is 0.9. Orbit inclination angles studied were 0° (maximum lunar shading), 5.5°, and 18.5° (minimum lunar shading).

2.30 Oxygen Temperatures at C/M Pressure Bulkhead

2.30.1 A thermal analysis of the oxygen lines was made from the point above the top bulkhead in the S/M where the oxygen lines join the water and glycol lines to the point where the lines enter the C/M at the pressure bulkhead. The purpose of the analysis was to determine the temperature of the oxygen at the pressure bulkhead for both normal and emergency flow rates. The results are presented in Table 2-16.

2.30.2 The analysis was based on flow rates of 0.2125 lbs/hr and 20 lbs/hr for normal and emergency flow, respectively. The surrounding temperatures used in the analysis were -80 F in the fairing region, 80 F in the aft compartment region of the command module and -170 F for the surface of the ablator section through which the lines pass.

2.31 Temperature Histories of the C/M RCS Propellant Tanks

2.31.1 Temperature analyses of the C/M RCS propellant tanks gave a maximum temperature in the RCS tanks of 77 F during translunar coast, with maximum solar heating on the outer surface. This condition existed with an aluminum wall temperature of 70 F in the vicinity of the tanks.

2.31.2 Figure 2-41 shows the temperature history for the case of an abort condition just before entering lunar orbit, which would be the worst case for hot temperature in the tanks.

2.32 Temperature Extremes of C/M Antennas in Space Flight

2.32.1 The C/M antenna space flight temperature extremes are presented in Table 2-17.

2.32.2 Preliminary estimates indicate maximum and minimum temperatures will be 250 F and -290 F, respectively.

2.33 Command Module Environmental Heat Exchanger (Various Mission Phases)

[redacted]

Table 2-13. Apex Lunar-Oriented (Positive X-Axis Pointed Toward Lunar Center at All Times)

Orbit Inclination	Surface Characteristics	Maximum Temperature (°F)	Minimum Temperature (°F)
18.5 degrees	$\alpha_s = 0.9$, $\epsilon = 0.9$ (Ablator)	163	-39
	$\alpha_s = 0.35$, $\epsilon = 0.75$ (White Paint)	72	-39
	$\alpha_s = 0.45$, $\epsilon = 0.4$ (Aluminum Paint)	110	-38
5.5 degrees	$\alpha_s = 0.9$, $\epsilon = 0.9$	163	-46
	$\alpha_s = 0.35$, $\epsilon = 0.75$	75	-49
	$\alpha_s = 0.45$, $\epsilon = 0.4$	109	-23
0 degrees	$\alpha_s = 0.9$, $\epsilon = 0.9$	167	-48
	$\alpha_s = 0.35$, $\epsilon = 0.75$	67	-54
	$\alpha_s = 0.45$, $\epsilon = 0.4$	86	-30

2.33.1 Heating rates for the C/M during space flight mission phase are shown in Figures 2-42 through 2-47. The data are presented in the form of curves showing heating rates as a function of the cabin temperature. All curves were drawn for energy conducted across the insulation only.

2.33.2 For Figures 2-42 and 2-43, a value of 0.050 Btu/in./hr-ft^2-F was used for the thermal conductivity of the insulation. For the transit-cold case (Figure 2-45), a value of 0.0127 Btu/in./hr-ft^2-F was used. The other figures, which are for transit-hot cases and lunar orbit, a thermal conductivity of 0.020 Btu/in./hr-ft^2-F was used.

[redacted]

~~CONFIDENTIAL~~

Table 2-14. Apex Orbit-Oriented (Positive X-Axis Pointed Along Orbit Path at All Times)

Orbit Inclination	Surface Characteristics	Maximum Temperature (°F)	Minimum Temperature (°F)
18.5 degrees	$\alpha_s = 0.9, \epsilon = 0.9$	184	-60
	$\alpha_s = 0.35, \epsilon\epsilon = 0.75$	90	-90
	$\alpha_s = 0.45, \epsilon = 0.4$	186	-50
5.5 degrees	$\alpha_s = 0.9, \epsilon = 0.9$	173	-55
	$\alpha_s = 0.35, \epsilon = 0.75$	95	-74
	$\alpha_s = 0.45, \epsilon = 0.4$	184	-12
0 degrees	$\alpha_s = 0.9, \epsilon = 0.9$	166	-58
	$\alpha_s = 0.35, \epsilon = 0.75$	100	-76
	$\alpha_s = 0.45, \epsilon = 0.4$	165	-19

Table 2-15. Base Sun-Oriented (Negative X-Axis Pointed Toward Sun at All Times)

Orbit Inclination	Surface Characteristics	Maximum Temperature (°F)	Minimum Temperature (°F)
0 degrees	$\alpha_s = 0.9, \epsilon = 0.9$	50	-80

[redacted]

Table 2-16. Oxygen Temperature at C/M Pressure Bulkhead

Type of Flow	Temperature at S/M Upper Bulkhead	Temperature at C/M Pressure Bulkhead
Normal	55 F	45 F
Emergency	-229 F	-189 F

Table 2-17. Antenna Temperature Extremes

Antenna	Type	Location	Range (°F)
Whip	I	In Parachute Compartment (attached to aluminum wall)	-25 to 250
Portable	II	In cabin	0 to 150

2.34 Command Module-LEM Docking Study - Space Heat Transfer Analysis

2.34.1 The minimum and maximum temperatures experienced by various structures and components will depend upon whether the docking mechanisms are internal or external to the C/M insulation. Internal components must be structurally mounted to internal structure (aluminum), and must not be exposed to the space environment, except during docking maneuvers. Those docking mechanisms external to C/M insulation, employing part of the LET may experience temperature limits of -350 F to +250 F.

2.34.2 Mechanisms internal to C/M insulation (within the C/M dome) may experience low temperatures of -100 F; however, only components of both small mass and large surface area will reach this value. The upper temperature limits for such items will be +250 F.

2.34.3 Insulation requirements to protect the ECS have been estimated as follows:

1. 1.0 inch of Q-felt (density: 6 lb cu ft) for the LEM tunnel exterior.
2. 0.8 inches of Q-felt for the interior of the dome.
3. 0.8 inches of Q-felt for all exposed interior CM and LEM surfaces after docking is accomplished.

[redacted]

[redacted]

2.35 Polaroid Filter Proposed for C/M Windows

2.35.1 The high temperature to be expected by the polaroid light filter assembly will be between 150 and 200 F, assuming that 96 percent of incident solar energy will be absorbed by the filter assembly.

2.35.2 Filters placed on the inner surface of the window assembly will still result in severe heat gains to the environmental control system, because any heat absorbed will be transferred to the cabin air, radiated to surrounding structure and components, and conducted away from the window area by the surrounding internal structure (aluminum). The most preferable means of controlling solar heat absorption is with a reflector placed between the inner and outer window assemblies. (If a reflector were placed on the inside surface of the inner window assembly, the panes of this window would absorb energy which will ultimately be transferred to the ECS system.)

2.36 Heat Loads Through C/M C-Band Antennas

2.36.1 An investigation indicates that the heat gains and losses of the C/M ECS through cables for the C-band antennas can be very high—290 and 1410 Btu/hr, respectively.

2.36.2 In a further study, the cable was made to travel six inches through the insulation before connection with the inner structure. The results of this study may be seen in Table 2-18. It will be noted that the heat gains and losses have been reduced considerably.

Table 2-18. Heat Gains and Losses Through C/M Antenna Cables

C-Band Antenna Cables	Heat Gain (Btu/hr)	Heat Loss (Btu/hr)
Small (one)	6.2	33
Large (four)	22.4	93
Total	28.6	126

[redacted]

[redacted]

2.37 Heat Loads to C/M

2.37.1 Listed in Table 2-19 are the revised maximum heat loads to the C/M, during space flight, that are a result of thermal heat shorts.

2.37.2 Part I of the heat gain table is for an orientation where the apex of the C/M is directed towards the sun. Part II is where the sun is normal to the conical surface at the -Z axis.

2.38 Temperature Extremes of C/M RCS Rocket Engines

2.38.1 An analysis was performed on the C/M RCS rocket engines to determine minimum and maximum temperatures which these engines will experience during space flight. For the analysis, a pair of the C/M RCS pitch rockets was studied, assuming the crew compartment to be pressurized and the service module fairing to be insulated.

Table 2-19. Heat Loads to C/M

Location	Btu/hr		
	Heat Loss	Heat Gain	
		Part I	Part II
4 Tower Wells	100	60	0
2 Jettison Fittings	28	6	0
4 Tension Ties	25	5	0
24 H. L. Frames	573	118	0
1 Small Antenna Cable	33	15	0
3 Large Antenna Cable	62	15	0
21 Crew Compartment Stringers	685	94	0
5 Windows	234	200	600
Umbilical Package	100	40	100
	1840	553	700

[redacted]

[redacted]

2.38.2 The study was divided into three cases: The first assumed no heat input to the rockets from external sources (solar); The second and third assumed heating due to solar radiation. Temperatures at different times are tabulated in Table 2-20 for both phases.

2.38.3 At the end of transearth coast the temperature of the injector plate can be as low as -102 F (Case 1). For full solar incidence on the injector plate during the entire transearth coast phase, the expected temperature is 245 F (Case 2). Since the slightest variation of the C/M attitude, with respect to the sun, will place the injector plate in the shadow, another analysis was performed. It was assumed that solar energy entering the mouth of the rocket was transiently distributed to different internal surfaces of the thrust chamber, while outer C/M surfaces in the vicinity of the rockets received a maximum of solar heating. For this condition, a maximum temperature of 207 F for the injector plate is expected.

2.39 Command Module Heat Shield Steady-State Circumferential Temperature Distributions in Space

2.39.1 Steady-state circumferential temperature distributions of the heat shield at $X_c = 23$ and $X_c = 112$ are shown in Figures 2-48 and 2-49. The curves describe circumferential temperature distributions as a function of angular location, θ , measured from maximum to minimum temperature. For X_c locations between 23 and 112, the temperature distributions along the meridian lines can be assumed to have a linear variation.

2.39.2 In the analysis the ablator was assumed to have a solar absorptivity and emissivity of 0.9, thermal conductivity of 0.07 Btu/hr-ft.°F, density of 35 pounds per cubic foot and a specific heat of 0.36 Btu/lb-°F.

2.40 Total Heat Loads to C/M

2.40.1 Total heat loads during various mission phases, for a crew compartment temperature of 75 F, are shown in Table 2-21.

2.41 Heat Transfer Coefficient Through C/M Walls

2.41.1 The overall conductance value between the crew compartment wall and the outer ablator surface is 0.0202 Btu/hr^2-°F. This value is representative for a cold-case condition; which implies no solar incidence on the conical surface of the C/M.

2.42 Command Module Space Flight Transient Circumferential Temperature Distribution

[redacted]

Table 2-20. C/M RCS Rocket Engine Temperature Distribution During Space Flight

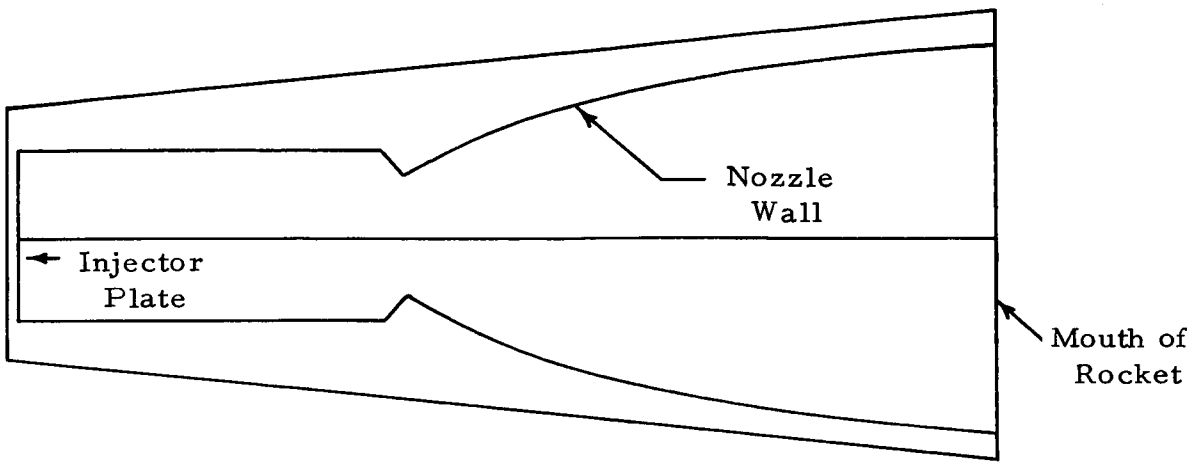

	Cold Case 1 Temperature (°F)		Extreme Heating Case 2 Temperature (°F)		Cyclic Heating Case 3 Temperature (°F)	
Time Hours	Nozzle Wall	Injector Plate	Nozzle Wall	Injector Plate	Nozzle Wall	Injector Plate
0	90	90	90	90	100	100
10	-88	30	188	101	184	149
25	-132	-8	212	176	195	185
50	-155	-59	222	228	201	200
84	-170	-102	225	245	207	207

2.42.1 Space flight transient circumferential temperature distributions for $X_c = 23$ are shown in Figures 2-50 and 2-51. Distributions for X_c locations 43, 56, 68, 81, 98 and 112 will be released as soon as they become available. Until that time it shall be assumed that the reported distribution holds for all other X_c locations.

2.42.2 The minimum temperatures anticipated for AFRM 011 at $X_c = 23$ are -80 F and -60 F for the ablator surface and for the steel-ablator interface, respectively.

Table 2-21. Total Heat Loads to C/M

	Heat Loads - Btu/hr		
	Command Module	Heat Shorts	Total
Earth Orbit Launch Time: June 21; 7 am	+120	+110	+230
Earth Orbit Launch Time: June 21; 12 am	-350	-175	-525
Translunar Mission (No LEM, Sun Makes 30-Degrees Angle, with Apex)	+20	+700	+720
Translunar Mission (No Sun on C/M	-740	-1840	-2580
Lunar Orbit (Apex of C/M Pointed Towards Moon)	-130	-180	-310
Transearth Mission (Apex Sun-Oriented)	+250	+550	+800

2.43 Minimum Temperature of Harmonic Drive Mechanism of Astro-Sextant Door

2.43.1 A preliminary thermal analysis was performed on the actuating and latching mechanism for the astro-sextant doors to determine the lowest temperature to be expected in the harmonic drive. (A lubricant is required for the harmonic drive mechanism, and temperature will grossly affect choice of a lubricant.)

2.43.2 A heat balance was set up for the drive mechanism, assuming that the crew compartment temperature was 0 F and the heat shield and astro-sextant doors were at -290 F. The control lines to the doors were assumed to be perfectly insulated (no heat transfer to heat shield or pressure vessel). Under these conditions the drive mechanism steady-state temperature was found to be -25 F.

2.43.3 It is important that the mechanical lines from the drive mechanism to the doors travel through the insulation (Q-felt) and not contact the heat shield or cabin walls between the attach points. This will prevent placing an excessive heat gain or loss on the ECS.

2.44 Space Flight Temperature Extremes of Scimitar Antenna

2.44.1 An analysis has indicated that the maximum temperature of the scimitar antenna under conditions of normal solar incidence will be 250 F. The minimum temperature during a cold-soak condition will reach -300 F.

2.45 Temperature Distributions Through the Heat Shield, About the C-Band Antenna Window

2.45.1 The temperature distributions through the heat shield, about the C-band antenna window, are shown in Figure 2-52 (17 sheets). The analysis was performed on the C-band antenna located at $X_c = 54$, but the resulting distributions can be assumed to hold for the other C-band antennas, except at X_c locations less than 20.

2.45.2 Sheet 1 through 8 show the transient heat shield temperature distributions, in space, about the C-band antenna window for heating from steady-state cold. Sheets 2-9 through 2-17 give the temperature distributions for cooling from steady-state hot. The distribution curves begin at the antenna-heat shield interface. Distances on the curves are measured radially outward from the center of the antenna.

2.45.3 Temperature Locations for Sheets 1 Through 17 are as follows:

Location 1 = surface of ablator
Location 2 = center of ablator
Location 3 = ablator-steel honeycomb bondline

2.45.4 Assumptions:

1. Ablator thickness = 1.45 inches (constant)
2. Configuration taken from Emertron drawing #72171
3. Heat shield solar absorptivity = 0.9; emissivity = 0.9
4. Antenna cable's first attachment to aluminum inner structure occurs 12 inches from antenna window
5. Cable travels through insulation without touching external structure

2.46 Steady-State Temperature Distribution for ECS Water Dump Line

2.46.1 A study was performed to find minimum temperature distributions in the ECS water dump line. The dump line was assumed to be centrally located within the 2-1/2-inch evaporator vent line and supported by four equally-spaced, nominal-sized stainless steel supports. Table 2-22 shows the steady-state longitudinal temperature distribution for the dump lines.

~~CONFIDENTIAL~~

Table 2-22. Steady-State Temperature Distribution for ECS Water Dump Line

Water Dump Line (Length in Inches From Cabin Wall)	Temperature (°F)
0	70.0
8	61.13
16	50.0
24	49.5
32	36.2
40	28.3
48	-5.2
52*	-53.7
* Approximate location of the vent port	

2.46.2 The maximum combined heat loss from the water dump line and the evaporator vent line for the condition shown above is 10.2 Btu/hr.

2.47 Temperature Extremes of Airlock Seals for Space Flight Conditions

2.47.1 A thermal analysis of the forward portion of the Apollo command module was performed to determine the temperature extremes of structure and components for worst case hot-soak and cold-soak conditions during various mission phases. This section reports temperatures of the airlock seal rings which are sensitive to extremes of temperature.

2.47.2 The two seal rings used, of an O-ring configuration, are compressed between the hatch cover and the access cylinder ring of the hatch assembly to prevent leakage of air from the crew compartment (Figure 2-53). The temperature of the seal rings therefore depends closely upon the temperature of the forward hatch assembly.

2.47.3 For this study it was assumed that the radome was not insulated. Solar absorptivity and emissivity of the aluminum forward hatch were assumed to be 0.4 and 0.15, respectively.

2.47.4 Figure 2-54 is a flow chart for the hot-soak mission and Figure 2-55 is a flow chart for the cold-soak mission. Figure 2-56 shows the results of the specific assumed orientations described in Figures 2-54 and 2-55.

2.47.5 The highest temperature of the seal rings was 158 F. The seals reached this temperature in the lunar-orbit-terminating-in-abort condition, in an interval of one hour with the radome open, and with sunshine normal to the hatch. The lower curve shows the lowest temperatures attained by the seal rings with the forward portion of the C/M under a constant cold-soak condition. The analysis did not include all the flight phases in sequence as in Figure 2-54, but only the translunar and transearth phases in that order, with an initial temperature of 80 F taken as the common temperature for all structure and parts.

2.47.6 The lowest temperature of the seals for any nominal mission did not fall below 30 F. A depressurized case was evaluated, which assumed no internal heat generation, to attempt to bound the minimum temperature which might occur. It was found that the forward section temperature dropped to -92 F.

2.47.7 Internal electrical components, however, generate energy at rates comparable to that which can be lost through the structure and insulation. It is therefore anticipated that depressurized case temperatures will be similar to pressurized case temperatures and the minimum allowable of -65 F for the seals will not be violated.

2.48 C-Band Antenna Window Temperatures in Space Flight

2.48.1 The temperature extremes anticipated for the C-band antennas are as follows:

1. The maximum expected space flight temperature is 250 F. This temperature applies to the entire antenna and antenna window.
2. The minimum temperature of the antenna has been modified to -200 F. This temperature is to be assumed applicable to the entire assembly.

2.49 Command Module Space Flight Transient Circumferential Temperature Distribution

2.49.1 An analysis was performed by cooling the heat shield from the initial temperature distribution, for the angle of 57.5 degrees between the sunline and the X-axis. Two initial conditions were evaluated:

1. The maximum temperature (+250 F) occurred on the -Z axis.
2. The maximum temperature (+250 F) occurred on the +Z axis.

2.49.2 Figures 2-57 and 2-58 show the temperatures at a given time after the start of cooling as a function of angular displacement (θ) around the X-axis, from the maximum temperature.

2.49.3 Description of cases (for Figures 2-57 and 2-58) are as follows:

Initial temperature distributions used in the analysis were for an angle of 57.5 degrees between the sunline and the X-axis.

Case 1: θ increases from $-Z_c$ to $+Z_c$, with maximum temperature (+250°F) occurring on $-Z_c$ axis.

Case 2: θ increases from $+Z_c$ to $-Z_c$, with maximum temperature (+250°F) occuring on $+Z_c$ axis.

The analysis was performed on $X_c = 23$.

2.50 Temperature Extremes of Parachutes During Space Flight Conditions

2.50.1 A detailed thermal analysis of the maximum and minimum parachute temperatures showed that the respective values of 120 F and -65 F were not violated.

2.50.2 In a thermal analysis of the forward part of the Apollo command module, consideration was given to the temperature distribution of the parachutes during the space flight phases of a hypothetical lunar mission. The mission was designed to give the most extreme upper and lower temperatures to be expected.

2.50.3 The conductivity value used, 0.02 Btu/hr-ft-°F, was one-half that value obtained by assuming that the ratio of parachute conductivity to solid nylon conductivity is directly proportional to the ratio of parachute bulk density to the density of solid nylon.

2.51 Insulation Requirements for the LES Tower-to-C/M Forward Heat Shield Pull-off Tubes

2.51.1 The minimum thickness of Buná-N ablative insulation required to prevent the four LES tower-to-C/M forward heat shield pull-off tubes from exceeding 550 F is 0.35 inch on the forward (windward) half of each tube and 0.075 inch on the rear (leeward) half of each tube. Figure 2-59 shows the location of the four pull-off tubes on the tower, as well as a typical tube cross-section with the required insulation.

2.51.2 It should be noted that if the tubes are to remain intact during a reentry from a high-altitude abort down to 25,000 feet, using the tower aerodynamic flap concept, additional insulation may be required to protect the subject tubes from reentry heating.

2.52 Temperature Distribution of the CM Structural I-Beam Spacer and Outer Structure for Space Operation.

2.52.1 An analysis to find the maximum temperature gradient through the command module fiberglass I-Beam and the minimum outer surface temperature of the structure was performed. These conditions occur during trans-lunar and trans-earth coast, with no solar energy incident on the outer surface. The results are listed in Table 2-23.

Table 2-23. Temperature Distribution of the CM I-Beam

Outer Surface Emissivity	Maximum Temp. Gradient in I-Beam (°F)	Minimum I-Beam Temperature (°F)	Minimum Outer Surface Temp. (°F)
0.90	256	-192	-266
0.75	250	-185	-257

2.52.2 The thermal conductivity of the fiberglass laminate used in the structural I-Beam spacer is considerably higher than that of Q-felt insulation. This allows for increased heat transfer from the crew compartment to the surface and thus increases the minimum surface temperature.

2.52.3 A detailed temperature distribution through the entire structure in the vicinity of the structural I-Beam is given in Figures 2-60 and 2-61, for outer surface emissivities of 0.90 and 0.75, respectively.

2.52.4 The analysis was performed under the following assumptions:

Crew compartment temperature held constant at 75°F.
50% contact between the fiberglass structural I-Beam and structure.
All heat loss from the surface of the command module was considered to be by radiation to space.

2.53 Thermal Data for Heat Shield Substructure and Attachments

2.53.1 The following discussion outlines the heat transfer effects of stringers, longerons, and other members and the insulation layer. In general, these members act as thermal shorts and decrease the thermal effectiveness of the insulation layer. The increased heat transfer through a stringer may cause the local temperature on the aluminum pressure vessel to exceed the design limit of 200 F. The stainless steel substructure panel will also be affected and is expected to be somewhat colder in the immediate attachment area of the stringer. The extent of these effects on the heat shield, caused by the substructure temperature distributions and the resulting thermally induced stresses, should be examined.

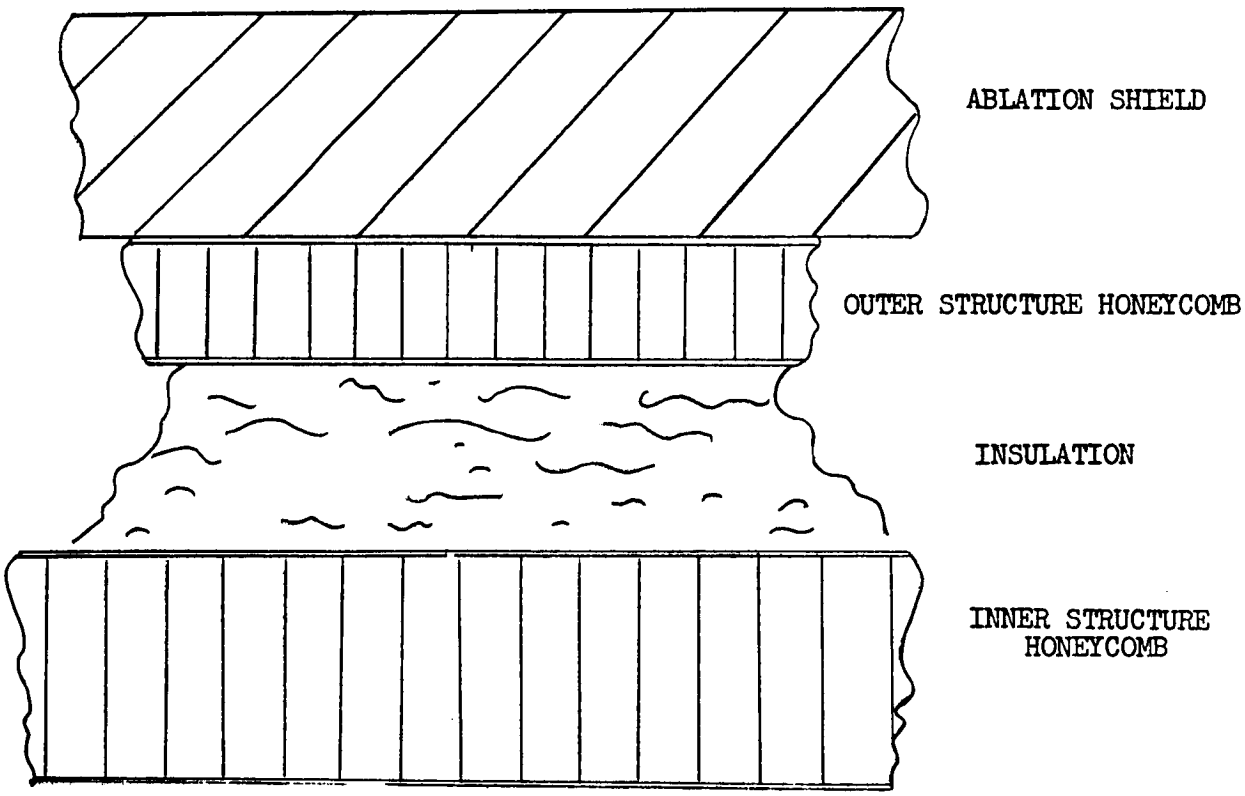

Figure 2-1. Typical Structure for Ablation and Transient Heat Transfer Analysis

[redacted]

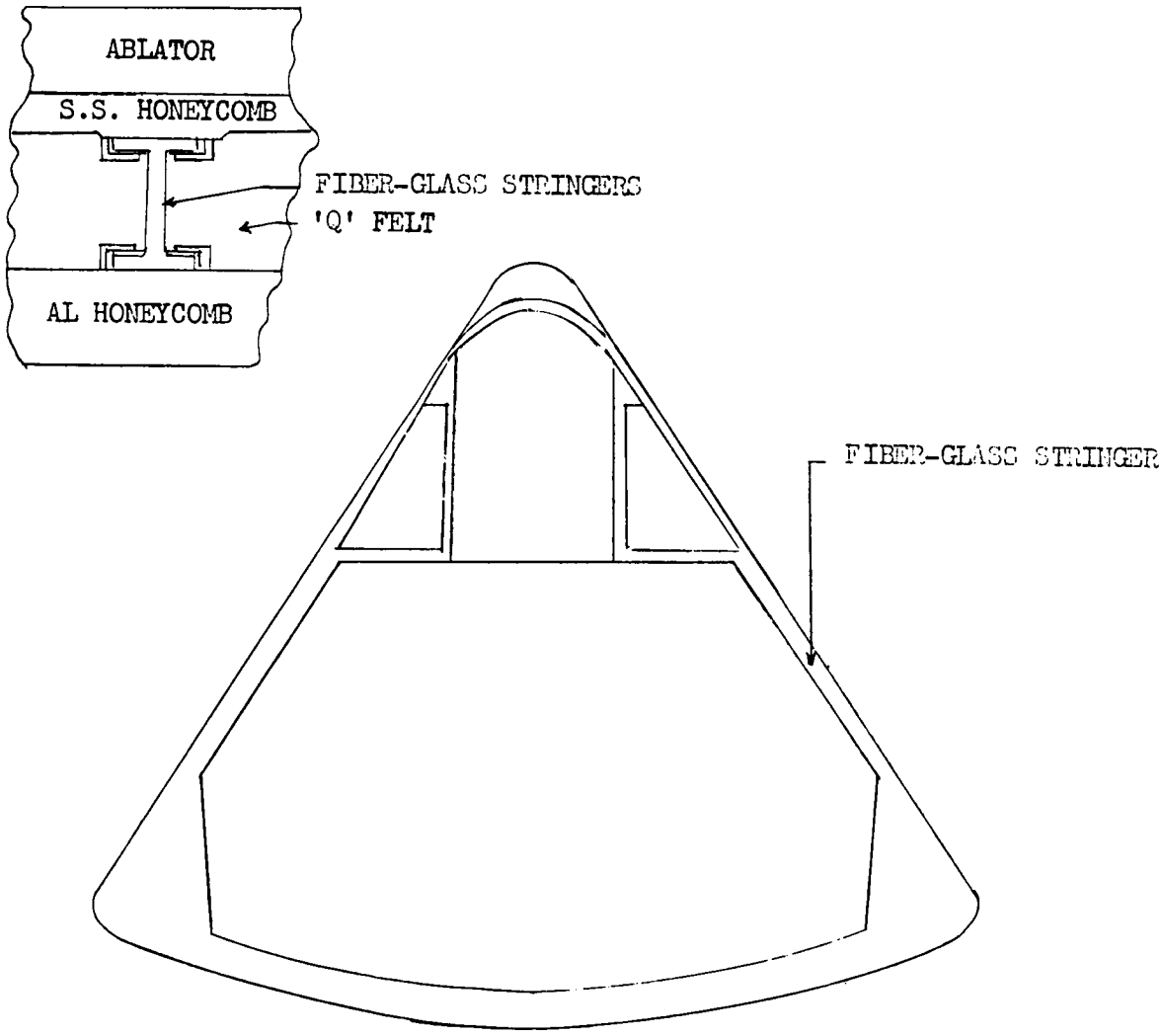

Figure 2-2. Schematic Diagram of the Command Module

[redacted]

~~CONFIDENTIAL~~

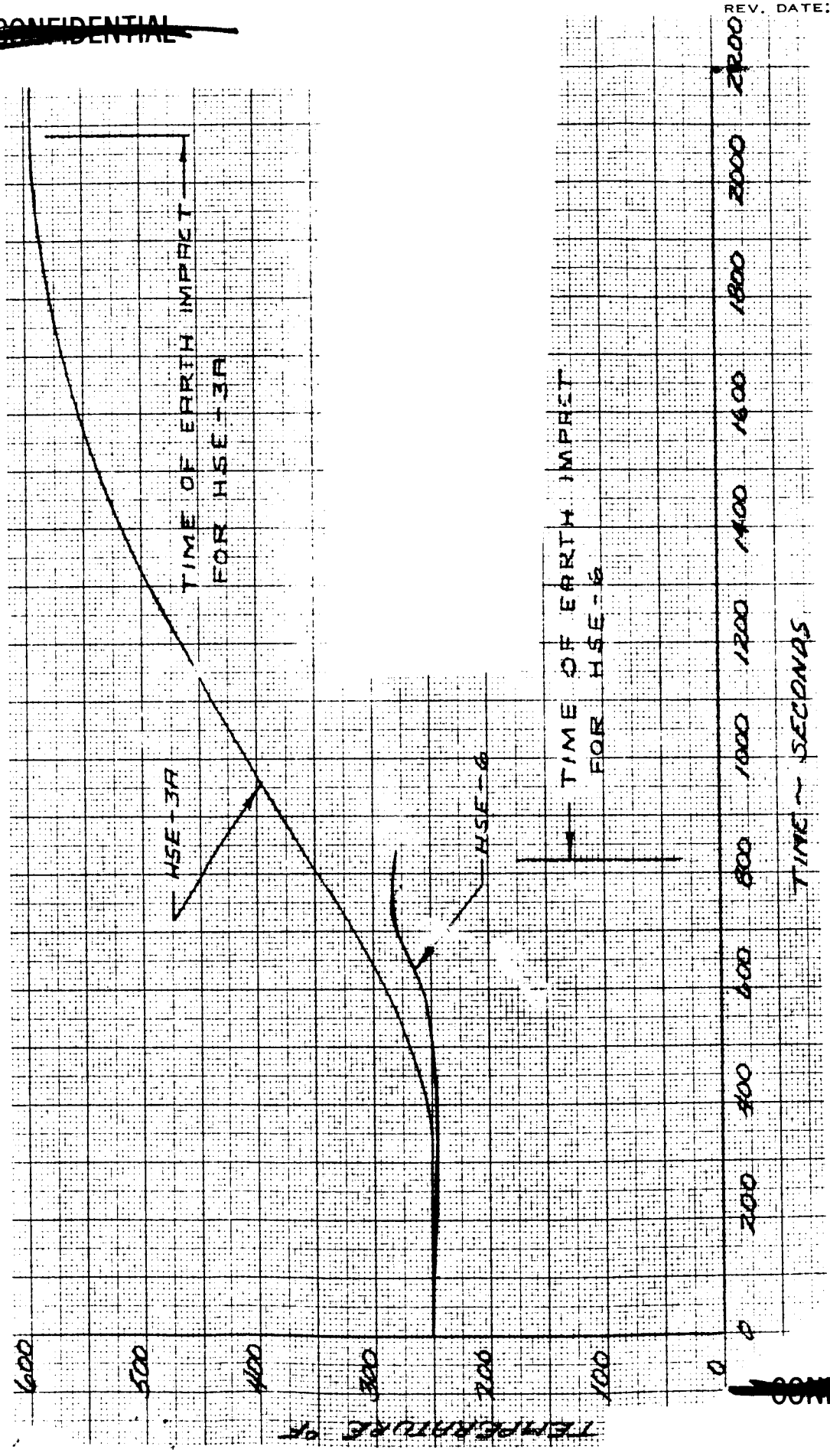

Figure 2-3. Command Module Ablator Stainless Steel Interface Temperature Histories for Reentry Trajectories (Indicated at Body Location 8)

~~CONFIDENTIAL~~

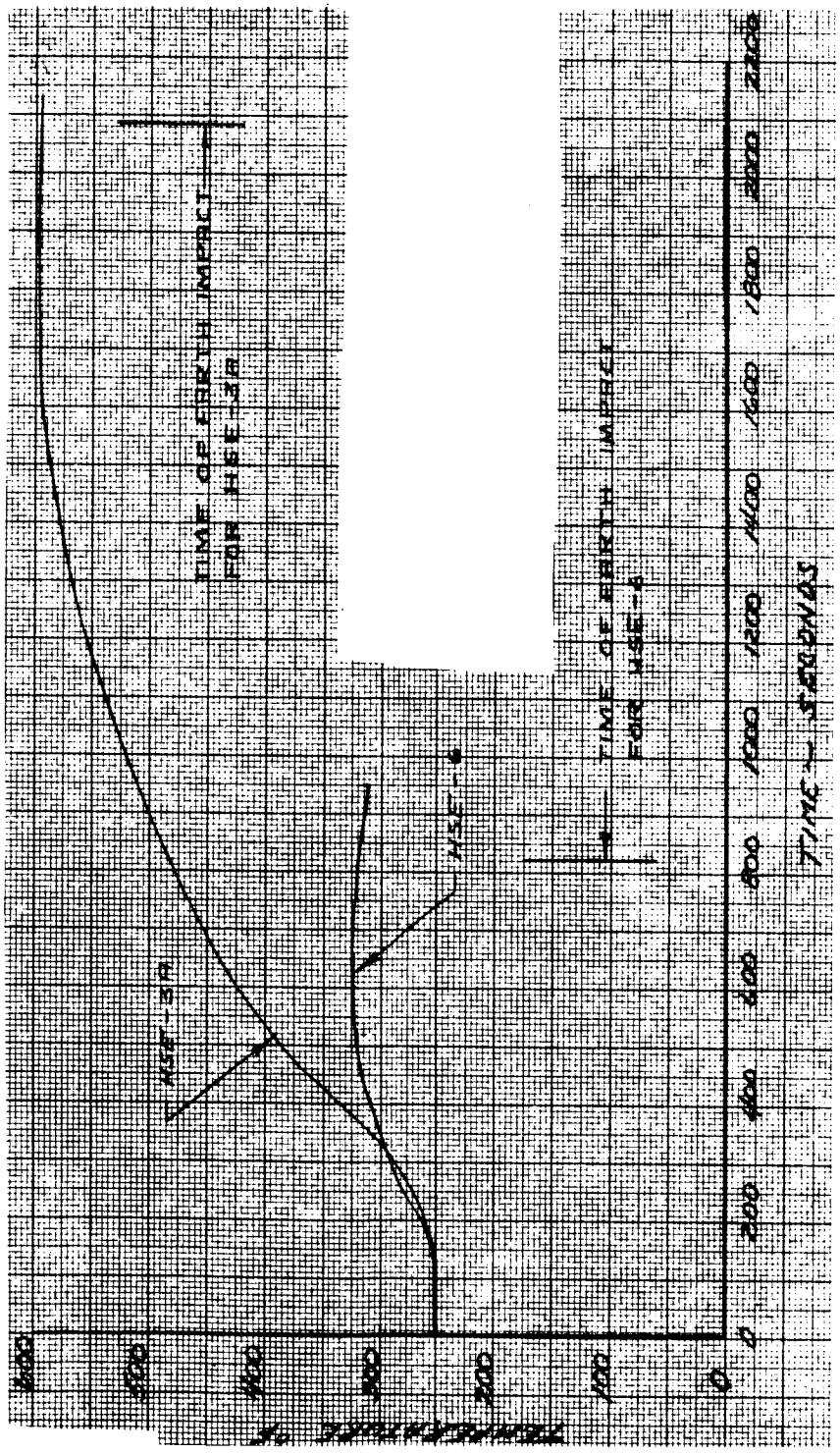

Figure 2-4. Command Module Ablator Stainless Steel Interface Temperature Histories for Reentry Trajectories (Indicated at Body Location 13)

~~CONFIDENTIAL~~

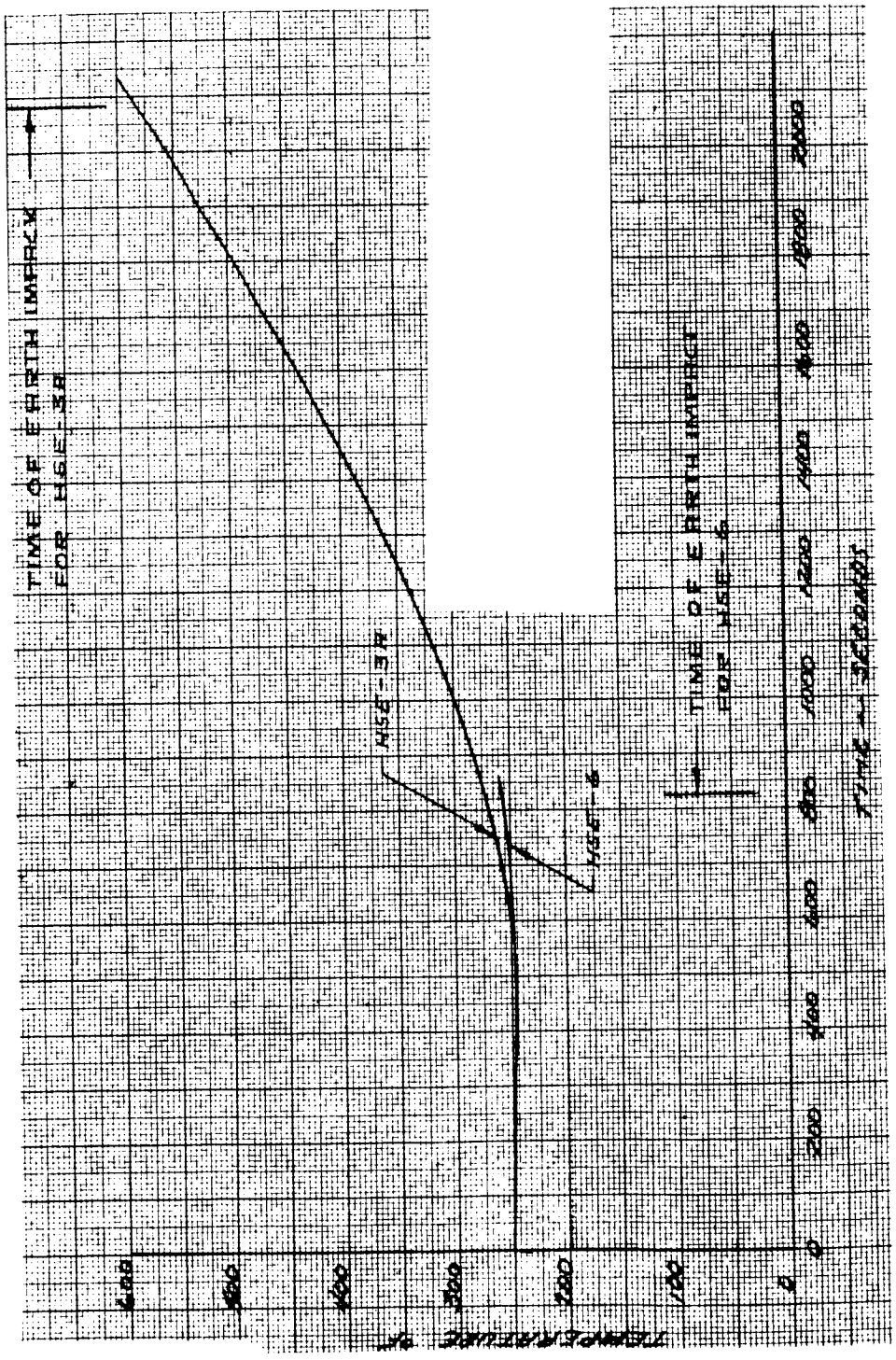

Figure 2-5. Command Module Ablator Stainless Steel Interface Temperature Histories for Reentry Trajectories (Indicated at Body Location 24)

~~CONFIDENTIAL~~

~~CONFIDENTIAL~~

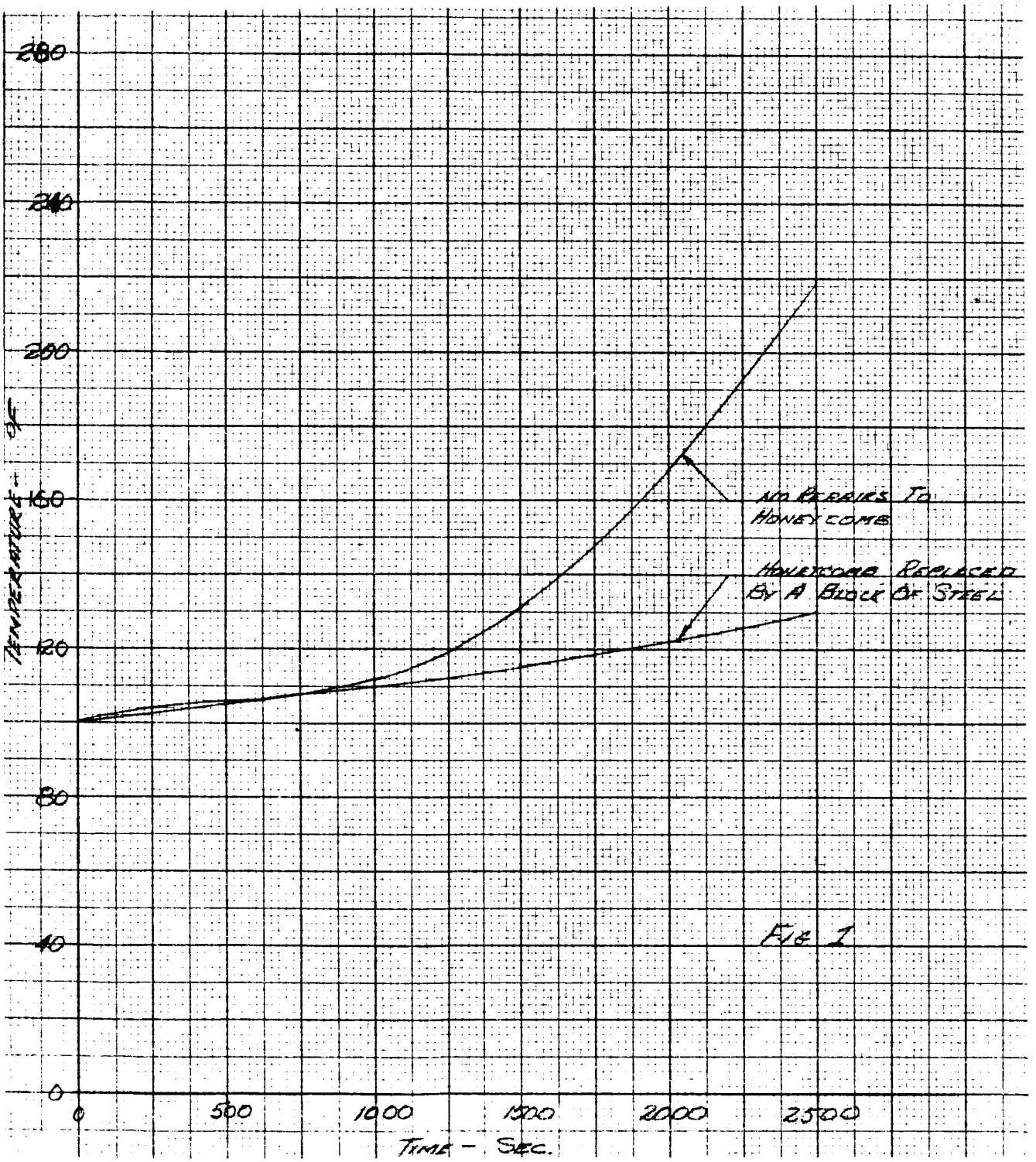

Figure 2-6. Temperature History at Inner Structure

~~CONFIDENTIAL~~

~~CONFIDENTIAL~~

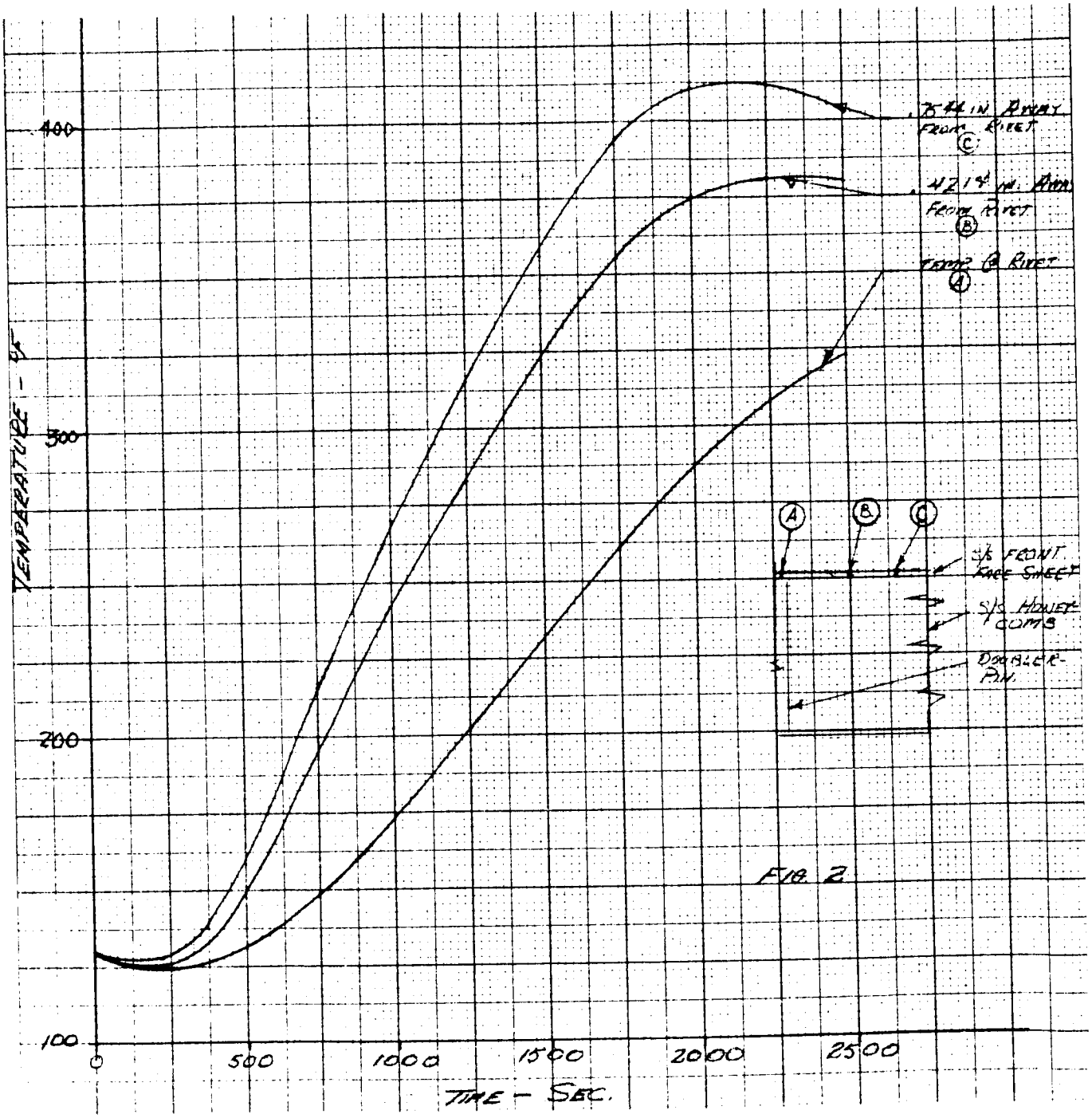

Figure 2-7. Temperature Histories of Front Face Sheet S/S Honeycomb as a Function of Distance From the Pin

[redacted]

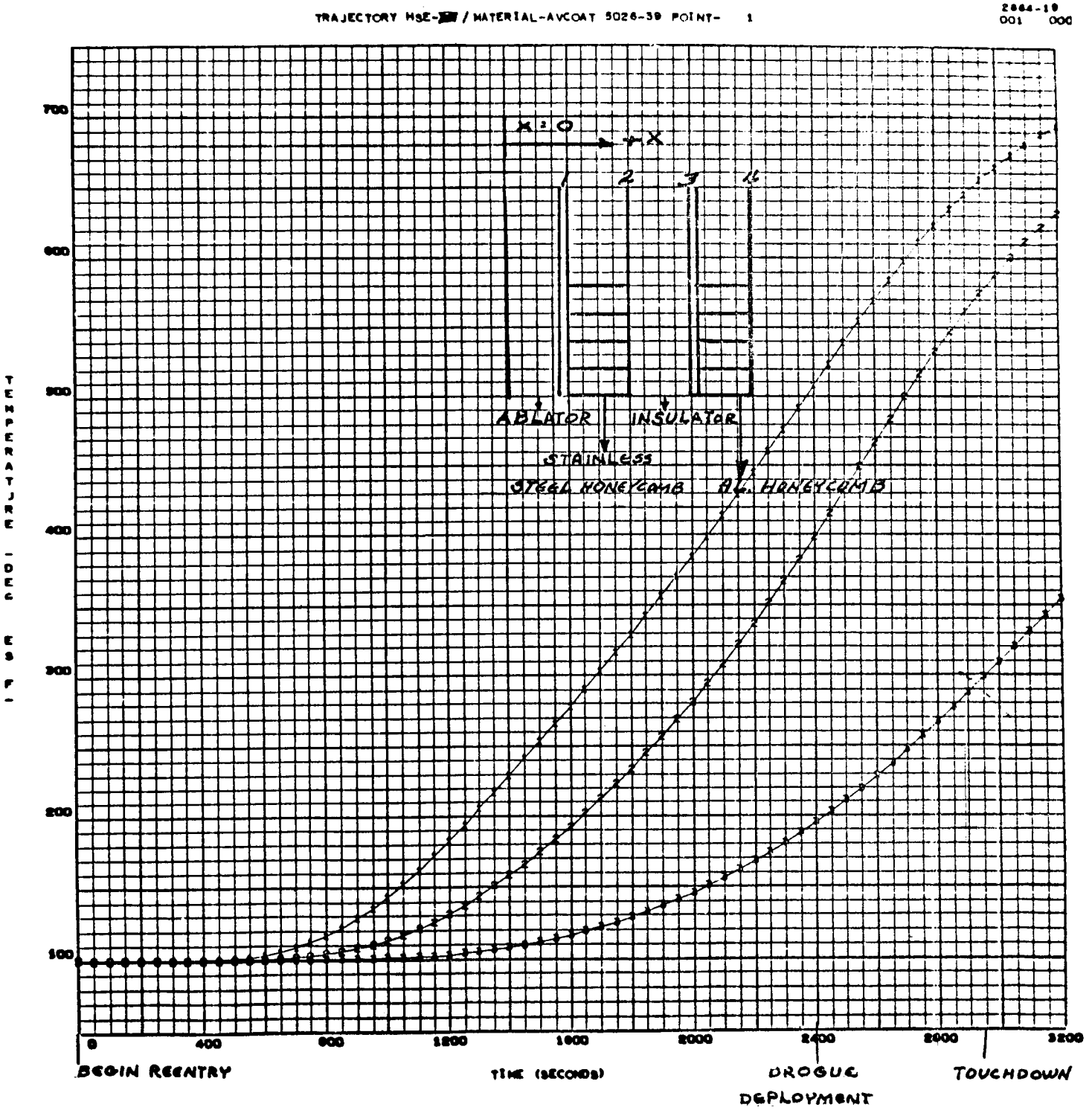

Figure 2-8. Temperature Versus Time
(Sheet 1)

[redacted]

[redacted]

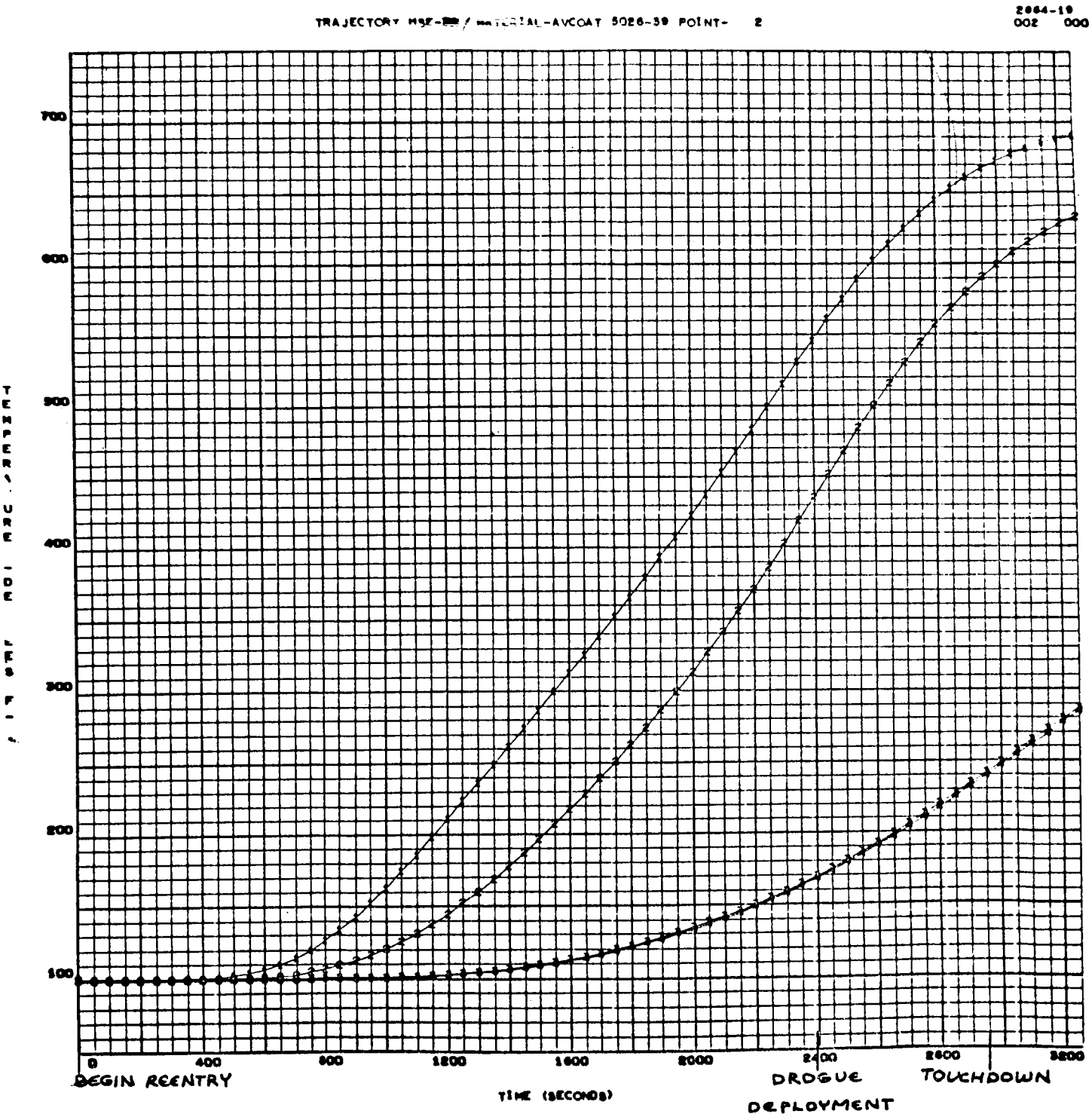

Figure 2-8. Temperature Versus Time
(Sheet 2)

[redacted]

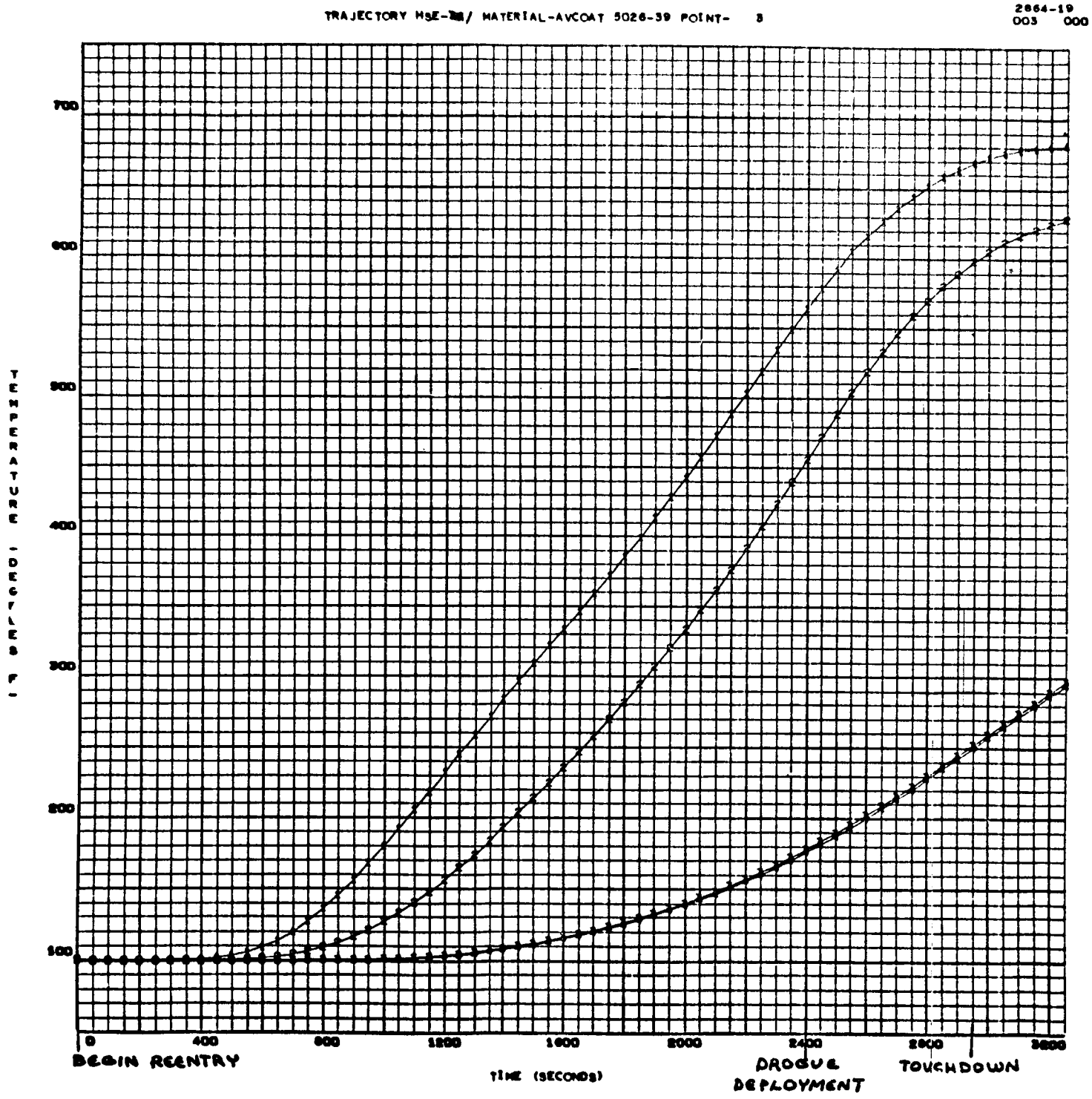

Figure 2-8. Temperature Versus Time
(Sheet 3)

[redacted]

[redacted]

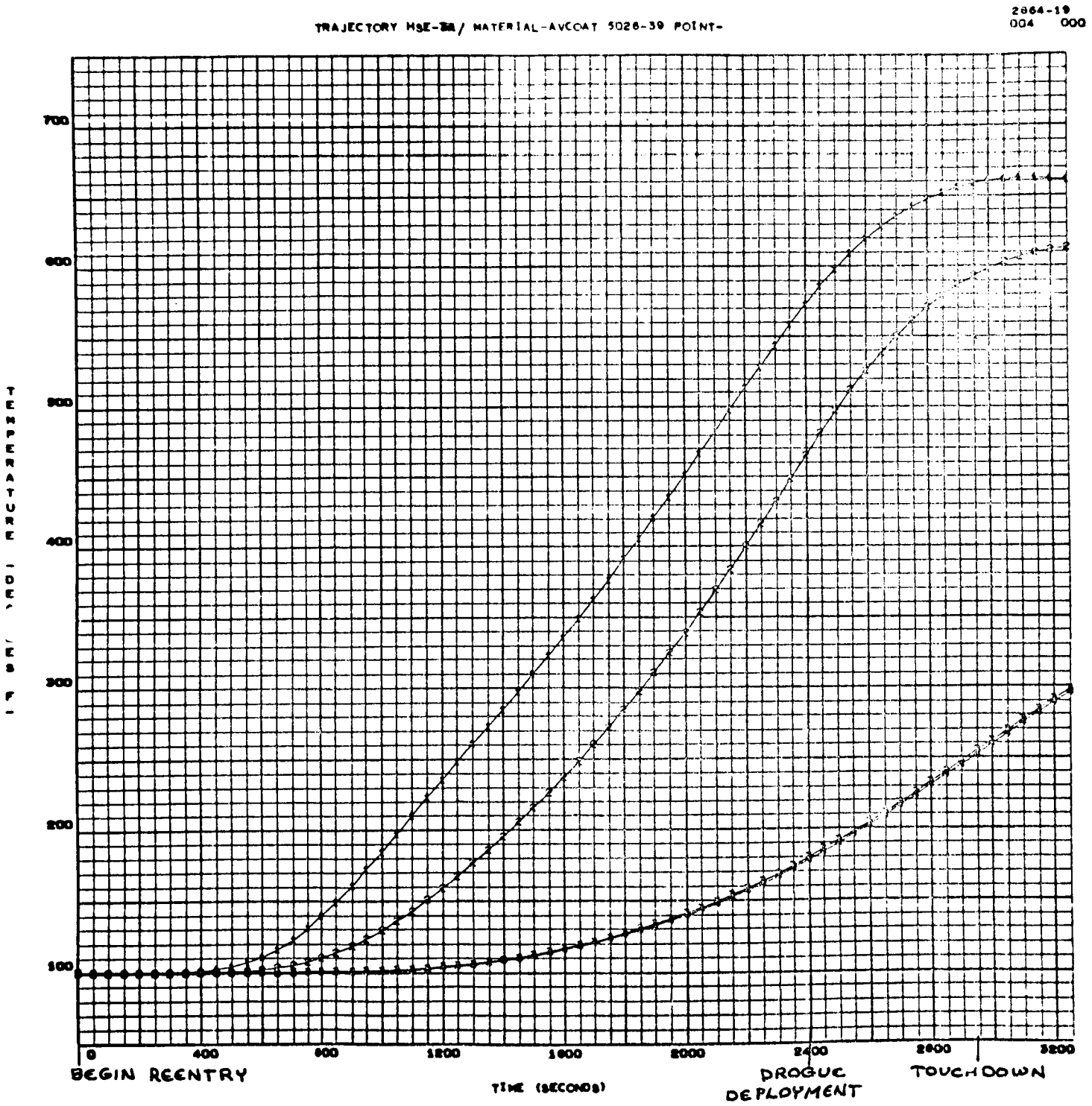

Figure 2-8. Temperature Versus Time
(Sheet 4)

[redacted]

[redacted]

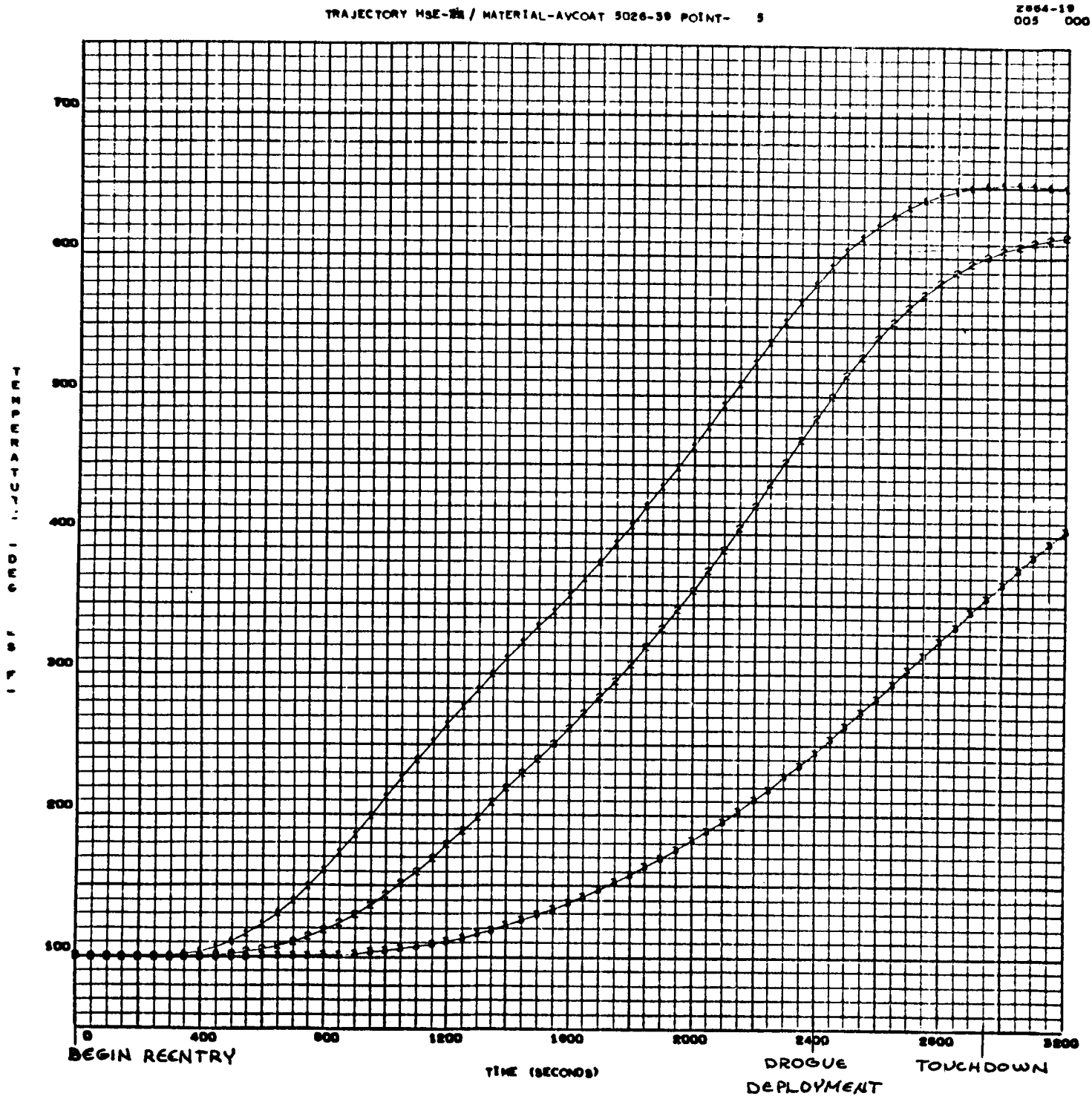

Figure 2-8. Temperature Versus Time
(Sheet 5)

[redacted]

[redacted]

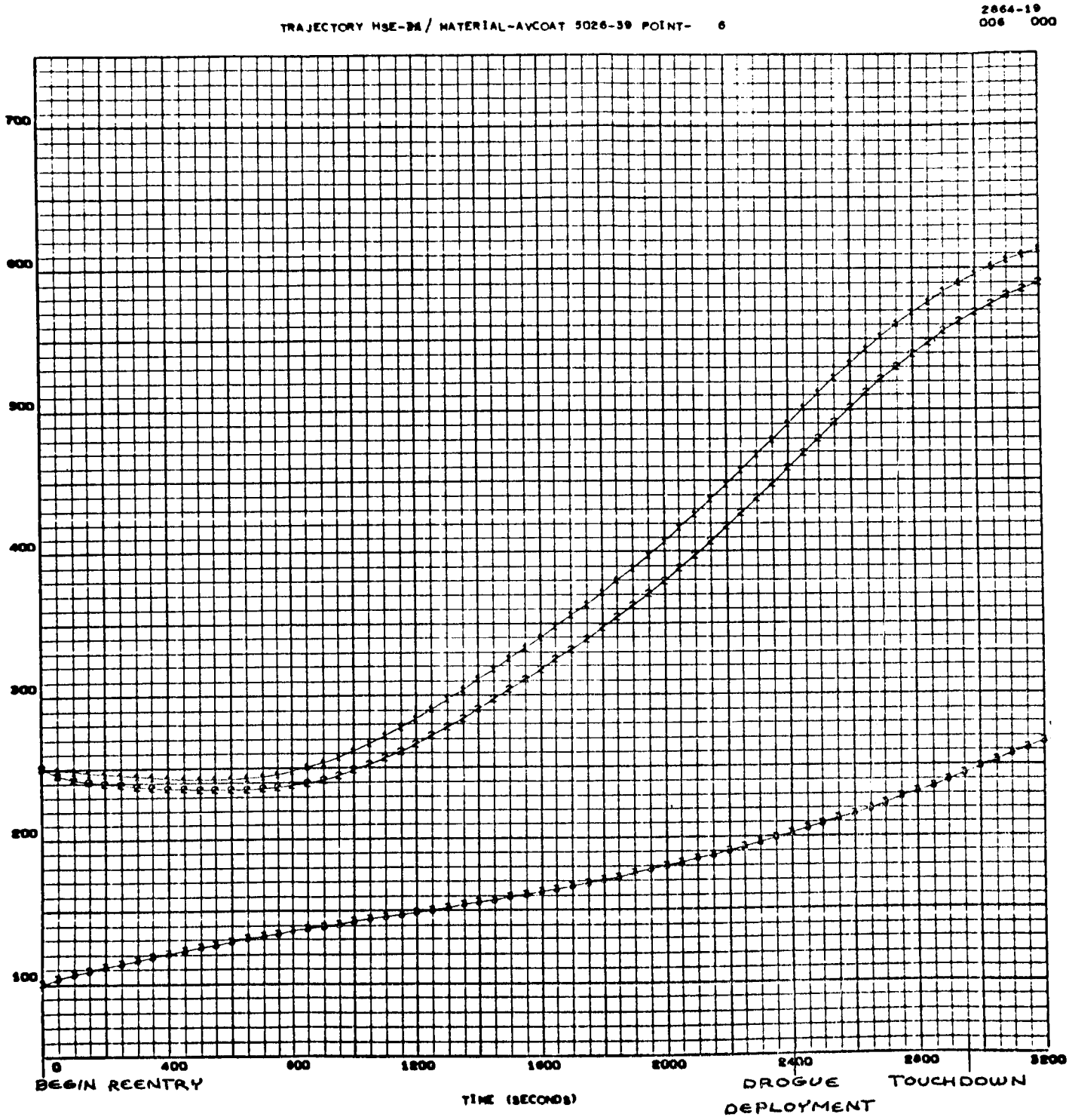

Figure 2-8. Temperature Versus Time
(Sheet 6)

[redacted]

~~CONFIDENTIAL~~

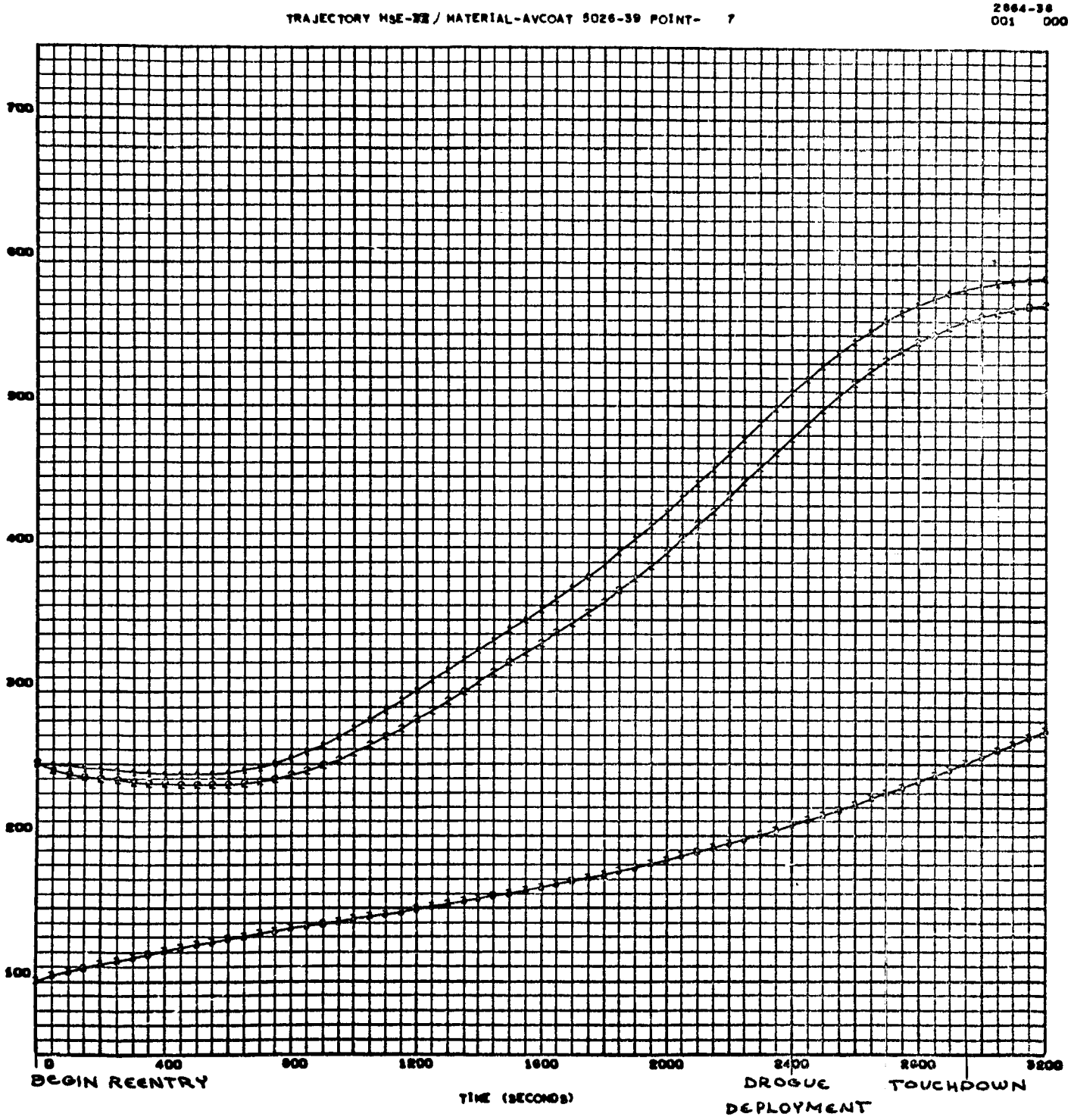

Figure 2-8. Temperature Versus Time
(Sheet 7)

[redacted]

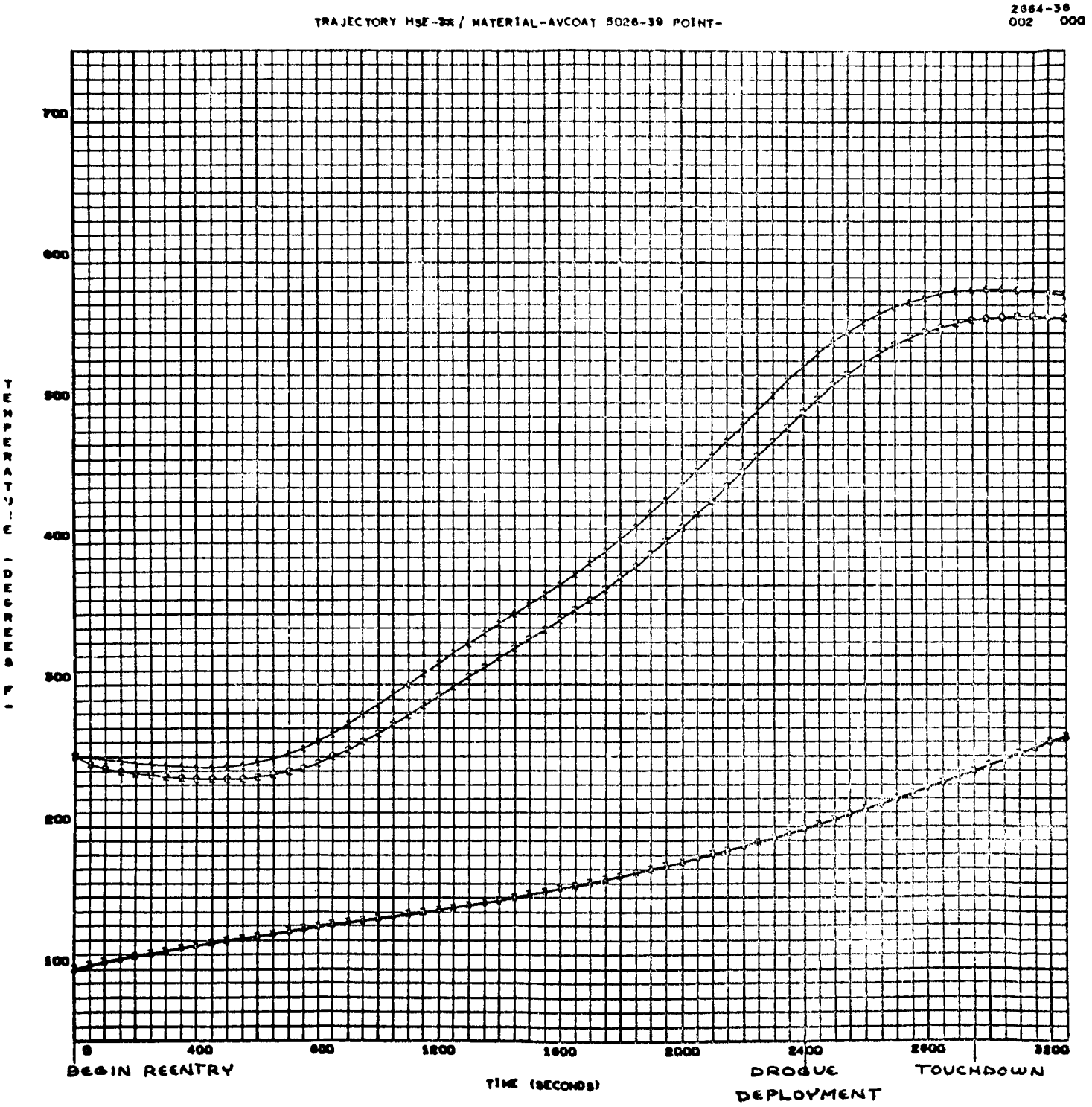

Figure 2-8. Temperature Versus Time
(Sheet 8)

[redacted]

[redacted]

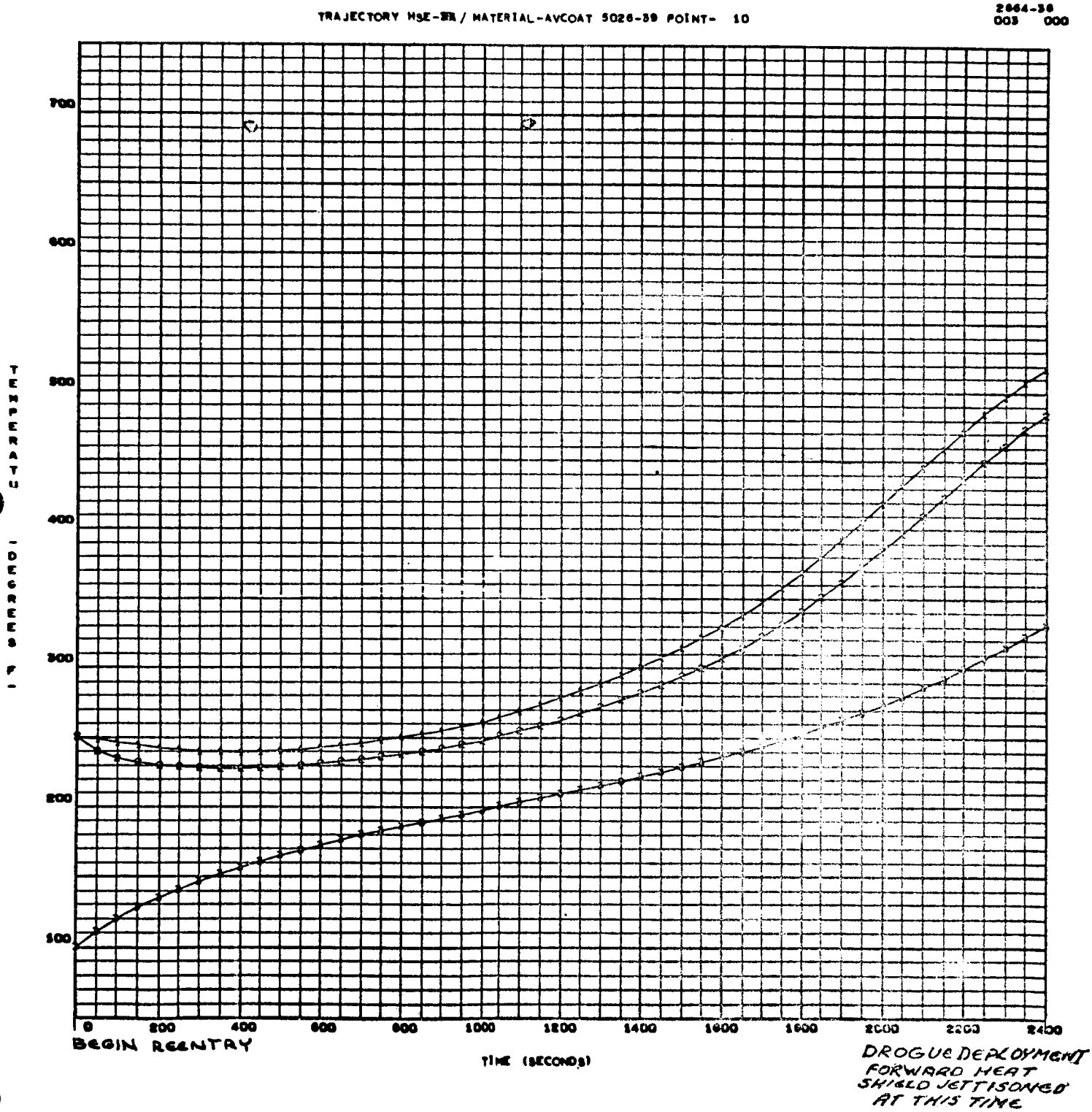

Figure 2-8. Temperature Versus Time
(Sheet 9)

[redacted]

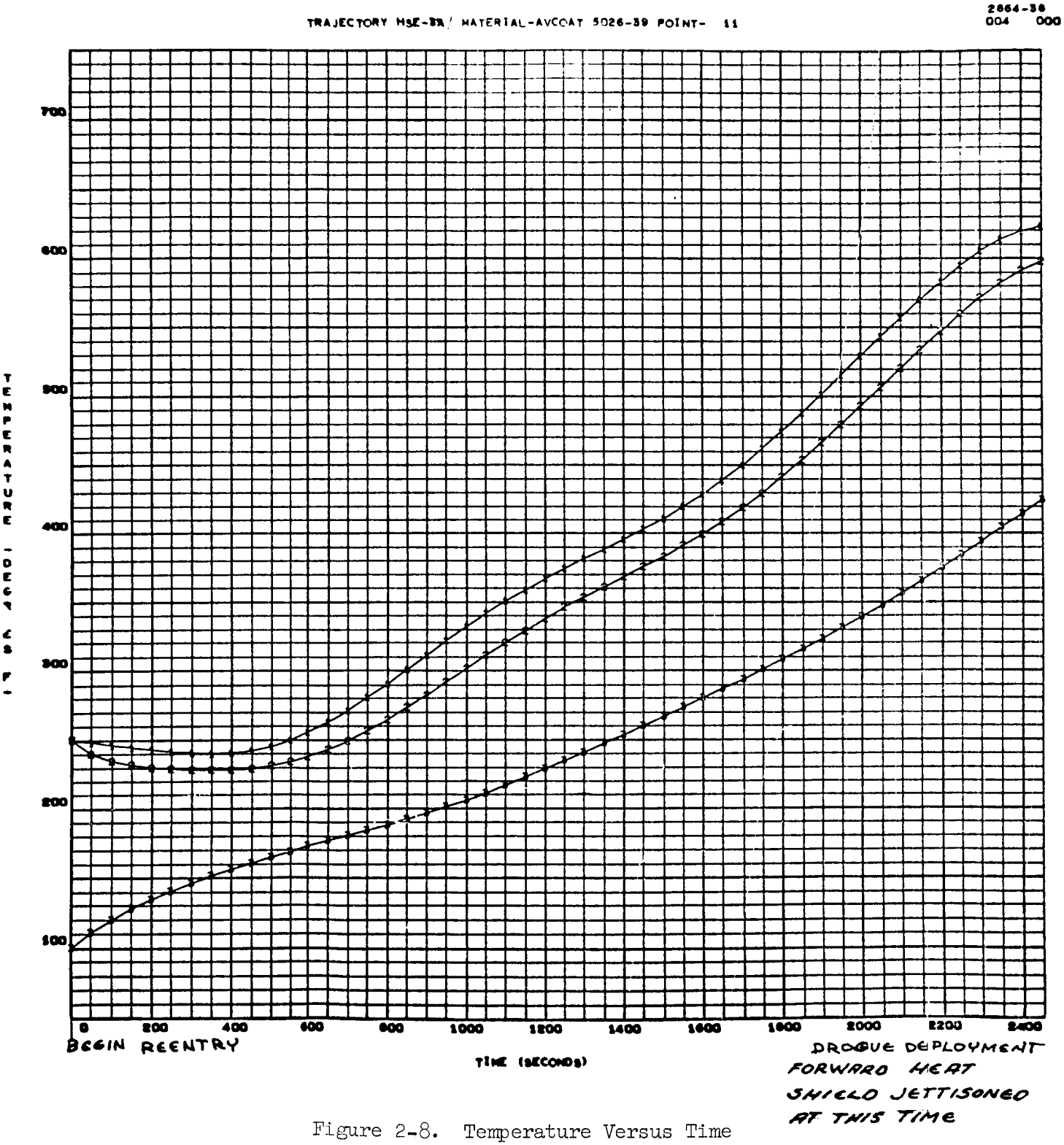

Figure 2-8. Temperature Versus Time
(Sheet 10)

~~CONFIDENTIAL~~

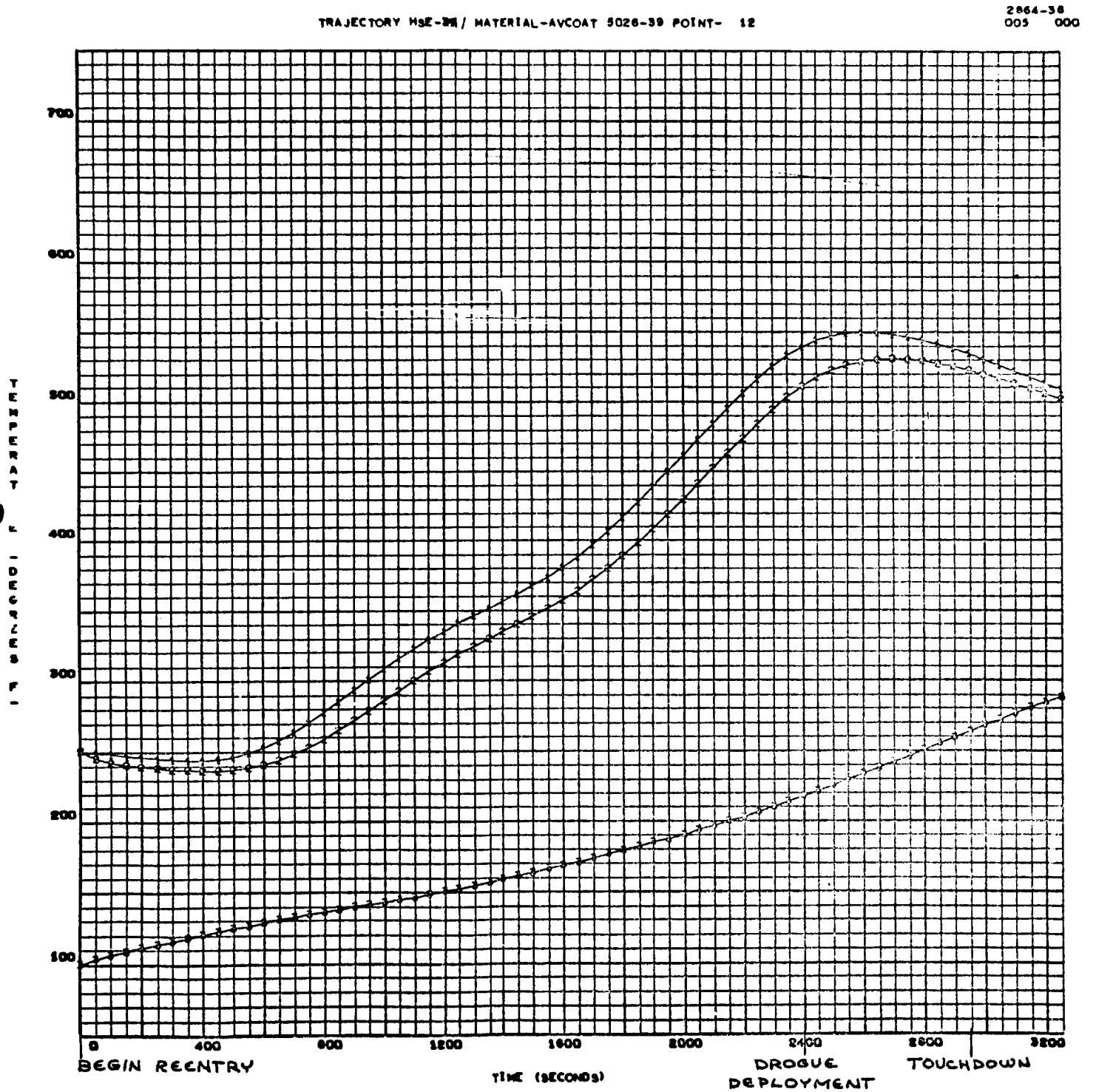

Figure 2-8. Temperature Versus Time
(Sheet 11)

[redacted]

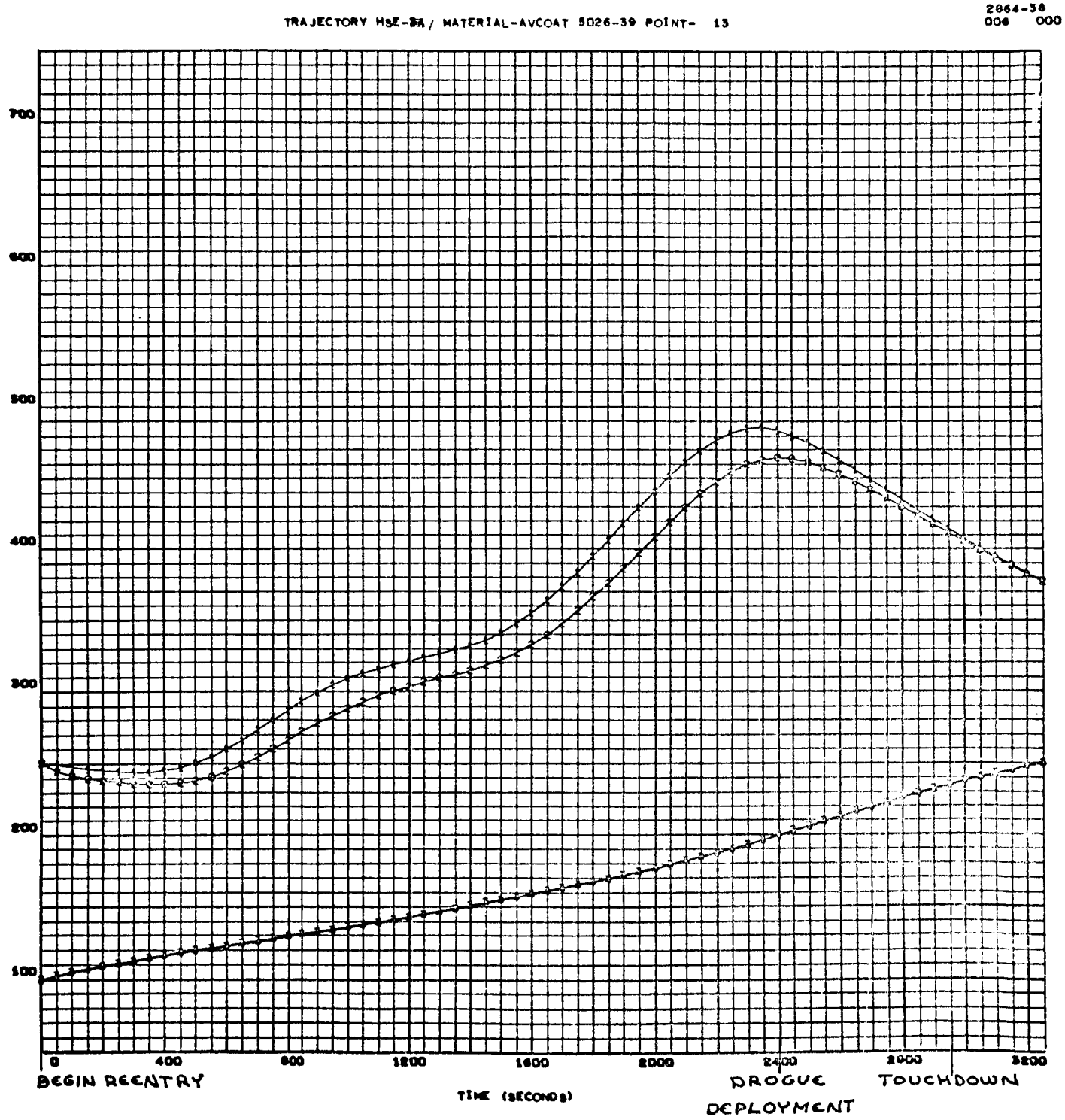

Figure 2-8. Temperature Versus Time
(Sheet 12)

[redacted]

[redacted]

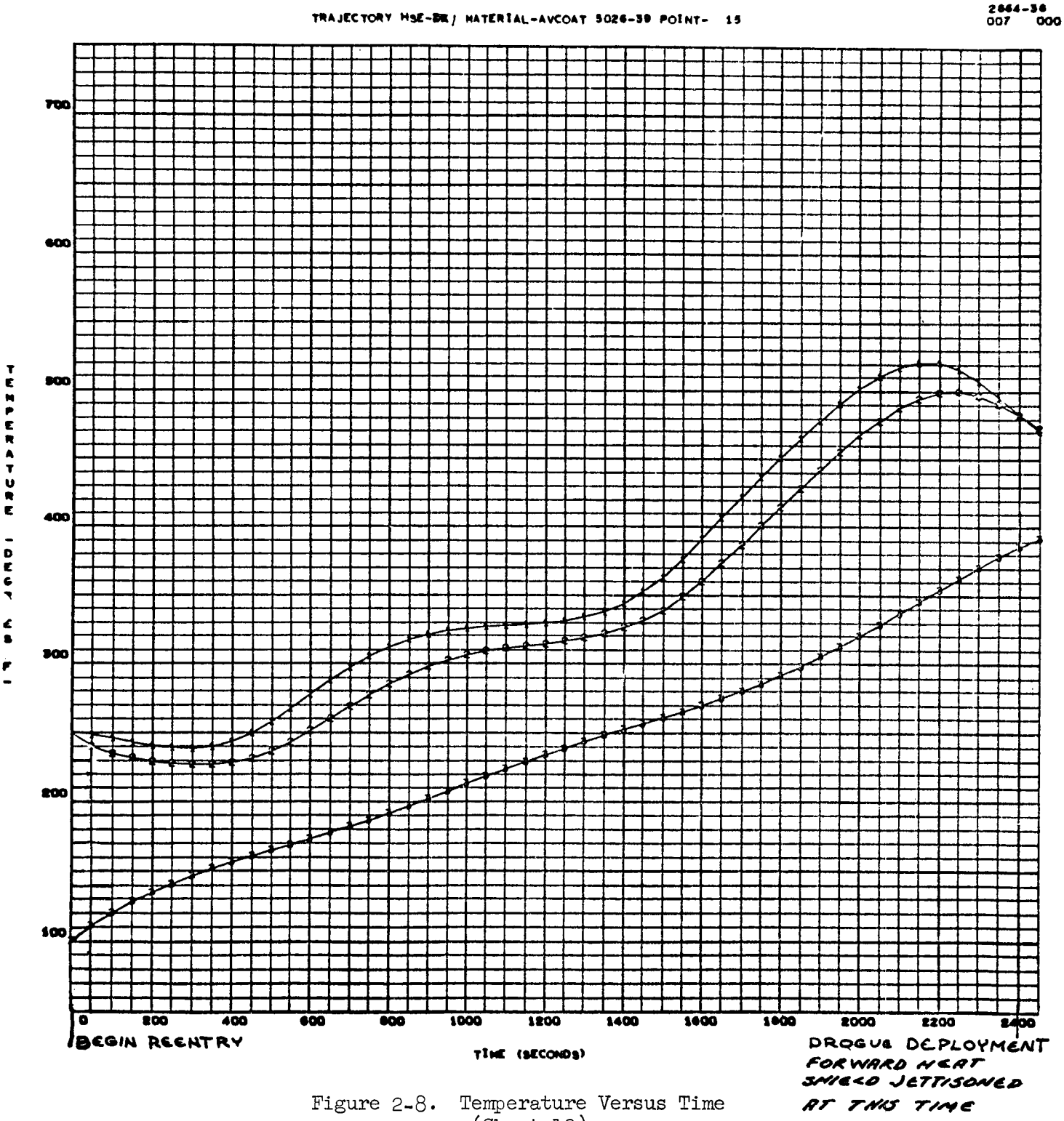

Figure 2-8. Temperature Versus Time
(Sheet 13)

[redacted]

~~CONFIDENTIAL~~

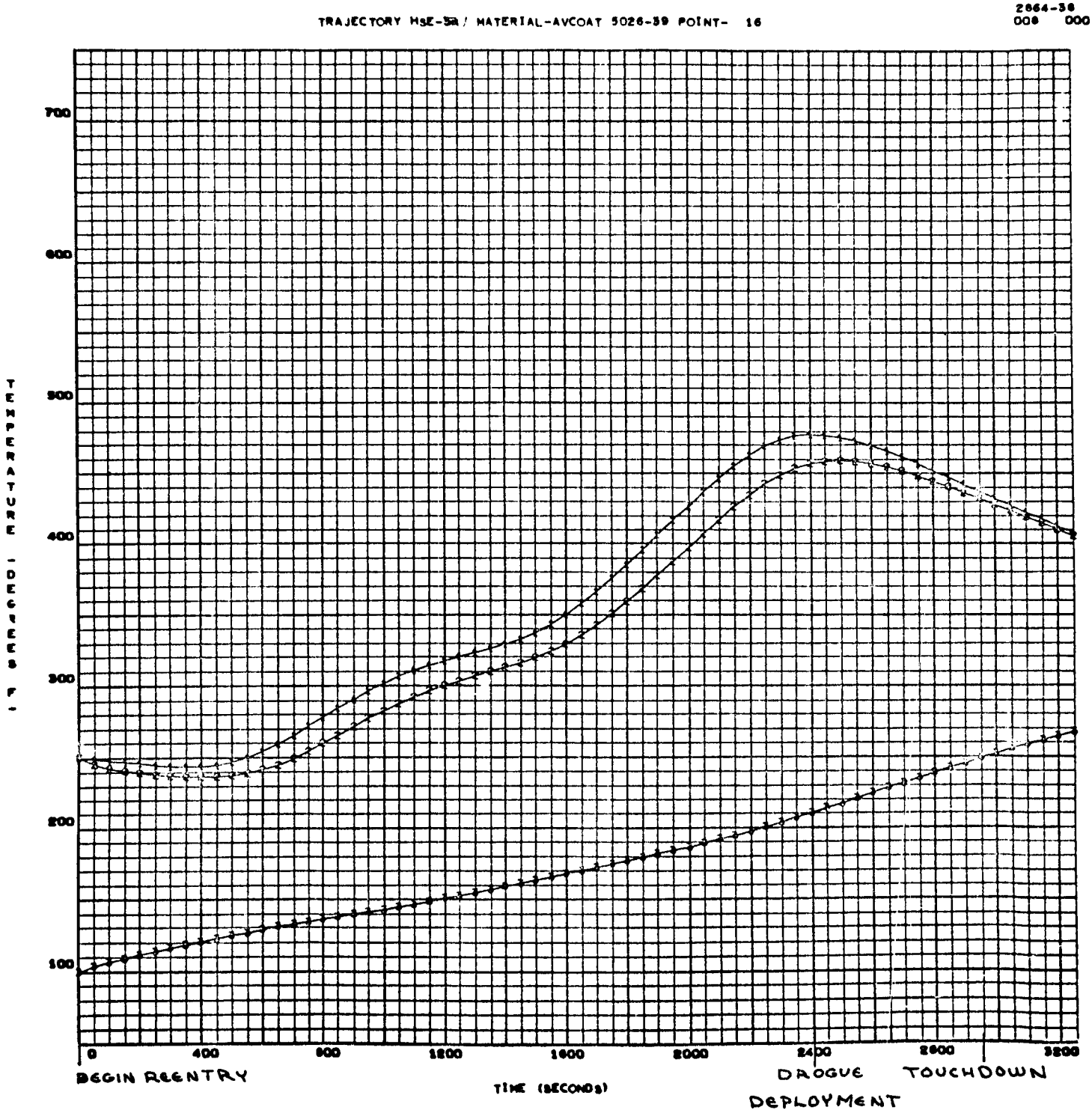

Figure 2-8. Temperature Versus Time
(Sheet 14)

[redacted]

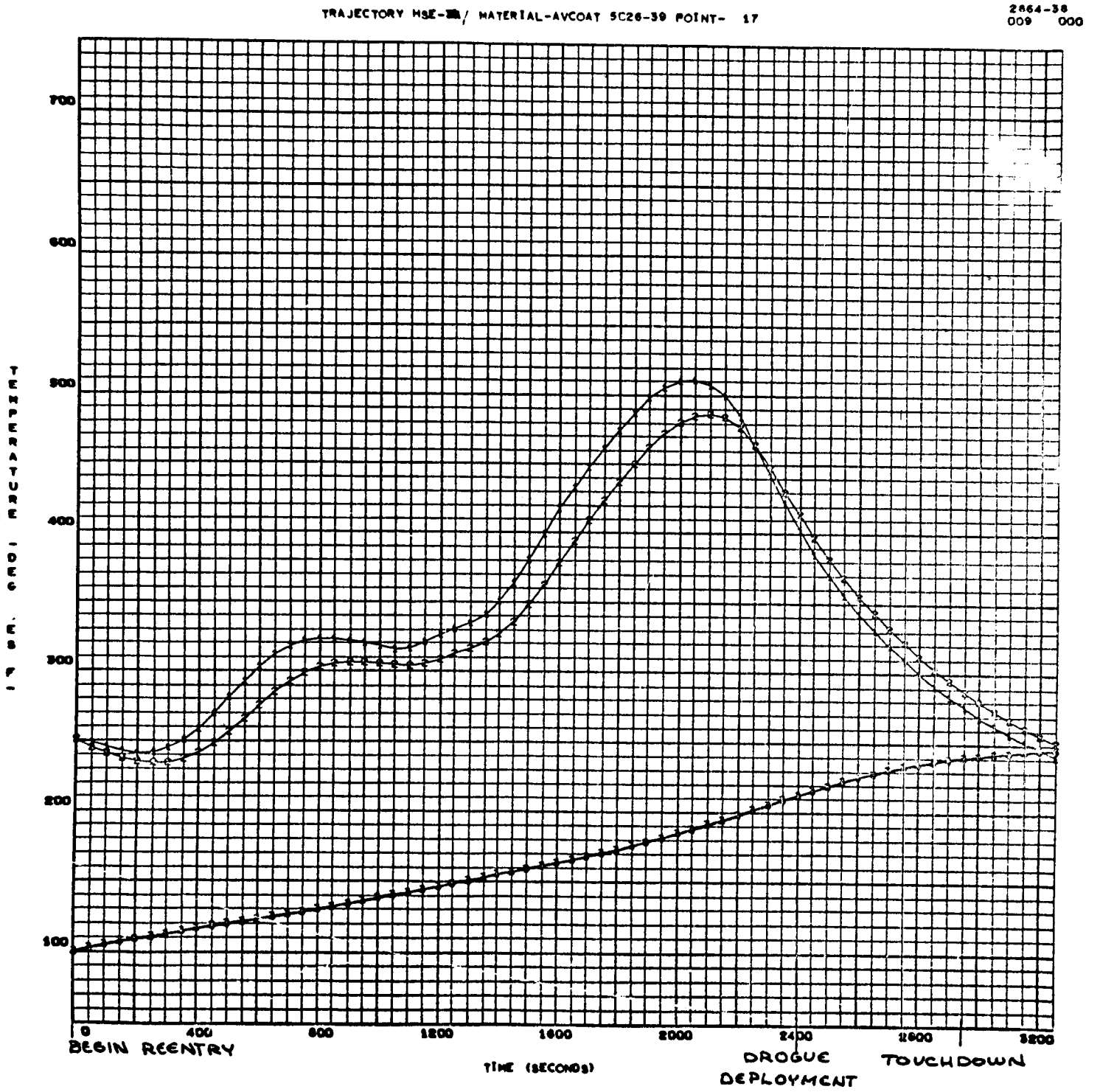

Figure 2-8. Temperature Versus Time
(Sheet 15)

[redacted]

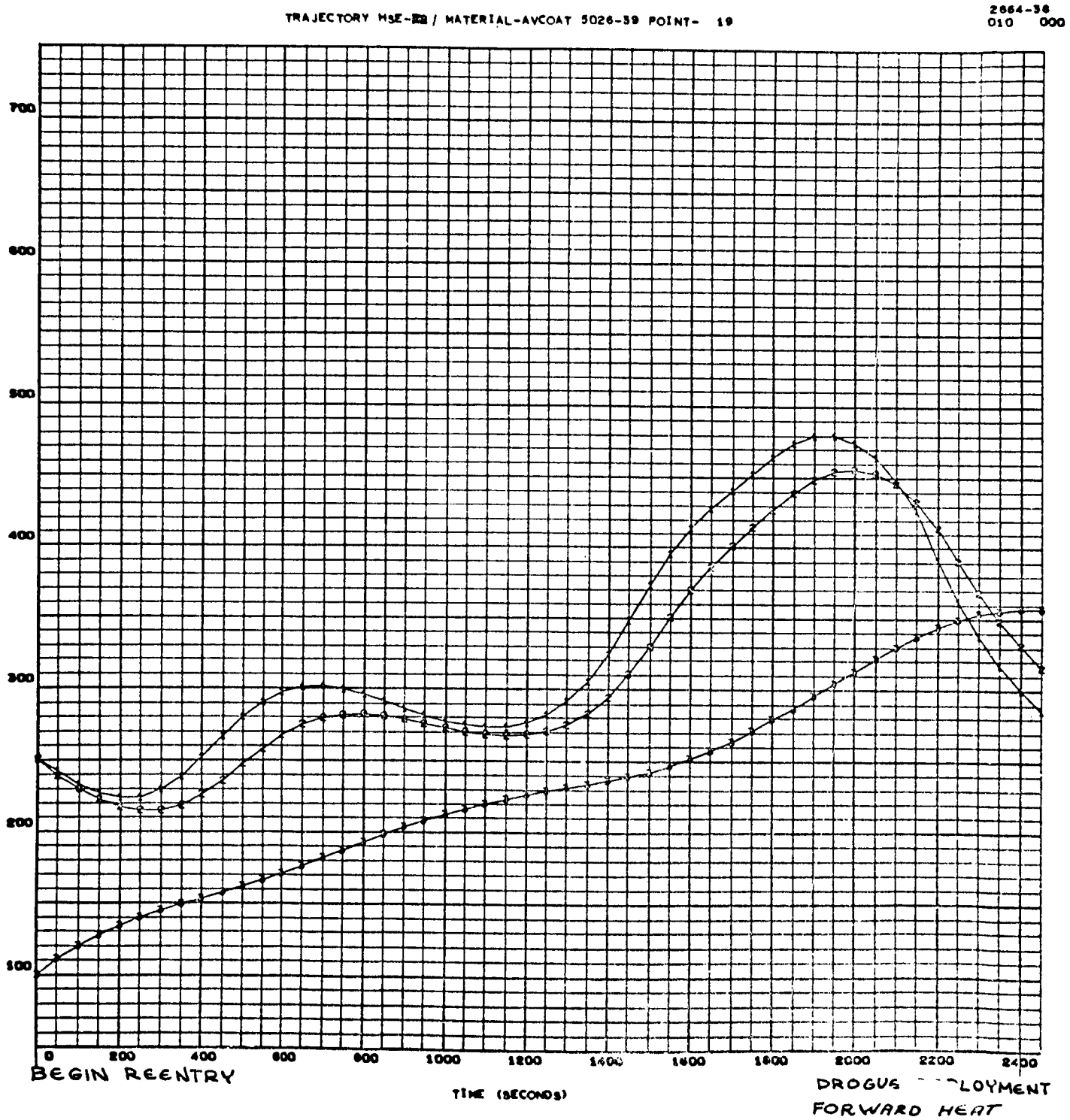

Figure 2-8. Temperature Versus Time
(Sheet 16)

[redacted]

[redacted]

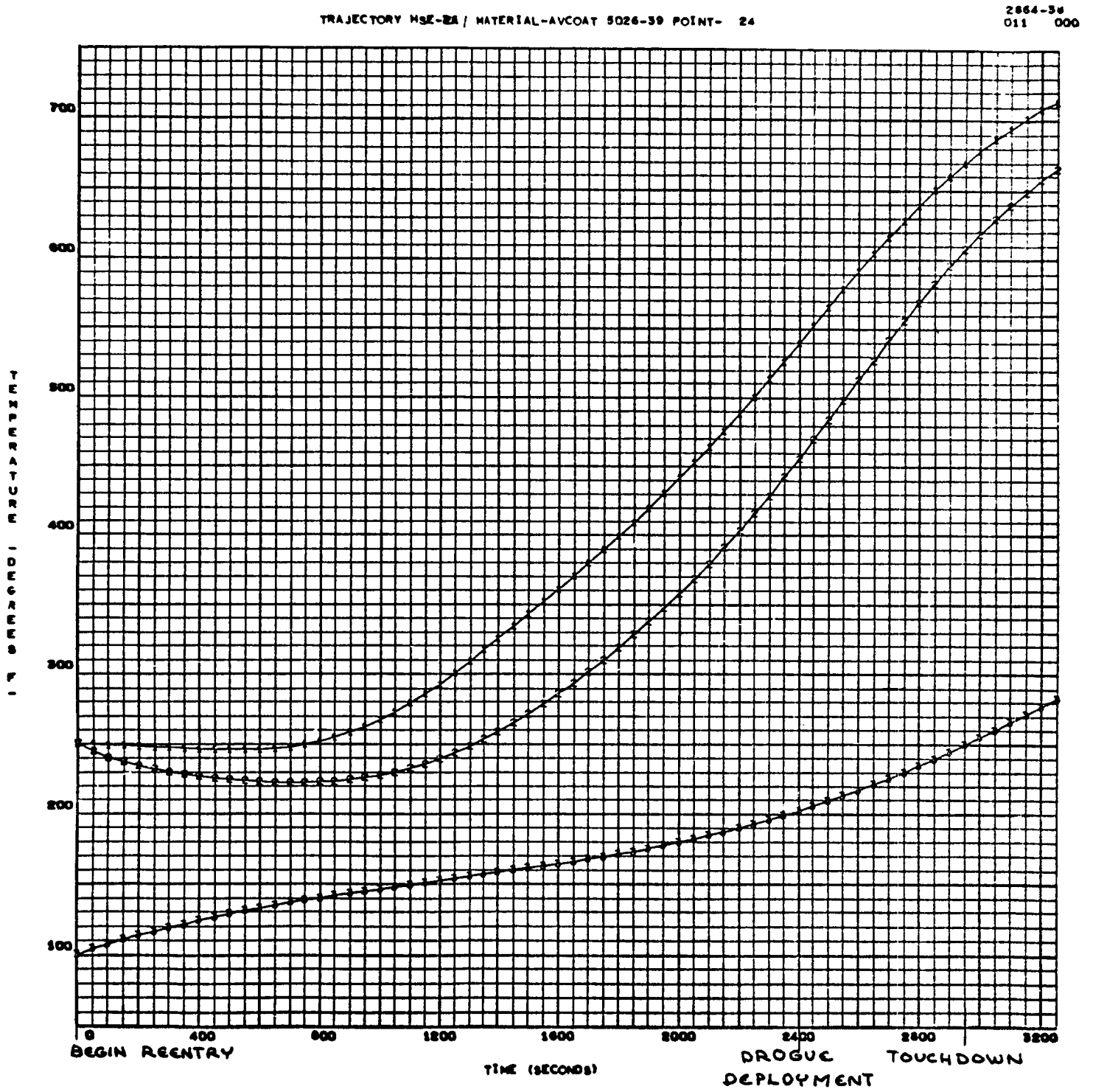

Figure 2-8. Temperature Versus Time
(Sheet 17)

[redacted]

[redacted]

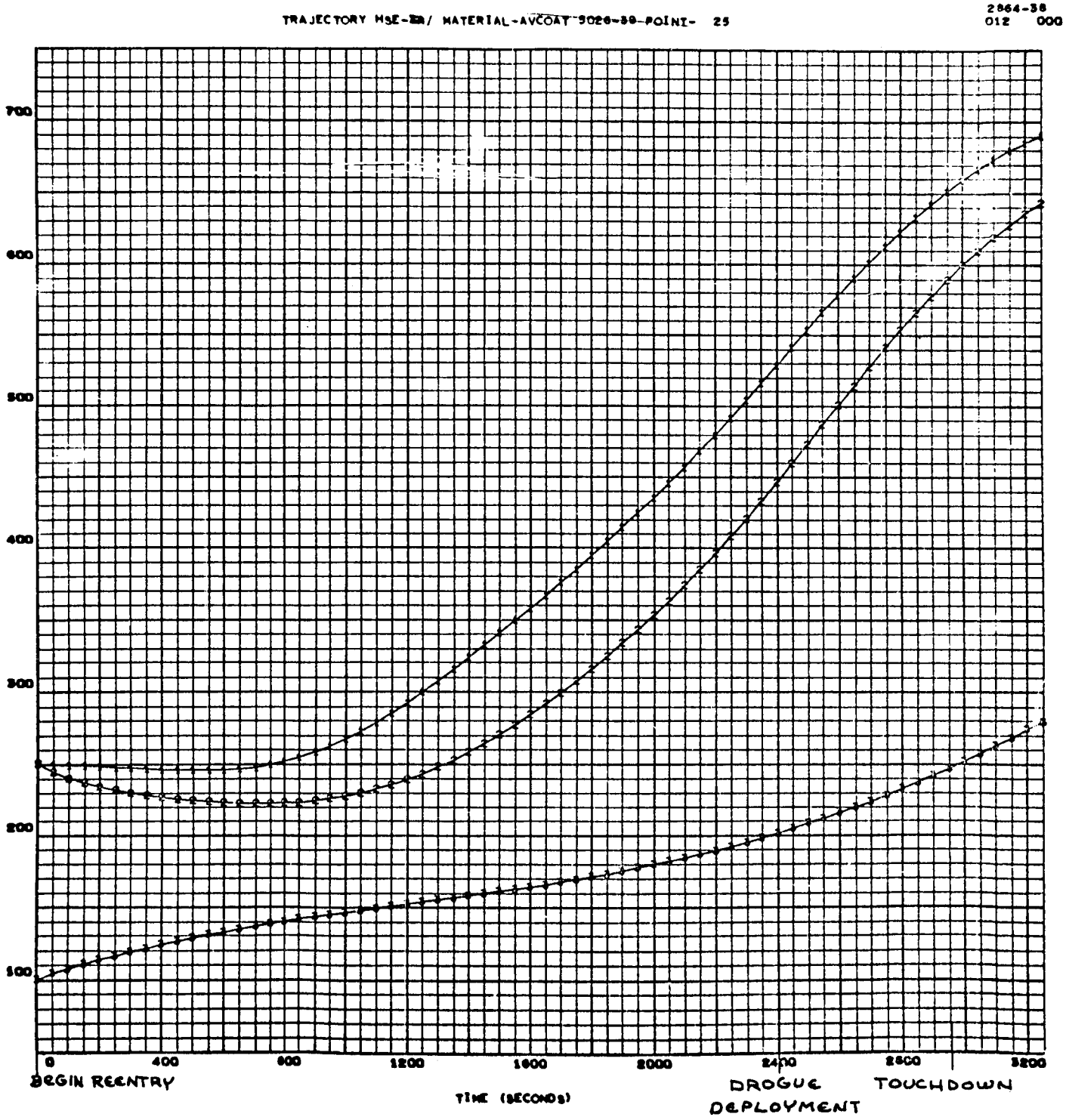

Figure 2-8. Temperature Versus Time
(Sheet 18)

[redacted]

[redacted]

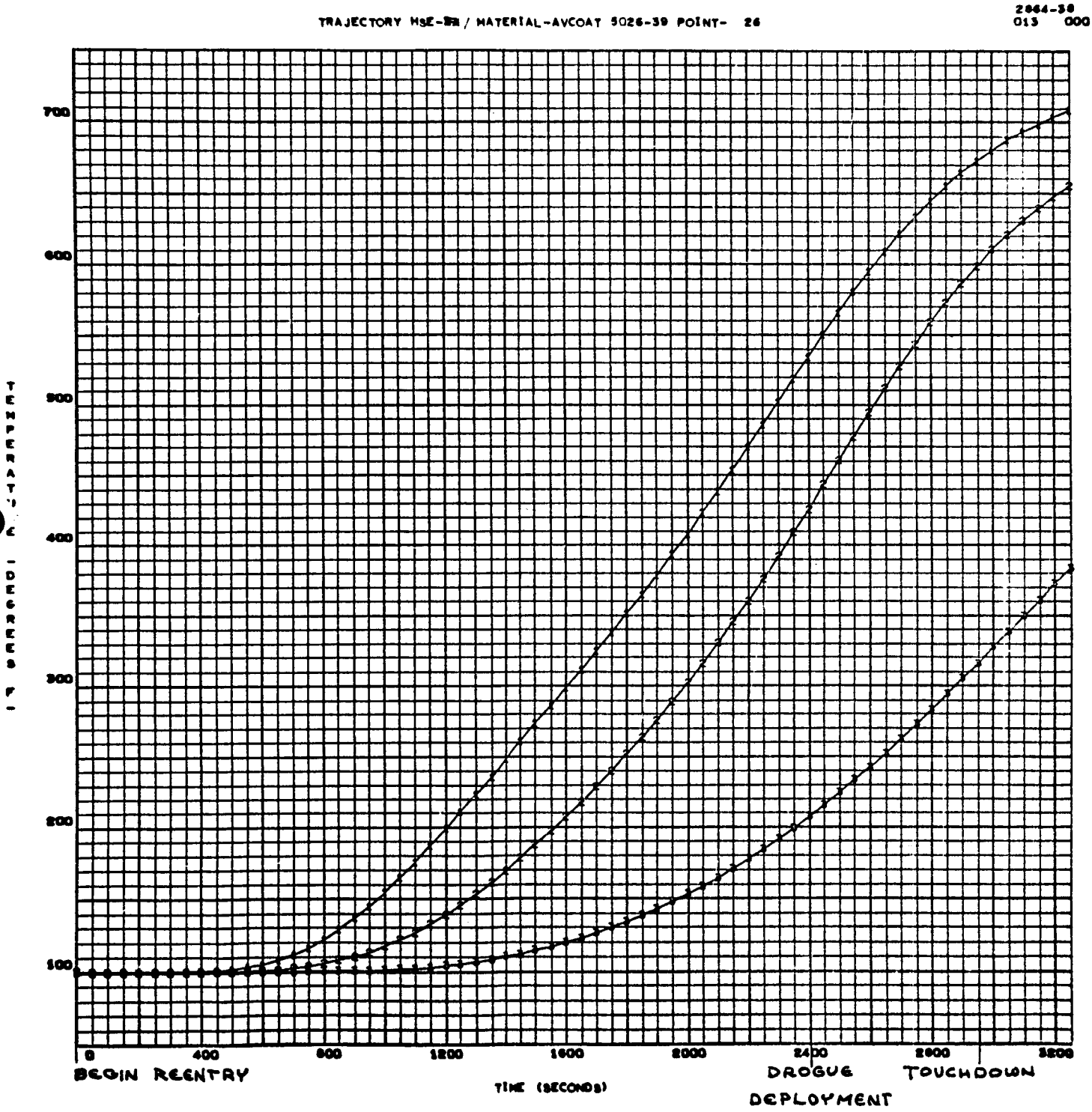

Figure 2-8 Temperature Versus Time
(Sheet 19)

[redacted]

~~CONFIDENTIAL~~

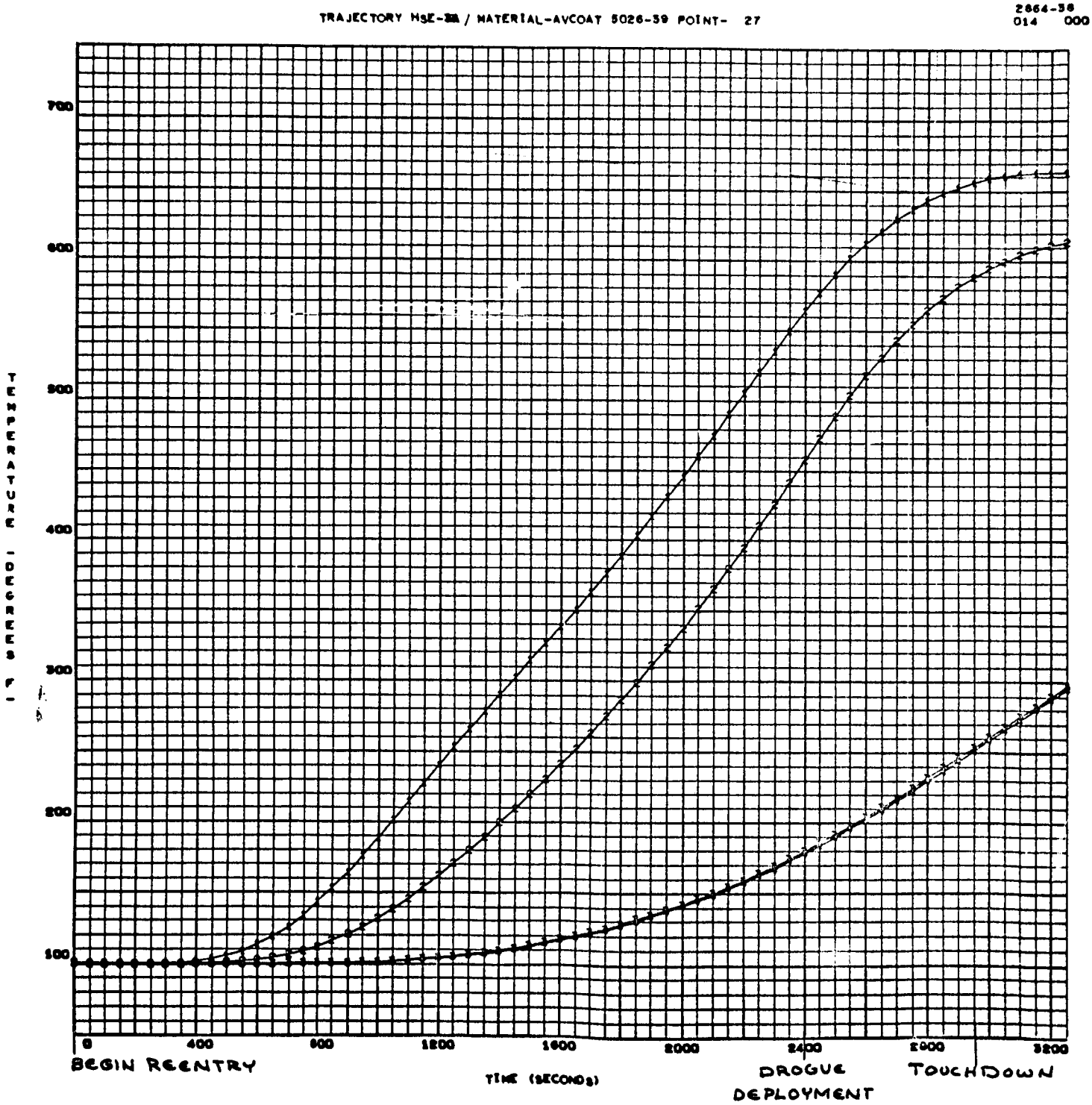

Figure 2-8. Temperature Versus Time
(Sheet 20)

[redacted]

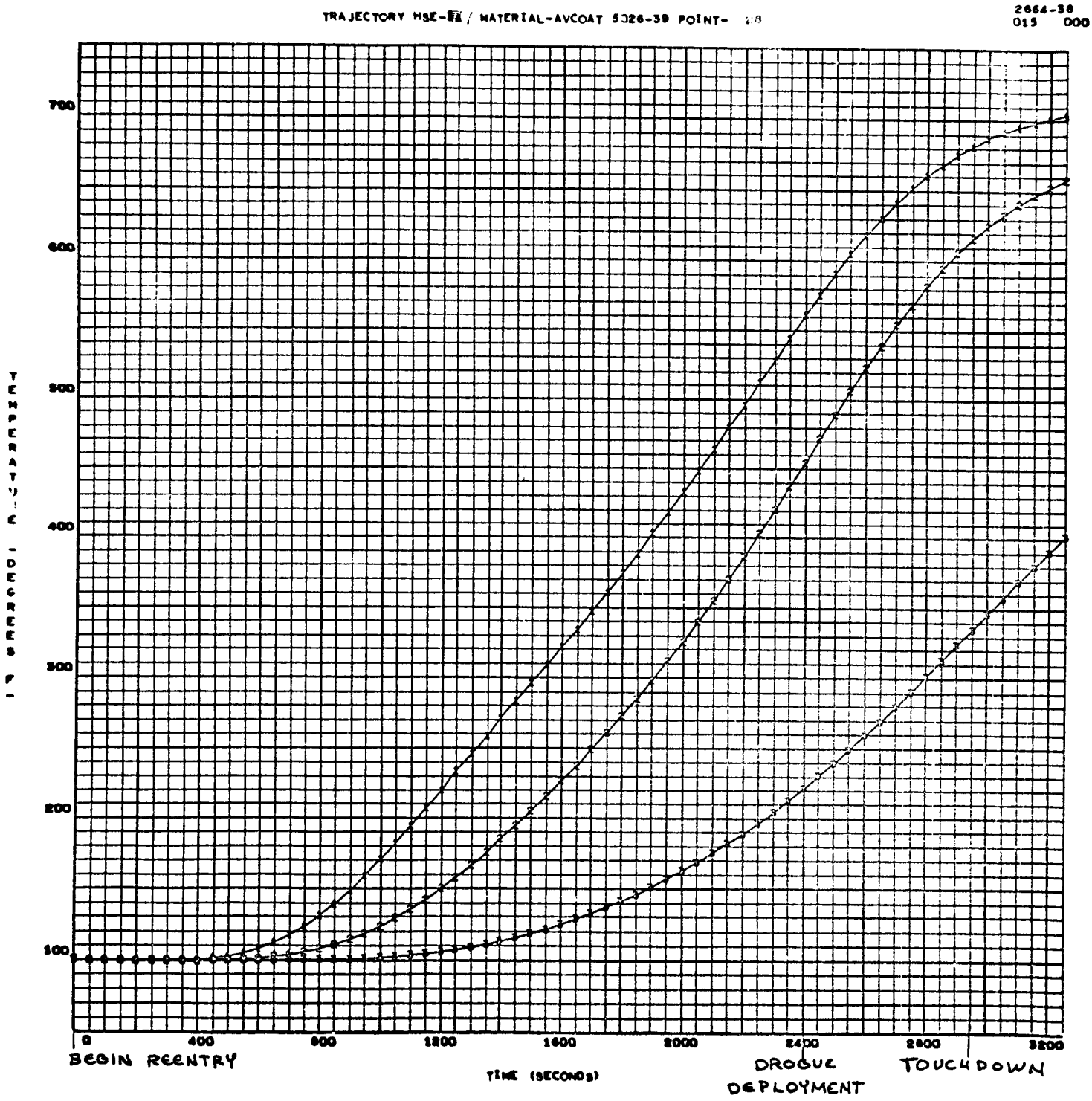

Figure 2-8. Temperature Versus Time
(Sheet 21)

[redacted]

[redacted]

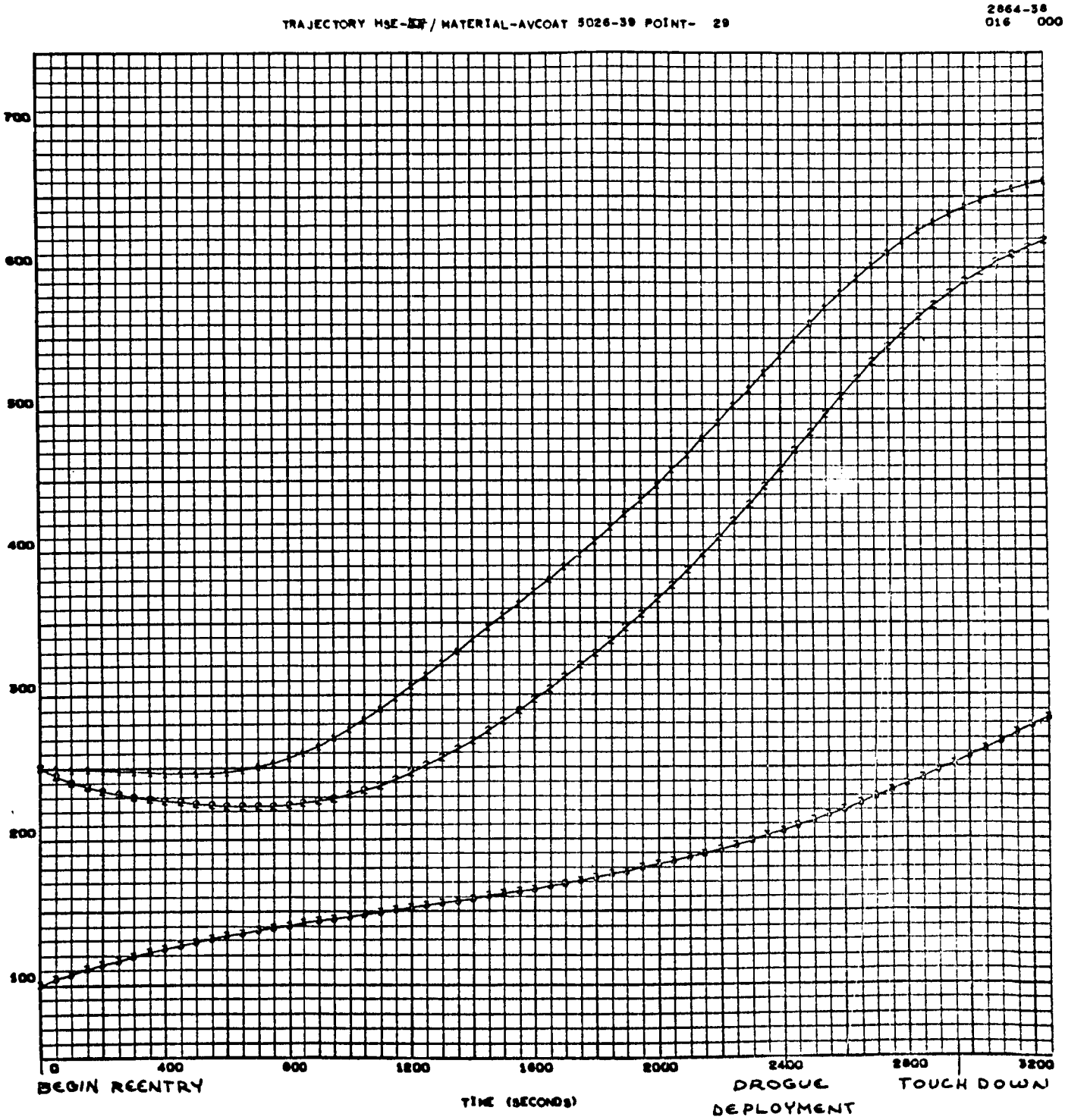

Figure 2-8. Temperature Versus Time
(Sheet 22)

[redacted]

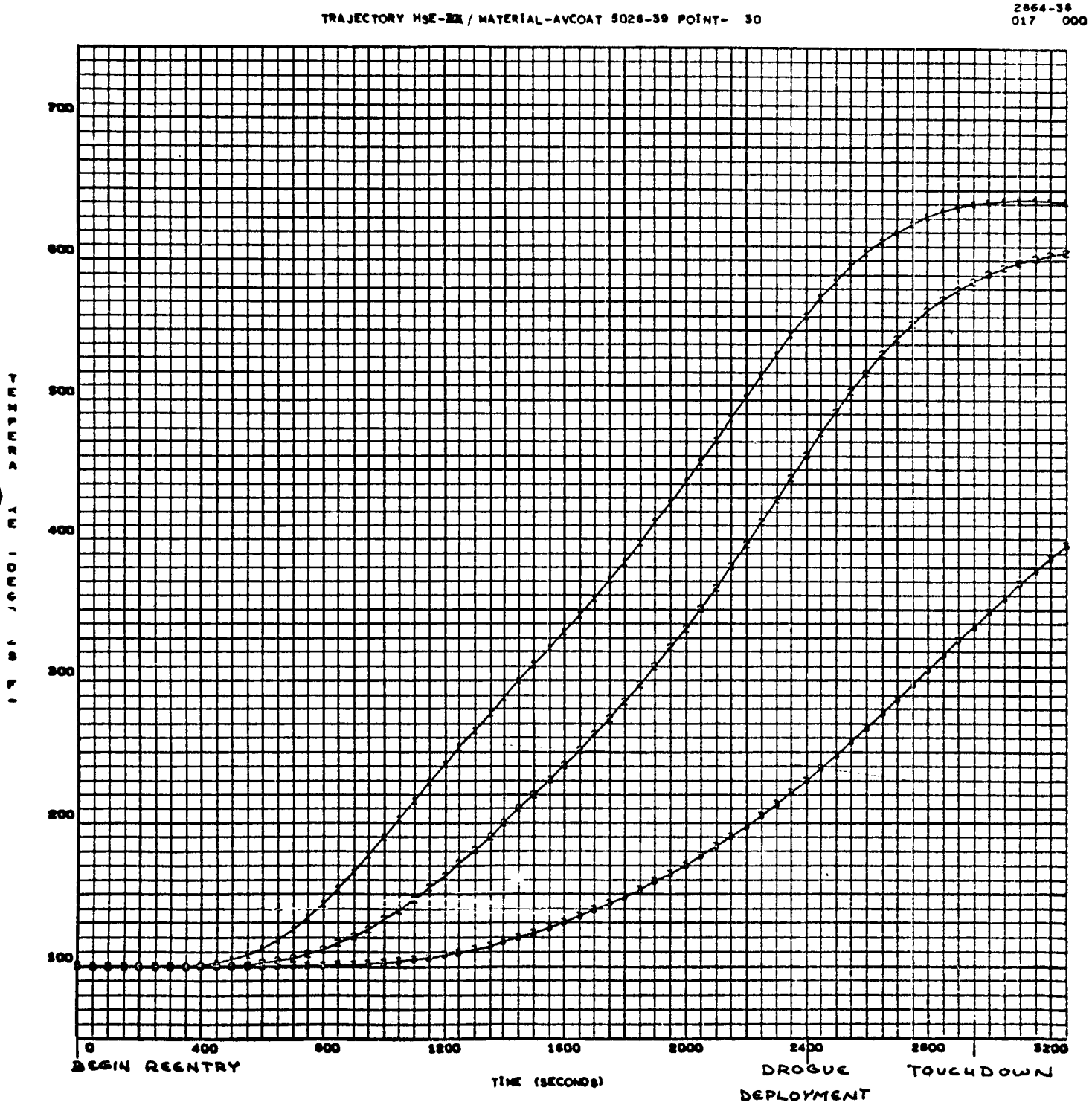

Figure 2-8. Temperature Versus Time
(Sheet 23)

[redacted]

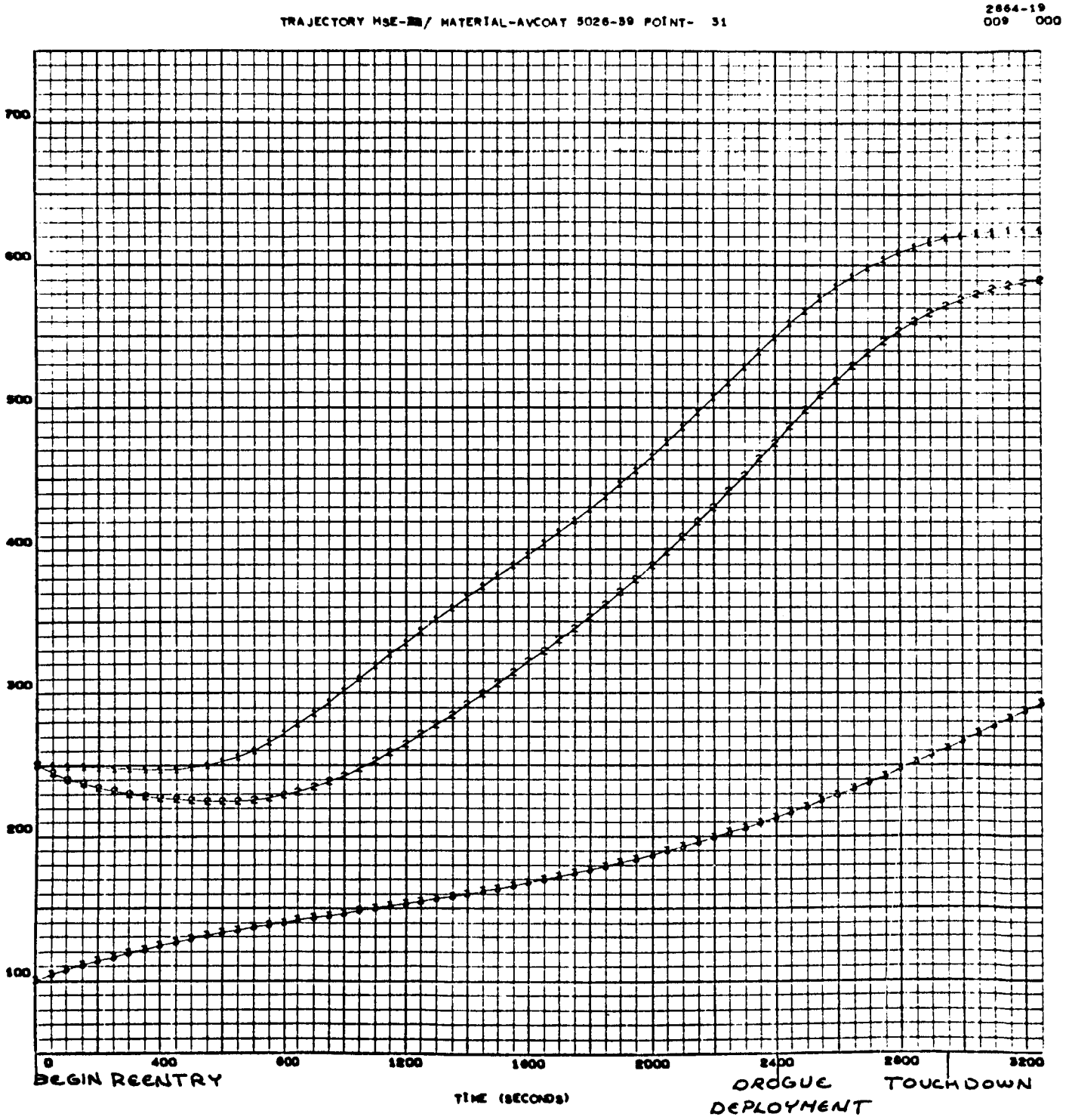

Figure 2-8. Temperature Versus Time
(Sheet 24)

~~CONFIDENTIAL~~

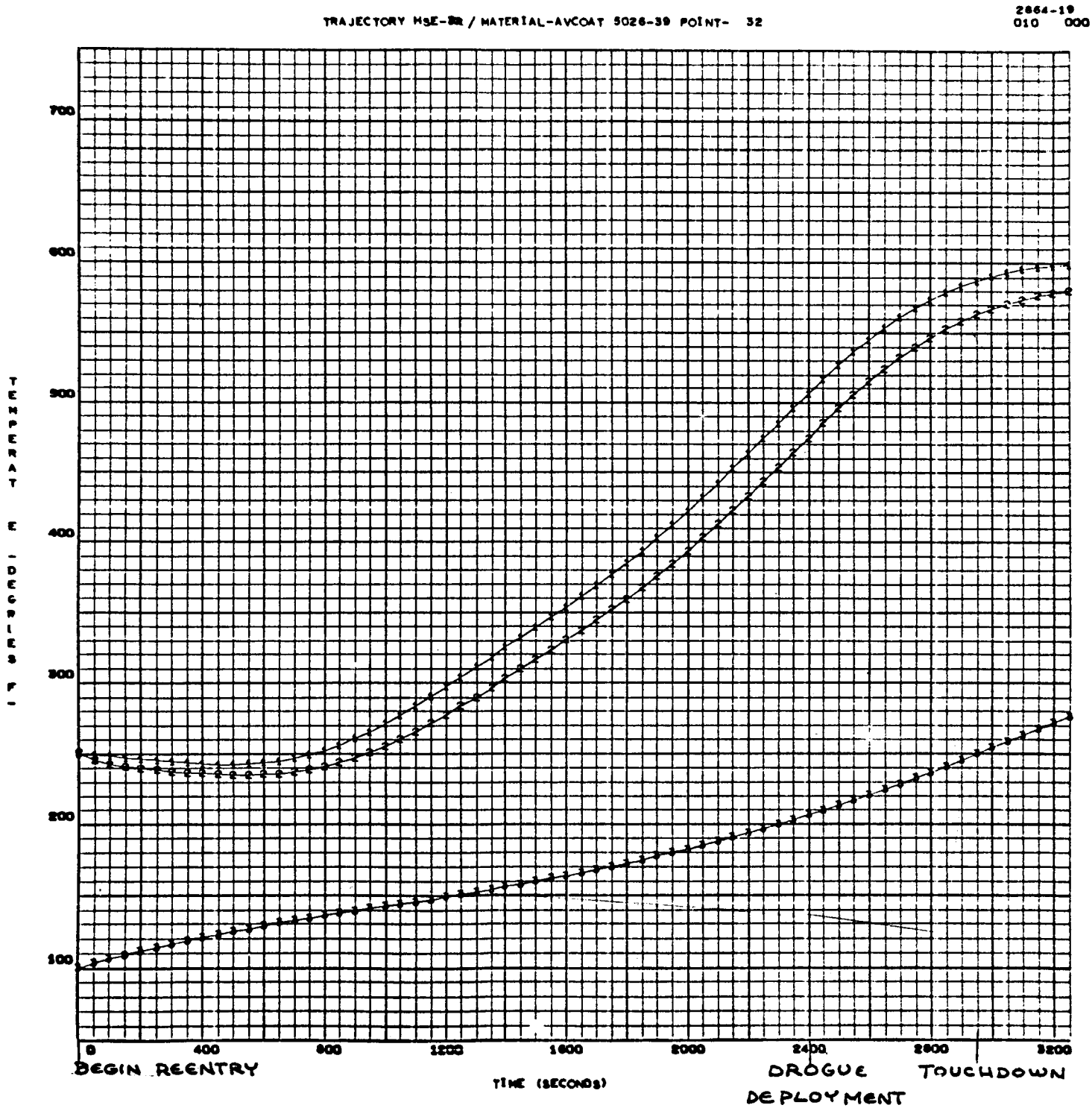

Figure 2-8. Temperature Versus Time
(Sheet 25)

[redacted]

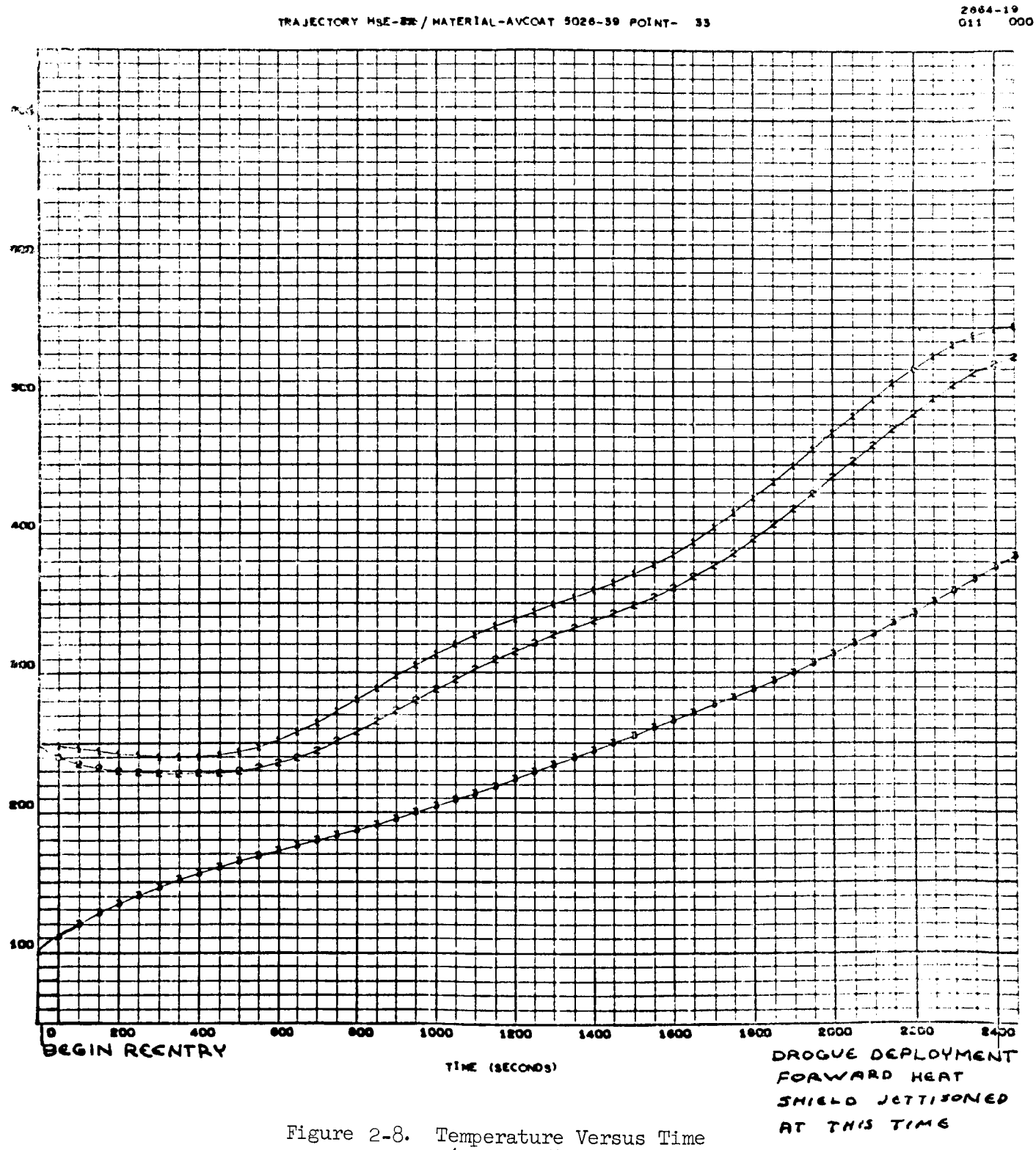

Figure 2-8. Temperature Versus Time
(Sheet 26)

[redacted]

[redacted]

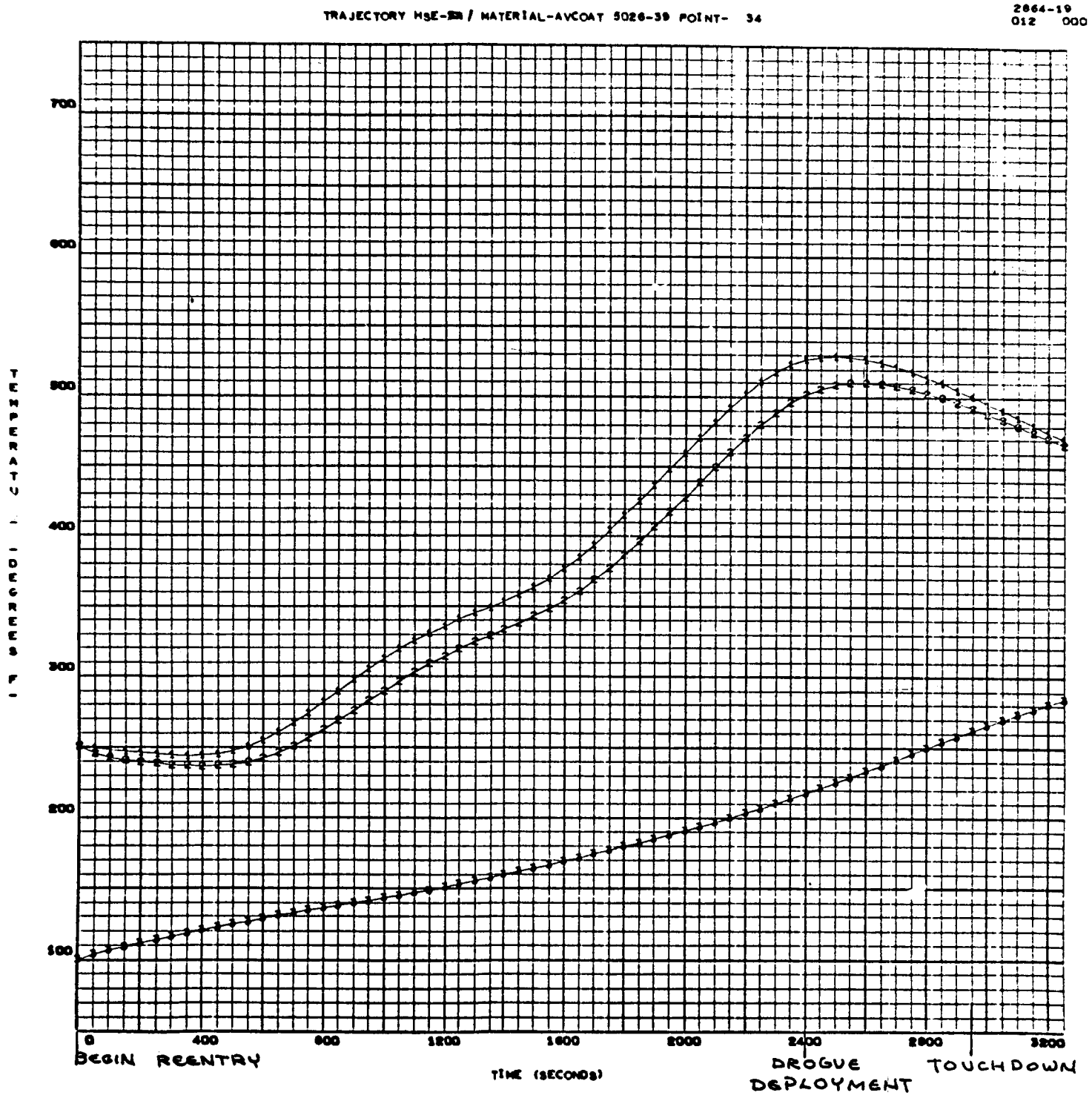

Figure 2-8. Temperature Versus Time
(Sheet 27)

[redacted]

~~CONFIDENTIAL~~

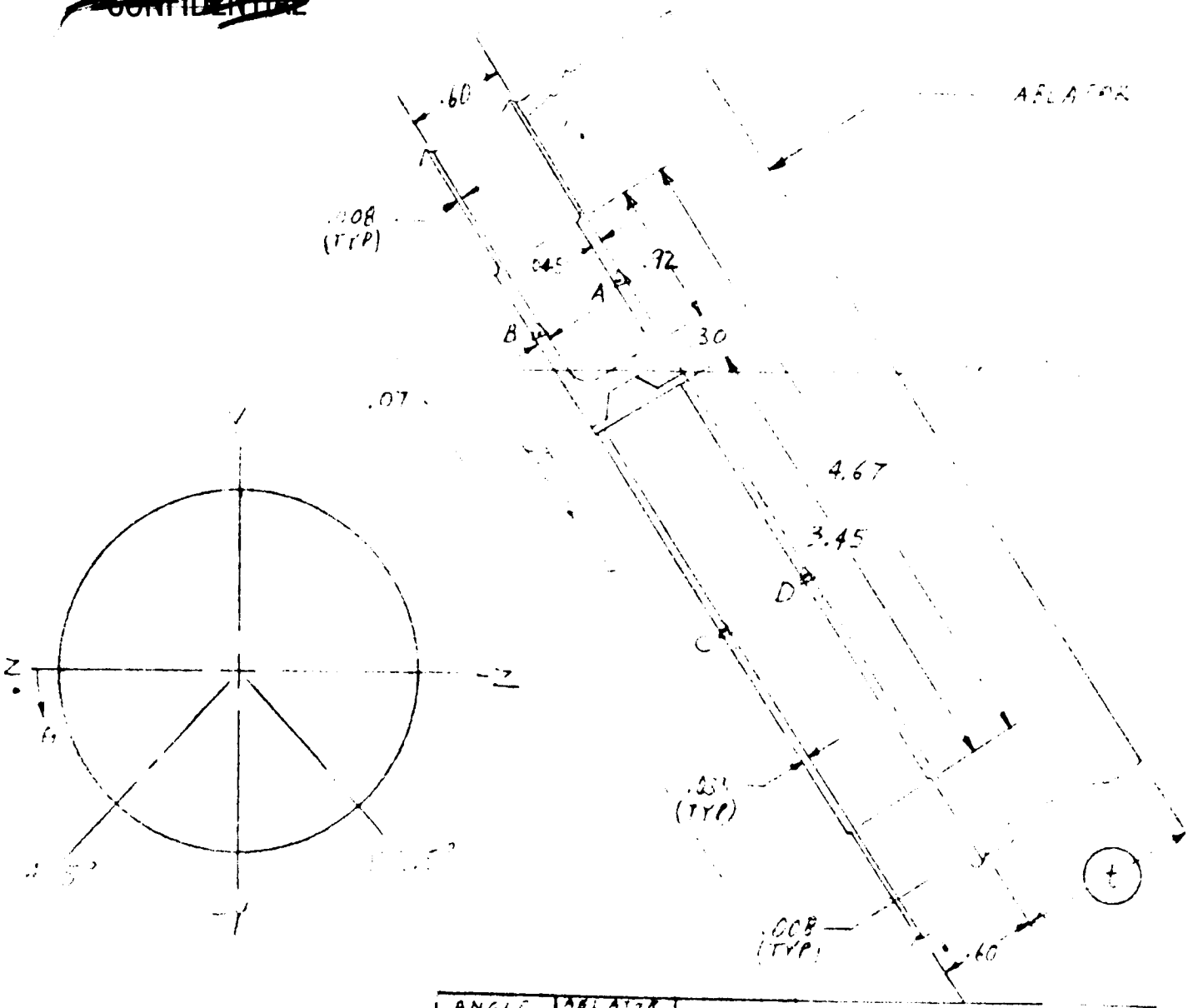

ANGLE θ	ABLATOR THICKNESS (t)	[illegible]			
		T_A	T_B	T_C	T_D
0°	1.16"	429	406	425	468
90°	.59"	428	417	449	469
180	.26	412	403	430	450

Figure 2-9 Forward Heat Shield Skin Panel
(Sheet 1 of 3)

~~CONFIDENTIAL~~

[redacted]

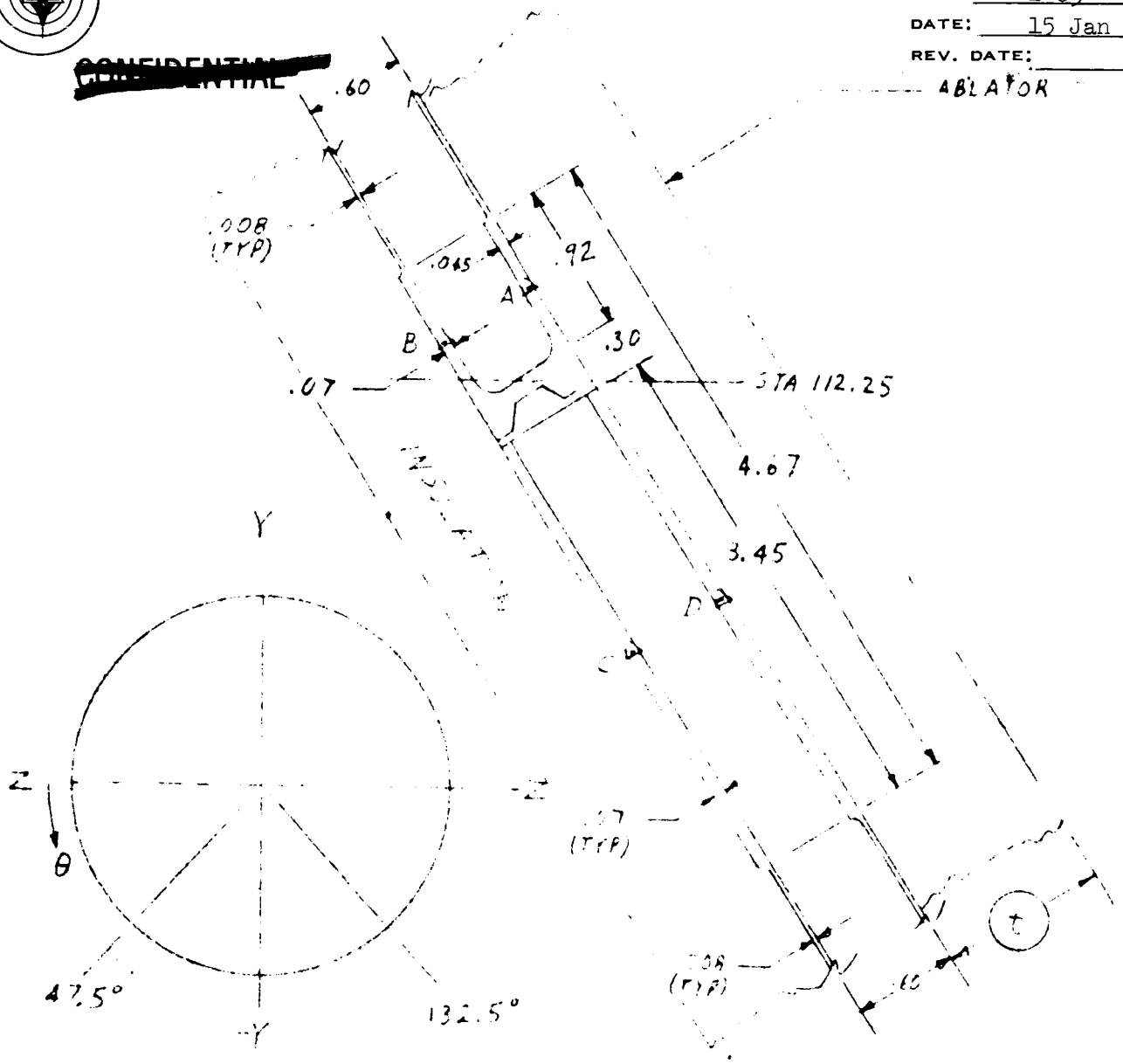

ANGLE θ	ABLATOR THICKNESS t	TEMPERATURE °F			
		T_A	T_B	T_C	T_D
47.5°	.97"	400	380	366	410
132.5°	.31"	461	447	449	474

Figure 2-9 Forward Heat Shield Skin Panel
(Sheet 2 of 3)

[redacted]

~~CONFIDENTIAL~~

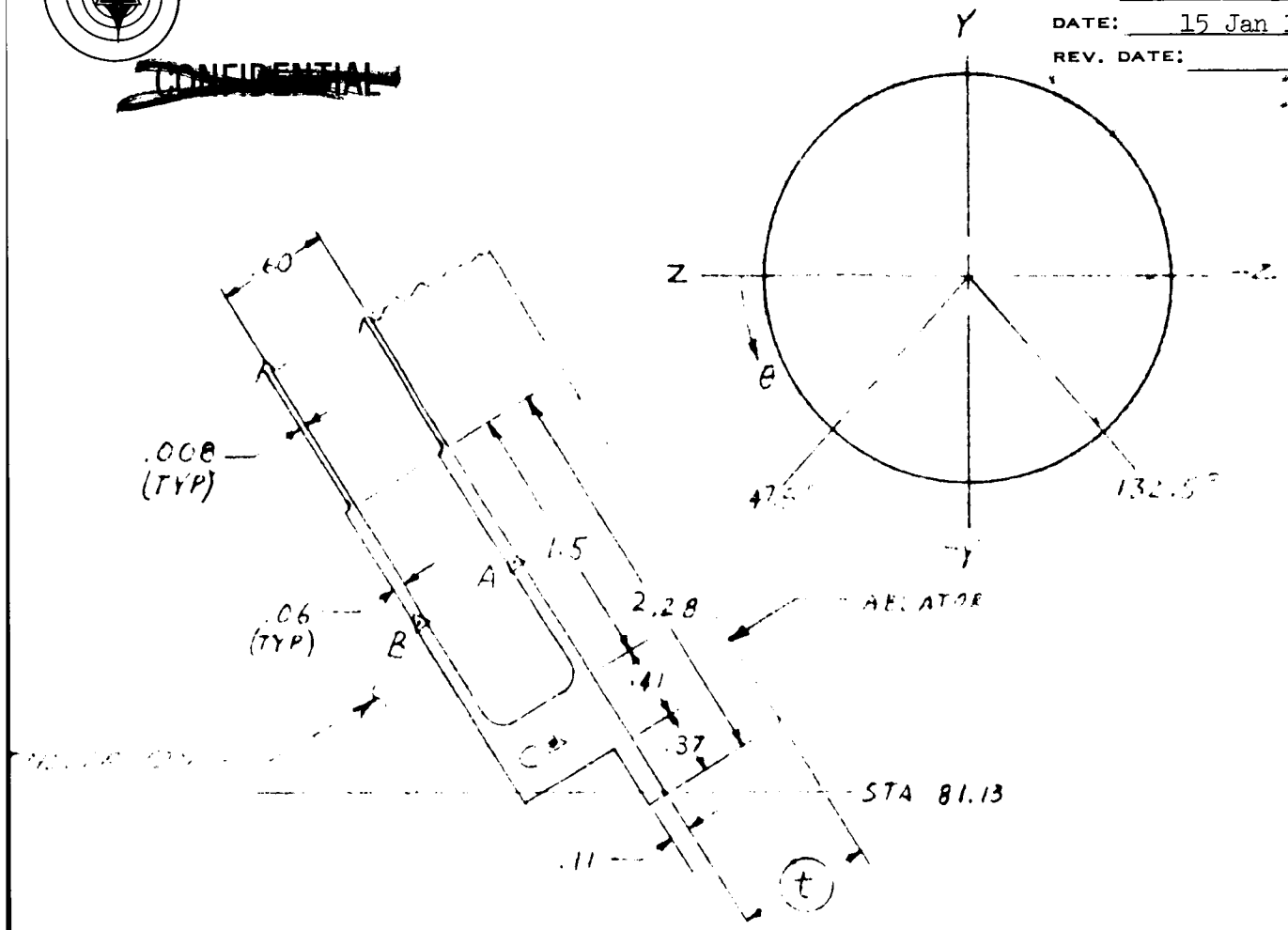

ANGLE θ	ABLATOR THICKNESS (t)	TEMPERATURE - °F T_A	T_B	T_C
0°	1.31"	420	395	398
47.5°	1.08"	332	306	307
90°	.70"	374	361	354
132.5°	.39"	403	390	385
180°	.32"	474	458	452

Figure 2-9. Forward Heat Shield Skin Panels (Sheet 3 of 3)

~~CONFIDENTIAL~~

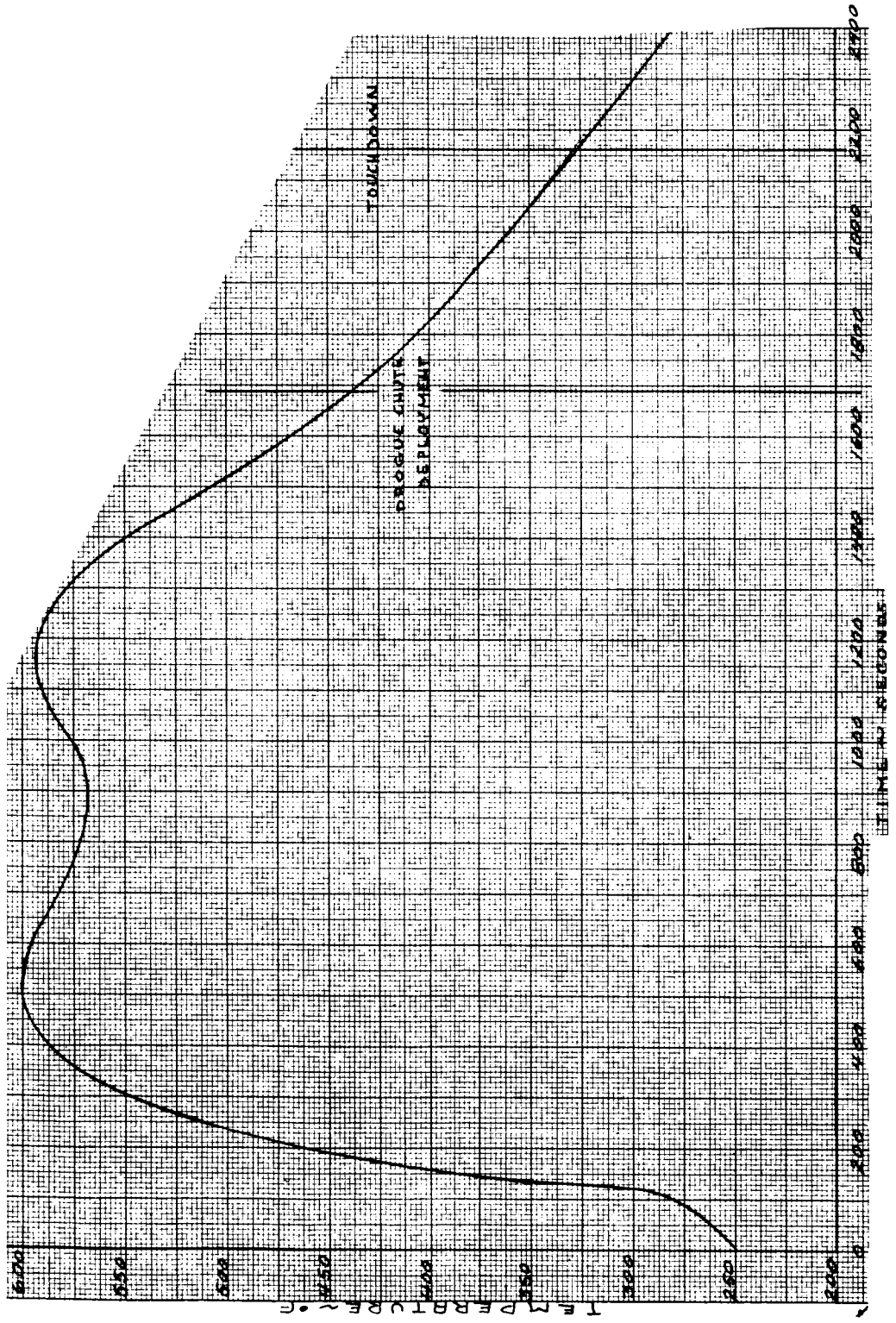

Figure 2-10. Bondline Temperature History HSE-3A
Body Point 17 Initial Temperature 250 °F

~~CONFIDENTIAL~~

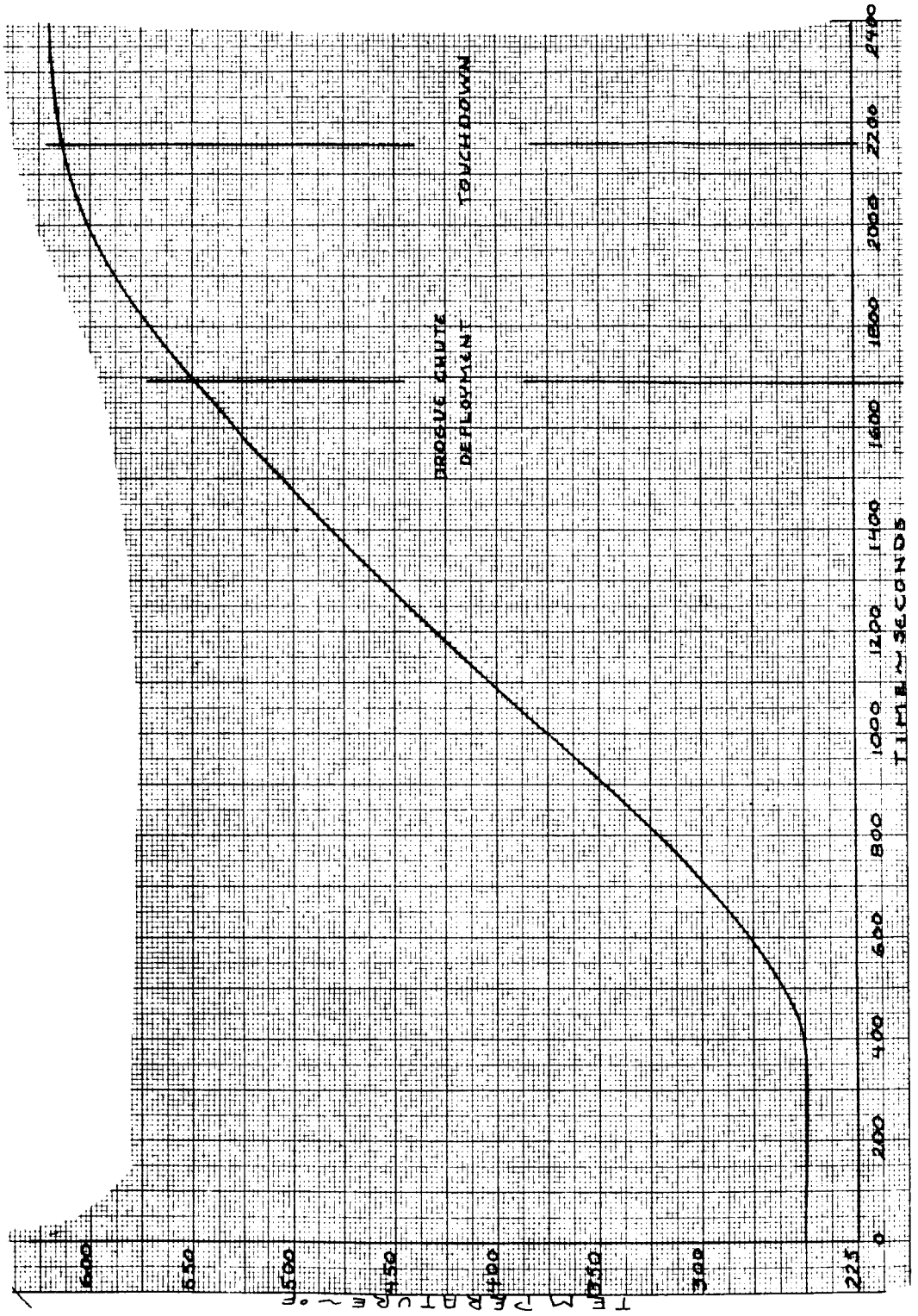

Figure 2-11. Bondline Temperature History HSE-3A
Body Point 31 Initial Temperature 250 °F

~~CONFIDENTIAL~~

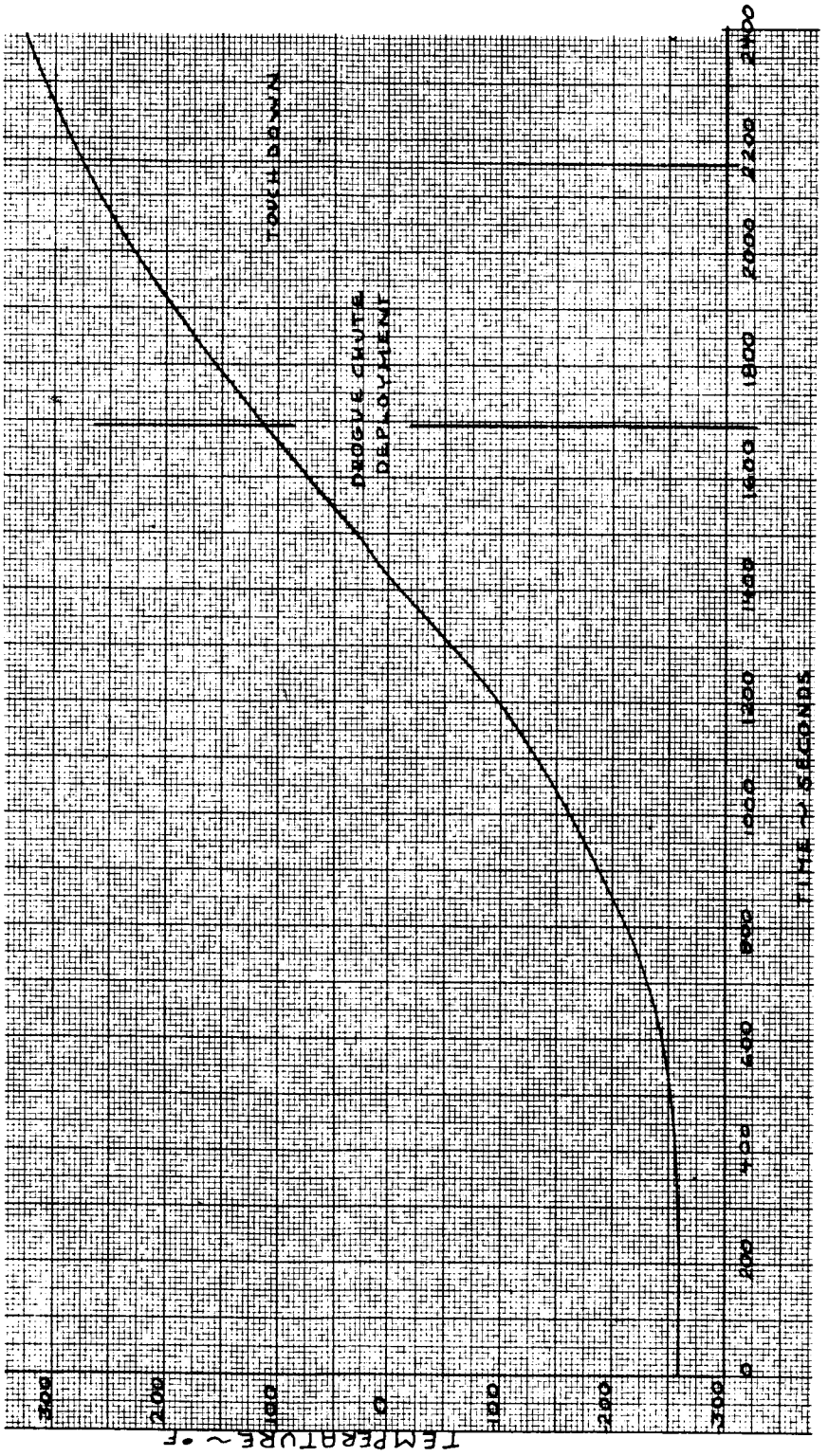

Figure 2-12. Bondline Temperature History HSE-3A
Body Point 24 Initial Temperature -260 °F

[redacted]

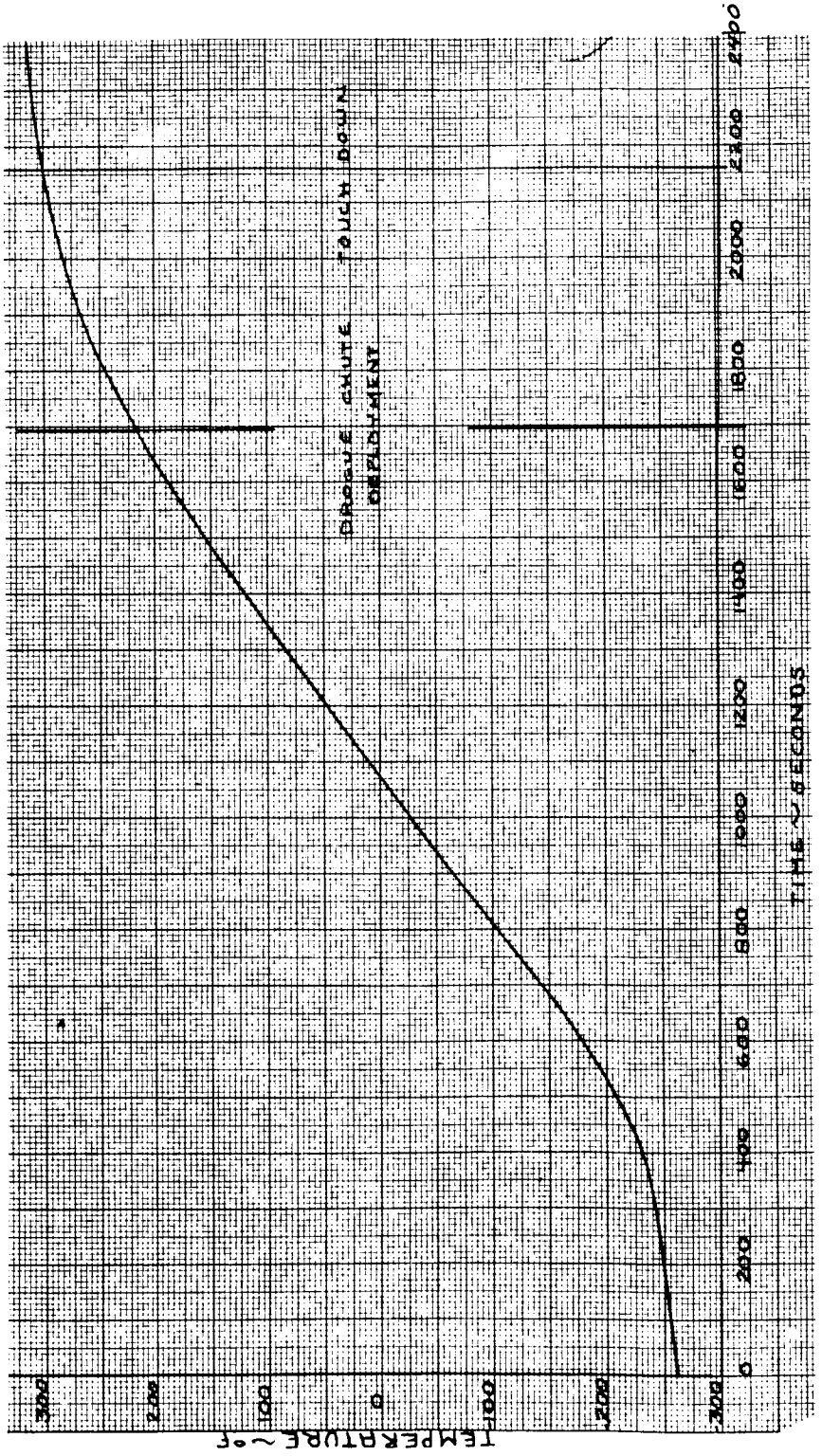

Figure 2-13. Bondline Temperature History HSE-3A
Body Point 8 Initial Temperature -260 °F

[redacted]

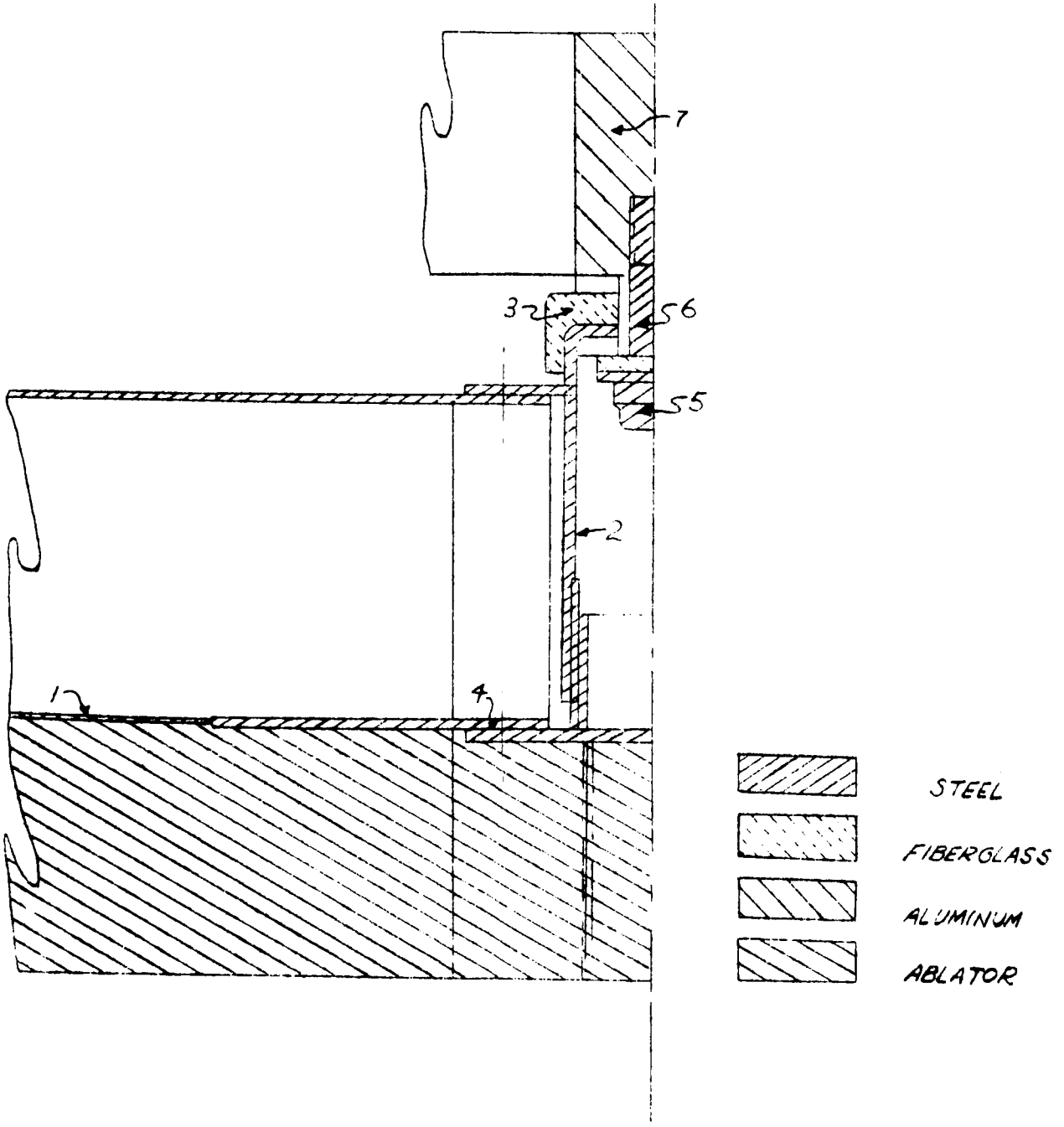

Figure 2-14. Sketch of Aft Heat Shield Tie-Down Bolt

[redacted]

[redacted]

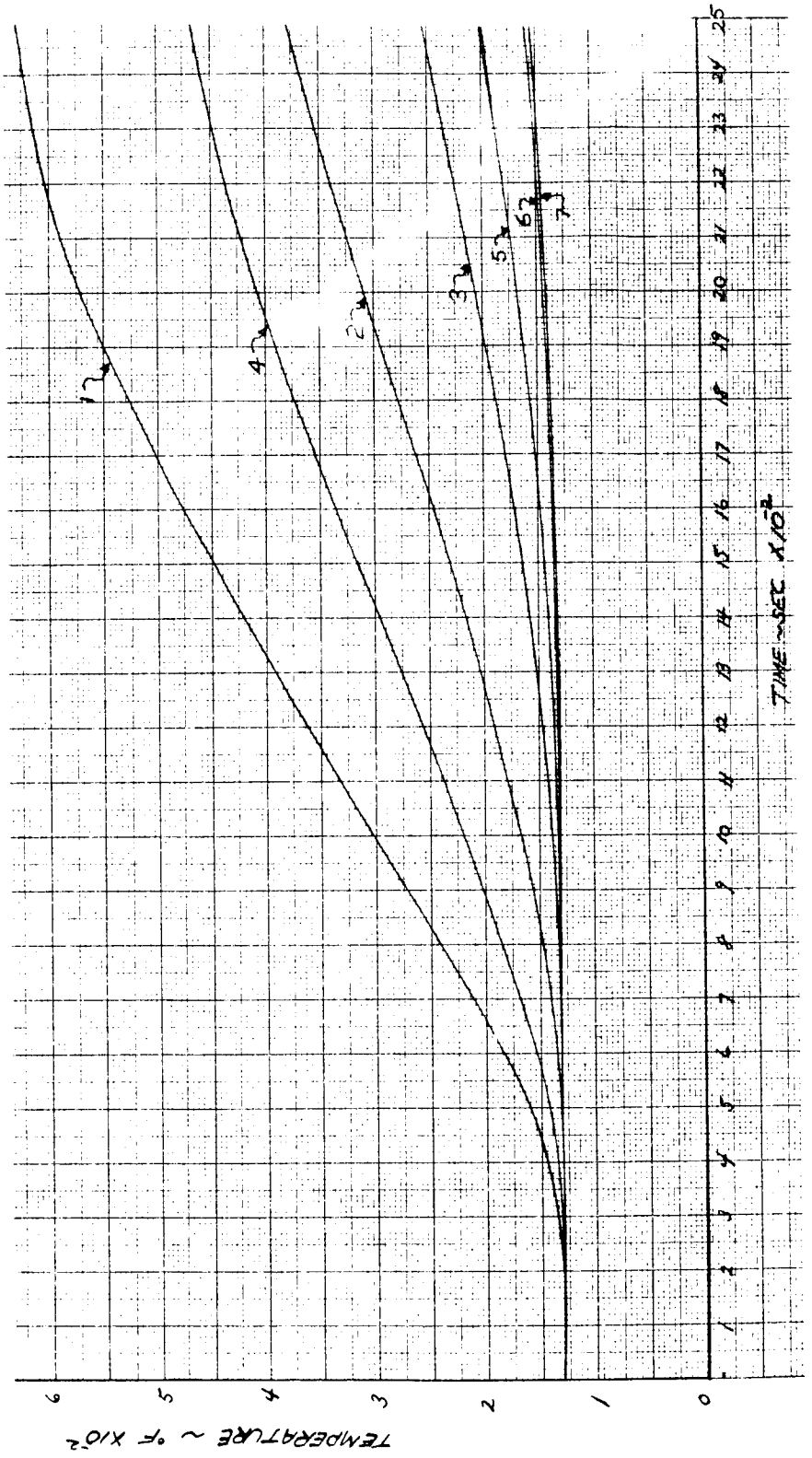

Figure 2-15. Temperature Histories of Aft Heat Shield Tie-Down Bolt and Supporting Substructure (See Figure 2-14 for Locations 1-7)

[redacted]

~~CONFIDENTIAL~~

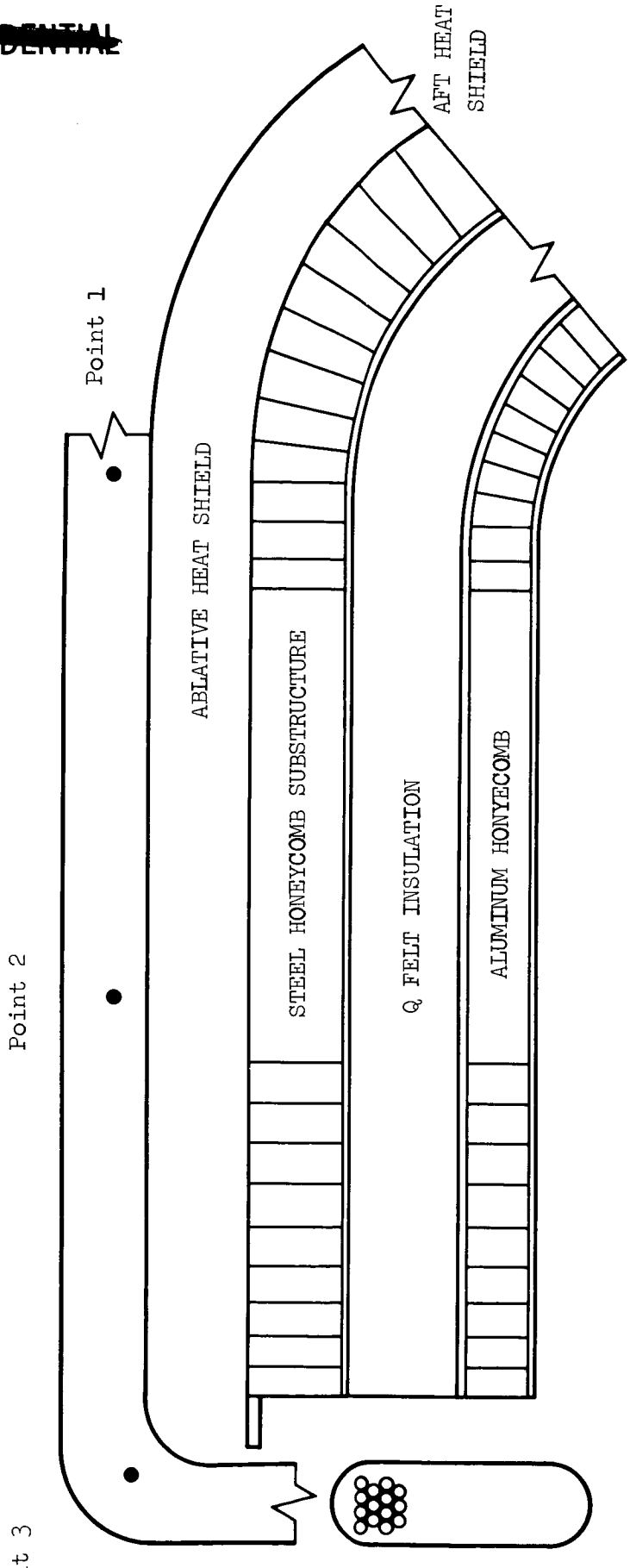

Figure 2-16. Sketch of C/M - S/M Umbilical Wire Package

~~CONFIDENTIAL~~

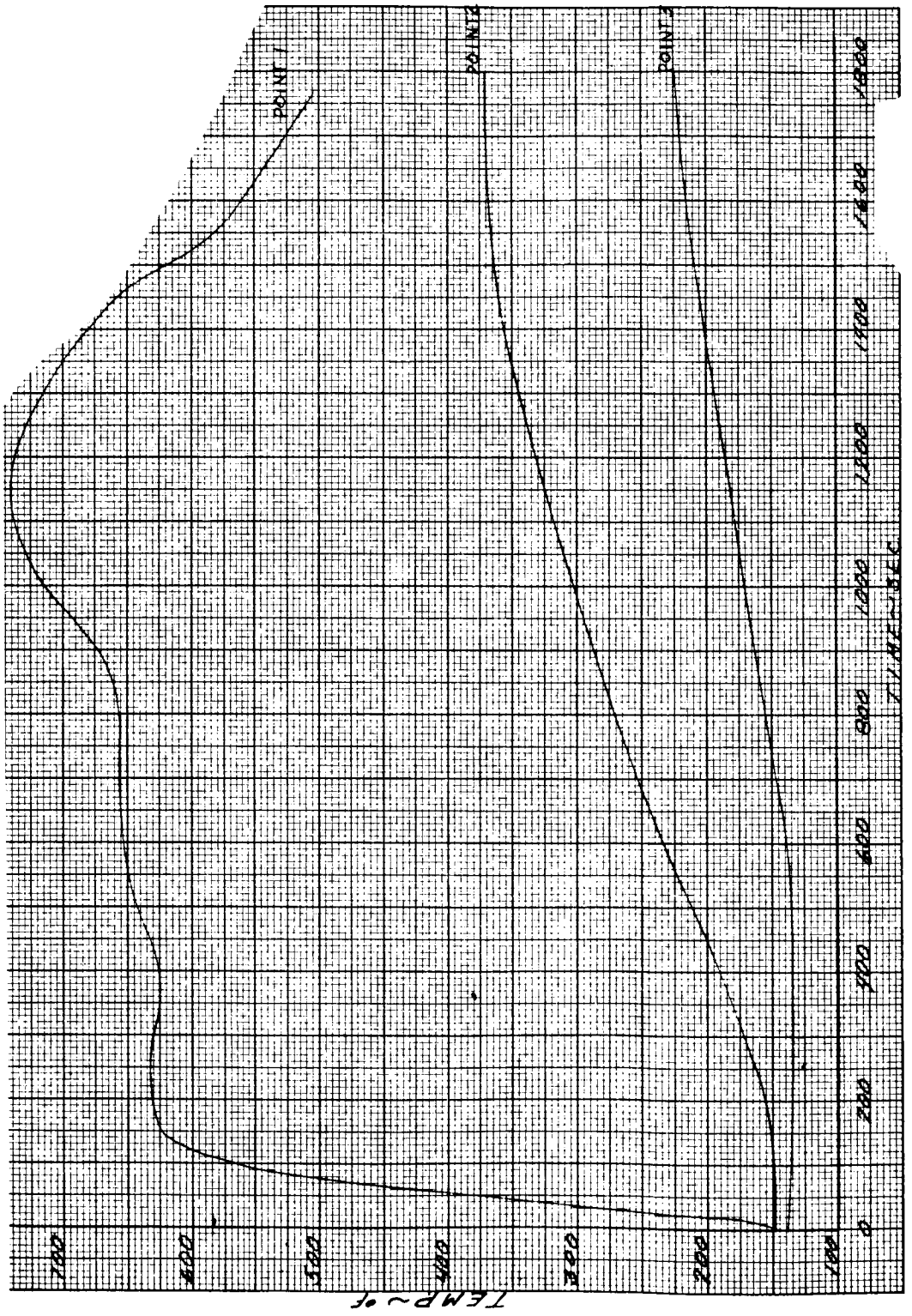

Figure 2-17. Temperature Histories of Referenced C/M to S/M Umbilical Locations

[redacted]

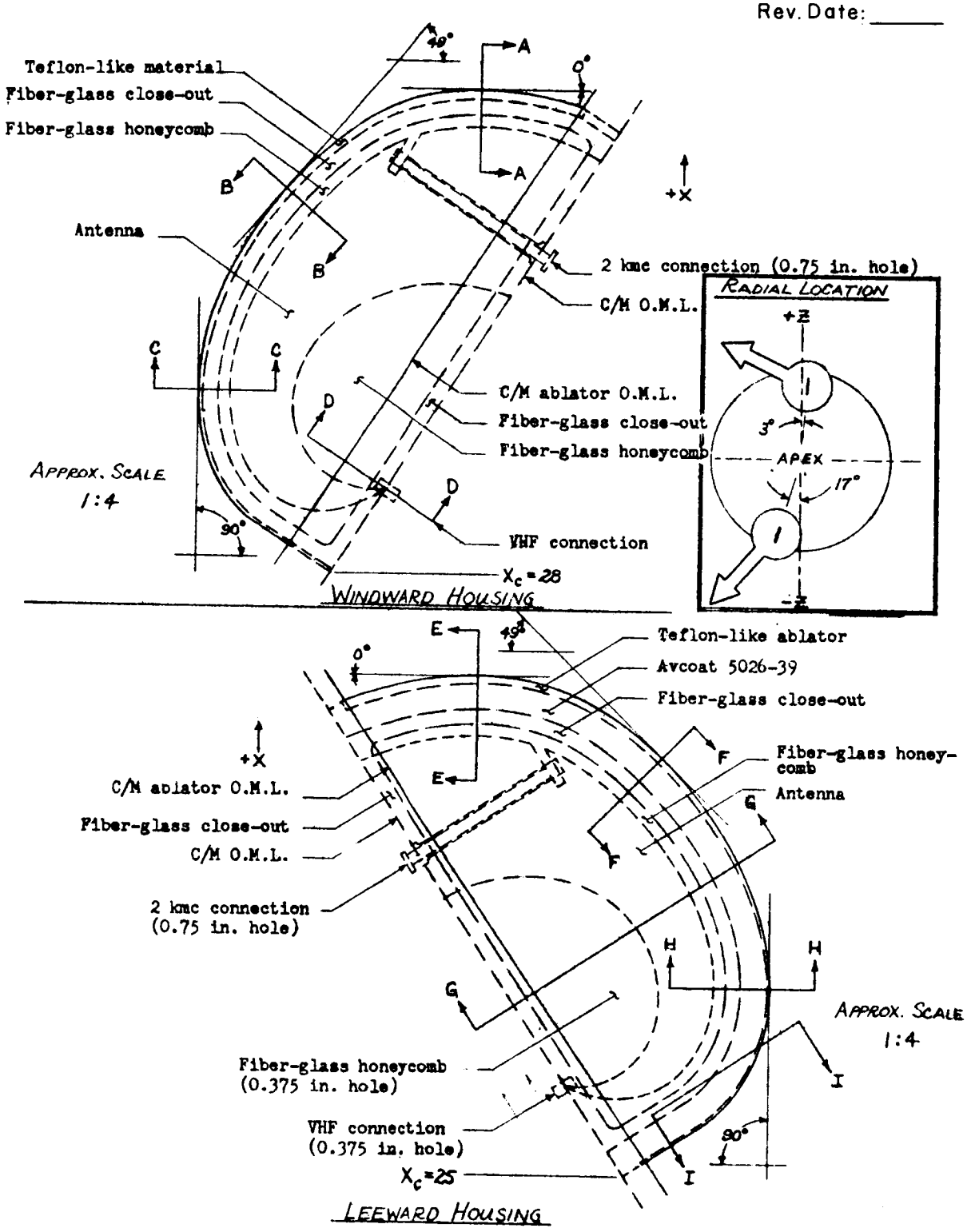

Figure 2-18 . Schematic Diagram of Scimitar Antenna Housings

[redacted]

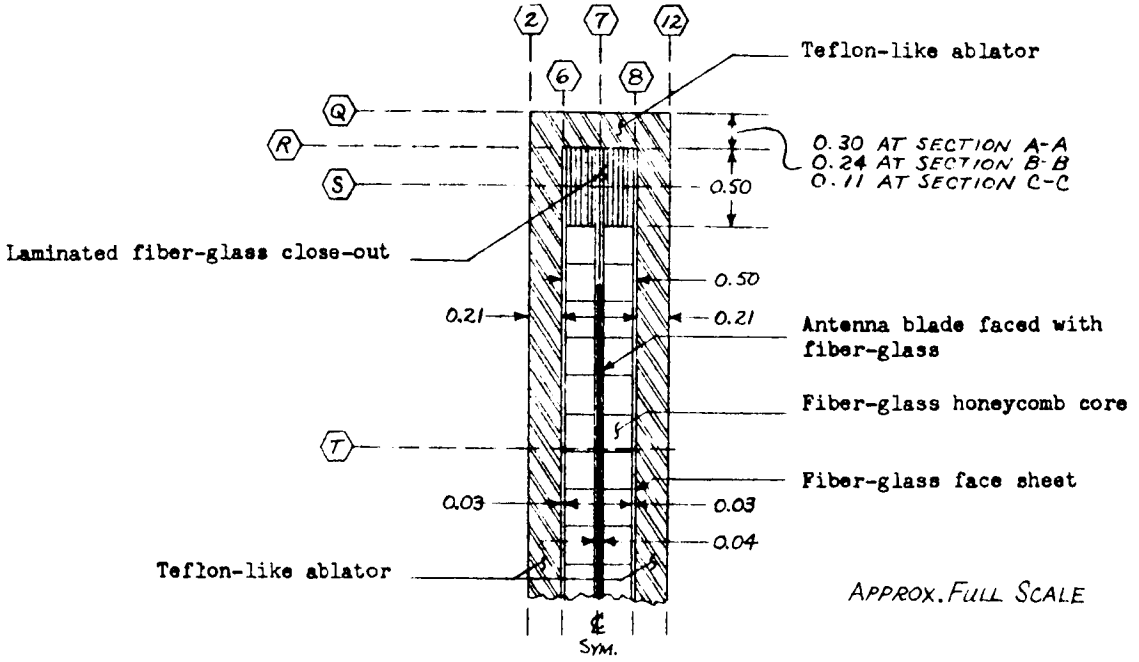

SECTIONS A-A, B-B AND C-C

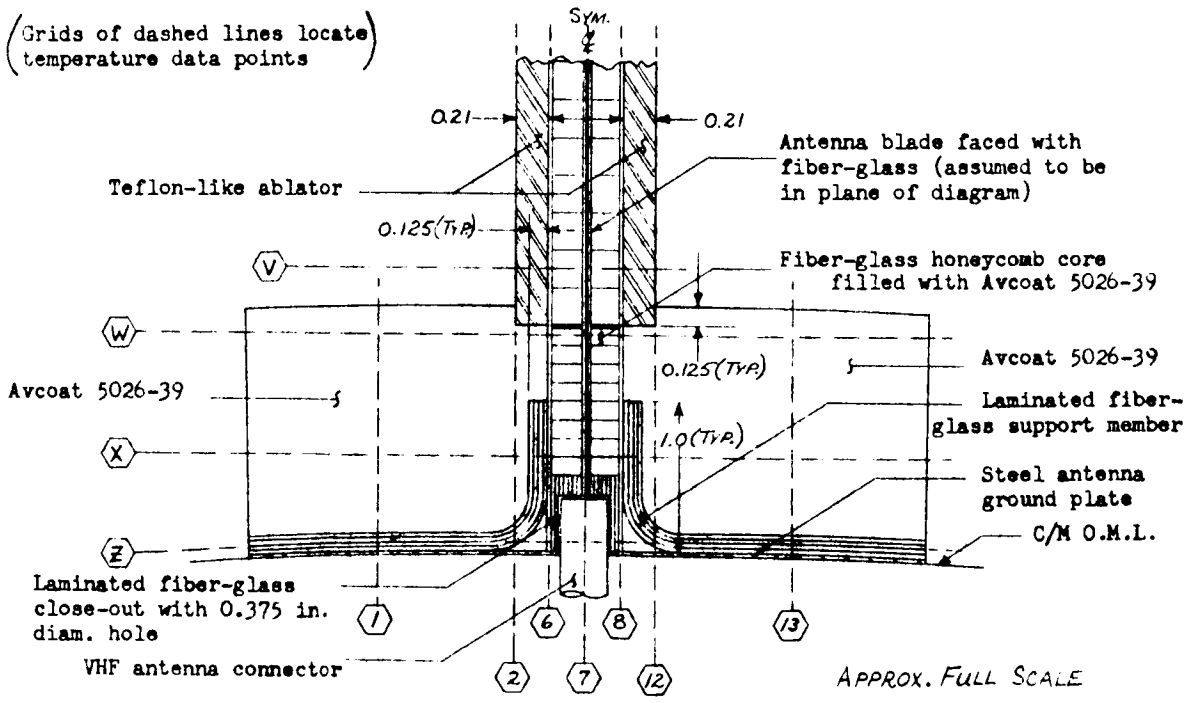

SECTION D-D

Figure 2-19. Sections Through Windward Antenna Housing

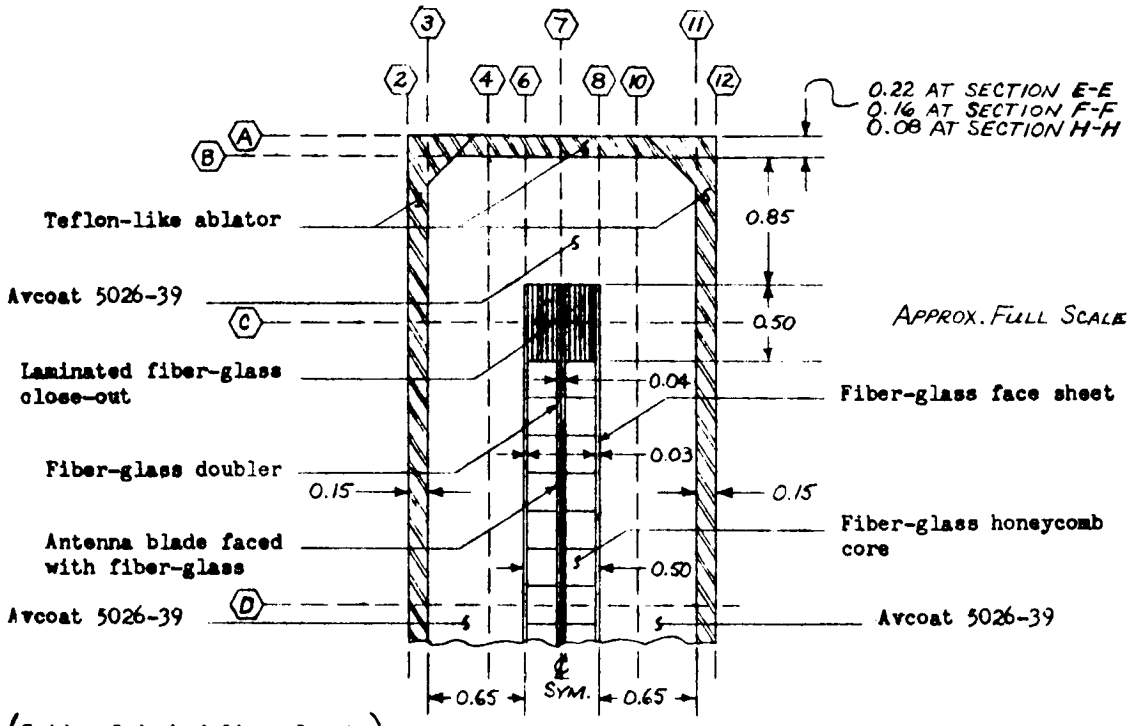

(Grids of dashed lines locate temperature data points)

SECTIONS E-E, F-F AND H-H

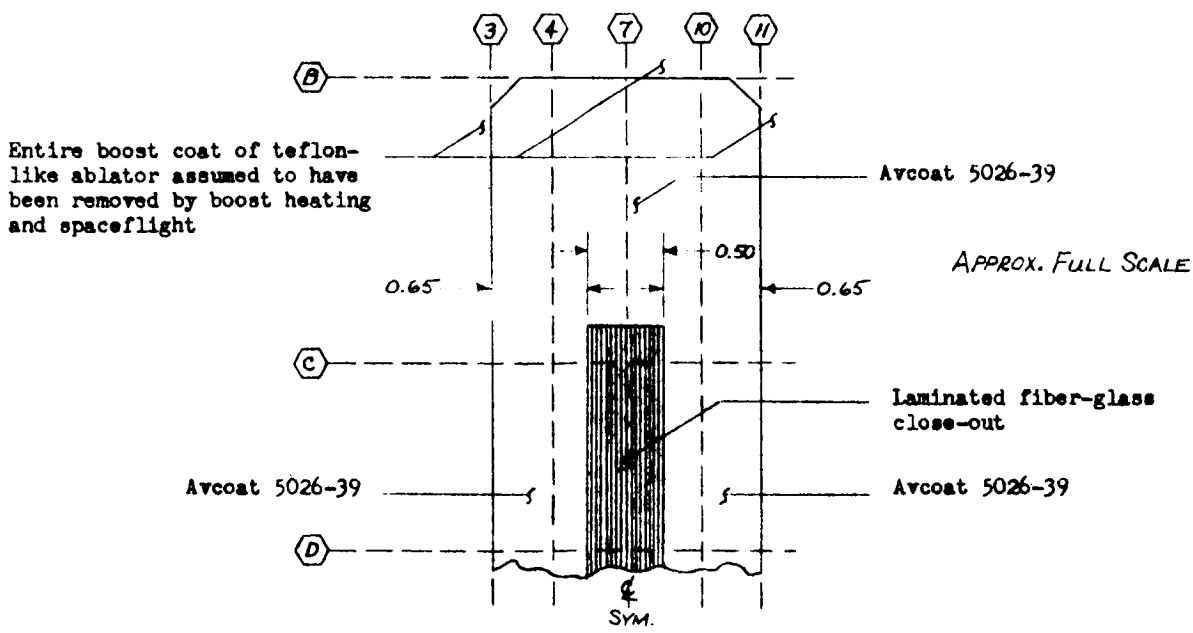

SECTION I-I

Figure 2-20. Sections Through Leeward Antenna Housing (Sheet 1)

~~CONFIDENTIAL~~

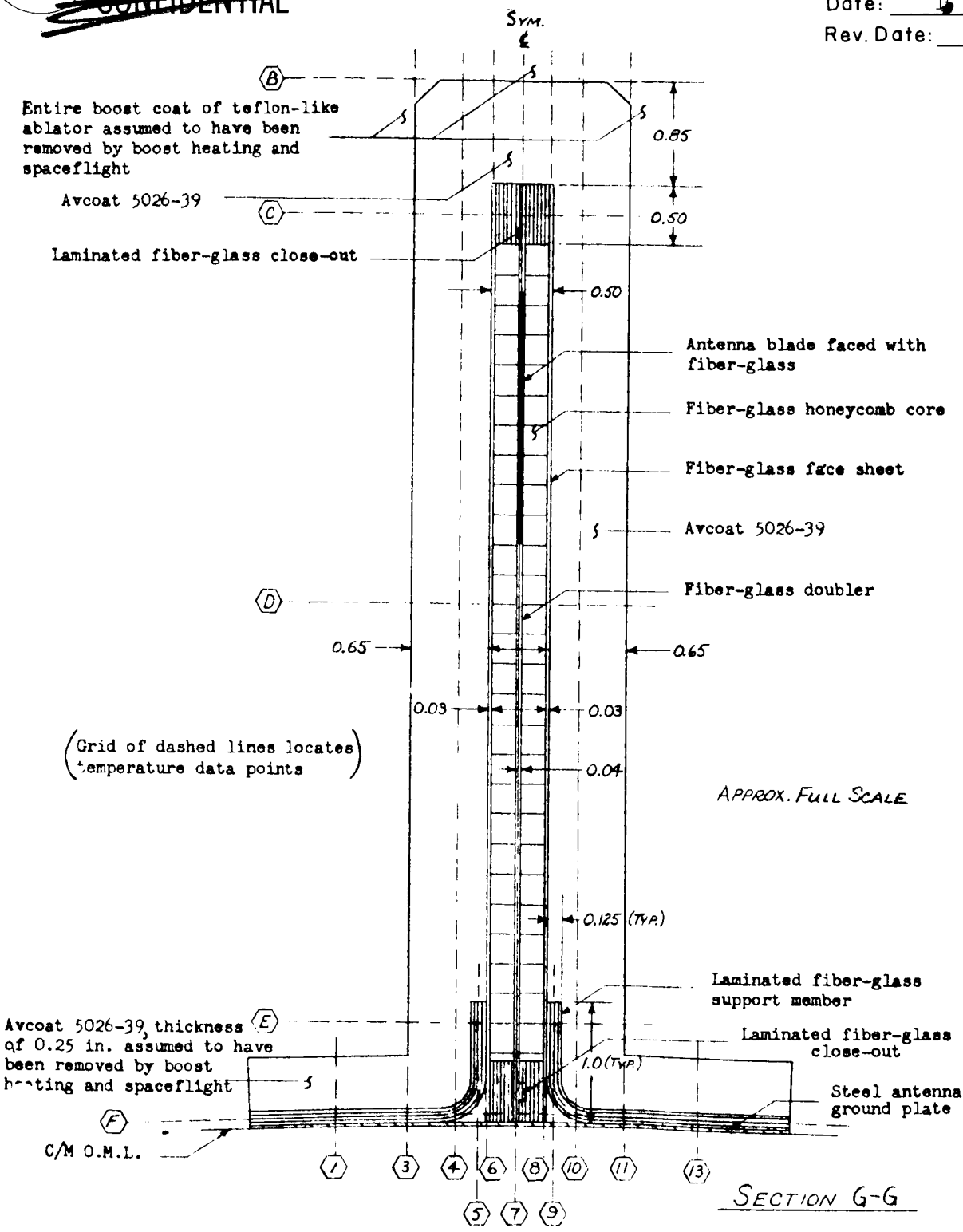

Figure 2-80. Sections Through Leeward Antenna Housing (Sheet 2)

~~CONFIDENTIAL~~

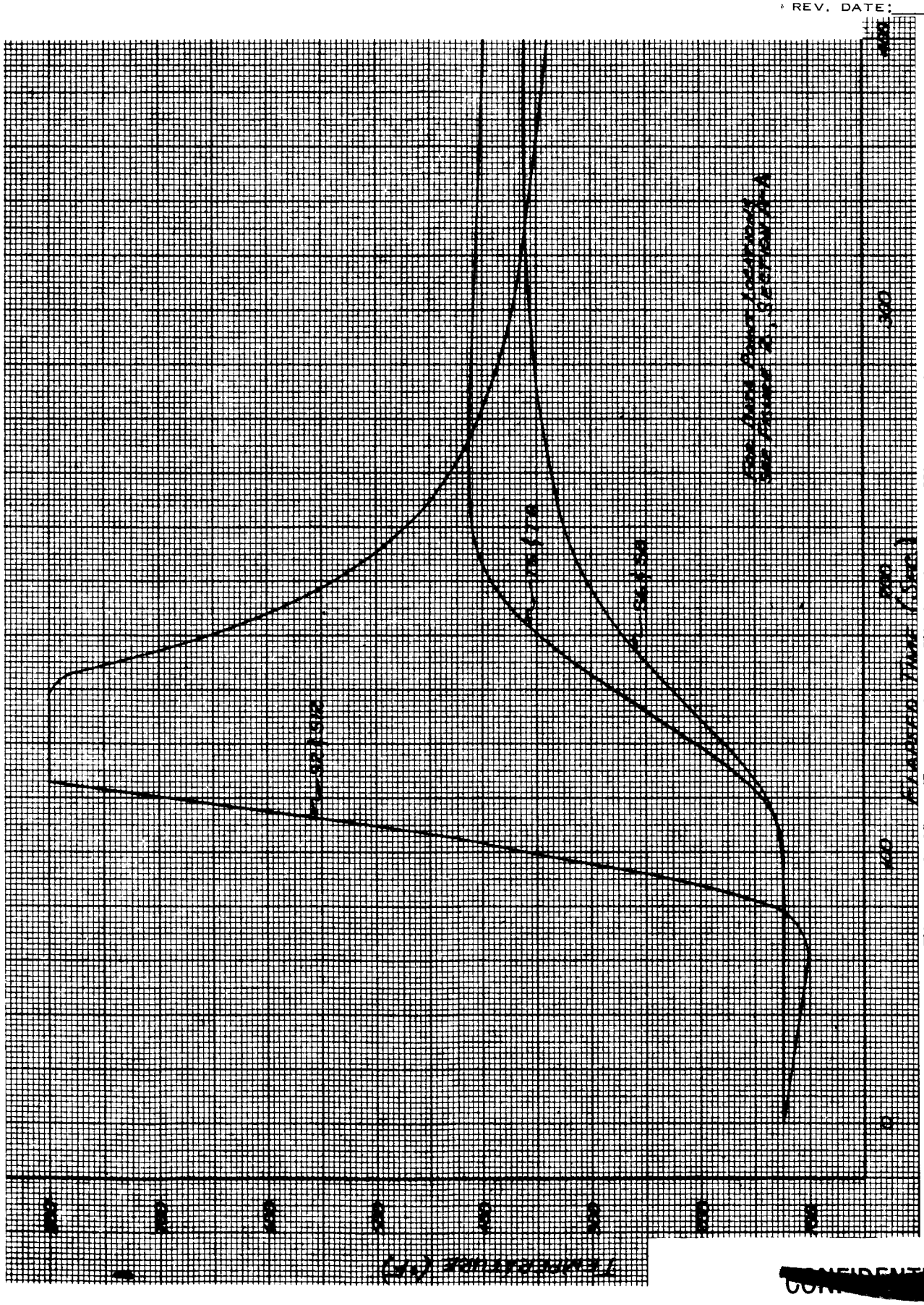

Figure 2-21. Temperature Histories for Windward Antenna Housing During S-V Boost (Sheet 1 of 4)

[redacted]

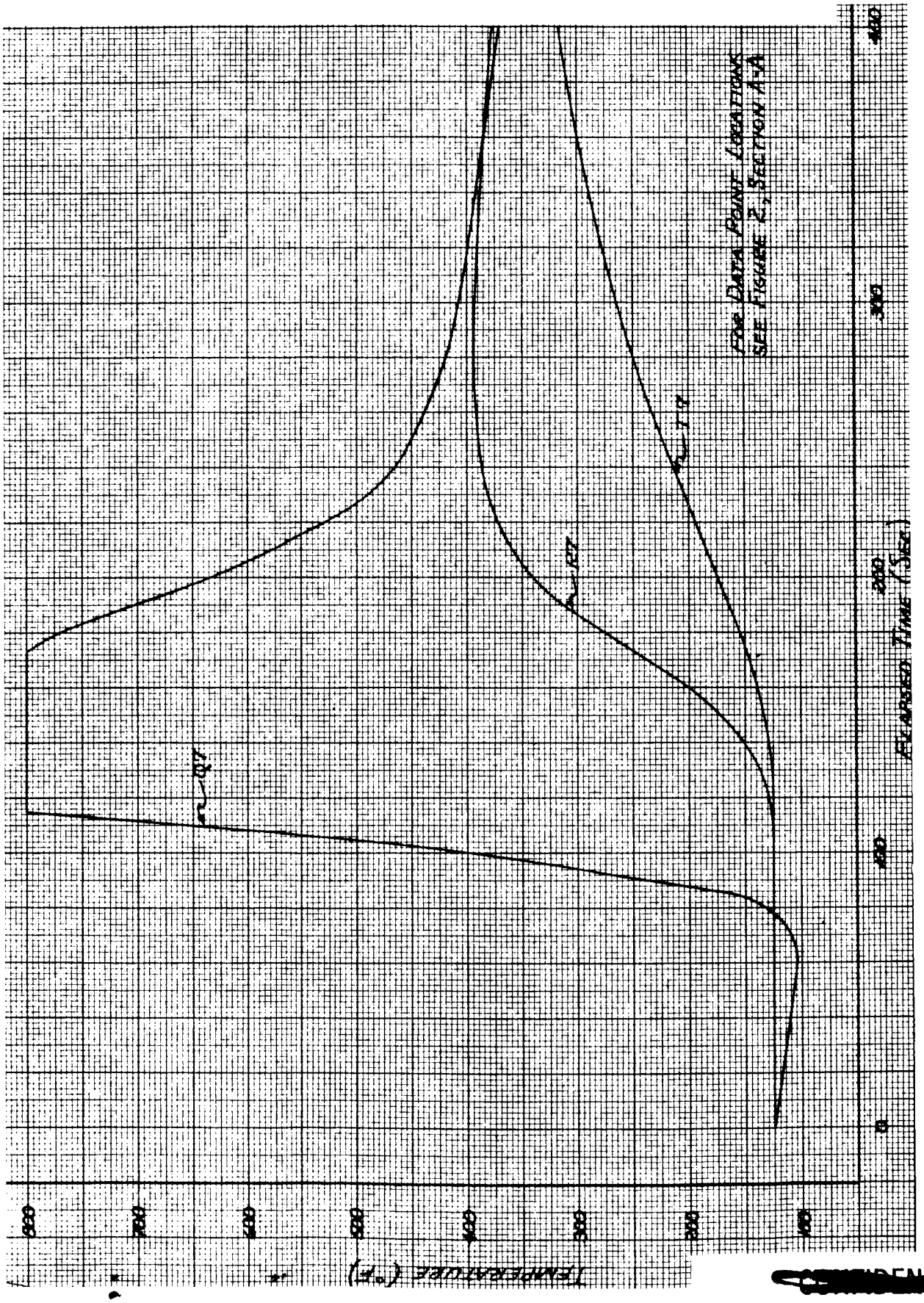

Figure 2-21. Temperature Histories for Windward Antenna Housing During S-V Boost (Sheet 2 of 4)

[redacted]

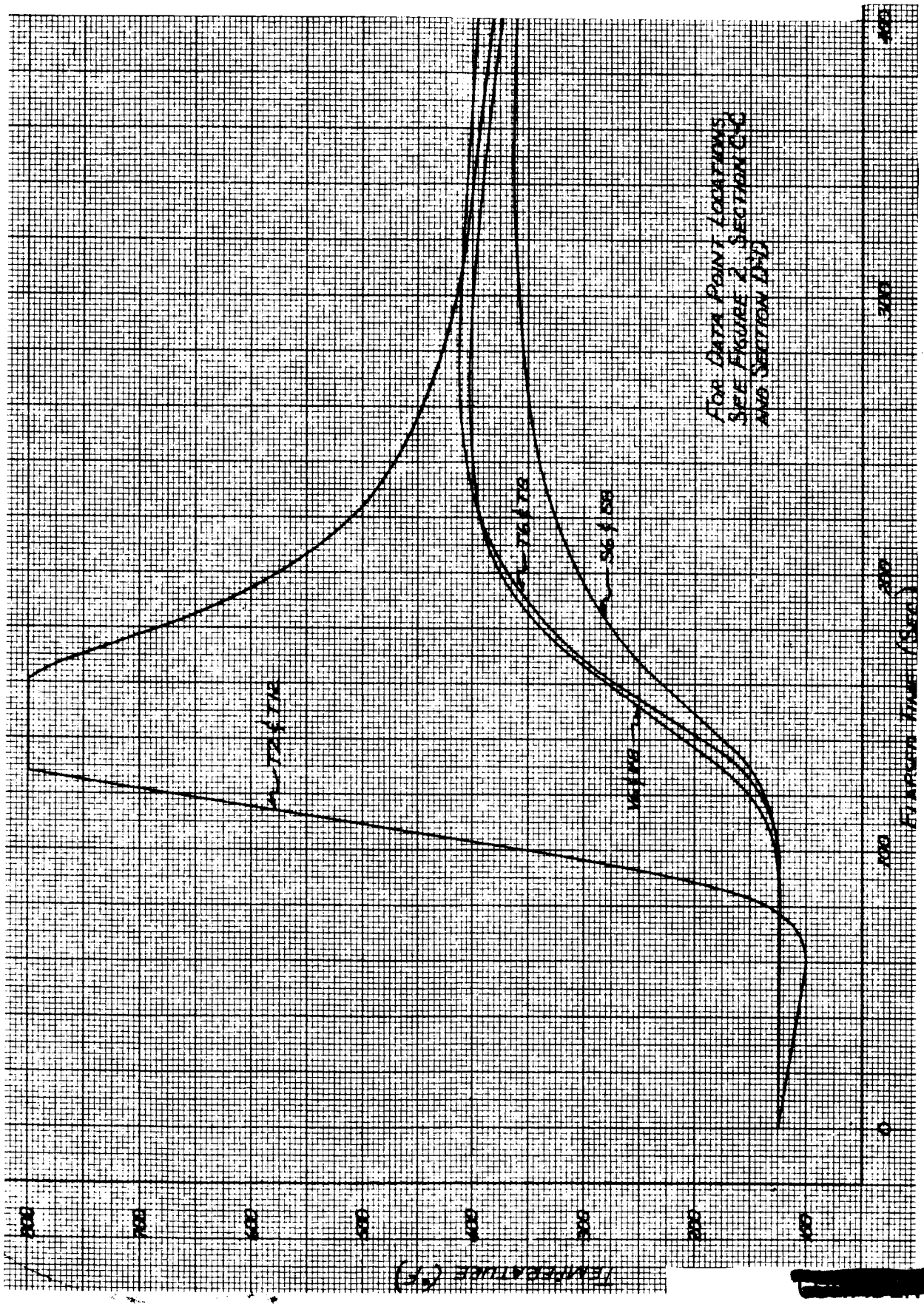

Figure 2-21. Temperature Histories for Windward Antenna Housing During S-V Boost (Sheet 3 of 4)

[redacted]

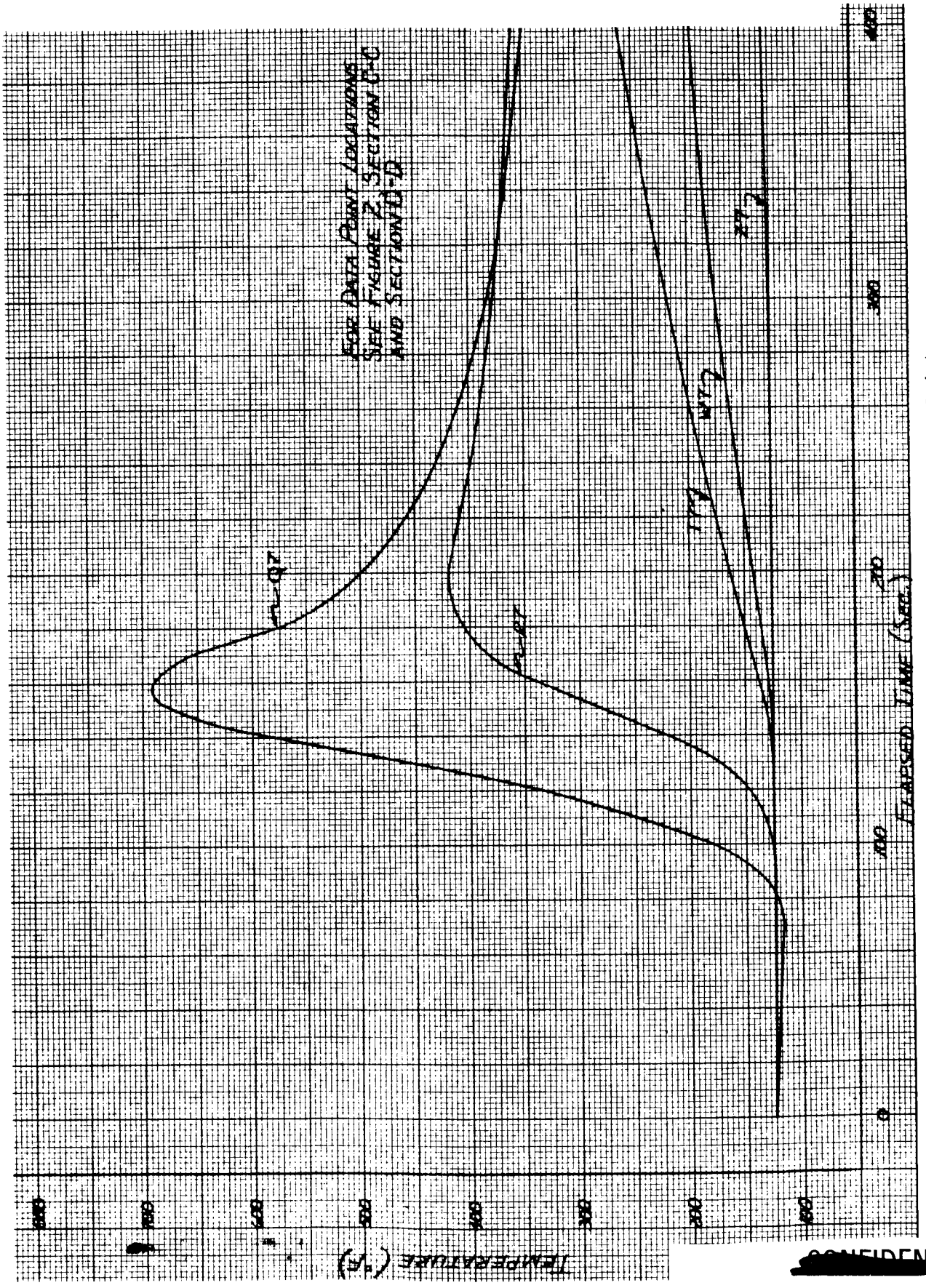
EGR DATA POINT LOCATIONS
SEE FIGURE 2, SECTION C-C
AND SECTION D-D
TEMPERATURE (°F)
ELAPSED TIME (SEC.)
0
100
200
300
400
500
600
700
800
900
1000
1100
1200
1300
1400
1500
1600
1700
1800
1900
2000
2100
2200
2300
2400
2500
2600
2700
2800
2900
3000
3100
3200
3300
3400
3500
3600
3700
3800
3900

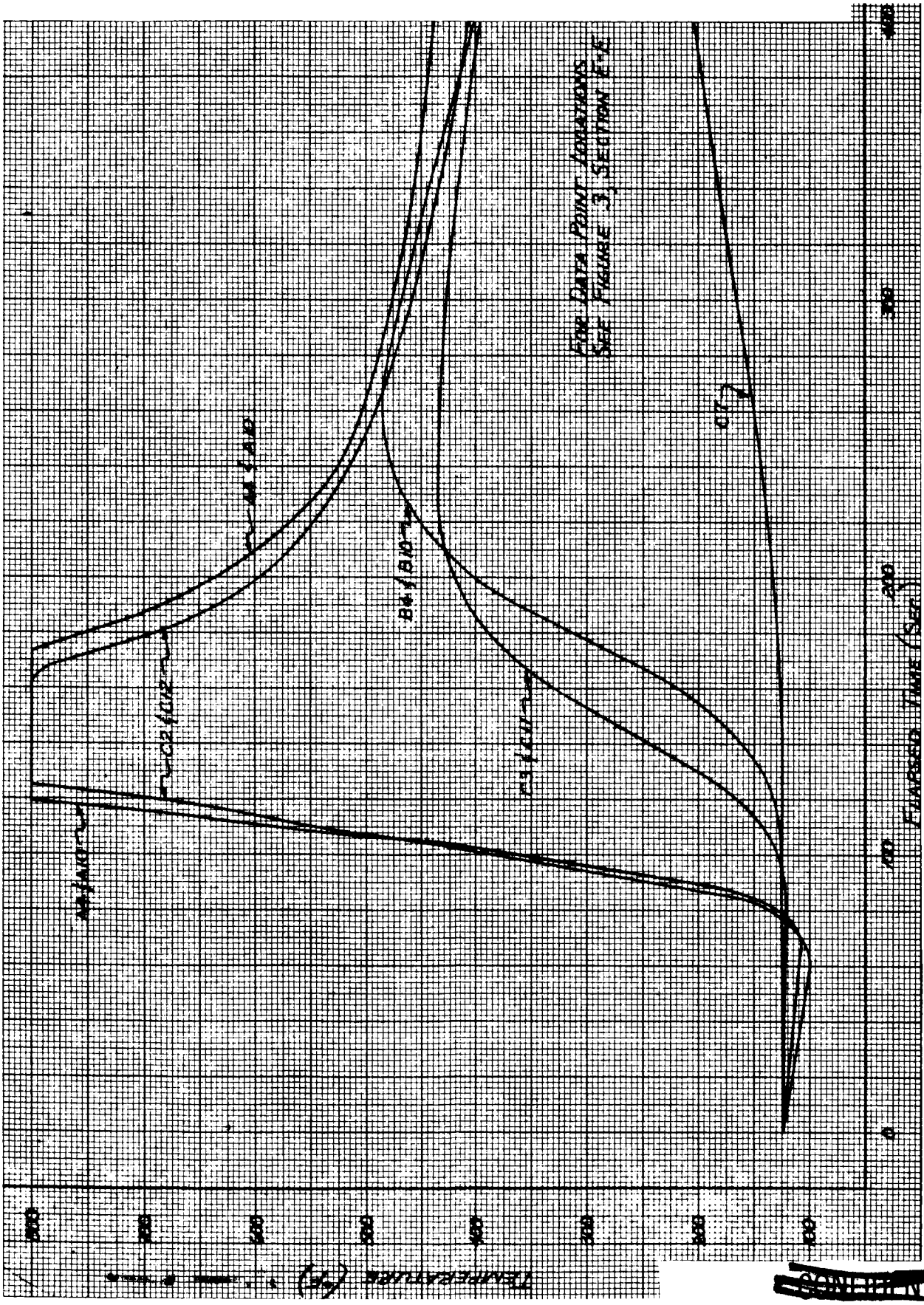

Figure 2-22. Temperature Histories for Leeward Antenna Housing During S-V Boost (Sheet 1 of 2)

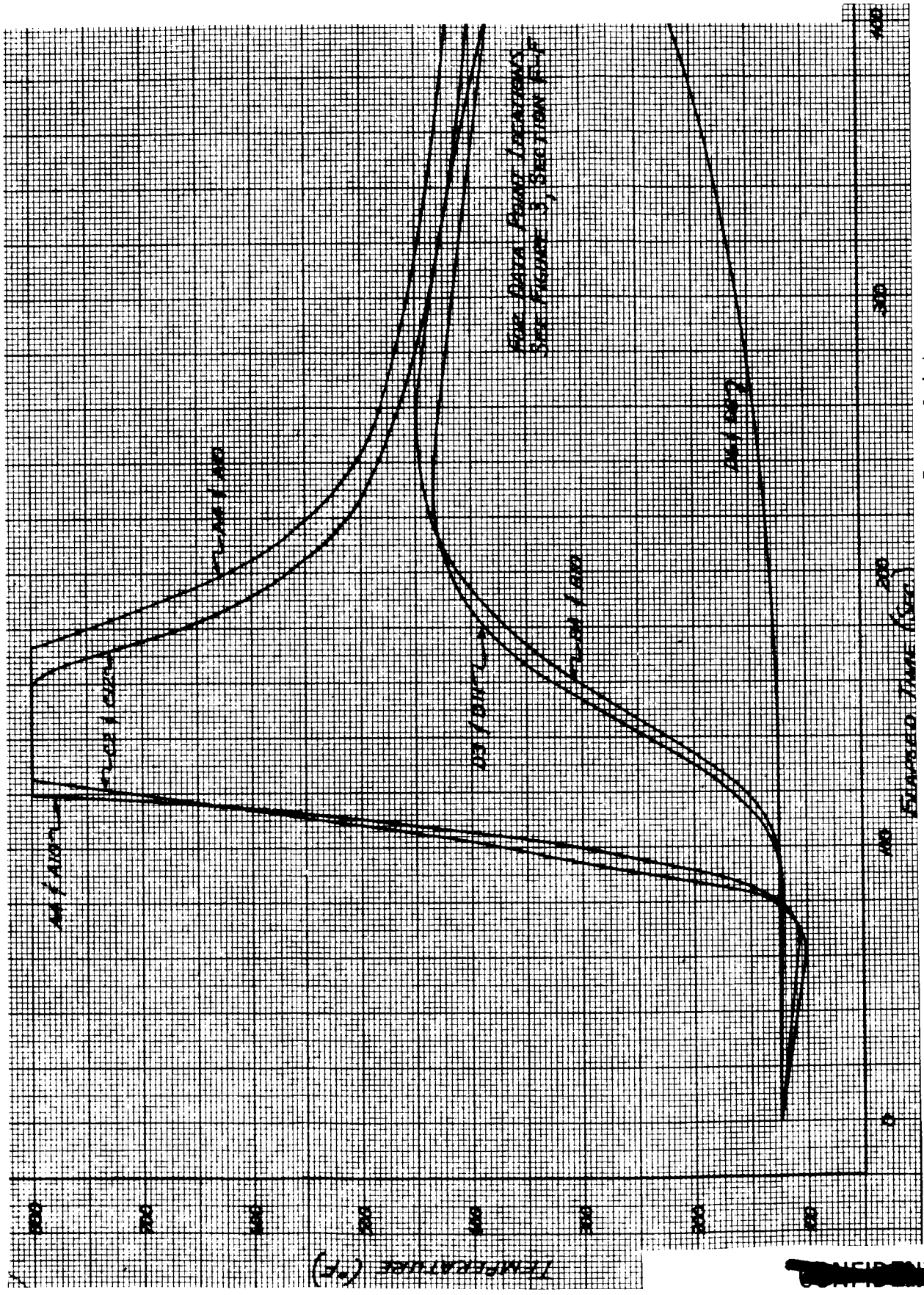

Figure 2-22. Temperature Histories for Leeward Antenna Housing During S-V Boost (Sheet 2 of 2)

[redacted]

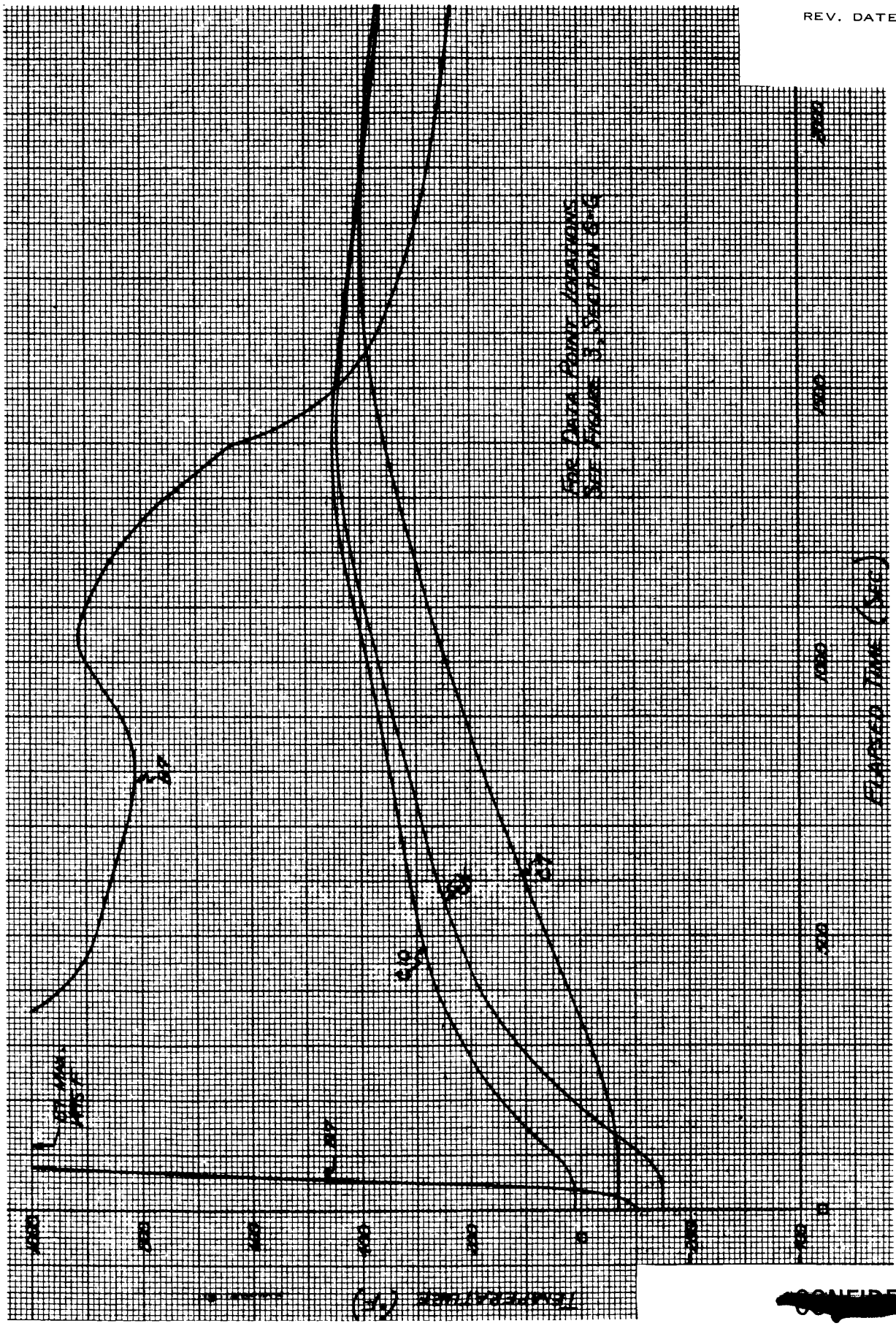

Figure 2-23. Temperature Histories With Severe Initial Gradients During Reentry Trajectory HSE-3A (Sheet 1 of 4)

[redacted]

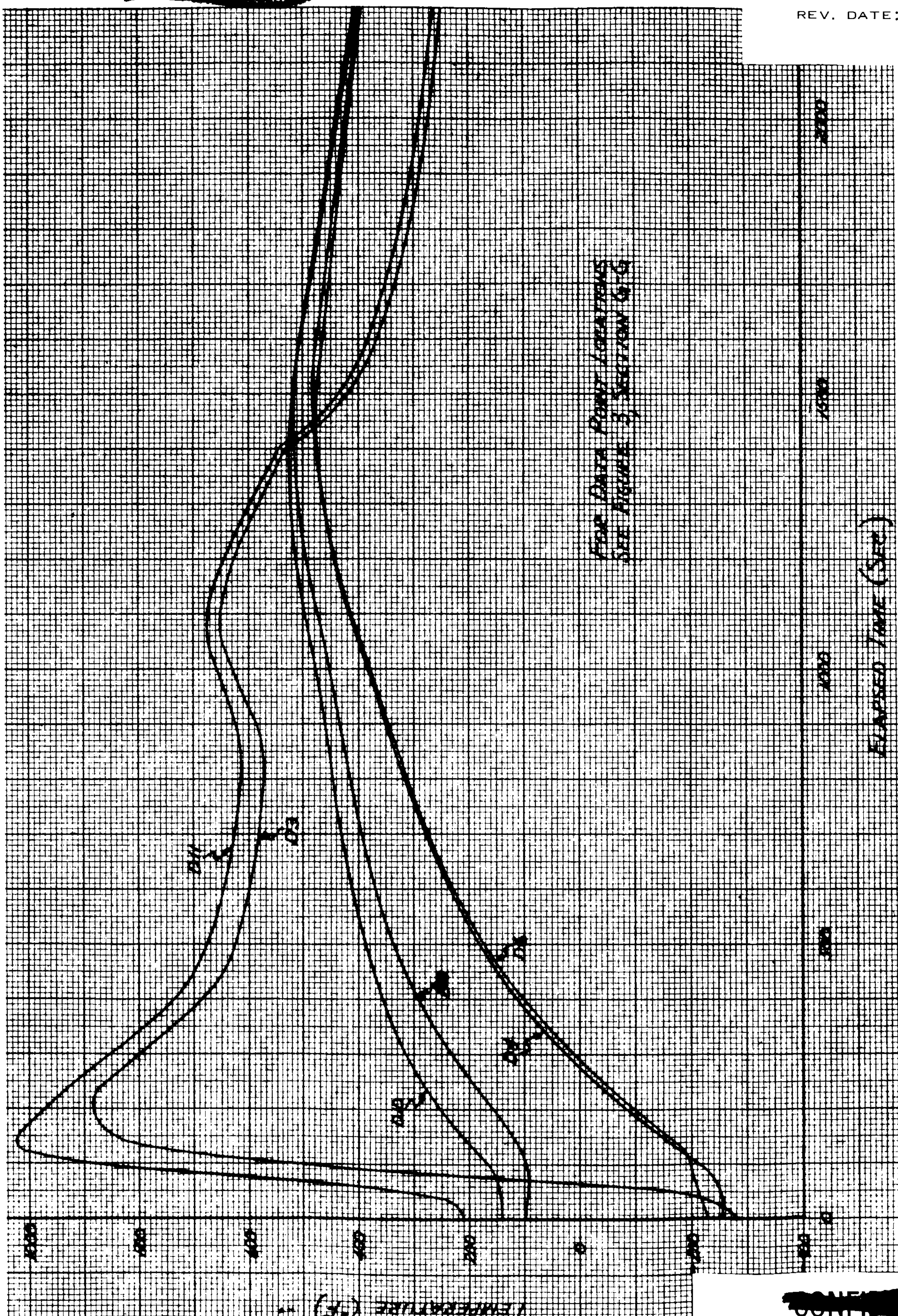

Figure 2-23. Temperature Histories With Severe Initial Gradients During Reentry Trajectory HSE-3A (Sheet 2 of 4)

[redacted]

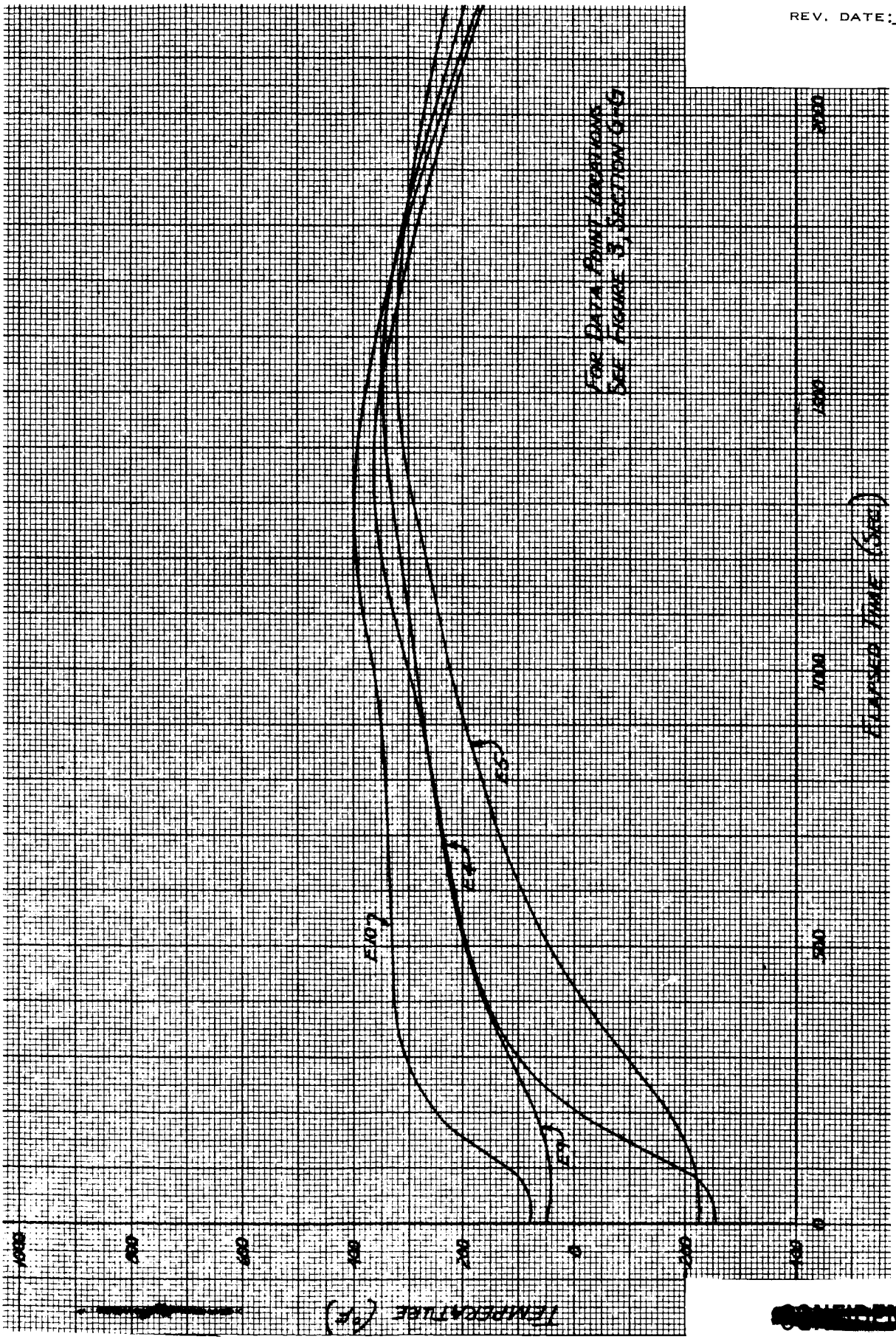

Figure 2-23. Temperature Histories With Severe Initial Gradients During Reentry Trajectory HSE-3A (Sheet 3 of 4)

[redacted]

~~CONFIDENTIAL~~

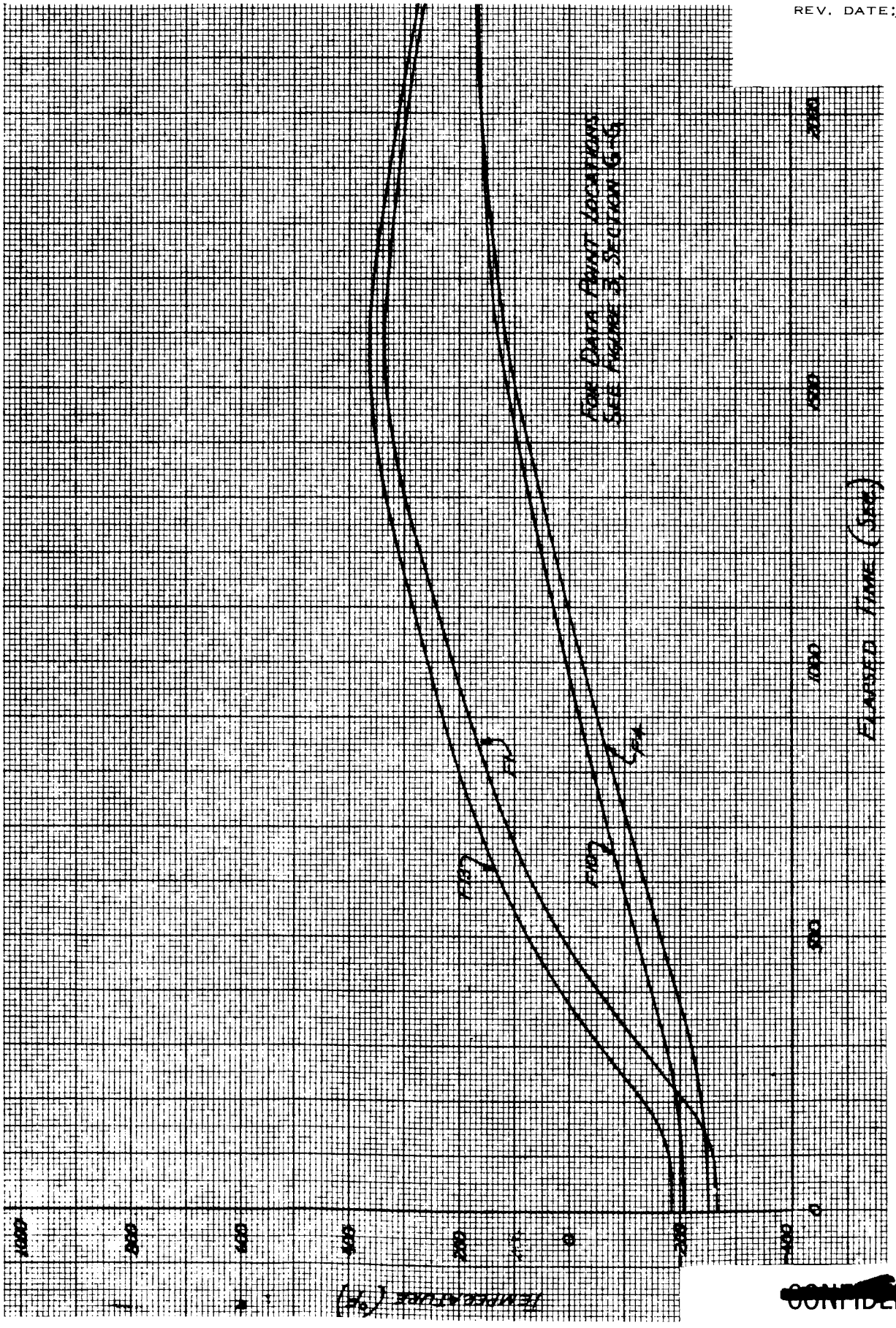

Figure 2-23. Temperature Histories With Severe Initial Gradients During Reentry Trajectory HSE-3A (Sheet 4 of 4)

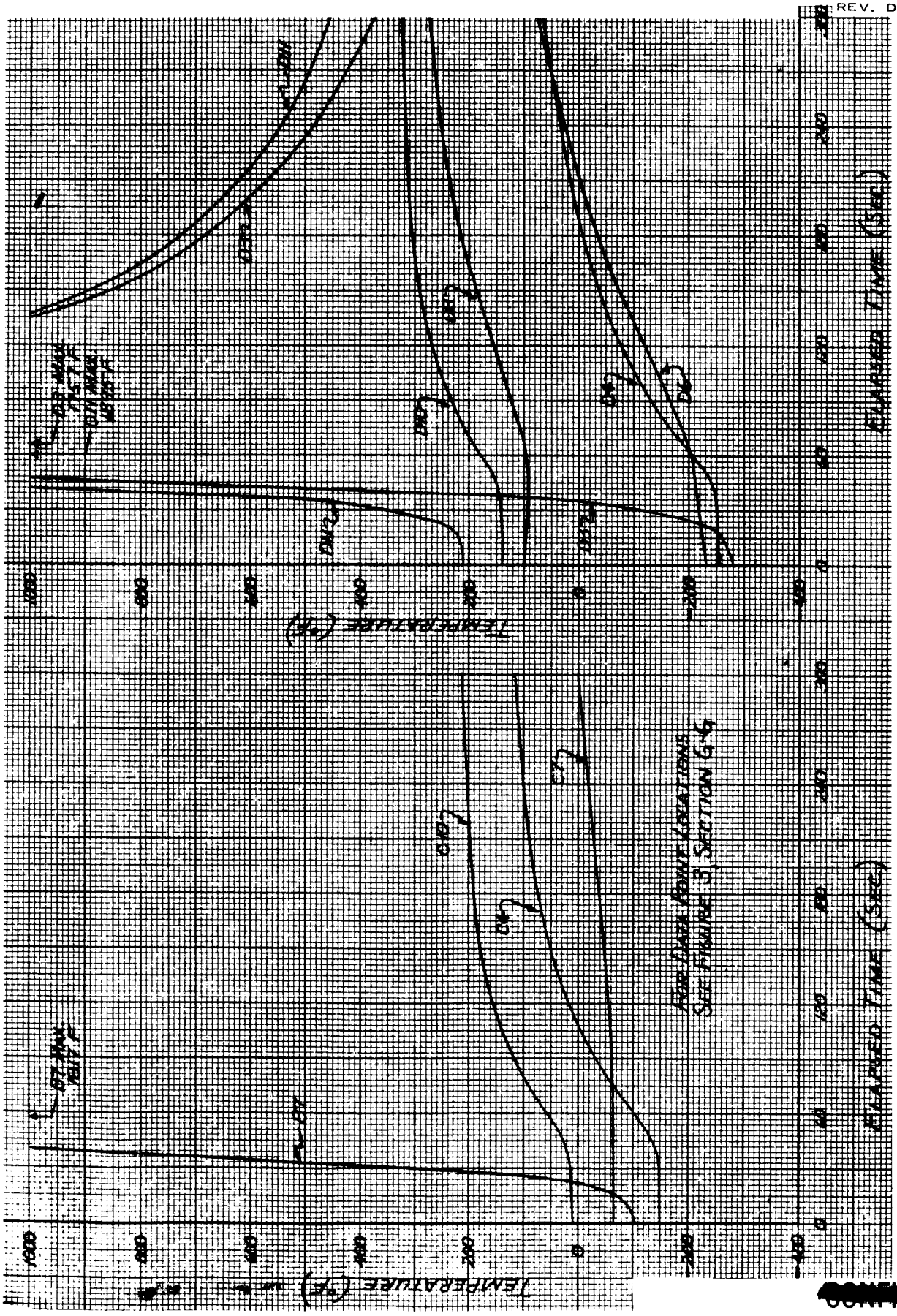

Figure 2-24. Temperature Histories With Severe Initial Gradients During Reentry Trajectory HSE-6 (Sheet 1 of 2)

[redacted]

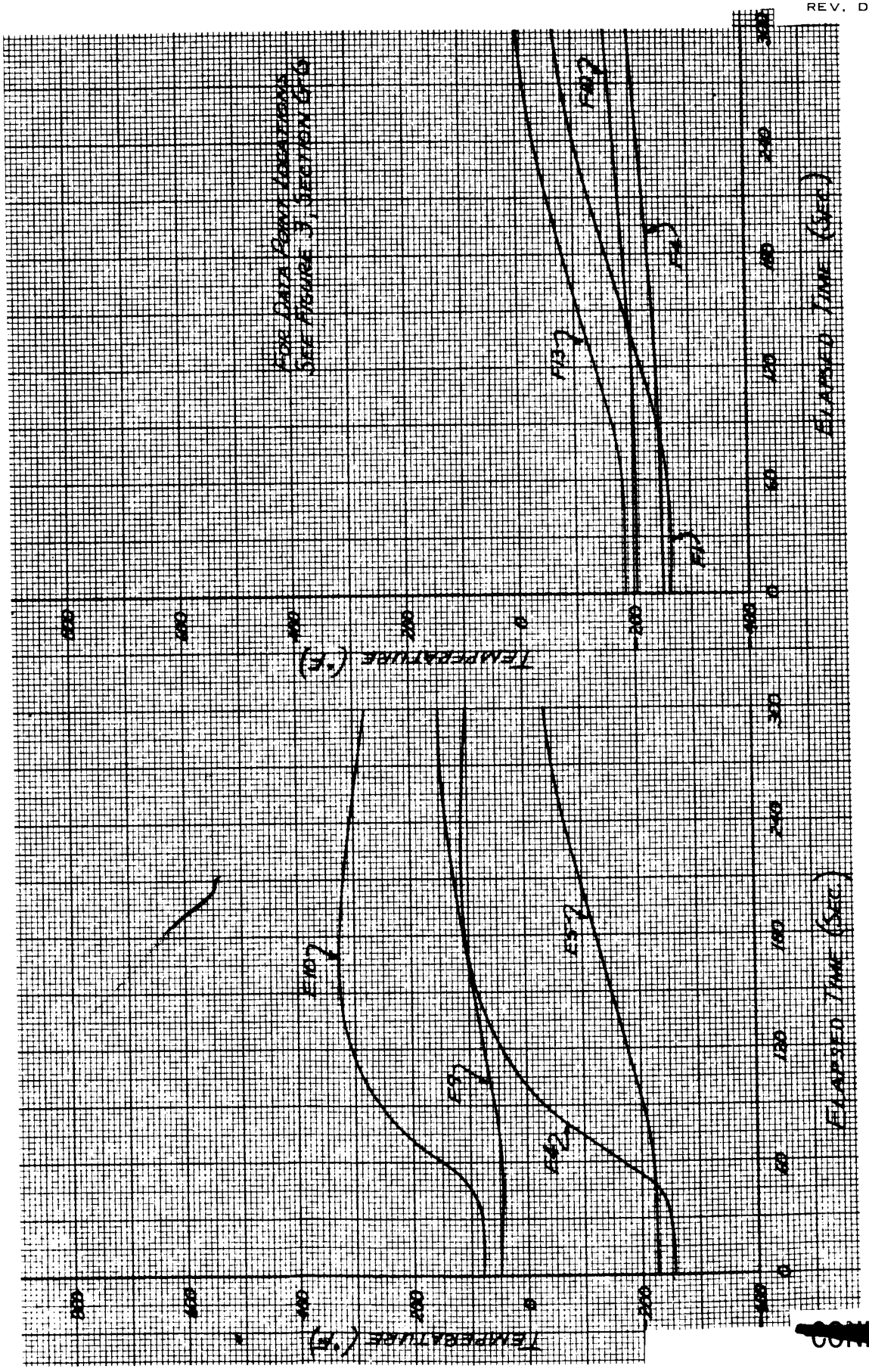

Figure 2-24. Temperature Histories With Severe Initial Gradients During Reentry Trajectory HSE-6 (Sheet 2 of 2)

[redacted]

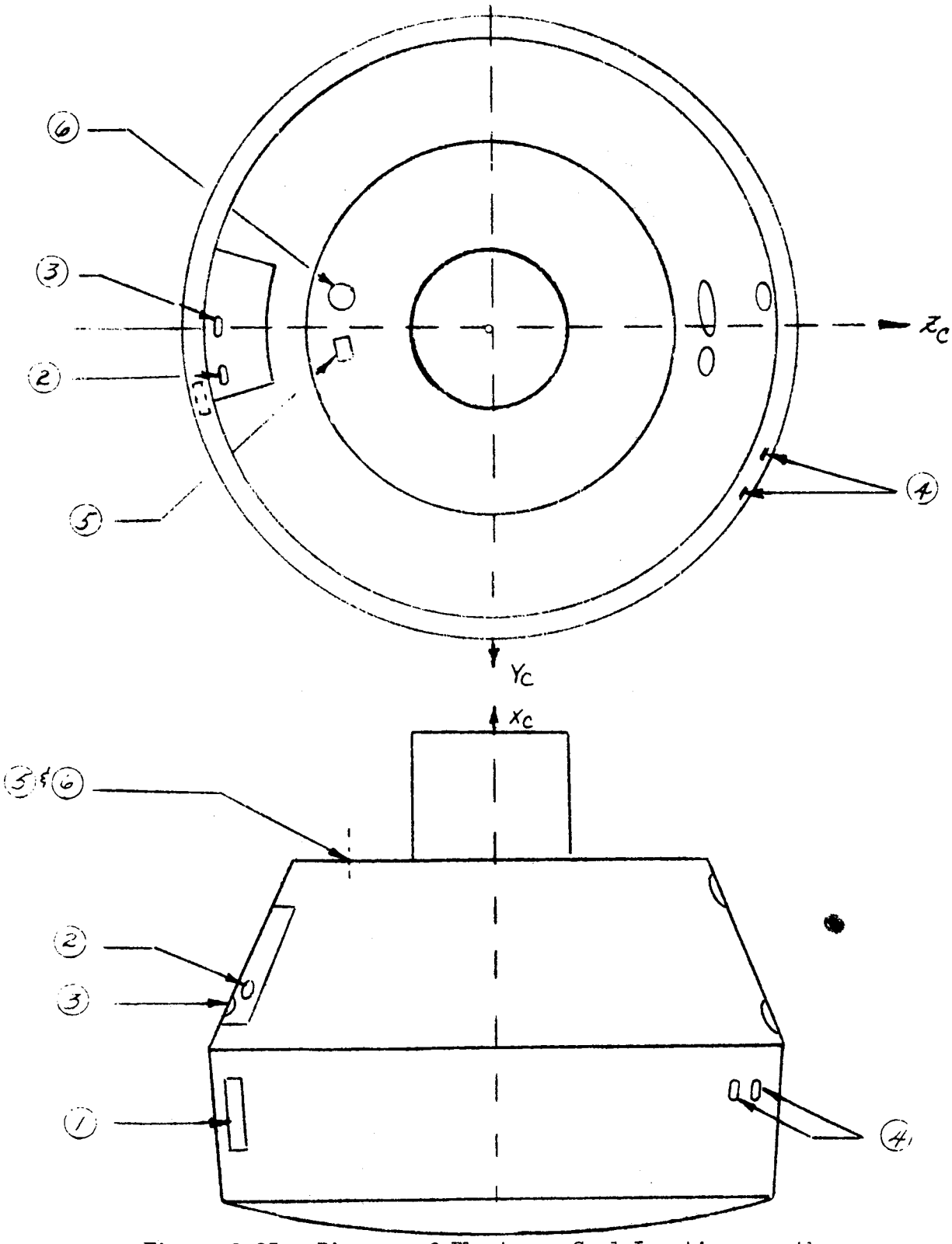

Figure 2-25. Diagram of Elastomer Seal Locations on the Command Module Inner Structure

[redacted]

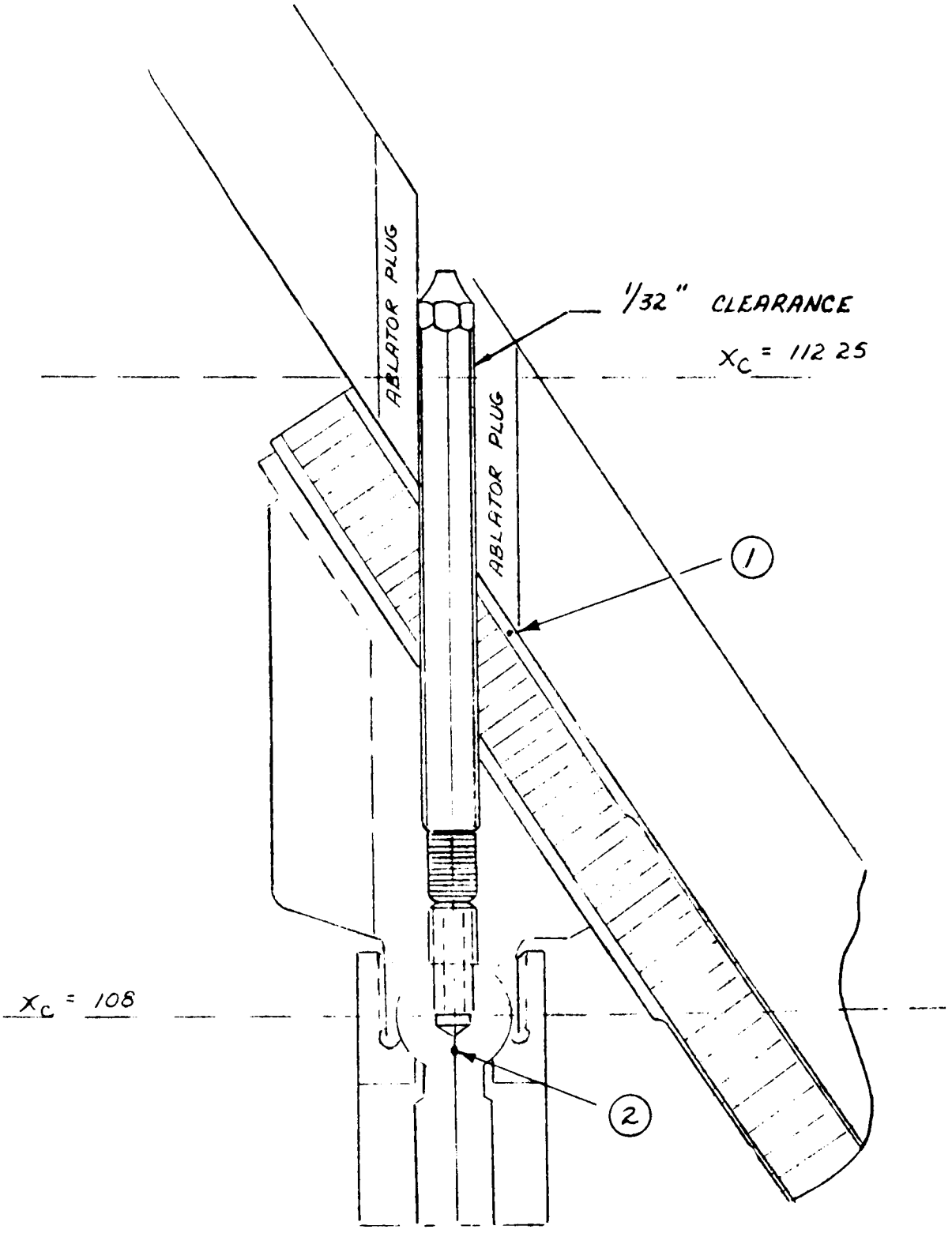

Figure 2-26. Forward Heat Shield Thruster

[redacted]

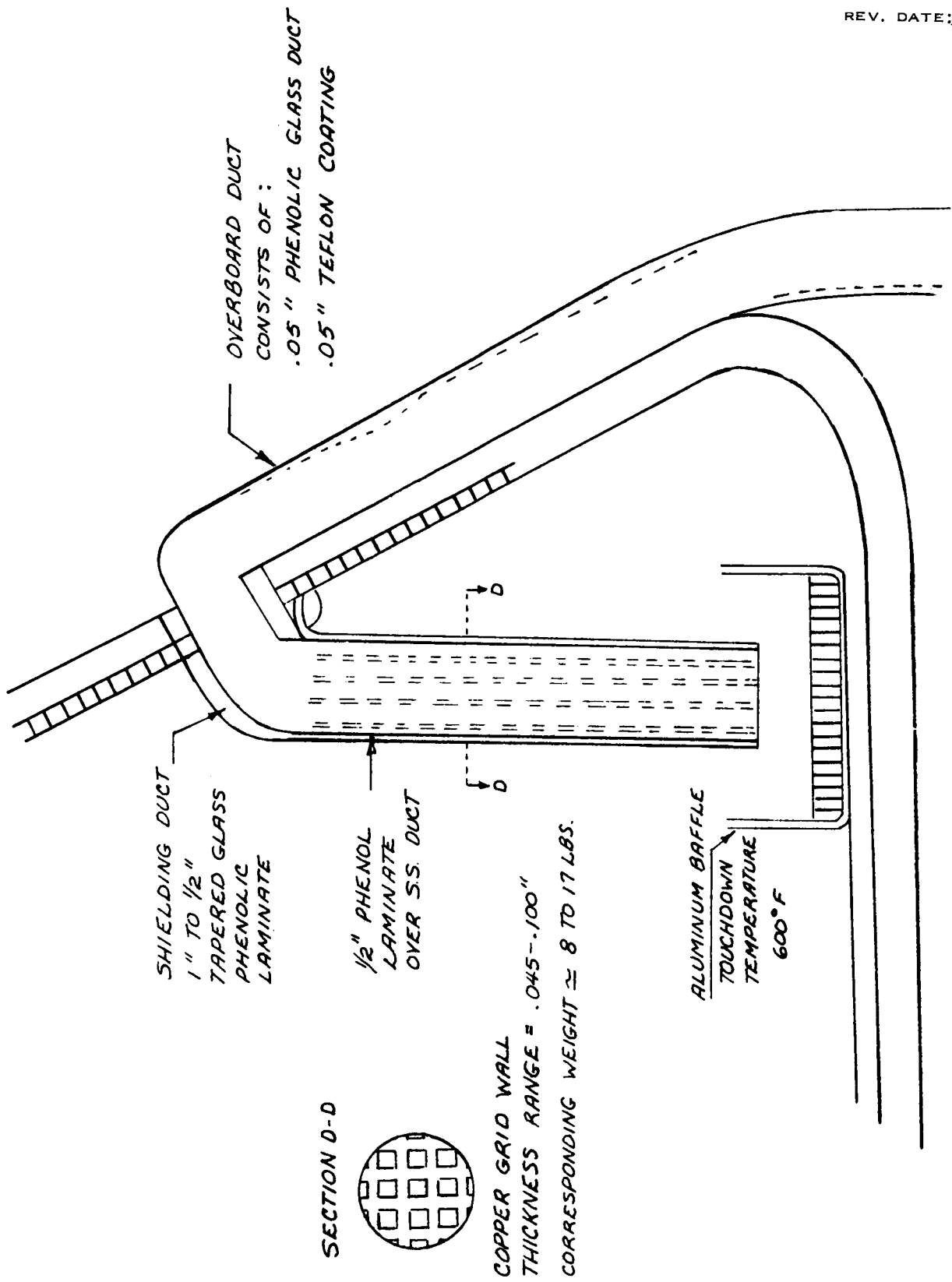

Figure 2-27. Schematic of the Command Module Air Vent Components

[redacted]

[redacted]

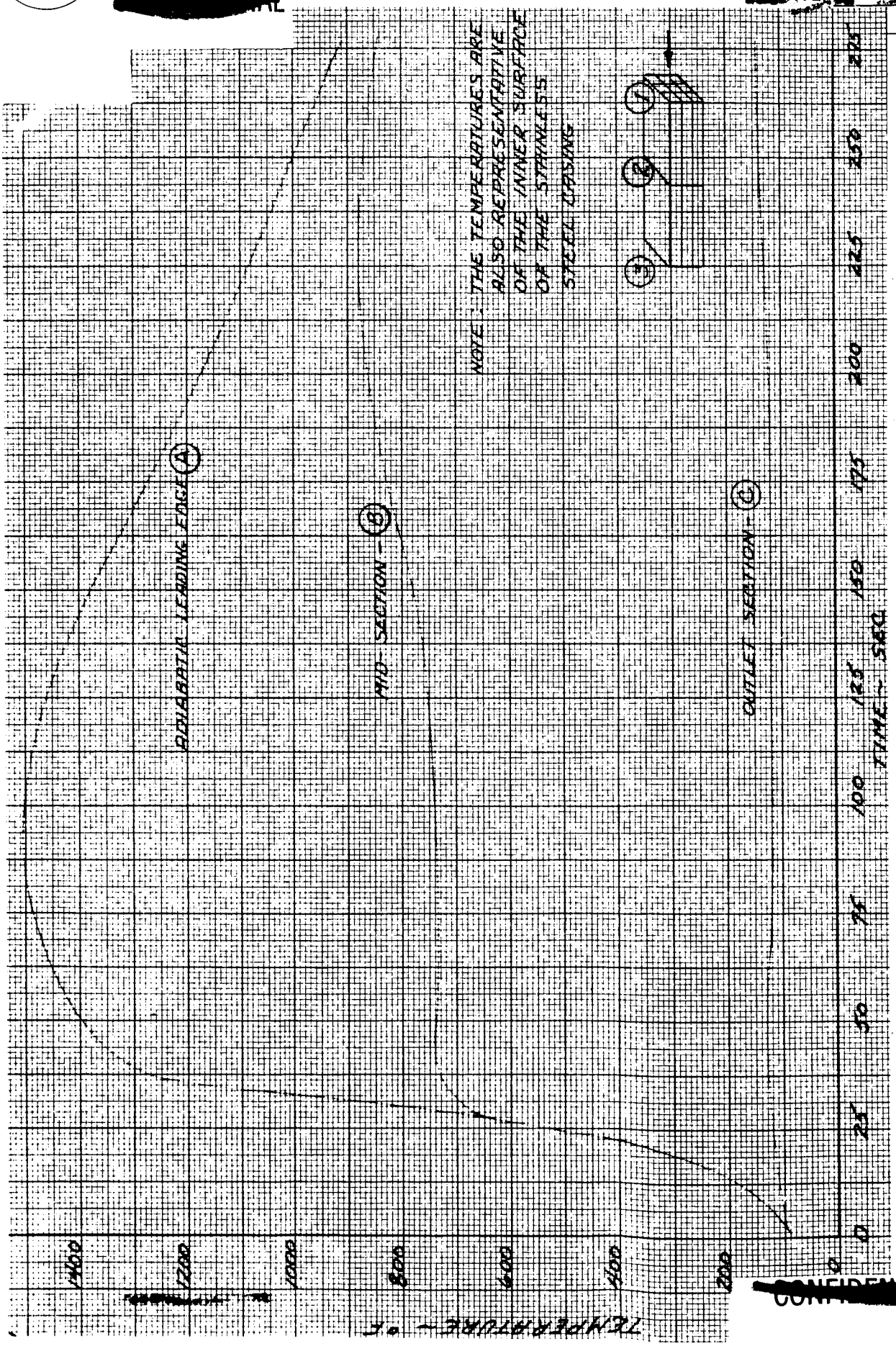

Figure 2-28. Typical Reentry Temperature Histories for the C/M Air Vent Copper Heat Exchanger—Trajectory HSE-6

[redacted]

[redacted]

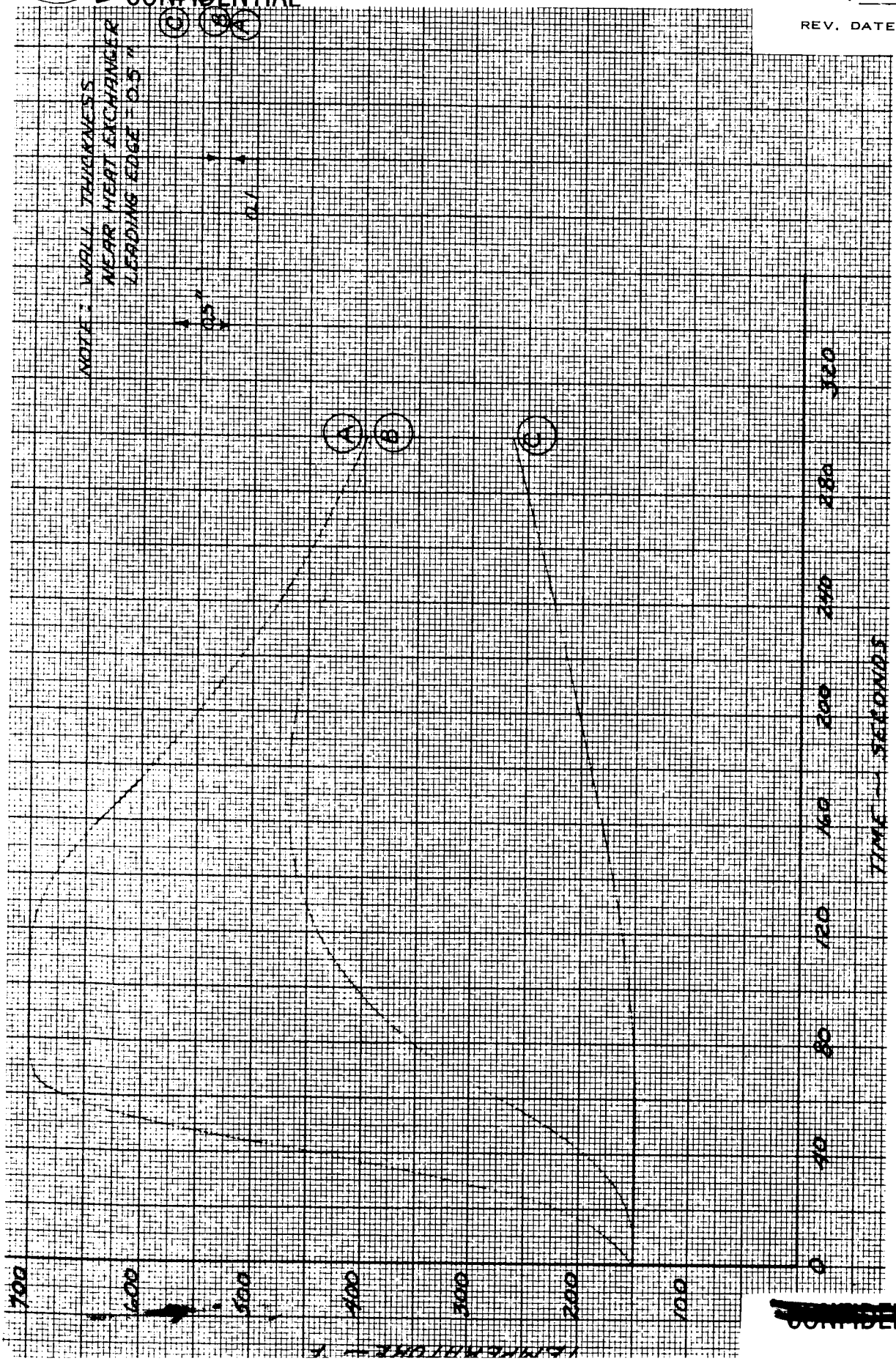

Figure 2-29. Typical Temperature Histories for the Tapered Ablation Outer Structure of the Air Vent Copper Grid Trajectory HSE-6

[redacted]

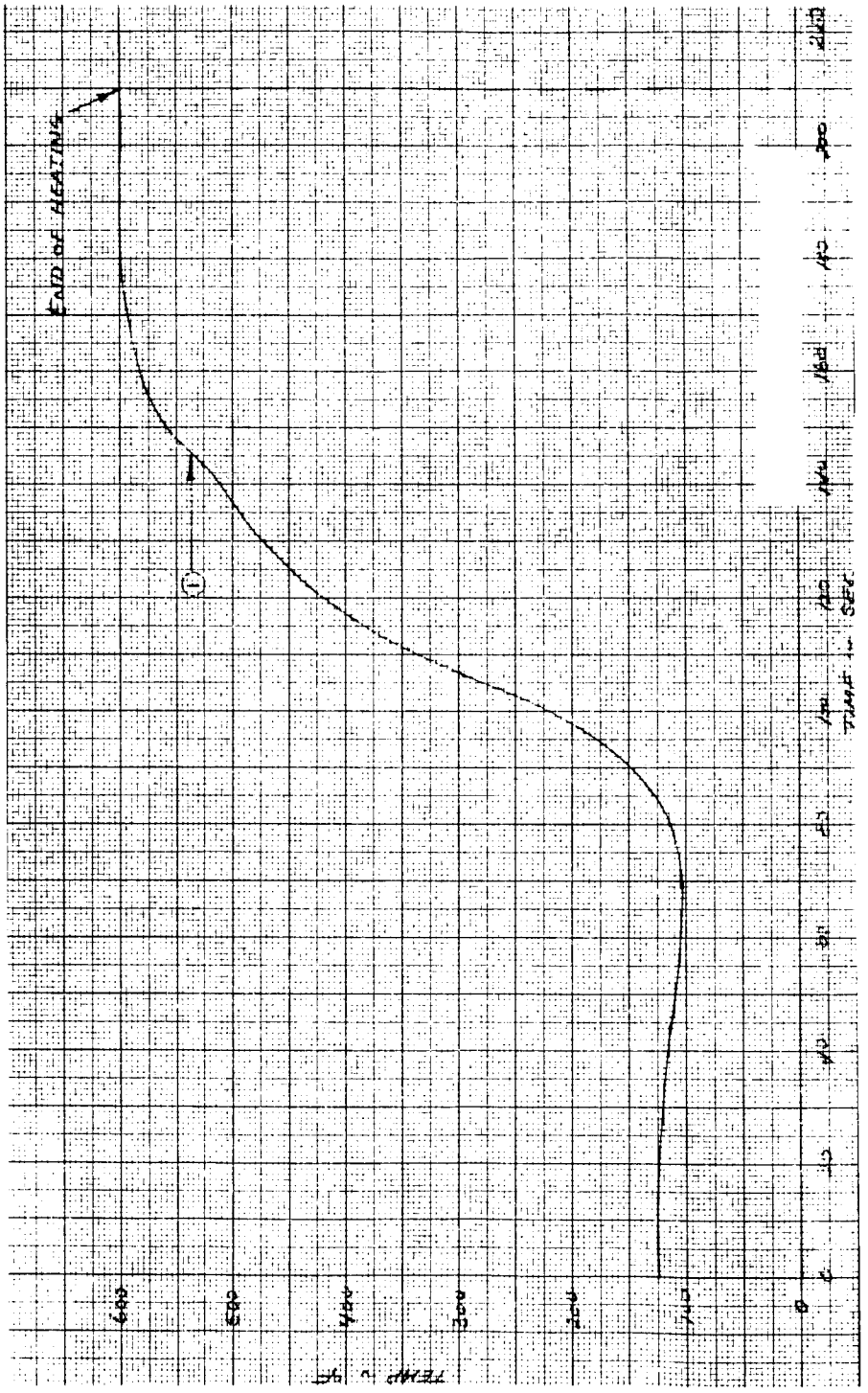

Figure 2-30. Vent Tube Bondline Temperature History of Point 1 for a Saturn V Boost (See Figure 2-29)

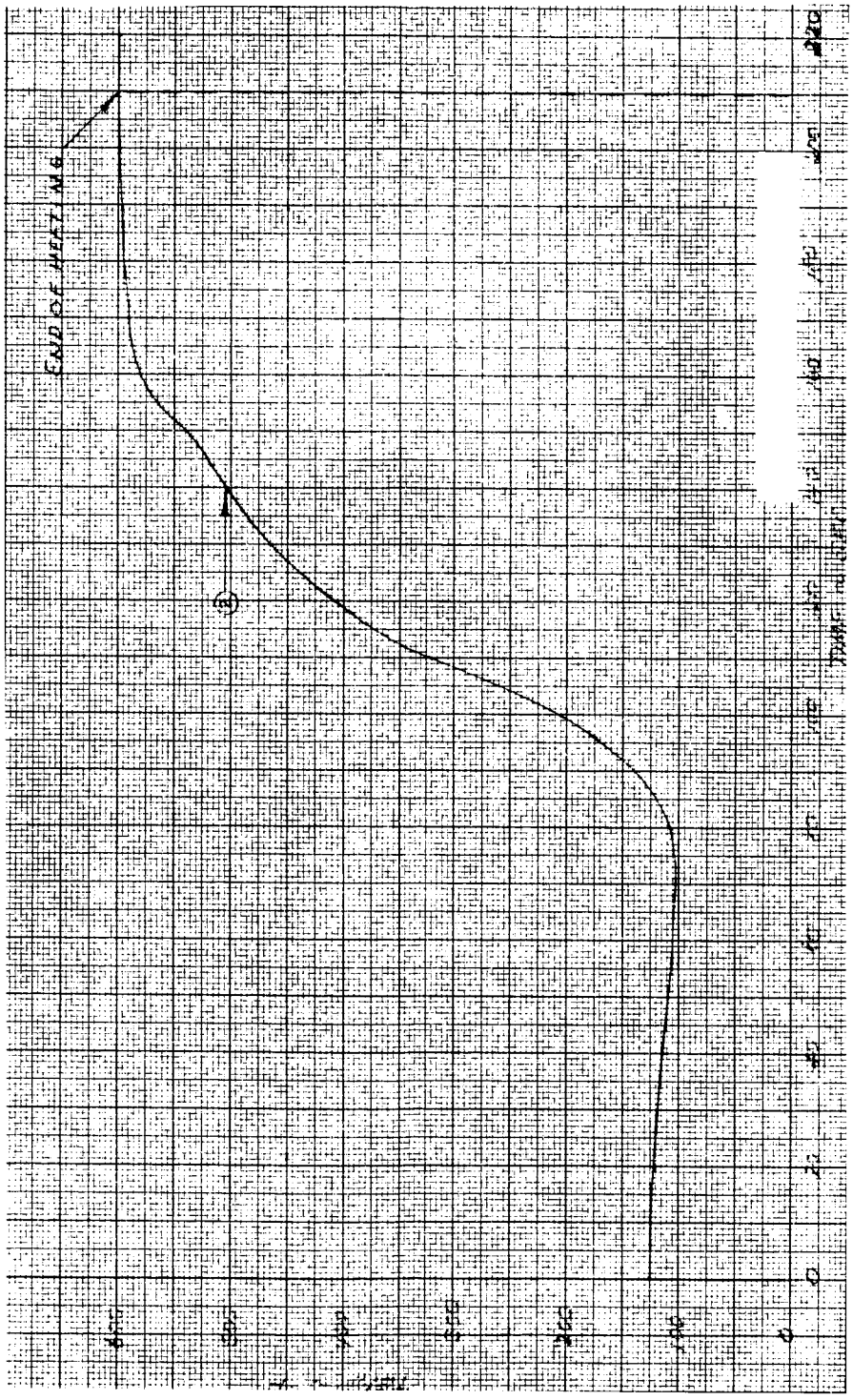

Figure 2-31. Vent Tube Bondline Temperature History of Point 2 for a Saturn V Boost (See Figure 2-29)

[redacted]

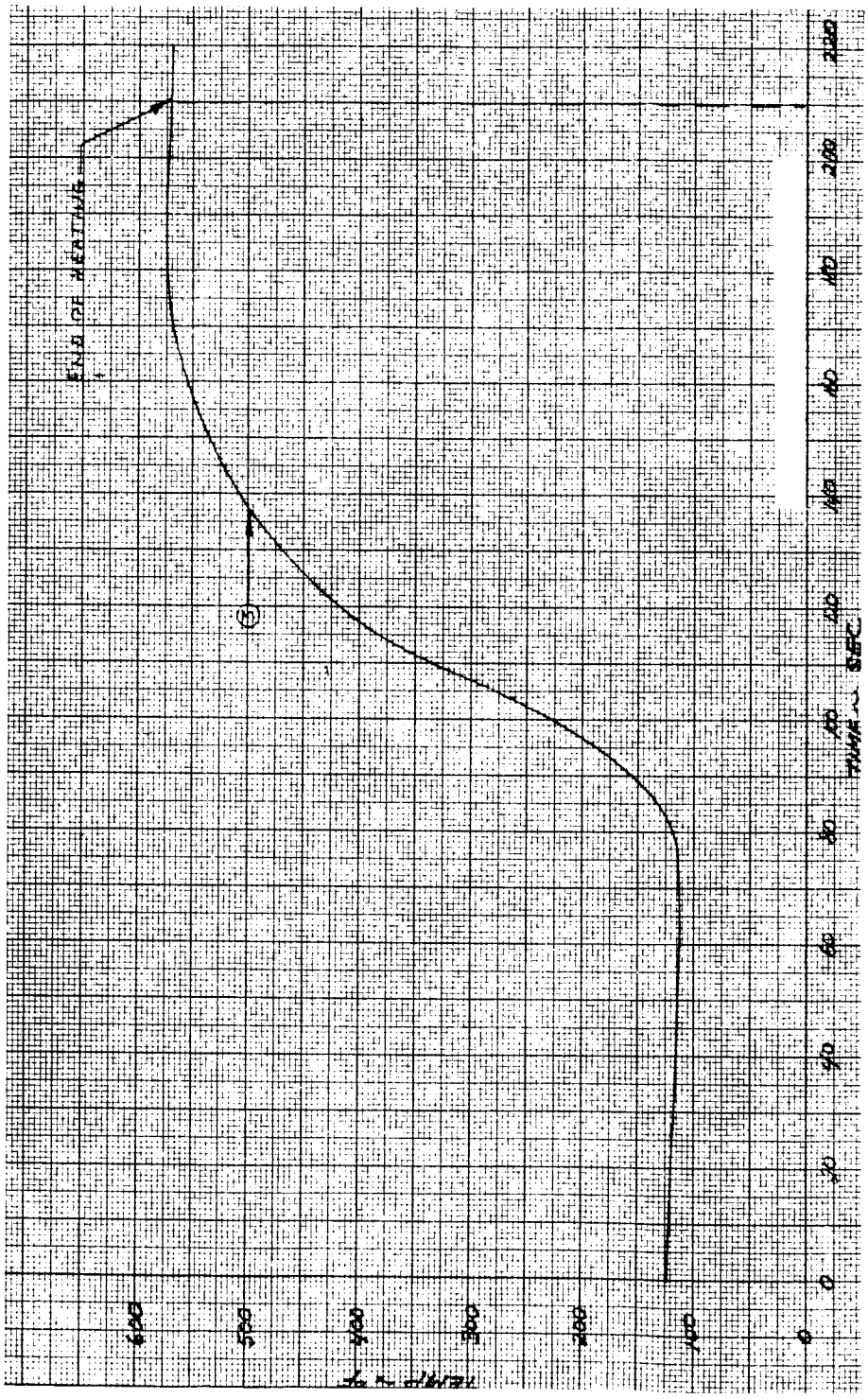

Figure 2-32. Vent Tube Bondline Temperature History of Point 3 for a Saturn V Boost (See Figure 2-29)

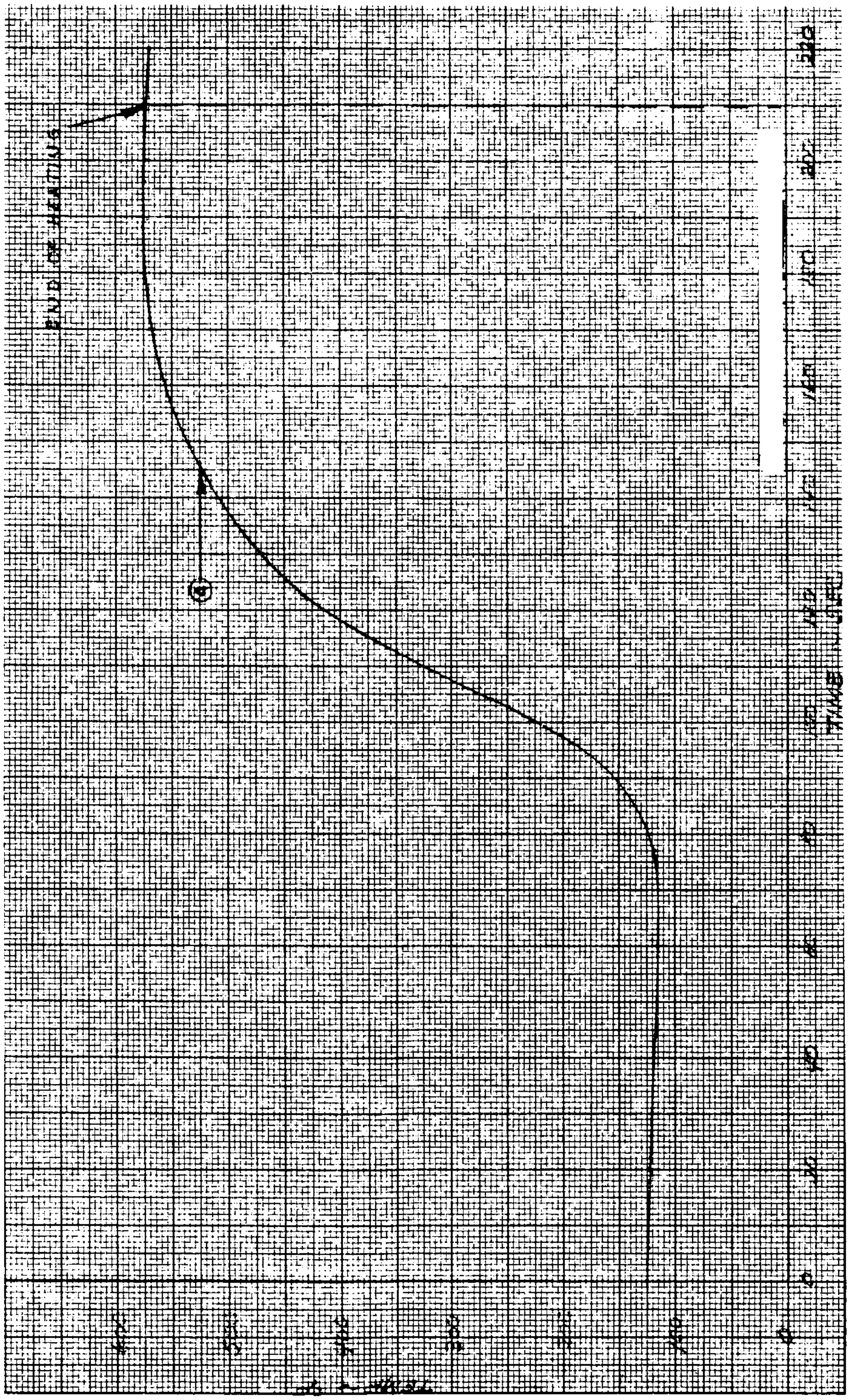

Figure 2-33. Vent Tube Bondline Temperature History of Point 4 for a Saturn V Boost (See Figure 2-29)

[redacted]

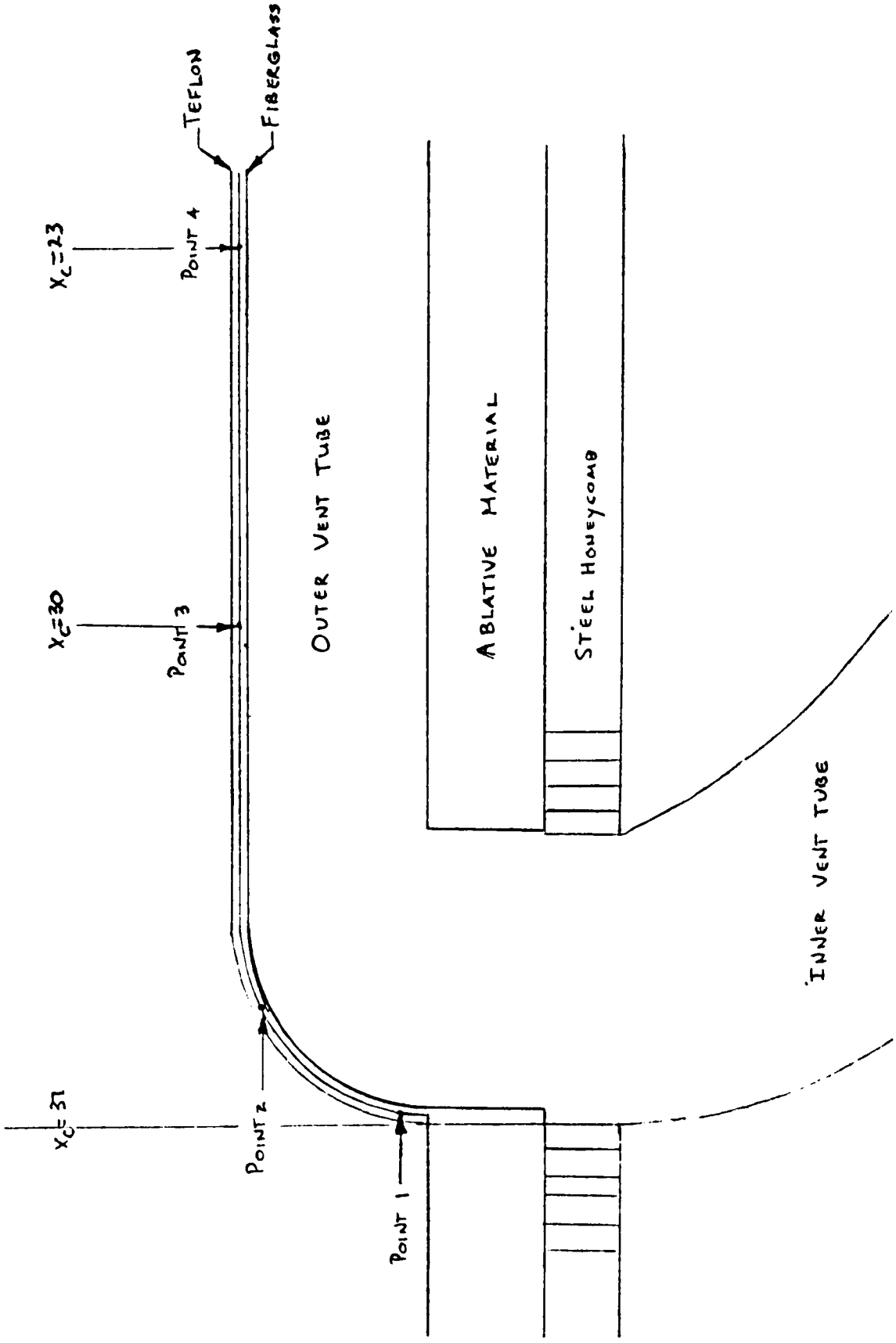

Figure 2-34. Command Module Air Vent System Sketch

[redacted]

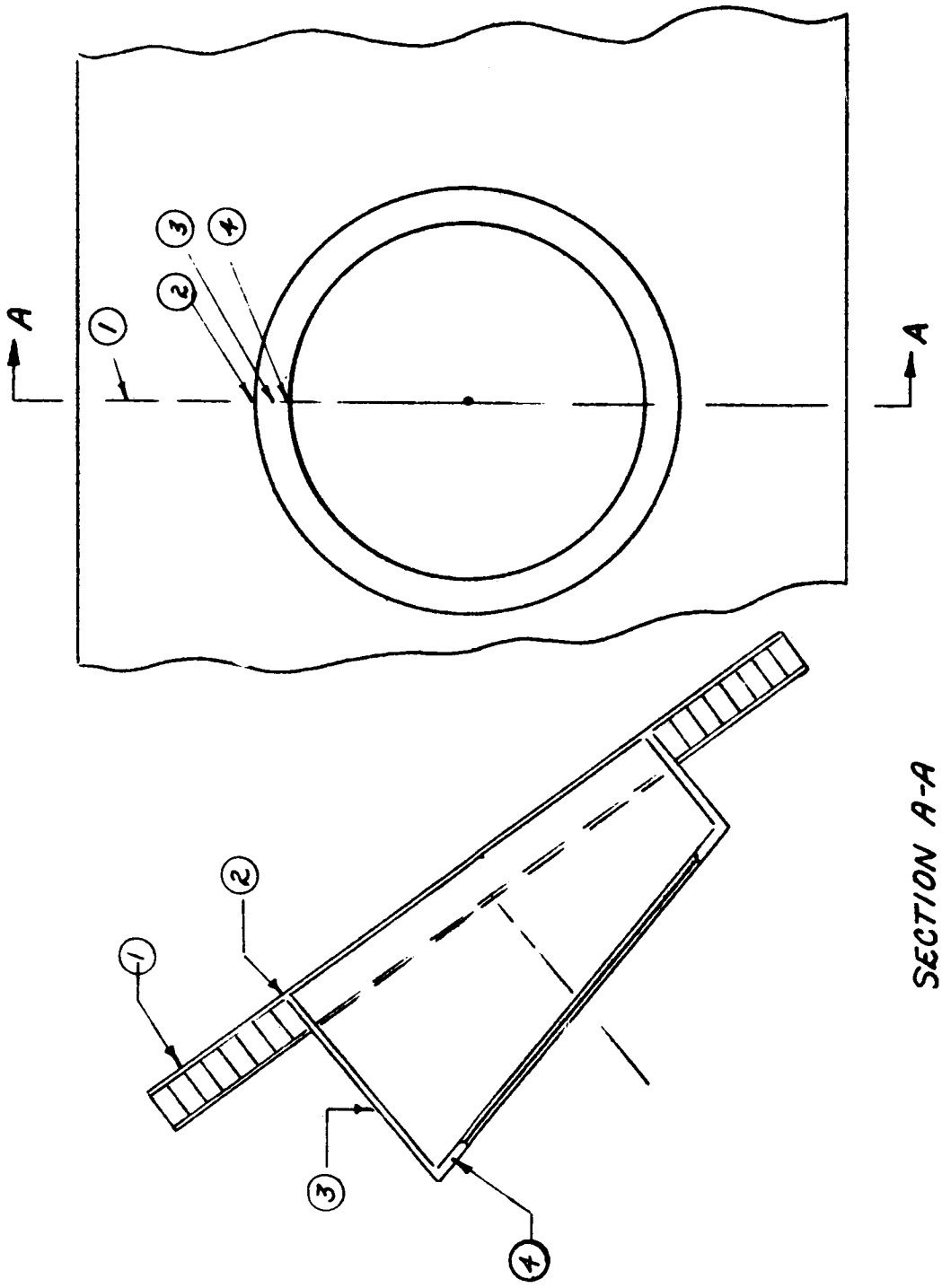

Figure 2-35. Typical Yaw Engine Mounting Can Configuration

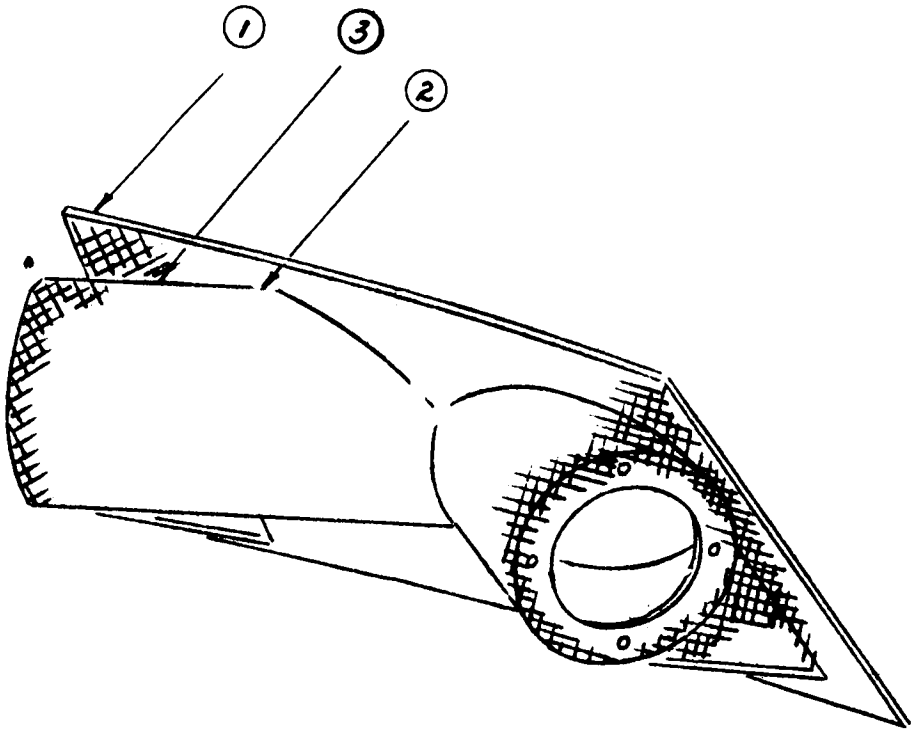

Figure 2-36. Typical Roll Engine Cast Mount Configuration

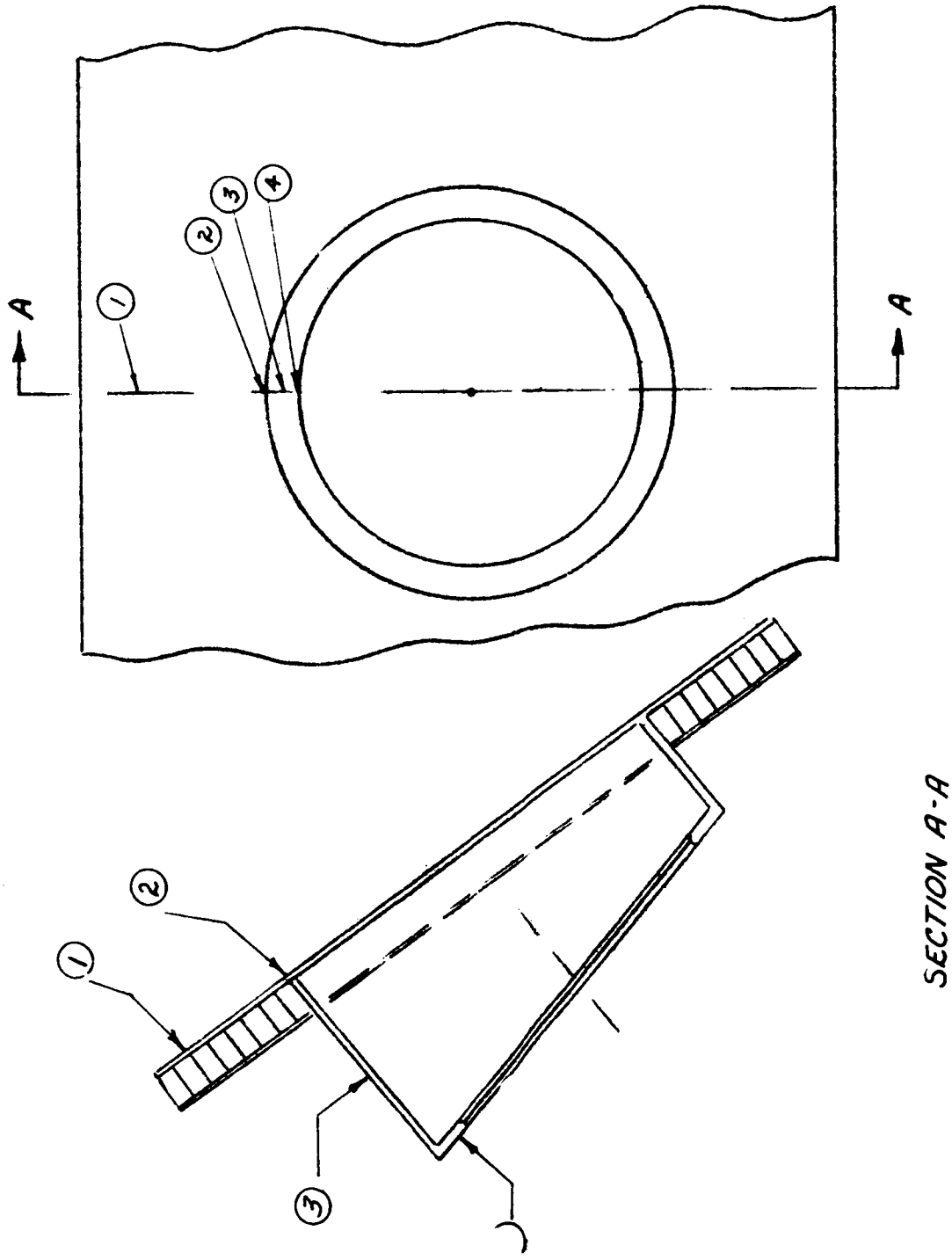

Figure 2-37. Typical Aft Pitch Engine Mounting Can Configuration

[redacted]

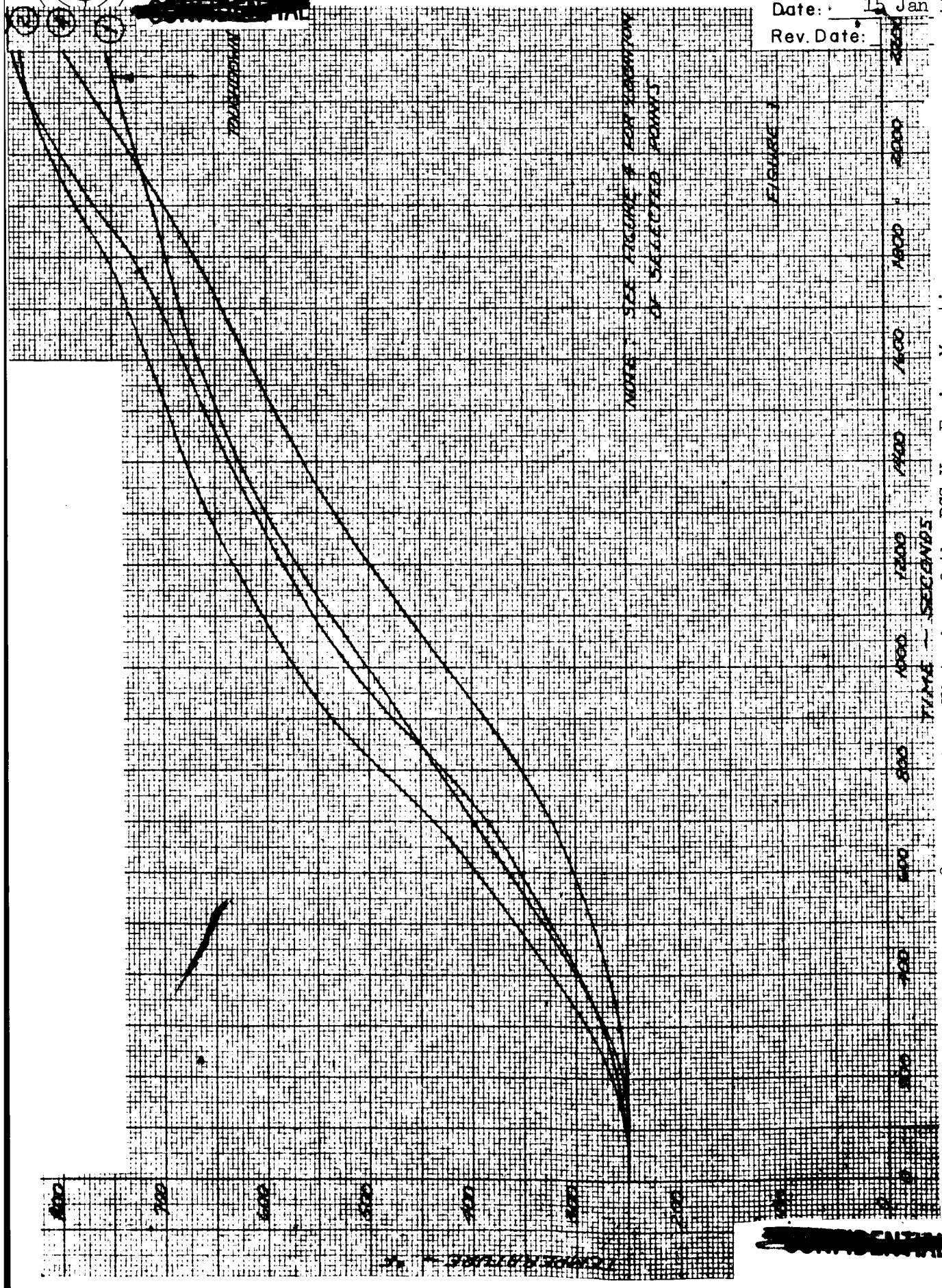

Figure 2-38. Temperature Histories of the RCS Yaw Engine Mounting Structure Reentry Trajectory HSE-3A

[redacted]

[redacted]

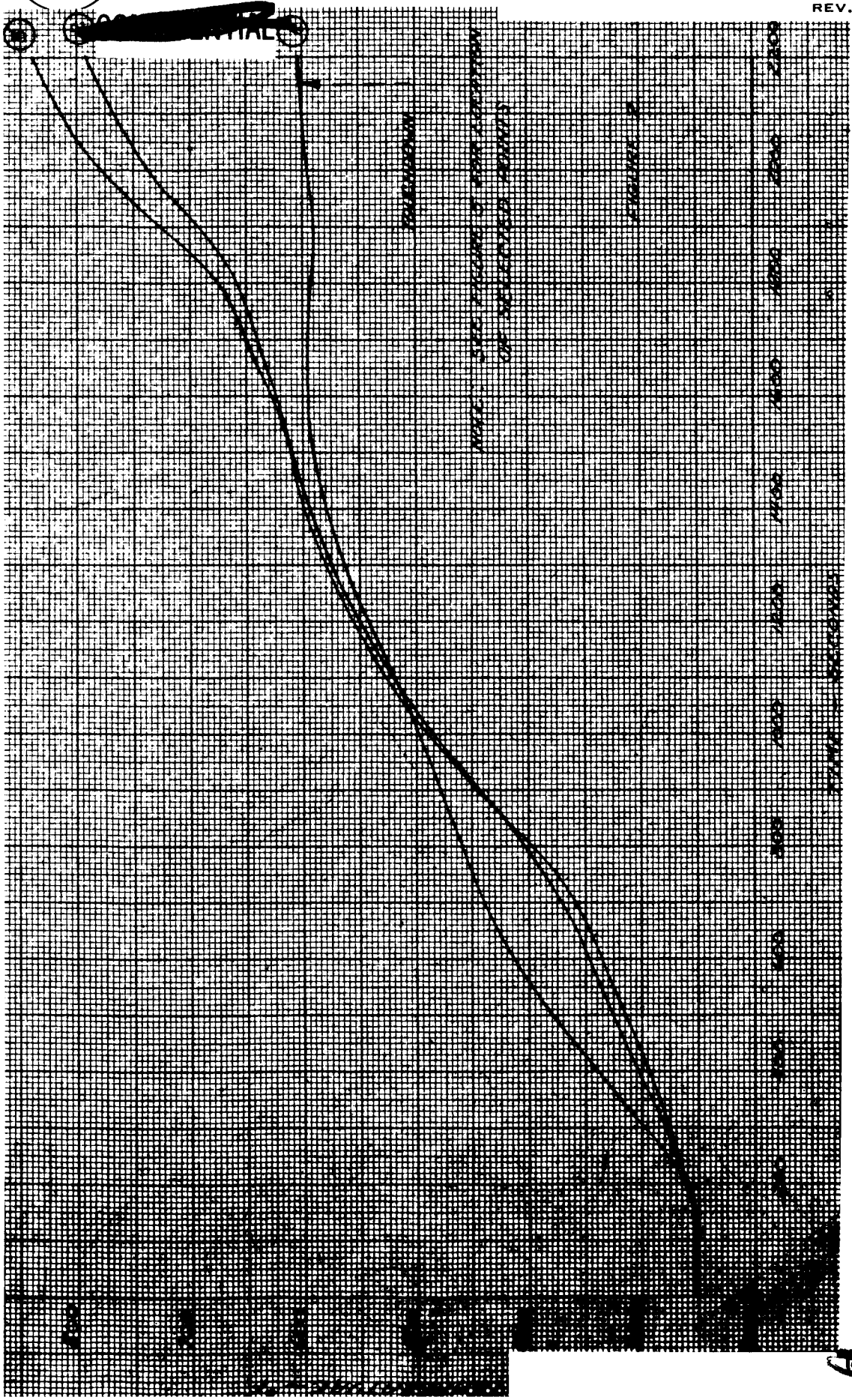

Figure 2-39. Temperature Histories of the RCS Engine Mounting Structure Reentry Trajectory, HSE-3A (Roll Engine) (Sheet 1 of 2)

[redacted]

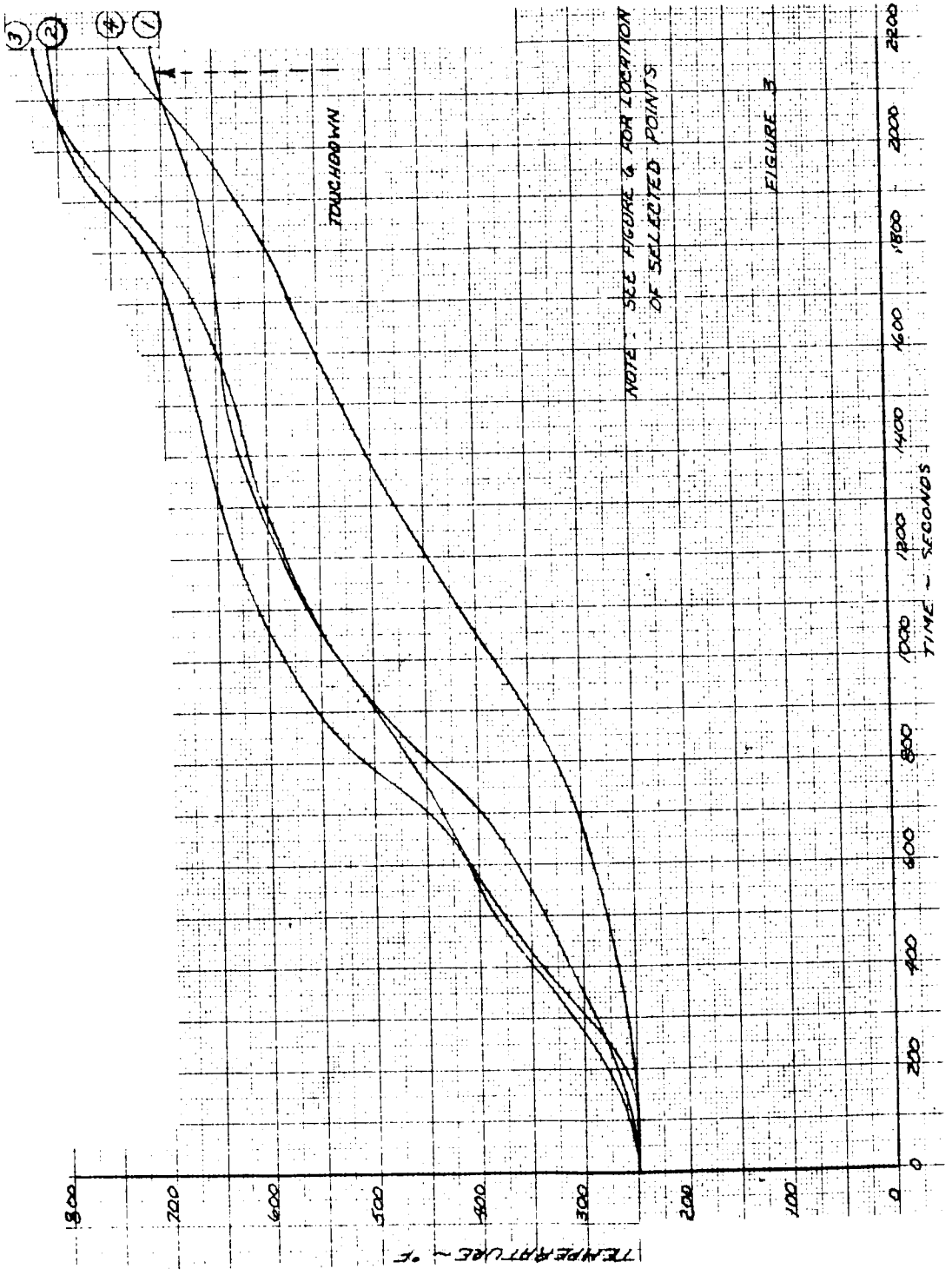

Figure 2-39. Temperature Histories of the RCS Engine Mounting Structure Reentry Trajectory HSE-3A (AFT Pitch Engine) (Sheet 2 of 2)

[redacted]

[redacted]

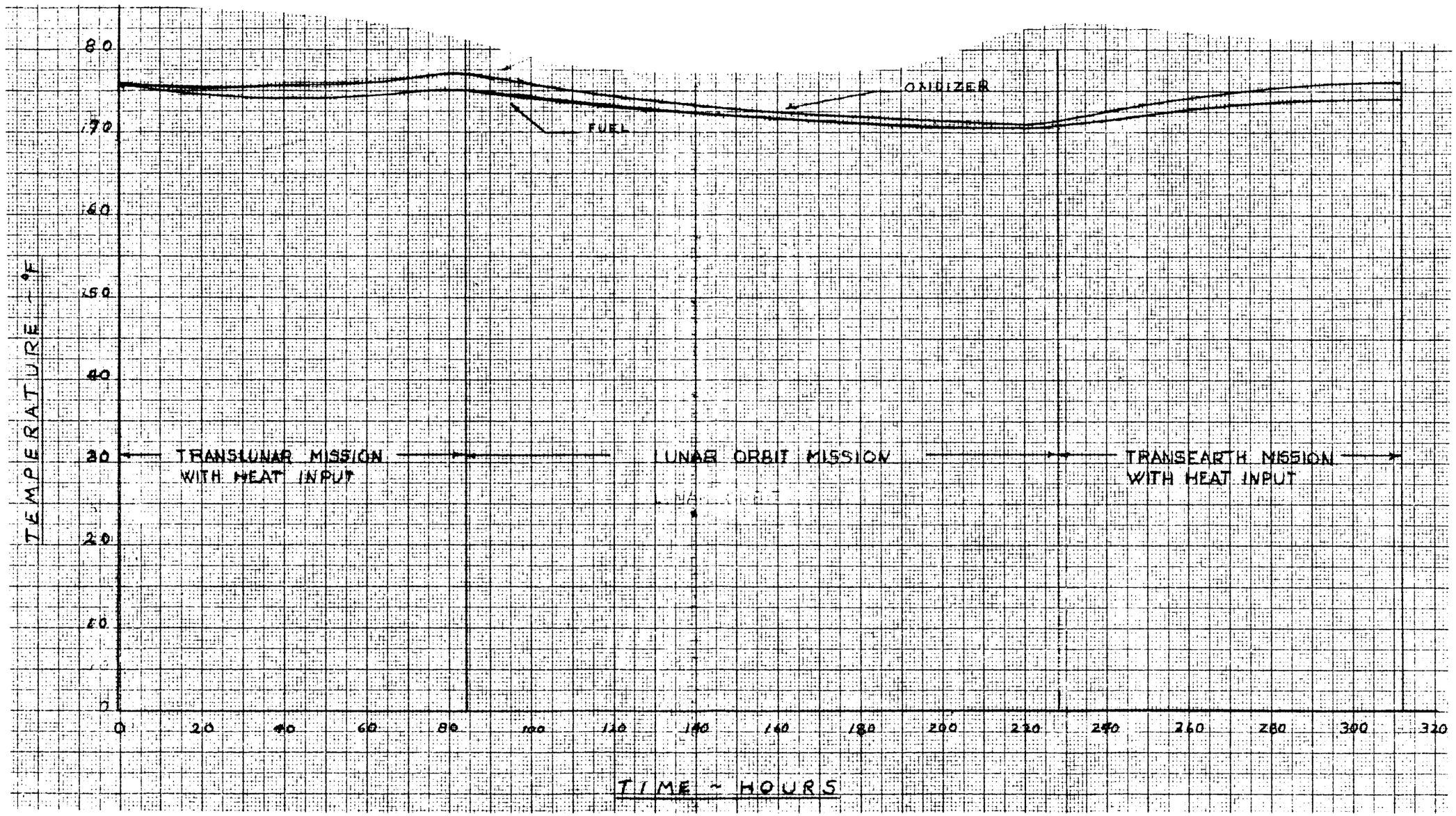

Figure 2-40. Command Module/RCS Temperatures (Helium Tanks During Space Flight - Hot Extreme) (Sheet 3 of 5)

[redacted]

[redacted]

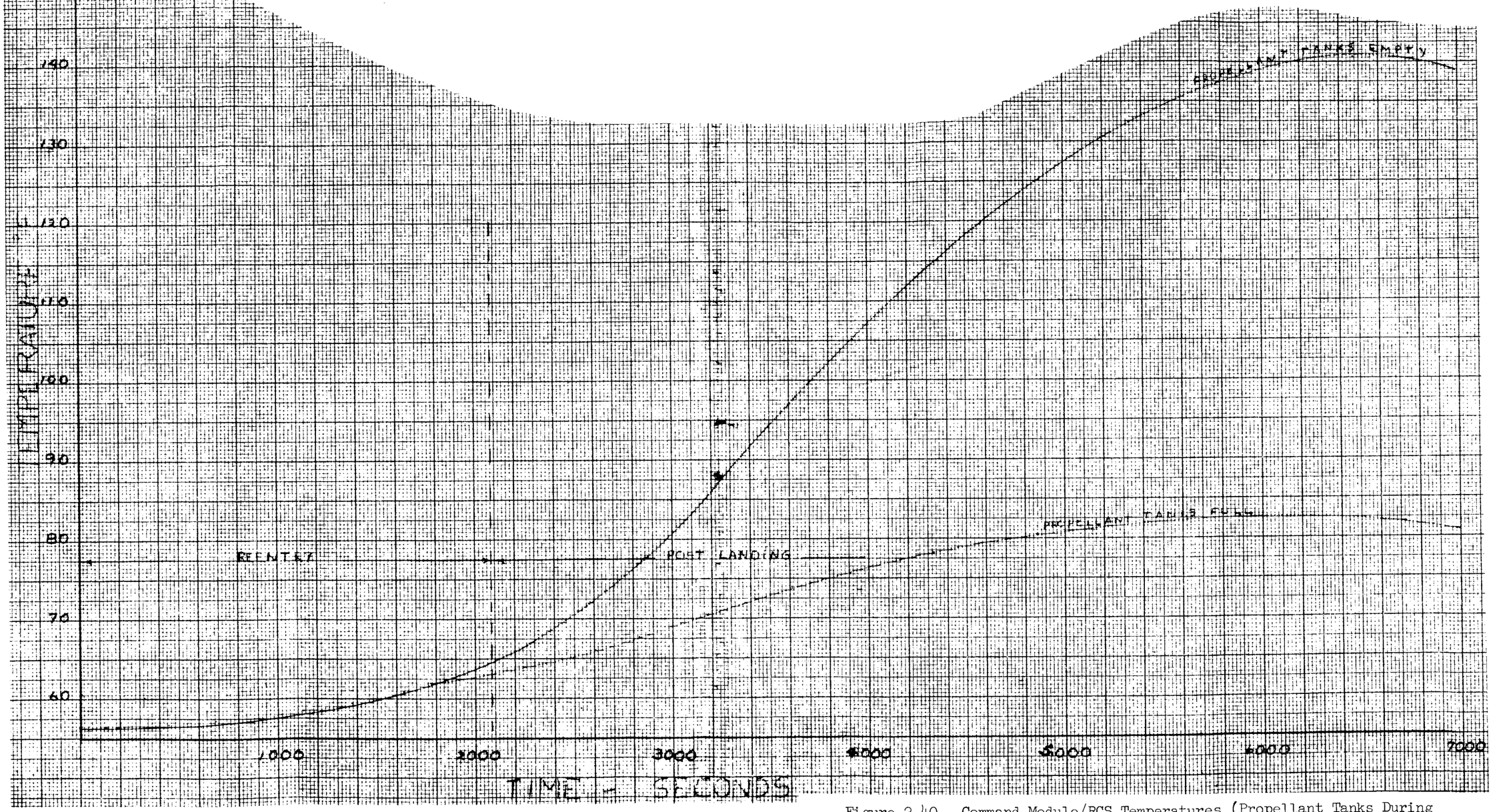

Figure 2-40. Command Module/RCS Temperatures (Propellant Tanks During Reentry) (Sheet 4 of 5)

[redacted]

[redacted]

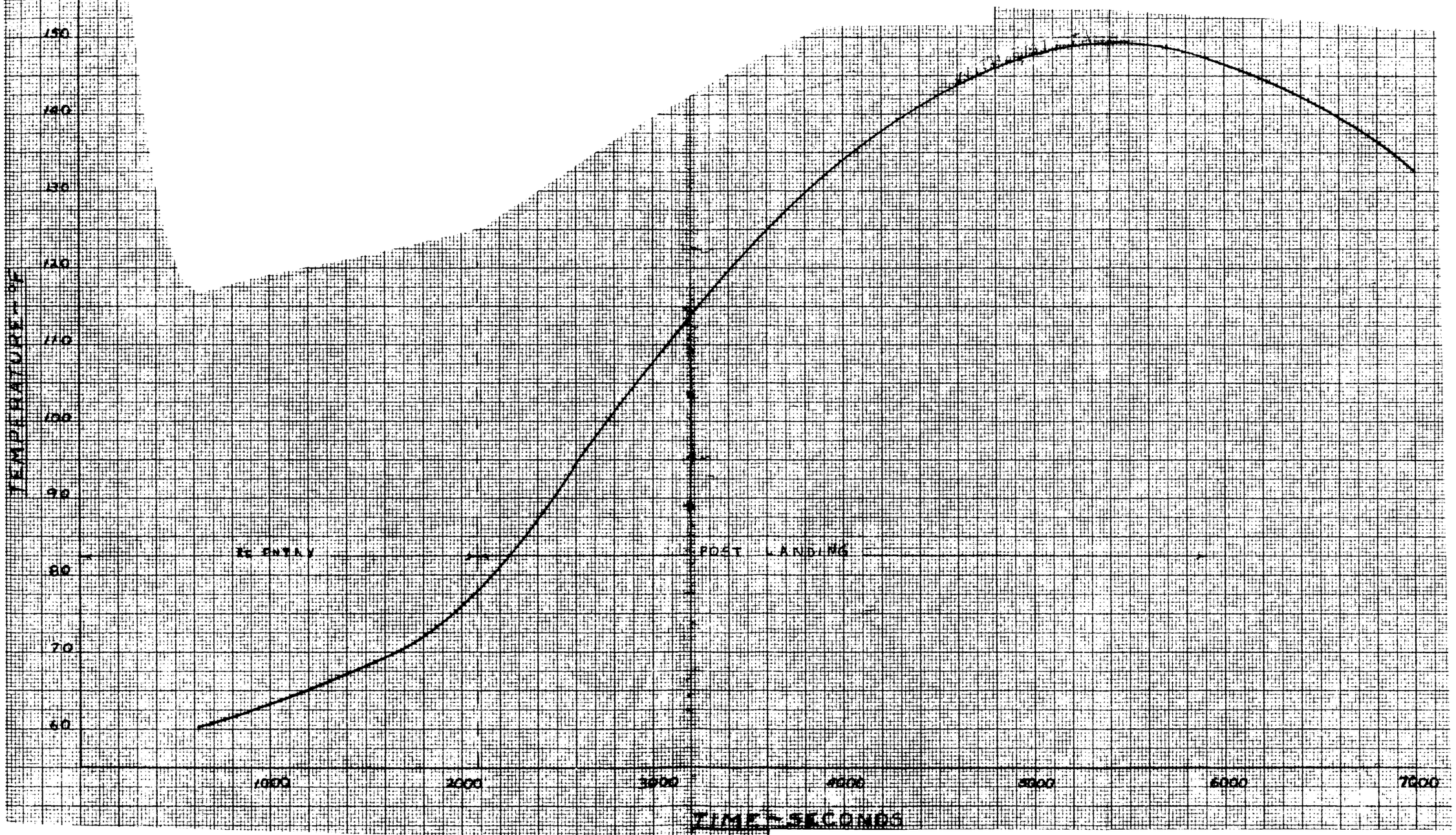

Figure 2-40. Command Module/RCS Temperatures (Propellant Lines During Reentry) (Sheet 5 of 5)

[redacted]

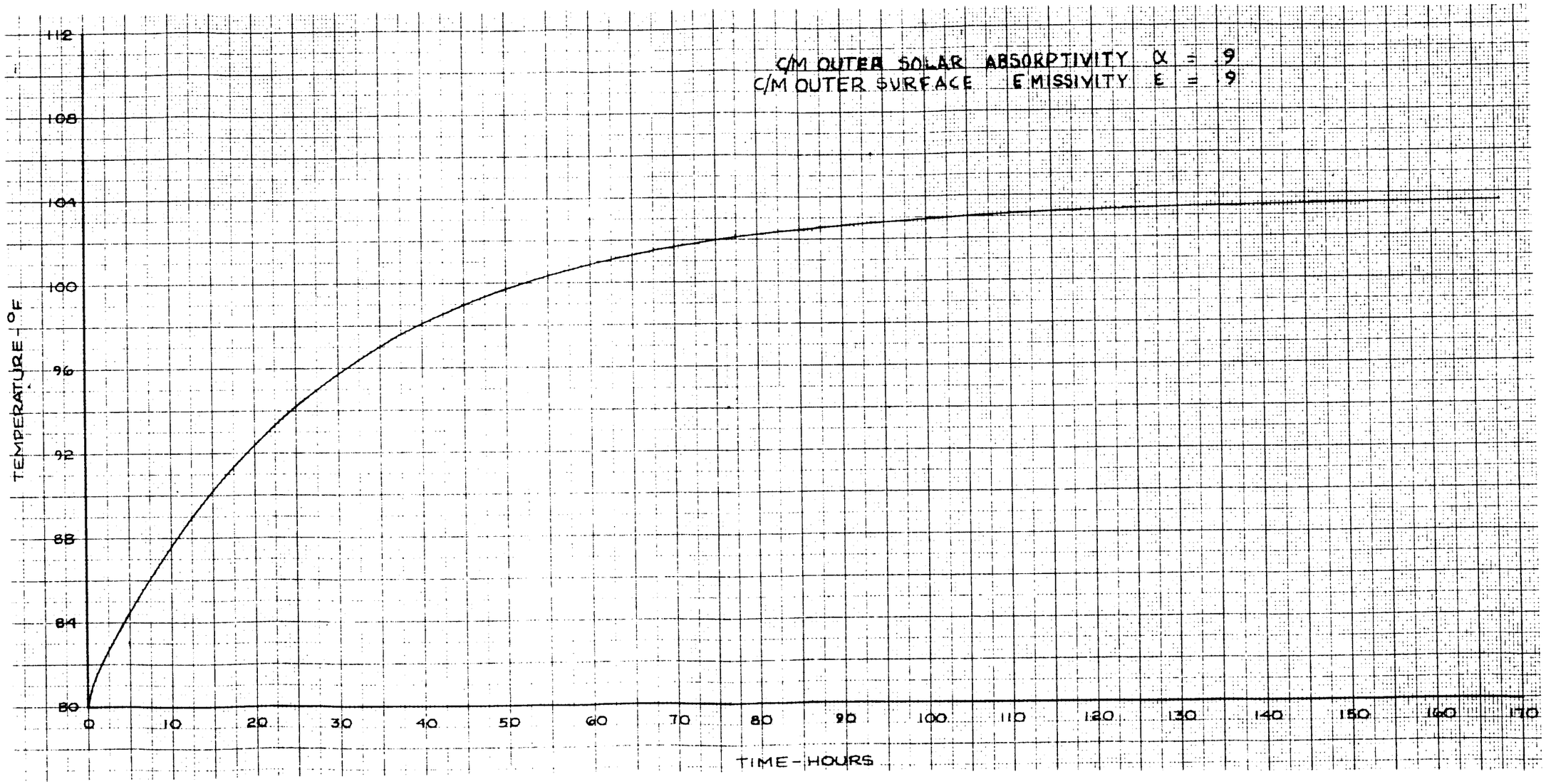

Figure 2-41. Command Module/RCS Propellant Tanks Temperature History

[redacted]

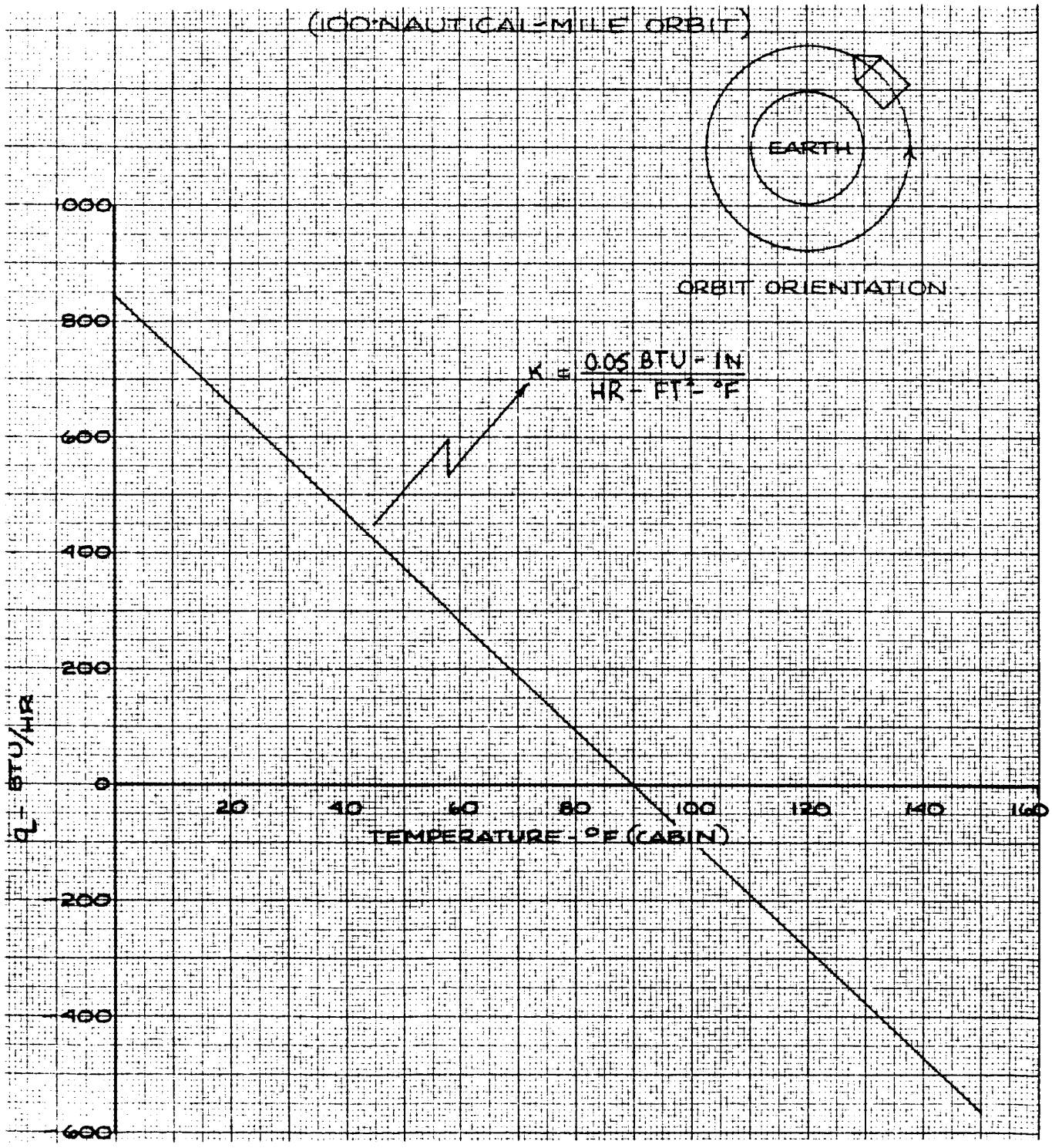

Figure 2-42. Command Module Environmental Heat Exchange, Earth Orbit (Launch Time: June 21, 7 AM)

~~CONFIDENTIAL~~

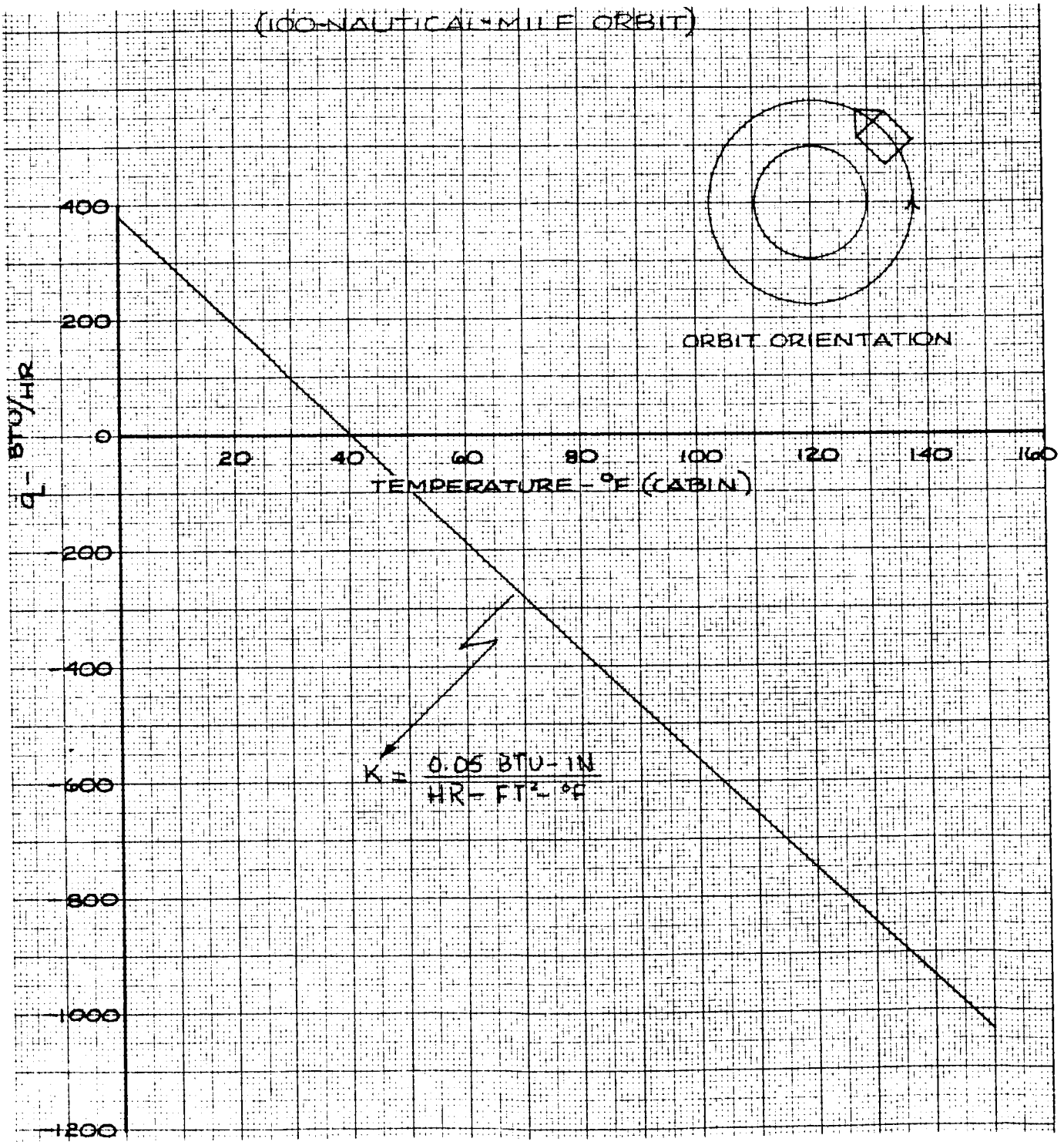

Figure 2-43. Command Module Environmental Heat Exchange, Earth Orbit (Launch Time: June 21, 12 AM)

[redacted]

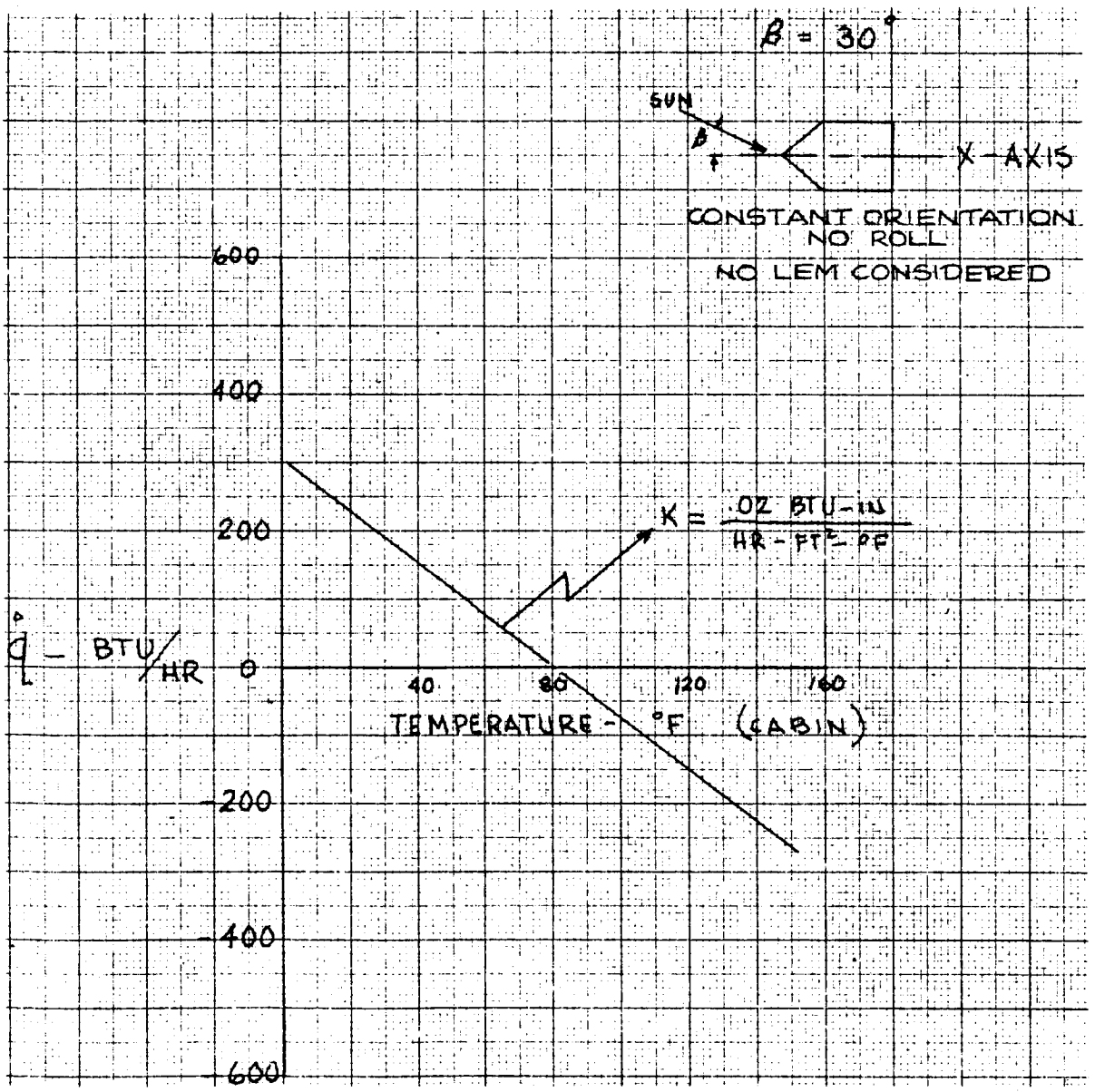

Figure 2-44. Command Module Environmental Heat Exchange, Translunar Mission

[redacted]

[redacted]

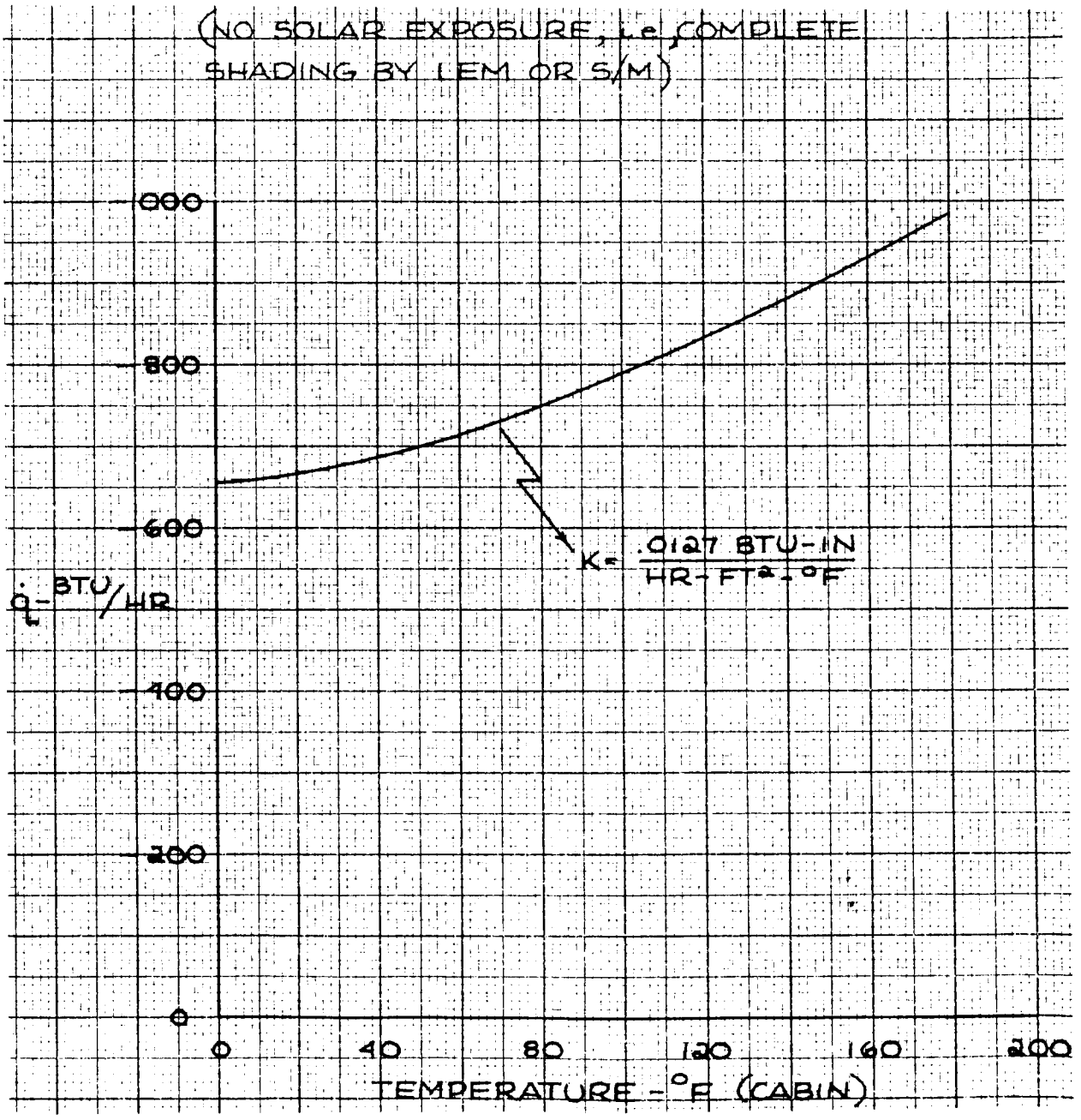

Figure 2-45. Command Module Environmental Heat Exchange, Transit - Cold Case

[redacted]

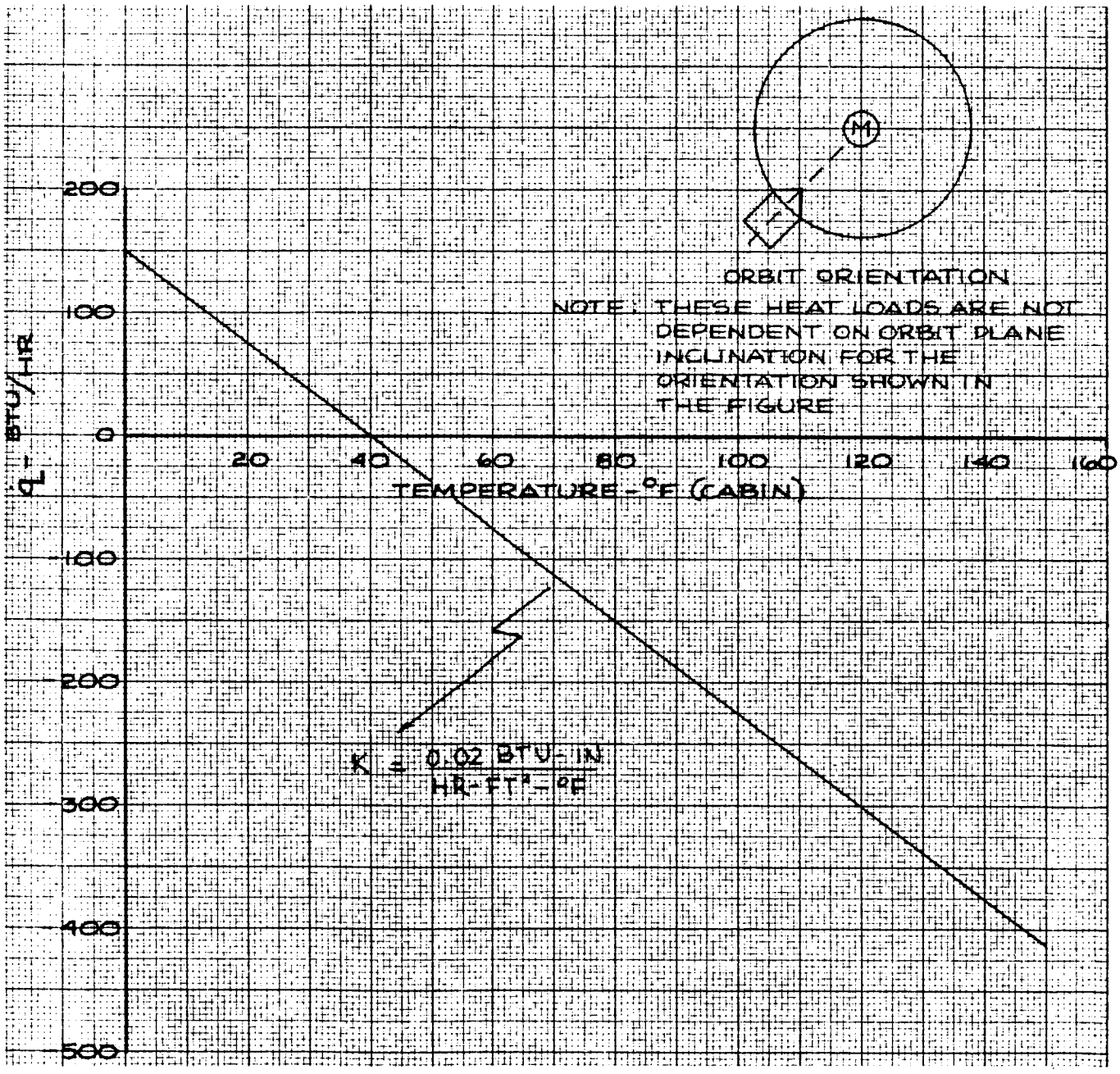

Figure 2-46. Command Module Environmental Heat Exchange, Lunar Orbit

[redacted]

[redacted]

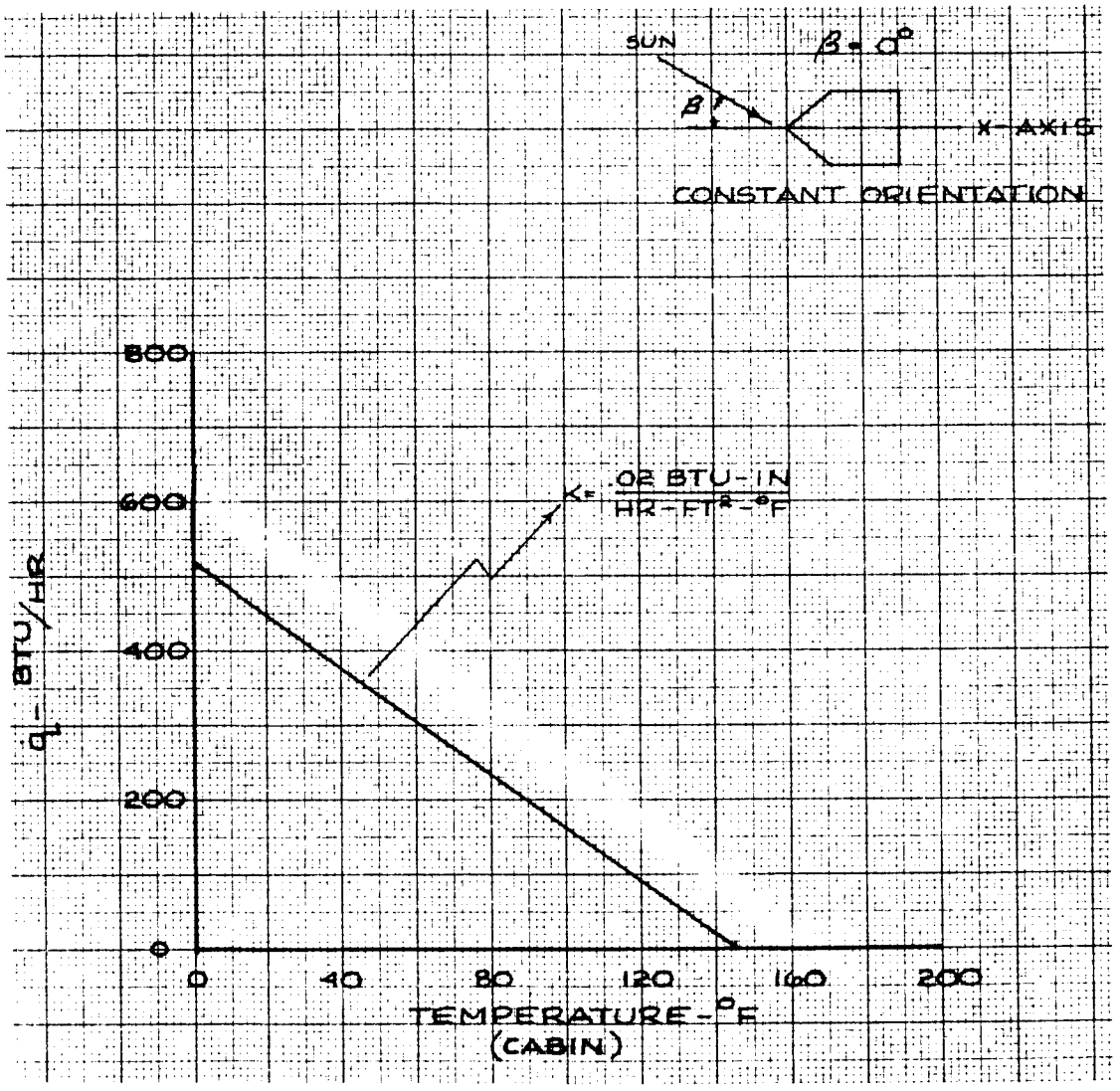

Figure 2-47. Command Module Environmental Heat Exchange, Transearth Mission

[redacted]

[redacted]

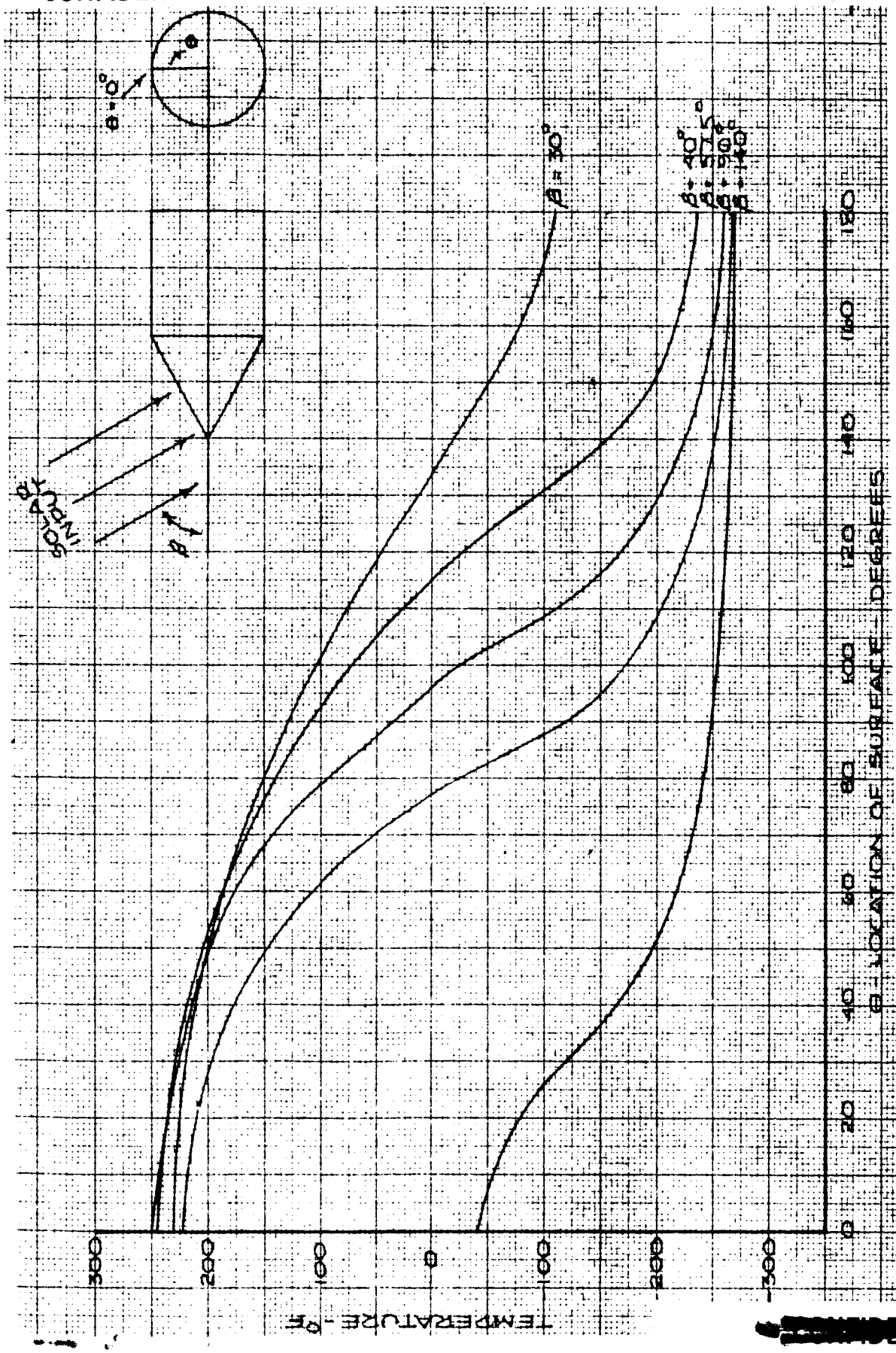

Figure 2-48. Command Module Steady-State Circumferential Temperature Distributions (at X_c = 23)

[redacted]

[redacted]

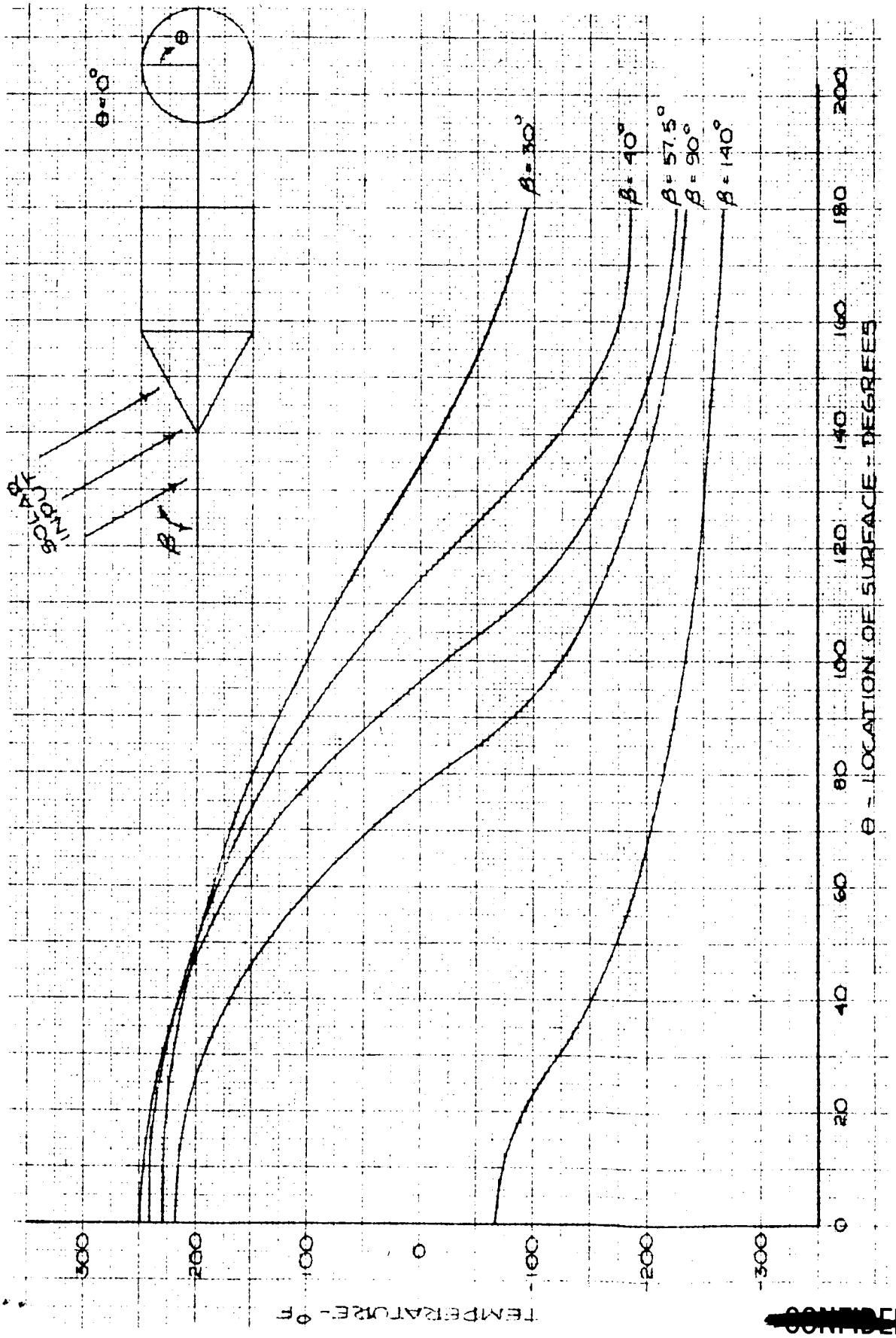

Figure 2-49. Command Module Steady-State Circumferential Temperature Distributions (at X_c = 112)

[redacted]

LOCATIONS OF REPORTED TEMPERATURES

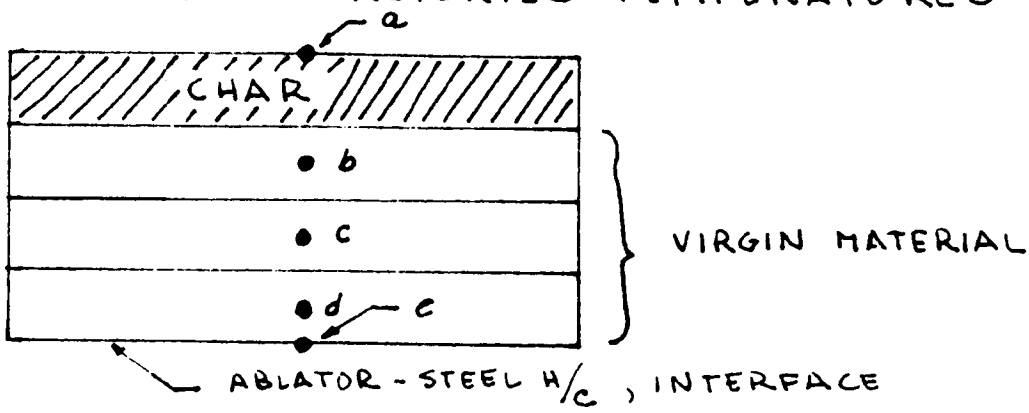

- t = TOTAL ABLATOR THICKNESS (CHAR AND VIRGIN) AS REPORTED IN "MASTER DIMENSIONS SPECIFICATION APOLLO MD-V14-16-600"
- CHAR THICKNESS ASSUMED CONSTANT 0.2 INCHES AFTER BOOST AS REPORTED IN "MINUTES OF NAA/AVCO TECHNICAL INTERCHANGE MEETING OF 21 AND 22 FEB. 1963."

$a = 0$ (OUTER SURFACE)

$b = (t - .2)\frac{1}{6} + .2$ (INCHES FROM OUTER SURFACE)

$c = (t - .2)\frac{1}{2} + .2$ (INCHES FROM OUTER SURFACE)

$d = (t - .2)\frac{5}{6} + .2$ (INCHES FROM OUTER SURFACE)

$e = t$ (INCHES FROM OUTER SURFACE)

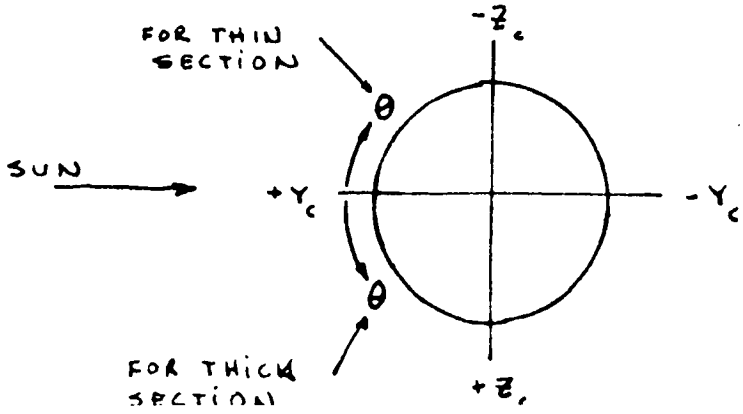

Figure 2-50. Forward Heat Shield Space Flight Transient Circumferential Temperature Distributions

[redacted]

~~CONFIDENTIAL~~

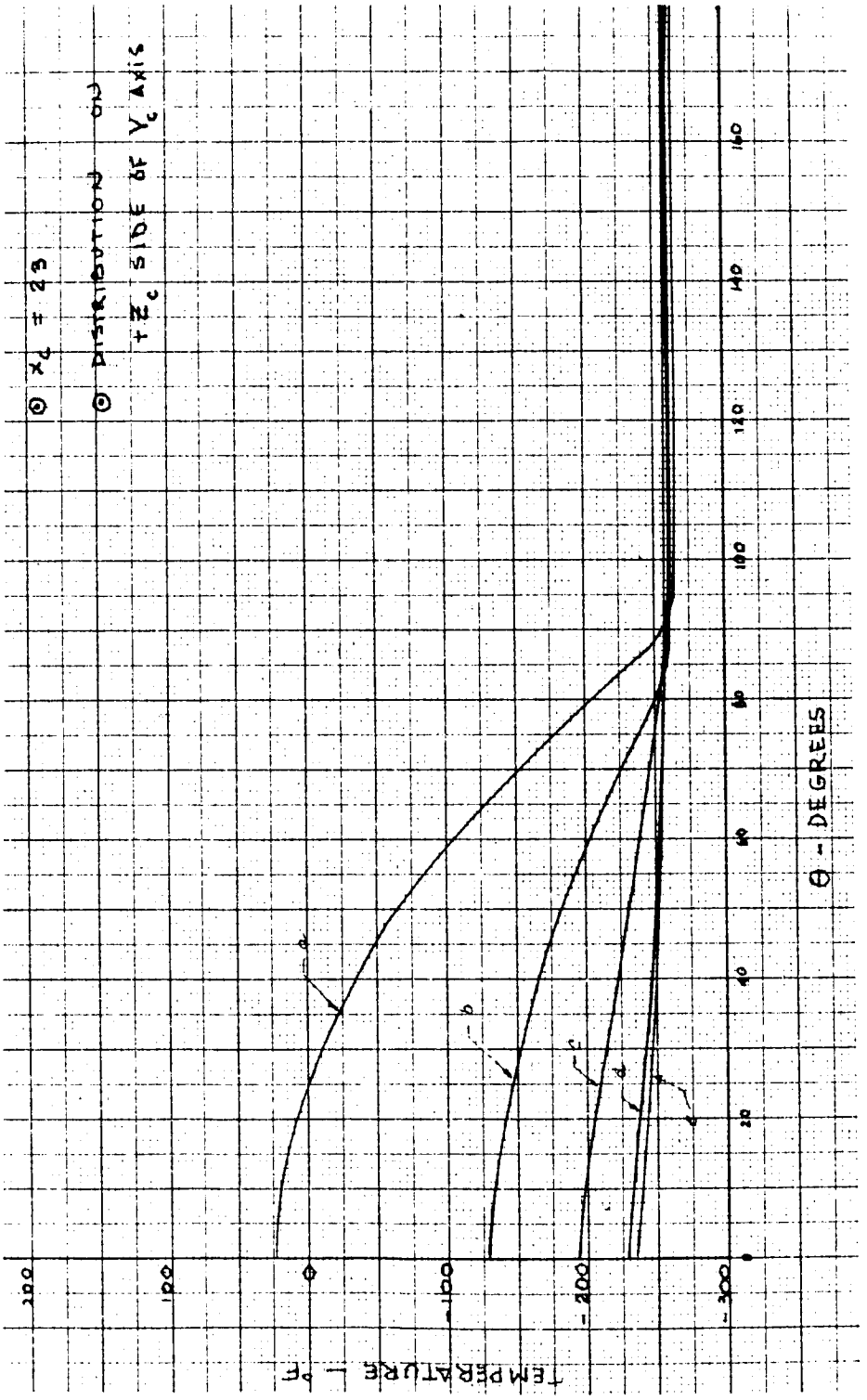

Figure 2-51. Forward Heat Shield Temperature Distribution After Start of Heating (From -260 F at 0.25 Hours) (Sheet 1 of 12)

~~CONFIDENTIAL~~

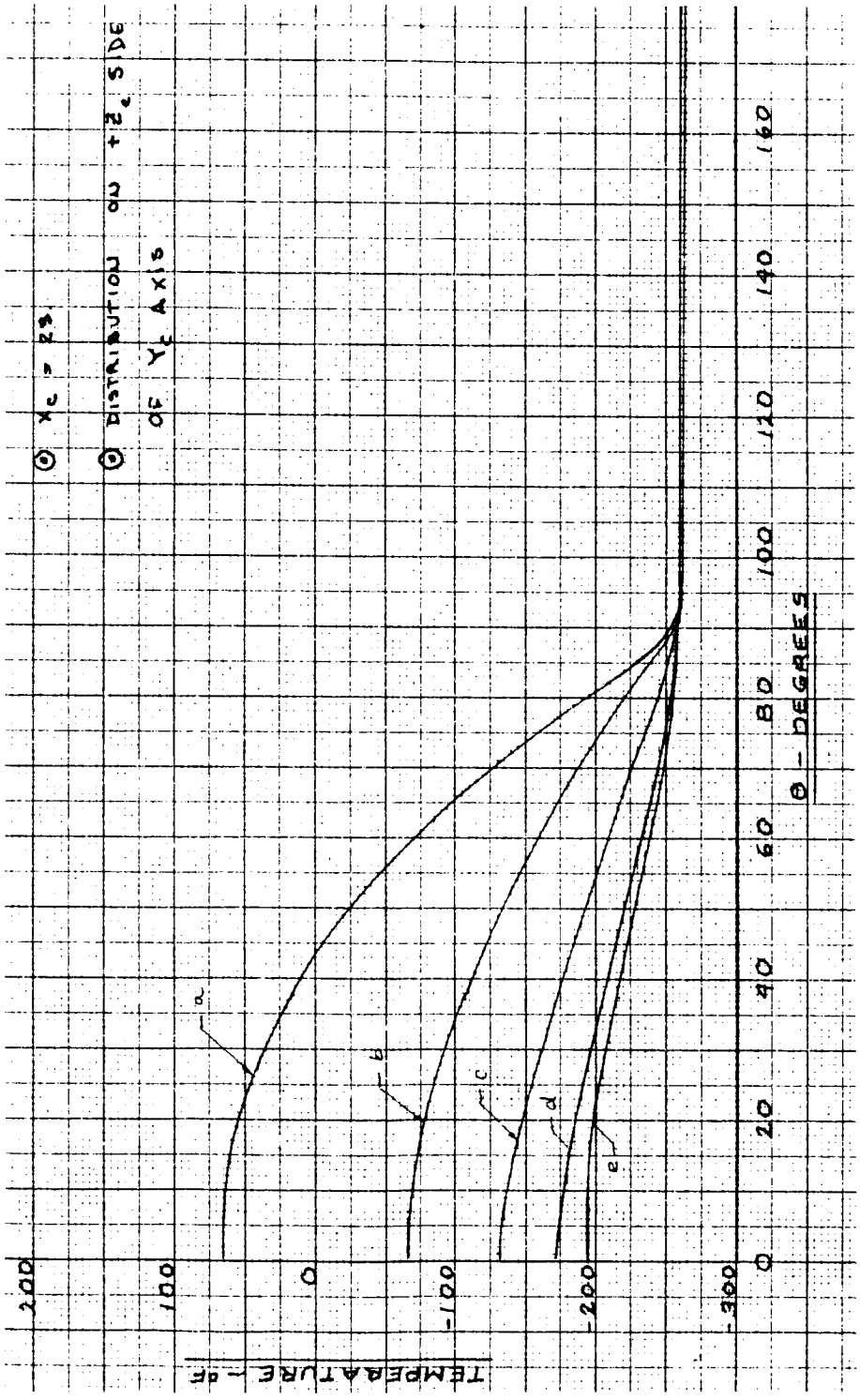

Figure 2-51. Forward Heat Shield Temperature Distribution After Start of Heating (From -260 F at 0.5 Hours) (Sheet 2 of 12)

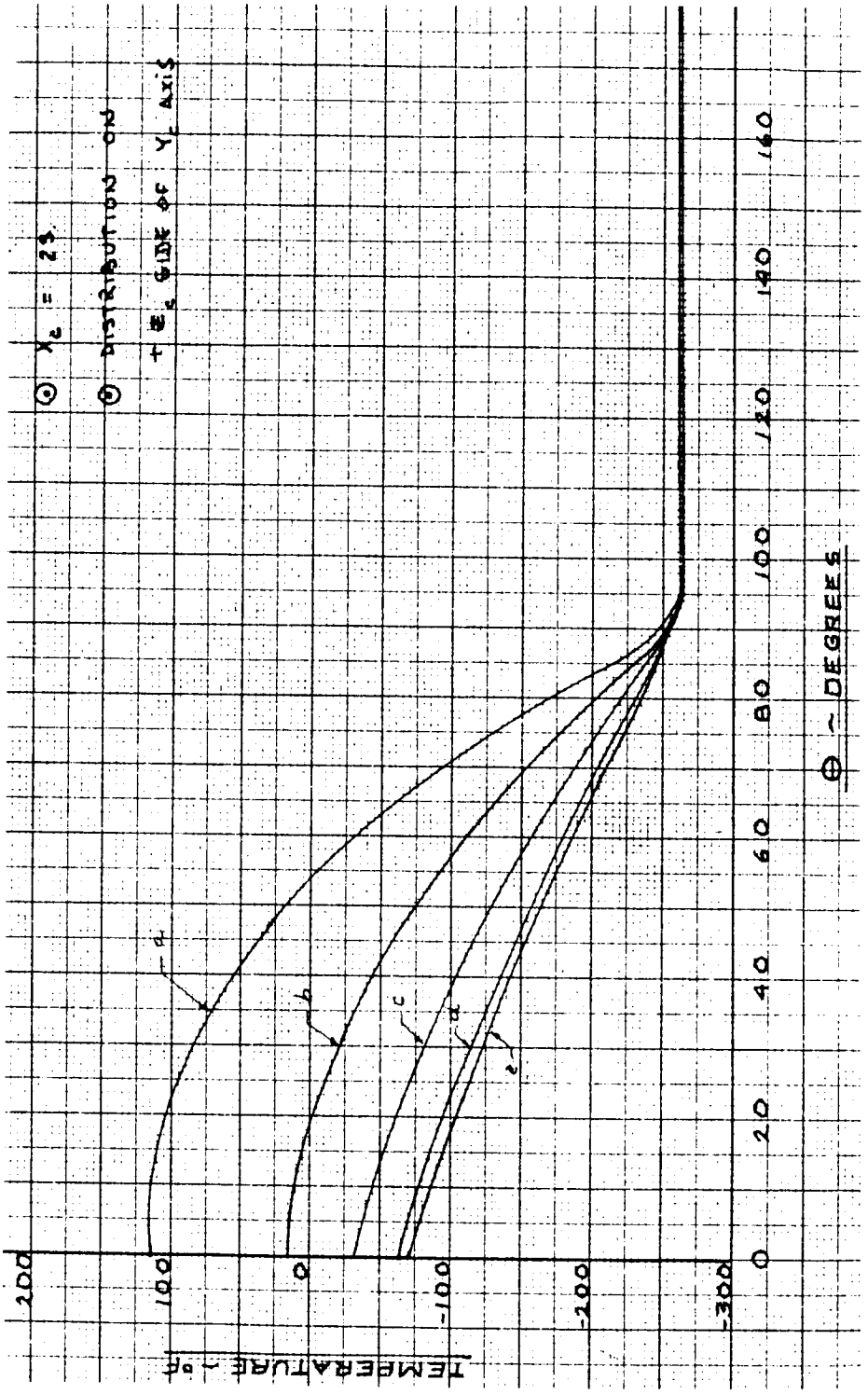

Figure 2-51. Forward Heat Shield Temperature Distribution After Start of Heating (From -260 F at 1.0 Hours) (Sheet 3 of 12)

[redacted]

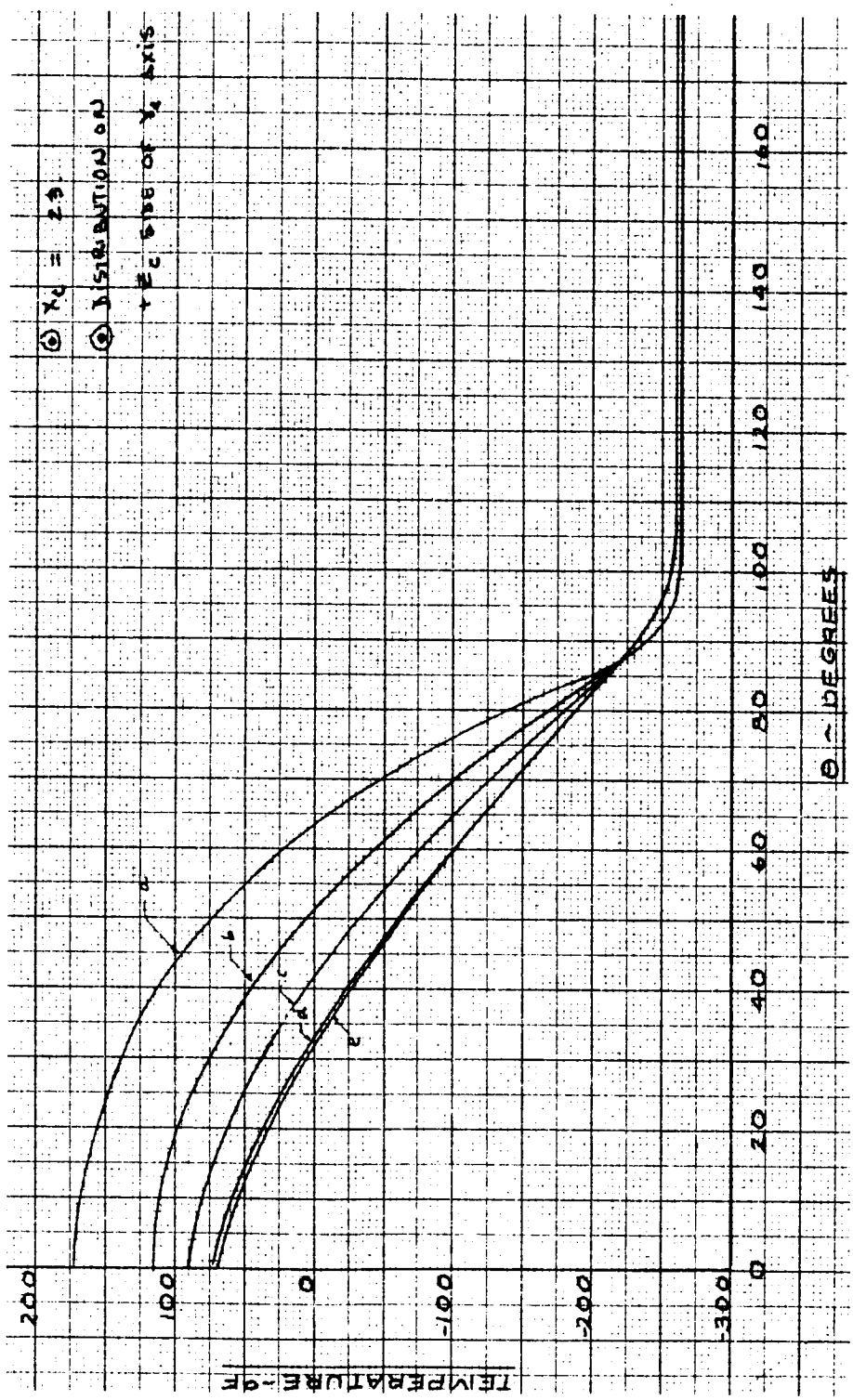

Figure 2-51. Forward Heat Shield Temperature Distribution After Start of Heating (From -260 F at 2.0 Hours) (Sheet 4 of 12)

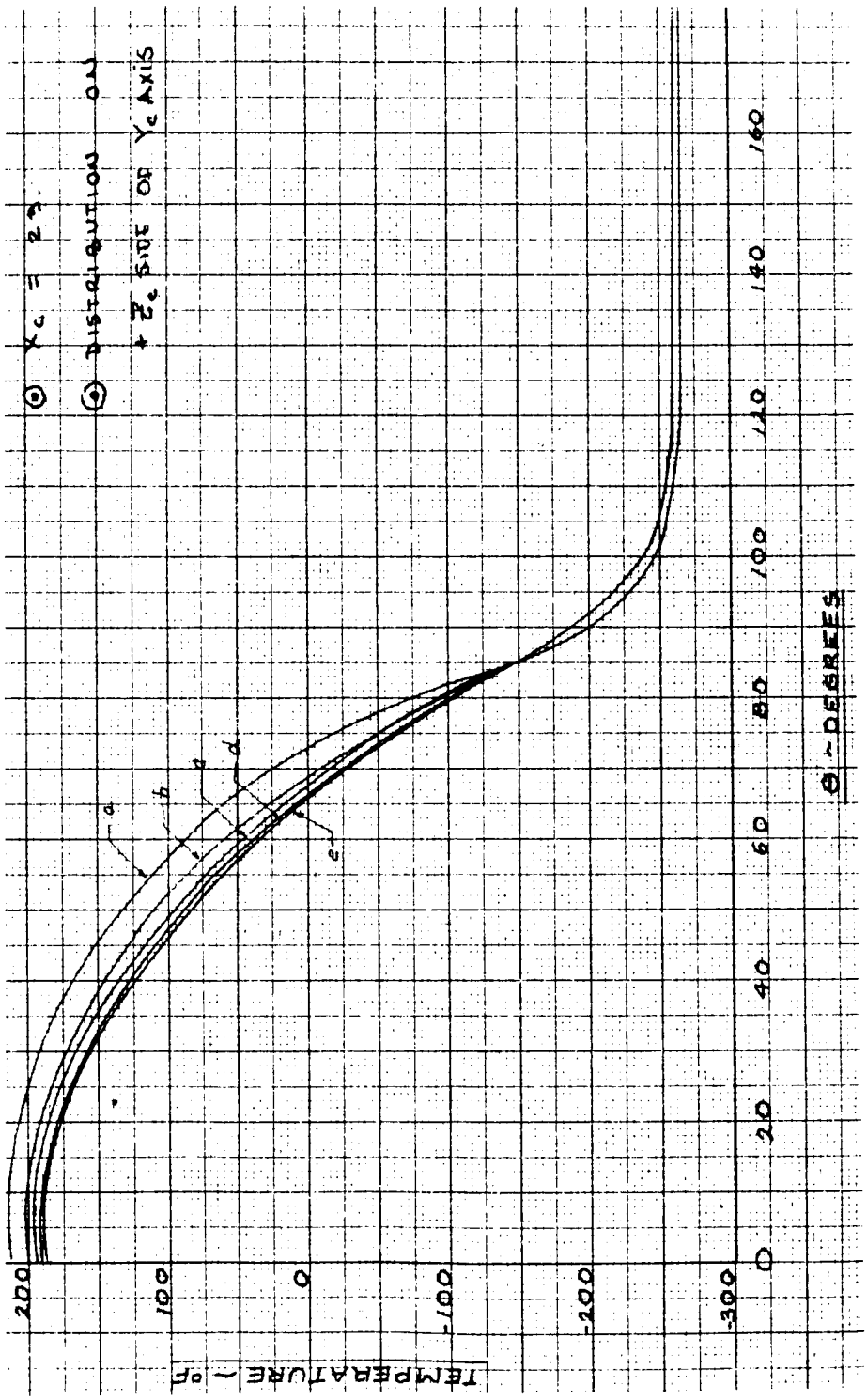

Figure 2-51. Forward Heat Shield Temperature Distribution After Start of Heating (From -260 F at 5.0 Hours) (Sheet 5 of 12)

[redacted]

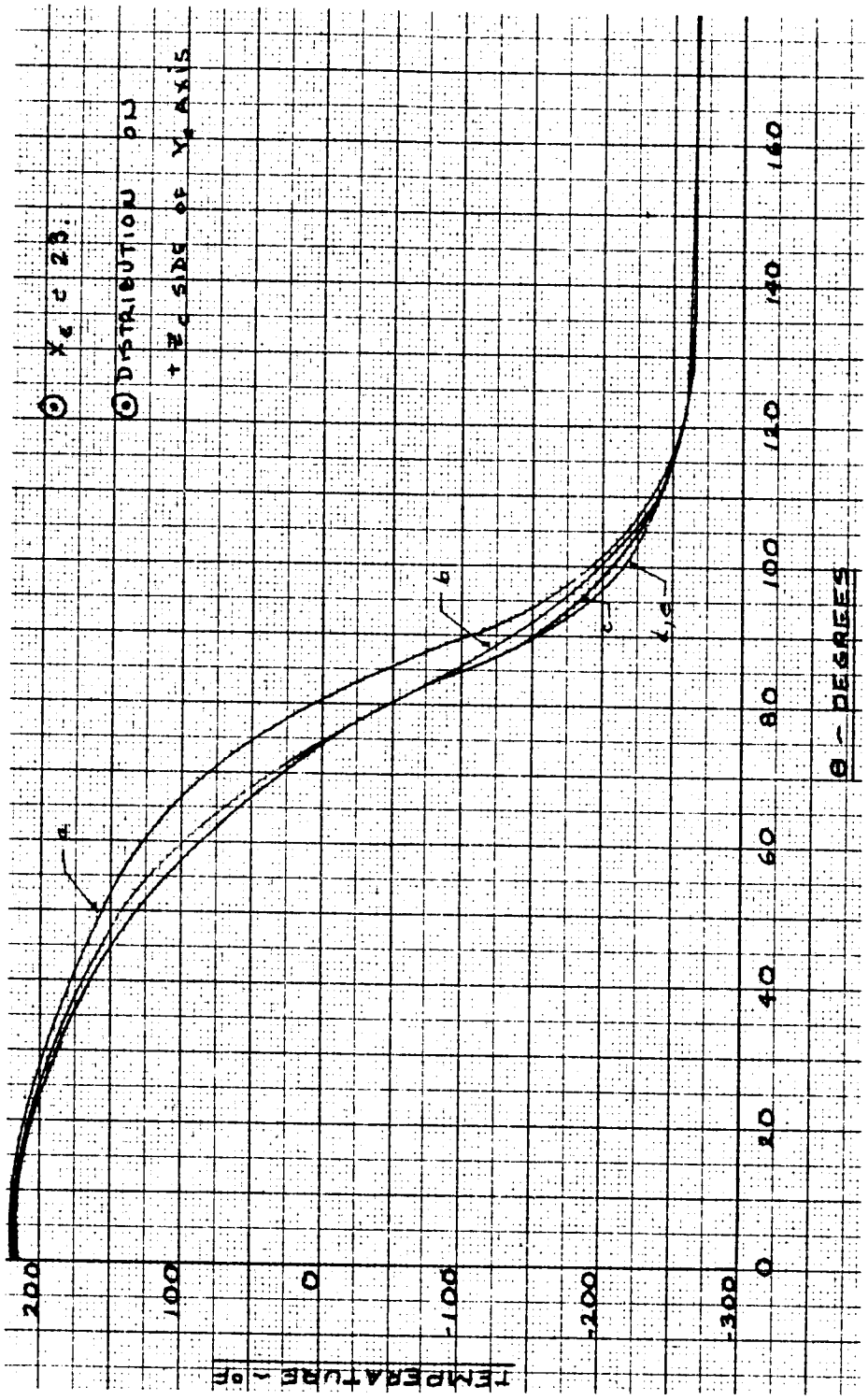

Figure 2-51. Forward Heat Shield Temperature Distribution After Start of Heating (From -260 F at 10.0 Hours) (Sheet 6 of 12)

[redacted]

[redacted]

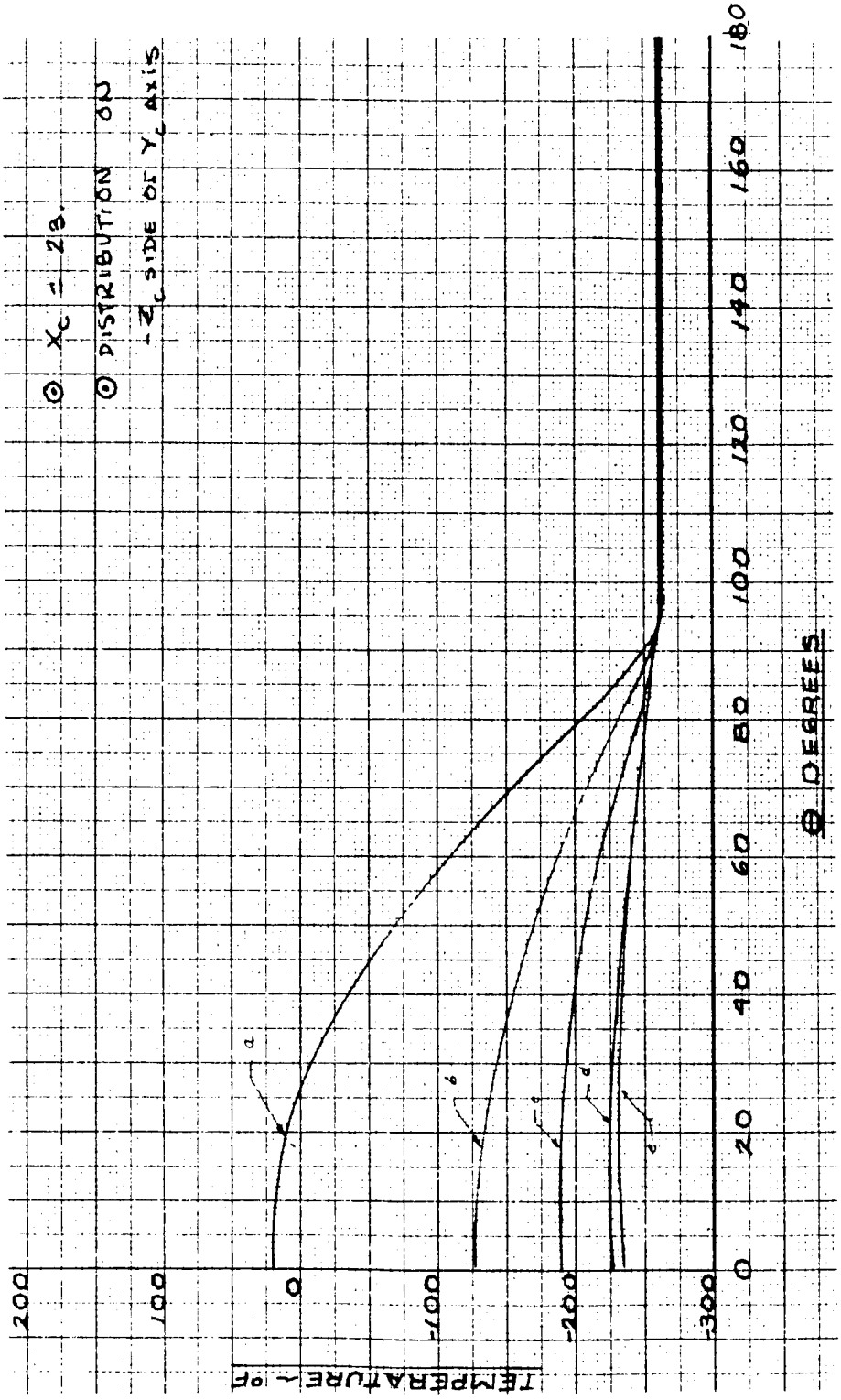

Figure 2-51. Forward Heat Shield Temperature Distribution After Start of Heating (From -260 F at 0.25 Hours) (Sheet 7 of 12)

[redacted]

[redacted]

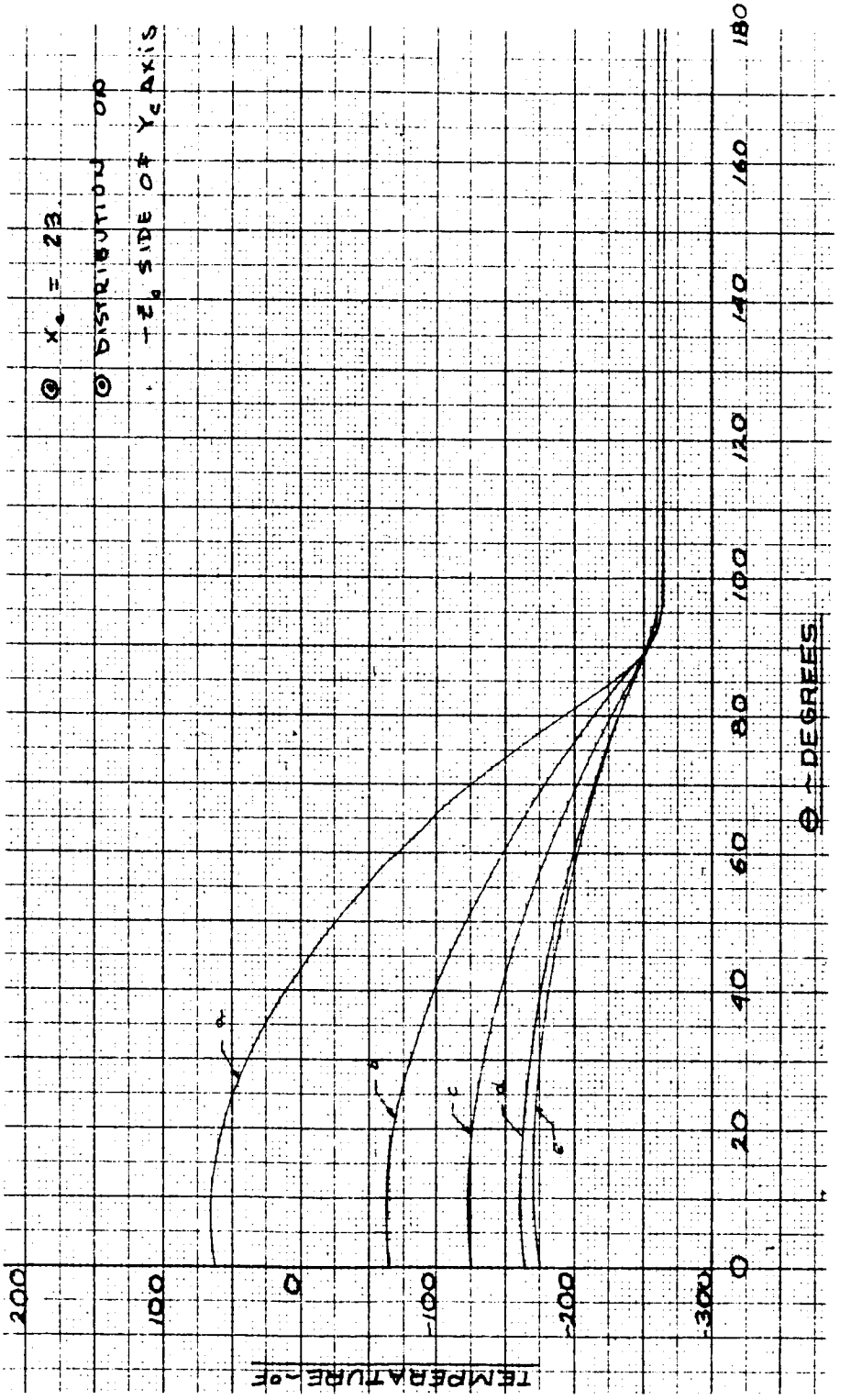

Figure 2-51. Forward Heat Shield Temperature Distribution After Start of Heating (From -260 F at 0.5 Hours) (Sheet 8 of 12)

[redacted]

~~CONFIDENTIAL~~

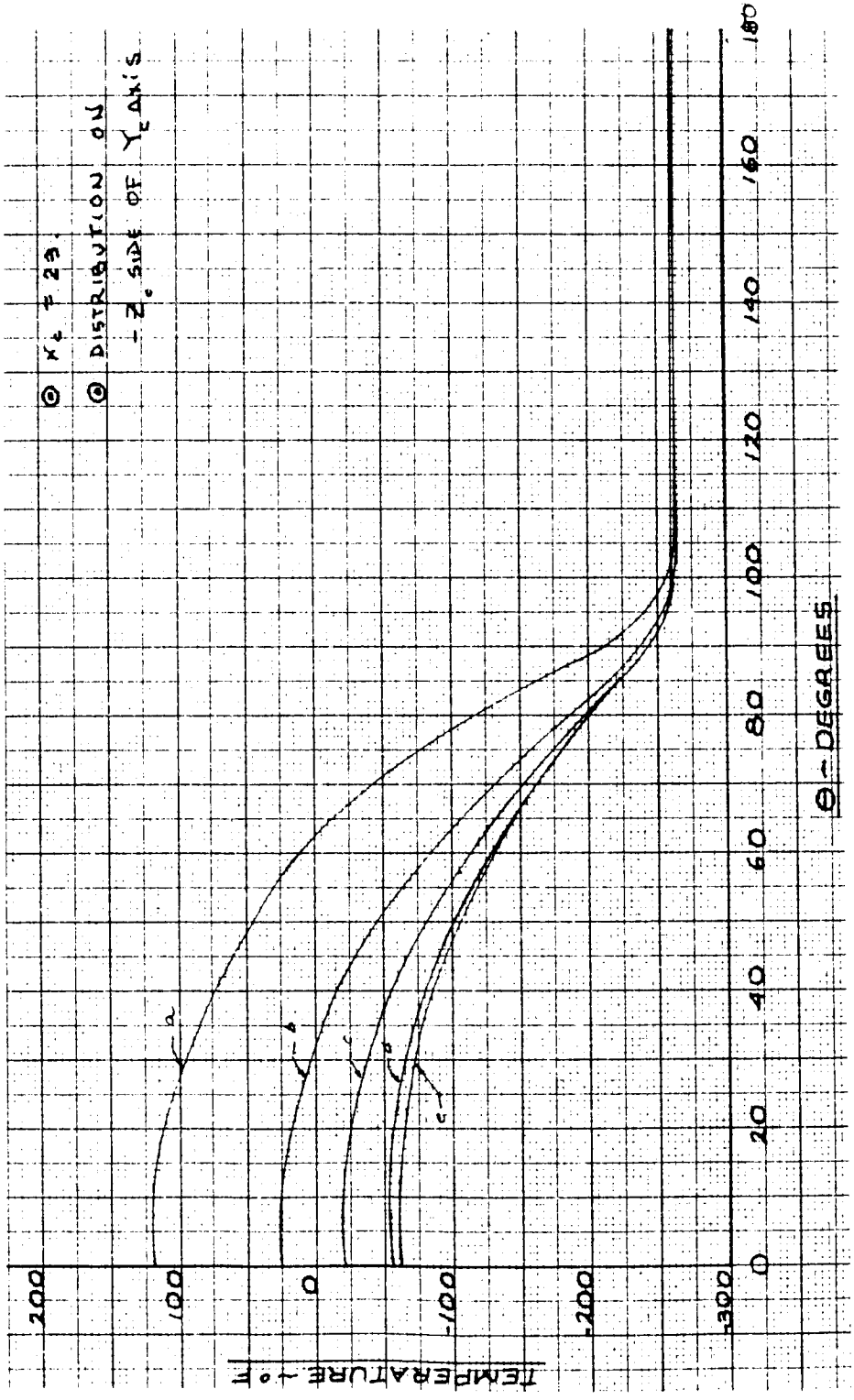

Figure 2-51. Forward Heat Shield Temperature Distribution After Start of Heating (From -260 F at 1.0 Hours) (Sheet 9 of 12)

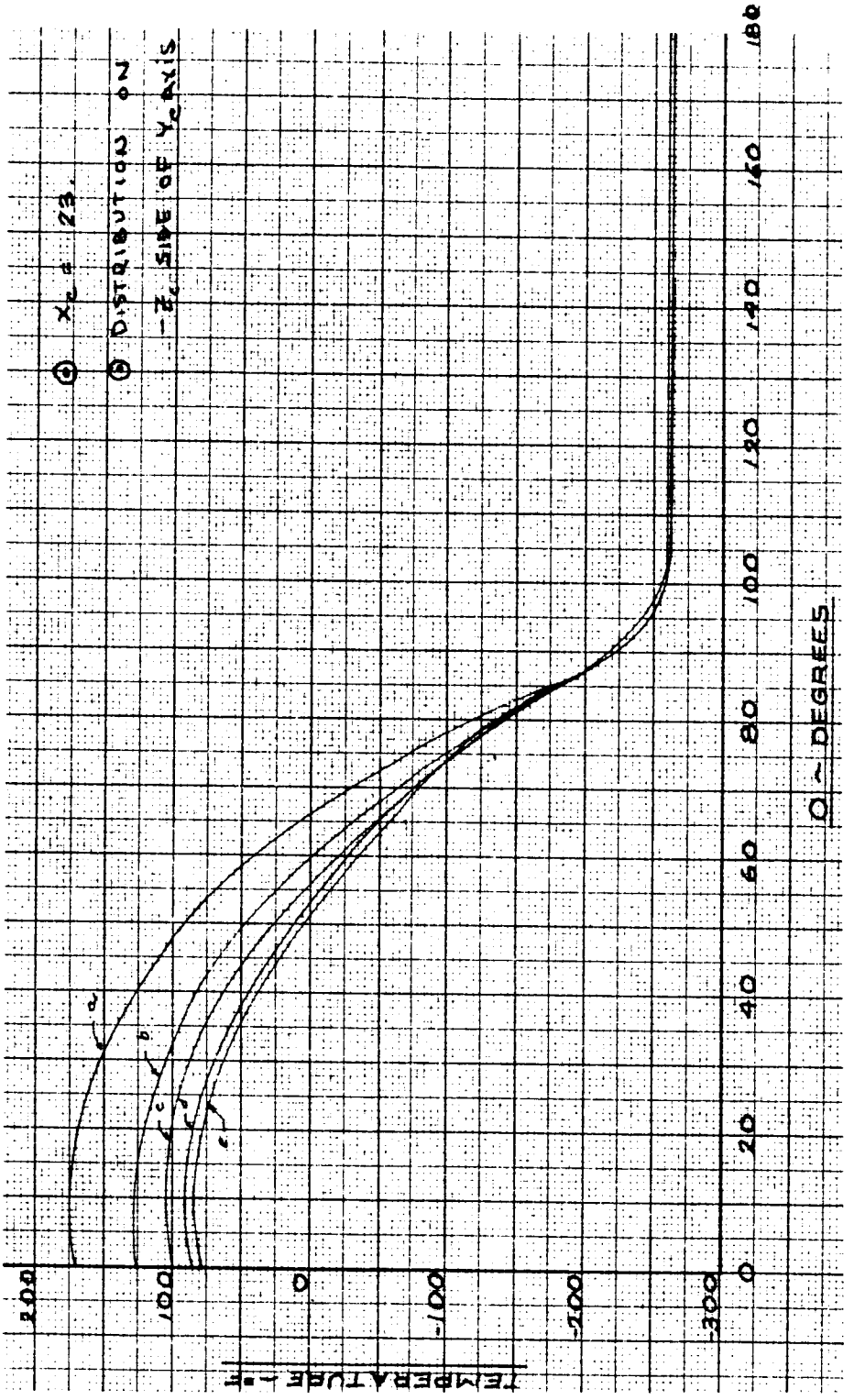

Figure 2-51. Forward Heat Shield Temperature Distribution After Start of Heating (From -260 F at 2.0 Hours) (Sheet 10 of 12)

~~CONFIDENTIAL~~

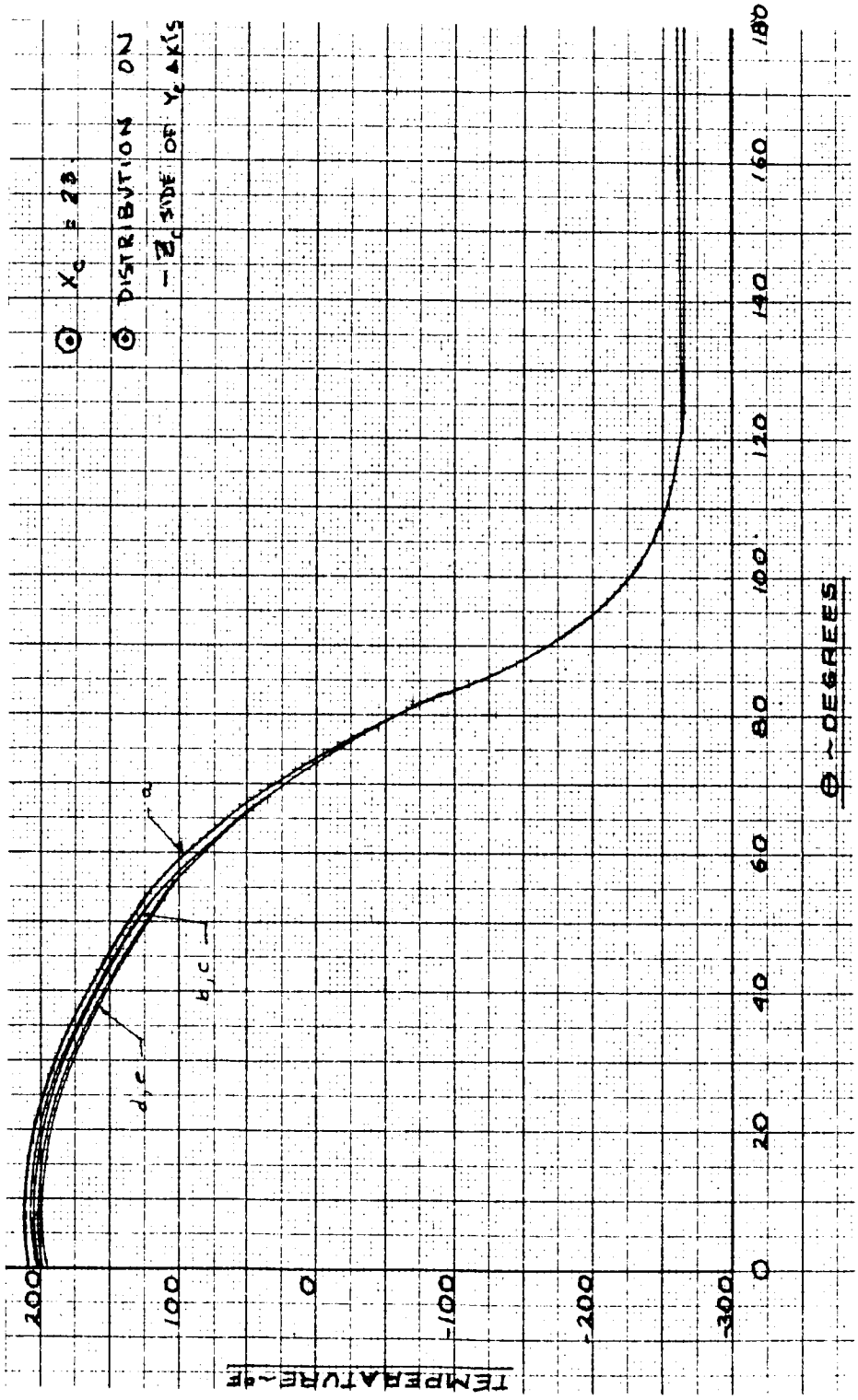

Figure 2-51. Forward Heat Shield Temperature Distribution After Start of Heating (From -260 F at 5.0 Hours) (Sheet 11 of 12)

~~CONFIDENTIAL~~

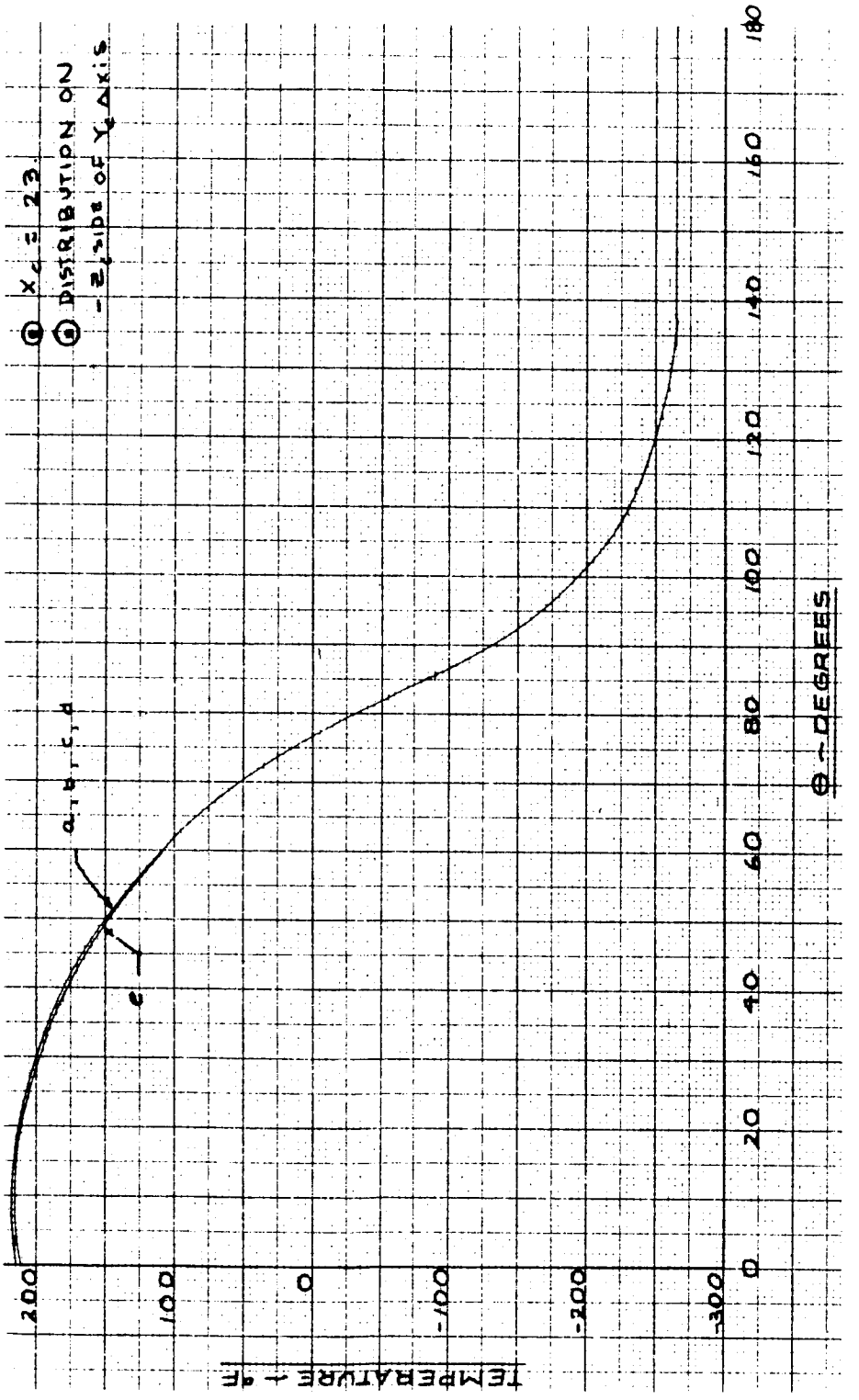

Figure 2-51. Forward Heat Shield Temperature Distribution After Start of Heating (From -260 F at 10.0 Hours) (Sheet 12 of 12)

[redacted]

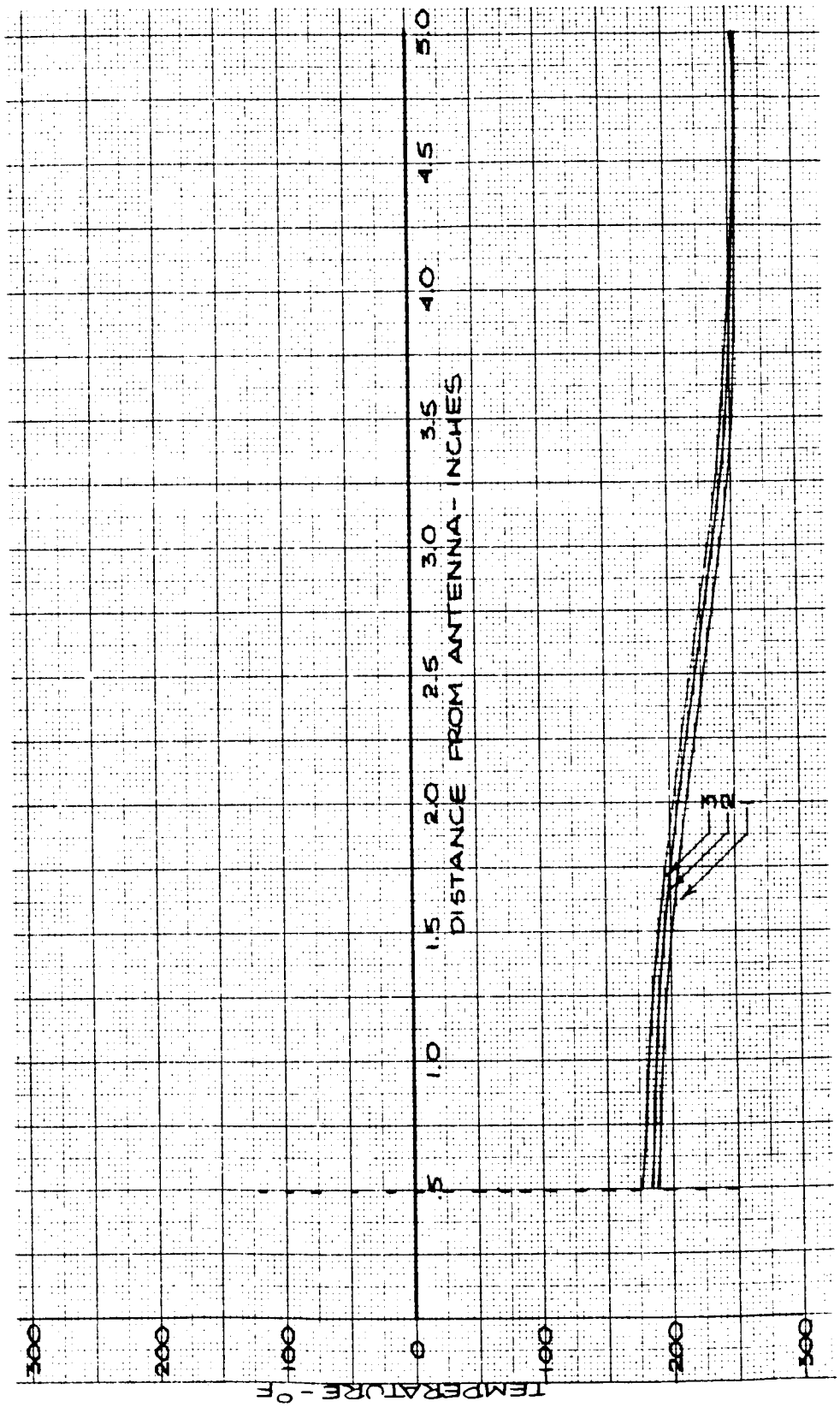

Figure 2-52. Distribution at 0 Hours: Heating From Steady-State Cold (Sheet 1 of 17)

[redacted]

[redacted]

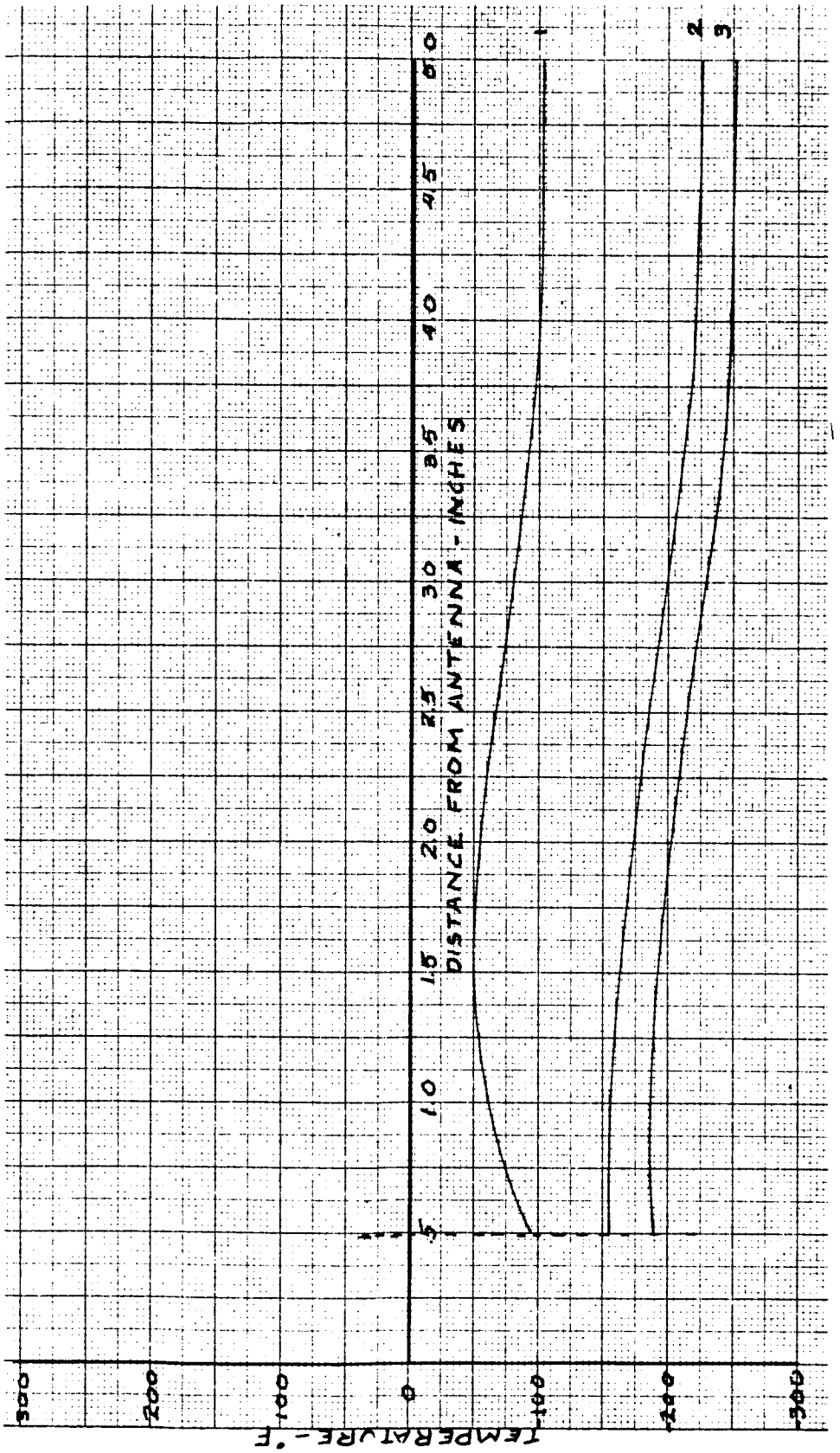

Figure 2-52. Distribution at 0 Hours: Heating From Steady-State Cold (Sheet 2 of 17)

[redacted]

~~CONFIDENTIAL~~

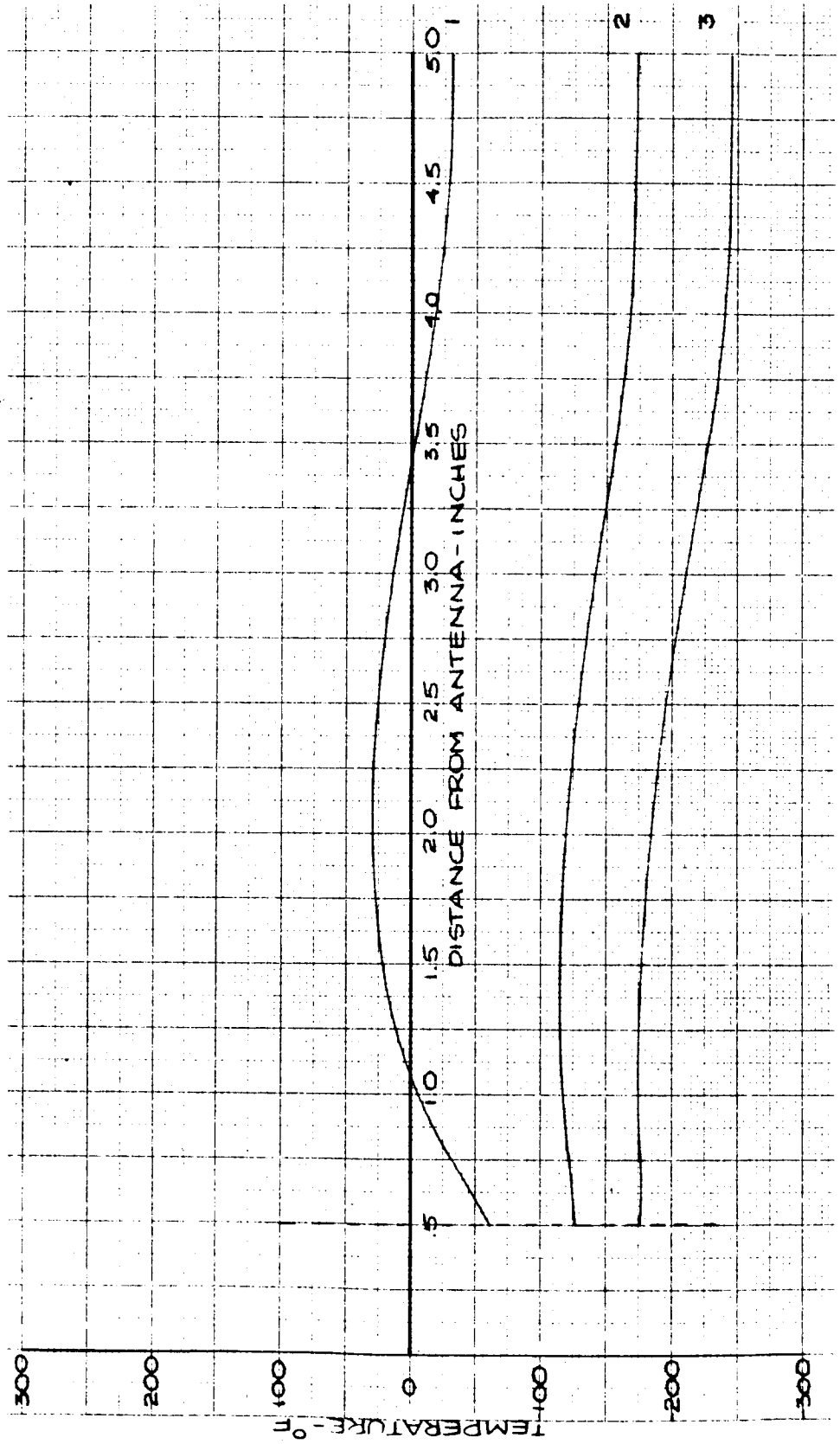

Figure 2-52. Distribution at 0 Hours:
Heating From Steady-State Cold (Sheet 3 of 17)

~~CONFIDENTIAL~~

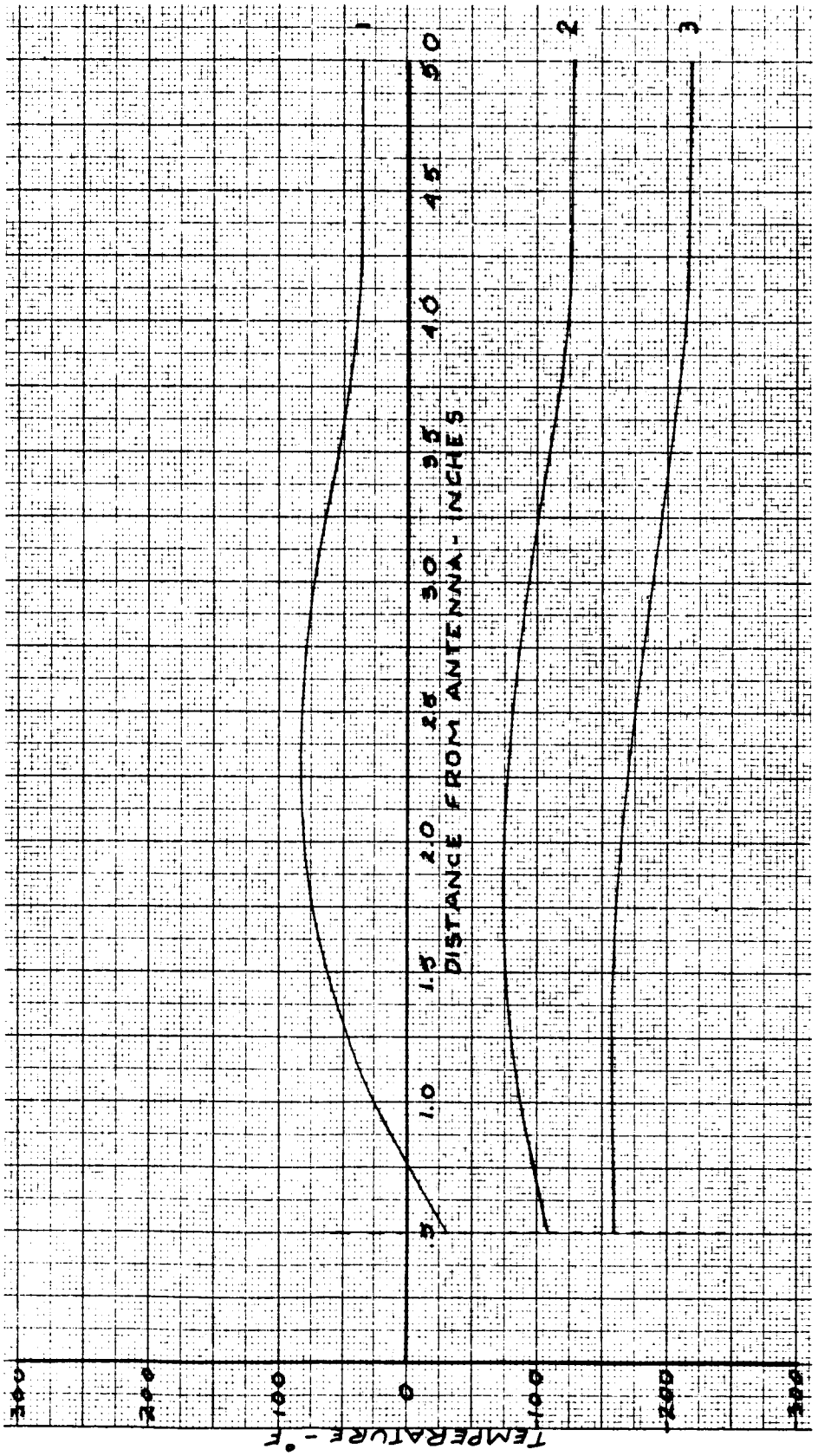

Figure 2-52. Distribution at 0 Hours: Heating From Steady-State Cold (Sheet 4 of 17)

~~CONFIDENTIAL~~

[redacted]

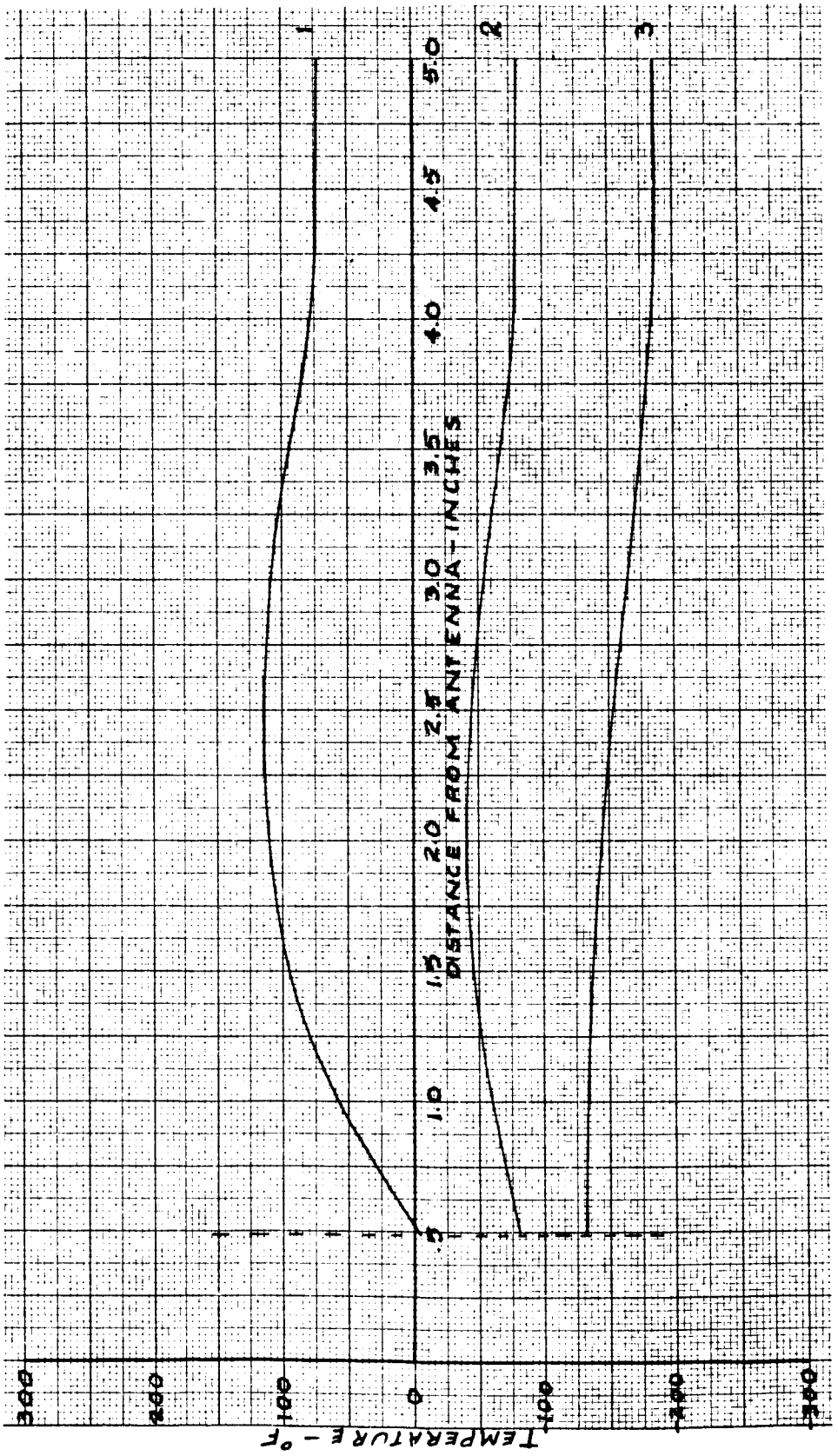

Figure 2-52. Distribution at 0 Hours:
Heating From Steady-State Cold (Sheet 5 of 17)

[redacted]

[redacted]

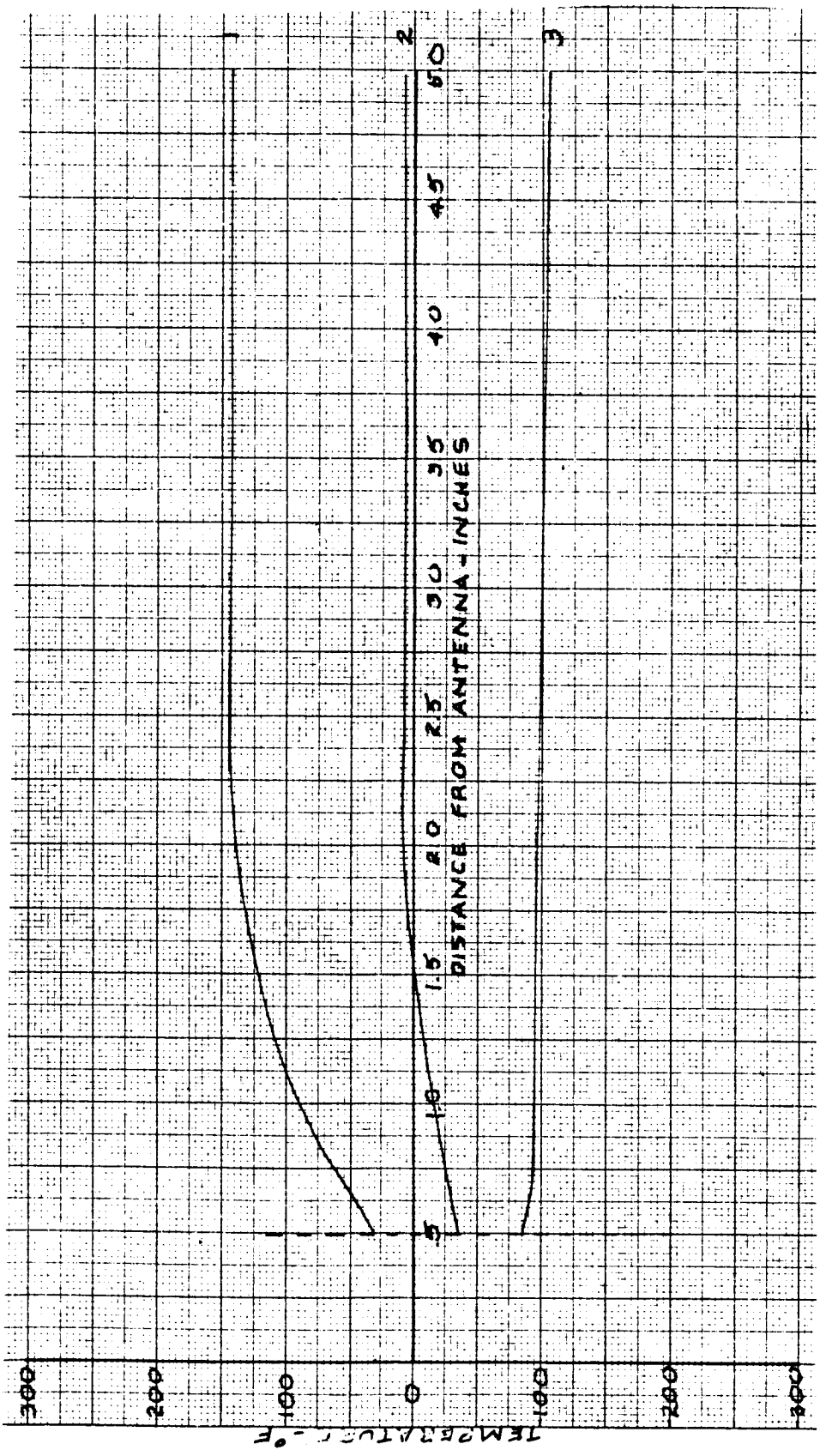

Figure 2-52. Distribution at 0 Hours: Heating From Steady-State Cold (Sheet 6 of 17)

[redacted]

[redacted]

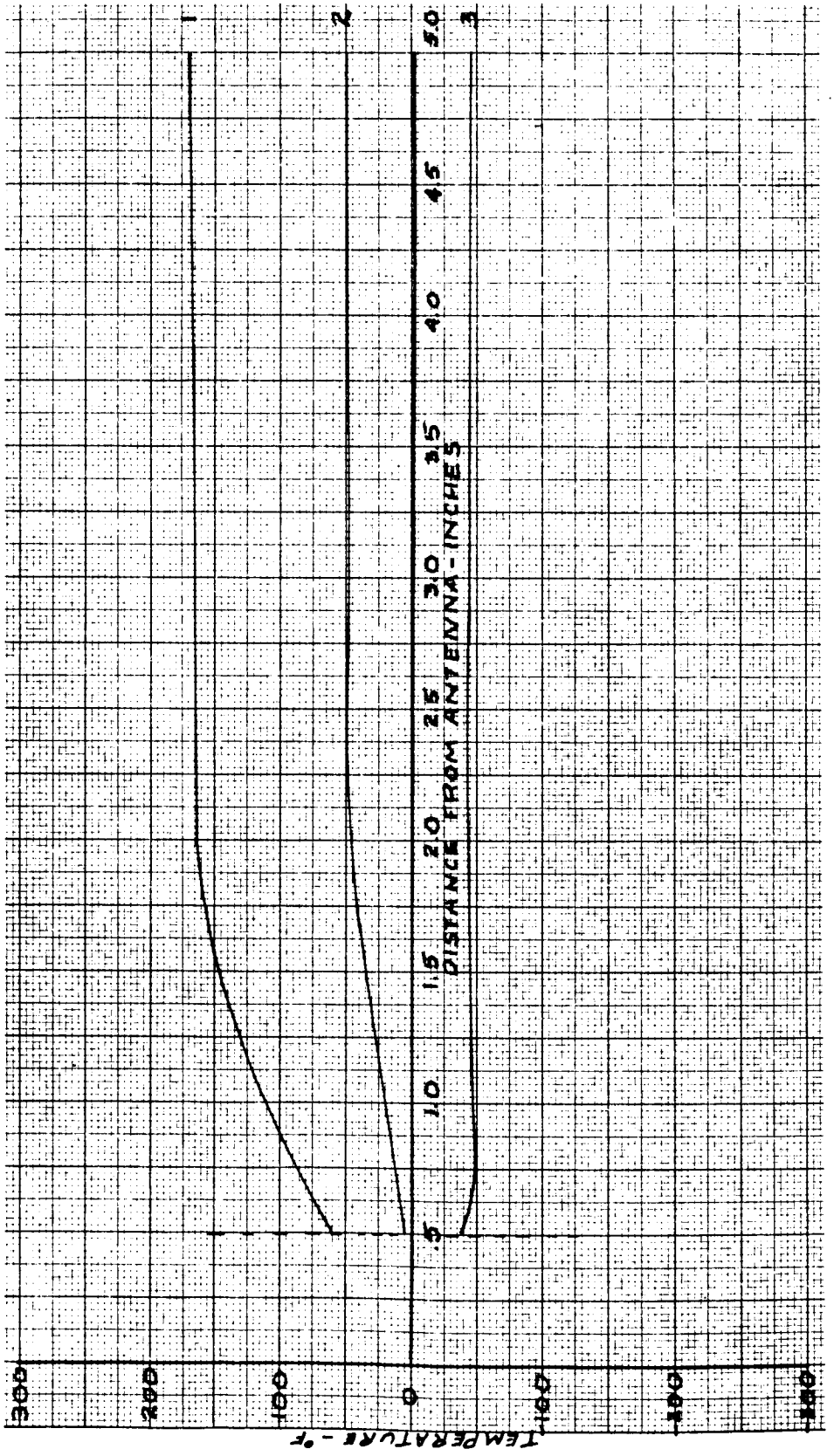

Figure 2-52. Distribution at 0 Hours: Heating From Steady-State Cold (Sheet 7 of 17)

[redacted]

[redacted]

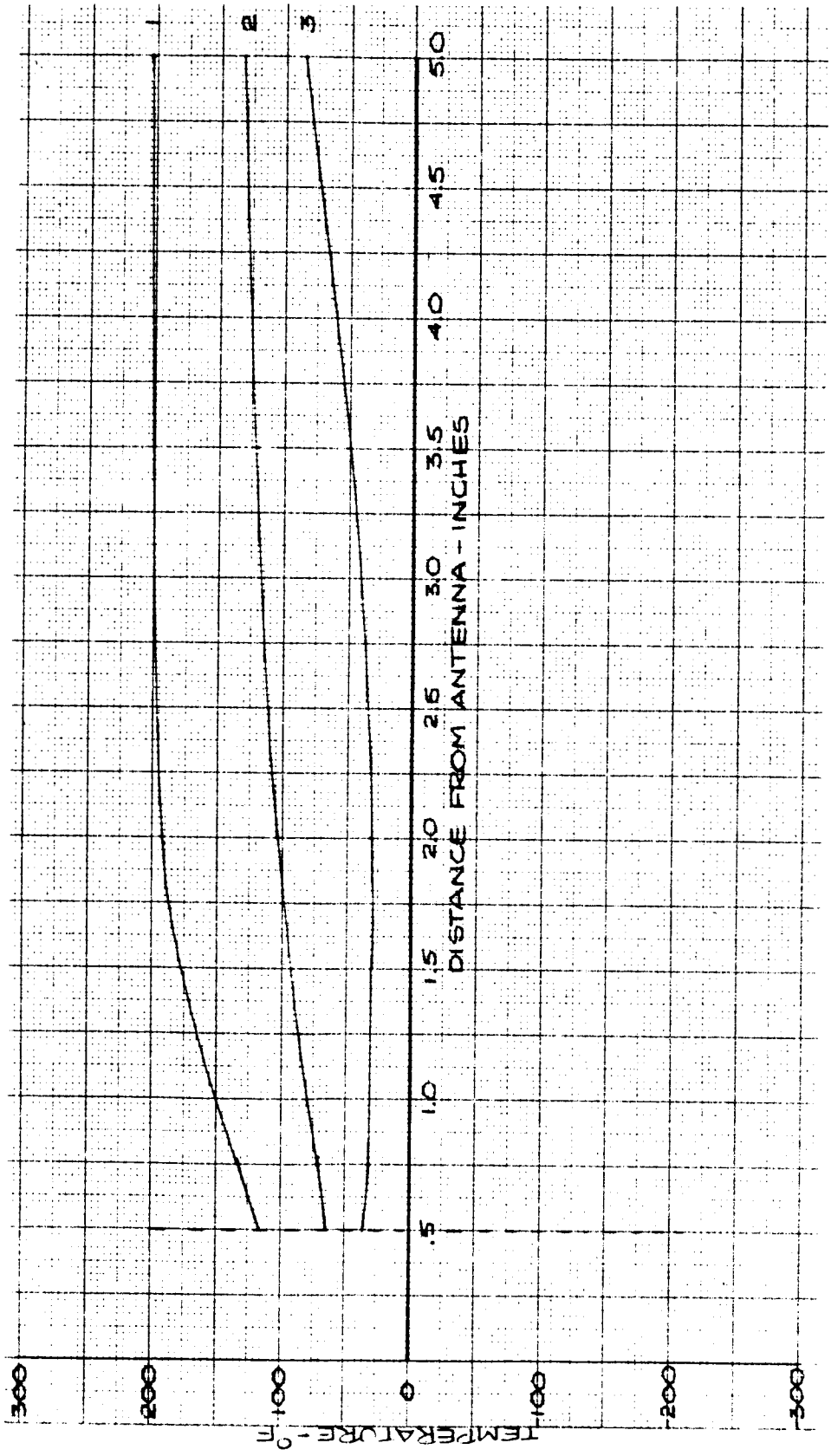

Figure 2-52. Distribution at 0 Hours: Heating From Steady-State Cold (Sheet 8 of 17)

~~CONFIDENTIAL~~

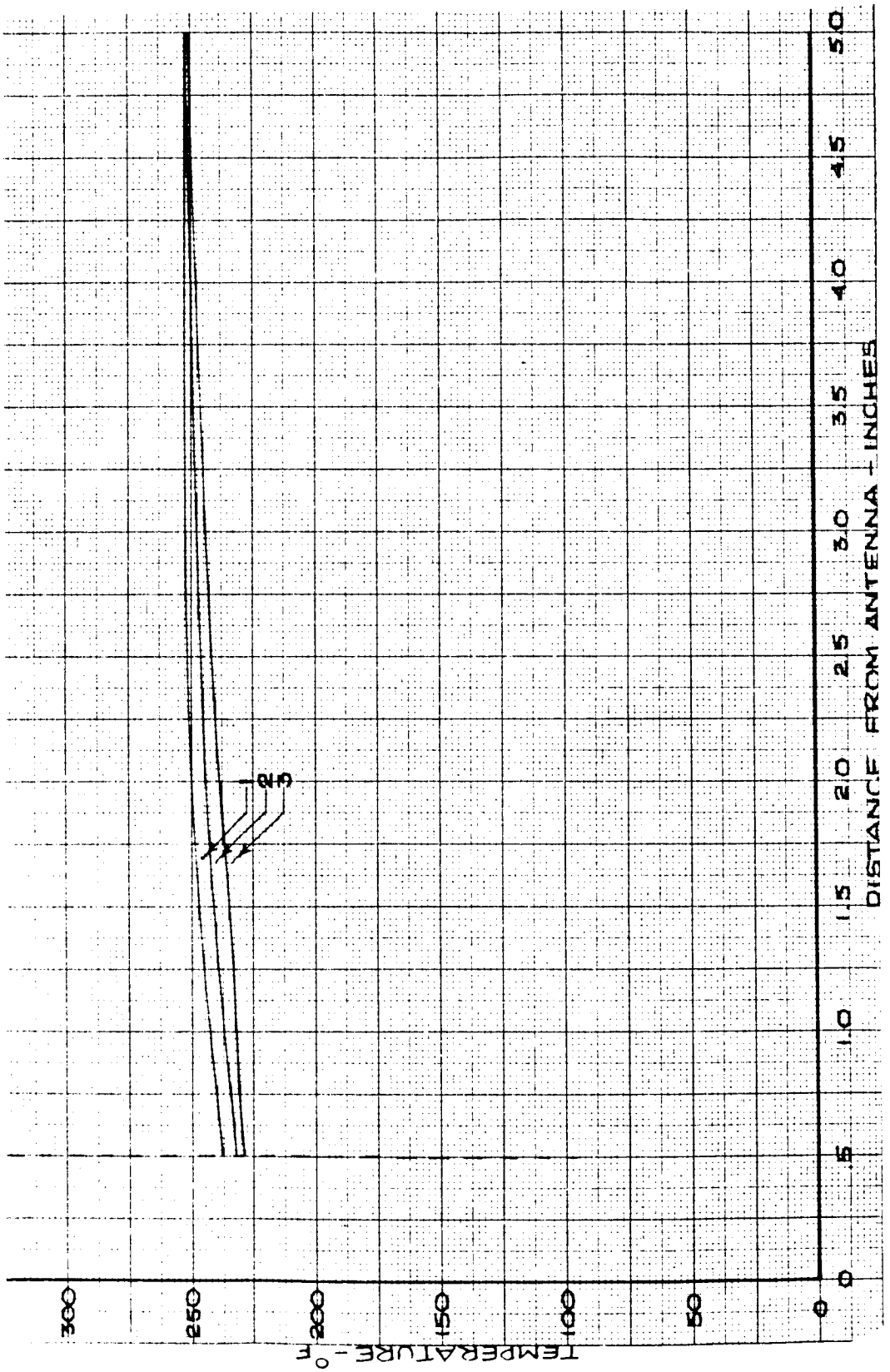

Figure 2-52. Distribution at 0 Hours:
Heating From Steady-State Cold (Sheet 9 of 17)

[redacted]

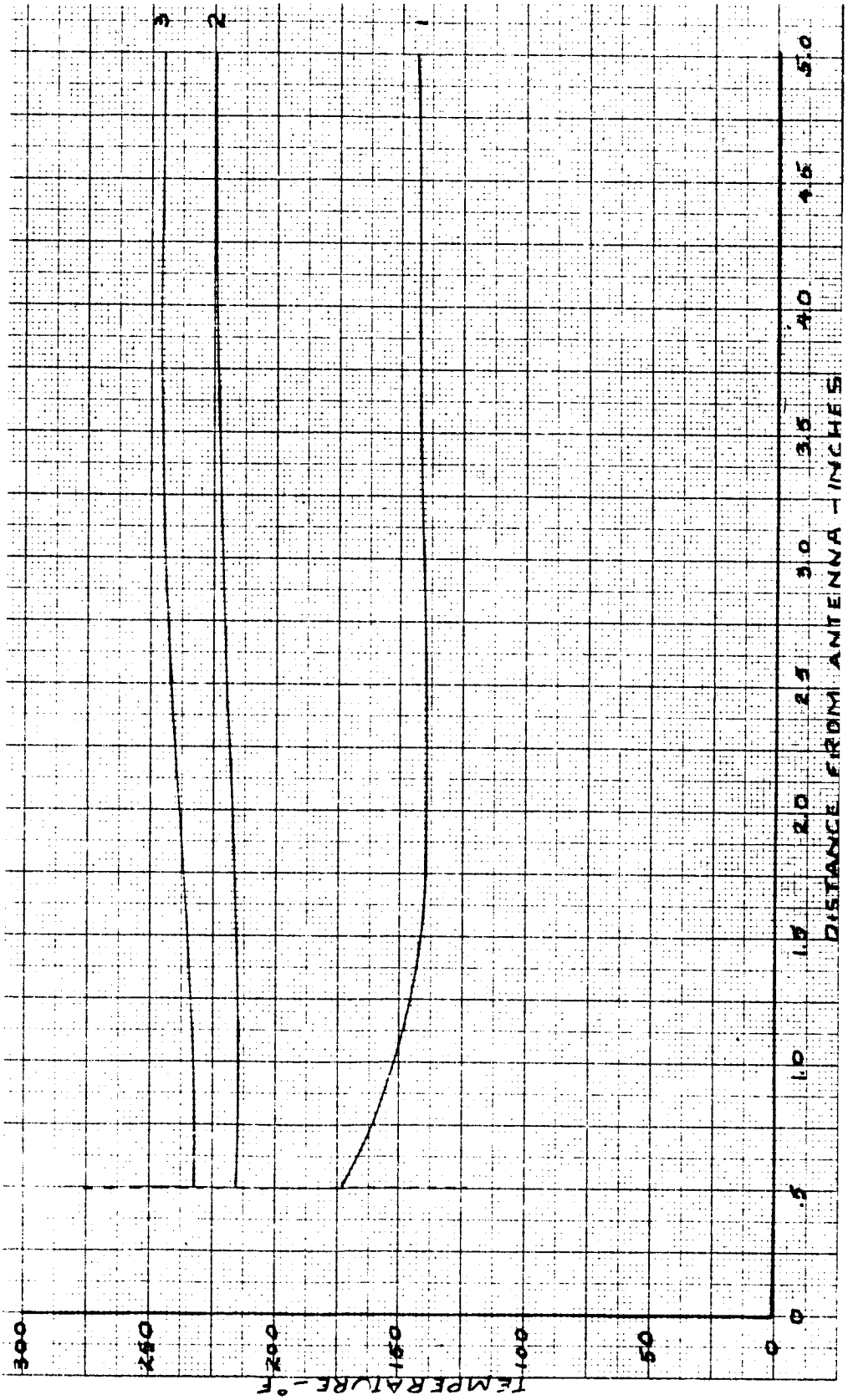

Figure 2-52. Distribution at 0 Hours: Heating From Steady-State Cold (Sheet 10 of 17)

[redacted]

[redacted]

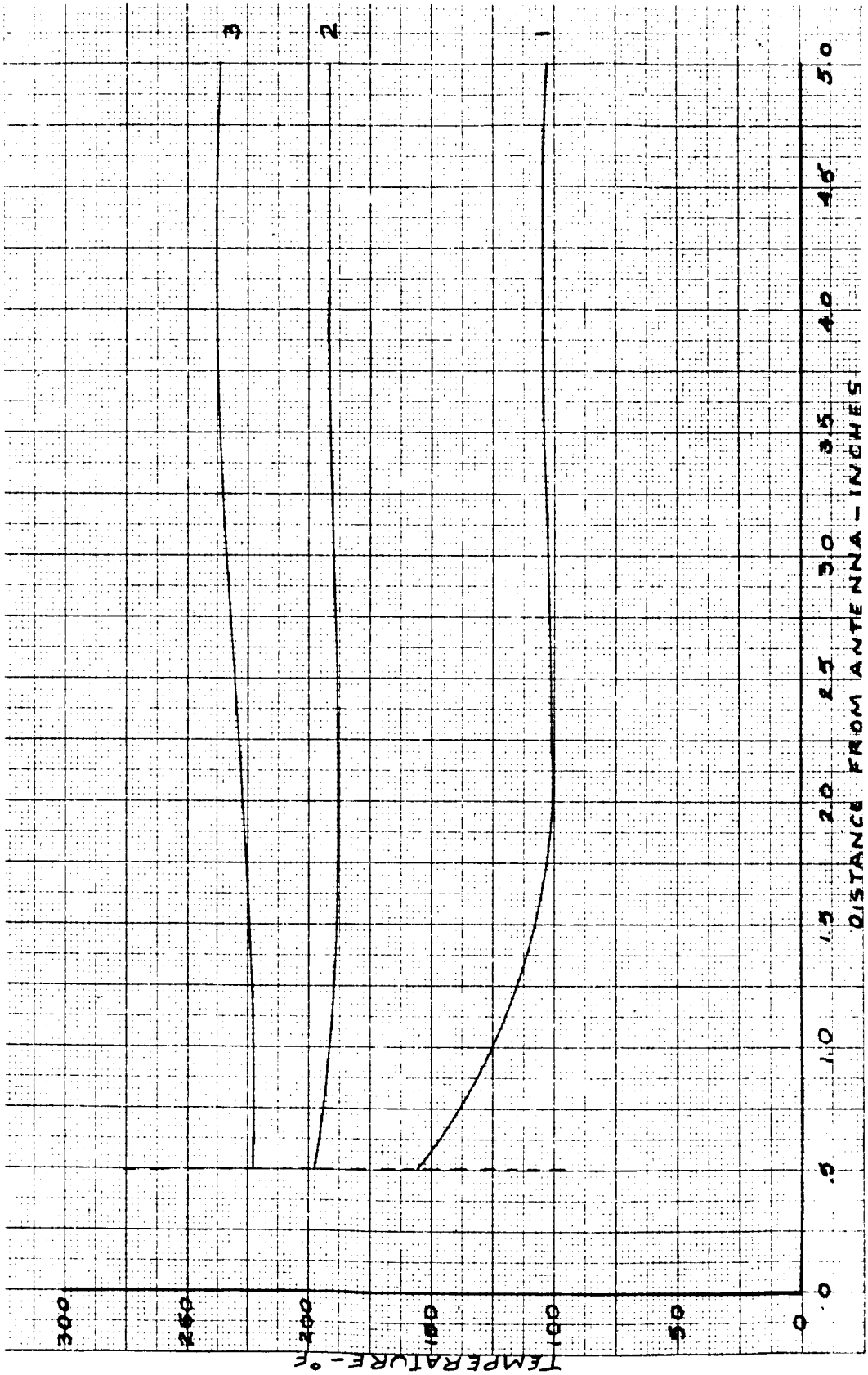

Figure 2-52. Distribution at 0 Hours:
Heating From Steady-State Cold (Sheet 11 of 17)

[redacted]

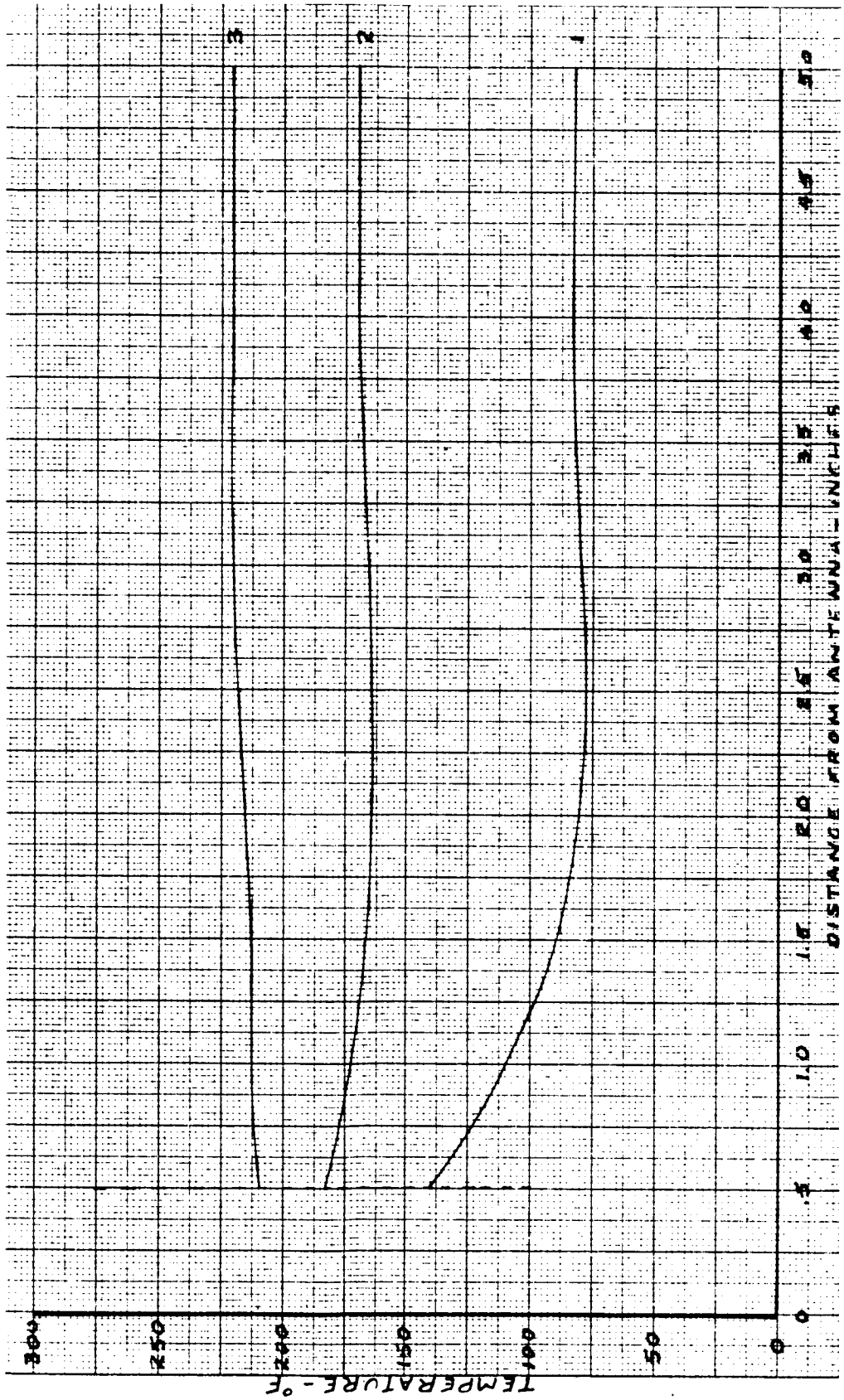

Figure 2-52. Distribution at 0 Hours:
Heating From Steady-State Cold (Sheet 12 of 17)

[redacted]

[redacted]

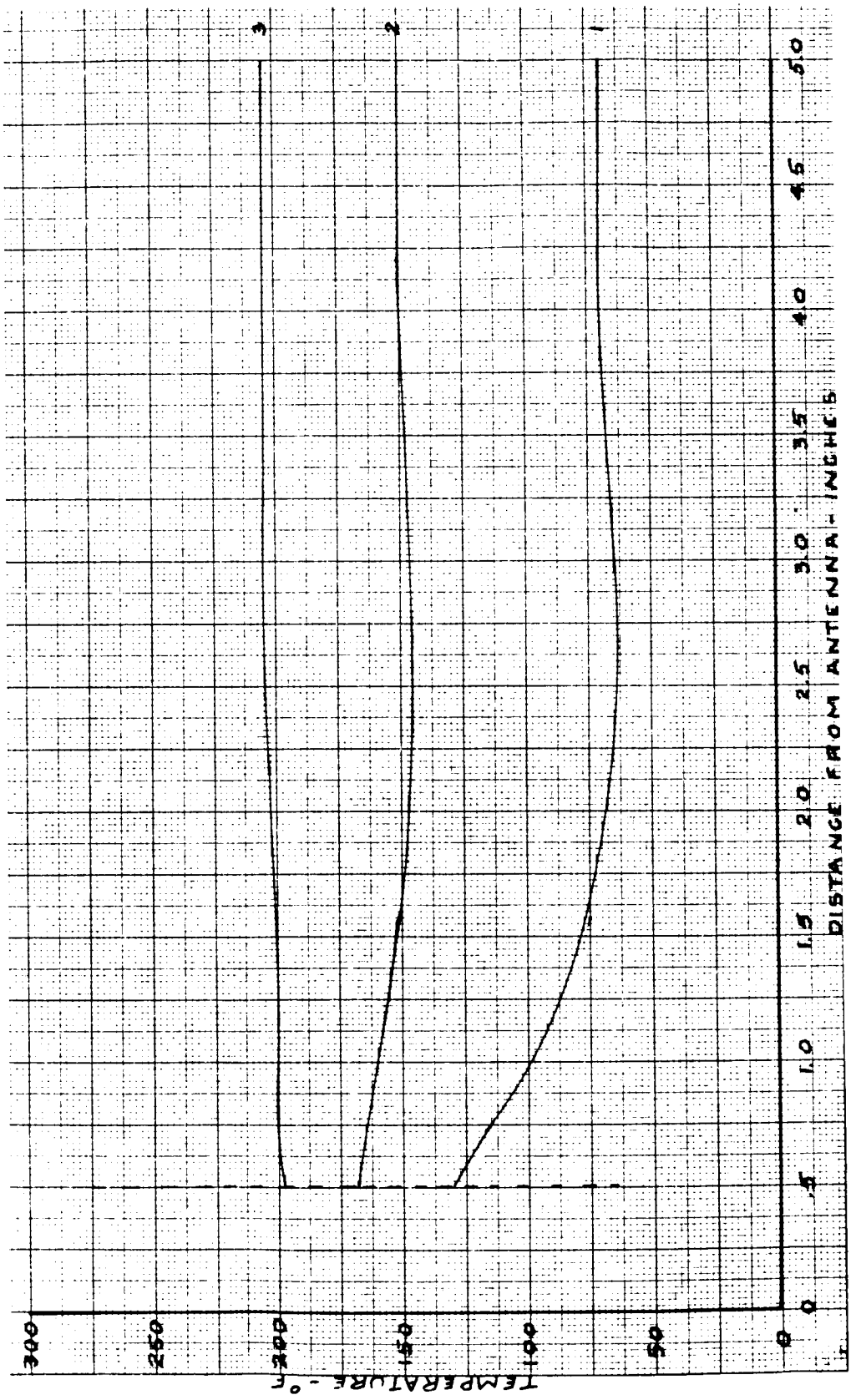

Figure 2-52. Distribution at 0 Hours:
Heating From Steady-State Cold (Sheet 13 of 17)

[redacted]

[redacted]

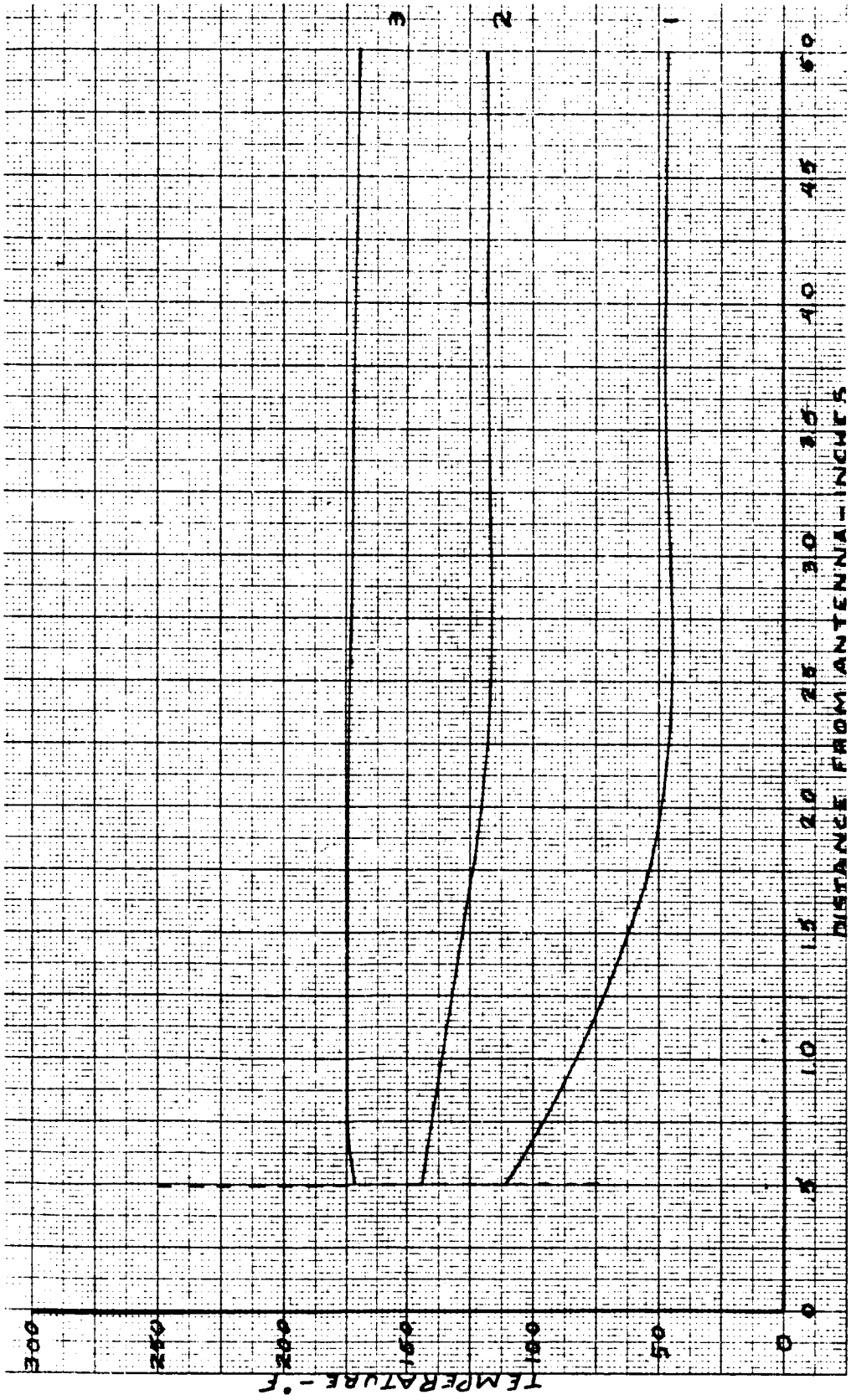

Figure 2-52. Distribution at 0 Hours:
Heating From Steady-State Cold (Sheet 14 of 17)

[redacted]

~~CONFIDENTIAL~~

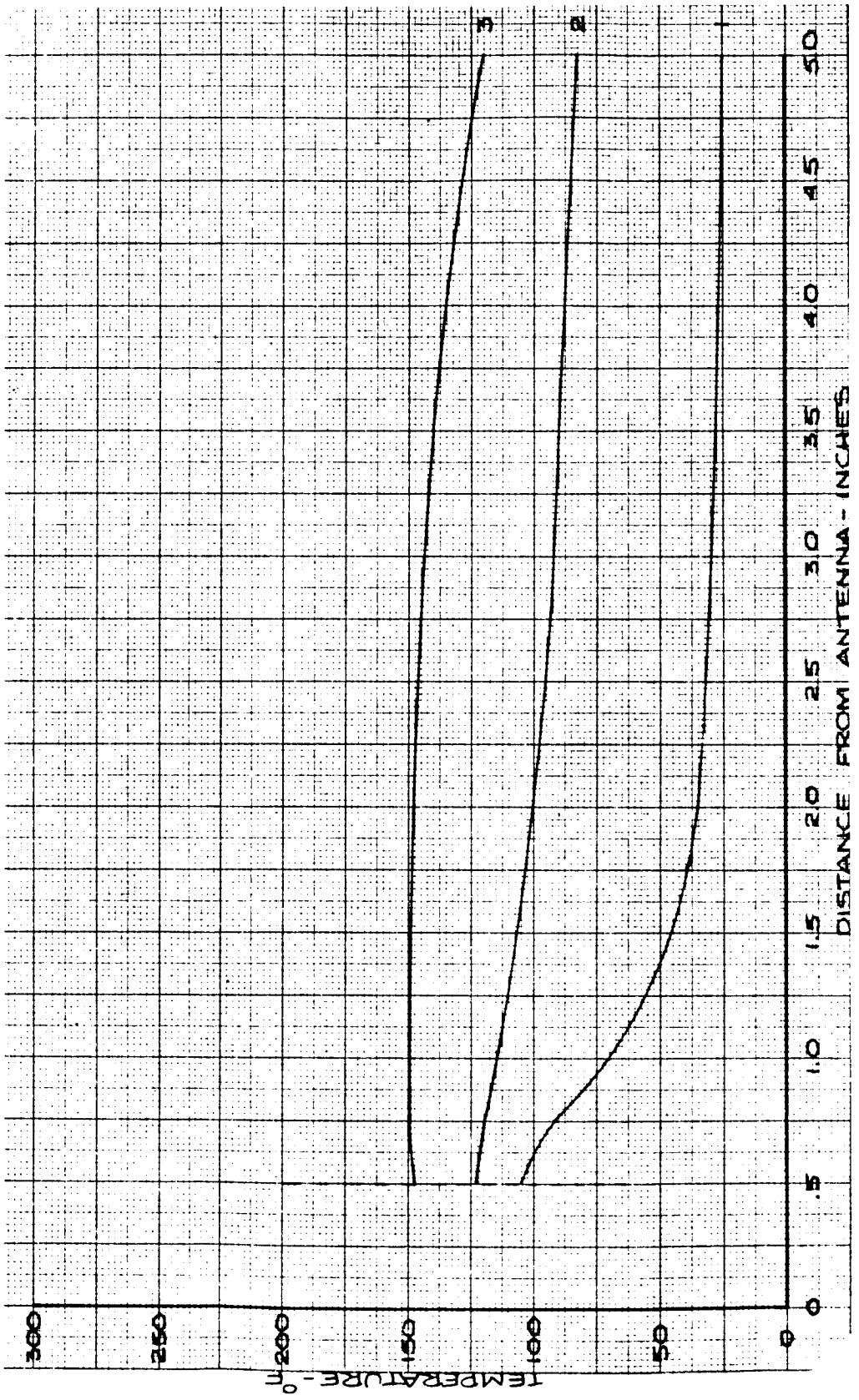

Figure 2-52. Distribution at 0 Hours: Heating From Steady-State Cold (Sheet 15 of 17)

[redacted]

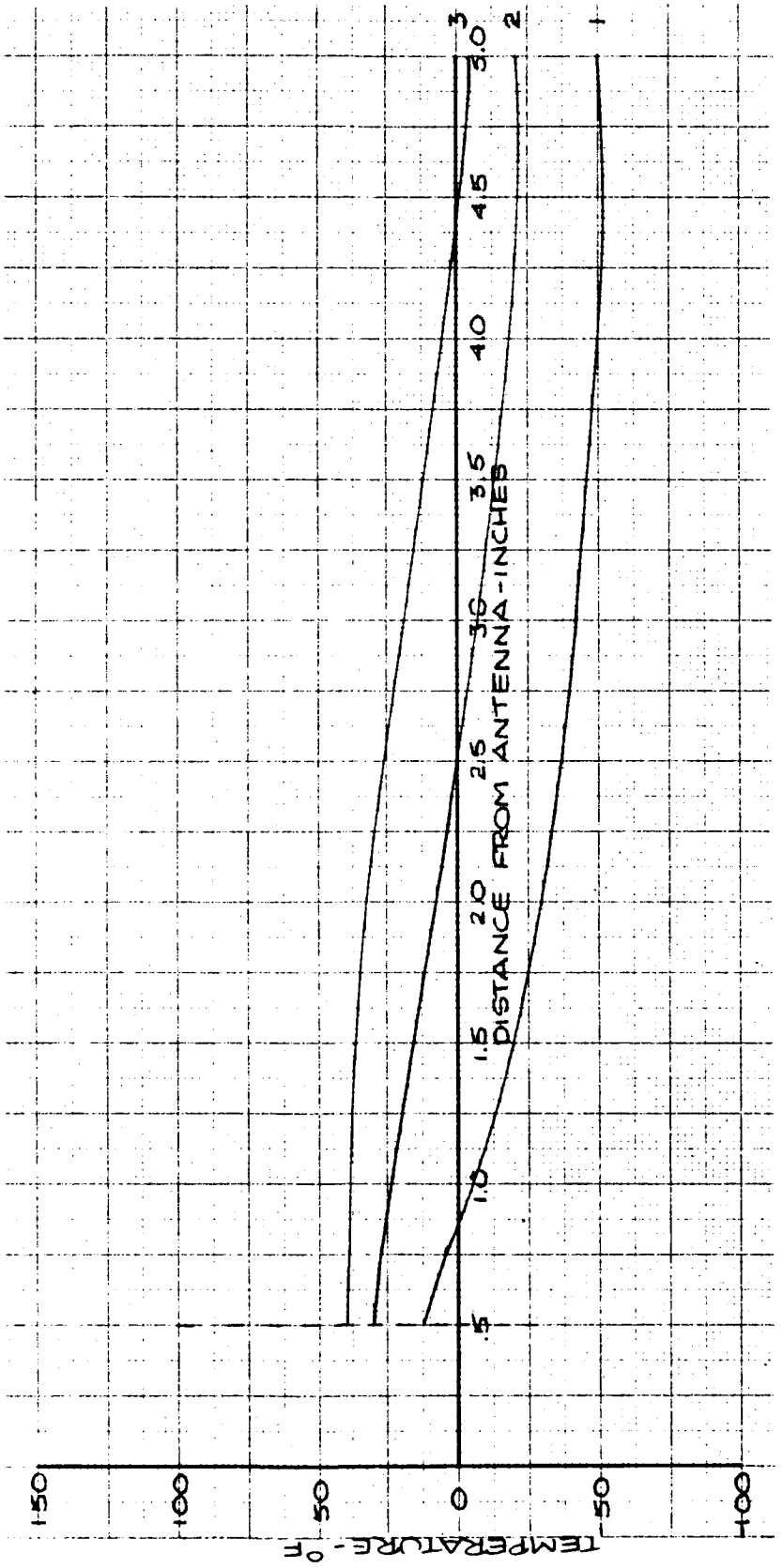

Figure 2-52. Distribution at 0 Hours: Heating From Steady-State Cold (Sheet 16 of 17)

~~CONFIDENTIAL~~

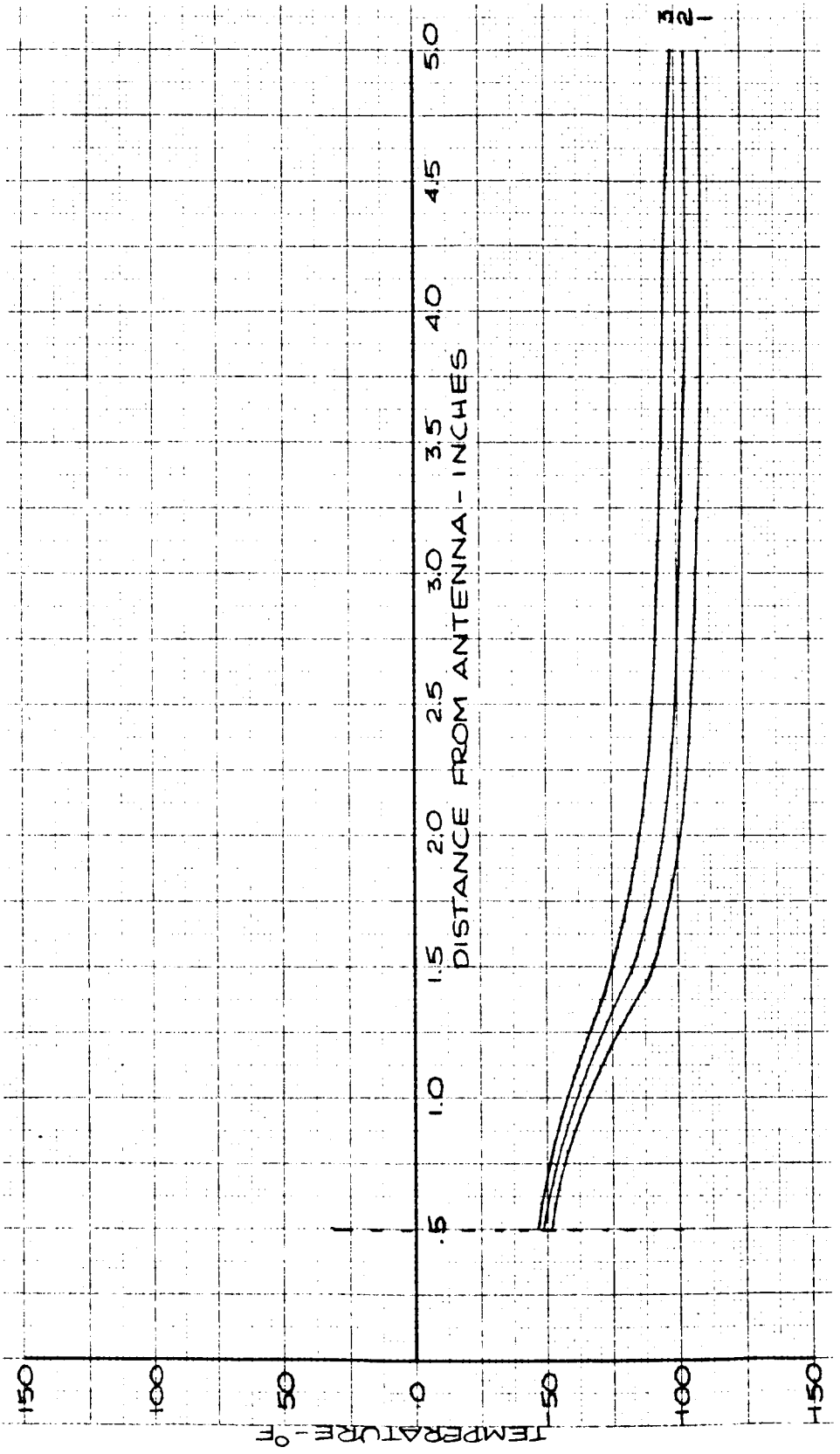

Figure 2-52. Distribution at 0 Hours: Heating From Steady-State Cold (Sheet 17 of 17)

~~CONFIDENTIAL~~

[redacted]

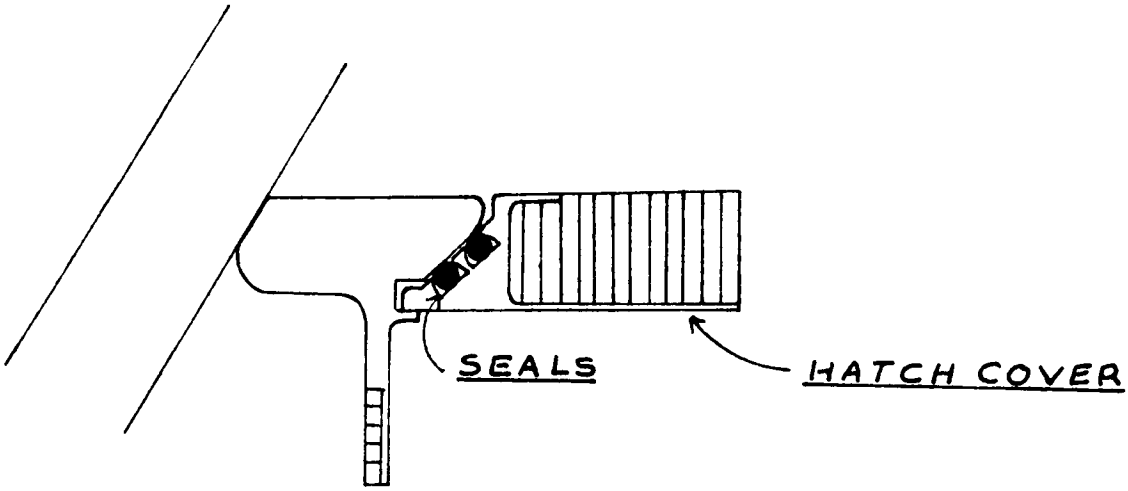

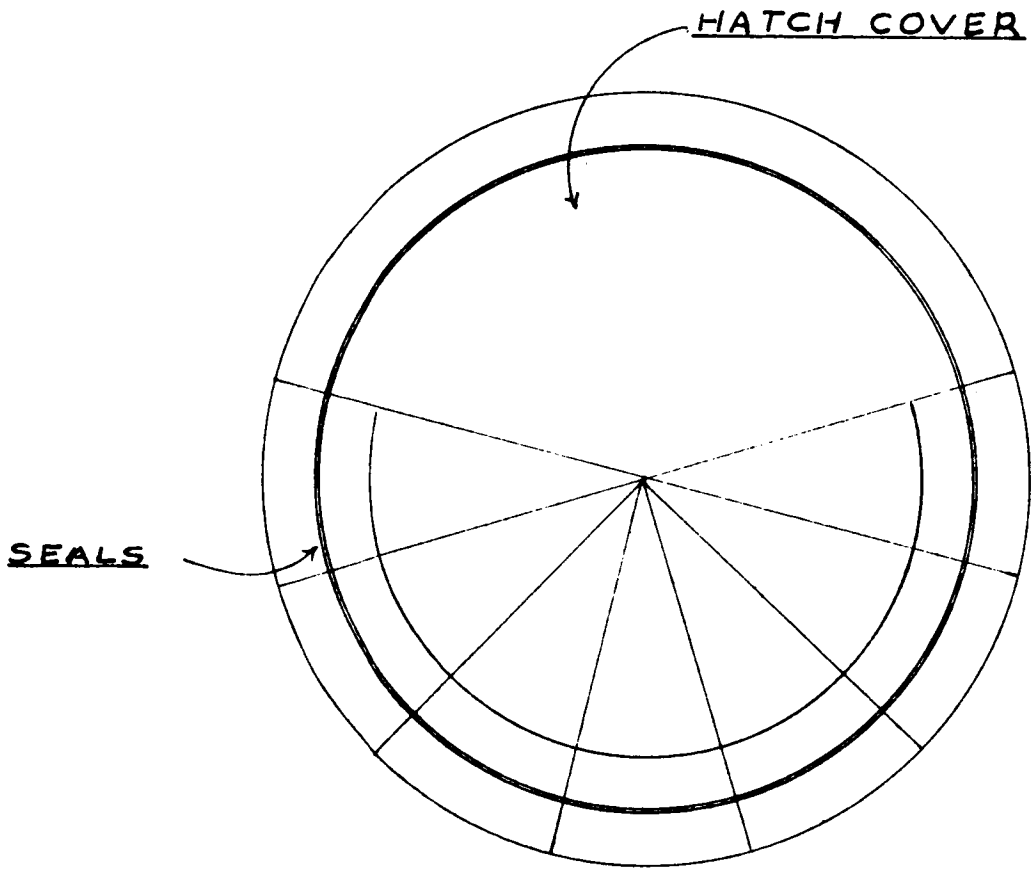

Figure 2-53. Forward Hatch Assembly Showing Location of Seals

~~CONFIDENTIAL~~

Translunar Injection

1. Solar incidence perpendicular to conic surface. *Angle = 137.5 deg
2. Radome closed.
3. Cabin pressurized.
4. Phase interval: 10 hours.

↓

Transposition of LEM

1. Solar incidence perpendicular to hatch cover.
2. Radome open.
3. Cabin pressurized.
4. Phase interval: 1 hour.

↓

Translunar Coast

1. Solar incidence perpendicular to conic surface. *Angle = 137.5 deg
2. Radome open.
3. Hatch cover assumed to be adiabatic wall.
4. Cabin pressurized.
5. Phase interval: 83 hours.

↓

Lunar Orbit - Abort

1. Solar incidence perpendicular to hatch cover.
2. Radome open.
3. Cabin depressurized.
4. Phase interval: 1 hour.

↓

Pressurized

Transearth

1. Solar incidence perpendicular to conic surface. *Angle = 137.5 deg
2. Radome closed.
3. Cabin pressurized
4. Phase interval: 84 hours.

De-Pressurized

Transearth

1. Solar incidence perpendicular to conic surface. *Angle = 137.5 deg
2. Radome closed.
3. Cabin depressurized.
4. No heat generated within cabin.
5. Phase interval: 84 hours.

* Angle measured from +Yc axis toward +Zc axis looking aft.

Figure 2-54. Hot-Soak Space Flight Conditions

[redacted]

Translunar Coast

1. Cold soak condition.
2. Radome closed
3. Cabin pressurized
4. Phase interval: 84 hours.

↓

Transearth Coast

1. Cold soak condition.
2. Radome closed.
3. Cabin de-pressurized.
4. Phase interval: 84 hours.

Special Conditions*

1. Cold soak condition.
2. Radome open.
3. Cabin de-pressurized.
4. Test run: 10 hours.

* These conditions pertain to "Transposition of LEM" and Lunar Orbit Abort" phases.

Figure 2-55. Cold-Soak Space Flight Conditions

~~CONFIDENTIAL~~

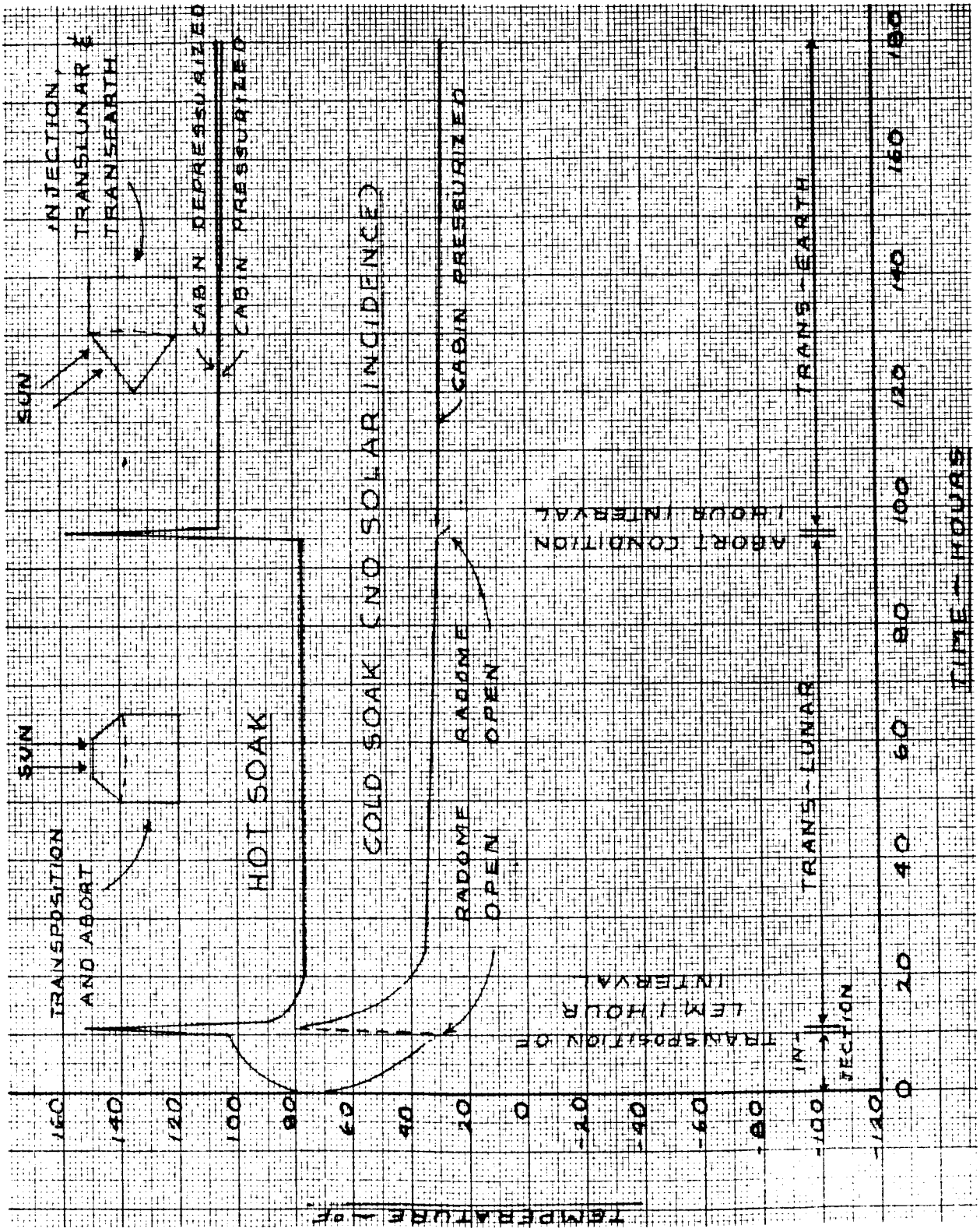

Figure 2-56. Airlock Seal Extreme Temperature History

~~CONFIDENTIAL~~

[redacted]

LOCATIONS OF REPORTED TEMPERATURES

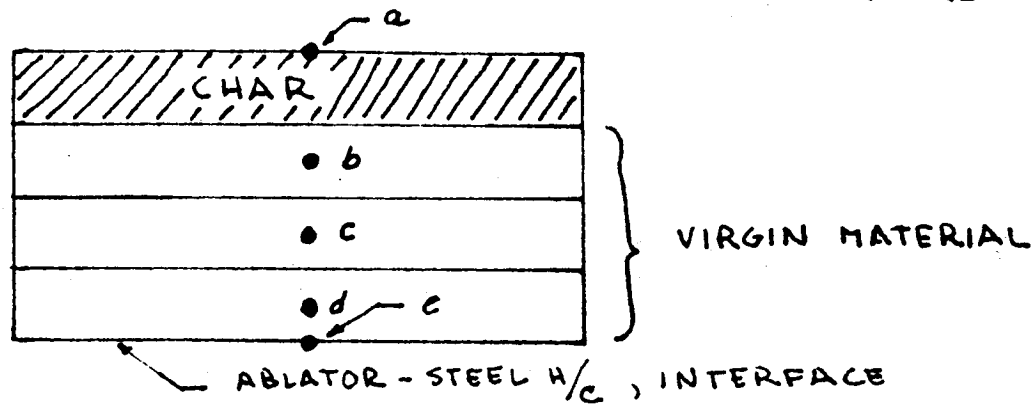

- t = TOTAL ABLATOR THICKNESS (CHAR AND VIRGIN) AS REPORTED IN "MASTER DIMENSIONS SPECIFICATION APOLLO MD - V14 - 16 - 600"
- CHAR THICKNESS ASSUMED CONSTANT 0.2 INCHES AFTER BOOST AS REPORTED IN "MINUTES OF NAA/AVCO TECHNICAL INTERCHANGE MEETING OF 21 AND 22 FEB. 1963."

$a = 0$ (OUTER SURFACE)

$b = (t - .2)\frac{1}{6} + .2$ (INCHES FROM OUTER SURFACE)

$c = (t - .2)\frac{1}{2} + .2$ (INCHES FROM OUTER SURFACE)

$d = (t - .2)\frac{5}{6} + .2$ (INCHES FROM OUTER SURFACE)

$e = t$ (INCHES FROM OUTER SURFACE)

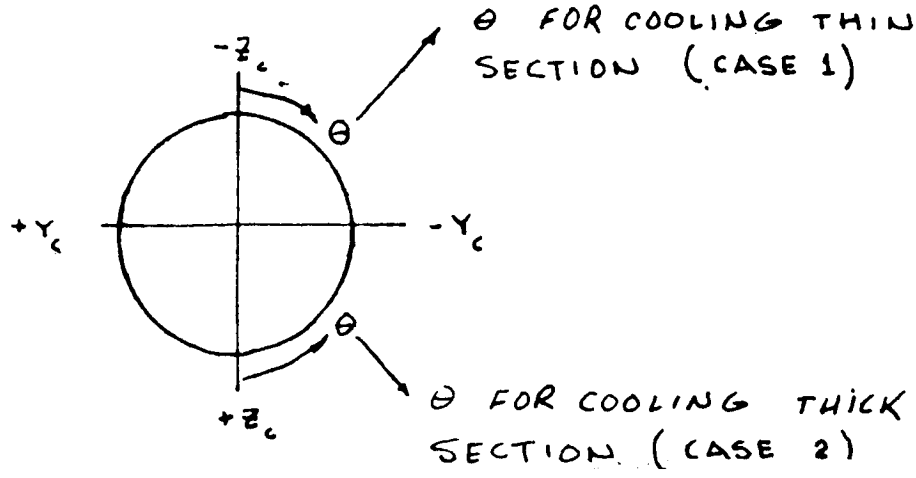

Figure 2-57. Forward Heat Shield Space Flight Transient Circumferential Temperature Distributions

[redacted]

[redacted]

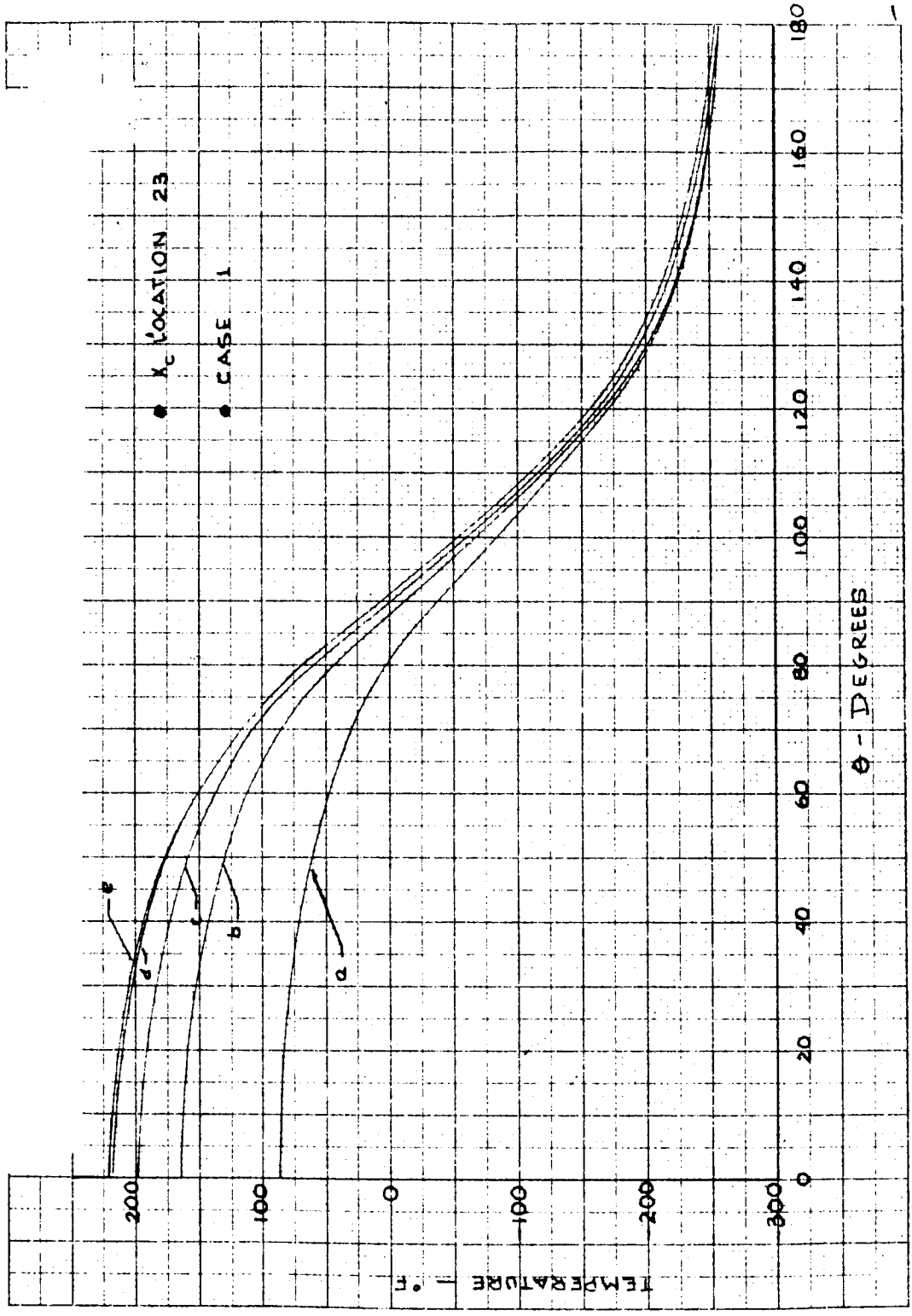

Figure 2-58. Forward Heat Shield Temperature Distribution After Start Cooling Period (0.25 Hours) (Sheet 1 of 14)

[redacted]

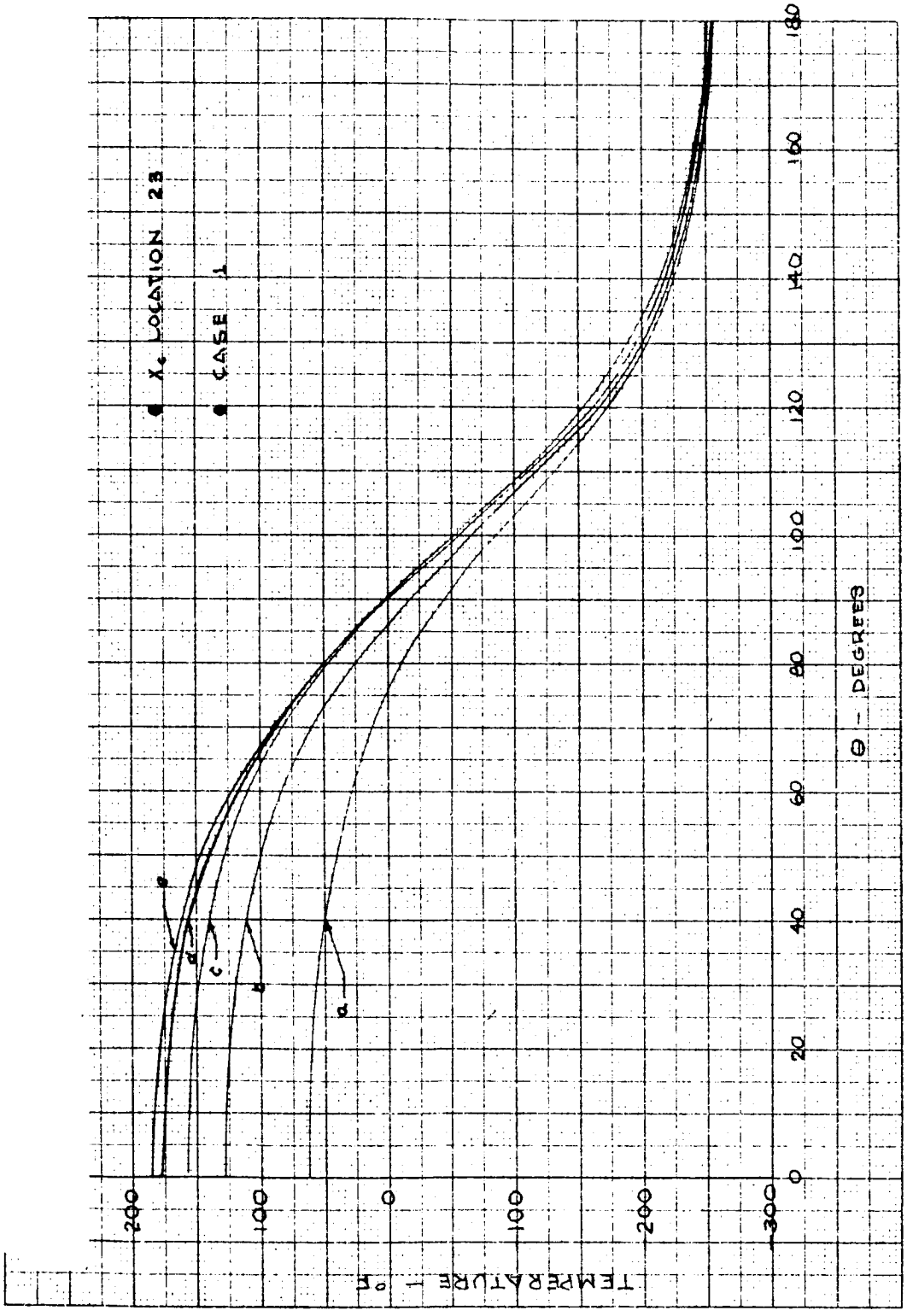

Figure 2-58. Forward Heat Shield Temperature Distribution After Start Cooling Period (0.5 Hours) (Sheet 2 of 14)

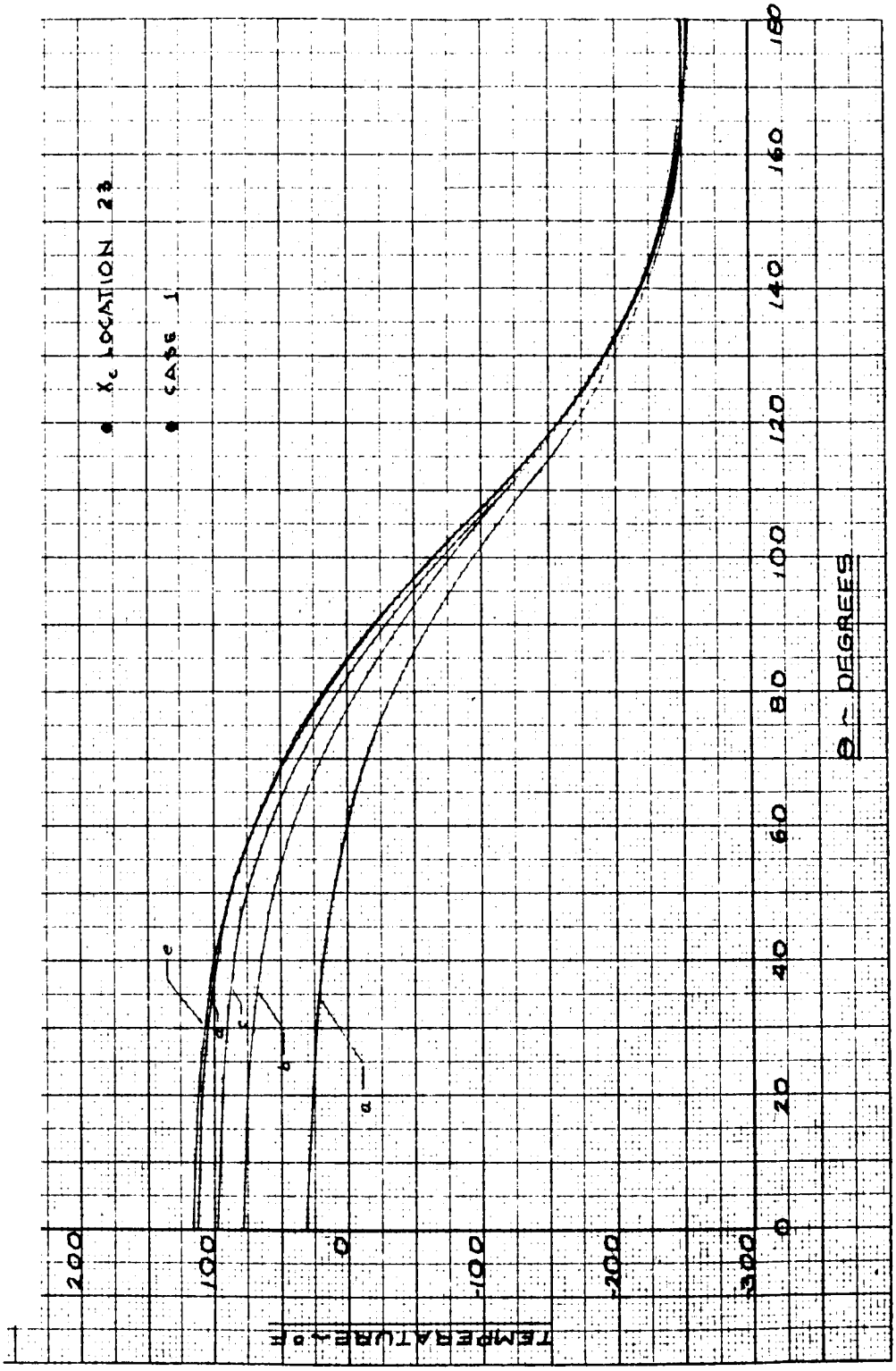

Figure 2-58. Forward Heat Shield Temperature Distribution After Start Cooling Period (1.0 Hours) (Sheet 3 of 14)

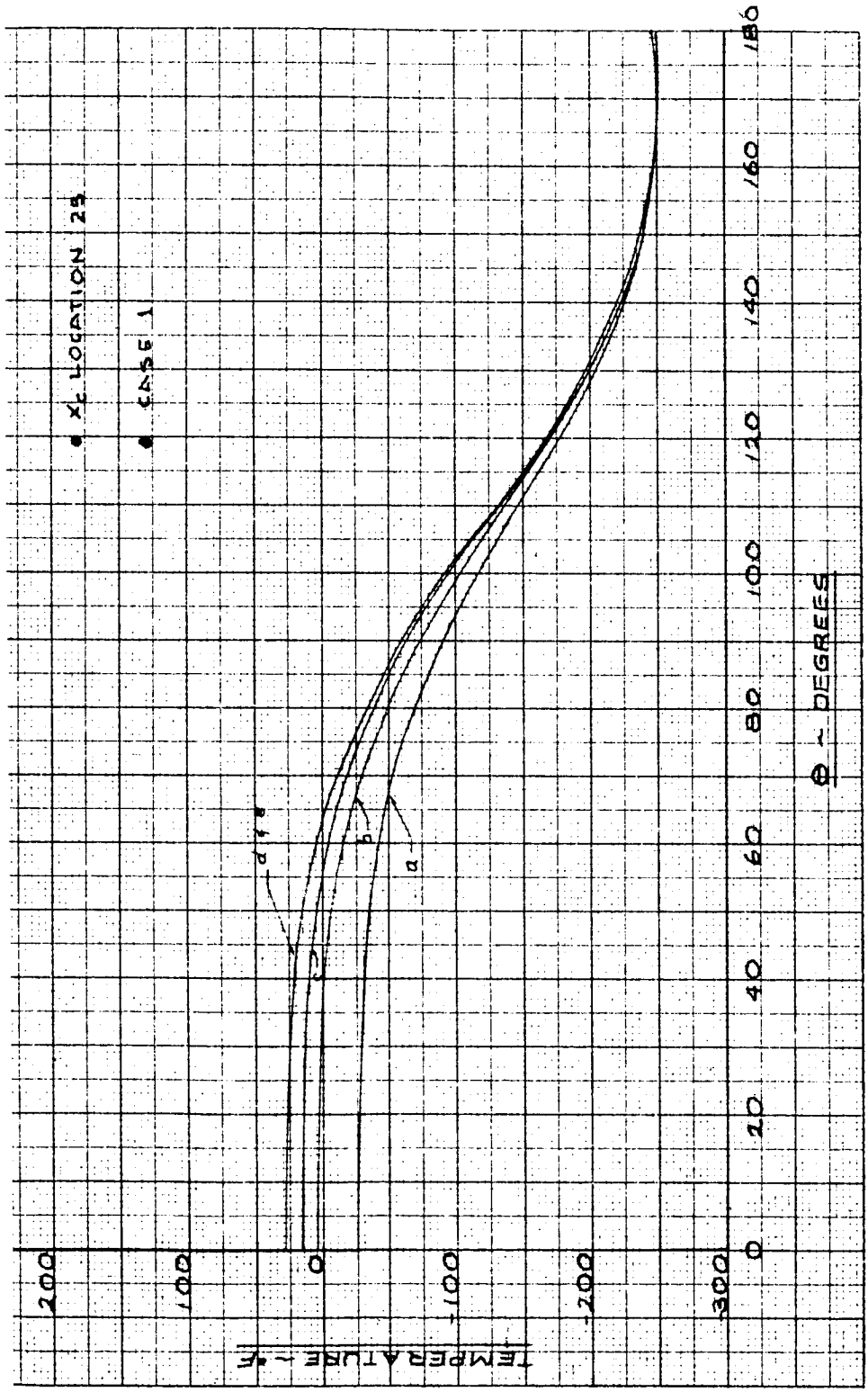

Figure 2-58. Forward Heat Shield Temperature Distribution After Start Cooling Period (2.0 Hours) (Sheet 4 of 14)

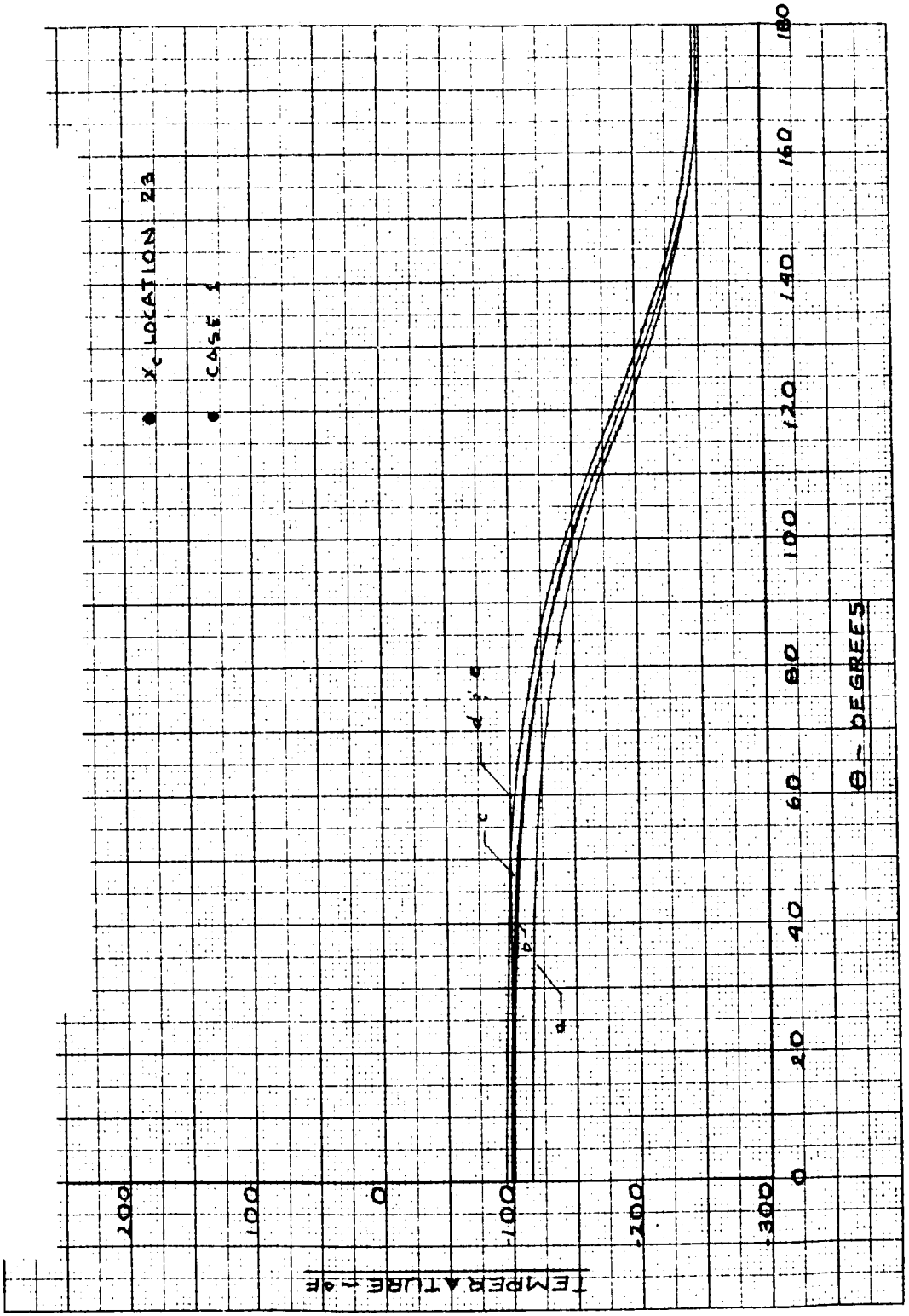

Figure 2-58. Forward Heat Shield Temperature Distribution After Start Cooling Period (5.0 Hours) (Sheet 5 of 14)

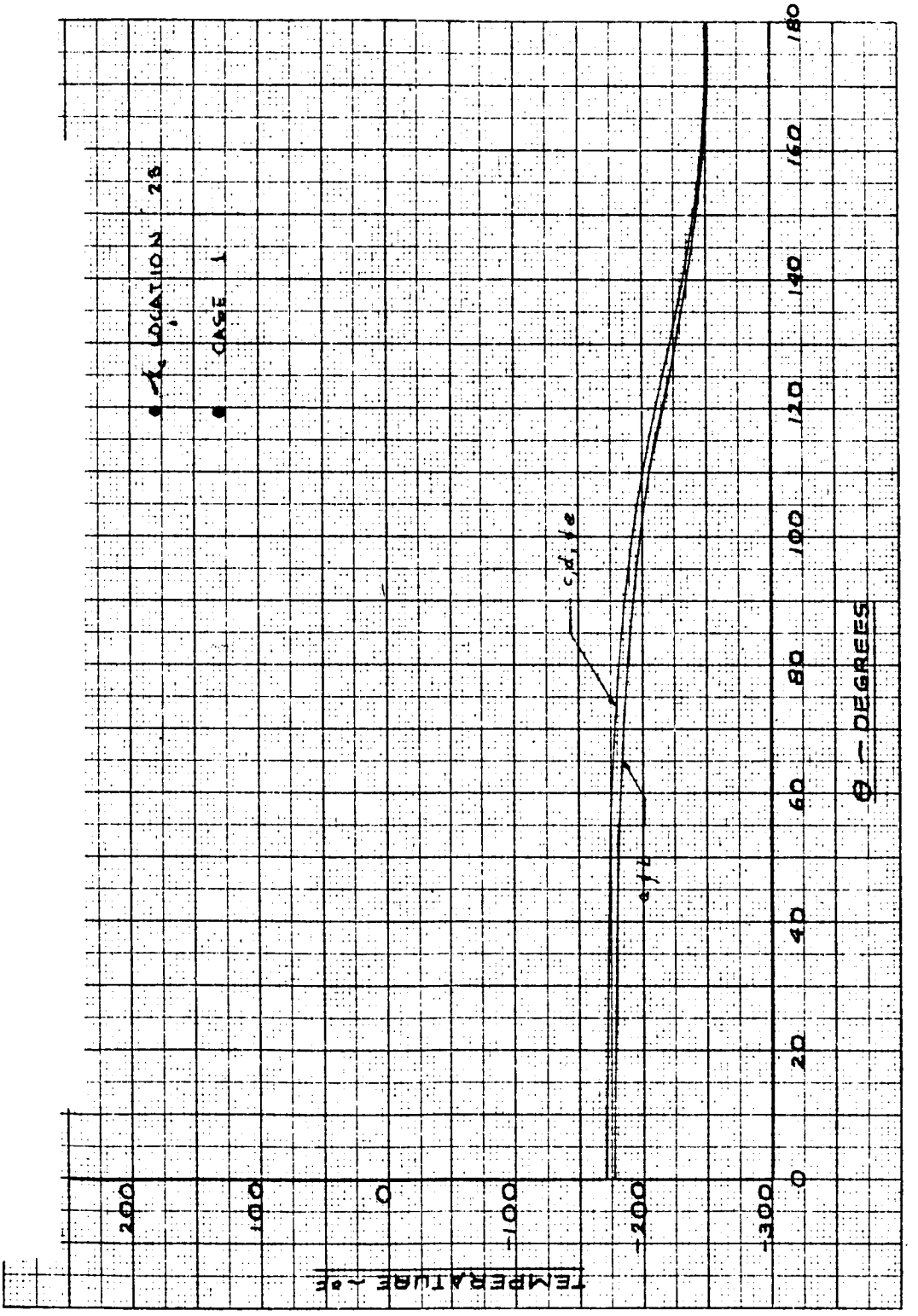

Figure 2-58. Forward Heat Shield Temperature Distribution After Start Cooling Period (10.0 Hours) (Sheet 6 of 14)

[redacted]

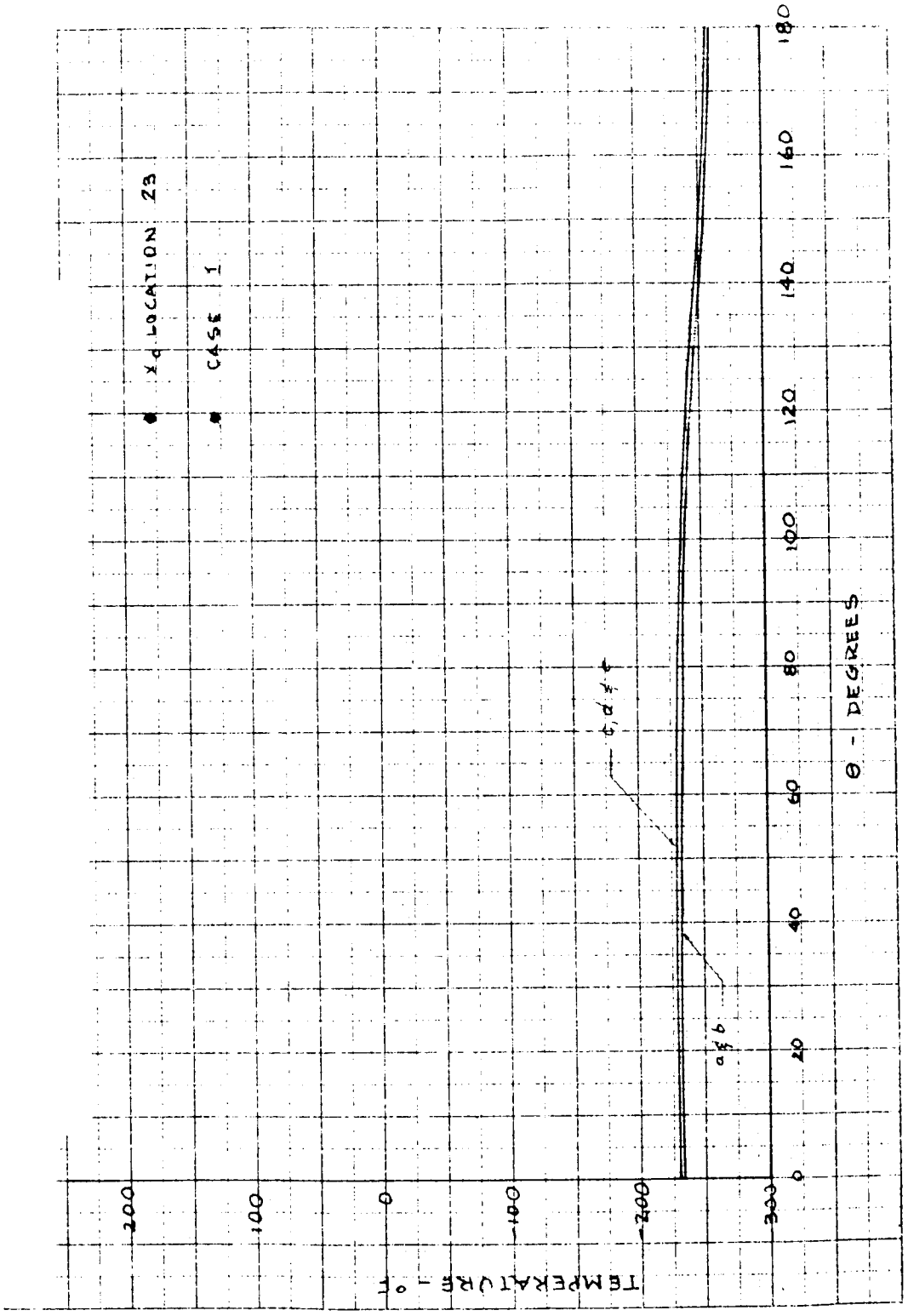

Figure 2-58. Forward Heat Shield Temperature Distribution After Start Cooling Period (20.0 Hours) (Sheet 7 of 14)

[redacted]

[redacted]

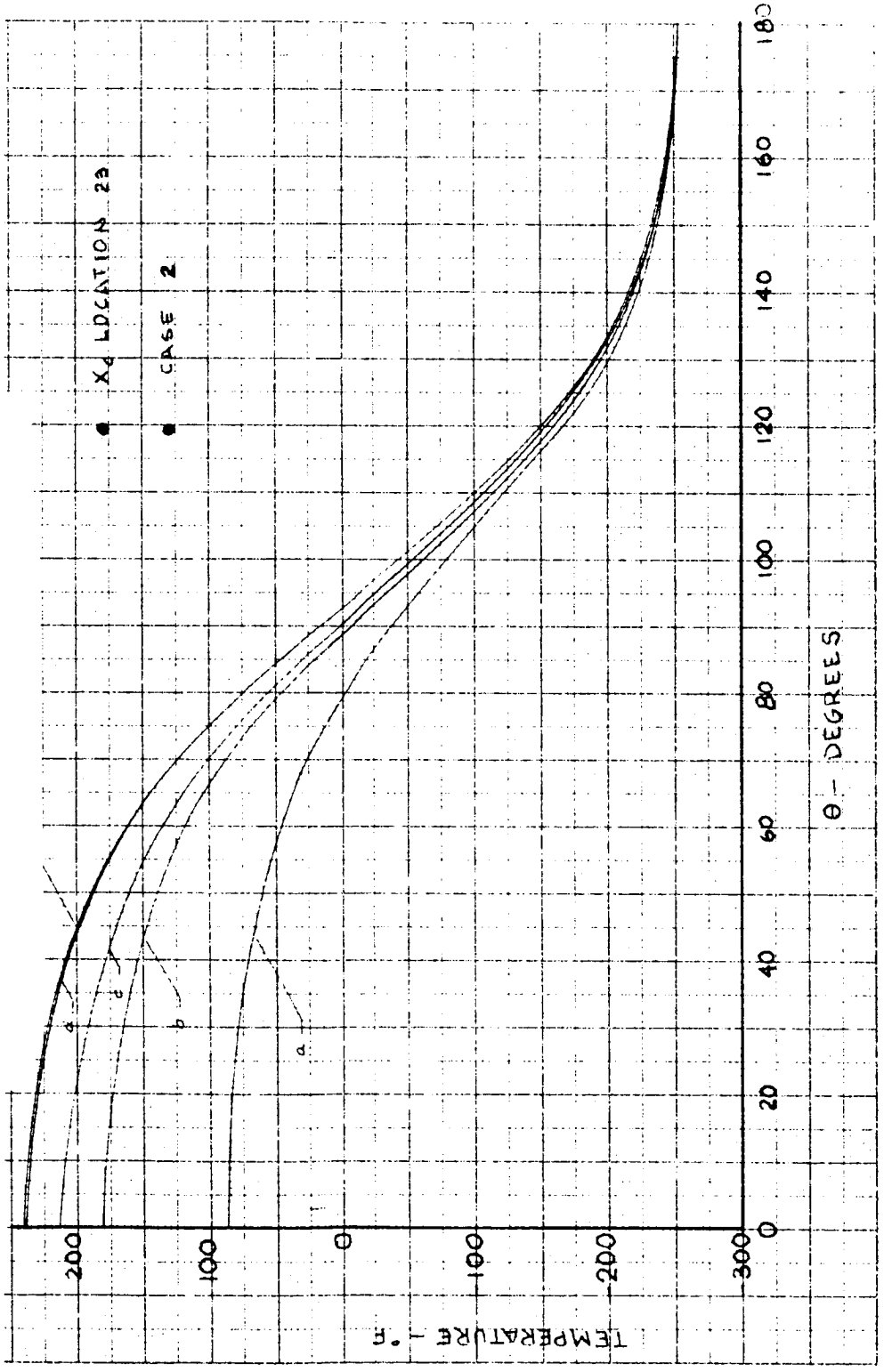

Figure 2-58. Forward Heat Shield Temperature Distribution After Start Cooling Period (0.25 Hours) (Sheet 8 of 14)

[redacted]

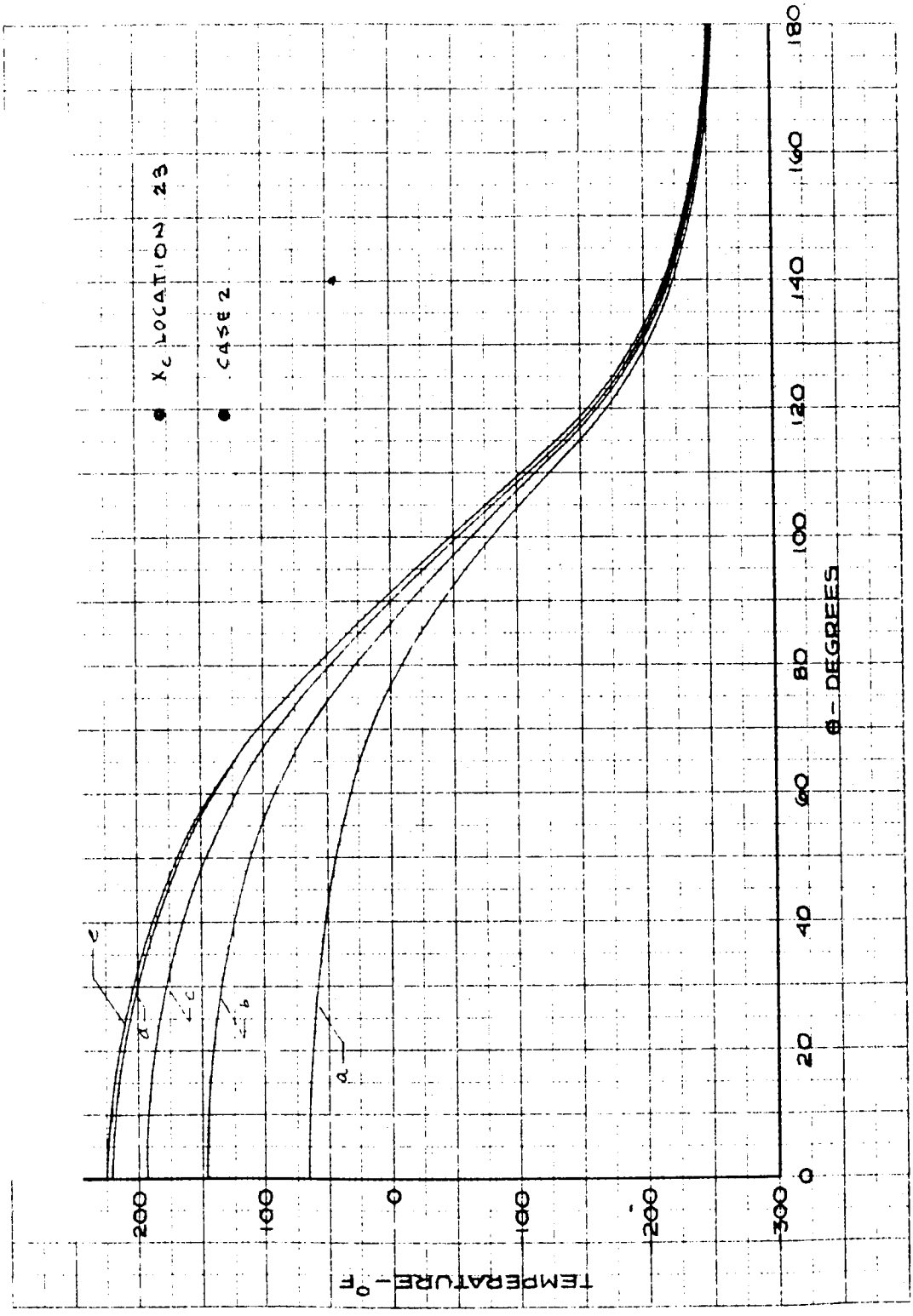

Figure 2-58. Forward Heat Shield Temperature Distribution After Start Cooling Period (0.5 Hours) (Sheet 9 of 14)

[redacted]

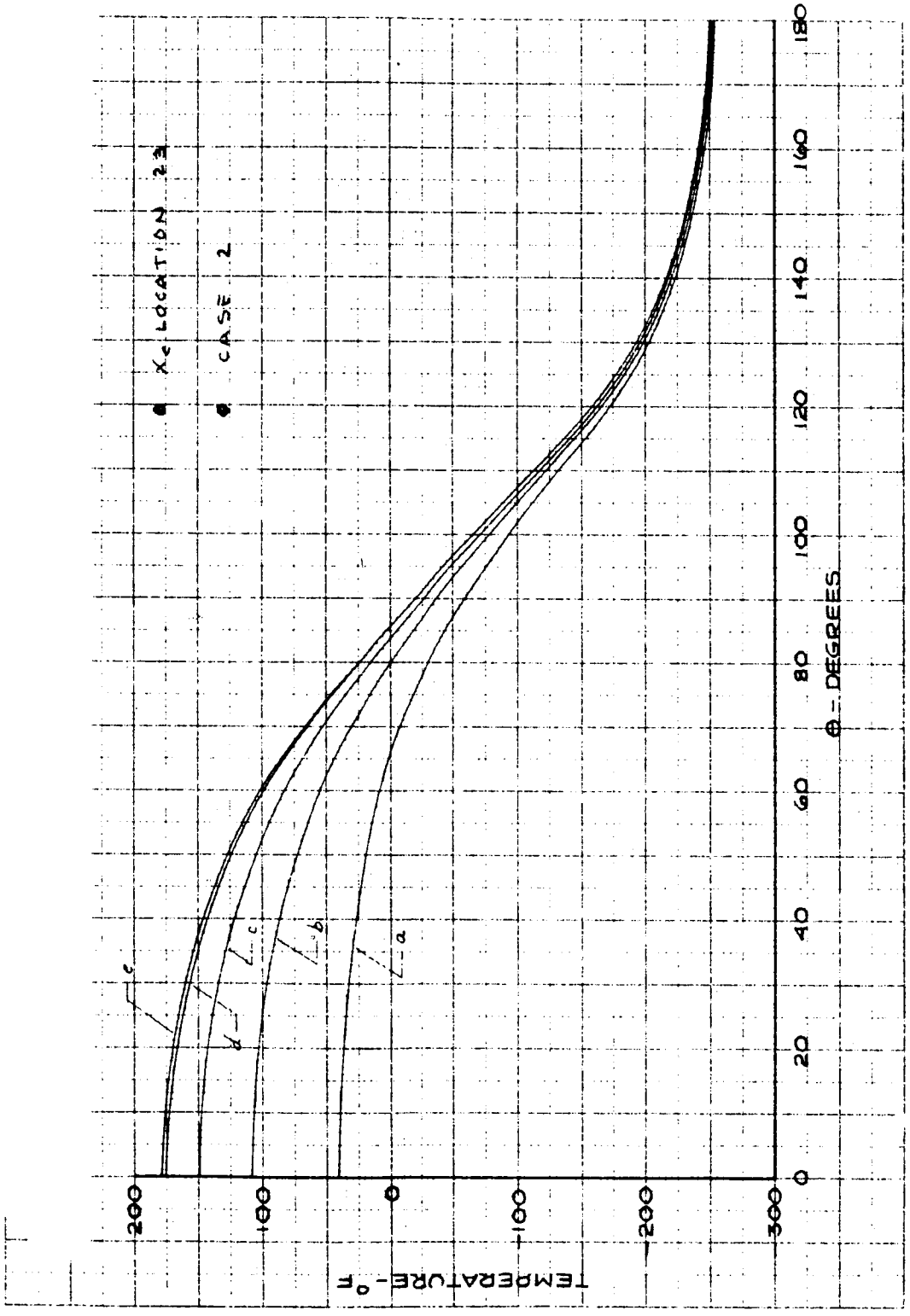

Figure 2-58. Forward Heat Shield Temperature Distribution After Start Cooling Period (1.0 Hours) (Sheet 10 of 14)

~~CONFIDENTIAL~~

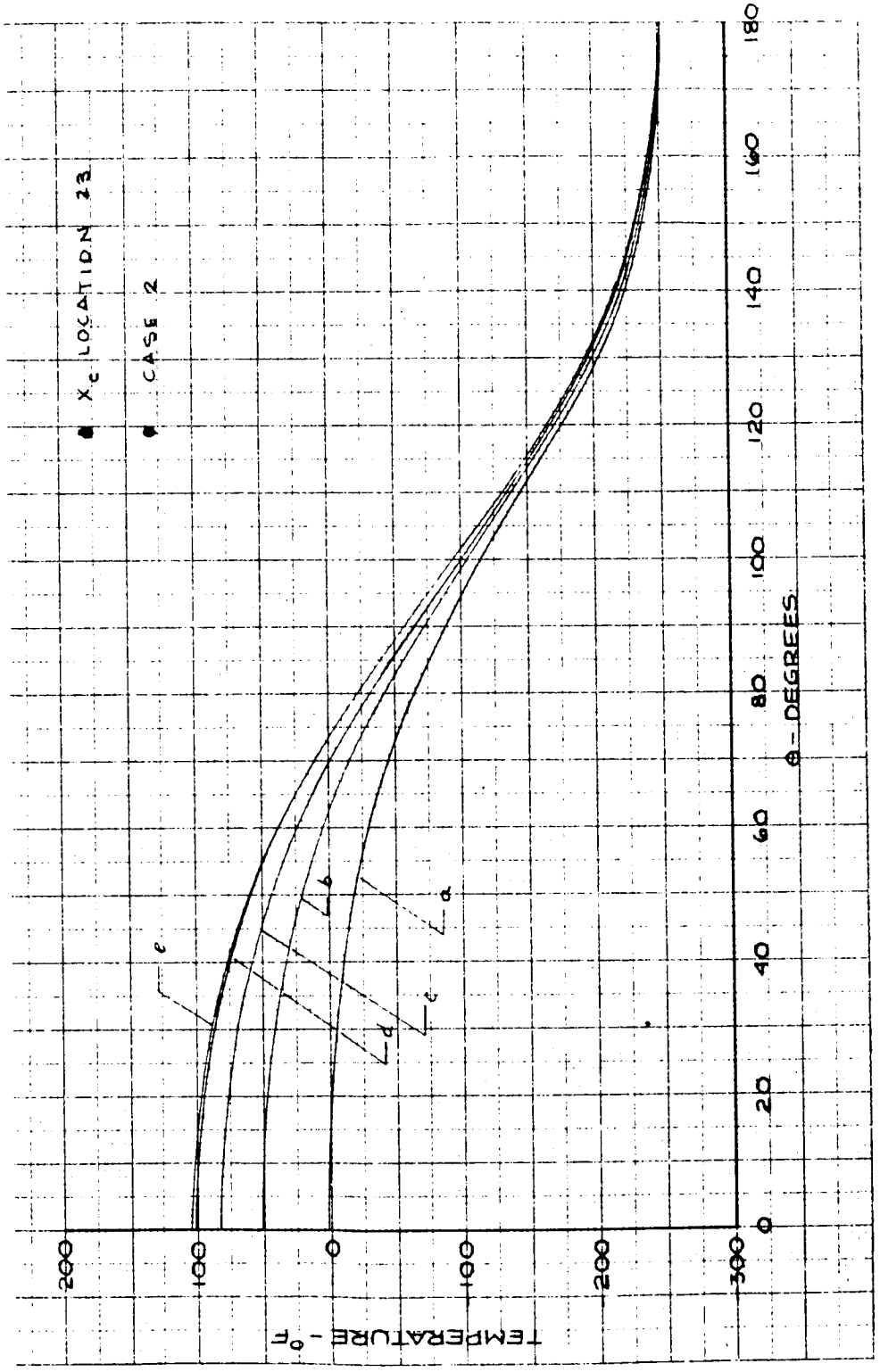

Figure 2-58. Forward Heat Shield Temperature Distribution After Start Cooling Period (2.0 Hours) (Sheet 11 of 14)

~~CONFIDENTIAL~~

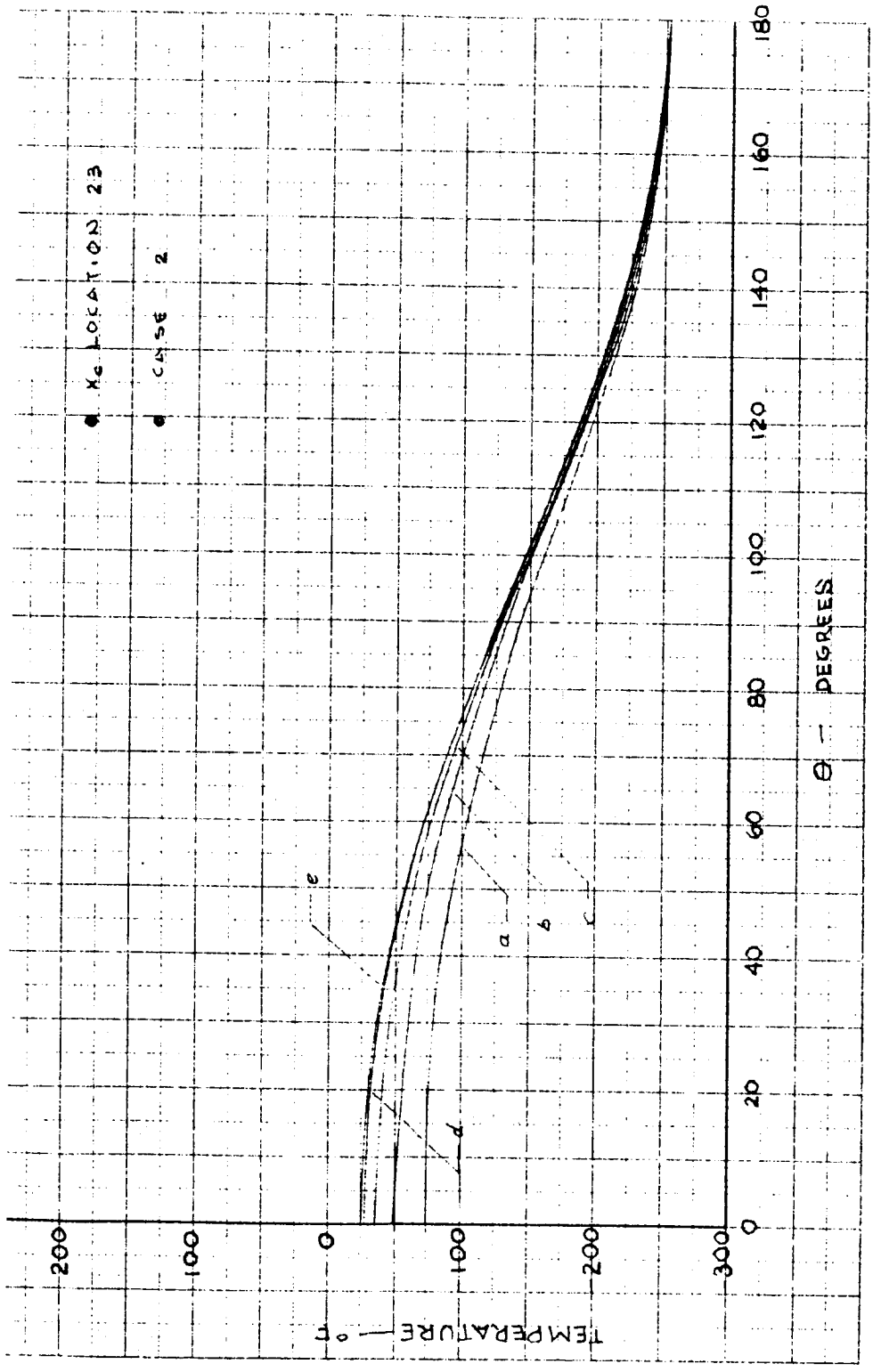

Figure 2-58. Forward Heat Shield Temperature Distribution After Start Cooling Period (5.0 Hours) (Sheet 12 of 14)

~~CONFIDENTIAL~~

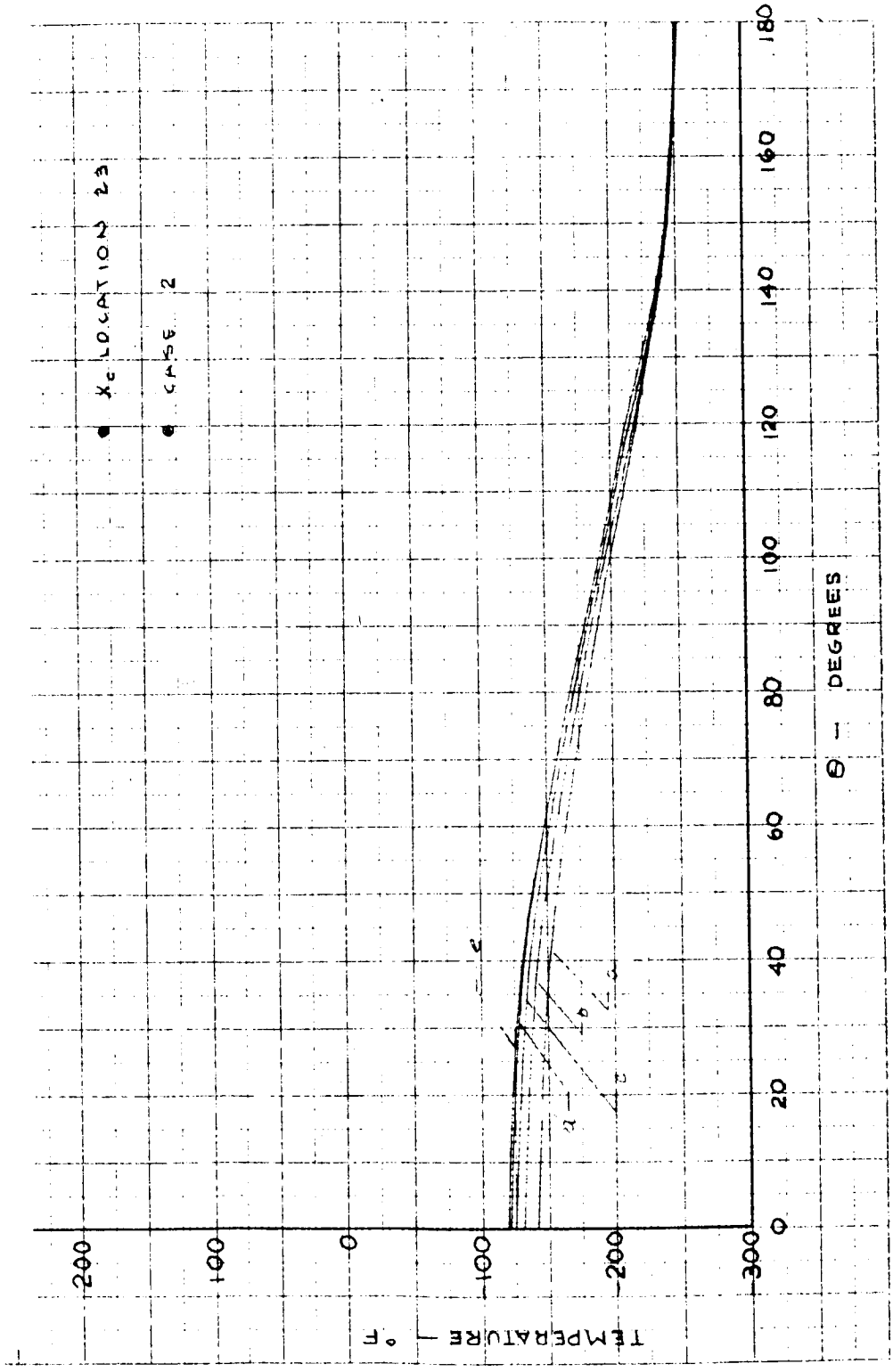

Figure 2-58. Forward Heat Shield Temperature Distribution After Start Cooling Period (10.0 Hours) (Sheet 13 of 14)

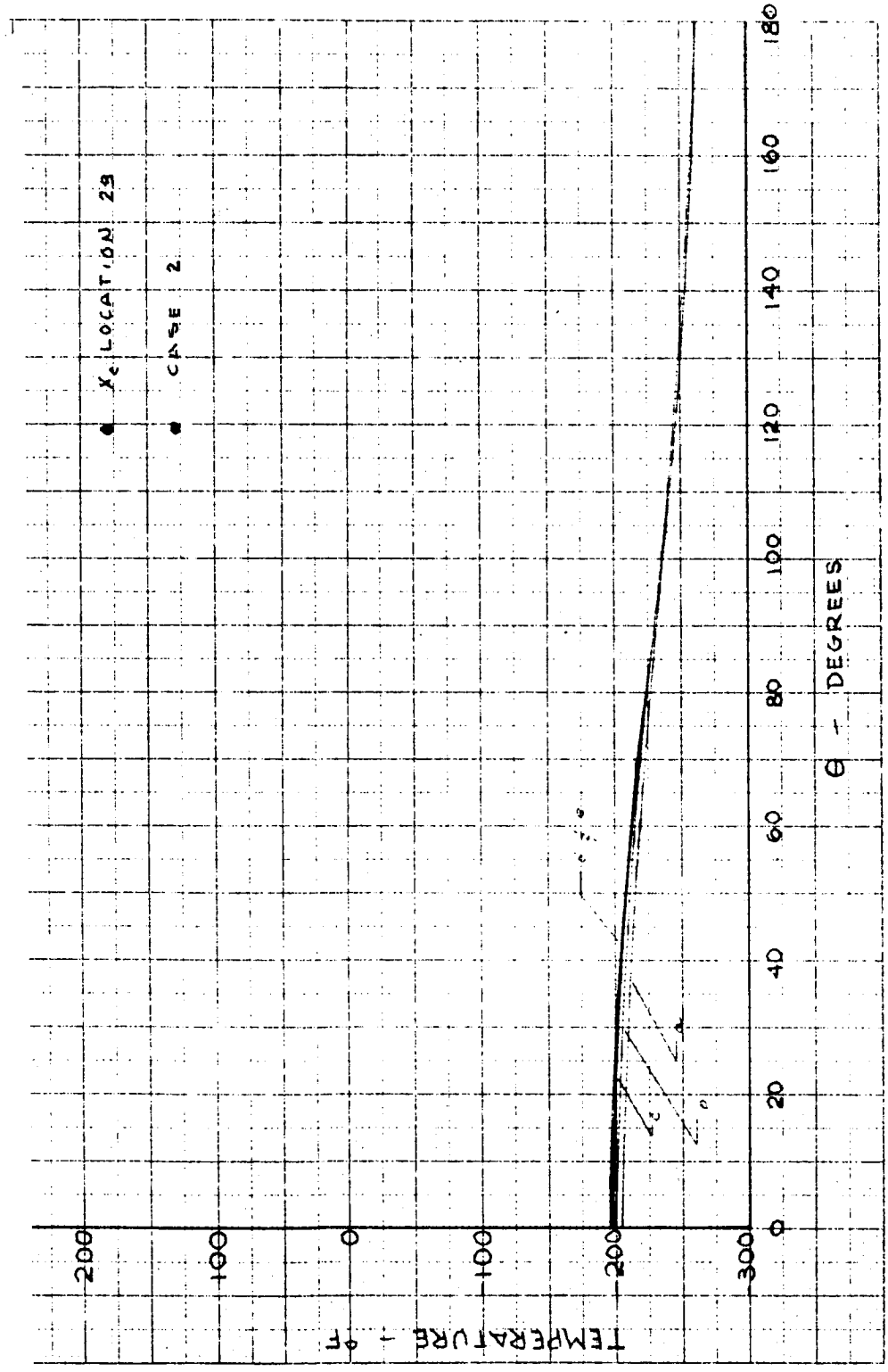

Figure 2-58. Forward Heat Shield Temperature Distribution After Start Cooling Period (20.0 Hours) (Sheet 14 of 14)

~~CONFIDENTIAL~~

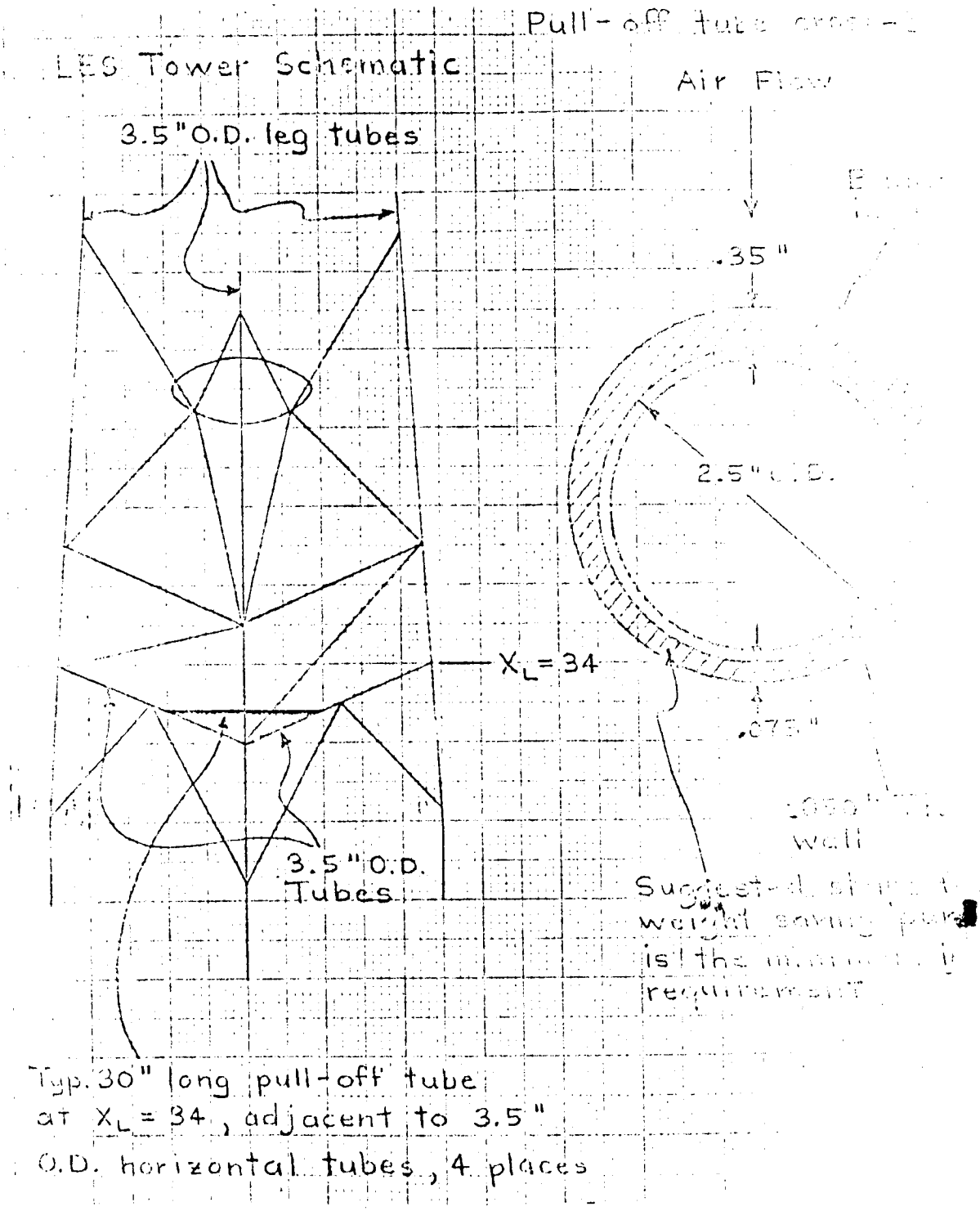

Figure 2-59. Schematic of the LES Tower, Showing the Location of the Forward Heat Shield Pull-off Tubes; and a Tube Cross-Section, Showing the Insulation Requirement for These Tubes

~~CONFIDENTIAL~~

[redacted]

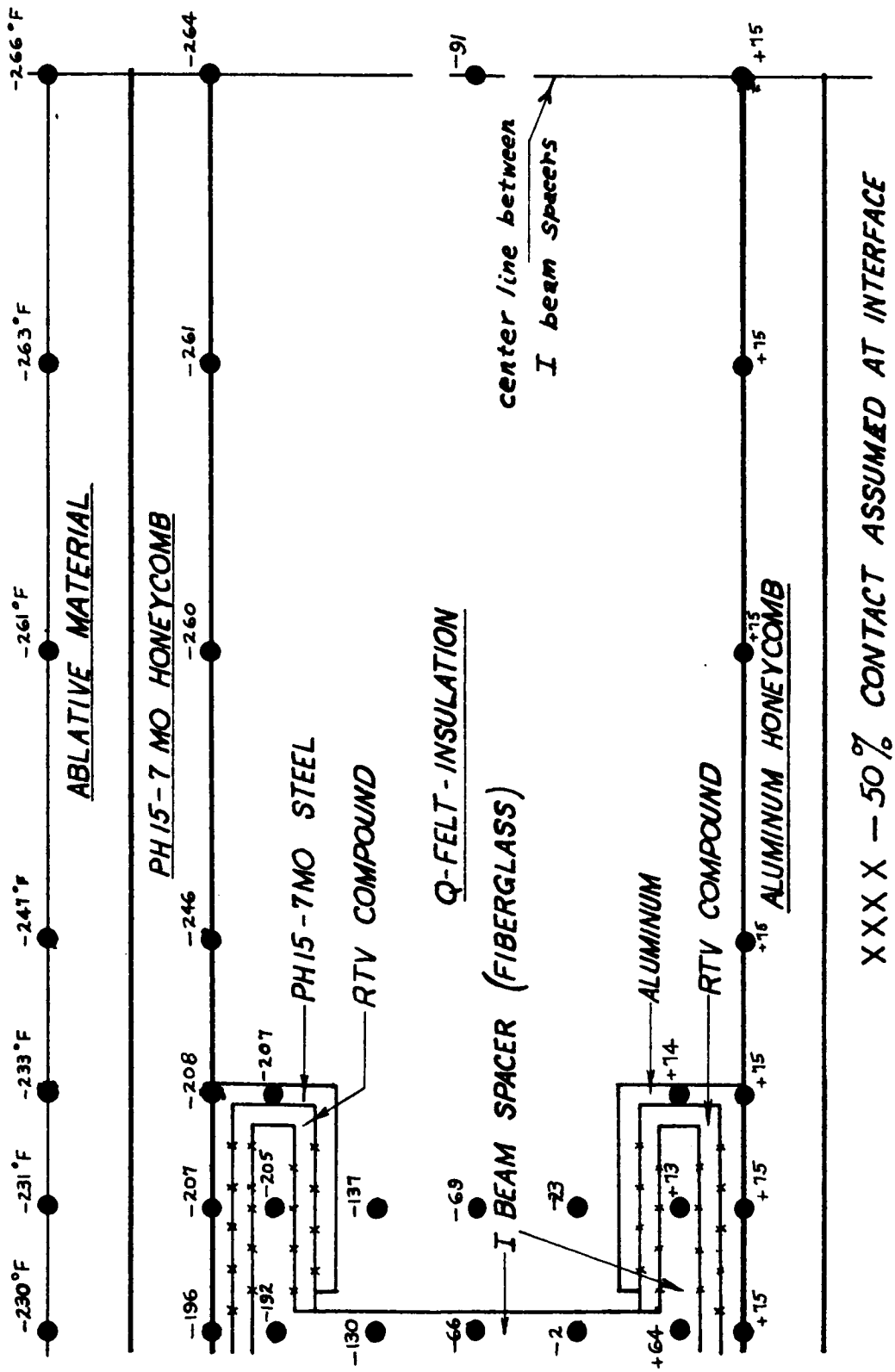

Figure 2-60. Command Module Steady-State Temperature Distribution of I-Beam Spacer for Space Flight

[redacted]

[redacted]

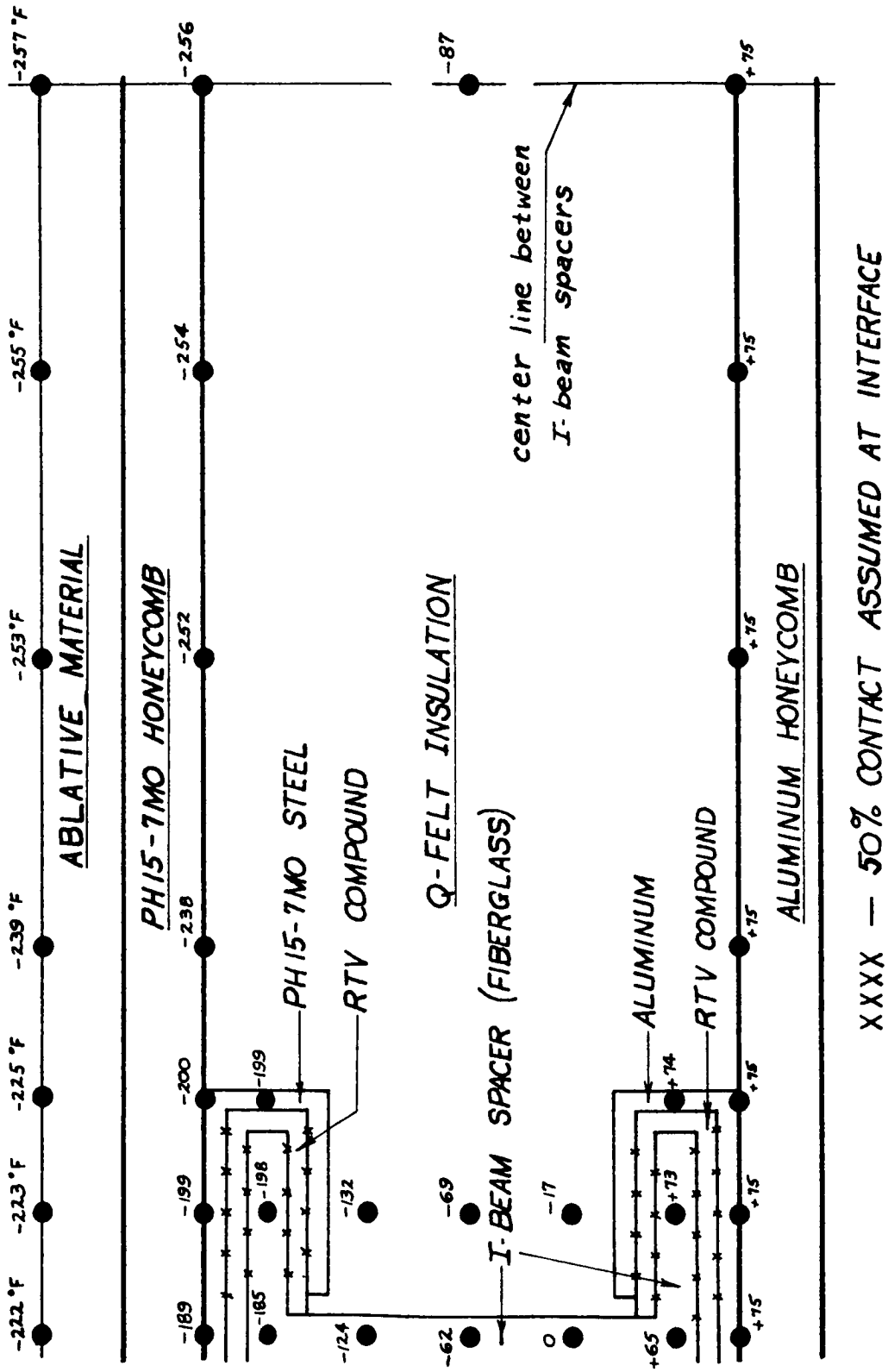

Figure 2-61. Command Module Steady-State Temperature Distribution of I-Beam Spacer for Space Flight

[redacted]

3.0 SERVICE MODULE

3.1 Expected Temperatures During Space Operations for the S/M Shell Structure and for Some Components

3.1.1 A summary of the expected temperatures, during space operations, for the S/M shell structure and for some of its components is tabulated in Tables 3-1 through 3-5. The results are presented in comparative form for two cases. In Case 1 the inside of the S/M shell and the radial shear panels were insulated to provide thermal protection for the SPS propellant. In Case 2 propellant thermal protection was provided by insulating the individual propellant storage tanks. The minimum insulation thickness required for propellant thermal protection can be considered to be 0.25 inches for each of the above mentioned cases. These results are based on a thermal conductivity of 3 x 10-5 Btu/hr-ft-°F for the insulation and an emissivity of 0.2 for the S/M's surface. In addition, it was assumed in the analysis that the S/M was shielded by the C/M during the translunar and transearth mission phases. (i.e., no solar radiation incident to the S/M's surface)

3.2 Service Module Honeycomb Shell Structure (Boost)

3.2.1 During boost the maximum expected face temperature of the S/M's aluminum honeycomb shell structure is 291 F. The maximum temperature gradient across the panel thickness is 93 F. Along the axial direction, a maximum temperature variation of 20 F is predicted.

3.2.2 The above values were based on an exposed 1.5-inch aluminum honeycomb shell structure with a face thickness of 0.032 inches. The 1/4-inch hexagonal core consisted of 0.0015-inch foil.

3.3 Thermal Requirements of Storable Propellants During Prelaunch Phase

3.3.1 Aside from ECS requirements, it appears that, due to the expected variation of weather conditions in Florida, some form of temperature control device such as air conditioning will be required in the S/M in order to maintain storable propellant temperature within allowable limits during the pre-launch phase. The conditioning air temperature is presently taken to be 70 ± 10 F. It is felt that the use of insulation during this phase will be ineffectual. Preliminary studies indicate that there will be no requirements for direct air conditioning of the command module equipment bay area. However, further studies will be necessary to substantiate these results.

3.4 Heating Requirement for the S/M Main Engine Injector Plate

3.4.1 When the honeycomb shell of the S/M is insulated, the power required to prevent the main engine injector plate from cooling below 40 F (during the lunar mission) will be as shown in Figure 3-1. The curve indicates a minimum heater capacity of 65 watts will be required during the mission.

[redacted]

Table 3-1. Expected Component Temperatures During Translunar Phase, S/M Surface (Part 1)

Case 1. Insulation on Inside of S/M Shell and on Radial Shear Panels

Expected Structure Temperature (°F)

Mission Phase	Relative Angular Distance - Degrees											
	0	30	60	90	120	150	180	210	240	270	300	330
Translunar	-84	-232	-220	-187	-99	-151	-98	-181	-201	-180	-97	-146
Lunar Orbit	35	110	146	146	110	35	6	52	80	80	52	6
Transearth	-112	-238	-227	-198	-126	-167	-125	-193	-209	-192	-124	-162
	Insulation Thickness 0.25 Inch											

Expected Structure Temperature (°F)

Mission Phase	Relative Angular Distance - Degrees											
	0	30	60	90	120	150	180	210	240	270	300	330
Translunar	-84	-243	-230	-193	-101	-154	-100	-186	-207	-185	-99	-149
Lunar Orbit	35	111	147	147	111	35	6	52	80	80	52	6
Transearth	-111	-247	-235	-203	-127	-168	-126	-196	-215	-196	-125	-163
	Insulation Thickness 0.4 Inch											

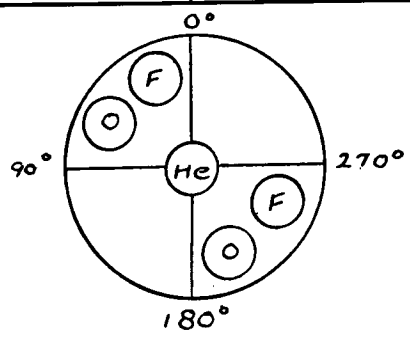

Where

F = Fuel
O = Oxidizer
He = Helium

[redacted]

Table 3-2. Expected Component Temperatures During Translunar Phase, S/M Surface (Part 2)

Case 2. Insulation on Propellant Tanks

Expected Structure Temperature (°F)

Mission Phase	Relative Angular Distance - Degrees											
	0	30	60	90	120	150	180	210	240	270	300	330
Translunar	-147	-160	-163	-160	-147	-155	-147	-160	-163	-160	-147	-155
Lunar Orbit	84	161	199	198	157	82	61	92	114	114	92	57
Transearth	-147	-160	-163	-160	-147	-154	-147	-160	-163	-160	-147	-154
	Insulation Thickness = 0.25 Inch											

Expected Structure Temperature (°F)

Mission Phase	Relative Angular Distance - Degrees											
	0	30	60	90	120	150	180	210	240	270	300	330
Translunar	-150	-163	-166	-163	-150	-157	-150	-163	-166	-163	-150	-157
Lunar Orbit	84	161	199	199	158	82	61	92	114	114	92	57
Transearth	-149	-162	-166	-163	-150	-156	-149	-162	-166	-163	-150	-156
	Insulation Thickness = 0.4 Inch											

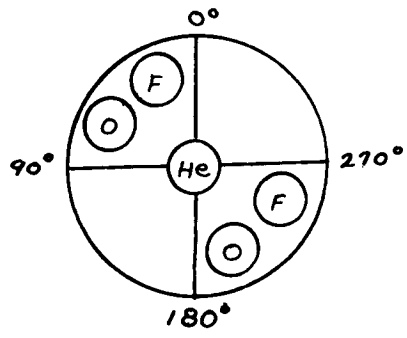

Where

F = Fuel
O = Oxidizer
He = Helium

[redacted]

[redacted]

Table 3-3. Expected Component Temperatures During Translunar Phase, S/M Surface (Part 3)

Case 1. Insulation on Inside of Service Module Shell and on Radial Shear Panels			
Component	Insulation Thickness		
	0	0.25	0.4
Radial Shear Panel		67.3	68.6
External Surface (minimum)		-232.2	-243.2
Helium Wall		68.2	69.1
Fuel		69.4	69.7
Oxidizer		69.3	69.7

Case 2. Insulation on Propellant Tanks			
Component	Thickness		
	0	0.25	0.4
Radial Shear Panel	9.6	-111.7	-114.6
External Surface (minimum)	-64.5	-162.6	-166.2
Helium Wall	29.2	-66.4	-68.8
Fuel	55.0	69.5	69.8
Oxidizer	52.8	69.4	69.7

[redacted]

Table 3-4. Maximum and Minimum Surface Temperatures of S/M Cryogenic Tanks During Lunar Mission (Part 1)

Case 1. Insulation on Inside of Service Module Shell and on Radial Shear Panel			
Component	Insulation Thickness		
	0	0.25	0.4
Radial Shear Panel		69.3	69.7
External Surface (maximum)		146.2	146.6
Helium Wall		69.2	69.6
Fuel		69.1	69.6
Oxidizer		69.1	69.6

Case 2. Insulation on Propellant Tanks			
Component	Insulation Thickness		
	0	0.25	0.4
Radial Shear Panel	79.0	102.7	102.9
External Surface (maximum)	75.9	198.6	198.7
Helium Wall	68.6	84.4	84.5
Fuel	61.6	69.2	69.7
Oxidizer	61.7	69.1	69.5

[redacted]

Table 3-5. Maximum Surface Temperatures of Honeycomb Adapter During Boost Heating

Case 1. Insulation on Inside of Service Module Shell and on Radial Shear Panel			
Component	Insulation Thickness		
	0	0.25	0.4
Radial Shear Panel		56.4	62.9
External Surface (minimum)		-238.2	-247.4
Helium Wall		59.8	64.7
Fuel		57.0	63.3
Oxidizer		57.0	63.2

Case 2. Insulation on Propellant Tanks			
Component	Insulation Thickness		
	0	0.25	0.4
Radial Shear Panel	-91.2	-111.3	-113.9
External Surface (minimum)	-140.1	-162.6	-165.7
Helium Wall	-50.3	-66.0	-67.7
Fuel	-82.0	51.5	59.7
Oxidizer	-82.0	51.0	59.3

3.4.2 The power requirement to the injector plate, when the main propellant tanks are insulated, is shown in Figure 3-2. When the surface emissivity of the injector plate (facing the propellant tanks) is reduced from 1.0 to 0.3, a 40 percent reduction in the required minimum heater capacity results.

3.4.3 The above information is preliminary in nature and should be used accordingly.

3.5 Maximum and Minimum Expected Surface Temperatures of the Service Module Cryogenic Tanks During the Lunar Mission

3.5.1 Table 3-6 shows the maximum and minimum expected temperatures for the outer surface of the cryogenic storage tanks during the lunar mission. The results are shown for the case when the S/M is shielded by the C/M (i.e., apex of C/M oriented towards the sun). Any other vehicle orientation would result in solar radiation incident on the S/M's surface and a subsequent increase in cryogenic tank surface temperatures. No consideration was given to possible X-axis inclination and vehicle rotation, which may be required due to the LEM concept.

Table 3-6. Maximum and Minimum Surface Temperatures of S/M Cryogenic Tanks During Lunar Mission (Part 2)

Mission	Oxygen Vessel		Hydrogen Vessel	
	T_1	T_2	T_1	T_2
Translunar	78	41	81	43
Lunar Orbit	65	41	67	43
Transearth	63	35	65	38

T_1 = Maximum Temperature

T_2 = Minimum Temperature

3.6 Heat Transfer Analysis of Solenoid Valve

3.6.1 The maximum duration of valve operation is specified as 5 minutes. In addition to this initial period of operation, intermittent operation is considered where the valve is operated for 30-second intervals, followed by 20-minute intervals of non-operation. The maximum temperature of the valve was calculated to be 172 F, which occurred at the end of the

initial 5-minute-period of operation. A constant heat generation of 56 watts was utilized in the analysis. Figure 3-3 shows the time/temperature history of the solenoid valve.

3.7 Expected Environmental Temperature Extremes for Electrical Cables

3.7.1 Table 3-7 shows the expected environmental temperature extremes. The temperature valves are preliminary in nature and should be used accordingly.

3.8 Thermal Data for Mechanical Docking Arms

3.8.1 A thermal analysis was made of the LEM mechanical transposition and docking configurations (Figure 3-4) to determine the expected temperature extremes for the tubular docking arms during spaceflight. The temperature extremes for the aluminum arms are -275 F and 275 F; temperature extremes for the titanium arms are -290 F and 199 F. Results of the thermal analysis are shown in Table 3-8.

3.8.2 The results indicate that the titanium tube attained the lowest temperature, while the aluminum tube attained the highest temperature. This situation is due to a higher emissivity and a lower capacitance for the titanium tube. The solar absorptivity of the titanium tube is 0.6; emissivity is 0.7. The solar absorptivity of the aluminum tube is 0.45; emissivity is 0.3. Because the titanium tube has a relatively low thermal conductivity and a thin wall, it is subjected to severe circumferential temperature gradients that could result in high thermal stresses. The aluminum tube has a negligible circumferential temperature gradient, due to its high thermal conductivity.

3.8.3 The heating from the RCS plume impingement resulted in a localized increase in temperature of approximately 5 F, due to the short duration of heating (5 seconds), and because the heating rates are low in the region that the arms pass through.

3.9 Service Module Outer Shell Temperatures During Translunar Flight

3.9.1 During this analysis the value used for the emissivity and solar absorptivity was 0.2. Insulation was considered to be on the inside of the S/M's shell and on both sides of the shear panels. The insulation thickness was 0.25 inches, with a thermal conductivity of 3.0 x 10-5 Btu/hr-ft-°F. The maximum circumferential temperature gradient expected during the above mentioned translunar mission is shown following Table 3-11. It is expected that circumferential temperature gradients, less severe than those shown, will occur when the effects of the ECS and EPS radiators are included.

[redacted]

Table 3-7. Summary of Expected Environmental Temperature Extremes For Electrical Cables in the C/M and S/M (Preliminary)

Service Module		
Cable Location	Maximum Environmental Temperature (°F)	Minimum Environmental Temperature (°F)
1. Attached to radial shear panels	200	-65
2. Adjacent to fuel cell	500	-
3. Service Module interior	depends upon specific location	-
4. Adjacent to RCS	275	0

Command Module		
Cable Location	Maximum Environmental Temperature (°F)	Minimum Environmental Temperature (°F)
1. Aft equipment compartment	600	-230
(a) Metal-to-metal attachment to outer honeycomb structure		
(b) Attached to outer honeycomb structure with fiberglass isolator	400	-230
(c) Attached to outside surface of pressure vessel	200	0
(d) Air temperature	180	-
2. Forward compartment	250	-60
3. Adjacent to RCS engines	275	-60

[redacted]

[redacted]

Table 3-8. Results of Thermal Analysis of Mechanical Docking Arms

Single Purpose (Aluminum Arms - Translunar Injection Only)				
Type of Data		Maximum Sun	No Sun	
Temperature Extremes		172 F	10 Hours	84 Hours
			-134 F	-275 F
Temperature Gradients	Circumferential	2 F/in.	0	
	Axial	0	0	

Double Purpose

Translunar Injection										Lunar Orbit	
Type of Data		Titanium			Aluminum			Titanium		Aluminum
		Max Sun	No Sun		Max Sun	No Sun				
Temperature Extremes		125 F	2 Hrs	84 Hrs	164 F	10 Hrs	84 Hrs	-22 F to 199 F per orbit		-15 F to 275 F per orbit
			-104 F	-290 F		-100 F	-256 F			
Temperature Gradients	Circum-ferential	8 F/in. to 17 F/in.	9 F/in. to 12 F/in.		2 F/in.	2 F/in.		Max	Avg	4 F/in.
								21 F/in.	13 F/in.	
	Axial	0	0		0	0		5 F/in.	3 F/in.	4 F/in.

Increase in Local Temperature Due to RCS Plume Heating	
Titanium Tube	Aluminum Tube
5.2 F	3.8 F

[redacted]

3.10 Summary of S/M SPS Propellant Thermal Protection Requirements

3.10.1 Initial results indicate that the insulation required to protect the propellant from extreme cold environmental conditions is also required for protection against the relatively high environmental temperatures which will result from solar radiation to the spacecraft. These insulation requirements, as summarized in Table 3-9, are designed to maintain propellant temperatures between the limits of 40 F to 80 F and to provide the best situation for temperature control of the SPS helium system.

Table 3-9. Summary of Insulation Requirements for S/M SPS Propellant Thermal Protection (1)

Location	Nominal Thickness
Inside of S/M shell	0.25
Radial shear panels (both sides)	0.25
Forward bulkhead, at X_s = 355 (both sides) (2)	0.25
Aft bulkhead, at X_s = 200 (forward side)	0.25
Inside of fairing (2)	0.25
Inside of combination meteorite-heat shield, and on aft side of bulkhead (X_s = 200) within the shield (3)	0.25

(1) Thermal conductivity of insulation = 3×10^{-5} Btu/hr-ft-°F; density = 3.5 pounds per cubic foot
(2) Insulation required on forward side of bulkhead and inside the fairing as thermal protection for the heat shield
(3) Design of combination meteorite - heat shield still pending

3.11 Service Module Surface Insulation Requirements Due to Plume Impingement From the Service Module RCS Engines

3.11.1 It was recommended that a composite material consisting of Min-K 2000 insulation with a stainless steel cover sheet be utilized as the S/M's thermal protection from RCS plume impingement heating. It was determined that by utilizing a composite material consisting of Q-felt insulation with a titanium cover sheet, a weight reduction of approximately 15 pounds can be realized.

3.11.2 The design parameters considered in this analysis included: (1) a maximum allowable surface temperature of the S/M of 400 F; (2) an aluminum honeycomb facesheet thickness of 0.017 inches; (3) an insulation cover sheet thickness of 0.005 inches; (4) an initial S/M surface temperature of 250 F prior to impingement; (5) a firing time of 60 seconds for the RCS engines; and (6) RCS engines located at X_s = 325, with an axial and roll nozzle cant of 10 degrees. Figure 3-5 shows the isothermal profile map utilized in the analysis; the surface of the S/M, where insulation is required, is shown in Figure 3-6. Table 3-10 presents a summary of the maximum temperatures and Q-felt insulation requirements for the S/M.

3.11.3 The total composite weight (cover sheet combined with insulation and bonding material) was 25.58 pounds when using Q-felt with a stainless steel cover sheet (emissivity = 0.25) and 19.04 pounds when using a titanium cover sheet (emissivity = 0.6). This compares with a total composite weight of 34.63 pounds when Min-K 2000 insulation is used with a stainless steel cover sheet. It is recommended that a composite insulation be used that consists of Q-felt with a 0.005-inch titanium cover. Table 3-11 presents a summary of the various composite insulation weights obtained for the Min-K and Q-Felt insulating materials.

3.12 Oxygen and Hydrogen Cryogenic Storage Tank Temperatures

3.12.1 An analysis was conducted to determine the maximum surface temperatures for the cryogenic storage tanks located in Sextant I of the S/M. Figure 3-7 shows the results of the study for the translunar mission. The spacecraft orientation considered was one in which there is maximum solar radiation incident to the surface of Sextant I. This condition results in the most extreme maximum expected temperatures for the surface of the cryogenic tanks.

3.13 Thermal Evaluation of 2 KMC Scimitar Antenna Located on the Service Module Fairing

3.13.1 A thermal evaluation of the 2 KMC scimitar antenna (Model C) was performed for a S-V boost trajectory and for a S/M RCS plume impingement environment. The two antenna locations considered were 22.5 and 45 degrees from the vertical axis of the RCS axial nozzle at station X_s = 365. Results of the evaluation indicate that the antenna temperature will not exceed 350 F when exposed to the S/M RCS plume impingement for 60 seconds. The maximum temperatures of an aluminum or steel antenna with either a fused silica or teflon surface plug for a S-V boost trajectory are shown in Table 3-12. The effect of changing the antenna thickness is also shown in Table 3-12.

Table 3-10. Summary of Maximum Temperature and Insulation Requirements for S/M Surface After 60 Seconds of RCS Plume Impingement

Identification Letter	Uninsulated S/M(1) (Surface Temperature - °F)	Q-Felt Insulation Requirements(2) (Inches)		Areas of Isothermal Zones (Ft^2)	Total Composite Thermal Protection Weight on S/M Surface(3)	
		Steel Cover	Titanium Cover		Steel Cover	Titanium Cover
A	300					
B	350					
C	400	0.125	0.125	19.4	4.559	2.883
D	590	0.250	0.125	26.3	7.002	3.908
E	985	0.500	0.500	11.26	3.802	2.729
F	1485	0.750	0.500	1.55	0.606	0.376
G	1720	0.750	0.500	0.218	0.085	0.052
H	300					
I	350					
J	400	0.125	0.125	3.2	0.752	0.475
K	430	0.125	0.125	1.21	0.284	0.179
L	460	0.125	0.125	0.655	0.154	0.097
Bonding Material (0.13 lb/ft^2)				63.79	8.340	8.340
				Total	25.584	19.039

(1) S/M aluminum face sheet thickness = 0.017 inches; initial temperature - 250 F
(2) To prevent the aluminum honeycomb surface from exceeding 400 F
(3) Consists of 0.005-inch cover sheet + Q-Felt + Bonding Material

[redacted]

Table 3-11. Comparison of Composite Insulation Weights of Min-K and Q-Felt

Type	Properties K Btu/Hr-Ft-°F (lbs/ft³)	Insulation Weight (lbs)	Cover Sheet(1) (lbs) Steel	Cover Sheet(1) (lbs) Titanium	Bonding Material (lbs)	Total Weight(2) (lbs)
Min-K	0.015 = K 20.0 = P	13.29	13.00		8.34	34.63
Q-Felt	0.02 = K 3.0 = P	4.24	13.00		8.34	25.58
Q-Felt	0.02 = K 3.0 = P	3.21		7.49	8.34	19.04

(1) 0.005 inch in thickness
(2) Not considering cover sheet fastener weight

Temperature Gradients: Translunar Mission
(See Para. 3.9.1)

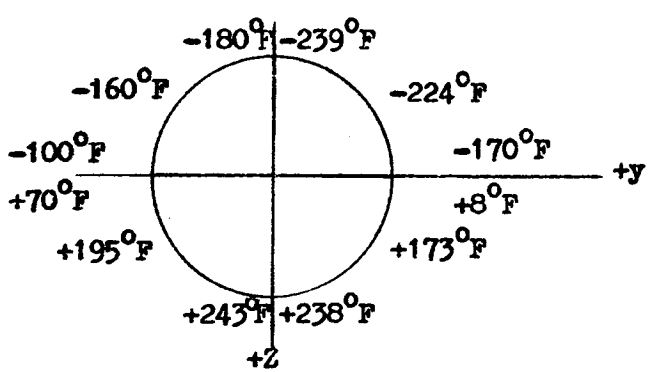

[redacted]

Table 3-12. Thermal Evaluation Results

Antenna Configuration	Maximum Temperature (°F)			Temperature Limit During Boost Trajectory* (degrees F)
	Antenna Thickness (1.0 in.)	Antenna Thickness (0.5 in.)	Antenna Thickness (0.25 in.)	
Aluminum Antenna	810	-	-	600
Silica Plug	670	-	-	600
Aluminum Antenna	835	-	-	600
Teflon Plug	550	-	-	600
Steel Antenna	660	1000	1500	1000
Silica Plug	510	630	765	600
Steel Antenna	670	1010	1510	1000
Silica Plug	461	600	755	600

*Values obtained from S/M Stress Dept. 695/411

3.14 Temperature Response of S/M RCS Composite Thermal Protection for Variable RCS Firings

3.14.1 A study was conducted to determine the effects of RCS plume impingement on the S/M's composite thermal protection, considering different retro-thrust firing cycles required for deorbiting. The maximum RCS retro-thrust firing cycle considered was 400 seconds.

3.14.2 Figure 3-8 presents a summary of temperatures reached at the end of various firing cycles. Figure 3-8 also shows the respective maximum temperature of the interface between the S/M's aluminum skin and RCS's composite thermal protection. The maximum temperatures occur after RCS firing has ceased, as a result of thermal soakback. Figure 3-9 shows the required time for the temperature of composite thermal protection interface to reach a maximum temperature as the RCS's retro-thrust period changes. For example, if the interface temperature at the end of a 400-second firing cycle is 678 F, then a maximum temperature of 719 F can be expected 88 seconds later.

3.15 Sensor Locations for AFRM 011, S/M

3.15.1 There are a total of 14 sensor locations being requested--two each on the S/M's aft heat shield and C/M-S/M adapter and ten on the S/M.

[redacted]

3.15.2 The locations on the C/M-S/M adapter are at the outer surface of the honeycomb at station X_S 370. Locations are 24 degrees CCW (view looking aft) from radial beams 2 and 5.

3.15.3 On the S/M the six shell locations are at X_S 280. Locations measured from the radial beams are listed below.

Sensor	Degree	Beam	Direction (view looking aft)
1	12.5	3	CCW
2	6	4	CCW
3	24	5	CCW
4	12.5	1	CCW
5	6	1	CCW
6	24	2	CCW

Sensor 1, 12.5 degrees CCW from beam 3, is located on the inside surface of the honeycomb; the other shell locations are on the outer honeycomb surface. There are sensor locations on beams 1, 3, 4 and 6 at X_S = 280. These sensors may be located on either side of the beam, 66 inches from the center of the S/M. On the S/M's aft heat shield, one location is on the stainless steel facesheet outer surface at X_S = 187.0; the other location is on the inner surface of super insulation at X_S = 188.28. Both sensor locations are 82.25 degrees CCW from +Z towards -Y, looking forward.

3.16 Thermal Analysis of Flexible Boot and Aft Heat Shield Attachment Techniques

3.16.1 A parametric analysis was performed to size the flexible boot aft of X_S = 200, which closes out the engine compartment. The results indicate that the flexible boot (now composed of three layers of M25 bolt) may be reduced to a single 0.25-inch layer of M25 bolt. The propellant lines directly exposed to the 0.25-inch boot must be insulated locally with 0.25 inches of NRC-2 insulation. The maximum temperatures reached by the outer and inner surfaces of the 0.25-inch boot after a 410-second engine firing are 1379 F and 646 F, respectively.

3.16.2 If the boot hangs below the flange, the effects of radiation interchange between the nozzle and boot will result in nozzle temperatures that exceed the maximum allowable design temperature of 240 F. It should be noted that this condition cannot be allowed to exist and that, if necessary, additional supports in the form of stiffeners or springs should be utilized to prevent the boot from hanging below the flange.

3.16.3 A study was also conducted to determine feasible attachment techniques between the stainless steel facesheet and the phenolic laminate heat

[redacted]

shield. Due to the degradation of the NRC-2 super insulation at temperatures above 400 F (for short durations), the maximum design temperature on the phenolic laminate heat shield has been set at 400 F for the purposes of this study. Figures 3-10 through 3-12 show the placement of the thermal protection required to isolate the heat shield structure from the high temperatures resulting during engine firing.

3.17 Thermal Design Requirements of the LEM Tracking Antenna

3.17.1 A S/M RCS rocket firing time of 60 seconds has been assumed and the antenna is located at X_s = 200 on the minus Y-axis. Figure 3-13 presents the dependence of the X-band antenna dish temperature on dish thickness and material at the end of a 60-second RCS firing. Figure 3-14 shows a temperature history of the VHF antenna, indicating the dependence of temperature on wall thickness and the type of material considered. This temperature is the maximum anticipated for the VHF tubes and occurs in the vicinity of the plumes stagnation point. Consequently, circumferential temperature gradients will exist in the tubes, becoming more severe as the wall is made thinner.

3.18 Temperature Histories of Service Module High-Gain Antenna and Boom During 60-Second Firing of RCS Rocket Engine

3.18.1 Figures 3-15 through 3-22 present results of a preliminary thermal analysis performed on the major components of the high-gain antenna and on the antenna boom. The antenna is located at X_s = 200, and is 10 degrees off the +Y axis toward the -Z axis. Temperatures predicted for the end-fire elements, the gimbal shield, and the earth sensor shield are the maximum values obtained and occur in the vicinity of the plume stagnation point.

3.18.2 Figures 3-15 and 3-16 present the temperature history of the end-fire elements. For an element made of Rene 41, a maximum temperature of 2380 F was obtained on the rim. An end-fire element made of columbium was found to reach a maximum rim temperature of 2160 F, as is indicated in Figure 3-16. The exceedingly fast temperature response of the end-fire element to plume heating is a consequence of its small thermal capacitance. Temperature histories of the gimbal housing and shield are shown in Figure 3-17. With a shield made of either columbium or stainless steel, the gimbal housing will reach a maximum temperature of 440 F. Figures 3-18 and 3-19 present temperature histories of the earth sensor. The sensor with a stainless steel shield (Figure 3-18) keeps the sensor at or below 680 F. The front objective lens is expected to reach a maximum of 550 F. For a shield made of columbium (Figure 3-19), the maximum housing temperature is 640 F and the front objective lens is 400 F. Boom temperature histories appear in Figures 3-20 through 3-22. For a stainless steel boom (Figure 3-20), the shield reached a maximum of 2100 F, while the cable is expected to stay below 200 F. Similarly, for a boom made of inconel (Figure 3-21), the shield reached 1660 F and the cable will stay below 280 F.

3.19 Service Module RCS Nozzle Radiation Reflector on the S/M's Surface

3.19.1 A study was initiated to determine if a parabolic reflector would be required below the S/M RCS nozzle to prevent excessive reradiation to the radiation-cooled RCS nozzle. The maximum temperatures during this test are shown in Figure 3-23. Results of the study indicate that reradiation, from the S/M's surface to the nozzle, does not significantly raise the maximum temperature of the nozzle. The results also indicate that thermal shielding is required to protect the service module surface from nozzle radiation. A composite shield, consisting of Q-felt insulation (0.30-inch in thickness) with a stainless steel cover sheet, coated on the outboard side to attain an emissivity of 0.15, was therefore investigated. The analysis was conducted on the basis of preventing the service module surface temperature from exceeding 400 F for an RCS firing cycle of 60 seconds.

3.19.2 Two other cases were considered to determine the temperatures resulting with an RCS firing cycle of 300 seconds and 500 seconds. The design parameters for this study are listed below.

1. Maximum allowable temperature on the service module surface of 400 F for an RCS firing cycle of 60 seconds

2. RCS firing times of 60, 300 and 500 seconds

3. Initial temperatures of the S/M and the RCS prior to RCS firing of 250 F; this represents a worst-case condition

4. Center of the RCS mount located at X_s = 320.9; axial and roll nozzle cant of 10 degrees

5. Q-felt insulation thickness for the shield of 0.30 inches

6. Heating of the S/M's surface, due to plume impingement is represented in the thermal network as temperature histories. (It is to be noted that the maximum plume heating rate used to obtain these temperature histories was 4.5 Btu/sec-ft^2. A new analysis has been initiated that will utilize revised plume heating rates. It is anticipated that the new analysis will result in lower RCS nozzle temperatures.)

7. An S/M aluminum honeycomb facesheet thickness of 0.017 inch

8. An insulation cover sheet of stainless steel (0.005 inch thick), coated on the outboard side to attain an emissivity of 0.15

3.19.3 Figure 3-24 shows the dimensions and relative location of the shield with respect to the RCS and S/M. A summary of the maximum S/M and RCS temperatures for an RCS firing time of 60 seconds is shown in Figure 3-25 for an RCS mount wall emissivity of 0.05, and in Figure 3-26 for

an RCS mount wall emissivity of 0.20. Figures 3-27 and 3-28 summarize the maximum service module and mount wall temperatures for an RCS firing time of 300 seconds with the RCS mount wall coated to emissivities of 0.05 and 0.20, respectively. Figures 3-29 and 3-30 show the maximum temperatures for a 500-second RCS firing cycle with RCS mount wall emissivities of 0.05 and 0.20, respectively. In Figure 3-29, it is seen that the RCS mount wall reaches 803 F, which is considered a maximum allowable temperature for an abort condition. Higher RCS mount wall emissivities will result in excessive temperatures as shown in Figure 3-30 for $\epsilon = 0.20$.

3.20 Service Module Interior Coating and Finish Requirements

3.20.1 From space flight thermal considerations, it appears desirable to have surfaces that exhibit highly reflective optical properties (low emissivity) as opposed to nonreflective properties (high emissivity). It is believed that any coating with an emissivity of 0.2 or less would be satisfactory for the interior aluminum surfaces. This requirement would be applicable to all exposed aluminum surfaces as well as those surfaces that are presently being covered with "super" insulation. These coating requirements are based on qualitative space flight thermal considerations.

3.21 Service Module SPS Nozzle Extension Temperatures During Abort Firing With S-IVB Adapter Attached

3.21.1 Extensive analyses performed on the SPS nozzle extension temperatures during engine firing have shown that a maximum temperature of 2400 F (design limit) can be expected when the engine is in its maximum gimballed position. Because the SPS engine has a radiation-cooled nozzle, maximum temperatures are governed by the magnitude of the nozzle view factor to space. The presence of the S-IVB adapter would greatly restrict this view factor and would result in overheating of the nozzle extension, exceeding the design temperature limit of 2400 F within 10 to 15 seconds.

3.22 Temperature Time History of RCS Tanks During Service Module Atmosphere Reentry

3.22.1 At approximately 223 seconds after reentry the RCS tank temperatures will increase to 430 F (Figure 3-31). The temperature response of the S/M RCS propellant during this period is negligible. In this analysis the propellant tanks were considered one-fourth filled.

3.23 Cooling Requirements for Service Module Reaction Control System Inboard Configuration

3.23.1 The maximum cooling requirements for the S/M RCS propellants during space flight, when the maximum allowable temperature of the propellant is raised 85 F to 100 F, is determined to be 315 Btu/hr per RCS package. This value is 390 Btu/hr per RCS package for a maximum propellant temperature of 85 F.

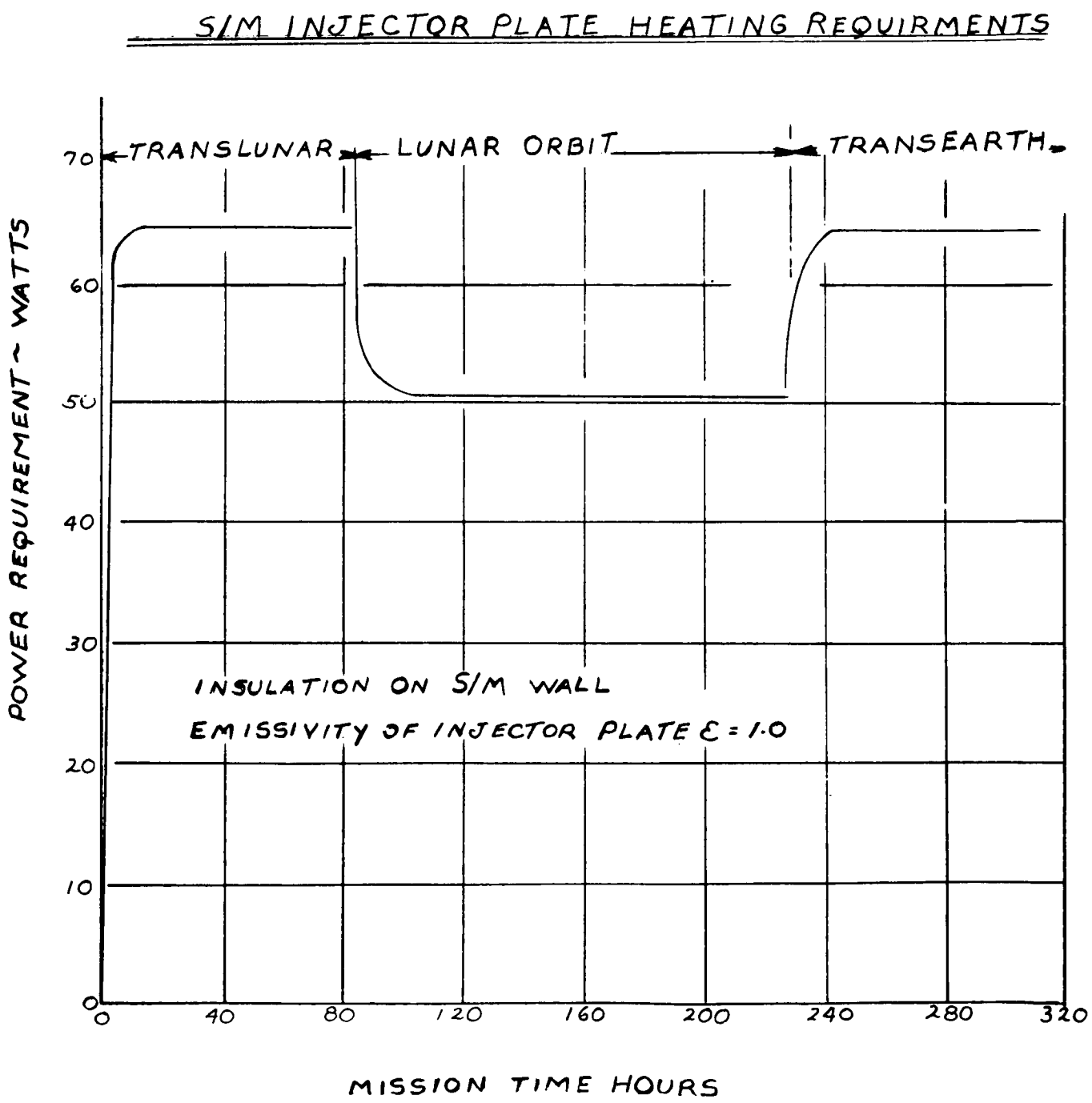

Figure 3-1. Heating Requirement for S/M Main Engine Injector Plate (Part 1)

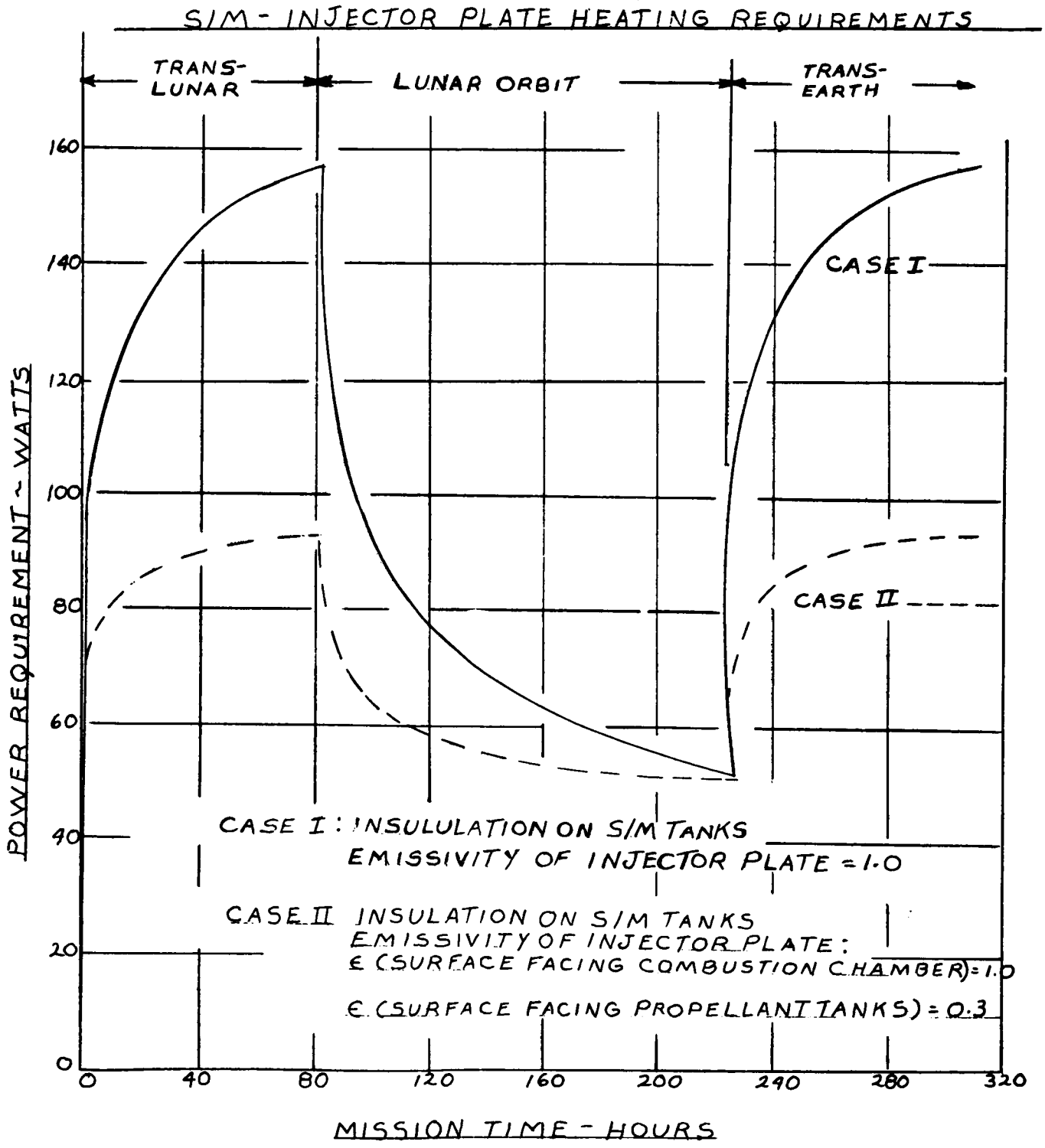

Figure 3-2. Heating Requirement for S/M Main Engine Injector Plate (Part 2)

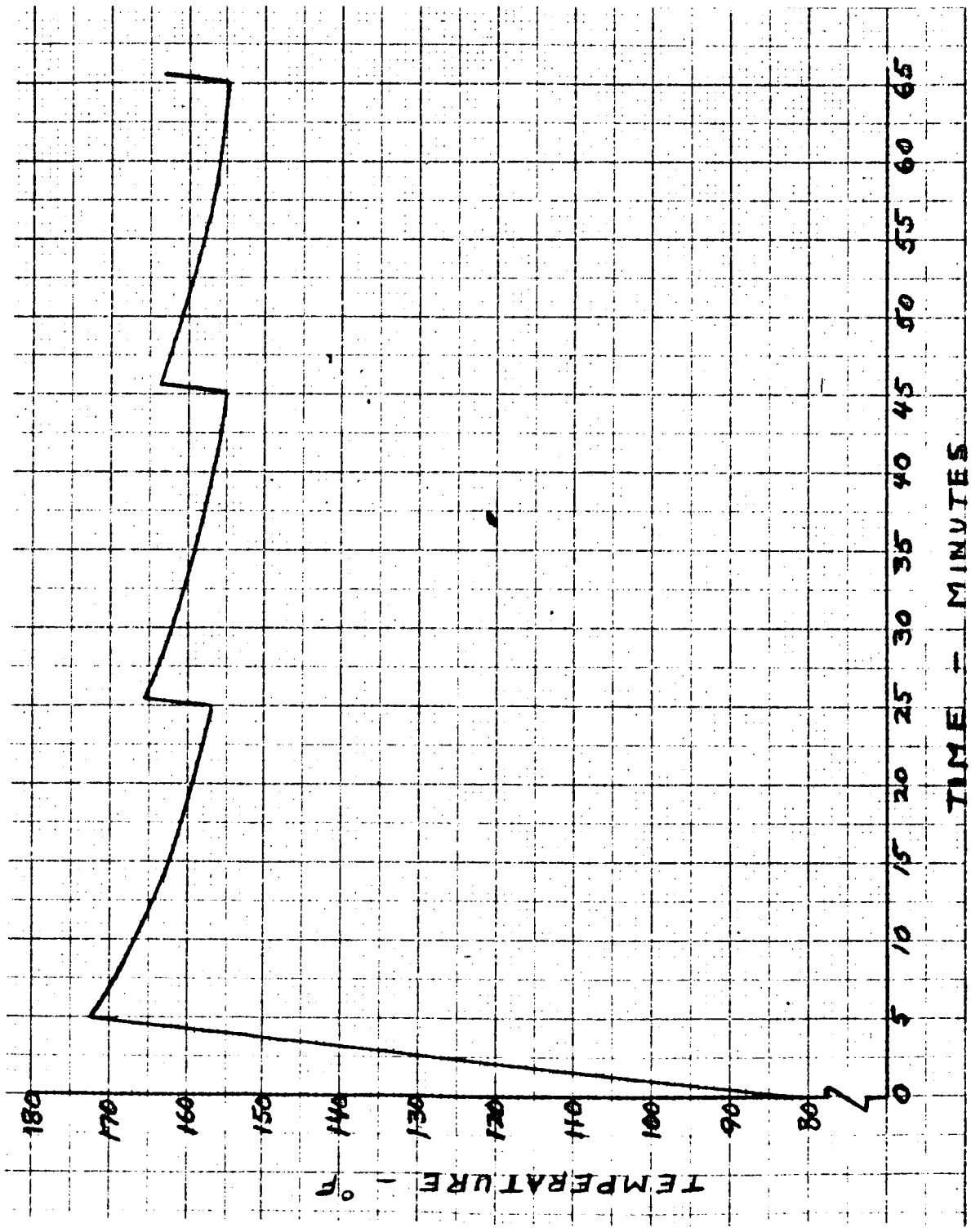

Figure 3-3. Time-Temperature History of Solenoid Valve

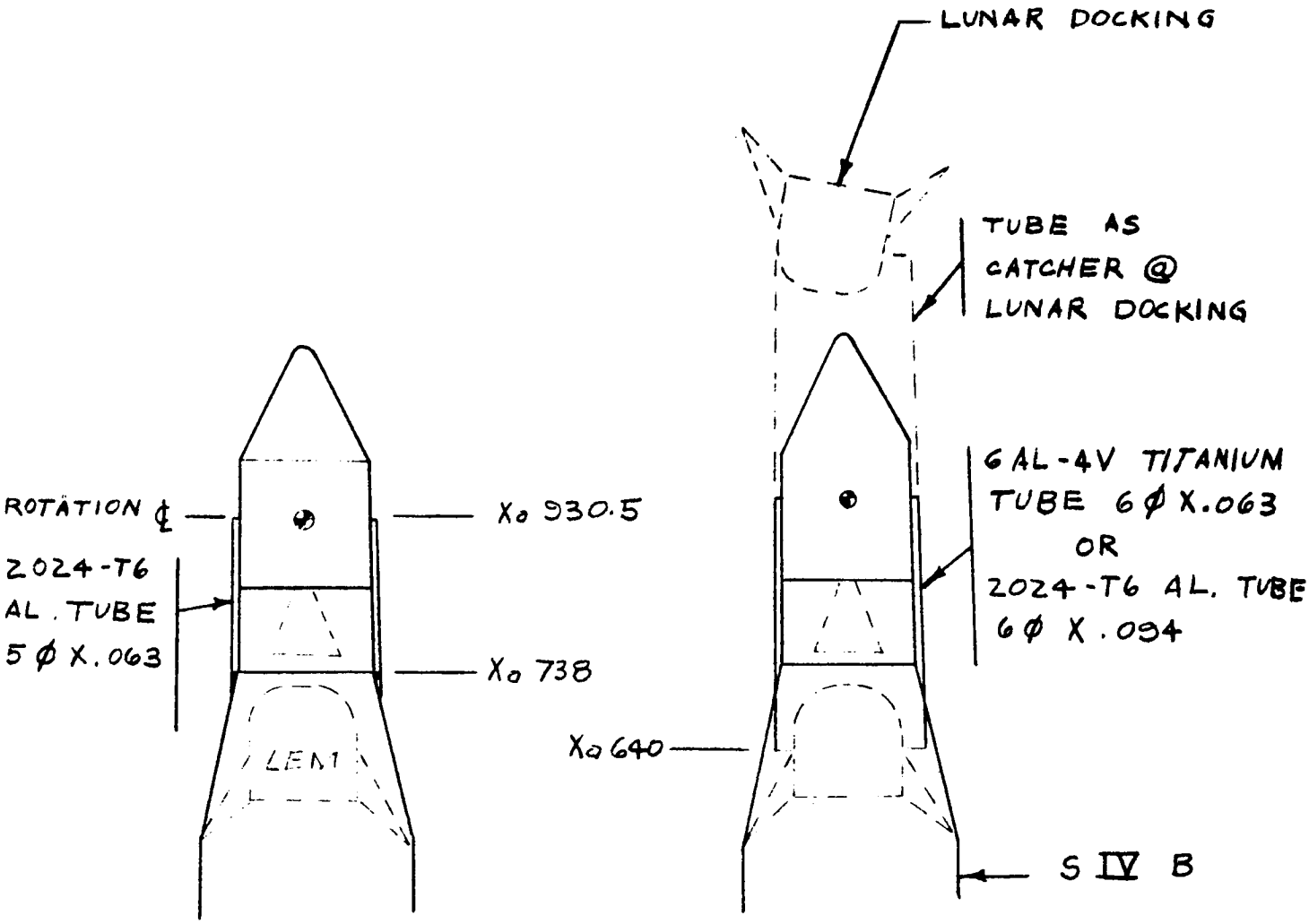

SINGLE PURPOSE
TRANSLUNAR INJECTION ONLY

DOUBLE PURPOSE
TRANSLUNAR INJECTION & LUNAR ORBIT DOCKING

Figure 3-4. Configurations Analyzed During Thermal Analysis

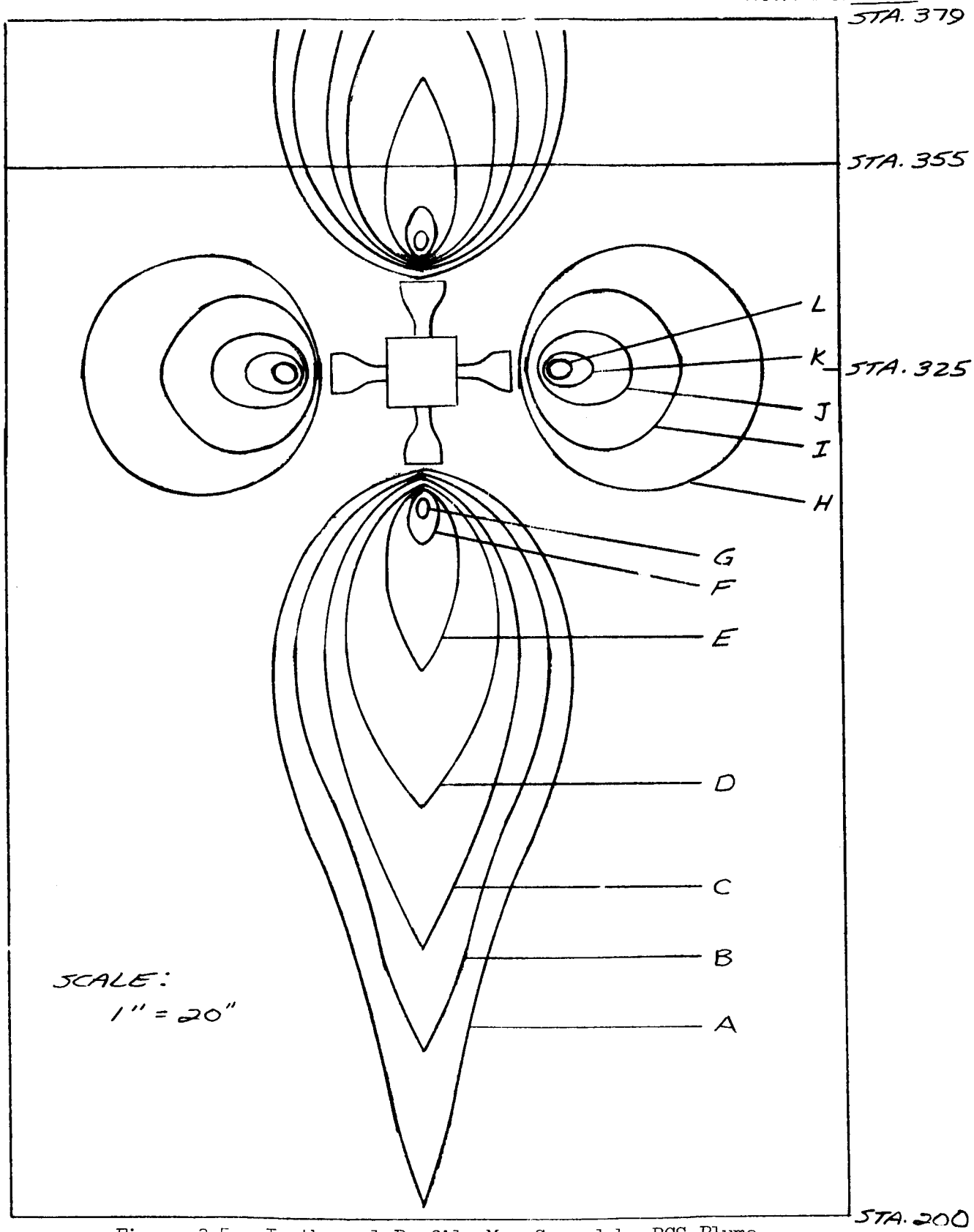

Figure 3-5. Isothermal Profile Map Caused by RCS Plume Impingement on S/M Surface

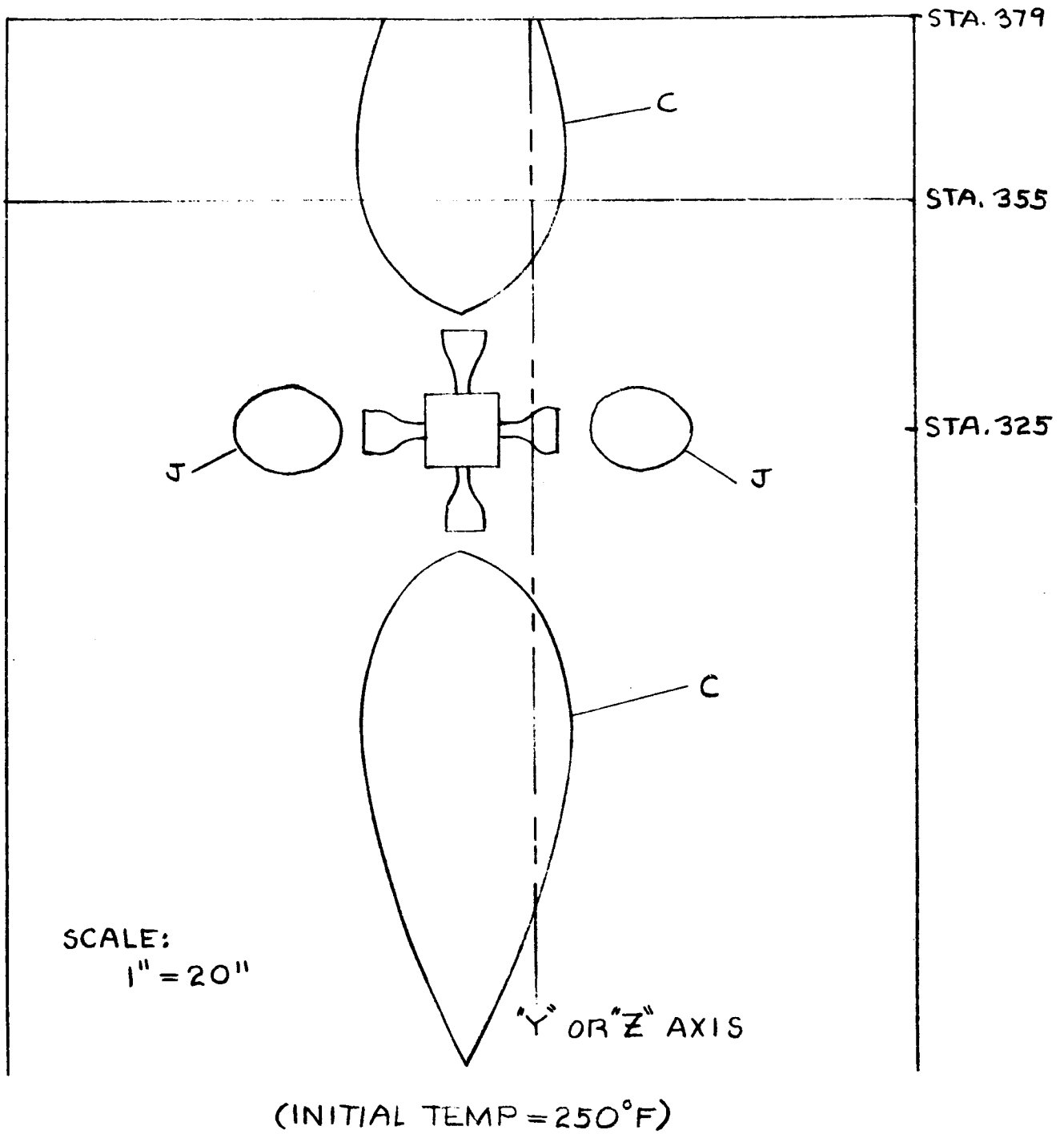

Figure 3-6. Area on S/M Covered by Q-Felt Plus Cover Sheet (Steel or Titanium) to Prevent the Surface Temperature of the Aluminum Honeycomb From Exceeding 400 F

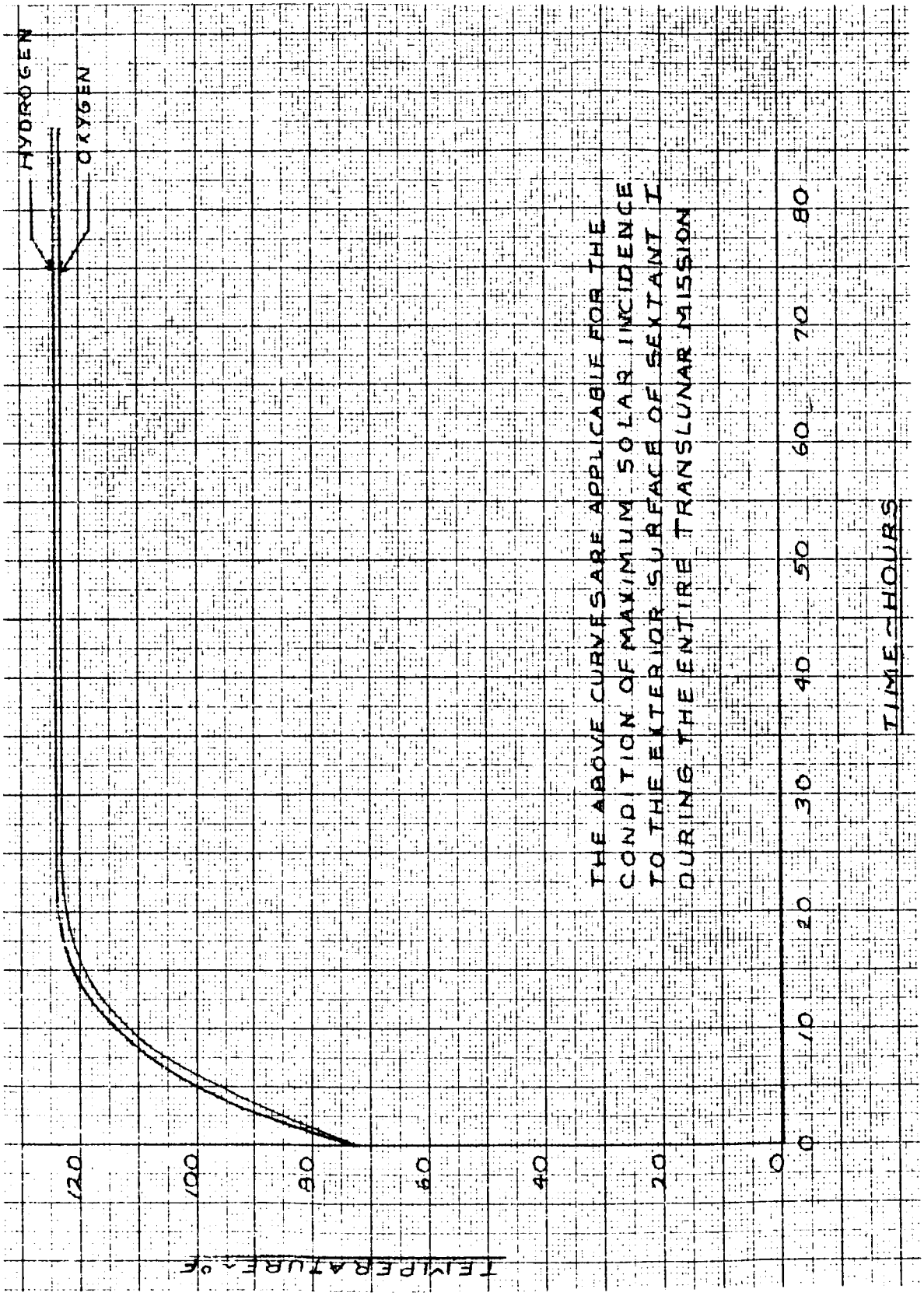

Figure 3-7. Temperature History for the Outer Surface of the Oxygen and Hydrogen Cryogenic Storage Tanks

COMPOSITE PROTECTION:
STEEL SHEET (0.005 INCHES)
+ Q-FELT INSULATION

	FIRING CYCLE - SECONDS 60	180	300	400
MAXIMUM TEMPERATURE - °F	381.5	531.0	644.2	719
TEMPERATURE AT END OF FIRING CYCLE - °F	266.1	422.7	582.6	678

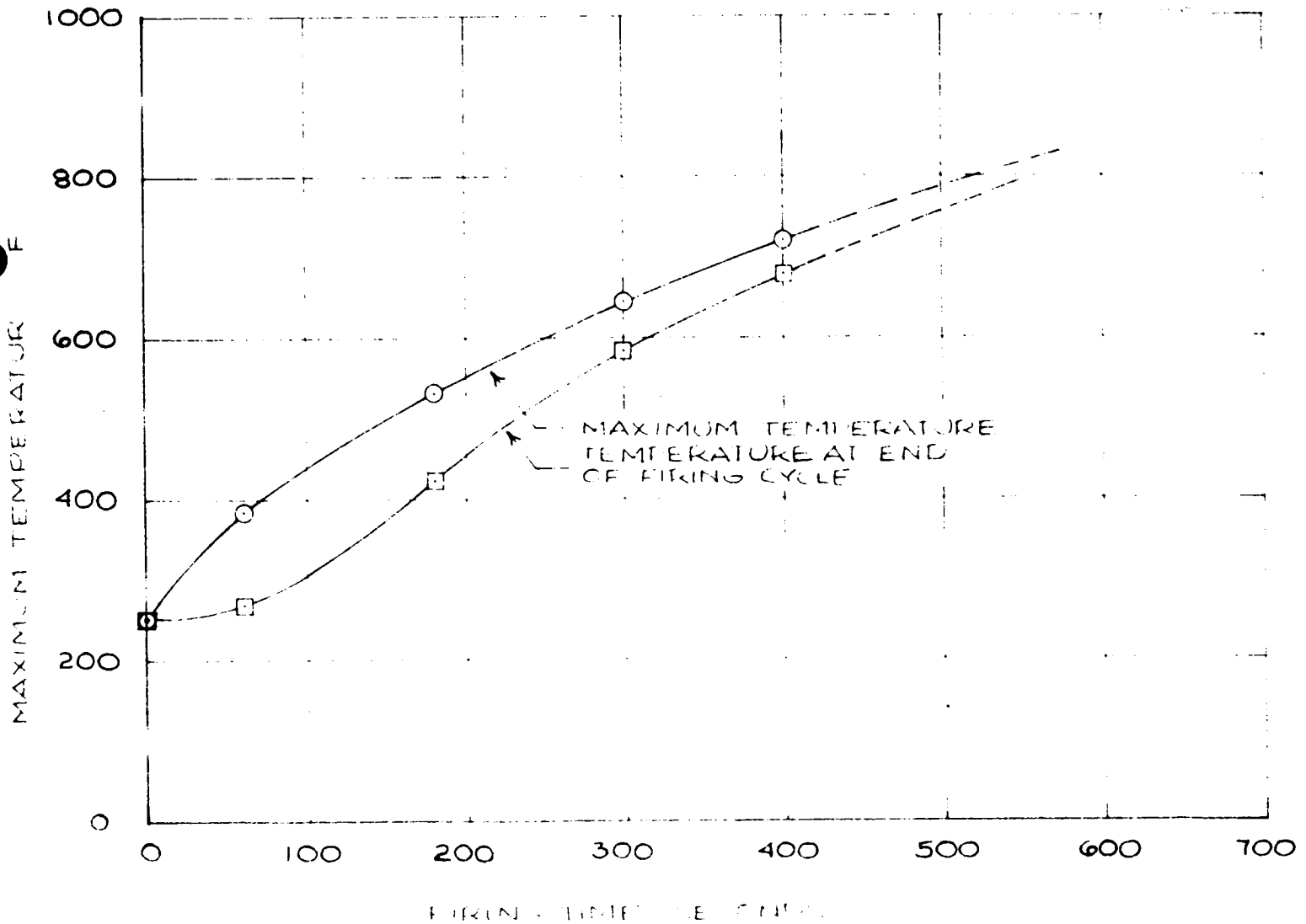

Figure 3-8. Temperature at End of Firing Cycle and Maximum Tem[illegible] of Interface Between Service Module and RCS Composite Ther[illegible] Protection as a Function of RCS Firing Time

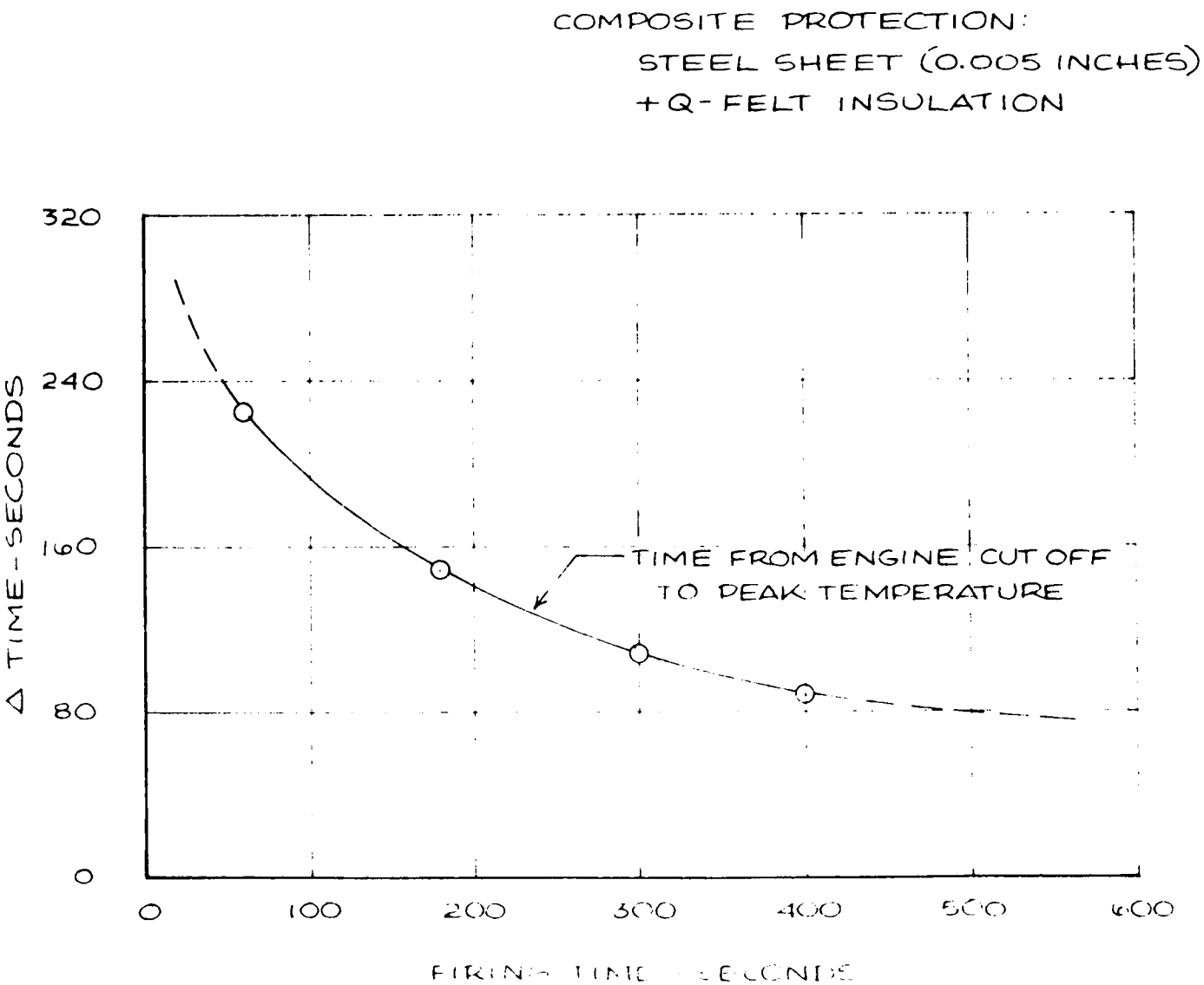

Figure 3-9. Time Required for the Temperature of Interface Between Service Module and RCS Composite Thermal Protection to Reach a Maximum as a Function of RCS Firing Time

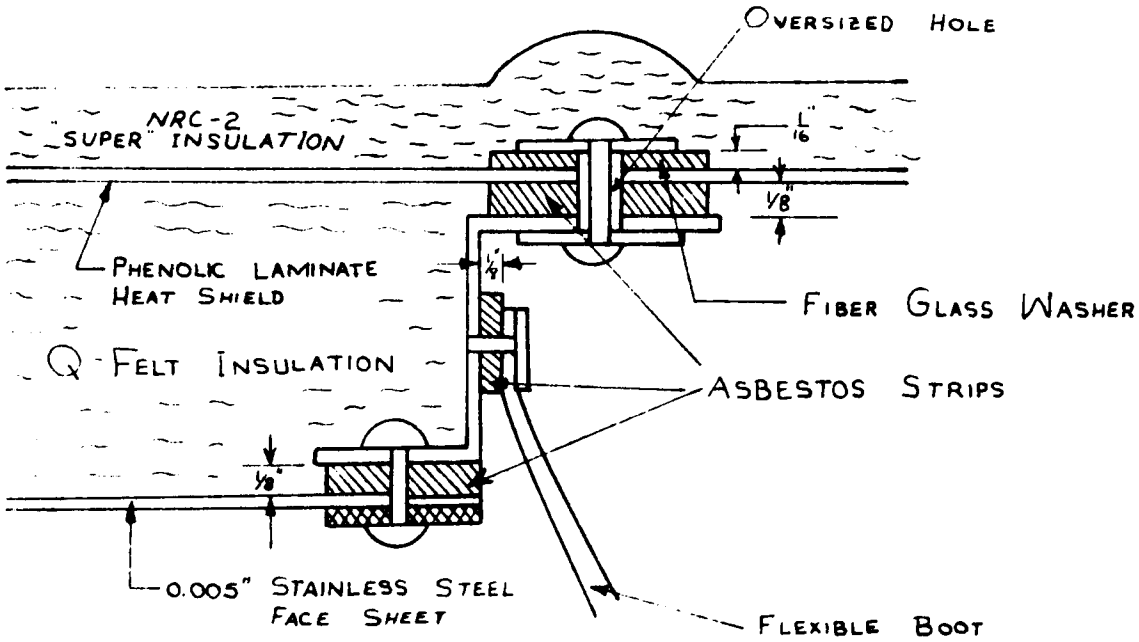

Figure 3-10. Placement of Insulation at Section E-E and All Similar Sections Shown in Drawing V17-931118

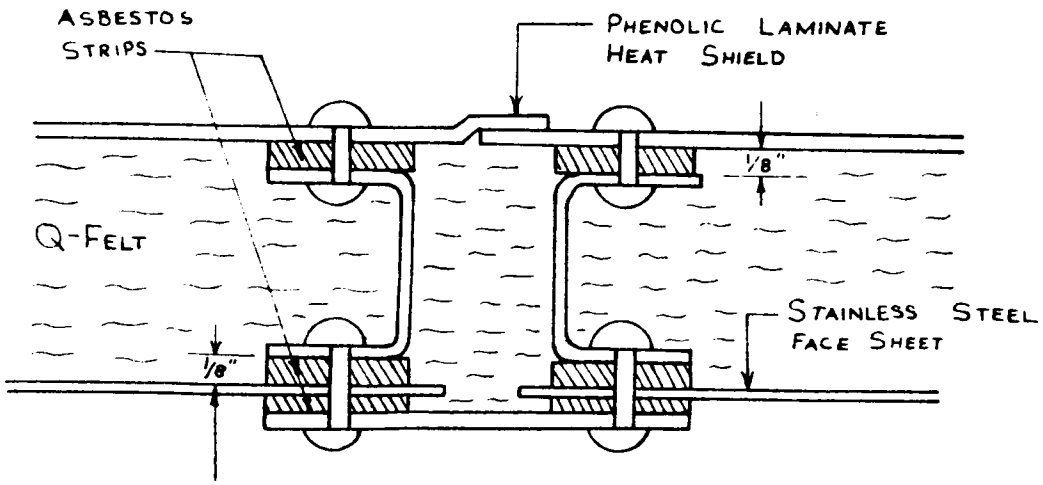

Figure 3-11. Placement of Thermal Protection for Section A-A and All Similar Sections Shown in Drawing V17-331739

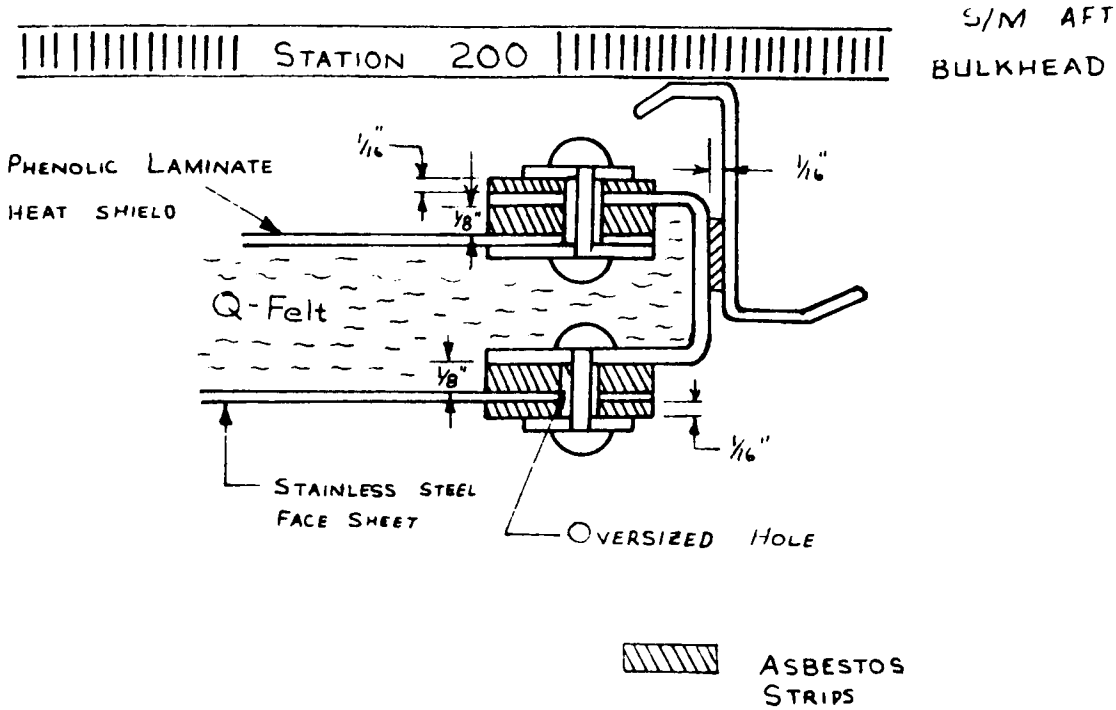

Figure 3-12. Placement of Thermal Protection for Section D-D and All Similar Sections Shown in Drawing V17-331739

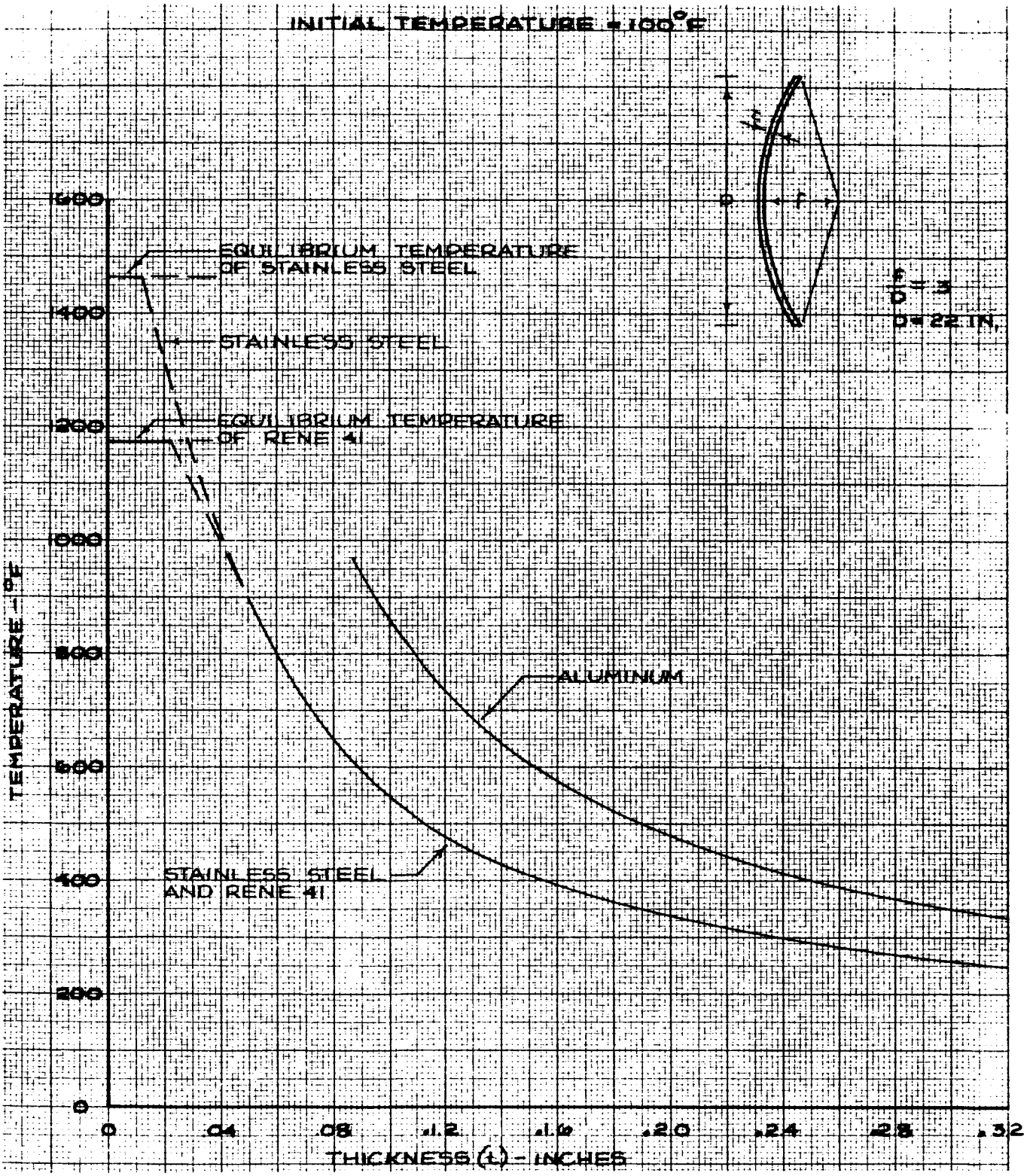

Figure 3-13. Thermal Design Criterion for the X-Band Radar Antenna Dish

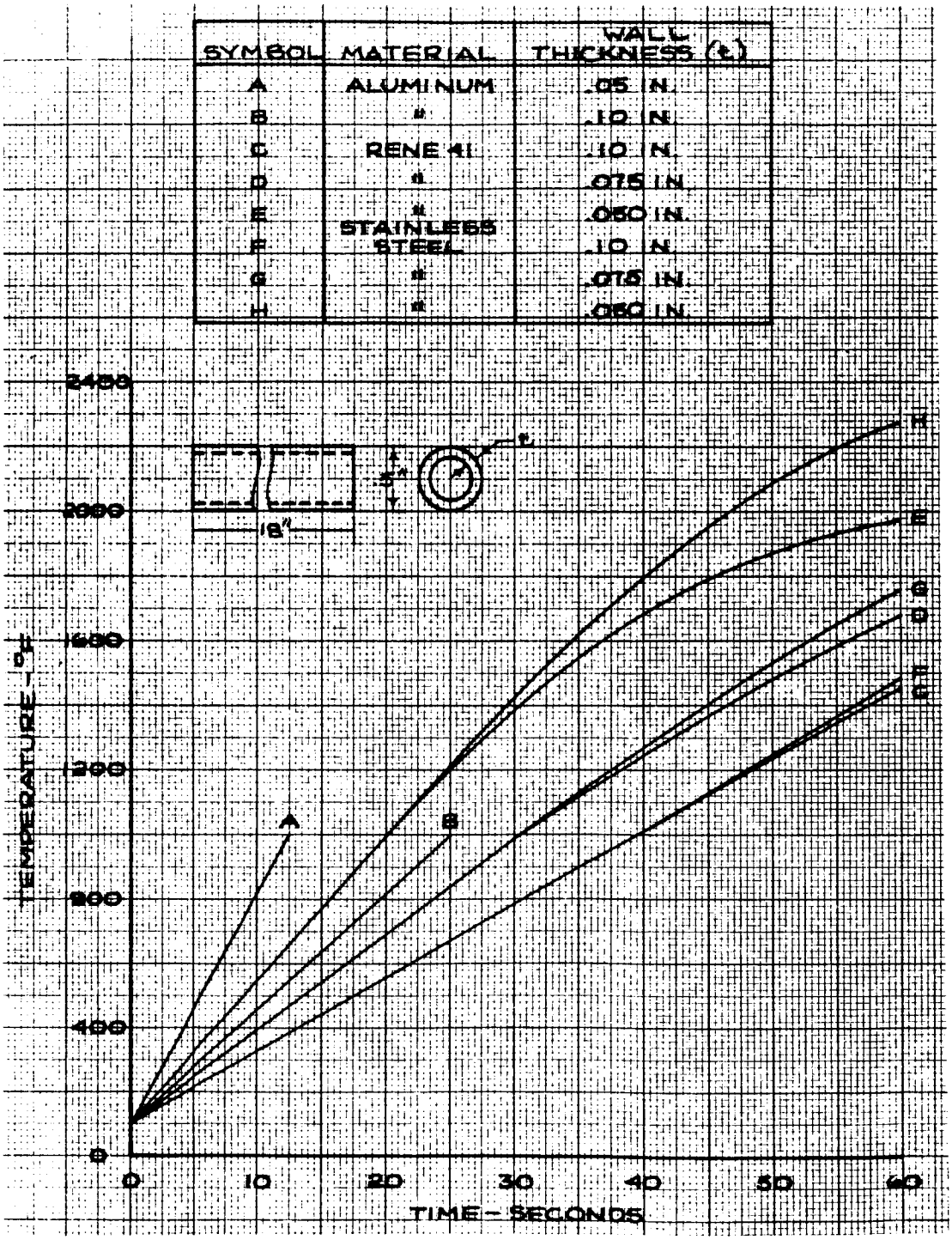

Figure 3-14. Thermal Design Criterion for the VHF Radar Antenna

~~CONFIDENTIAL~~

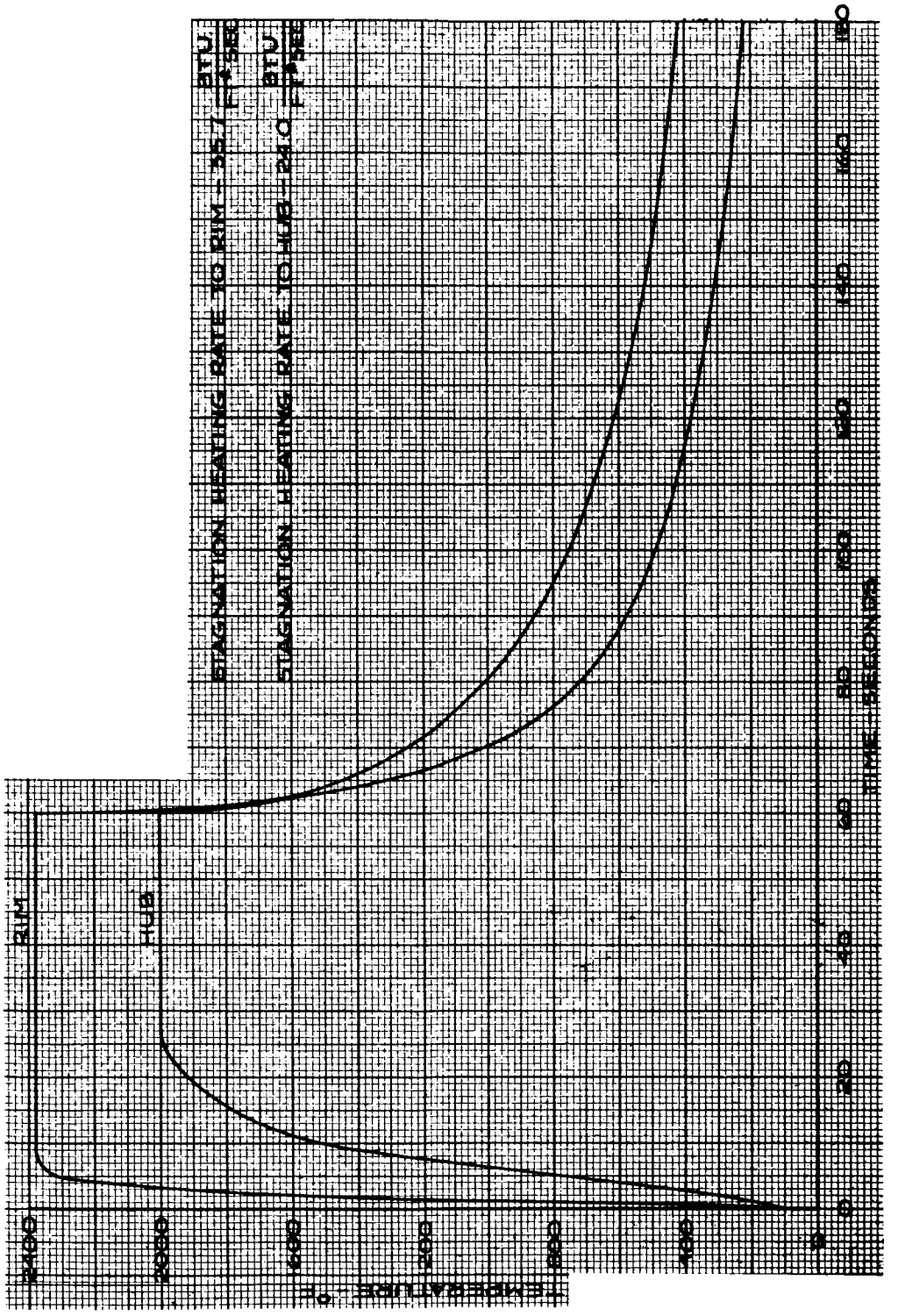

Figure 3-15. Temperature History of End Fire Element - René 41

~~CONFIDENTIAL~~

[redacted]

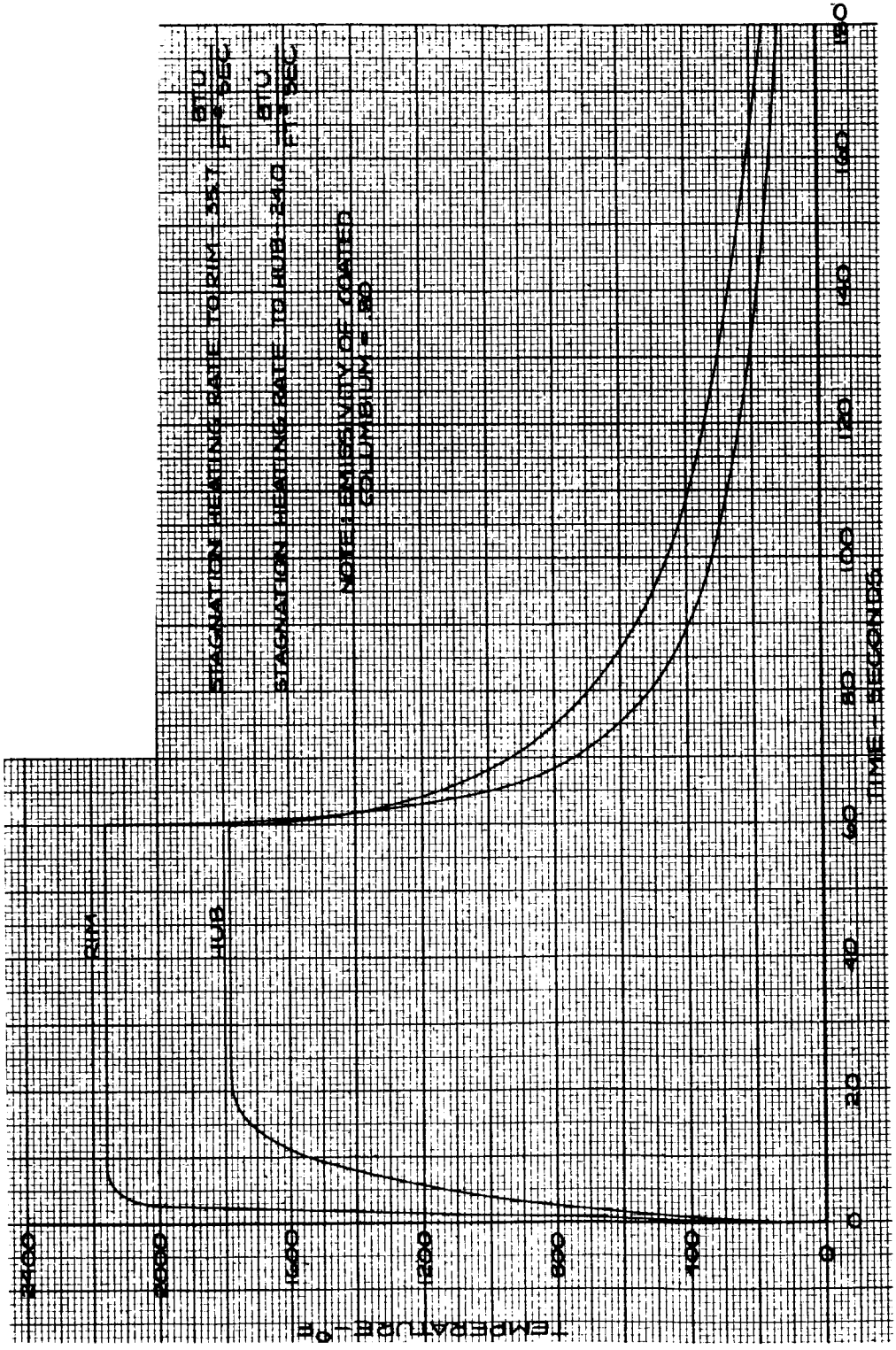

Figure 3-16. Temperature History of End Fire Element - Columbium

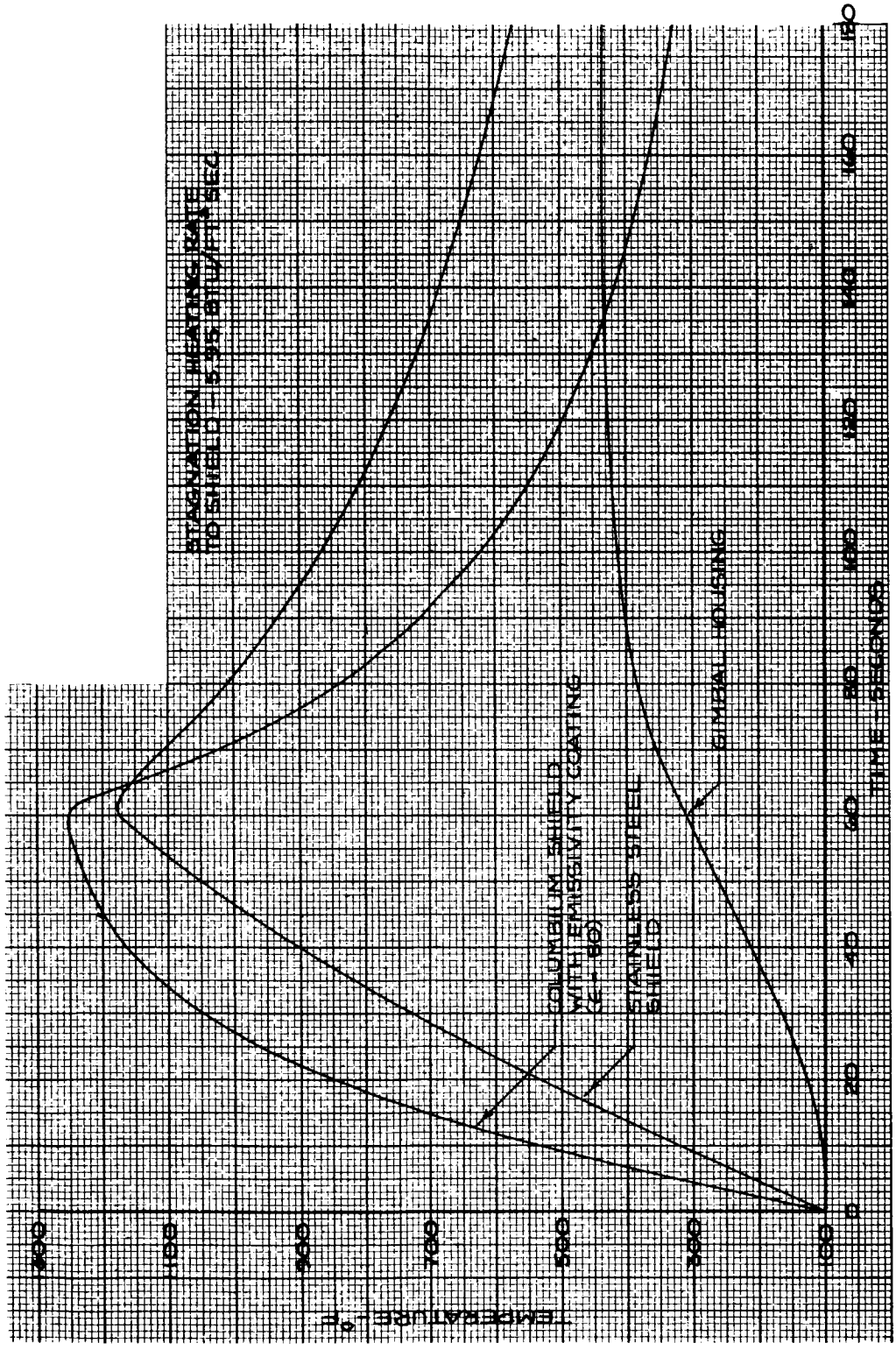

Figure 3-17. Temperature History of Gimbal Housing and Shield

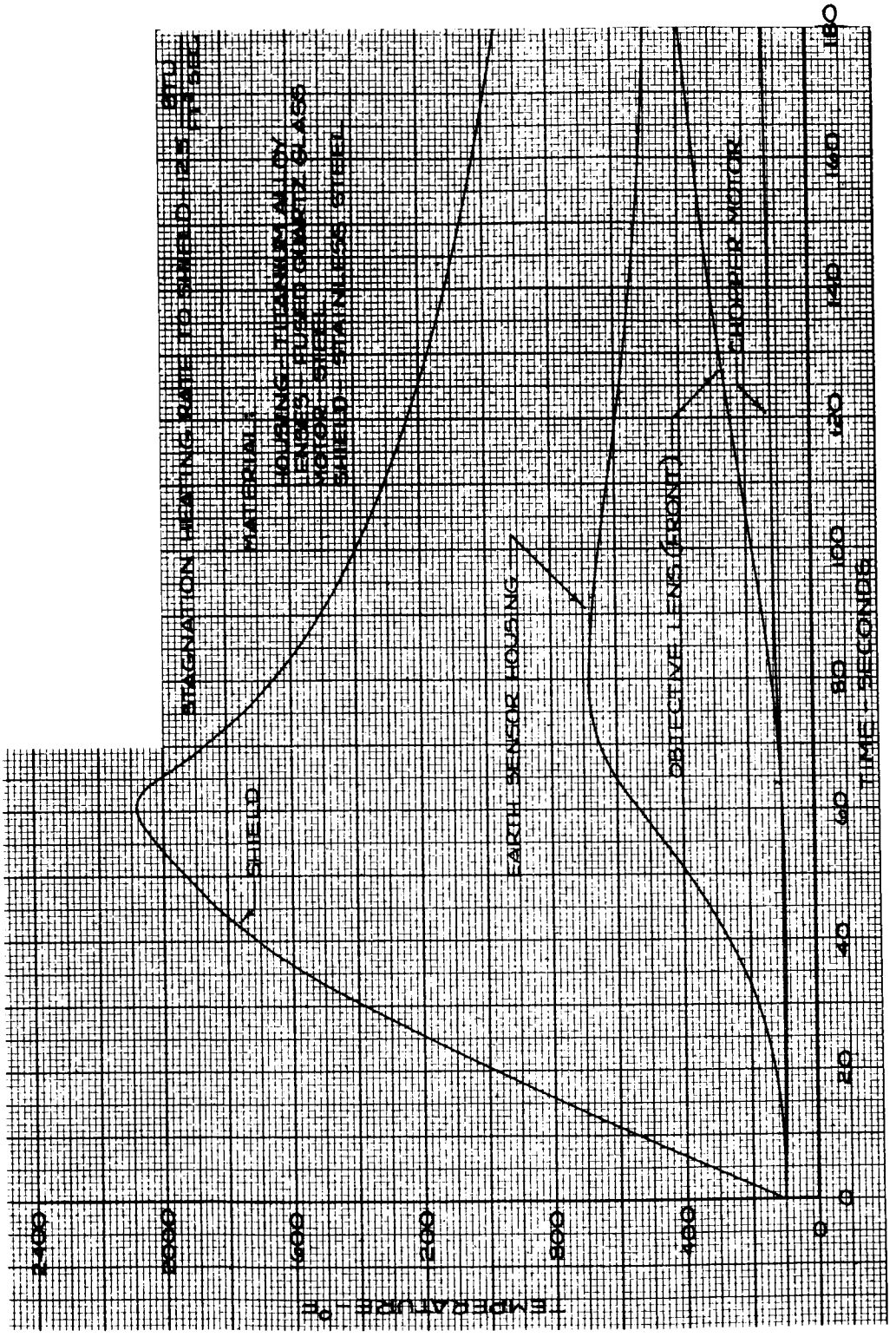

Figure 3-18. Temperature History of Earth Sensor With Stainless Steel Shield

~~CONFIDENTIAL~~

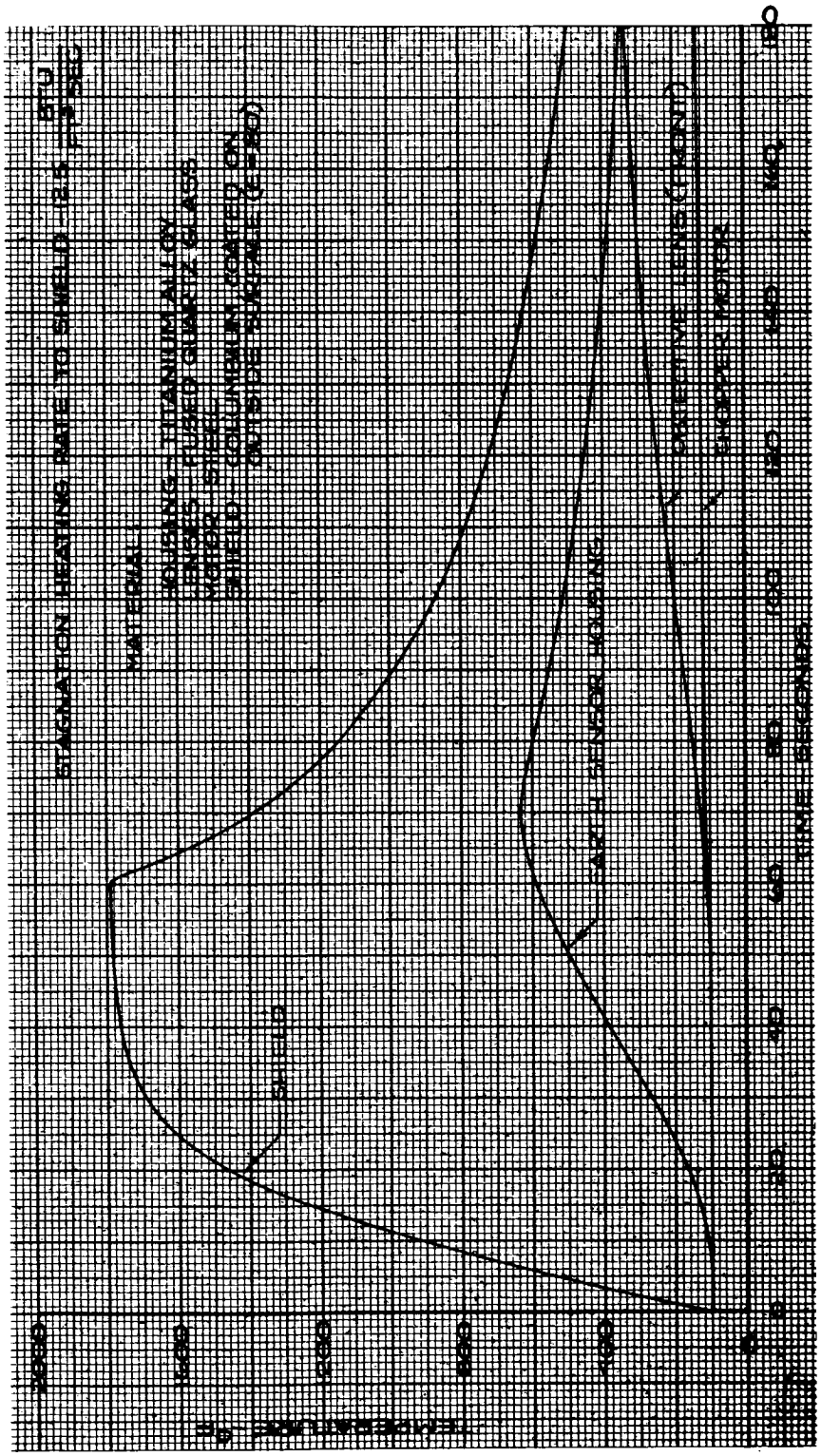

Figure 3-19. Temperature History of Earth Sensor With Columbium Shield

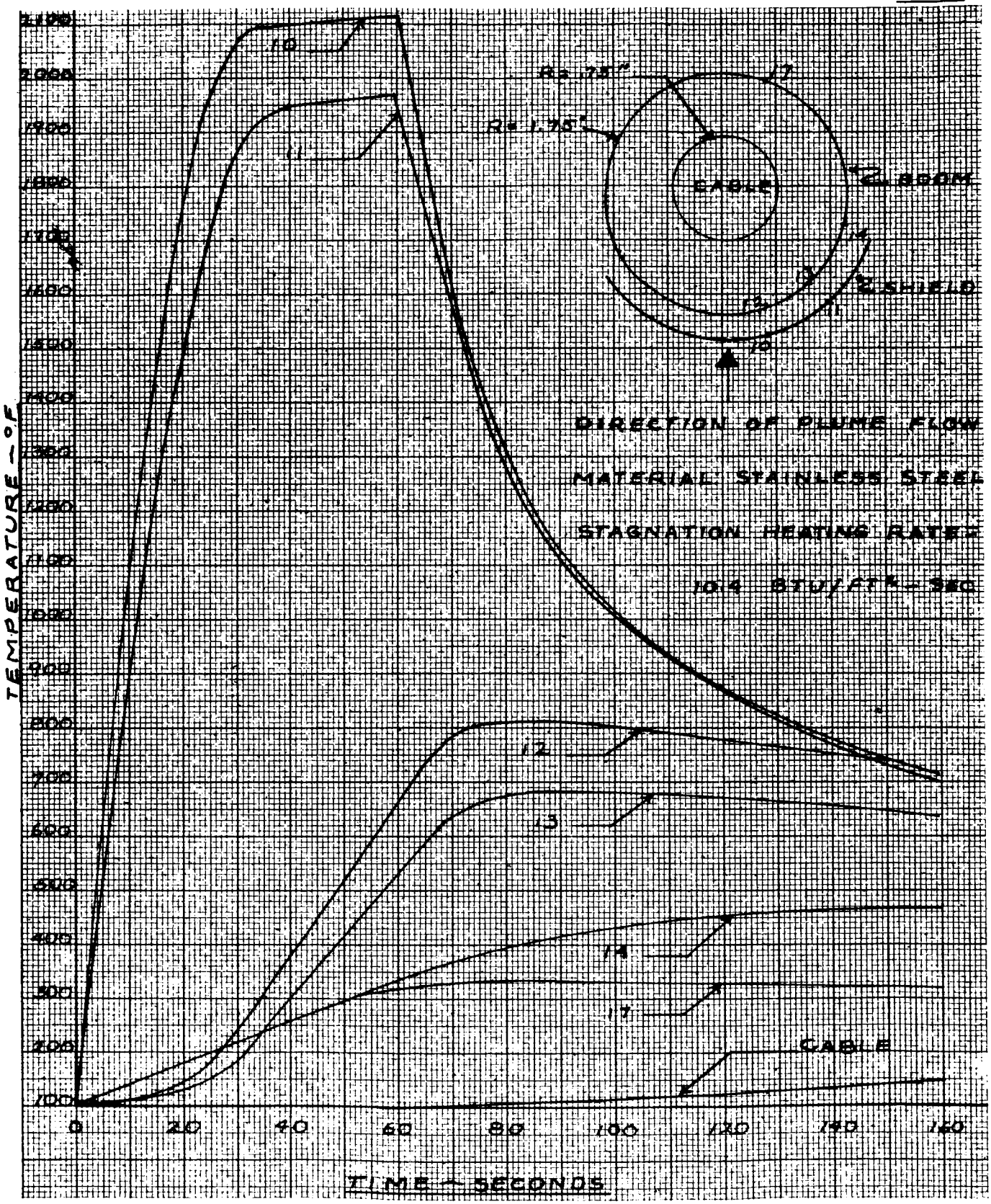

Figure 3-20. Temperature History of Antenna Boom, Stainless Steel

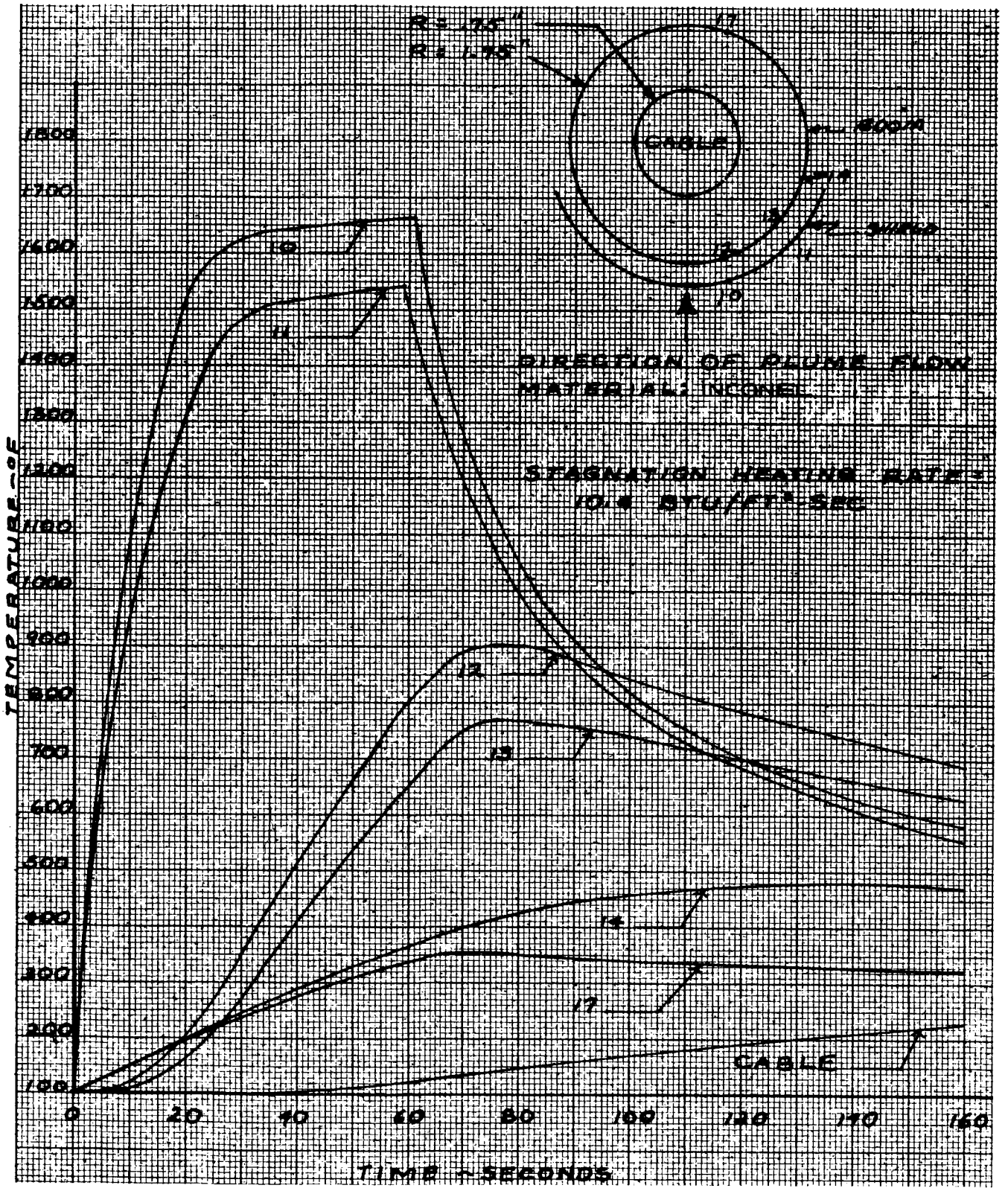

Figure 3-21. Temperature History of Antenna Boom, Inconel

[redacted]

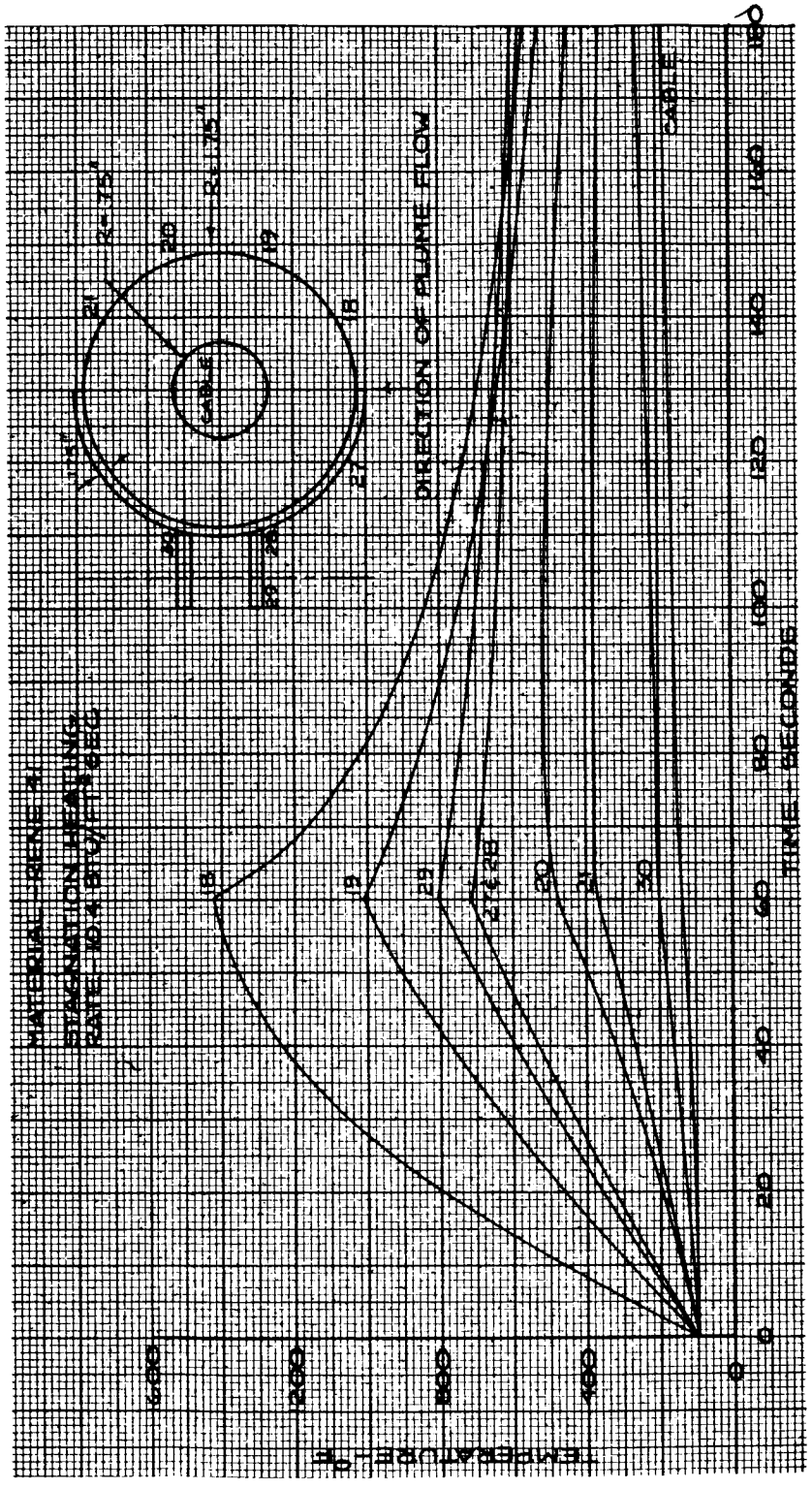

Figure 3-22. Temperature History of Antenna Boom at Deployment Point - No Shield

[redacted]

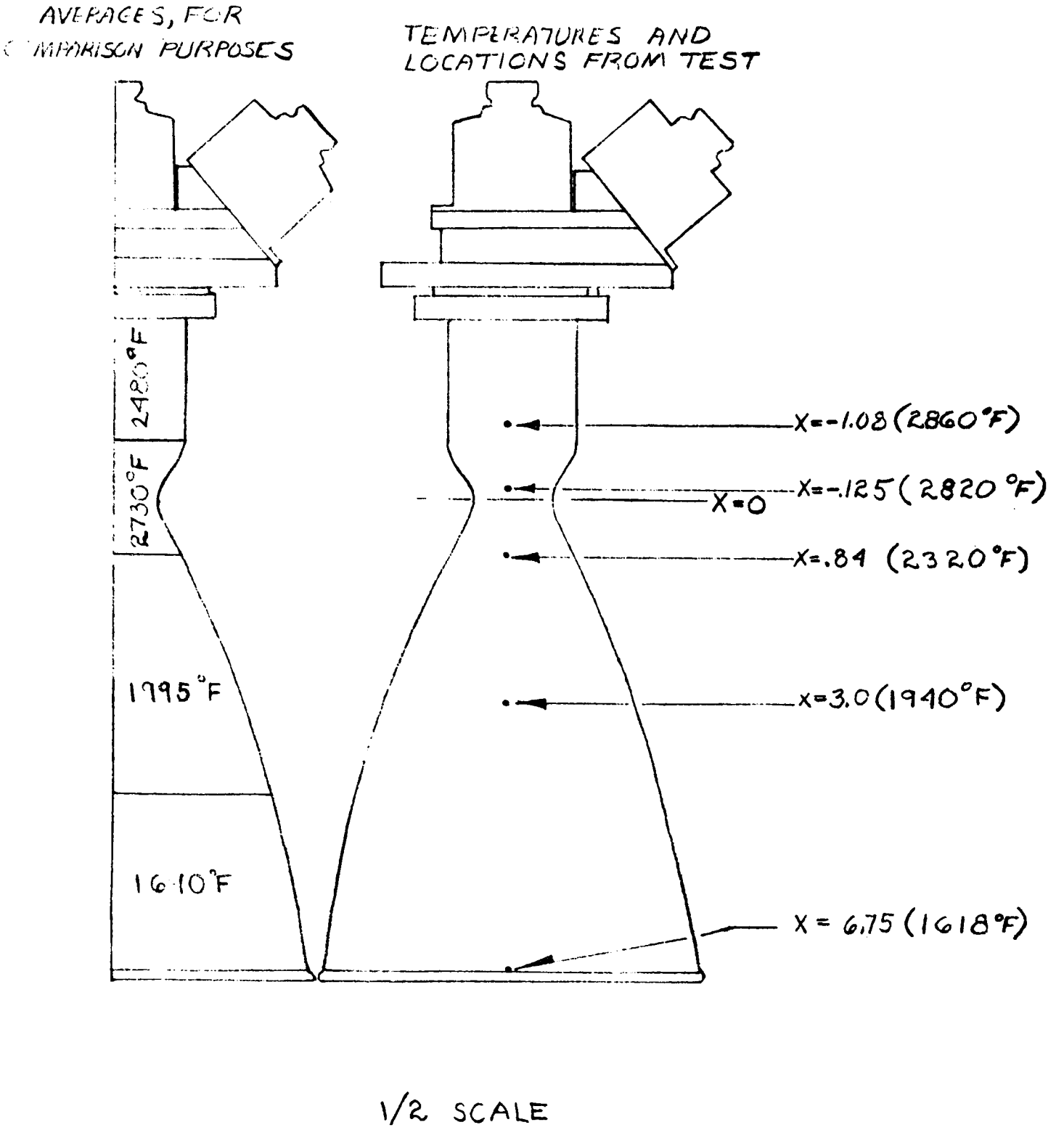

Figure 3-23. S/M RCS Nozzle Temperatures From Marquardt Test (Run 467, 12 July 1962)

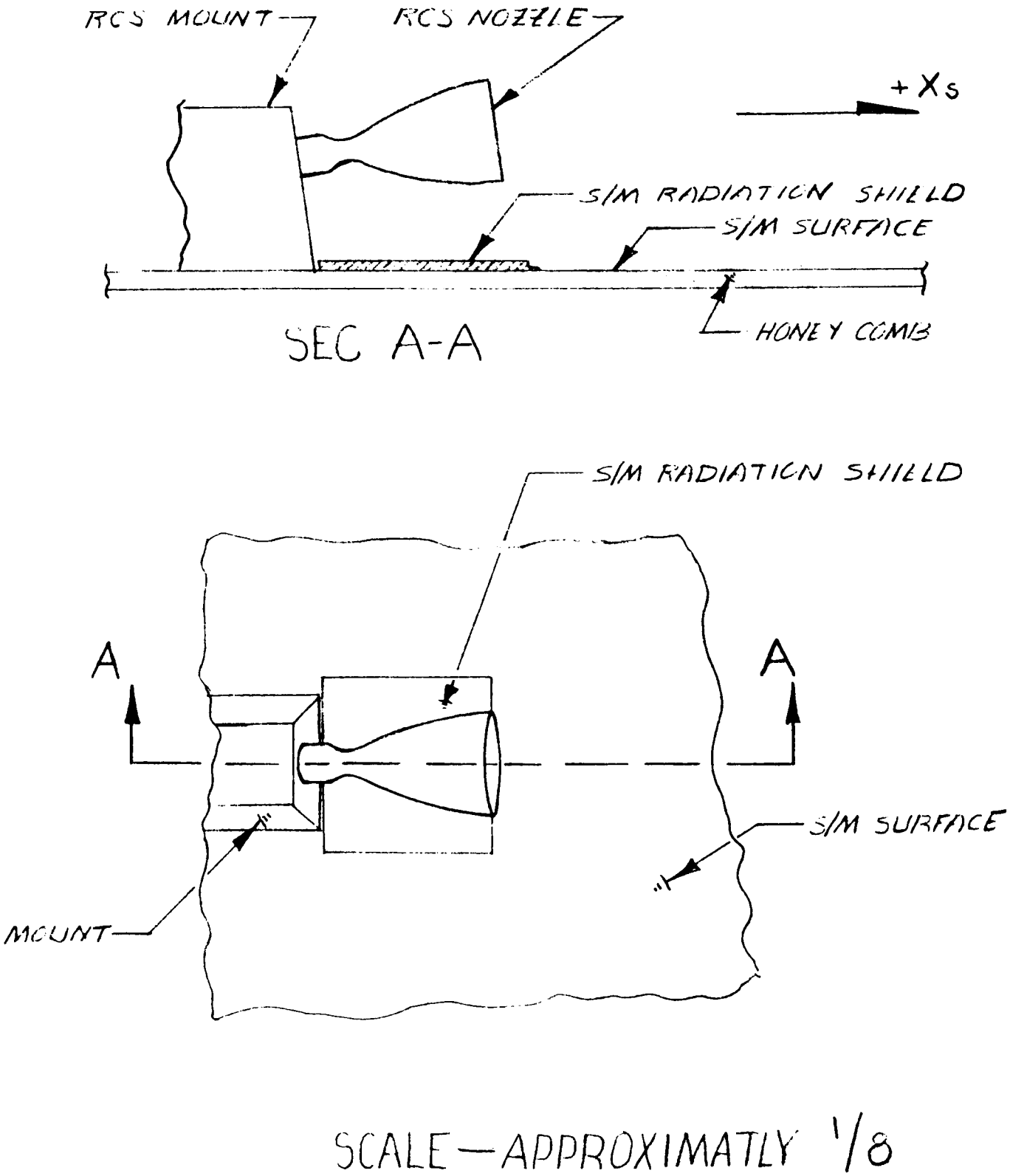

Figure 3-24. S/M Radiation Shield Configuration

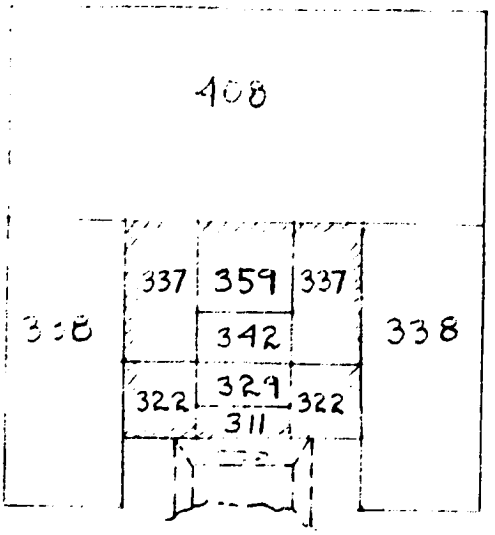

S/M SURFACE TEMPERATURES
SCALE – 1/8

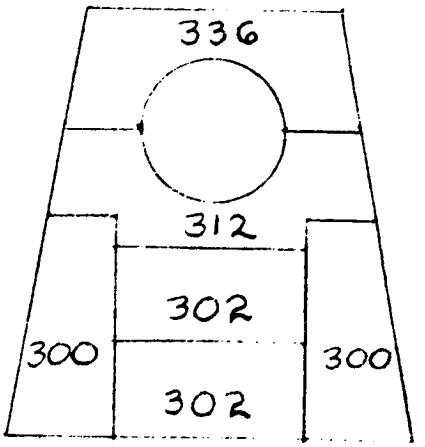

RCS MOUNT WALL TEMPERATURES
SCALE – 1/4

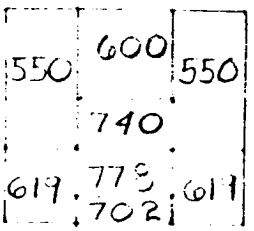

S/M SHIELD TEMPERATURES
SCALE – 1/8

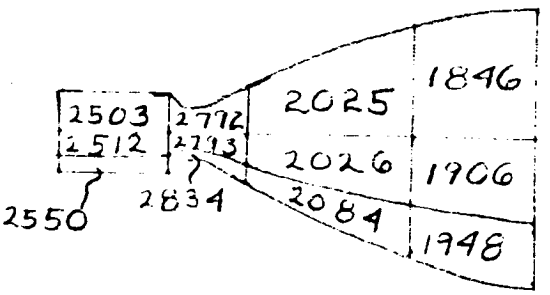

RCS NOZZLE TEMPERATURES
SCALE – 1/4

Figure 3-25. Summary of RCS and S/M Temperatures for a 60-Second RCS Engine Fire Cycle, With an RCS Mount Wall ε of 0.05

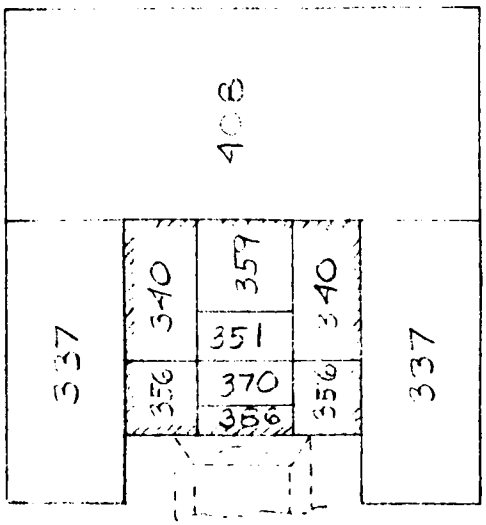

S/M SURFACE TEMPERATURES
SCALE — 1/8
SHADING SHOWS AREA
COVERED BY SHIELD

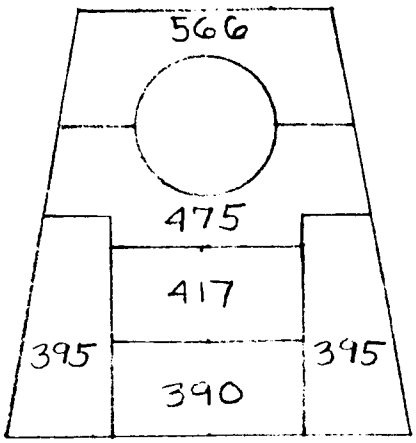

RCS MOUNT WALL TEMPERATURES
SCALE — 1/4

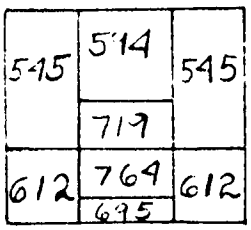

S/M SHIELD TEMPERATURES
SCALE — 1/8

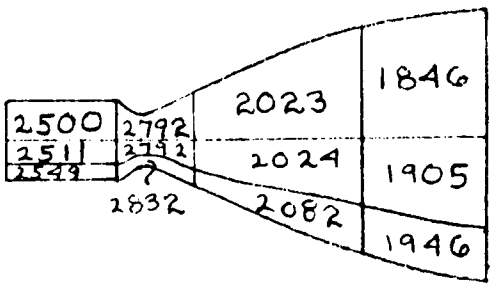

RCS NOZZLE TEMPERATURES
SCALE — 1/4

Figure 3-26. Summary of RCS and S/M Temperatures for a 60-Second RCS Engine Fire Cycle, With an RCS Mount Wall ϵ of 0.20

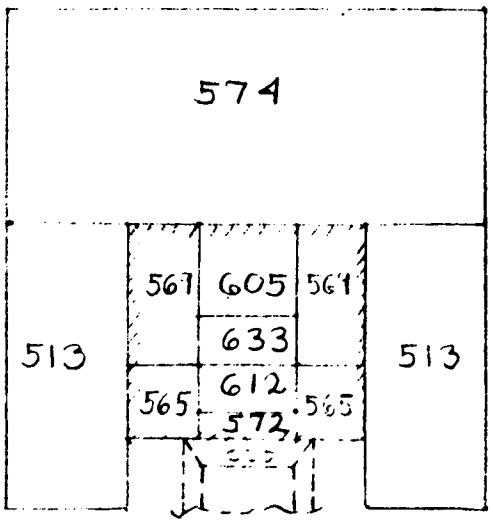

S/M SURFACE TEMPERATURES
SCALE — 1/8

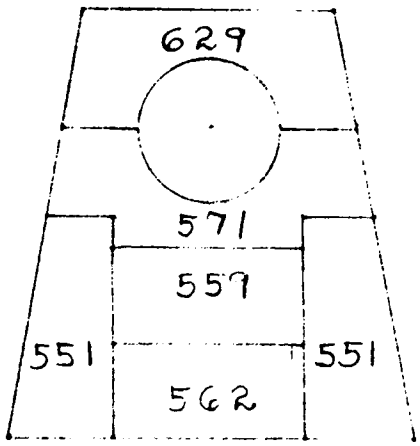

RCS MOUNT WALL
TEMPERATURES
SCALE — 1/4

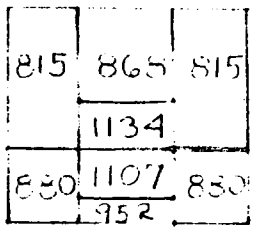

S/M SHIELD TEMPERATURES
SCALE — 1/8

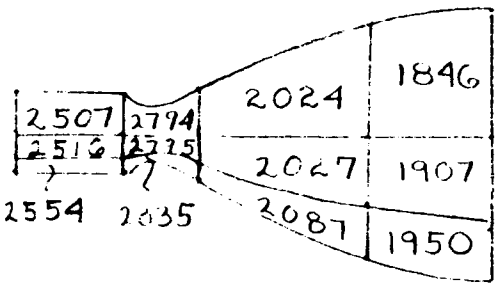

RCS NOZZLE TEMPERATURES
SCALE — 1/4

Figure 3-27. Summary of RCS and S/M Temperatures for a 300-Second RCS Engine Fire Cycle, With RCS Mount Wall ε of 0.05

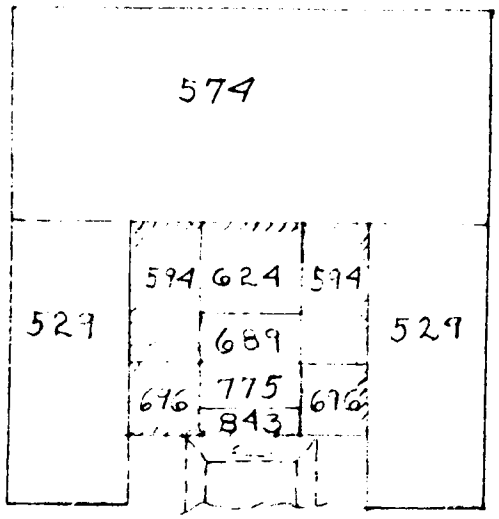

S/M SURFACE TEMPERATURES
SCALE – 1/8

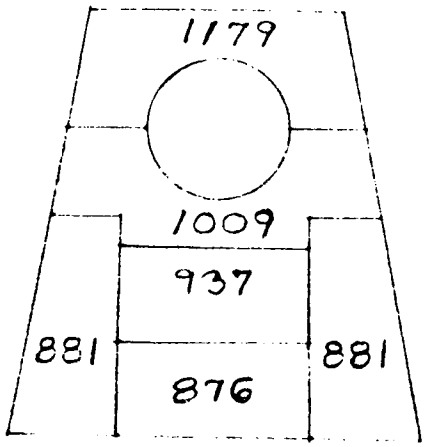

RCS MOUNT WALL TEMPERATURES
SCALE – 1/4

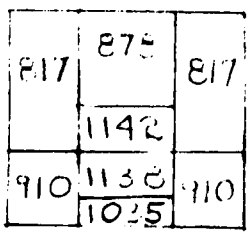

S/M SHIELD TEMPERATURES
SCALE – 1/8

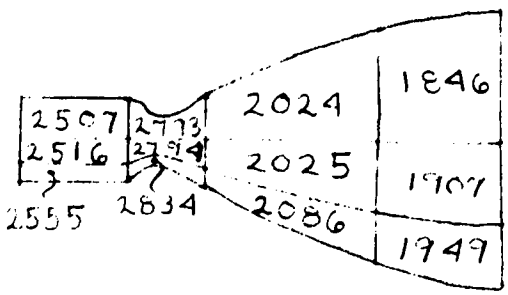

RCS NOZZLE TEMPERATURES
SCALE – 1/4

Figure 3-28. Summary of RCS and S/M Temperatures for a 300-Second RCS Engine Fire Cycle, With RCS Mount Wall ϵ of 0.20

~~CONFIDENTIAL~~

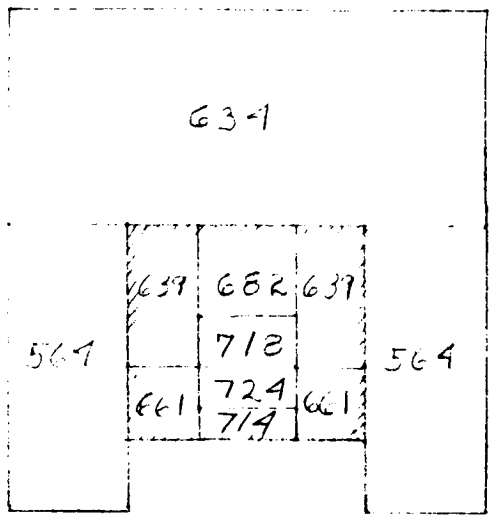

S/M SURFACE TEMPERATURES
SCALE — 1/8

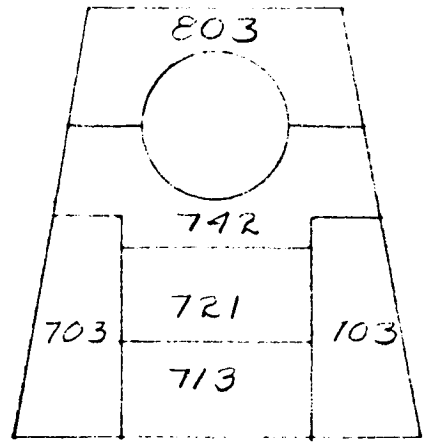

RCS MOUNT WALL TEMPERATURES
SCALE — 1/4

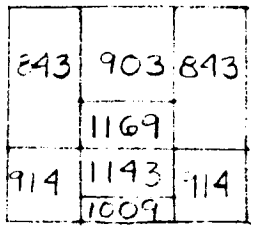

S/M SHIELD TEMPERATURES
SCALE — 1/8

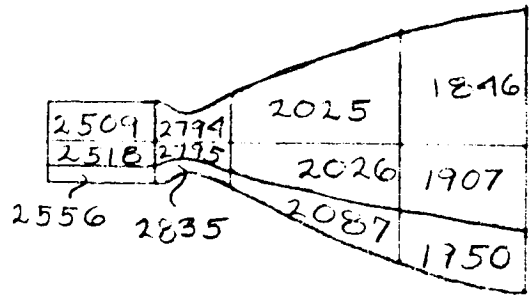

RCS NOZZLE TEMPERATURES
SCALE — 1/4

Figure 3-29. Summary of RCS and S/M Temperatures for a 500-Second RCS Engine Fire Cycle, With an RCS Mount Wall ϵ of 0.05

~~CONFIDENTIAL~~

~~CONFIDENTIAL~~

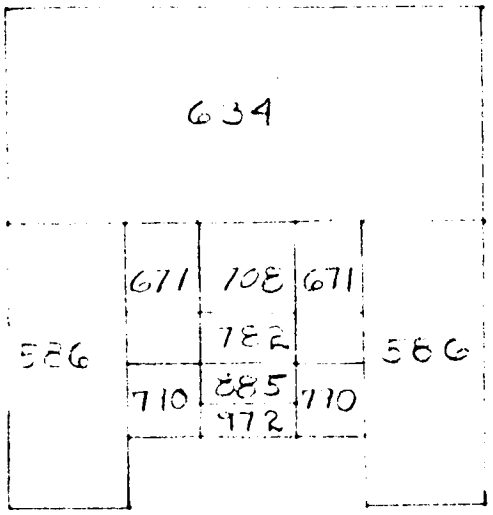

S/M SURFACE TEMPERATURES
SCALE — 1/8

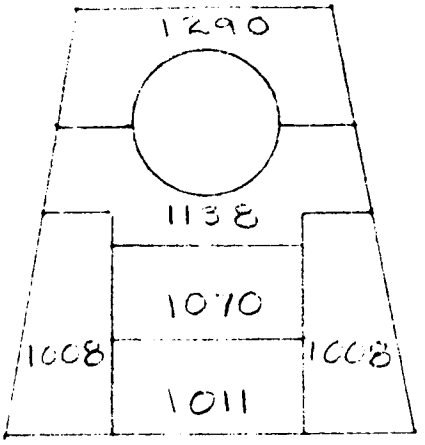

RCS MOUNT WALL TEMPERATURES
SCALE — 1/4

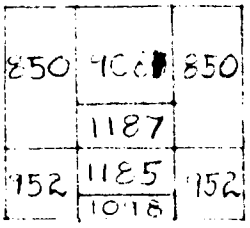

S/M SHIELD TEMPERATURES
SCALE — 1/8

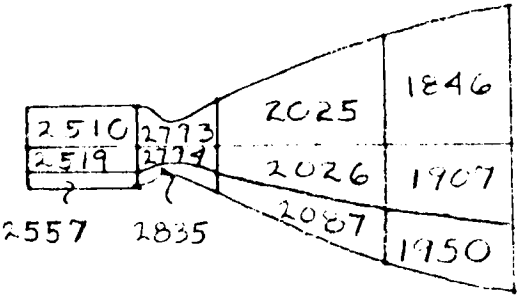

RCS NOZZLE TEMPERATURES
SCALE — 1/4

Figure 3-30. Summary of RCS and S/M Temperatures for a 500-Second RCS Engine Fire Cycle, With an RCS Mount Wall ϵ of 0.20

~~CONFIDENTIAL~~

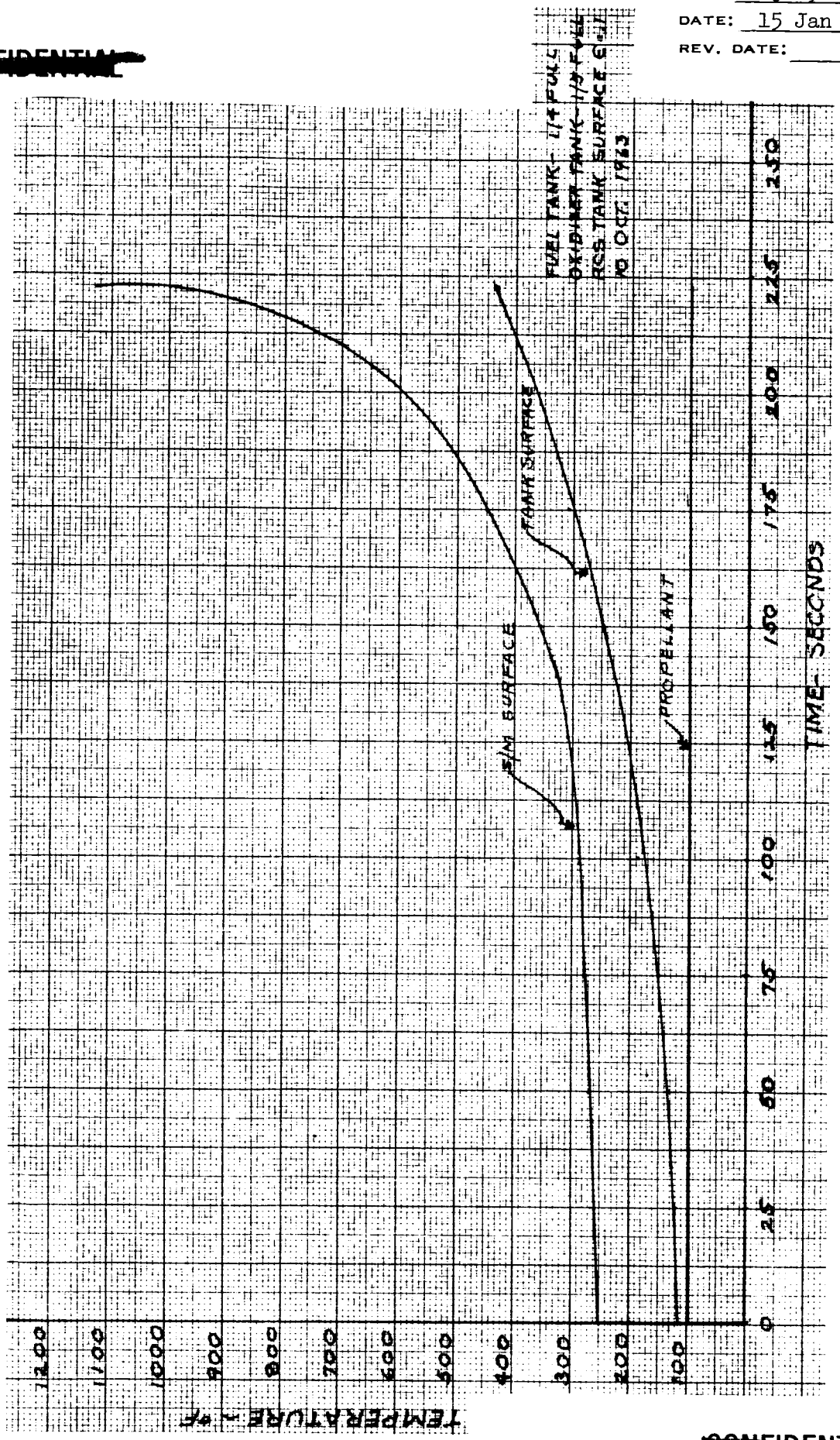

Figure 3-31. Temperature-Time History of RCS Tanks for S/M Reentry Temperature

~~CONFIDENTIAL~~

4.0 INTERFACE

4.1 Maximum Surface Temperatures of the Honeycomb Adapter During Boost Heating

4.1.1 Listed in Table 4.1 are the maximum expected temperatures of the S/M adapter during boost heating, for wetness, face thickness and core densities.

Table 4-1. Maximum Surface Temperatures of the Honeycomb Adapter During Boost Heating

Core Density	2 lb/ft^3		3 lb/ft^3	
Face Thickness	T_1 °F	T_2 °F	T_1 °F	T_2 °F
0.015 in.	422	395	388	351
0.016	408	381	378	340
0.017	396	368	369	330
0.018	385	357	361	321
0.019	375	346	353	313
0.020	366	336	346	305
0.021	358	327	339	297
0.022	350	319	330	291
0.023	342	311	327	284
0.024	335	304	321	278
0.025	329	297	316	272

T_1 = Temperature of outer face
T_2 = Temperature of inner face

5.0 BOILERPLATES

5.1 Thermal Requirements During C-1 Boost (Boilerplates 9, 13, 15, 16 and 18)

5.1.1 Results of atmospheric heat transfer and thermo and fluid dynamics studies indicate that the boilerplate skins will greatly exceed the allowable temperature of 250 F during a C-1 boost. Table 5-1 supplies the minimum thermal requirements for Boilerplates 9, 13, 15, 16 and 18.

Table 5-1. Minimum Thermal Requirements (Various Boilerplates)

Location (in inches)	Aluminum (Thickness in inches)	Avcoat II (Thickness in inches)	Buna-N (Thickness in inches)	Thermolag T-500 (Thickness in inches)	Cork (Thickness in inches)
X_c = 23.873	0.19	0.24	0.15	0.15	0.12
X_c = 82.750	(2)	0.28	0.24	0.25	0.15
X_c = 115.938	0.08	0.28	0.24	0.25	0.15
X_c = 133.723	0.03	0.03(3)	0.03(3)	0.03(3)	0.03(3)

(1) There is a linear relationship from one location to another for ablator requirements.

(2) At X_c = 82.750 the aluminum skin thickness changes from 0.19 to 0.08 inches.

(3) Requirements for Boilerplate 9 only.

5.1.2 Boilerplate 9 will require insulation from locations X_c = 115.938 to X_c = 133.723. The additional requirement occurs because an aluminum skin will be fabricated especially for this particular boilerplate. The skin replaces the Collins Radome that will be used on all other boilerplates mentioned.

5.1.3 Figure 5-1 shows the general configuration of the boilerplates, giving the X_c locations considered in the studies. Figures 5-2 and 5-3 furnish typical temperature histories for the boilerplate skins during a C-1 boost, with and without the use of thermal protection.

[redacted]

5.2 Temperature Histories of the C-Band Antenna Windows (at X_c = 77) During Maximum-Q and High-Altitude Abort Missions

5.2.1 A thermal analysis determined that the maximum temperatures the C-band antenna windows would experience during the Little Joe II maximum-q abort (36,500 feet), if located at X_c = 77, would be 400 F. The study was carried out for a Duroid 5650 antenna window which was 0.064 inches thick at that particular station.

5.2.2 Figure 5-4 is a schematic diagram of a C-band antenna. Figures 5-5 and 5-6 show the data which was gathered for the antenna windows from boost through abort of both Little Joe II maximum-q abort and high-altitude abort missions.

5.3 Boilerplate Shell Structure Temperatures During C-1 Boost

5.3.1 During a C-1 boost, the maximum expected temperature on the shell structure of either the service module, insert, or adapter, for Boilerplates 9, 13, 15 and 16, is 200 F. Figure 5-7 graphs the temperatures at various time intervals from launch. A design consisting of a 0.16-inch-thick aluminum skin was assumed for each structure.

5.4 Shell Structure Temperatures During the Little Joe II Boost (Boilerplate 12, 22 and 23)

5.4.1 The maximum expected temperature, during a Little Joe II boost, of the shell structure of either the S/M or the extension on Boilerplate 22 (high-altitude abort) is 187 F. Figure 5-8 gives the temperature profile of this boilerplate's shell structure, assuming a 0.134-inch-thick steel skin for each structure. For Boilerplates 12 and 23 (maximum-q aborts), lower temperatures are expected.

5.5 Command Module Forward Heat Shield Separation Bolt Temperature Histories (Boilerplates 6 and 12)

5.5.1 Temperature histories were determined for the C/M's forward heat shield separation bolt (Figure 5-9) during pad abort and abort at 19,000 feet. In both cases the temperatures were found to be equivalent; also, in both instances, the heat flux was due to radiation from the LES rocket plumes. The material assumed for the analysis was A286 steel on all components.

5.5.2 The temperature histories at three points along the bolt are shown in Figures 5-10 to 5-12. The maximum temperature of the necked section was 176 F at 51 seconds after initial firing.

5.6 Maximum Temperatures of the LES, Nose Cone, Motor Casing and Structural Skirt Skin (Boilerplate 22)

5.6.1 The maximum expected temperatures of the LES's nose cone, motor casing (at three locations) and structural skirt skin are given in Figure 5-13, for the new Boilerplate 22 boost-abort. This new mission, a Little Joe II boost followed by a 60,000-foot abort, stands in contrast to the previous 180,000-foot abort trajectory.

5.7 Thermal Analysis of the C/M R & D Radome (Boilerplates 13, 15 and 18)

5.7.1 The maximum expected temperature of the C/M R & D radome outer fiberglass honeycomb laminate is 780 F for Boilerplate 13, 805 F for Boilerplate 15, and 3390 F for Boilerplate 18. Since fiberglass chars at approximately 600 F, these temperatures are for the charred materials.

5.7.2 The locations of four data points on the C/M radome are shown in Figure 5-14. Maximum expected temperatures, during boost or boost-abort missions, for Boilerplates 13, 15 and 18 are given for each of these points in Table 5-2. Temperature histories are to be found in Figures 5-15 through 5-18.

Table 5-2. Maximum Expected Temperatures for Four Data Points (of Figure 5-14)

Data Point	Location	Maximum Temperature (°F) for Boilerplates:		
		3	5	18
A	Outer laminate at nose	445	625	3390
B	Inner laminate at nose	230	260	1560
C	Outer laminate at base	780	805	1980
D	Inner laminate at base	430	440	850

5.8 Thermal Protection for Boilerplates 12 and 23

5.8.1 The possibility exists that rocket plume impingement from the LES motor on the C/M will occur during a maximum-q abort (at 18,000 feet) on Boilerplates 12 and 23. Should this happen, it would raise the temperatures of the boilerplate skins above the design limit of 250 F, thus requiring 0.15-inch-thick cork insulation from X_c = 24.12 to X_c = 82.75 and 0.07-inch-thick cork insulation from X_c = 82.75 to X_c = 133.72.

5.8.2 If no insulation is applied to the boilerplate, maximum temperatures of 770 F above and 1115 F below station X_c = 82.75 can be expected. In order to prevent the skins from exceeding the design limit of 250 F, a cork insulation thickness of 0.15 inches must be applied from X_c = 24.12 to X_c = 82.75, and a cork thickness of 0.07 inches applied from X_c = 82.75 to X_c = 133.72.

5.8.3 Figure 5-19 is a diagram of the C/M boilerplates showing skin thicknesses for various X_c locations. Figures 5-20 and 5-21 give predicted temperature histories for C/M boilerplate skins during the Little Joe II boost and abort conditions.

5.9 Thermal Protection for C/M-to-S/M Umbilical Cover on Boilerplate 13

5.9.1 Results indicate that minimum cork thicknesses of 0.20 inches from X_c = 43.9 to X_c = 40.2 and 0.15 inches from X_c = 40.2 to X_s = 356.5 will be required in order to prevent the C/M-to-S/M umbilical cover of Boilerplate 13 from exceeding the 250 F design limit during Saturn-I boost. If no insulation is used, maximum temperatures of 1490 F from X_c = 43.9 to X_c = 40.2 and 722 F from X_c = 40.2 to X_s = 356.5 can be expected.

5.9.2 Figure 5-22 is a schematic of the umbilical cover on Boilerplate 13. This cover is made from polyester fiberglass laminates and is 0.25 inches in thickness. Figures 5-23 and 5-24 show temperature histories of the umbilical cover at various locations.

5.10 Thermal Analysis of Selected Points on the C/M of Boilerplate 15 (During Boost)

5.10.1 A thermal analysis was performed on selected points of the C/M of Boilerplate 15 to determine if any additional thermal protection would be required as a result of using a live LES escape rocket. Figure 5-25 shows what locations were under consideration. Temperature conditions of 120 F were used.

5.10.2 The study indicates that the only modification required will be at X_c = 88.00. In this instance, the thermal protection (cork) must be increased from 0.15 inches to 0.18 inches to limit the aluminum skin and bondline (cork and aluminum) to a maximum of 250 F. Figure 5-26 graphs both temperature histories at this location.

[redacted]

5.11 Minimum Insulation Requirements of the LES Tower-to-C/M Umbilical Conduit and Shroud

5.11.1 Because Buna-N ablative insulation is recommended for the LES tower-to-C/M umbilical conduit and shroud (Figure 5-27), it was used for the ensuing study. The design temperature of 300 F for the wires and connector was used in obtaining the results. The heating rates used were: Saturn-I boost for Boilerplates 13, 15, 16 and 26; Little Joe II boost/high altitude (60,000 feet) abort for Boilerplate 22; Saturn-I boost/high-altitude abort for Boilerplate 18 and Airframes 009 and 011; and Saturn-V boost/high-altitude abort for the Saturn-V spacecraft mission.

It should be noted that if the new concept of using the LES tower aerodynamic flaps to stabilize the C/M during reentry from a high-altitude abort is adopted, and the tower-to-C/M umbilical is allowed to remain operative until tower jettison, reentry heating on the umbilical installation will have to be considered on those missions affected by this change.

5.11.3 Results for these boilerplates, airframes and the typical spacecraft mission show that the most insulation required for any flight condition is 0.30 inches covering the umbilical wire conduit and 0.10 inches covering the umbilical connector shroud.

5.11.4 Table 5-3 gives the minimum Buna-N ablative insulation thicknesses required to cover the LES tower-to-C/M umbilical wire conduit and connector shroud.

Table 5-3. Minimum Buna-N Ablative Insulation Requirements of the LES Tower-to-C/M Umbilical Conduit and Shroud (See Figure 5-27)

Boilerplate or AFRM*	Minimum Buna-N Thickness (inches) Required to Prevent Part From Exceeding 300 F	
	Conduit	Shroud
13	0.22	0.05
15	0.22	0.05
16	0.22	0.05
18	0.30	0.10
22	0.20	0.10
26	0.22	0.05
009	0.30	0.10
011	0.30	0.10
Saturn-V Spacecraft Mission	0.30	0.10

*Boilerplates contain only two digits in their numerical designation; AFRM's have three.

[redacted]

[redacted]

5.12 Thermal Analysis of the C/M Tower Leg Wells for Boilerplates 13, 15, 16, 18 and 26

5.12.1 The maximum expected temperature of the C/M tower leg wells for Boilerplates 13, 15, 16, 18 and 26, without insulation, is 1100 F. This temperature has been calculated for the Boilerplate 18 well fairing and is shown in Figure 5-28.

5.12.2 In order to prevent any well part from exceeding 250 F in any of the boilerplates under consideration, cork thicknesses varying from zero to 0.14 inches are required on all exposed well surfaces. However, since some uncertainties exist in regards to abort plume heating from the LES exhaust (i.e., plume bending), it is recommended that 0.20 inches of cork be used to cover all exposed surfaces of the Boilerplate 18 wells.

5.12.3 Table 5-4 tabulates the maximum temperatures and minimum required insulation for three well locations. Figure 5-28 also shows the data point locations, and Figures 5-29 through 5-34 profile temperature histories (for various boilerplates) of the C/M tower leg well.

Table 5-4. Maximum Temperatures and Minimum Insulation Requirements for the C/M Tower Leg Well

Boilerplate	Data Point	Maximum Temperature (F) No Insulation	Minimum Cork Thickness (inches) Required To Maintain Part Below 250 F
13, 16, 26	A	680	0.13
	B	220	None
	C	425	0.08
15	A	690	0.13
	B	225	None
	C	430	0.08
18	A	1100	0.14*
	B	295	0.03*
	C	620	0.09*

*0.20-inch cork recommended on all exposed surfaces of the Boilerplate 18 wells.

[redacted]

5.13 Thermal Protection for Boilerplate 22

5.13.1 The recommended thermal protection requirements for Boilerplate 22 are shown in Table 5-5.

Table 5-5. Thermal Protection Requirements for Boilerplate 22

Location* (on C/M)	Structure Thickness (inches)	Cork Insulation (inches)	
		Recommended	Minimum
X_c = 24.12 to X_c = 82.75	0.19 aluminum	0.20	0.05
X_c = 82.75 to X_c = 115.94	0.08 aluminum	0.20	0.10
Nose Cone	0.08 aluminum	0.20	0.05
Tower Leg Wells	0.04 aluminum	0.20	0.10
C-band Antenna Window	0.065 fiberglass	0.20	0.10
Telemetry Antenna Window	0.38 fiberglass	0.20	0.10

*The aft heat shield is not expected to exceed the design limit of 250 F.

5.13.2 The minimum insulation requirements, to prevent the skins of the C/M of Boilerplate 22 from exceeding 250 F, are also given in Table 5-5. These are new requirements and are due to the new heating rates resulting from the revision of test conditions to a 60,000-foot abort.

5.13.3 The amount of insulation recommended is twice that calculated for the minimum in order to prevent its skin from exceeding the 250 F limit. This provision was made to avoid any future schedule slippage resulting as a consequence of a higher heating environment than the one considered. Such an environment may be created primarily, though not exclusively, by an increase in plume impingement effect. The possible increase in plume impingement could, in turn, be caused by high angles of attack experienced by the C/M and LES during abort initiation, excessive plume bending, etc.

5.13.4 Figure 5-35 is a schematic of the C/M boilerplate, showing the locations considered in the study. Figures 5-36 through 5-38 show typical temperature histories for these locations.

[redacted]

5.14 Insulation Requirements for the LES Tower-to-C/M Forward Heat Shield Pull-Off Tubes

5.14.1 The minimum thickness of Buna-N ablative insulation required to prevent the four LES tower-to-C/M forward heat shield pull-off tubes from exceeding 550 F is 0.35 inches on the forward (windows) half of each tube and 0.075 inches on the rearward (leeward) half of each tube. Figure 5-39 shows the location of the four pull-off tubes on the tower as well as a typical tubular cross-section with the required insulation.

5.14.2 It should be noted that if the tubes are to remain intact during a reentry from a high-altitude abort down to 25,000 feet (as in the tower-aerodynamic flap concept), additional insulation may be required to protect the tubes from reentry heating.

5.15 Temperature Histories of Telemetry Antenna Cover on Boilerplate 22

5.15.1 Temperature histories were determined for the telemetry antenna cover on Boilerplate 22, with a Little Joe II boost/60,000-foot-abort considered for the study. The results are given in Figure 5-40, which shows the design and the approximate locations of the Teflon covers, and in Figure 5-41, which profiles the temperature histories for both the outer and inner surfaces of the Teflon cover.

5.16 Maximum Temperatures of S/M RCS Fiberglass Nozzles for a Saturn-I Boost Trajectory of Boilerplates 13 and 15

5.16.1 An analysis of the fiberglass S/M RCS nozzles during the Saturn-I boost trajectory (for Boilerplate 13 and 15) revealed that these nozzles will reach maximum temperature at approximately 150 seconds after lift-off (Figure 5-42). The maximum dynamic load on the nozzles will occur at 66 seconds after lift-off and the maximum nozzle temperature of 1600 F will be approximately 200 F at that time. A fiberglass nozzle thickness of 0.020 inches was used in this analysis.

5.17 Shaped Charges for C-1 Adapter

5.17.1 A thermal analysis determined the expected temperature extremes for the shaped charges in the S/M adapter configuration. The results are given in Table 5-6, for the first ten hours of spaceflight.

[redacted]

Table 5-6. Temperature Extremes for Shaped Charges of C-1 Adapter

	Maximum Temperature of Change	Minimum Temperature of Change
Absorptivity = 0.3 (White Paint) Emissivity = 0.75	121 F	-98 F
Absorptivity = 0.25 (Aluminum Paint) Emissivity = 0.22	190 F	-80 F
Absorptivity = 0.3 (Weathered Aluminum) Emissivity = 0.9	112 F	-102 F

5.17.2 It should be noted that these figures are not applicable for boost conditions. It was assumed in the analysis that the shaped charges had survived the effects of boost history, and that initial temperatures for the shaped charges and the surface of the adapter were 275 F and 375 F, respectively.

5.18 Environmental Temperature Extremes for the LEM Adapter

5.18.1 The expected space temperature extremes for the LEM adapter are 275 F and -200 F. These extremes would be experienced after six earth orbits and twenty-four minutes of translunar injection. For this analysis it was assumed the insulation would have ablated away during boost, resulting in a solar absorptivity of 0.9 and an emissivity of 0.9 for the outer adapter surface. An inner surface emissivity of 0.25 was assumed for radiation interchange with the LEM.

5.19 Thermal Environment of Radiation Sensor During Lunar Mission

5.19.1 The radiation sensor temperature history for the lunar mission may be seen in Figure 5-43. For the translunar and transearth mission phases, maximum solar incidence was considered to the fairing, where the sensor is located. The orientation assumed for the lunar orbit was one in which the positive X axis of the spacecraft was pointed towards the center of the moon. A value of 0.25 was used for the solar absorptivity and emissivity of the fairing surface.

5.20 Thermal Characteristics of the Forward Heat Shield/Launch Escape Tower Ejection System

5.20.1 The ablator material of the forward heat shield considered in this

analysis was 0.5 inches in thickness with an α/E ratio of one, ($\delta = \alpha = 0.9$). Two thermal environment conditions were considered: a hot case (maximum solar input), for which the equilibrium temperature of the heat shield was taken as 250 F; and a cold case (no solar input), for which the equilibrium temperature was taken as -290 F. The temperature of the airlock in the forward compartment was assumed to be a constant 40 F.

5.20.2 For the cold case, heat loss from the airlock was determined to be 3.0 Btu/hr/ejector. For the hot case, the heat gained by the airlock was 2.5 Btu/hr/ejector. These heating rates represent thermal loads on the environmental control system of the CM for steady-state conditions.

5.20.3 Thermal effects of breaking the tension tie rod (Figure 5-44) at a point outside of the forward heat shield ablator material, in this case one inch beyond the ablator material surface, produced a temperature change of the tie rod of only a few degrees, a change which resulted in insignificant heat flow changes.

5.20.4 Table 5-7 supplies the temperature summary of this analysis.

Table 5-7. Temperature History of Tension Tie Rod

Location	Hot Case (°F)	Cold Case (°F)
Ablator surface:		
at 0.30 inches from rod	229	-203
at 1.00 inches from rod	236	-226
at 2.00 inches from rod	243	-258
Exposed end of rod	213	-181
Inside surface of cylinder assembly	57	12
Outside surface of cylinder assembly	50	25
Gusset	41	39

5.21 Parametric Thermal Analysis of the LEM Adapter During Boost

5.21.1 A parametric analysis was performed to determine the insulation requirement (cork) for the LEM adapter, shown schematically in Figure 5-45.

5.21.2 Figures 5-46 and 5-47 represent the maximum temperature of the LEM adapter (aluminum honeycomb) facesheet as a function of cork insulation and honeycomb facesheet thickness. Two honeycomb core depths of 1.5 inches and 2.5 inches were considered.

5.21.3 For example, an insulation (cork) and honeycomb (facesheet) thickness of 0.030 inches and 0.0163 inches, respectively, will result in a maximum facesheet temperature of 400 F during a Saturn-V trajectory (core depth = 1.5 inches). Figures 5-48 through 5-50 represent typical temperature histories of the front and back facesheets of the LEM honeycomb during the boost heating. The interior surface of the LEM adapter was considered to be adiabatically insulated.

5.22 Heating Rates for C/M During a 100-Nautical-Mile Tumbling-Earth Orbit

5.22.1 The C/M's earth orbital heating rates for a 100-nautical-mile tumbling orbit are given in Table 5-8. These results show that the average heating rates range between 25 and 198 Btu/hr/ft^2 for an orbit time of 1.55 hours. The conical surface of the C/M was divided into 12 segments, each being equal in area. Two computer runs were made, the first with the apex of the C/M pointed toward the sun during orbit, and the second with the base of the command module directed toward the sun. These two vehicle orientations resulted in the maximum heating rates, respectively, for the conical portion. An average of the heating rates on the 12 segments was made for each of the vehicle orientations. These two results were then averaged to obtain the results. (These heating rates are applicable to Boilerplates 13, 15, 16 and 18.)

Table 5-8. Command Module Average Heating Rates During 100-Nautical-Mile Tumbling-Earth Orbit

Orbit Time Hours	Degrees	Heating Rate Btu/hr/ft^2
0.000	0	198
0.086	20	196
0.172	40	189
0.258	60	172
0.344	80	159
0.452	105	148
0.474	110	26
0.603	140	26
0.689	160	25
0.775	180	25
0.860	200	25
1.080	250	25

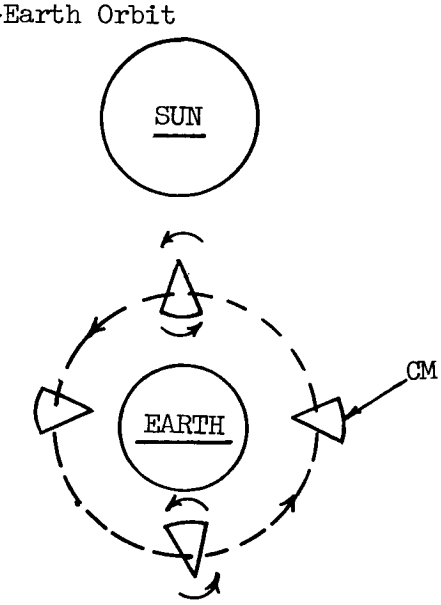

[redacted]

Table 5-8. Command Module Average Heating Rates During 100-Nautical-Mile Tumbling-Earth Orbit (Cont)

Orbit Time Hours	Degrees	Heating Rate Btu/hr/ft^2
1.10	255	148
1.21	280	153
1.29	300	170
1.38	320	187
1.46	340	194
1.55	360	198

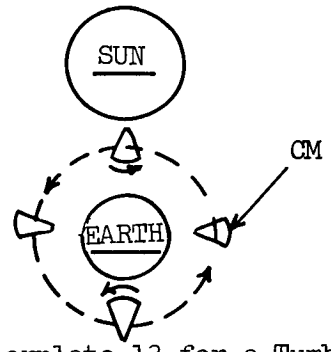

5.23 Expected Inside Wall Temperatures of Boilerplate 13 for a Tumbling-Earth Orbit

5.23.1 A maximum temperature of 219 F and a minimum of 115 F are expected for the inside wall of Boilerplate 13 during a random tumbling earth orbit.

5.23.2 A 500-pound instrument package was assumed to be in the vehicle, generating a constant energy output of 1200 watts. Surface properties used in the analysis were an emissivity of 0.75 and a solar absorptivity of 0.35.

[redacted]

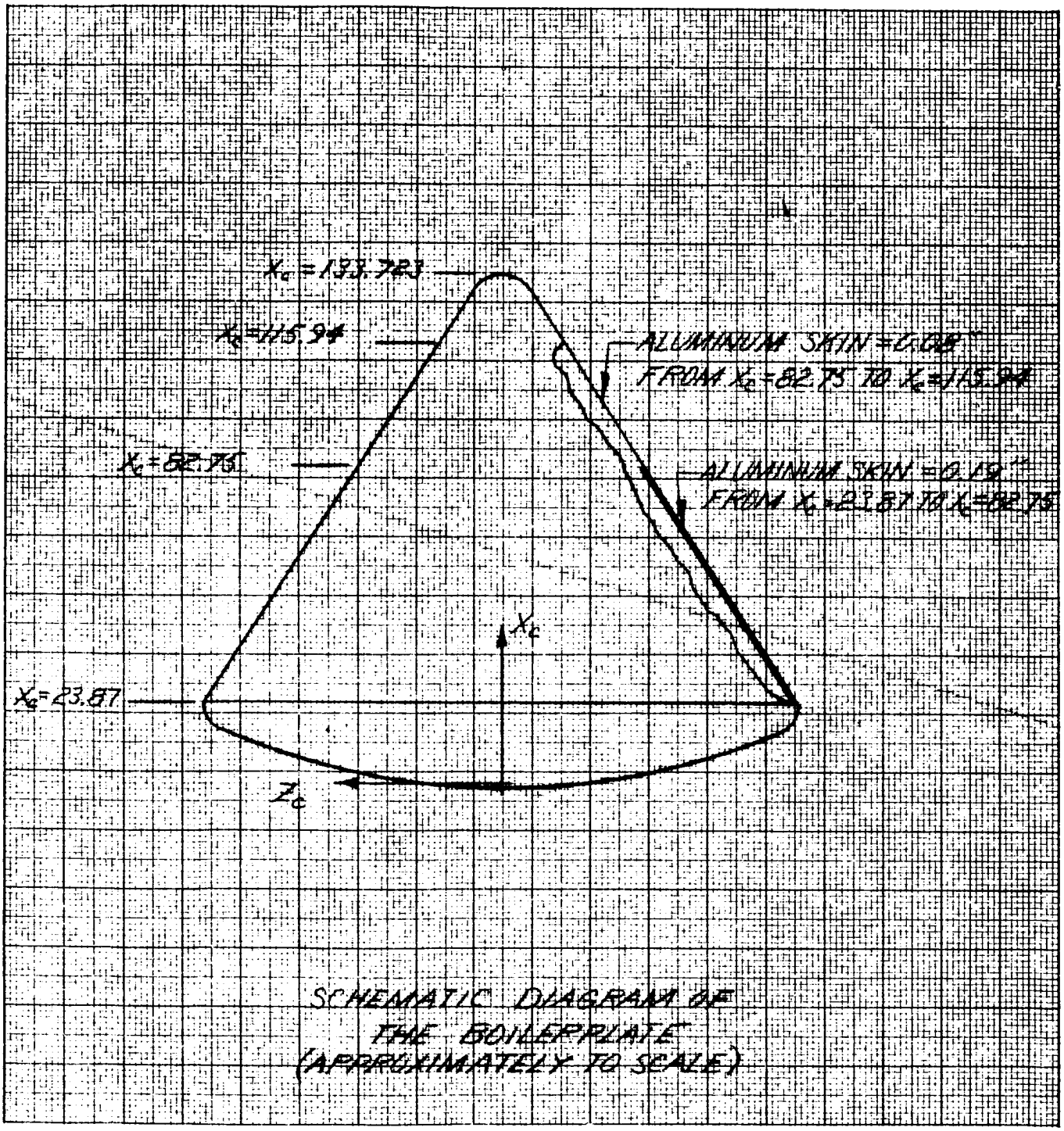

Figure 5-1. Typical Boilerplate (With X_c Locations Shown)

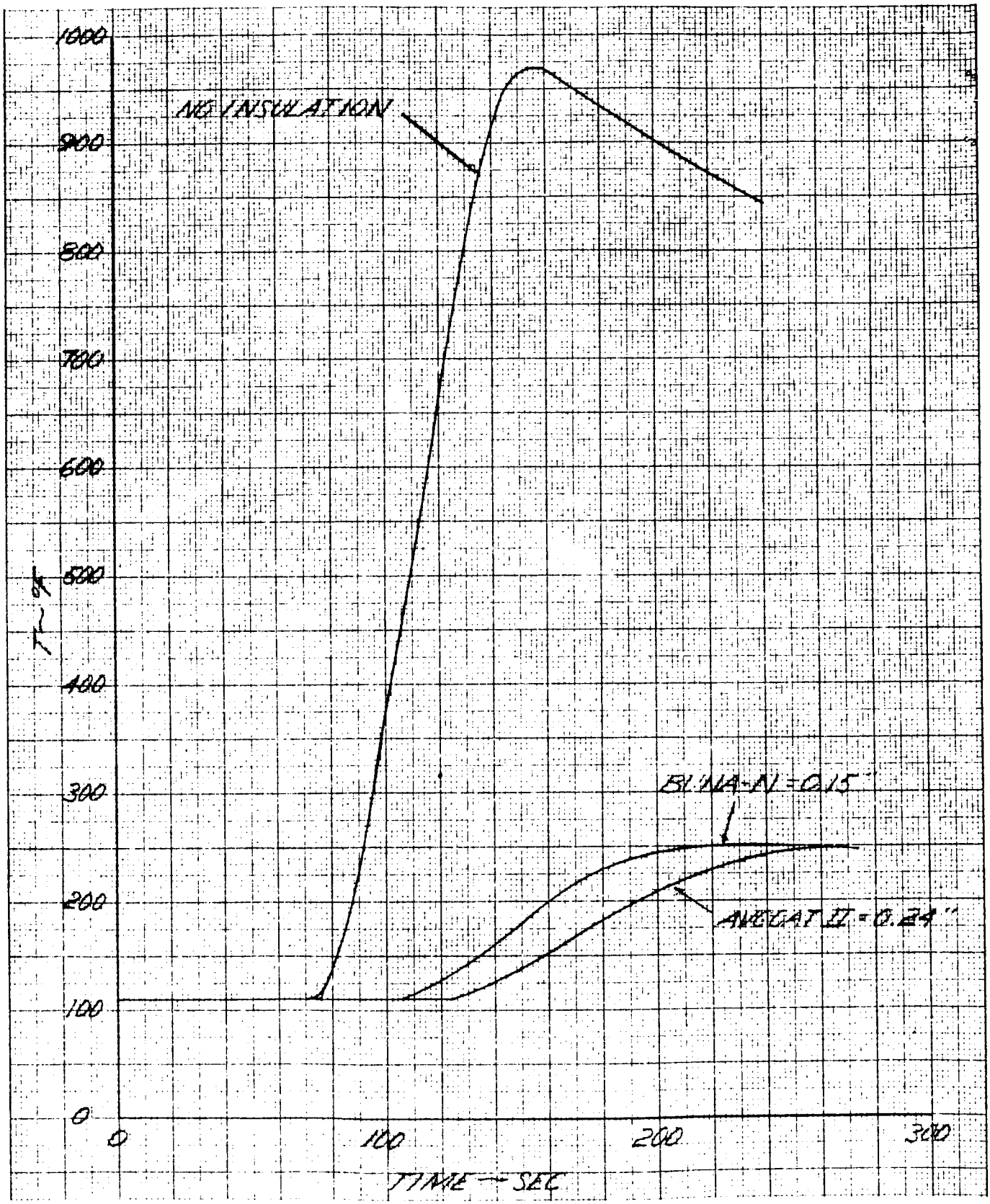

Figure 5-2. Temperature History of Aluminum Skin During a C-1 Boost (X_c = 23.87)

[redacted]

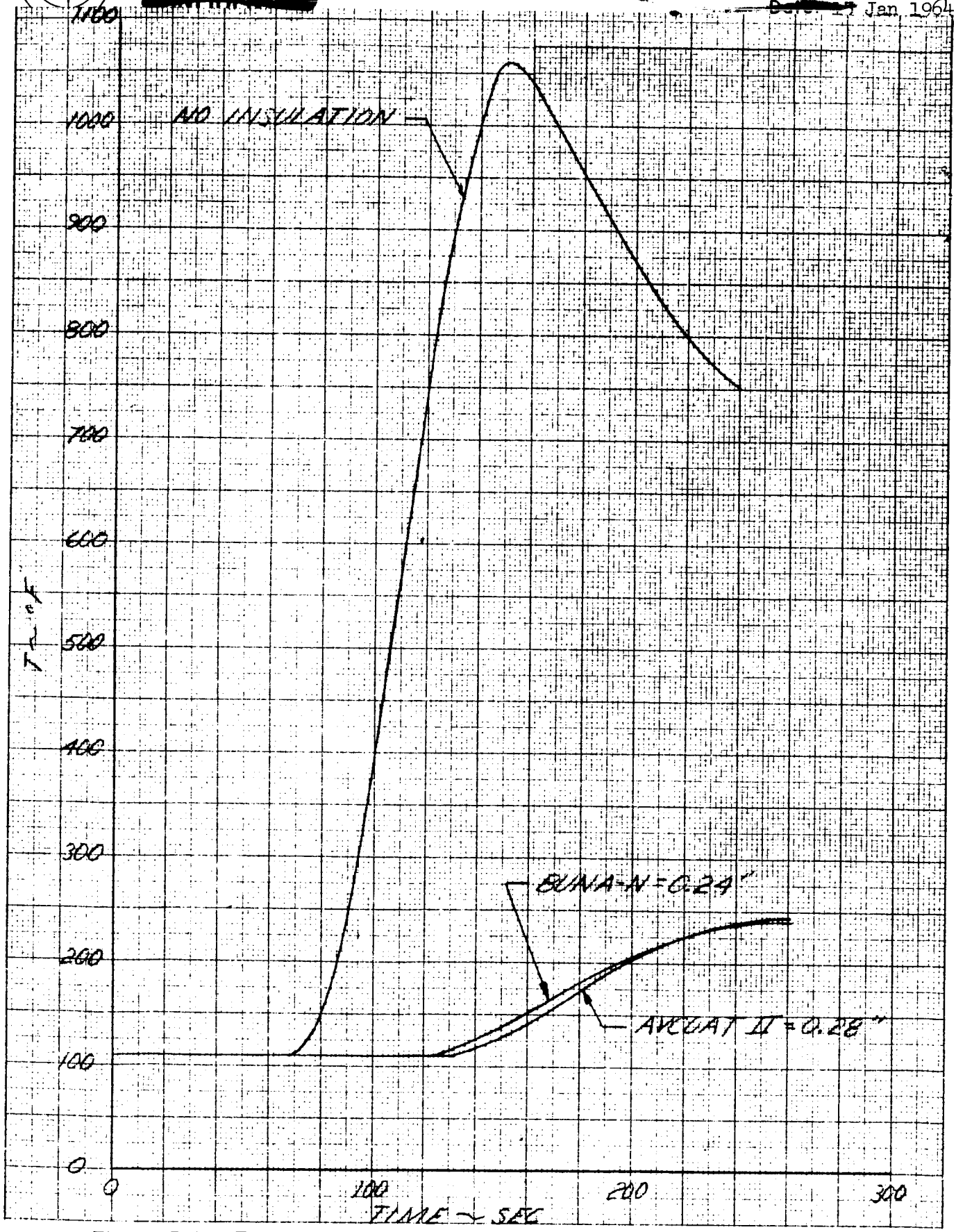

Figure 5-3. Temperature History of Aluminum Skin During a C-1 Boost (X_c = 115.938)

[redacted]

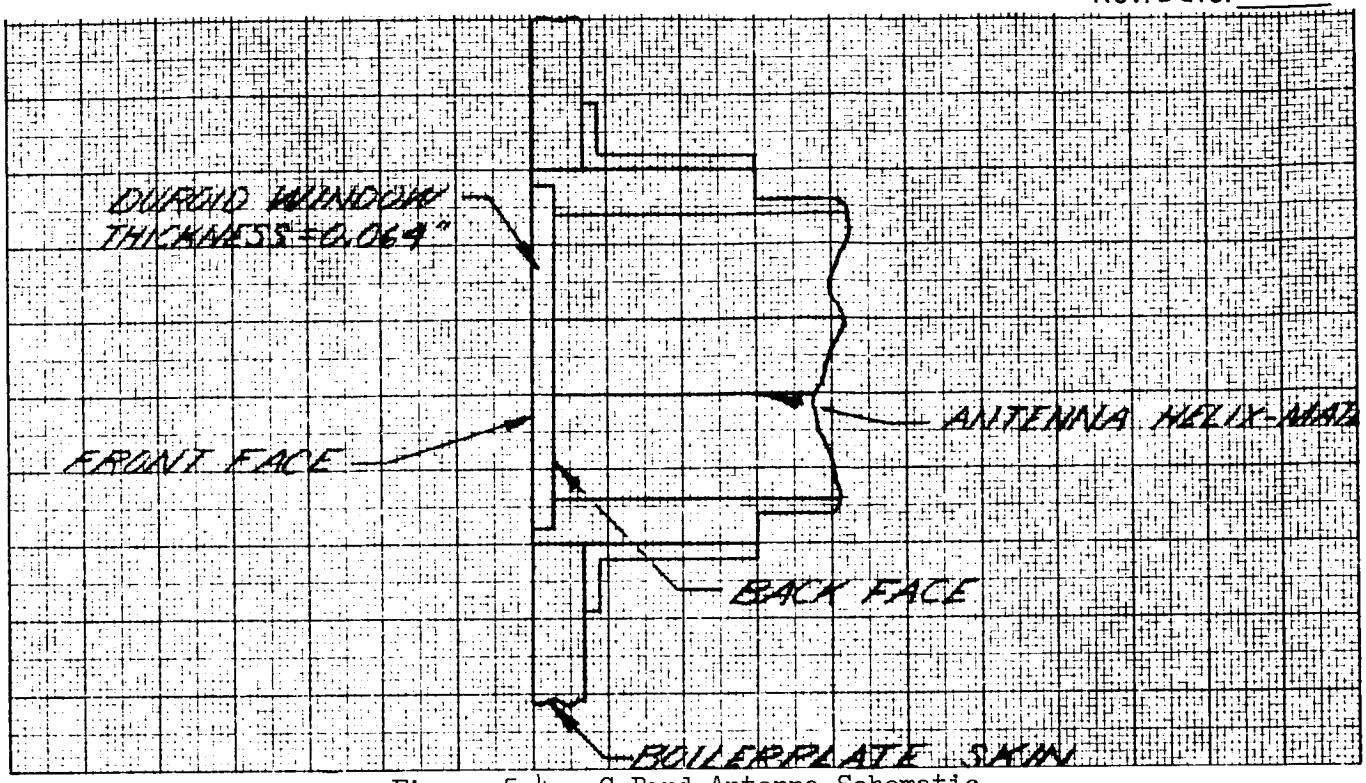

Figure 5-4. C-Band Antenna Schematic

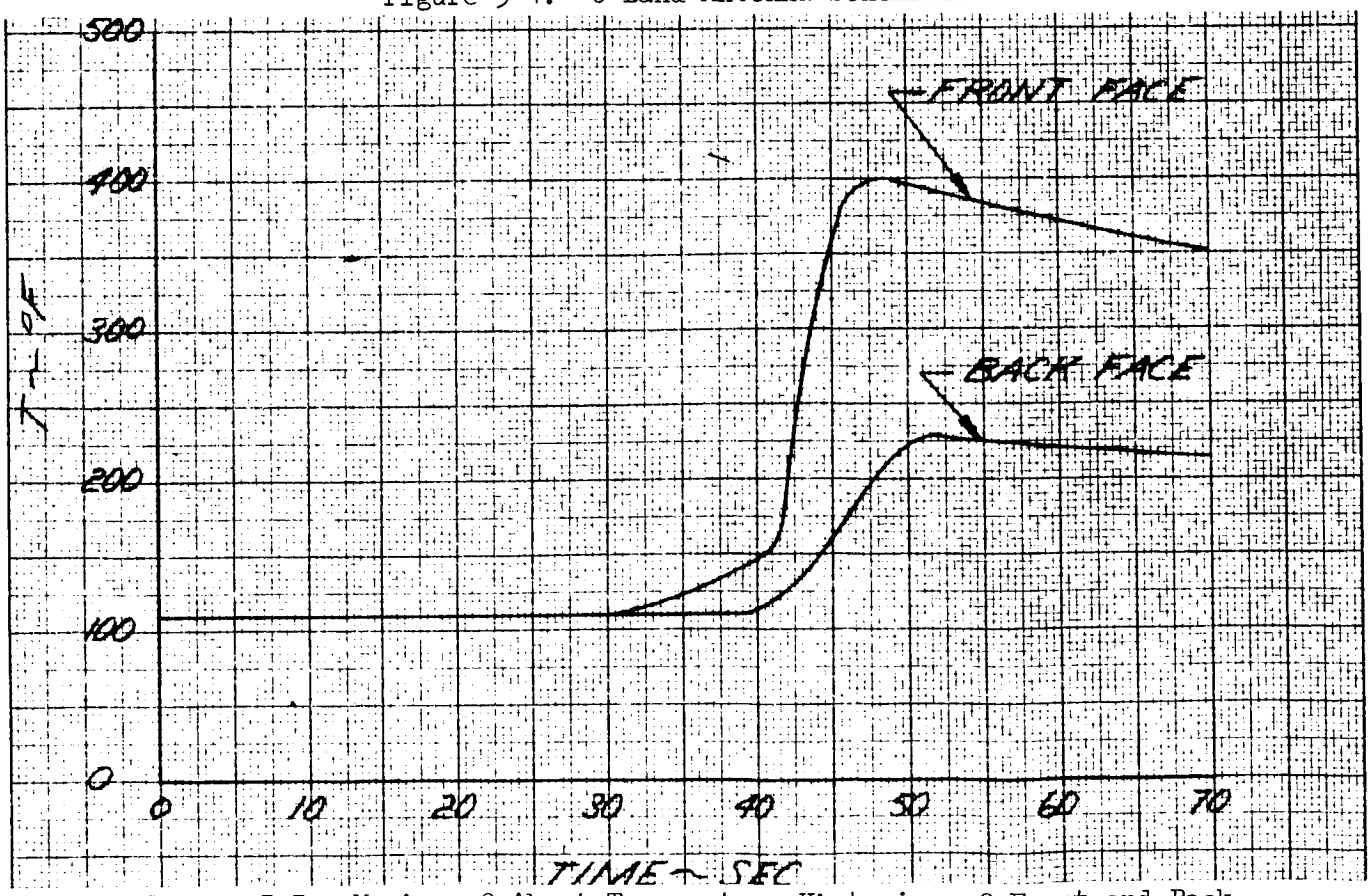

Figure 5-5. Maximum-Q Abort Temperature Histories of Front and Back Faces of C-Band Antenna Windows (X_c = 77)

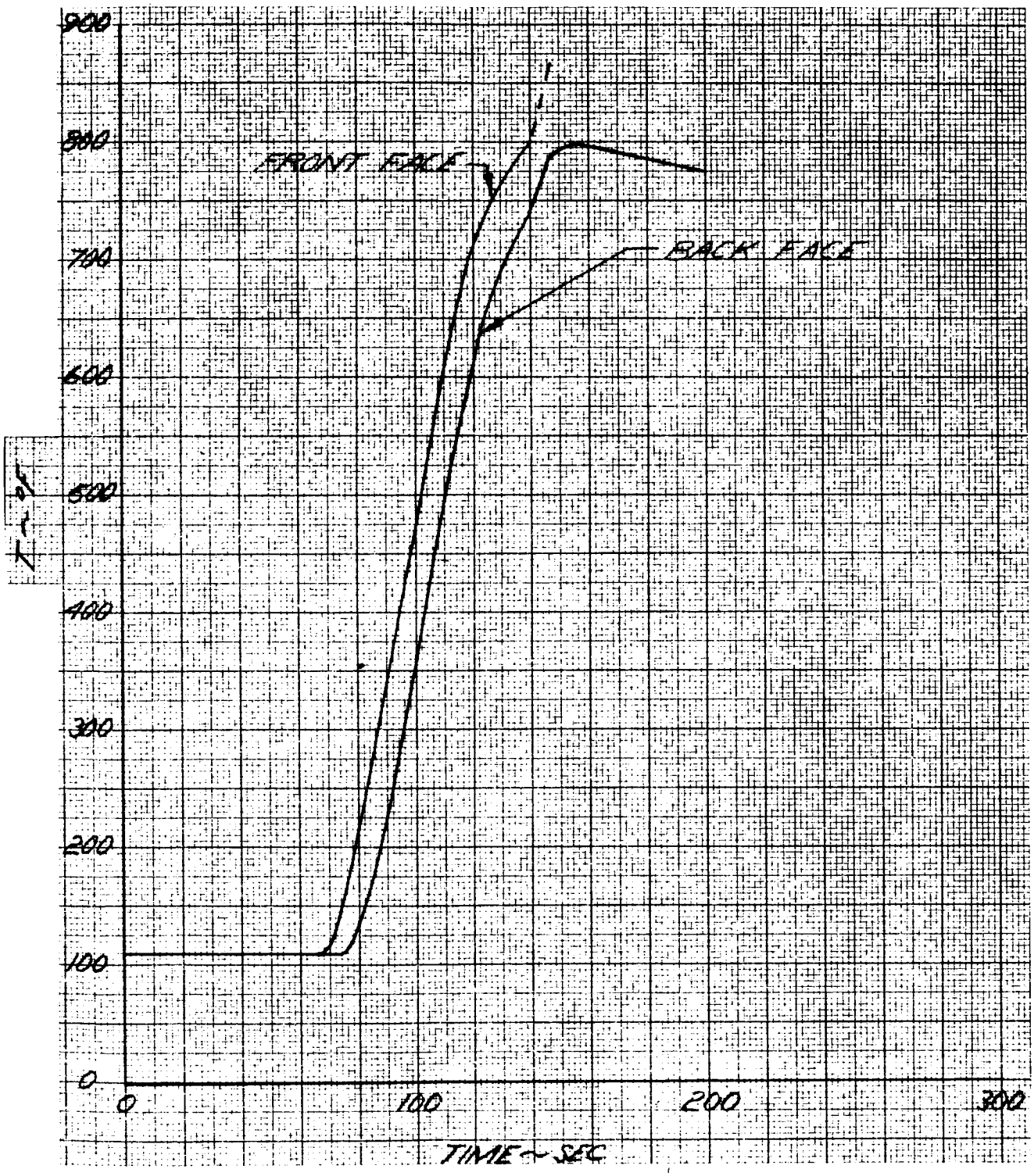

Figure 5-6. High-Altitude Abort Temperature Histories of Front and Back Faces of C-Band Antenna Windows (X_c = 77)

[redacted]

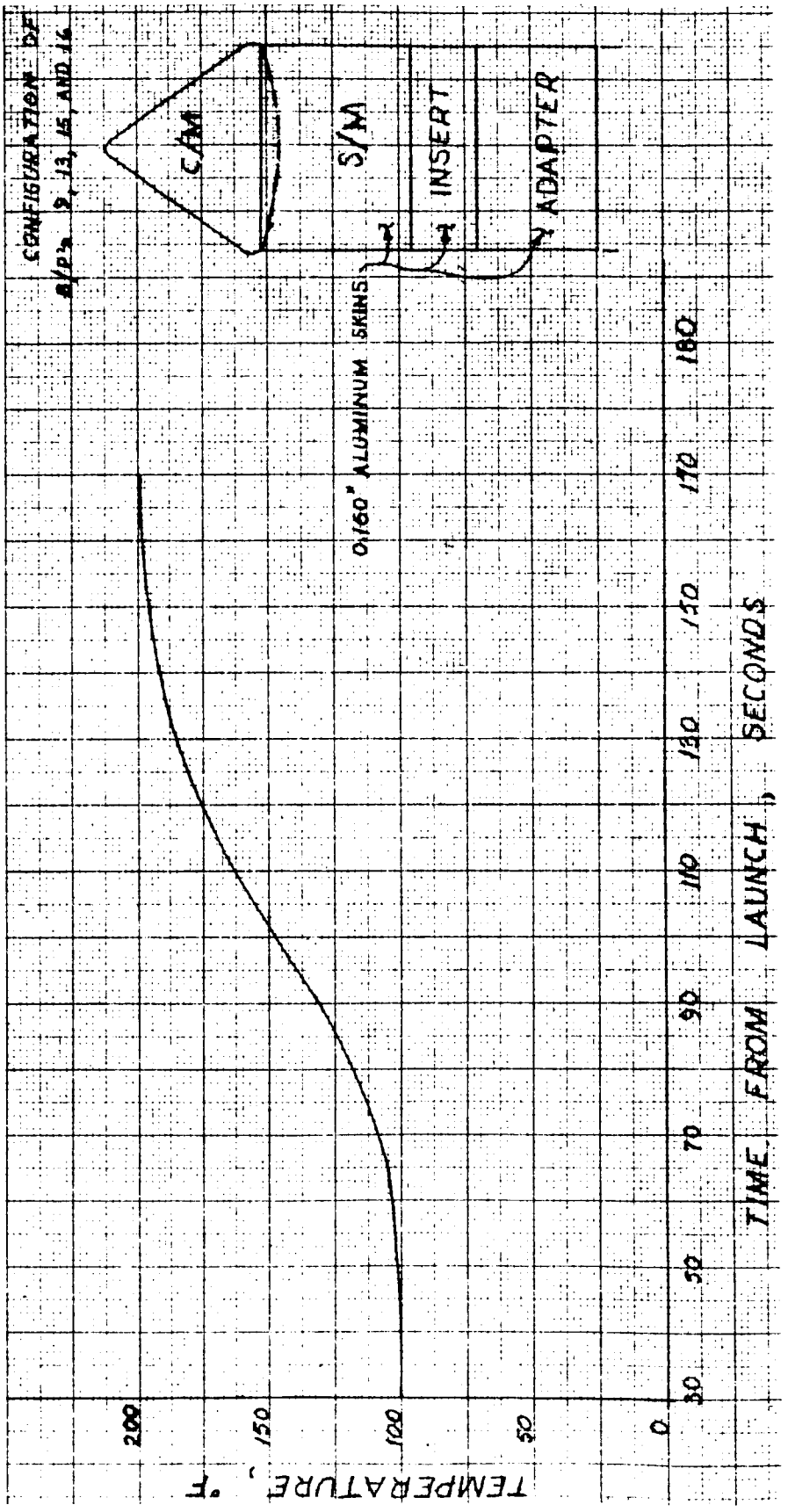

Figure 5-7. Temperature Profile of Boilerplate Shell Structure During C-1 Boost

[redacted]

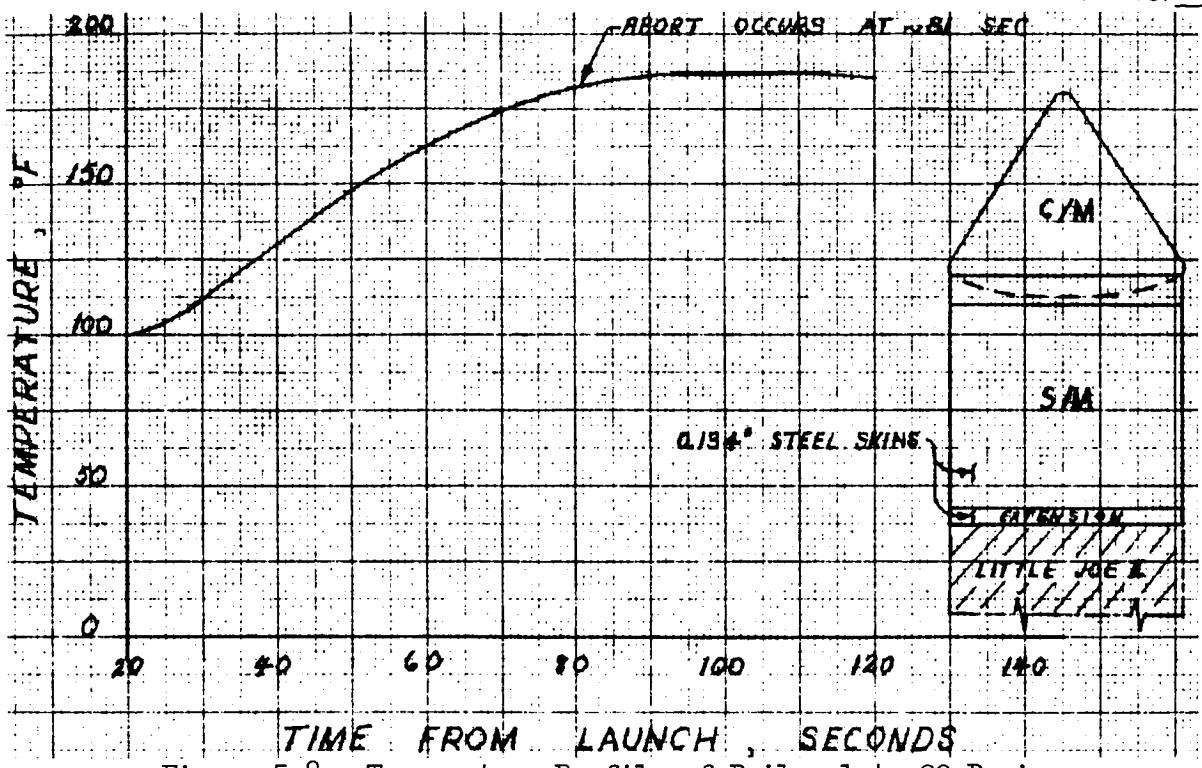

Figure 5-8. Temperature Profile of Boilerplate 22 During Little Joe II Boost

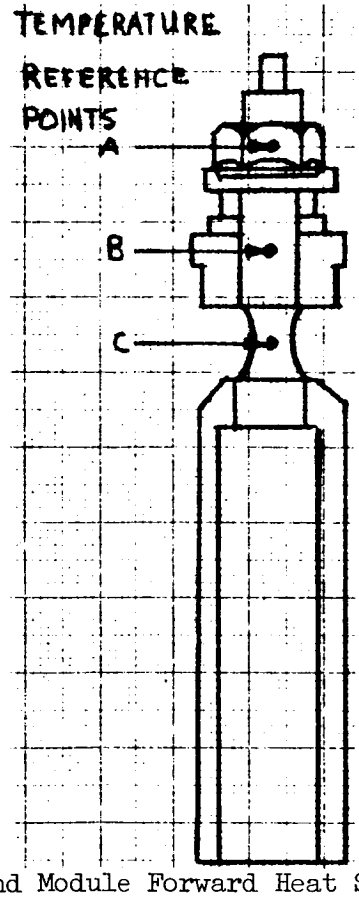

Figure 5-9. Command Module Forward Heat Shield Separation Bolt

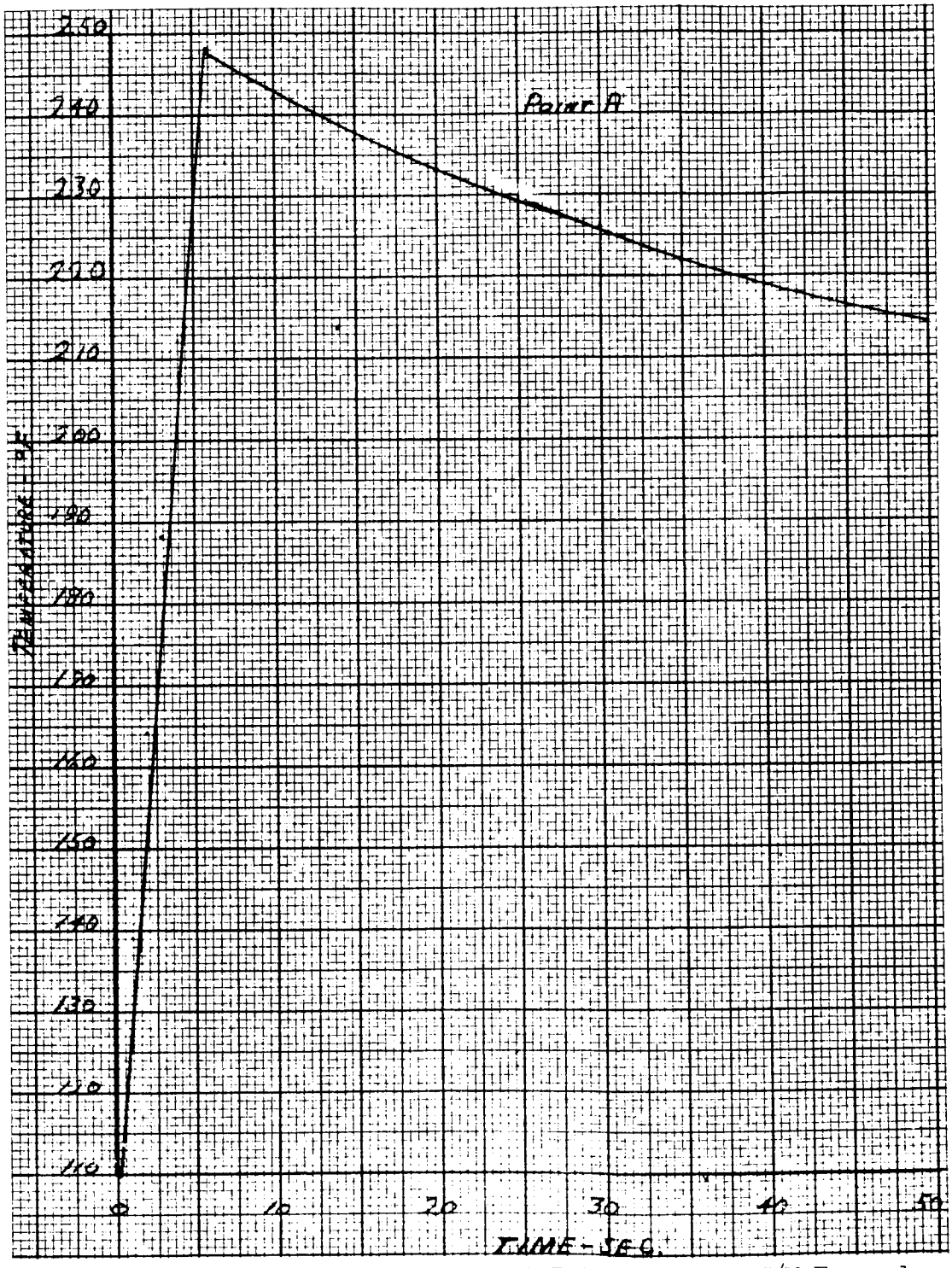

Figure 5-10. Temperature History at Point A of the C/M Forward Heat Shield Separation Bolt During a Pad Abort

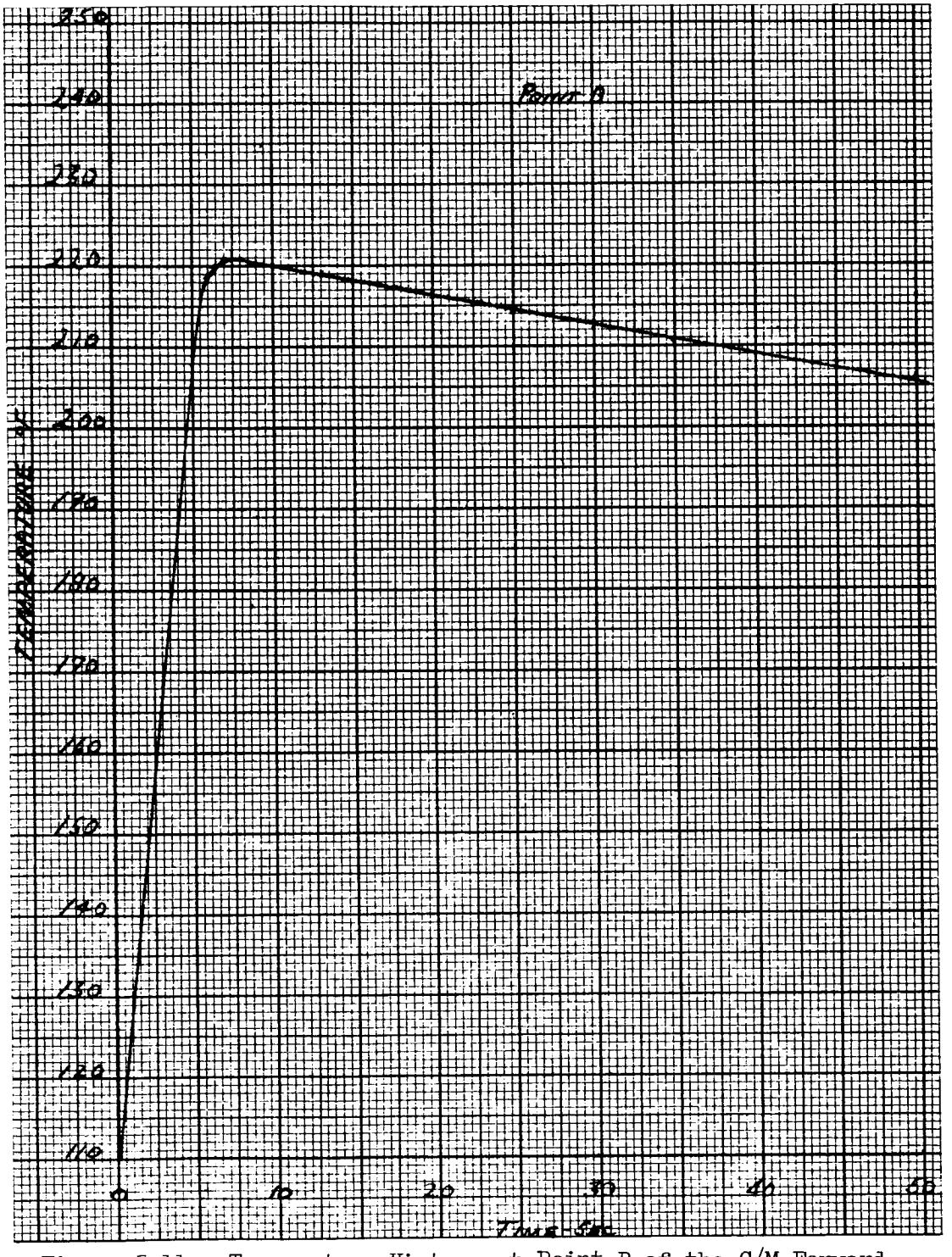

Figure 5-11. Temperature History at Point B of the C/M Forward Heat Shield Separation Bolt During a Pad Abort

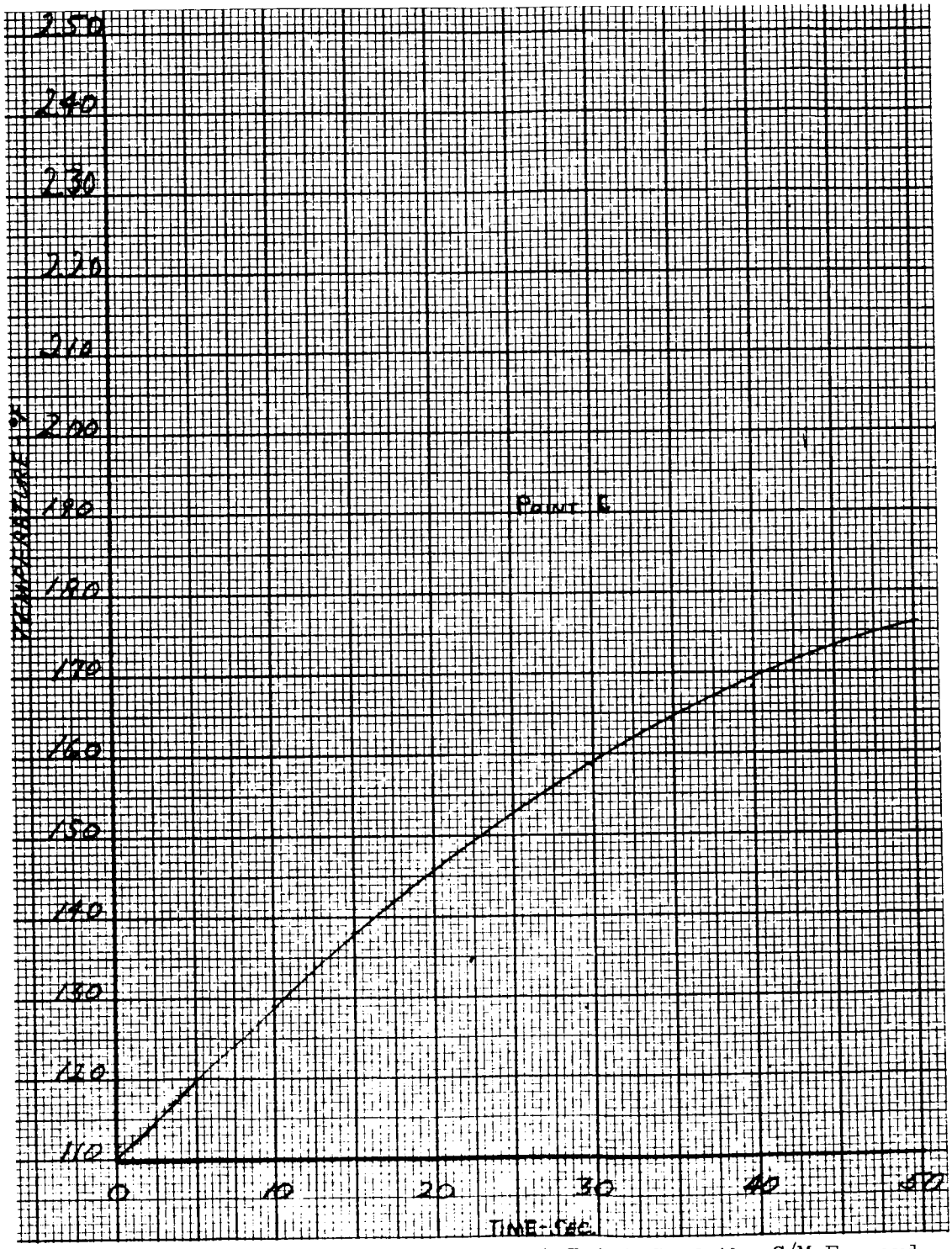

Figure 5-12. Temperature History at Point C of the C/M Forward Heat Shield Bolt During a Pad Abort

LES motor assembly showing data points

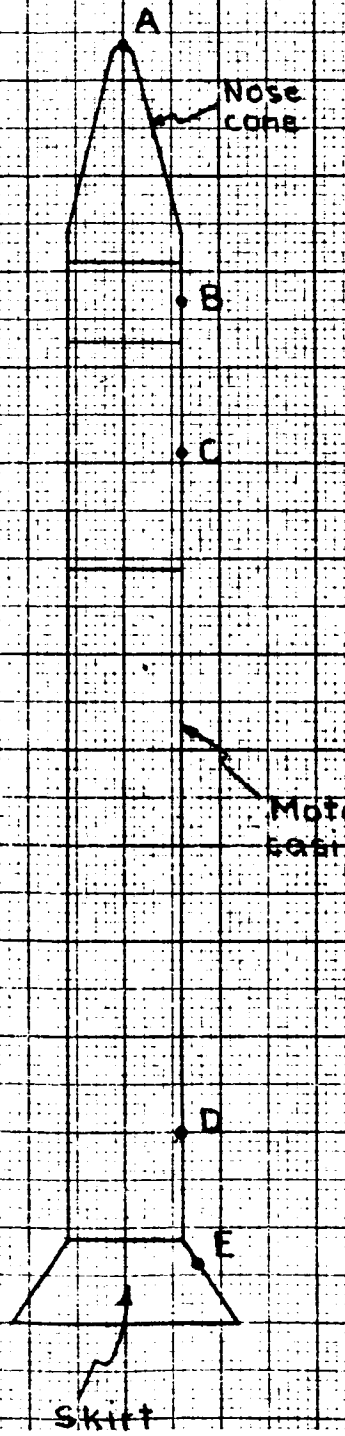

Table of maximum expected casing (skin) temperatures

Point	Location	X_L (in.)	Max. temp. (°F)
A	Nose cone	400	220
B	Pitch motor	366	210
C	Jettison motor	345	180
D	Escape motor	165	140
E	Skirt skin	130	260

Figure 5-13. Maximum Expected Temperatures of the LES Nose Cone, Motor Casing and Skirt Skin

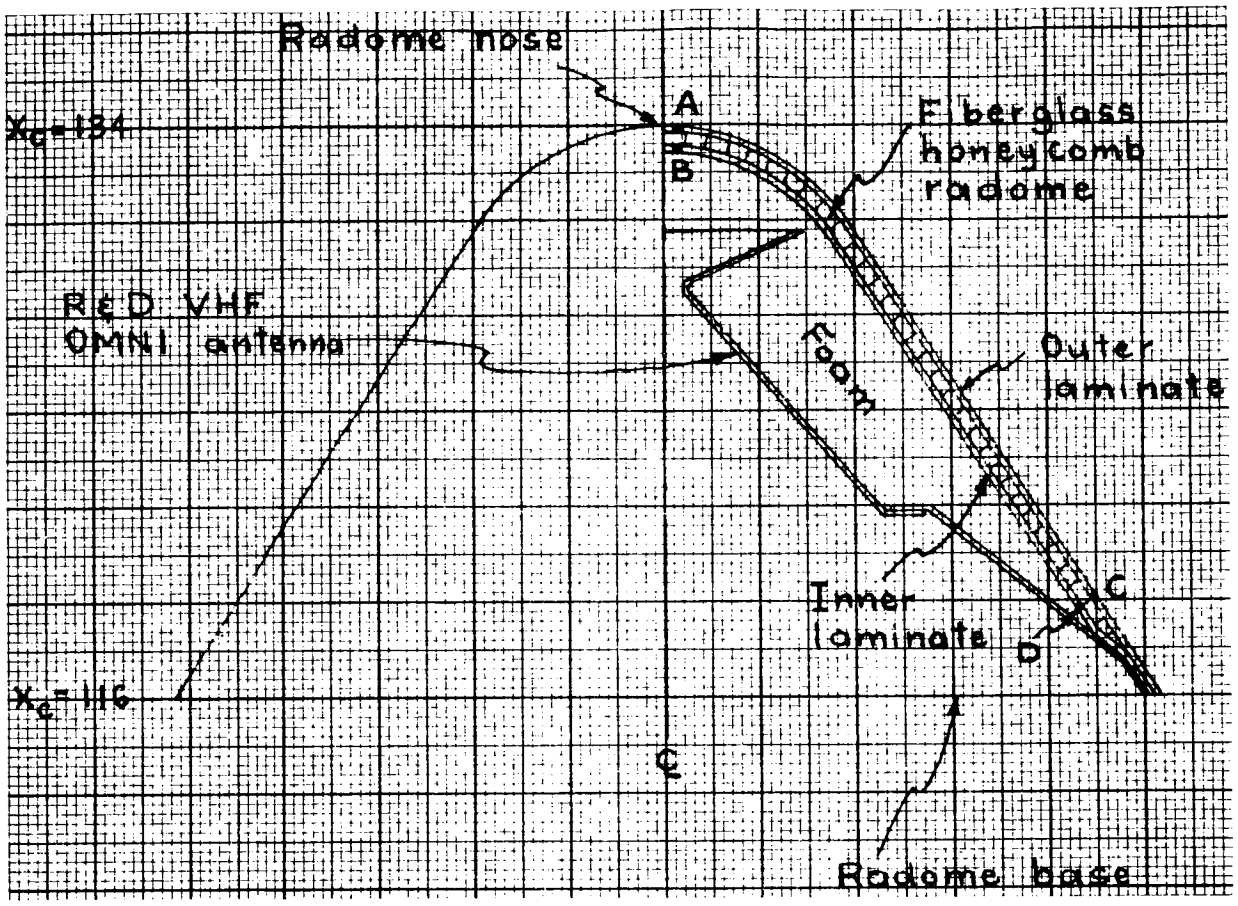

Figure 5-14. Schematic of the C/M Radome for Boilerplates 13, 15 and 18, Showing Locations of Four Data Points

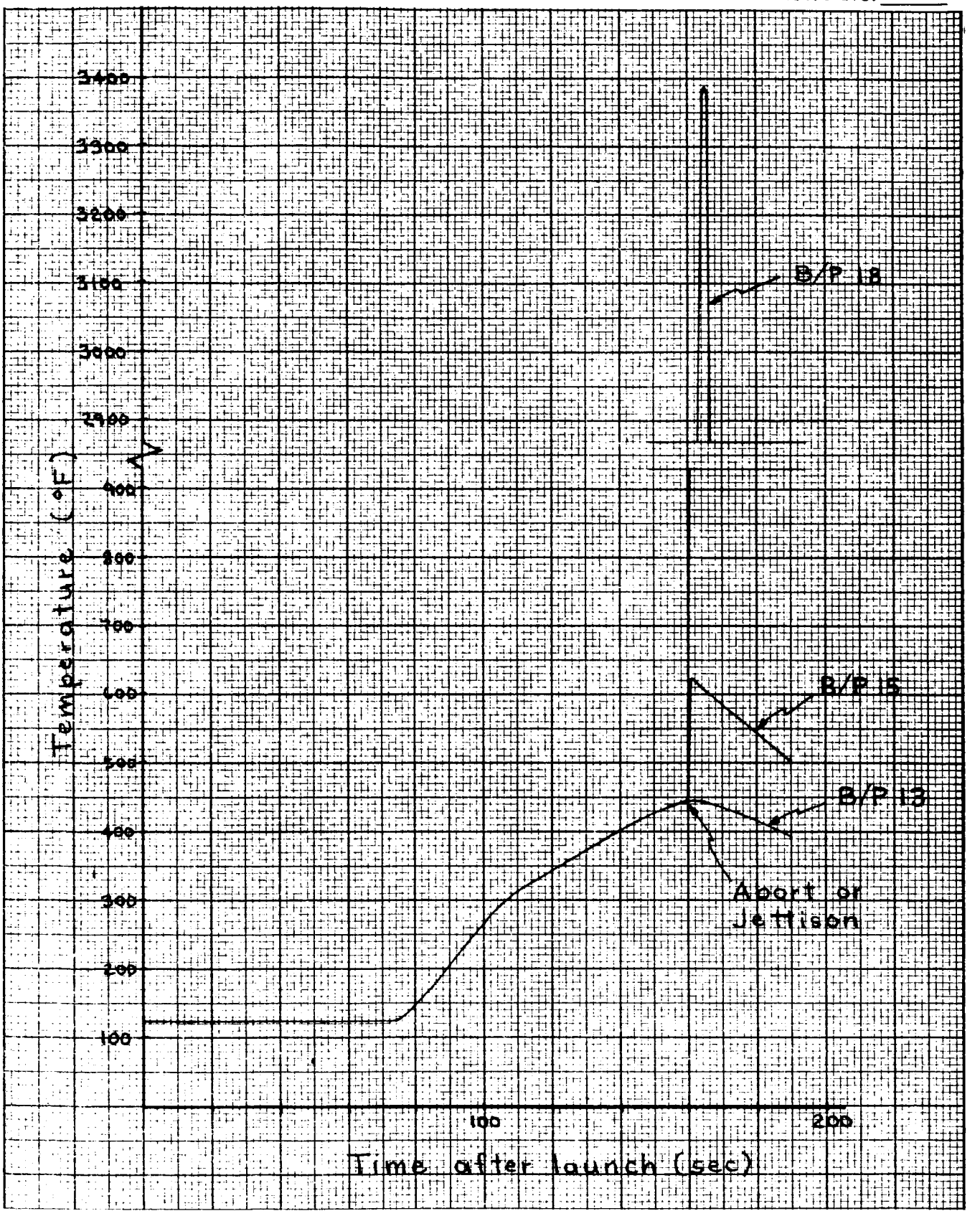

Figure 5-15. Temperature History at Point A of Figure 5-14

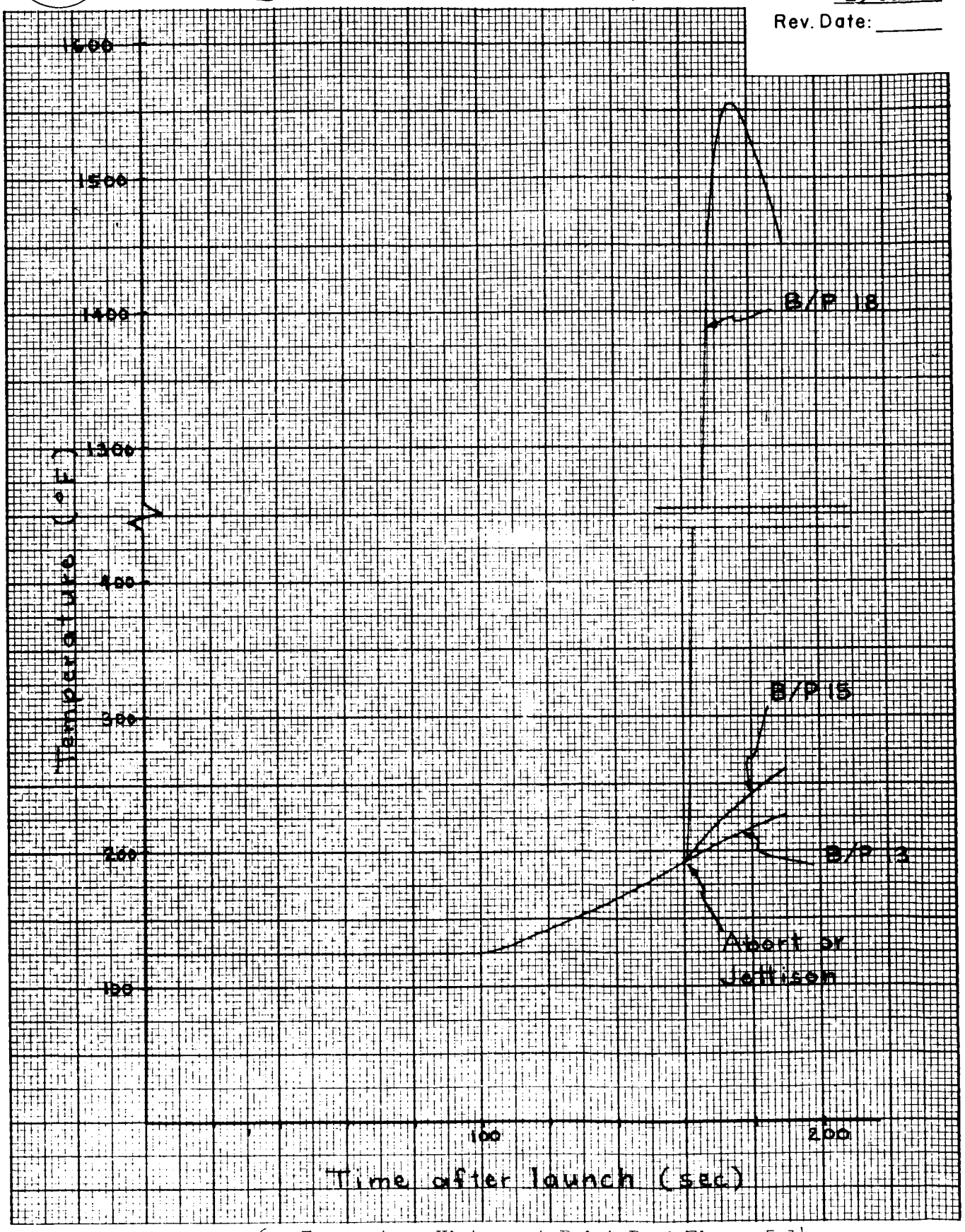

Figure 5-16. Temperature History at Point B of Figure 5-14

[redacted]

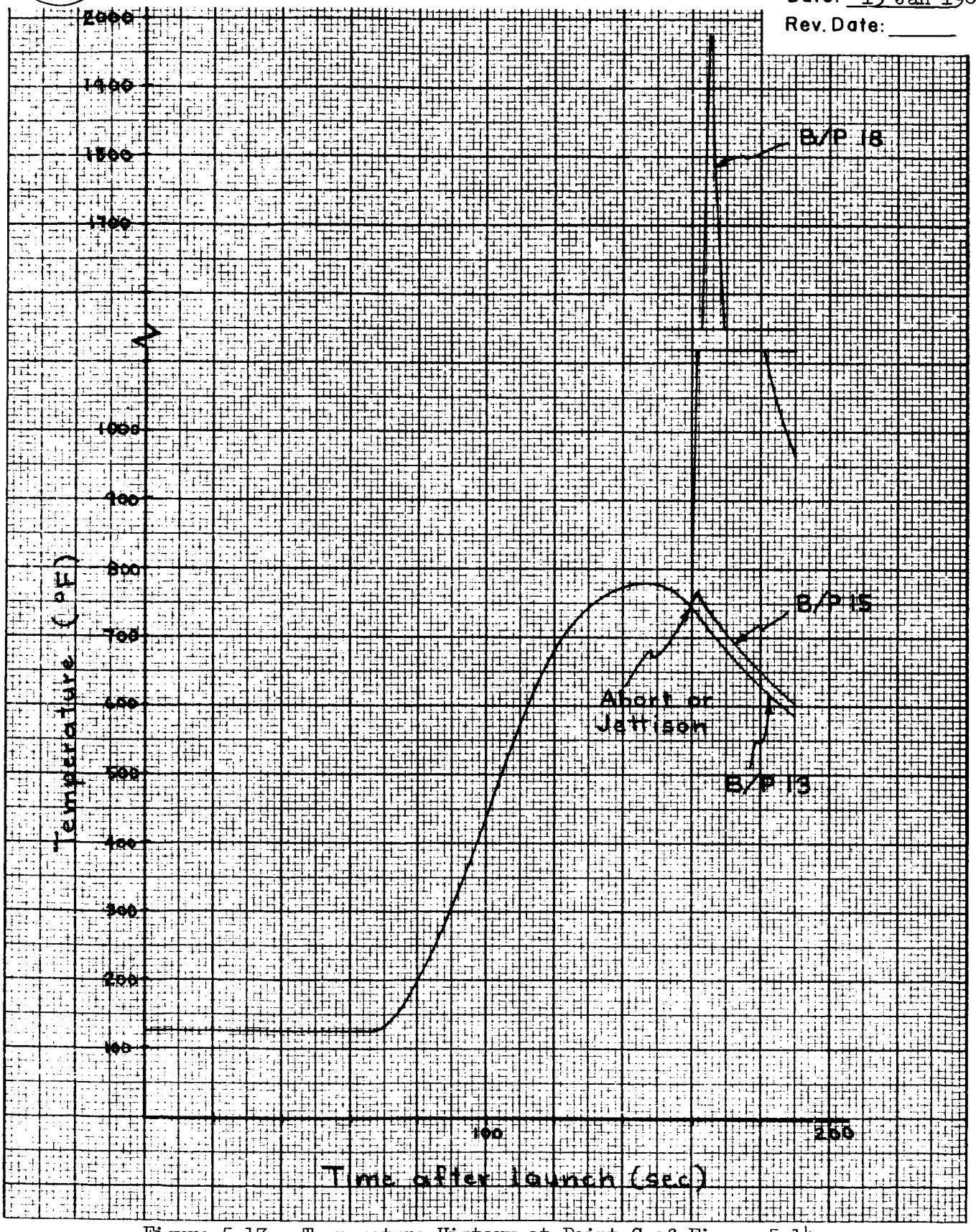

Figure 5-17. Temperature History at Point C of Figure 5-14

[redacted]

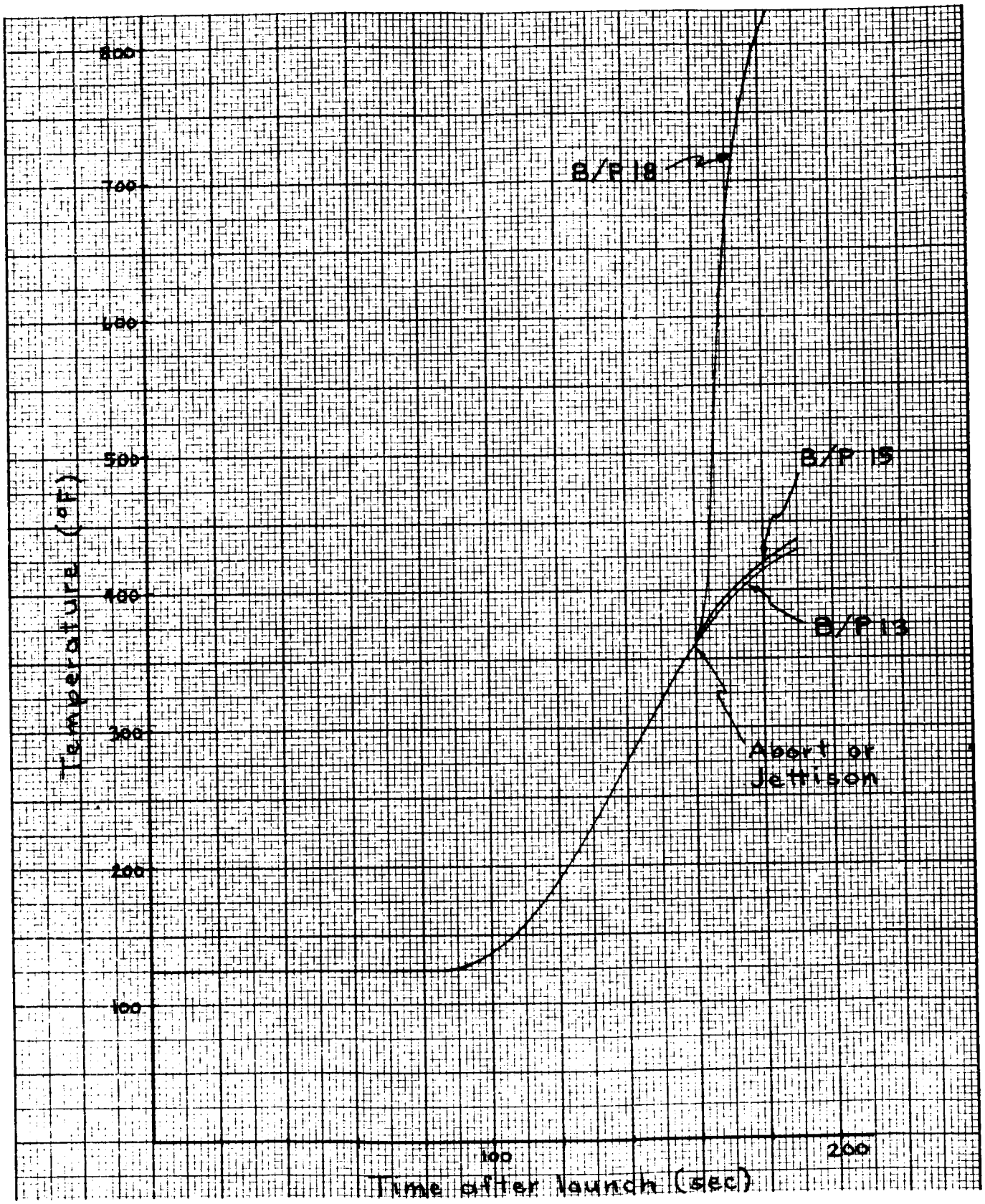

Figure 5-18. Temperature History at Point D of Figure 5-14

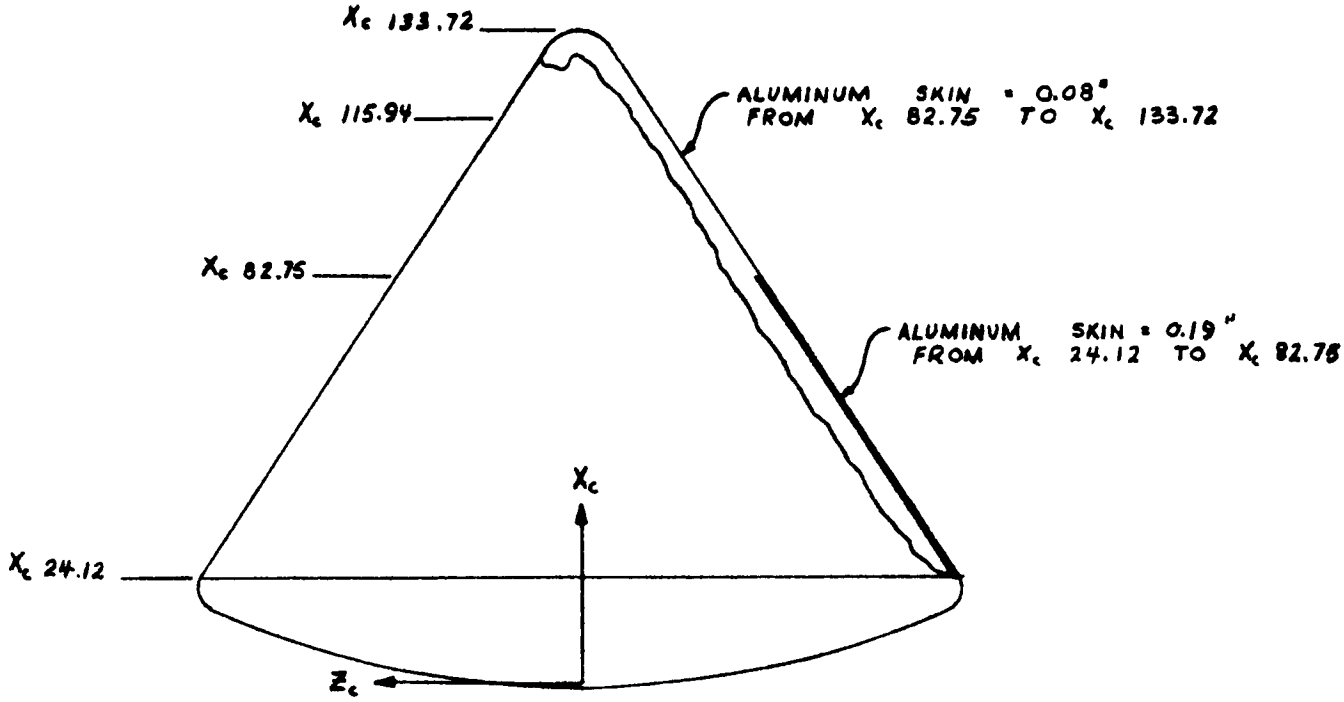

Figure 5-19. Diagram of the C/M Boilerplate, Showing X_c Locations

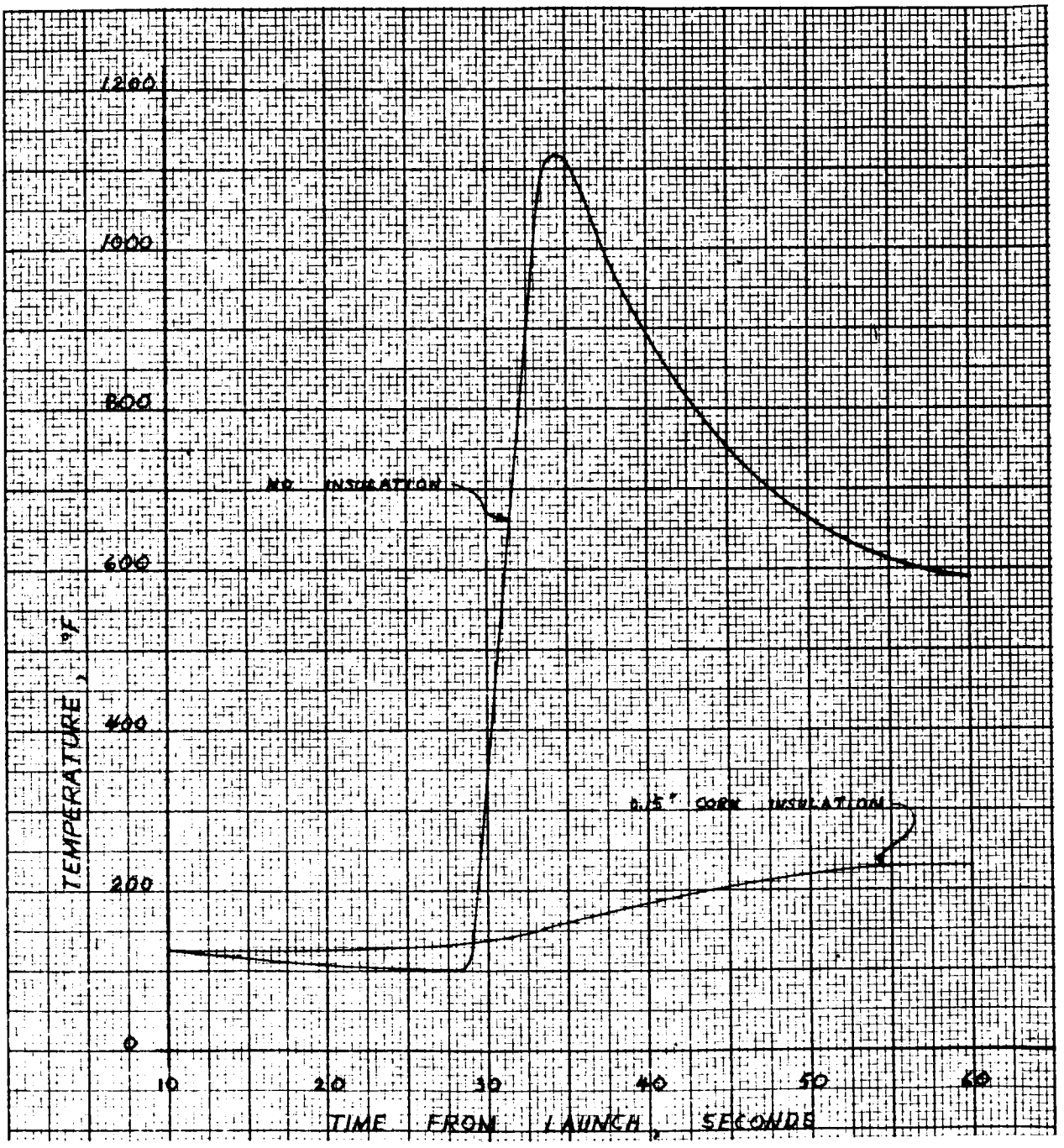

Figure 5-20. Temperature History of Aluminum, 0.08-Inch Skin (With and Without Thermal Protection), During Little Joe II Boost/Maximum-Q Abort

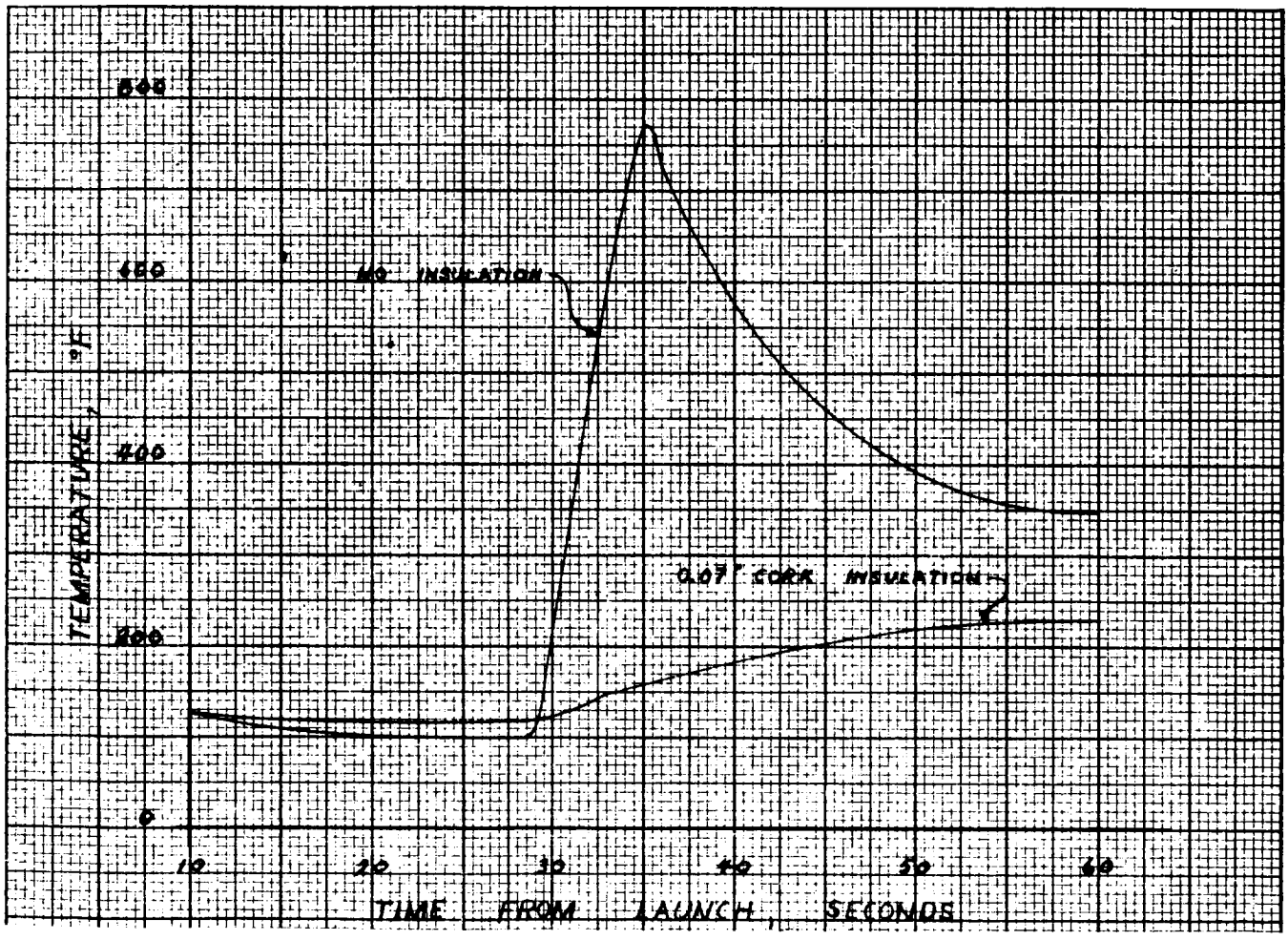

Figure 5-21. Temperature History of Aluminum, 0.19-Inch Skin (With and Without Thermal Protection), During Little Joe II Boost/Maximum-Q Abort

[redacted]

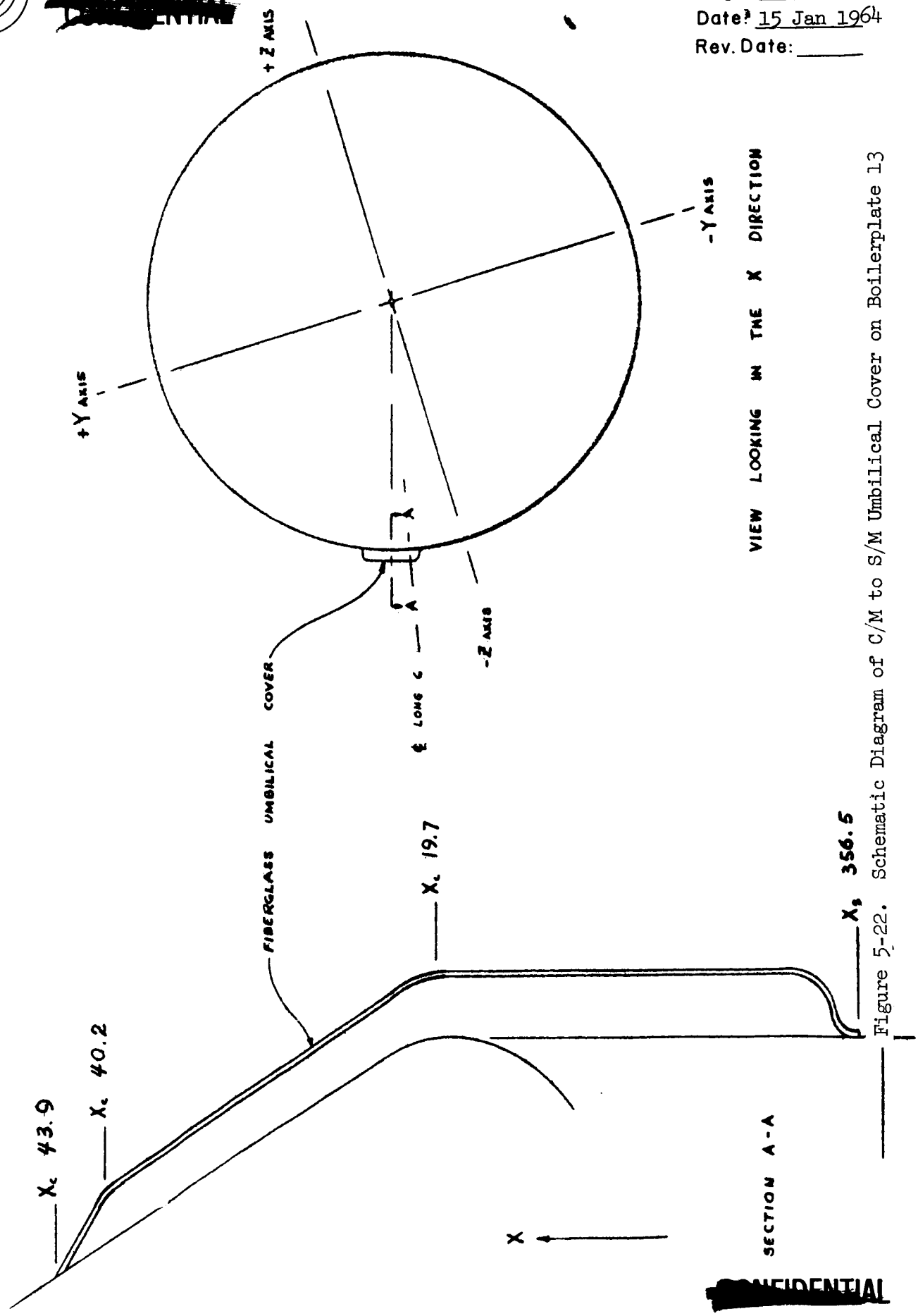

Figure 5-22. Schematic Diagram of C/M to S/M Umbilical Cover on Boilerplate 13

[redacted]

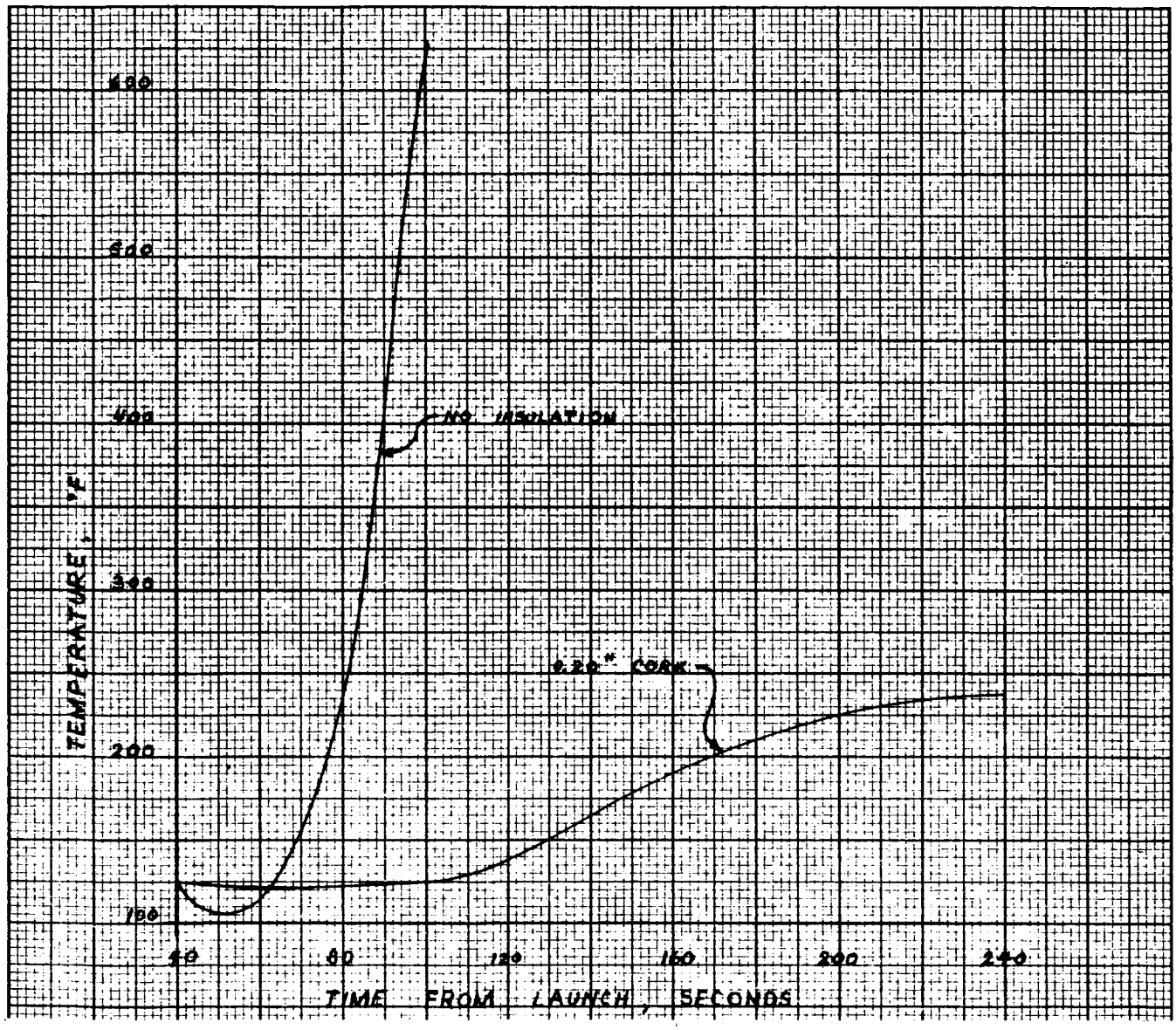

Figure 5-23. Temperature History of the Umbilical Cover, From $X_c = 43.9$ to $X_c = 40.2$

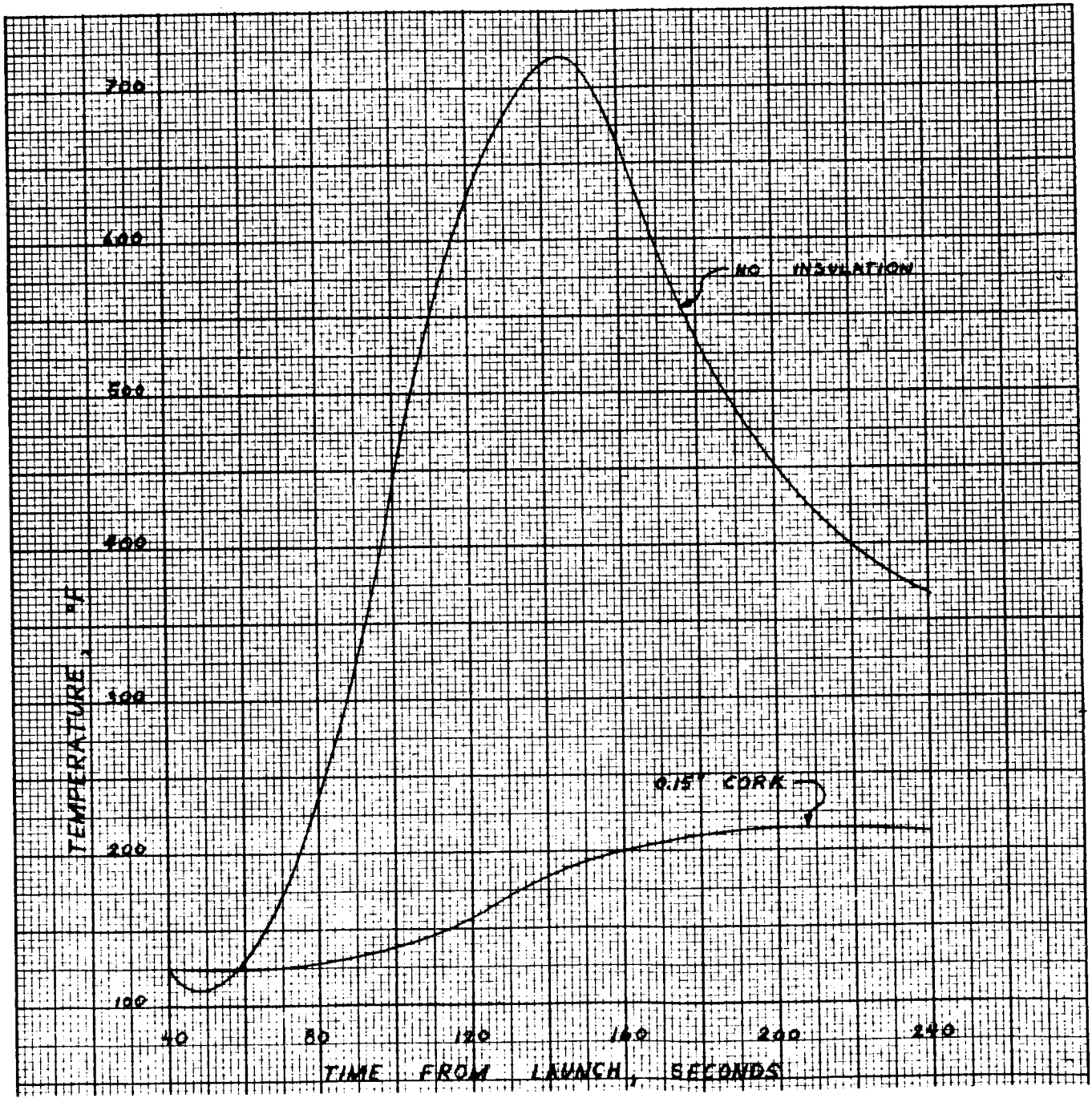

Figure 5-24. Temperature History of the Umbilical Cover, From X_c = 40.2 to X_c = 356.5

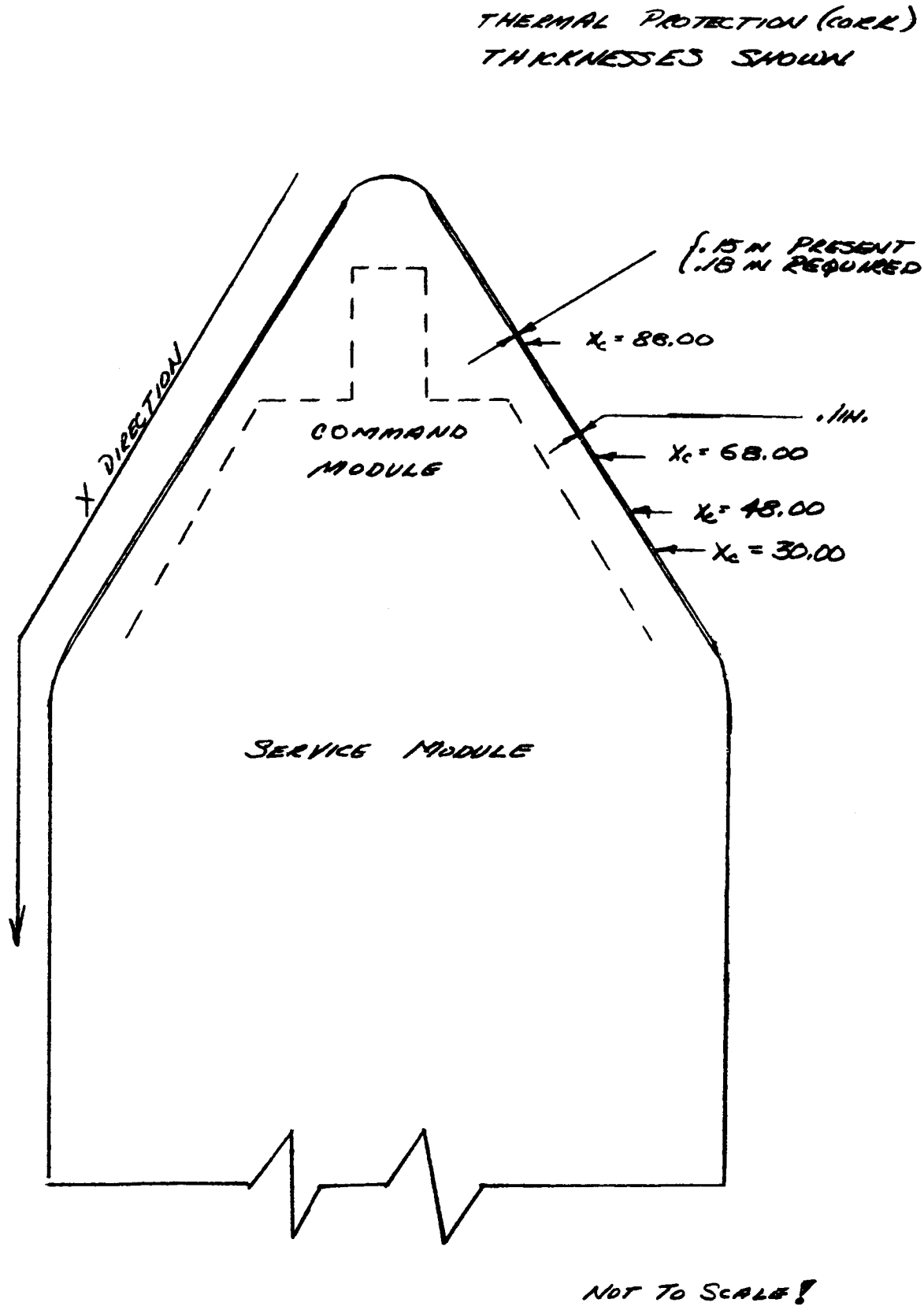

Figure 5-25. Locations for Thermal Analysis on Boilerplate 15

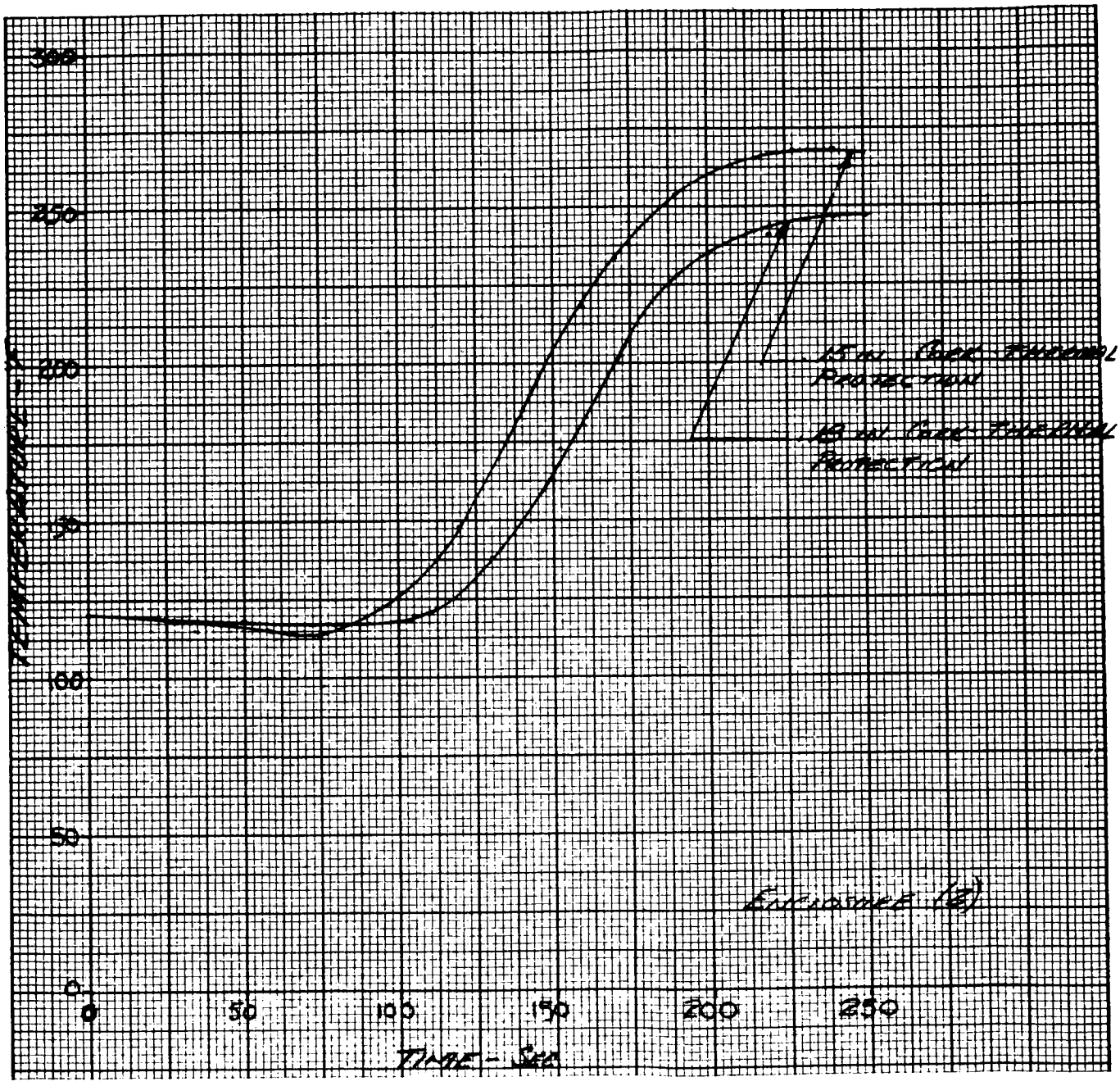

Figure 5-26. Temperature Histories of Bond Lines at X_c = 88.00

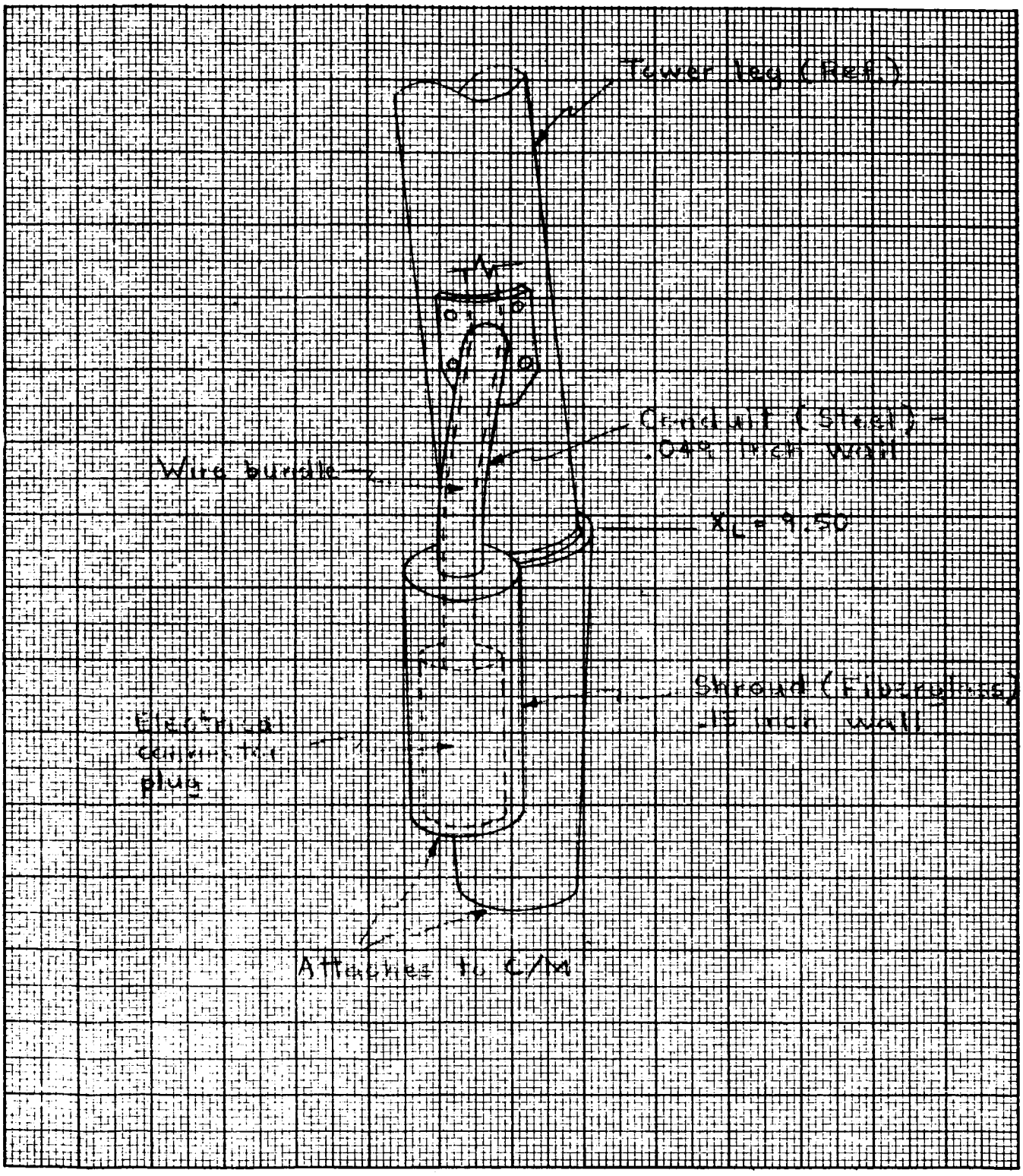

Figure 5-27. Schematic of the LES Tower-to-C/M Umbilical Electrical Installation, Showing the Locations of the Wire Conduit and Connector Shroud

[redacted]

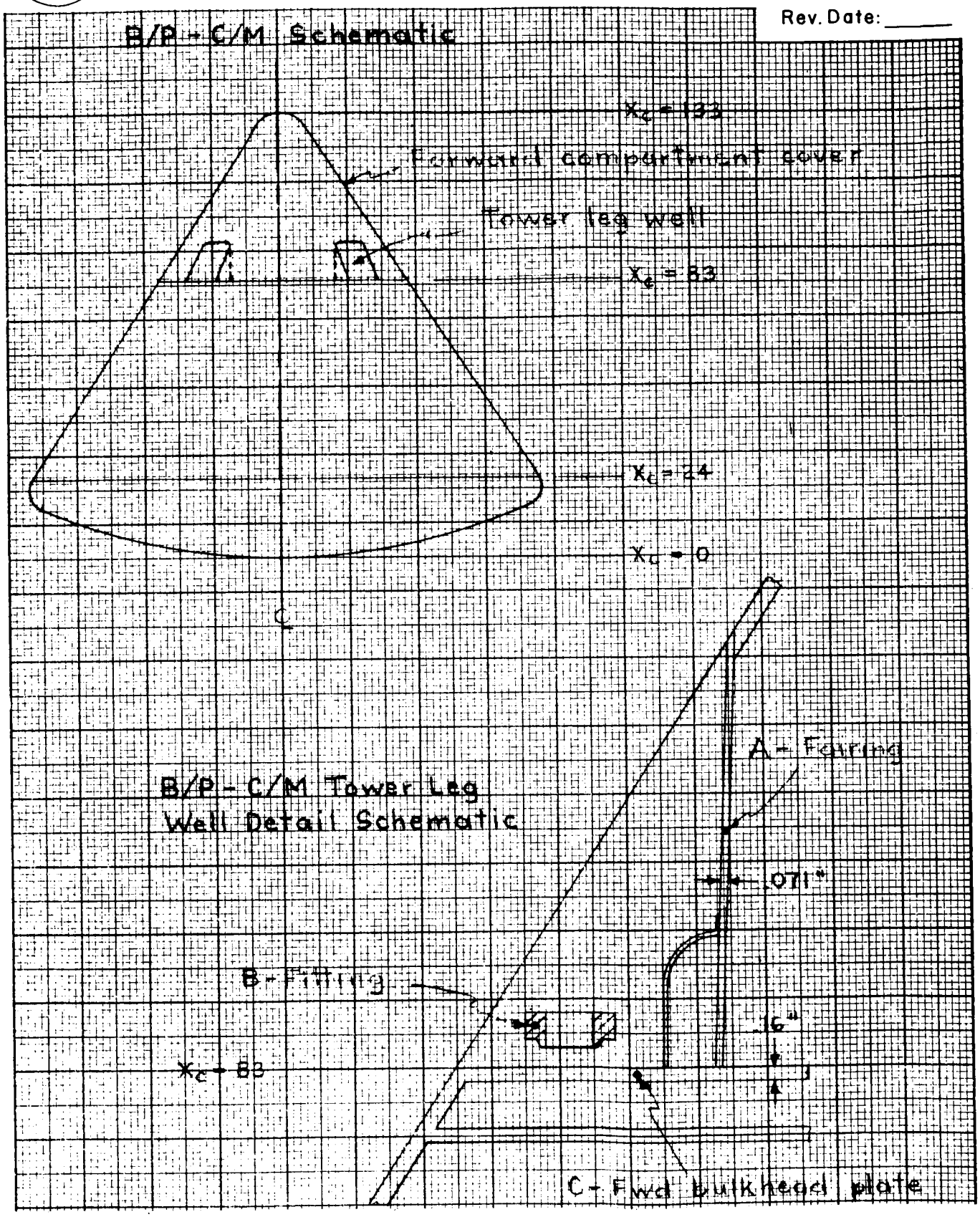

Figure 5-28. Locations of Data Points on the C/M Tower Leg Well

[redacted]

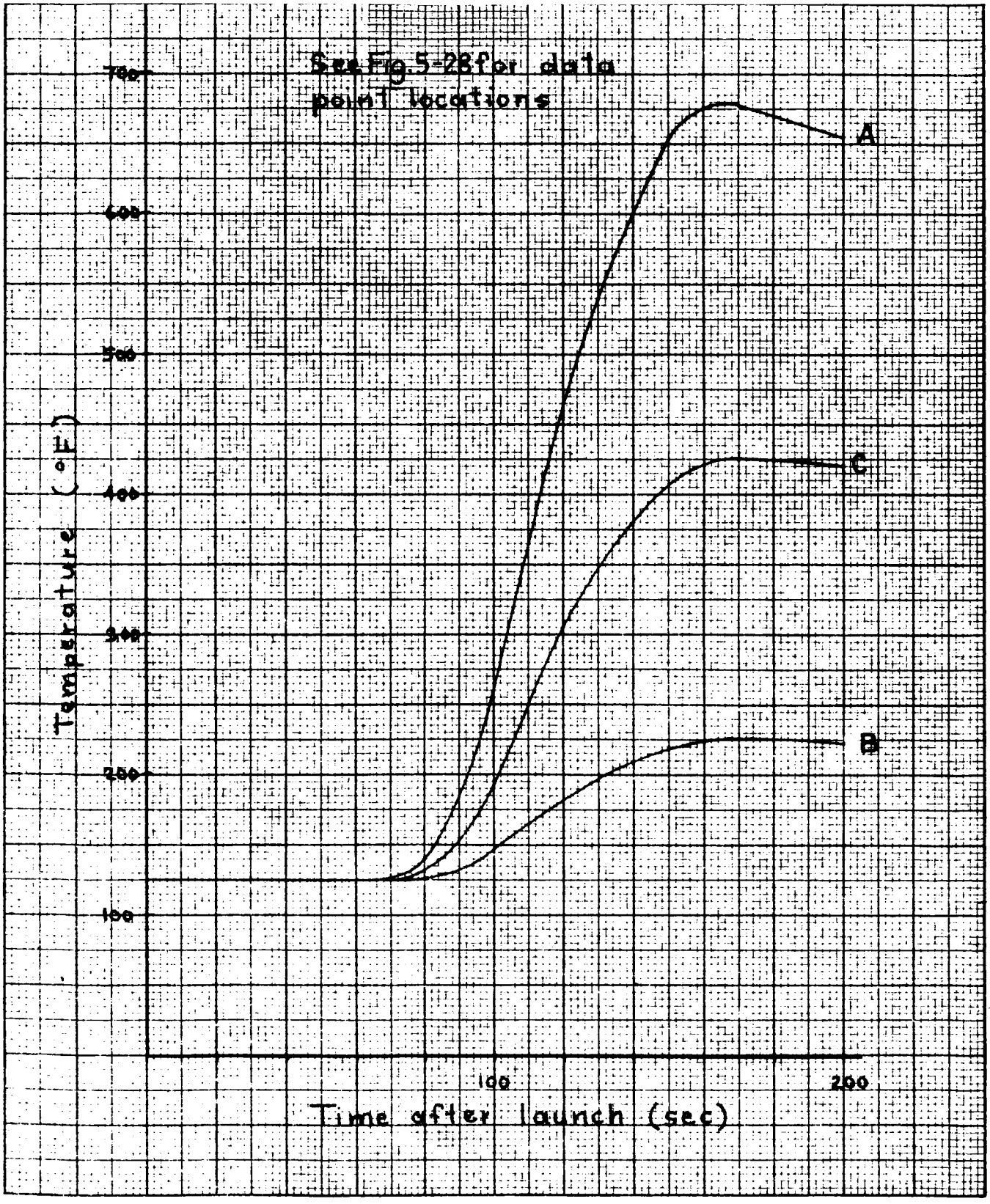

Figure 5-29. Temperature History of the C/M Tower Leg Well For Boilerplates 13, 16 and 26 (No Insulation)

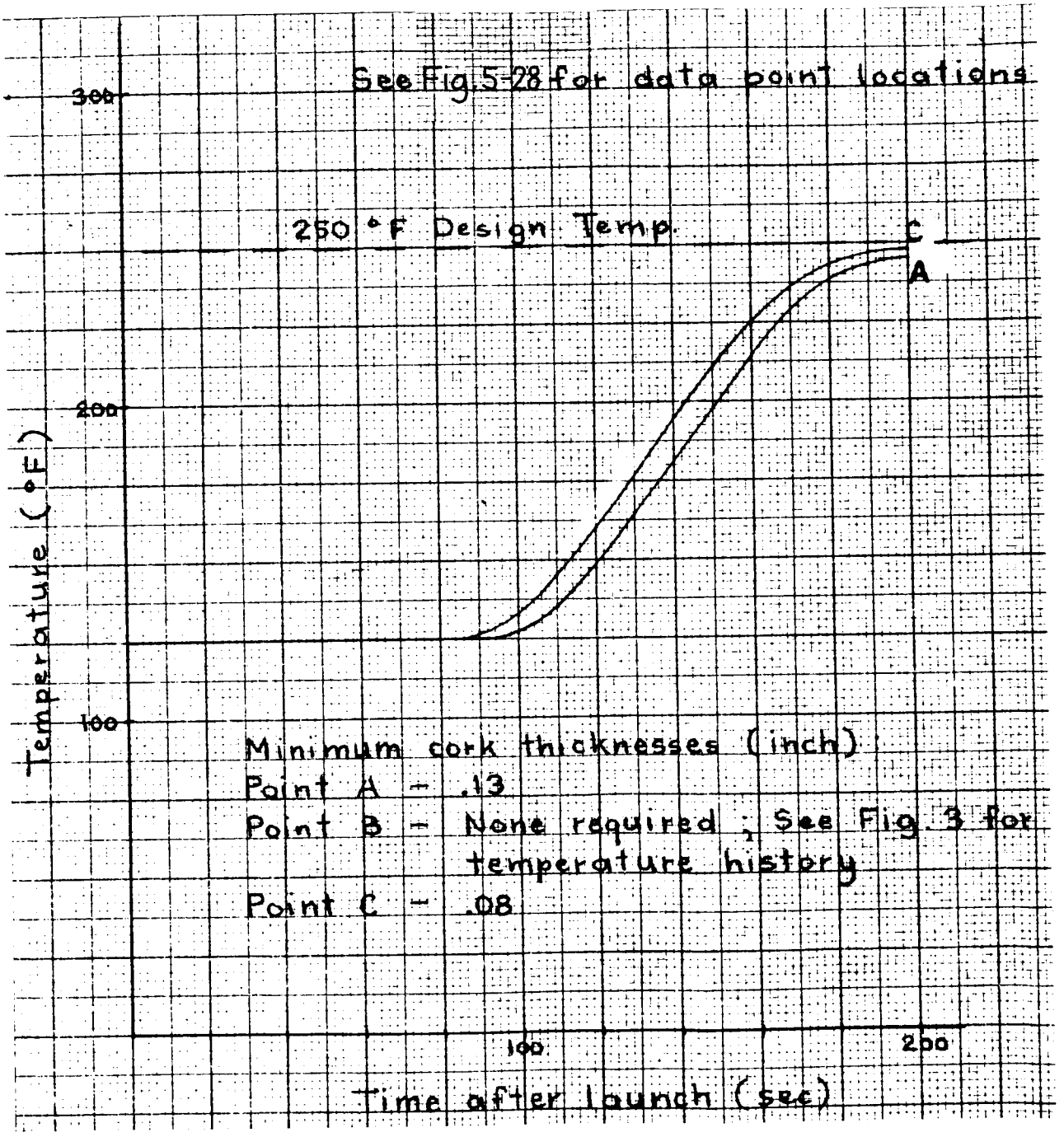

Figure 5-30. Temperature History of the C/M Tower Leg Well For Boilerplates 13, 16 and 26 (Minimum Insulation)

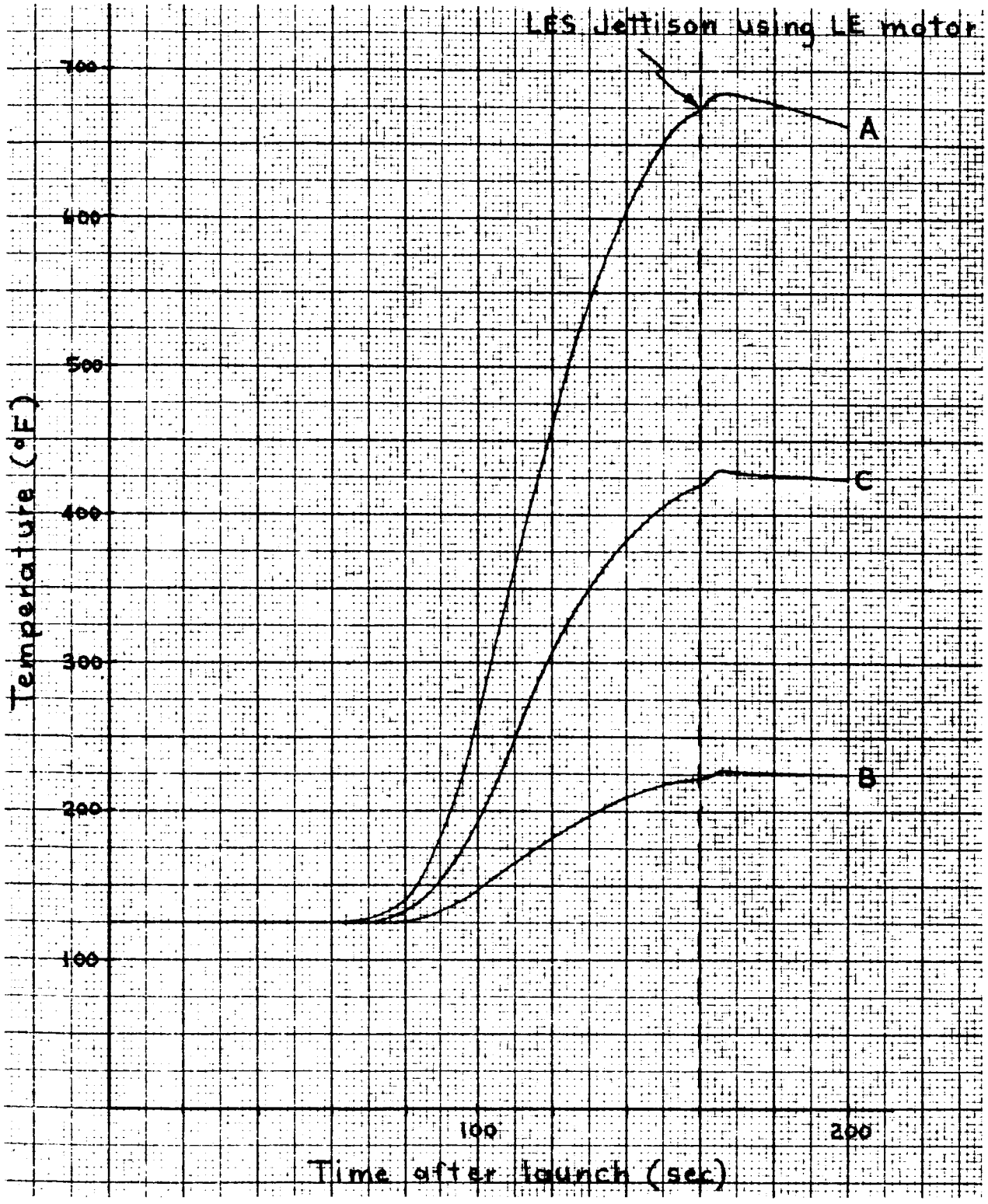

Figure 5-31. Temperature History of the C/M Tower Leg Well For Boilerplate 15 (No Insulation)

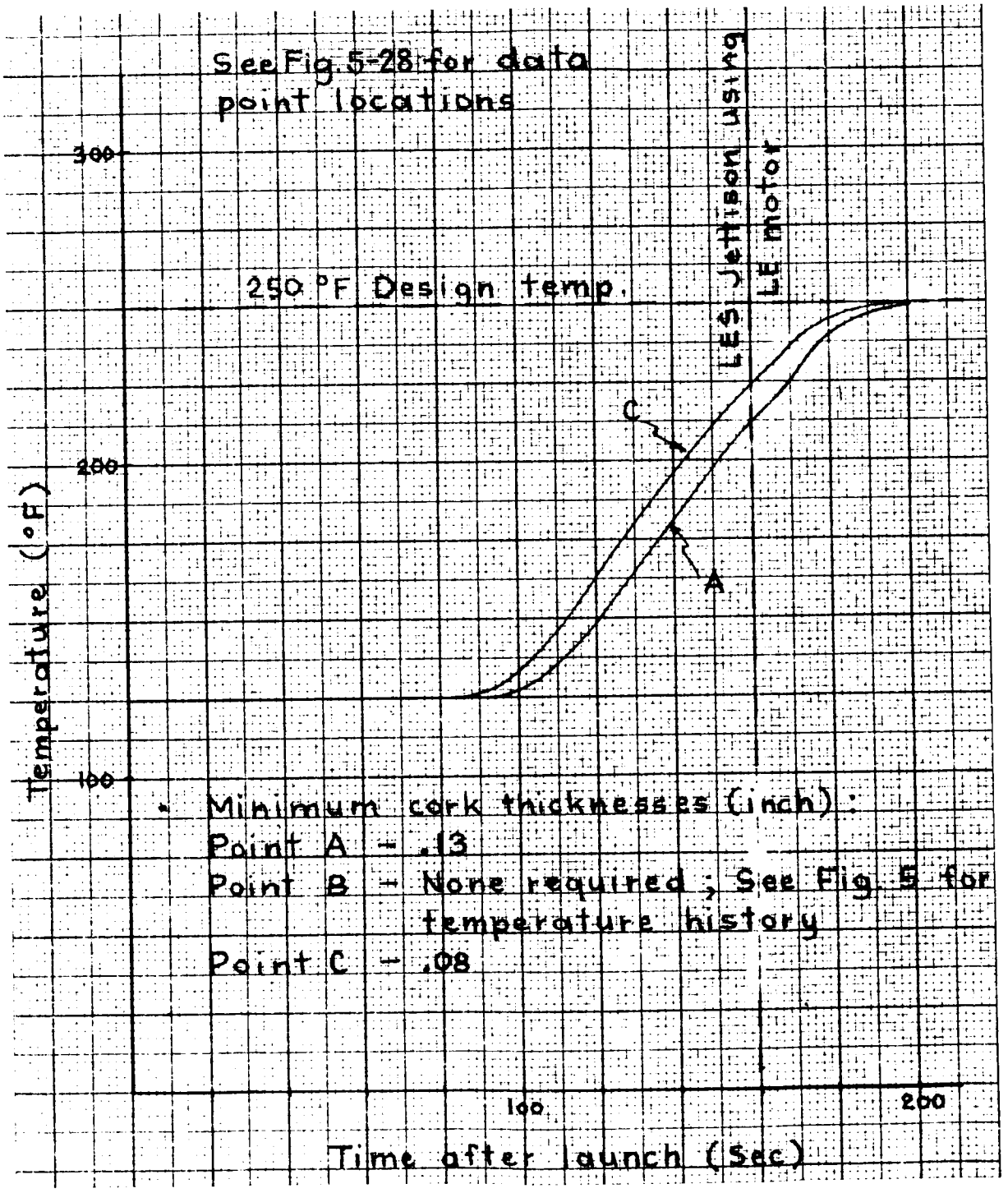

Figure 5-32. Temperature History of the C/M Tower Leg Well For Boilerplate 15 (Minimum Insulation)

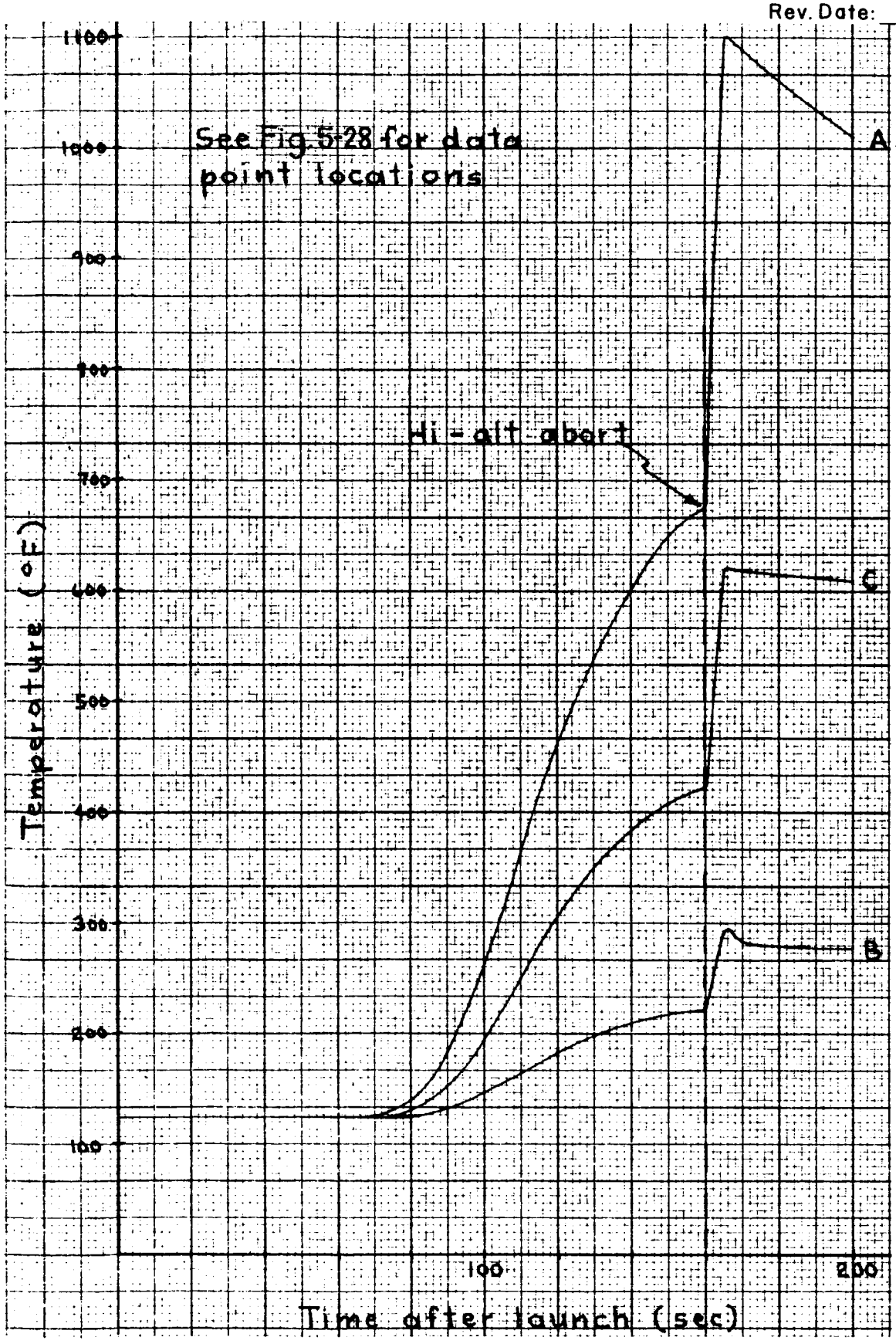

Figure 5-33. Temperature History of the C/M Tower Leg Well For Boilerplate 18 (No Insulation)

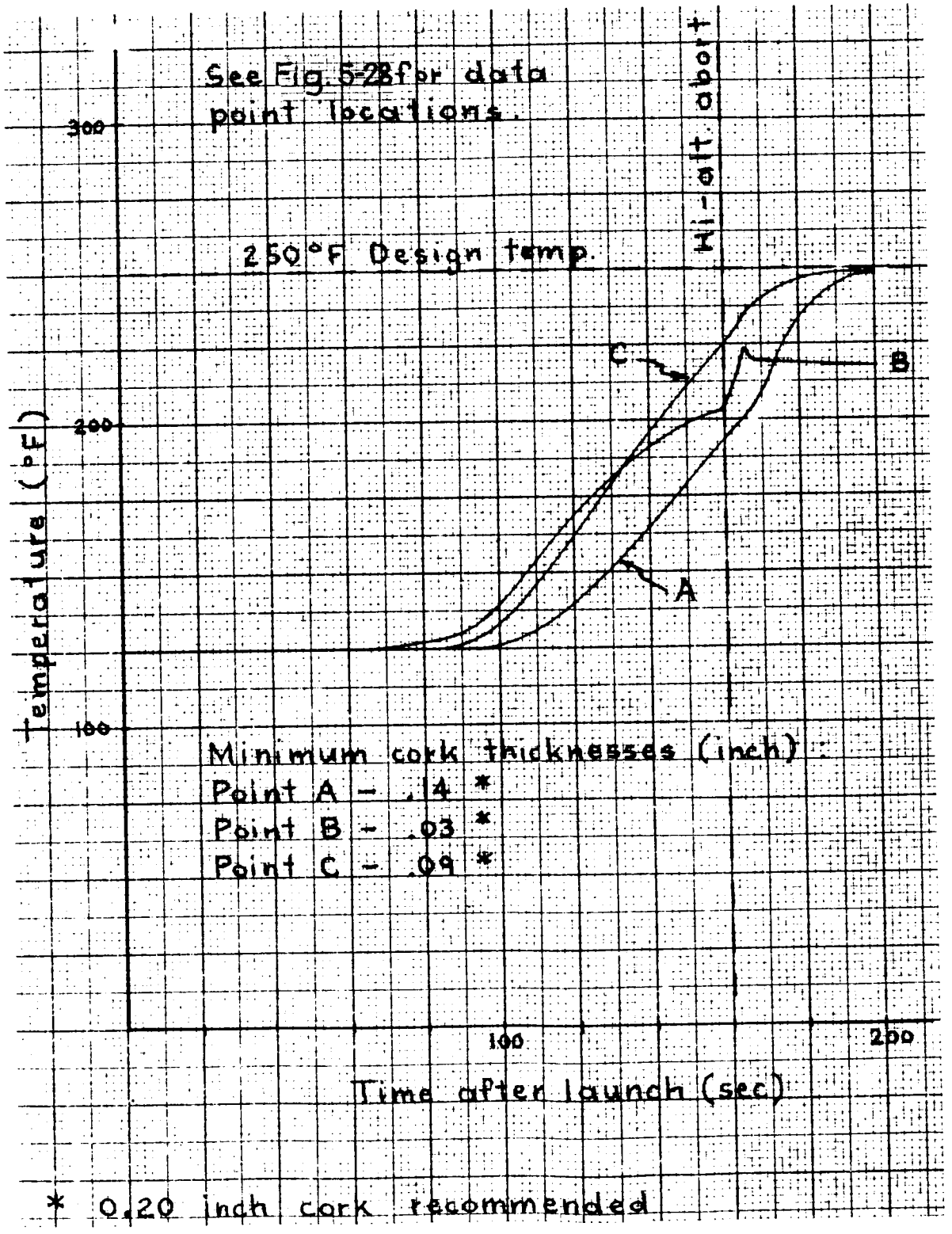

Figure 5-34. Temperature History of the C/M Tower Leg Well For Boilerplate 18 (Minimum Insulation)

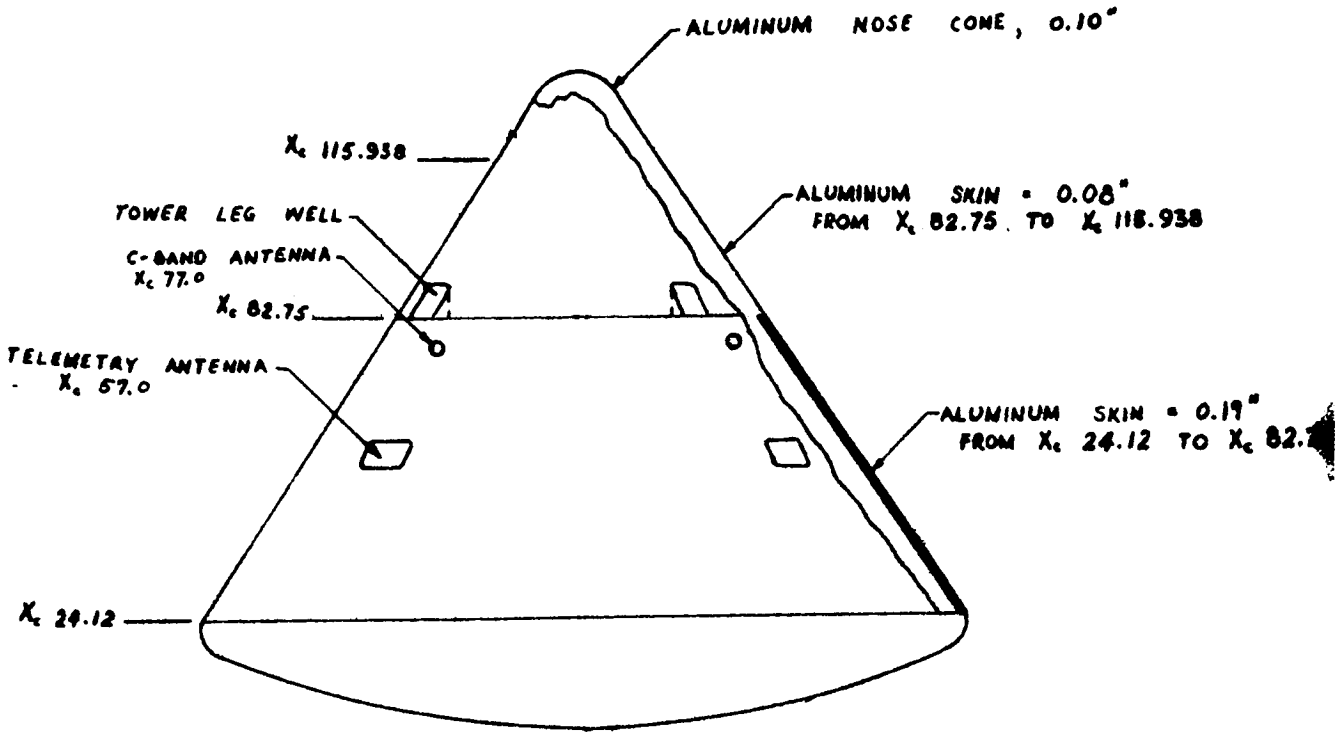

Figure 5-35. Diagram of the C/M Boilerplate

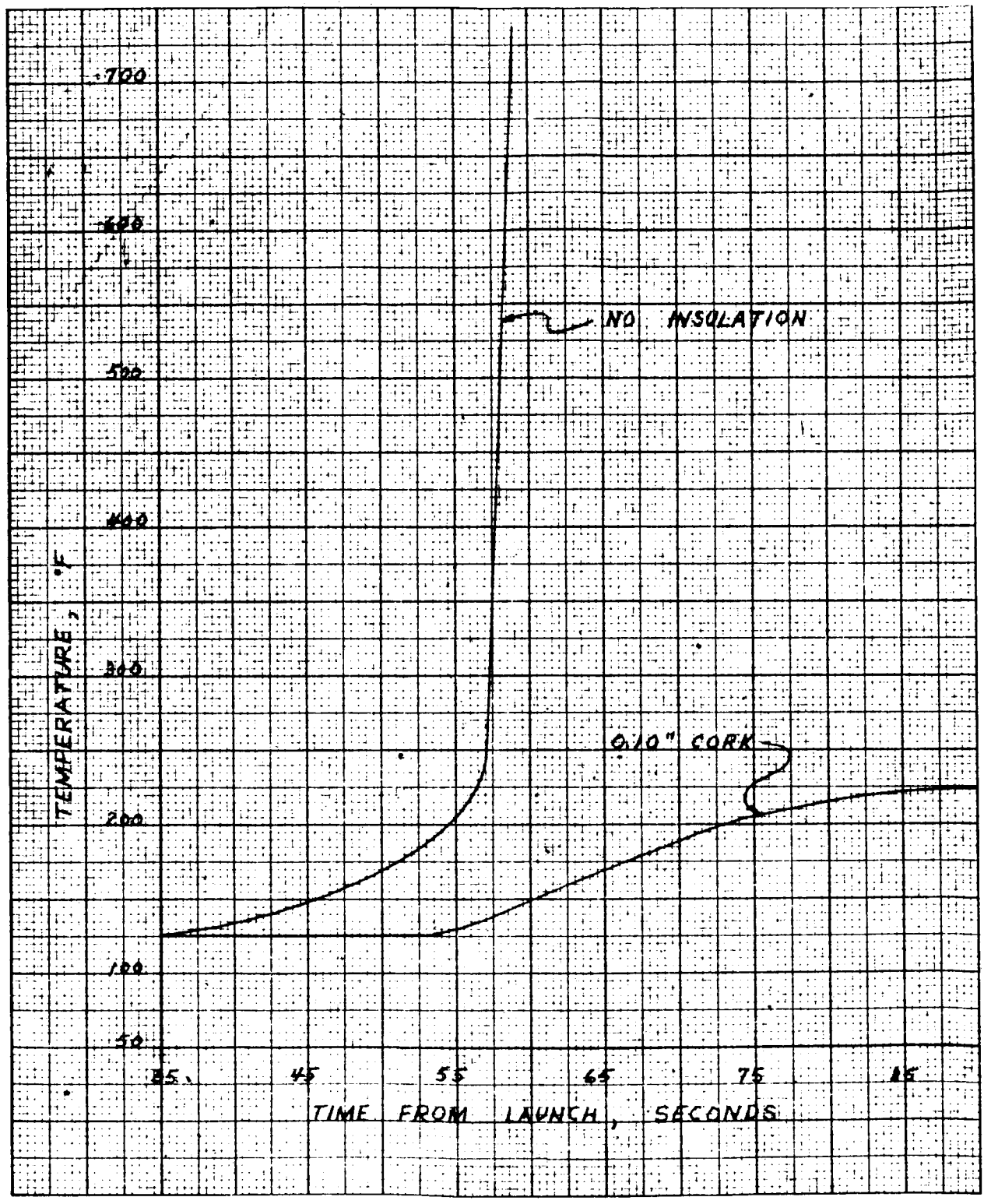

Figure 5-36. Temperature History of Aluminum Skin - With and Without Thermal Protection - (X_c=115.938) During Little Joe II Boost/60,000-ft Abort

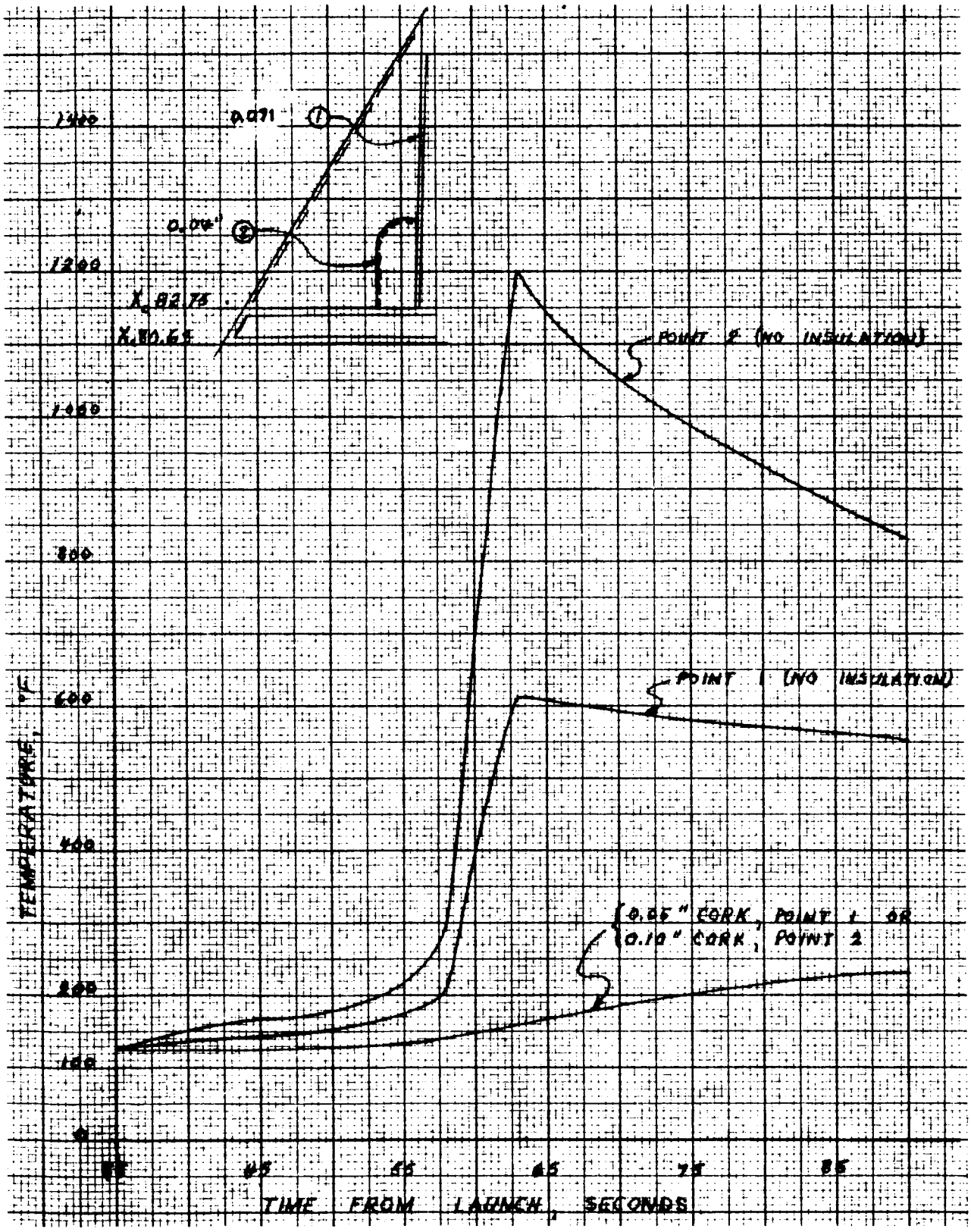

Figure 5-37. Temperature History of Tower Leg Well - With and Without Insulation - During Little Joe II Boost/60,000-ft Abort

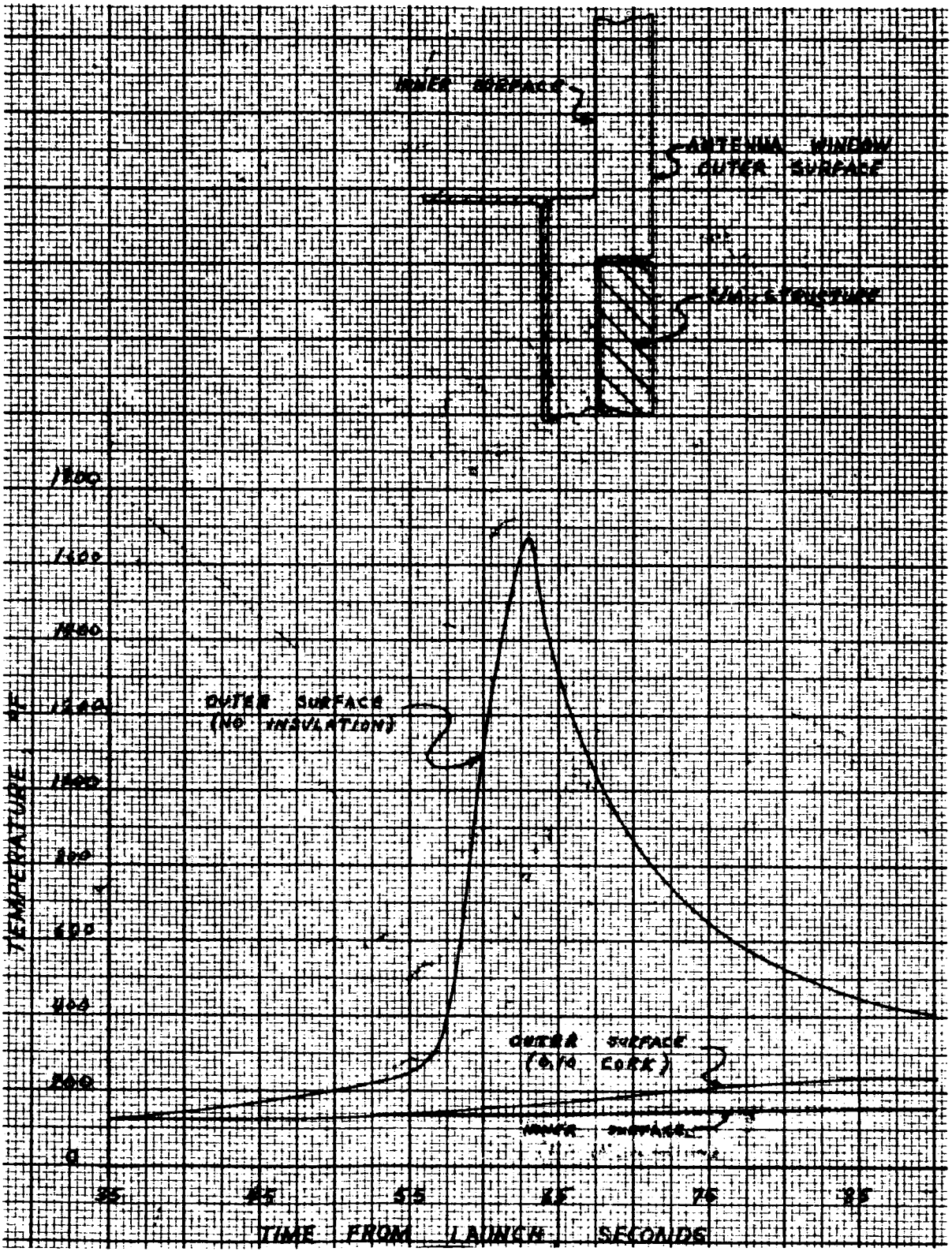

Figure 5-38. Temperature History of the Telemetry Antenna Window Surfaces - With and Without Insulation - During Little Joe II Boost/60,000-ft Abort

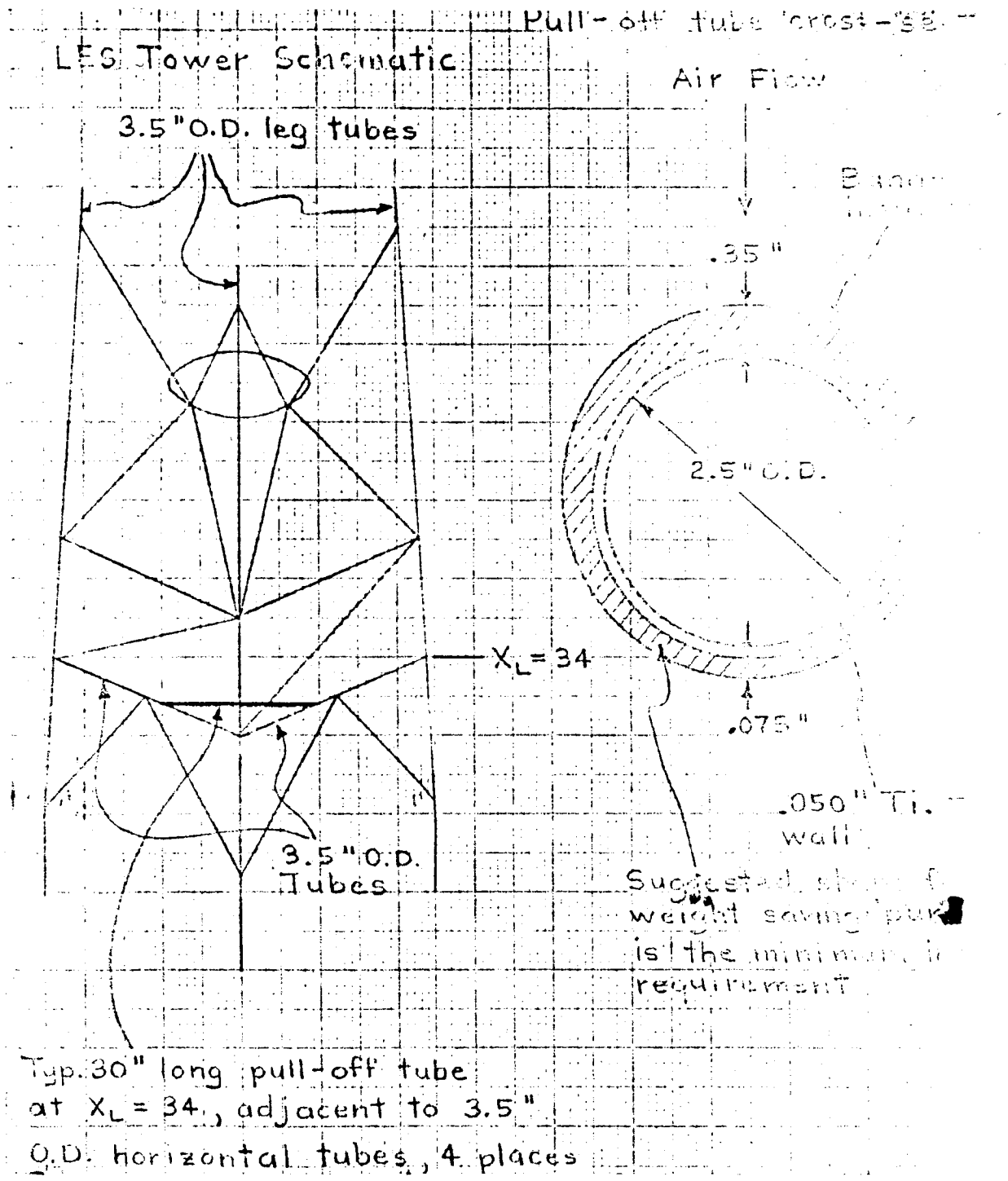

Figure 5-39. Schematic of the LES Tower (Showing the Location of the Forward Heat Shield Pull-Off Tubes) and a Tubular Cross-Section (Showing the Insulation Requirement for These Tubes)

[redacted]

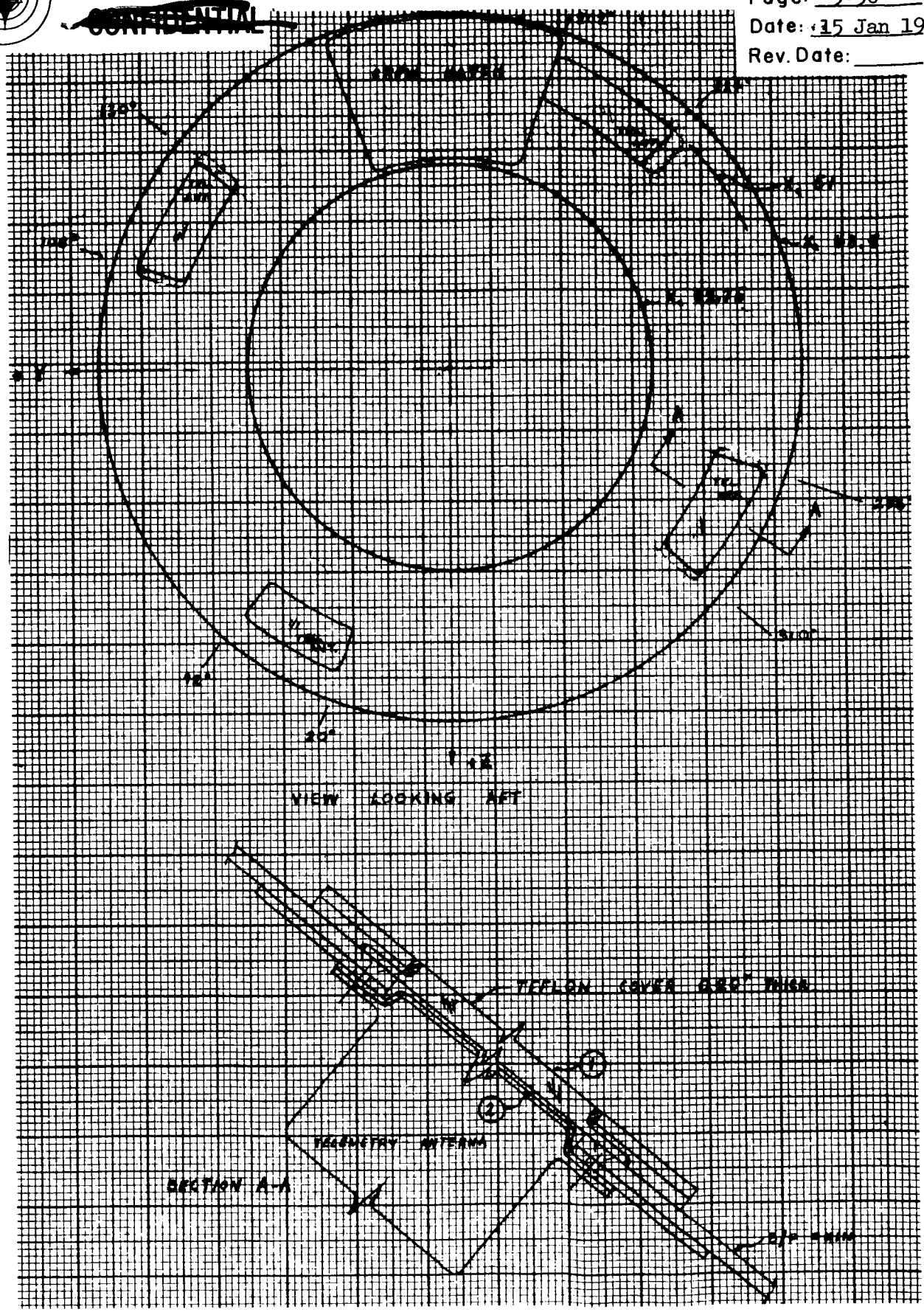

Figure 5-40. Approximate Location of Telemetry Antennas for Boilerplate 22

[redacted]

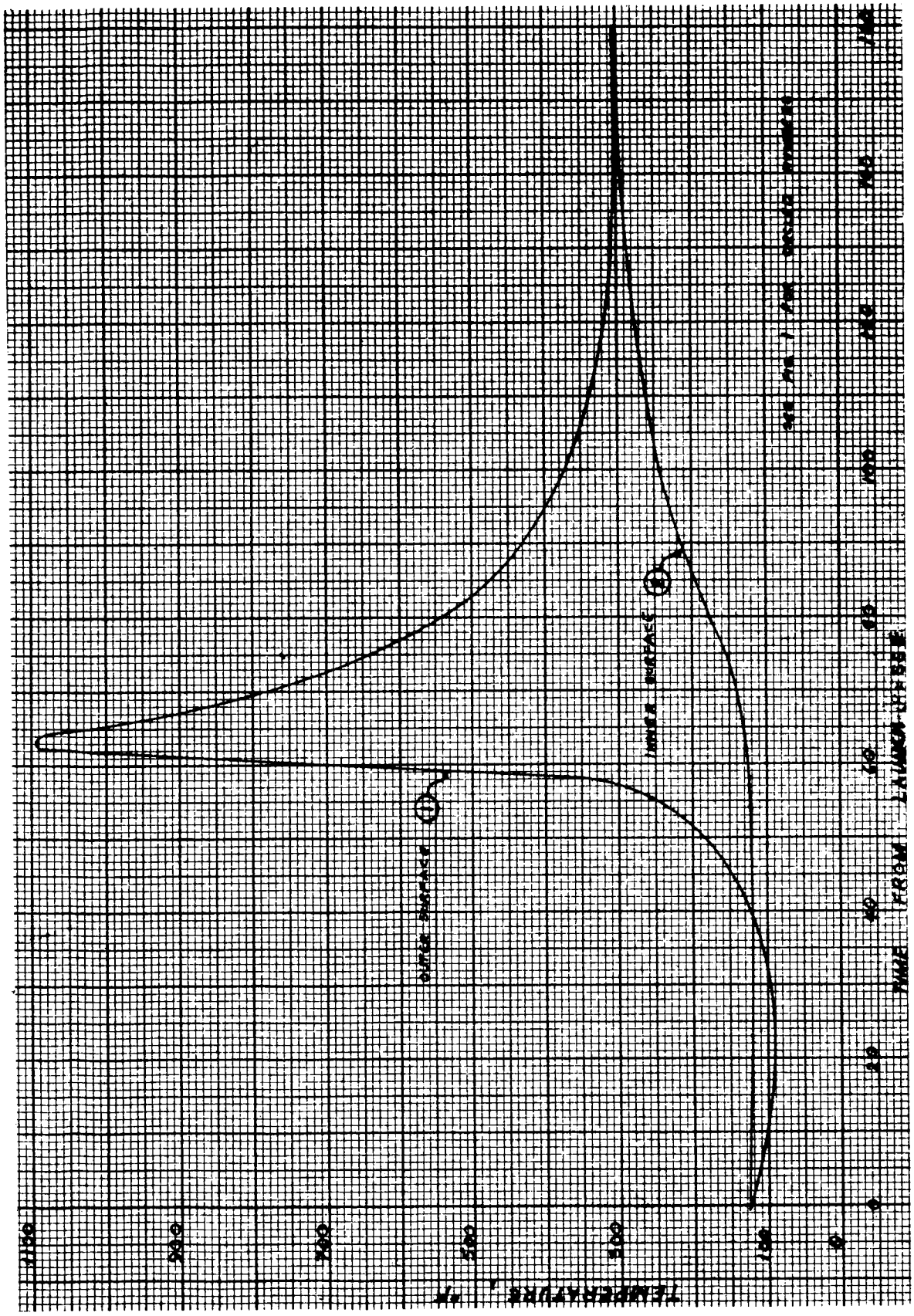

Figure 5-41. Temperature Histories of Teflon Cover of Telemetry Antenna for Boilerplate 22 (Little Joe II Boost/60,000-ft Abort)

[redacted]

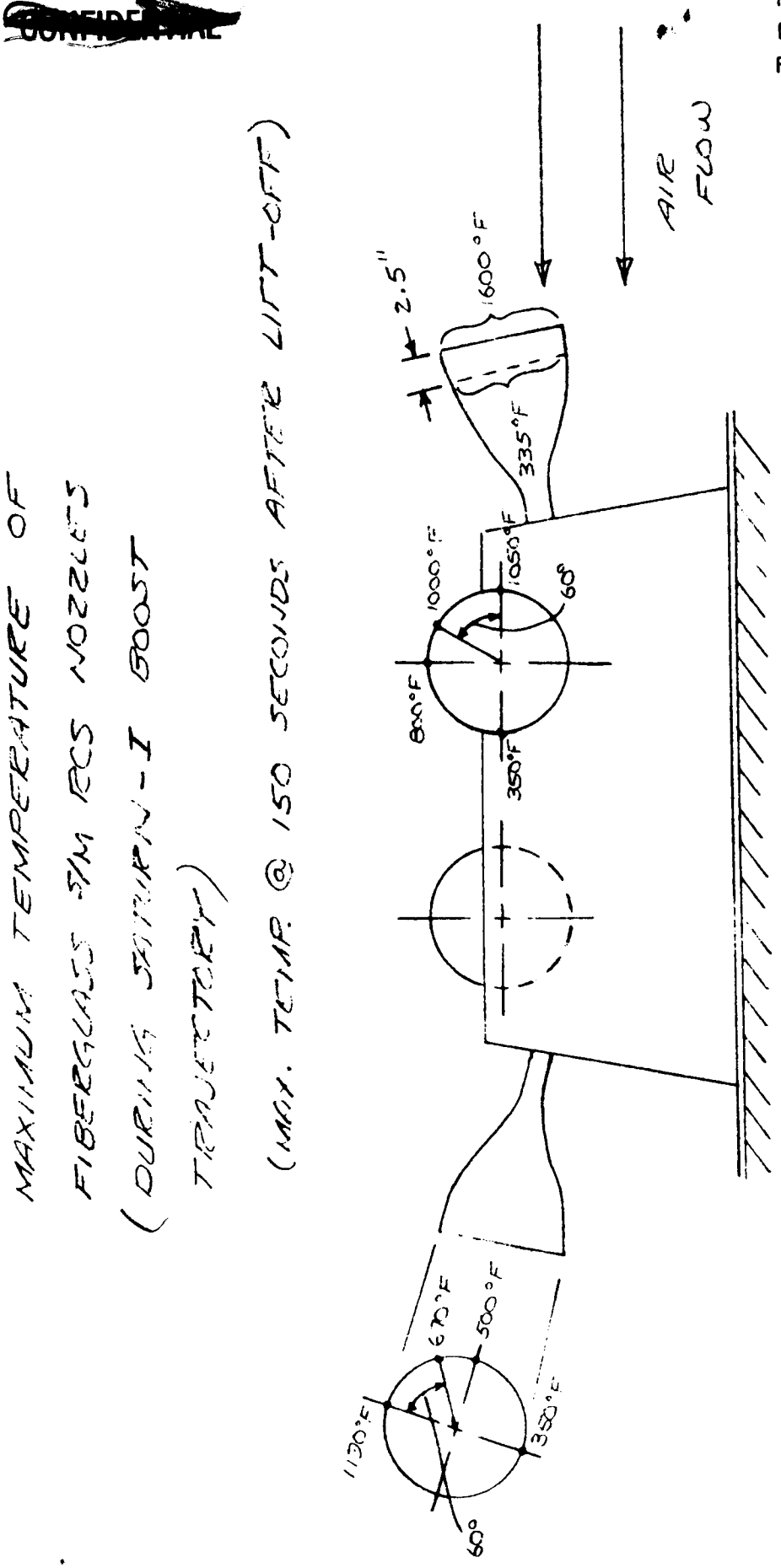

Figure 5-42. Maximum Temperature of Fiberglass S/M RCS Nozzles (During Saturn-I Boost Trajectory)

[redacted]

[redacted]

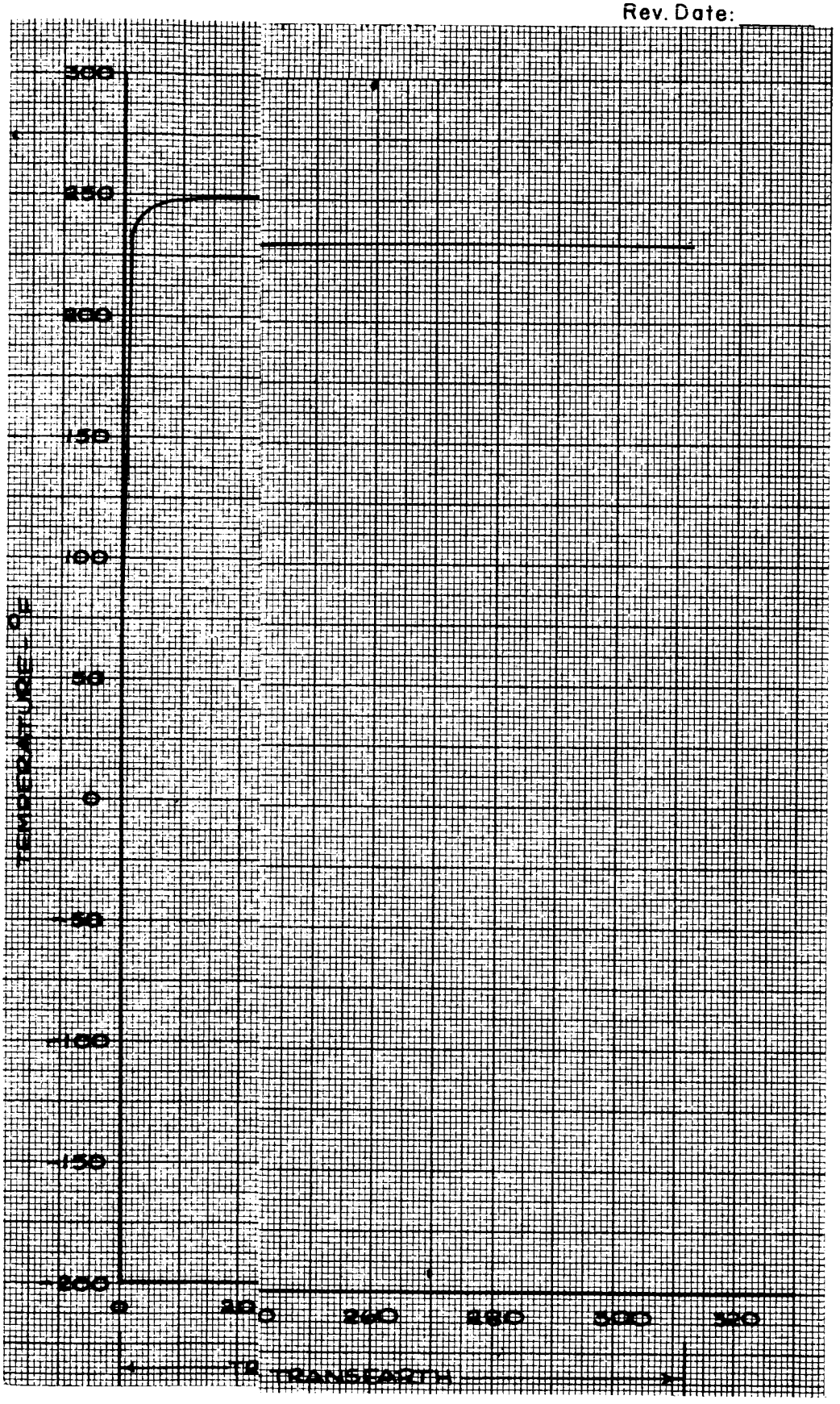

ture History, Lunar Mission

[redacted]

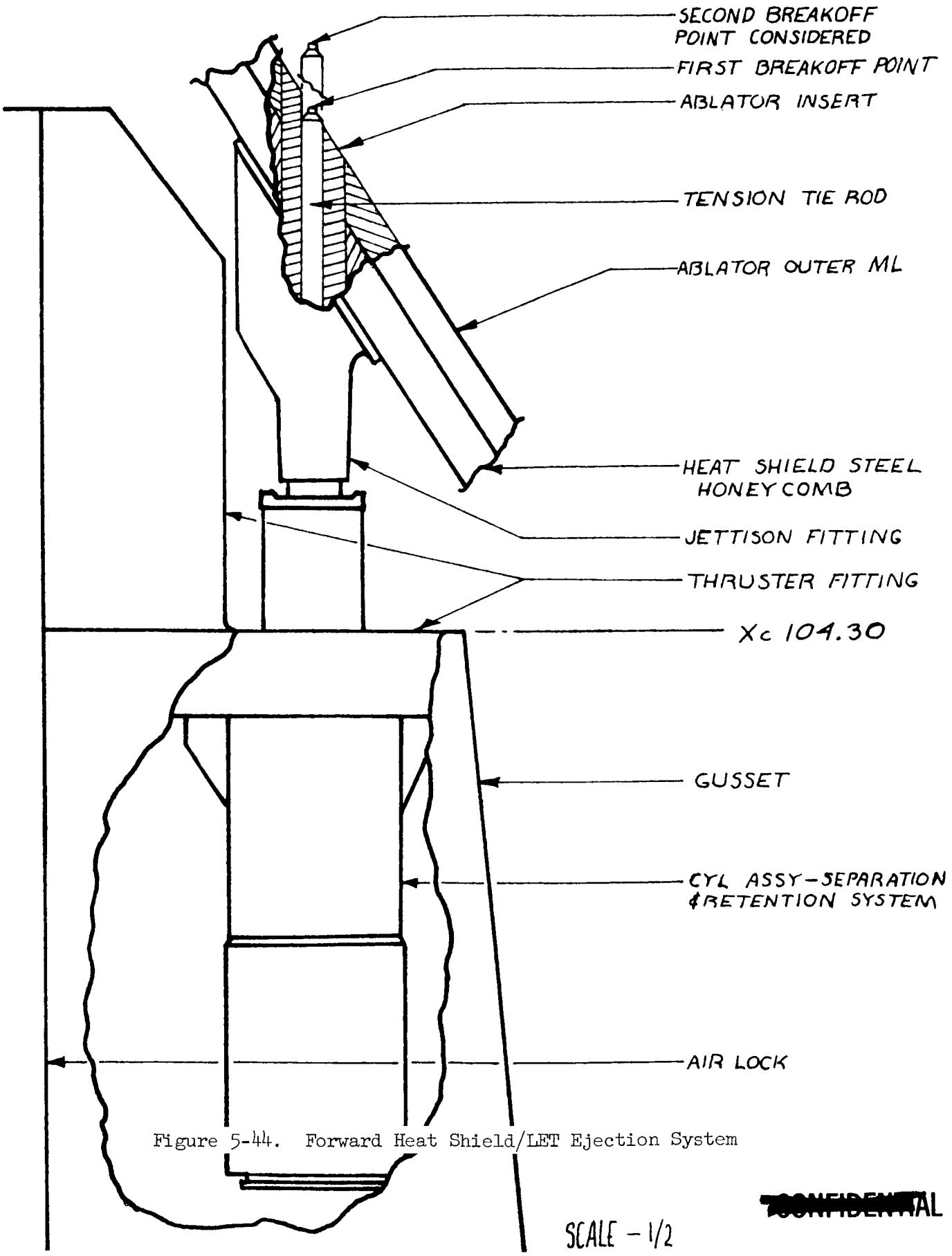

Figure 5-44. Forward Heat Shield/LET Ejection System

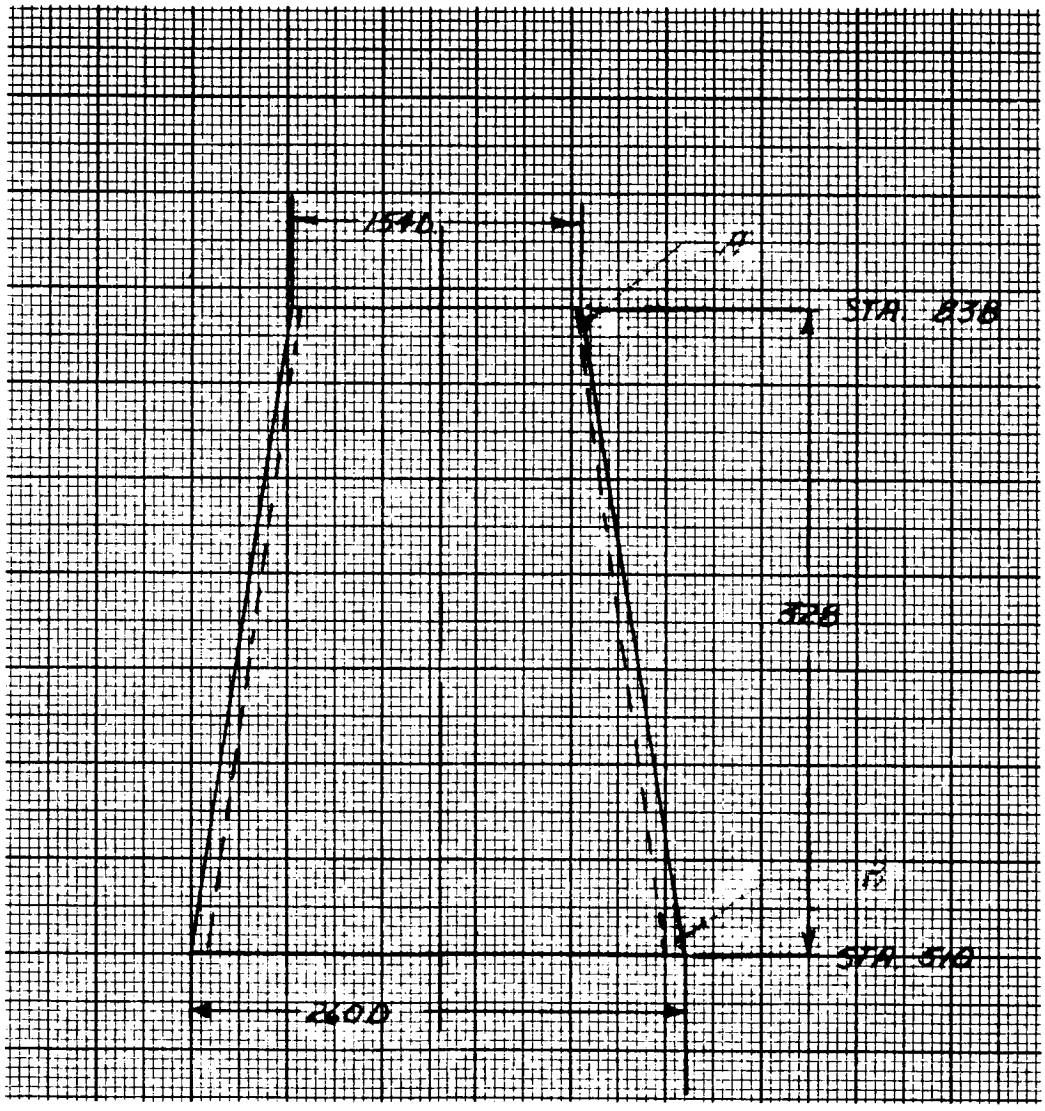

Figure 5-45. Schematic Diagram of the LEM Adapter

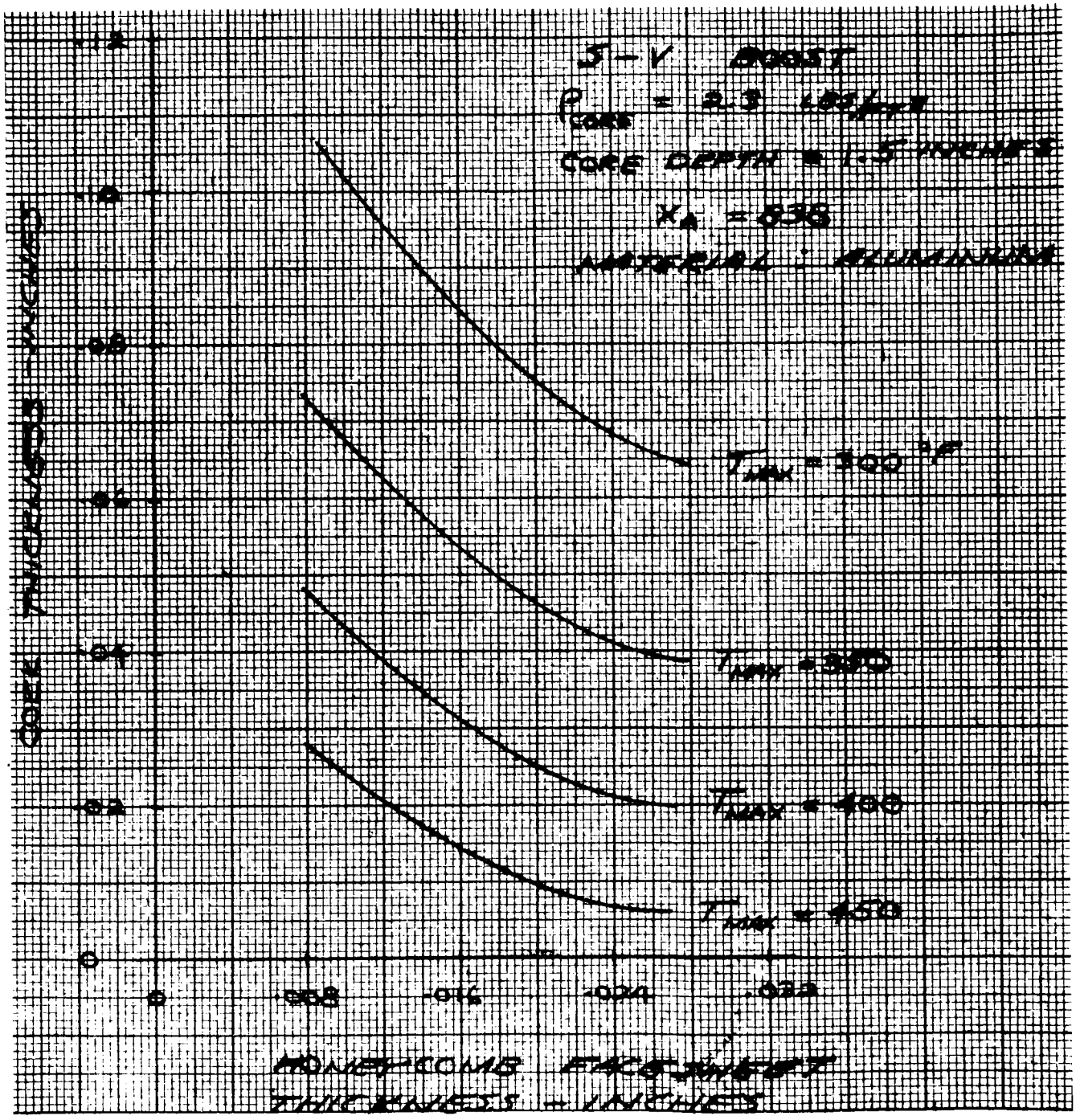

Figure 5-46. Maximum Temperature of LEM Adapter: Honeycomb Surface Facesheet Versus Insulation (Cork) Thickness & Facesheet Thickness (X_a = 838)

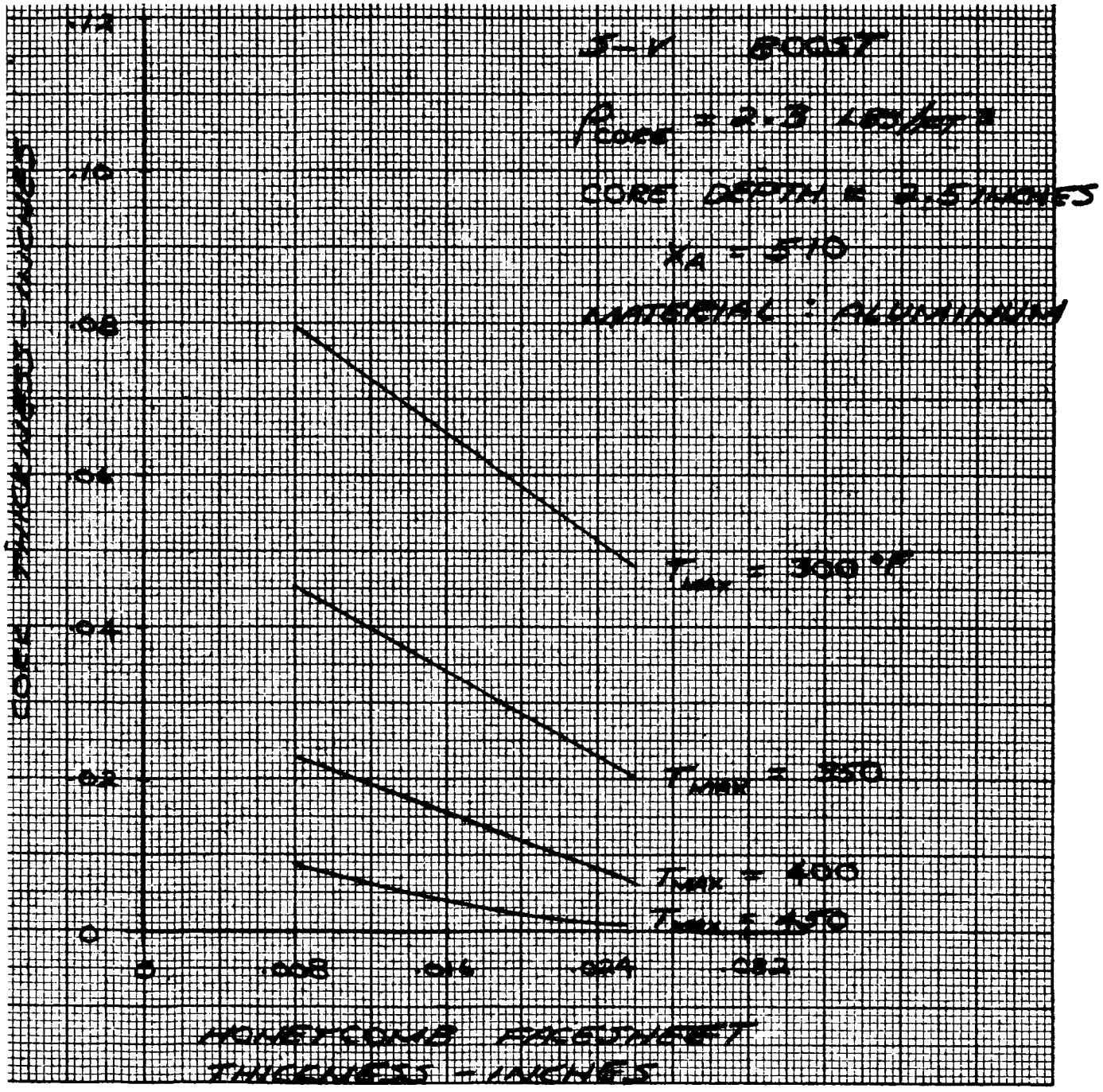

Figure 5-47. Maximum Temperature of LEM Adapter: Honeycomb Surface Facesheet Versus Insulation (Cork) Thickness & Facesheet Thickness (X_a = 510)

~~CONFIDENTIAL~~

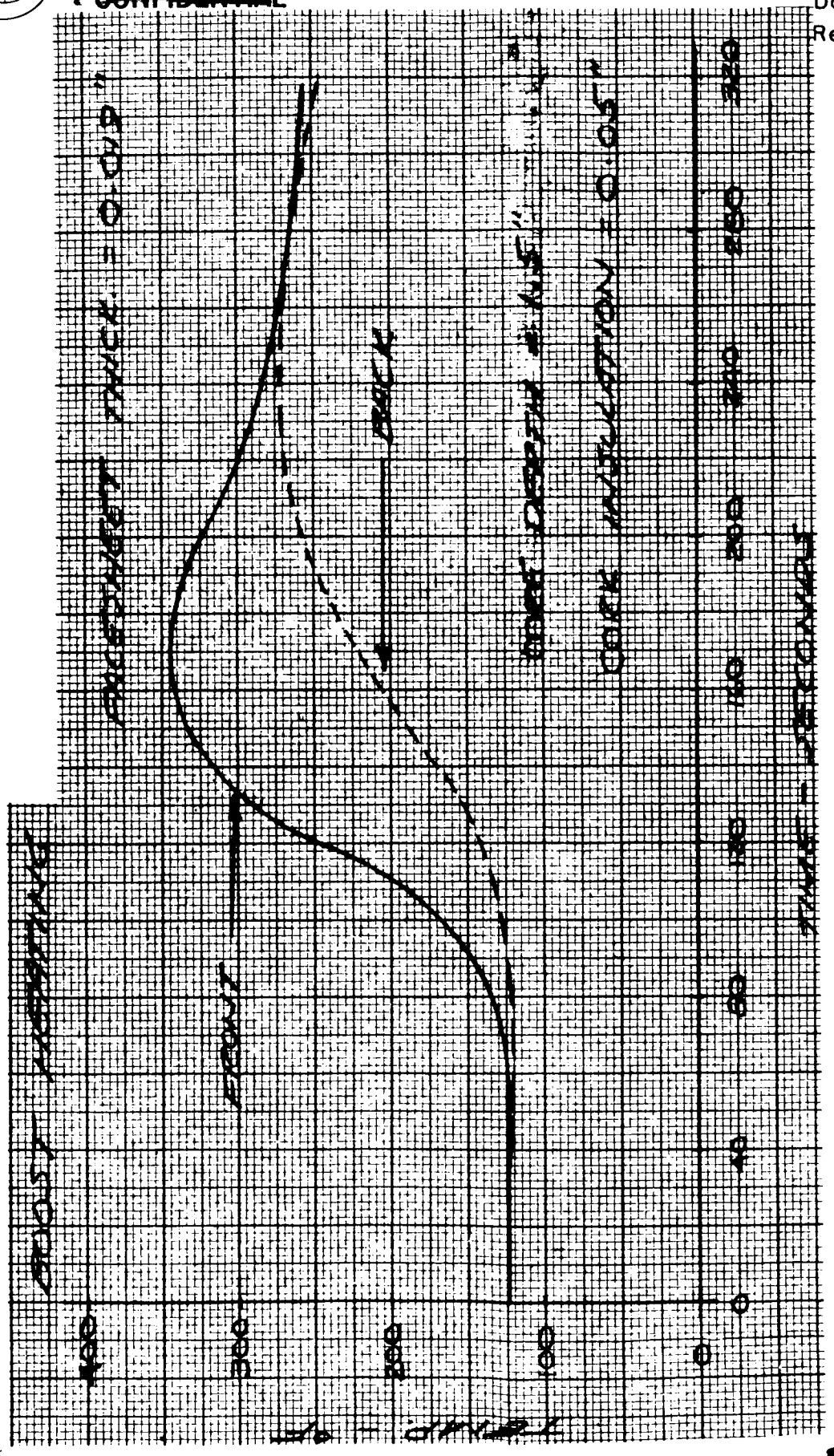

Figure 5-48. Temperature History of LEM Adapter: Aluminum Honeycomb Facesheet During Saturn-V Boost Heating (Sheet 1 of 3)

~~CONFIDENTIAL~~

[redacted]

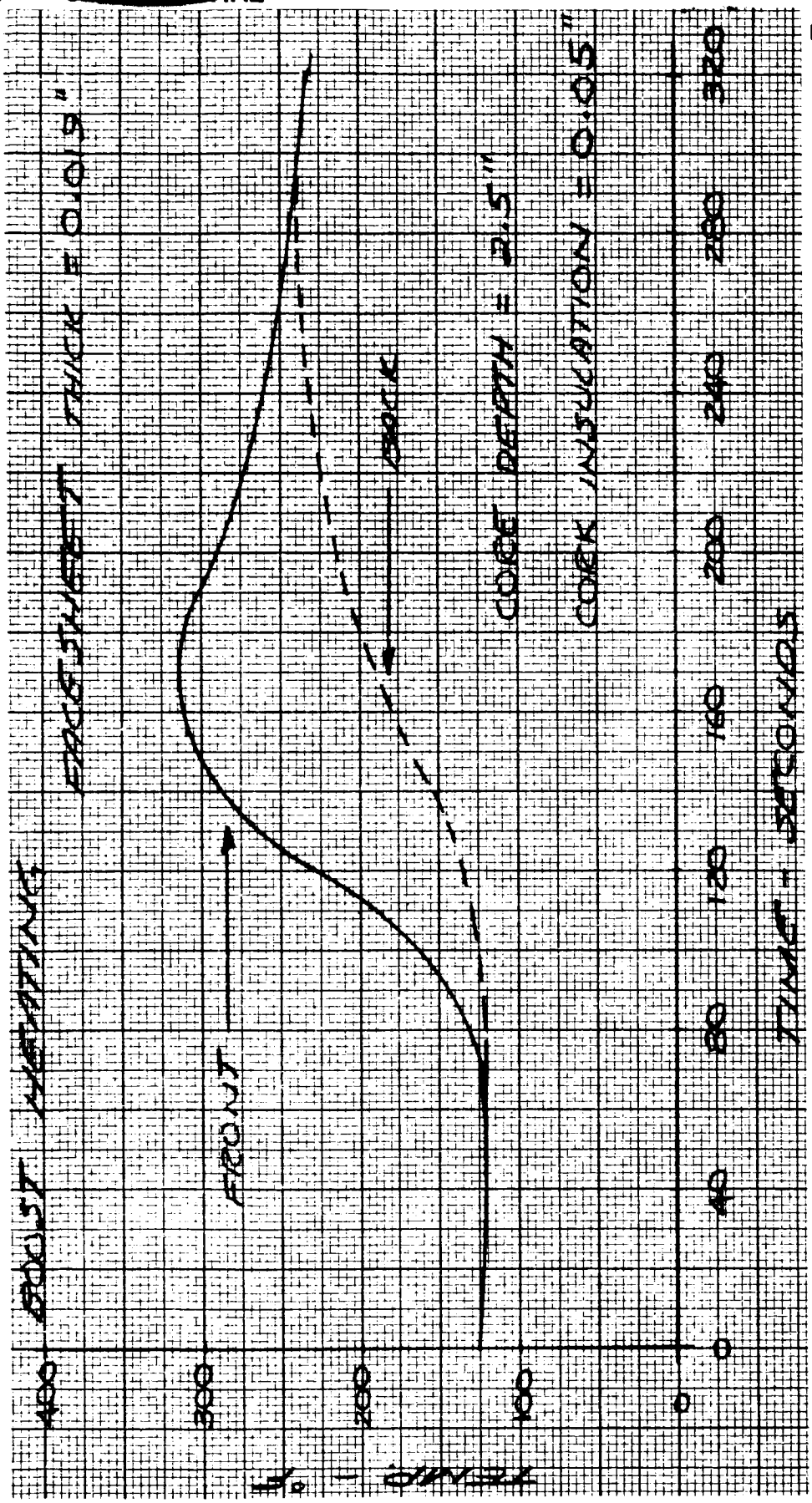

Figure 5-48. Temperature History of LEM Adapter: Aluminum Honeycomb Facesheet During Saturn-V Boost Heating (Sheet 2 of 3)

[redacted]

[redacted]

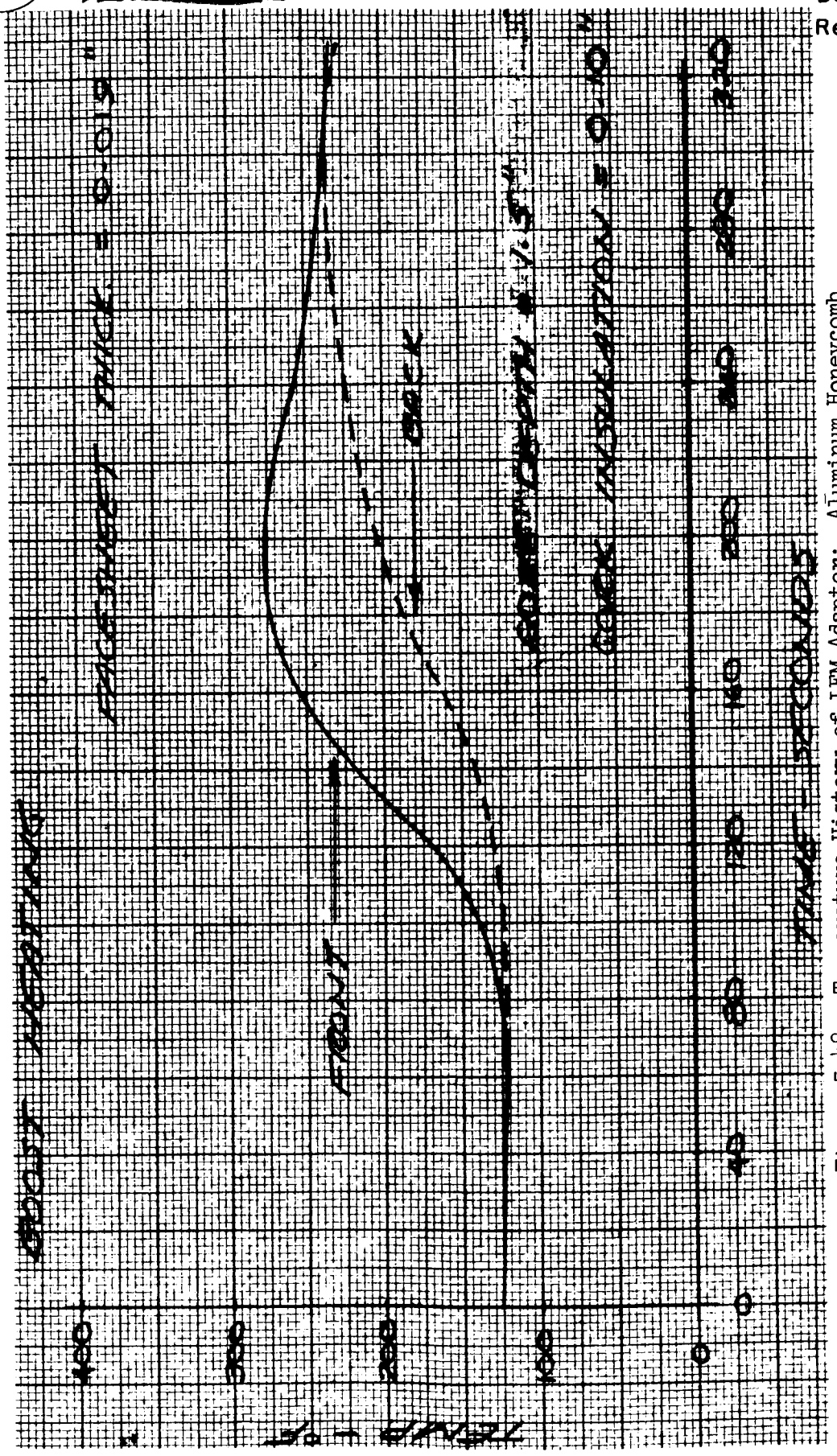

Figure 5-48. Temperature History of LEM Adapter: Aluminum Honeycomb Facesheet During Saturn-V Boost Heating (Sheet 3 of 3)

[redacted]

[redacted]

6.0 GROUND SUPPORT EQUIPMENT

Note: This material is currently being prepared. It will be distributed to all manual holders by IOL, when available.

GROUP (4)
DOWNGRADED AT 3 YEAR INTERVALS; DECLASSIFIED AFTER 12 YEARS.

[redacted]